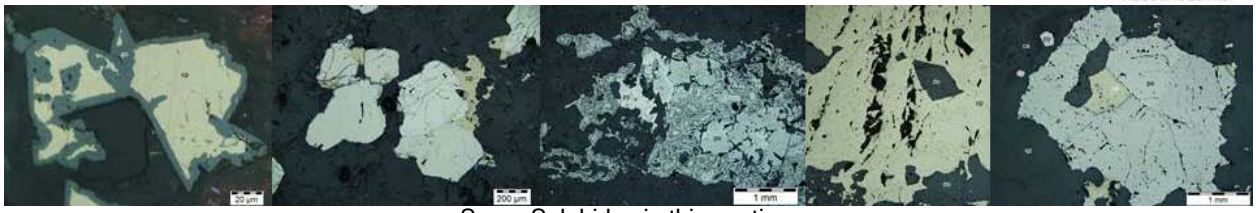

Sagar Sulphides in thin section.

Exploration Report

(February-March and July-August 2013 Program)
on the

Sagar Property

Romanet Horst, Labrador Trough, Québec, Canada

Latitude, 56°22'N and Longitude 68°00'W
NTS Map sheets 24B/05 and 24C/08

February, 2014

Prepared for

ENERGIZER RESOURCES INC.

Toronto, Ontario

By

Jean-Philippe Desrochers, P.Geo.
Craig Scherba, P.Geo.
Jean-François Montreuil
Quentin Yarie, P.Geo.

2. Table of Contents

2. Table of Contents 2
3. Summary 6
4. Introduction 8
5. Reliance on Other Experts 11
6. Property Description and Location 12
    6.1 Location 12
    6.2 Company Name Change 12
    6.3 Property Title and Tenure 12
    6.4 Terms of Option agreement on Sagar property 12
7. Accessibility, Climate, Local Resources, Infrastructure and Physiography 29
    7.1 Accessibility 29
    7.2 Climate 30
    7.3 Local Resources 30
    7.4 Infrastructure and Physiography 30
8. Exploration History 32
9. Geological Setting 35
    9.1 Regional Geology 35
    9.2 Labrador Trough Stratigraphy 37
    9.3 Local Geology 37
    9.4 Large Igneous Provinces (LIPs) 40
10. Deposit Types 41
    10.1 Labrador Trough Deposit Types 41
    10.2 Iron-Oxide Copper Gold (IOCG) Deposit Model 42
11. Mineralization 44
    11.1 Mistamisk Boulder Field 44
    11.2 Gold-Uranium Mineralization, Northern Part of the Romanet Horst 45
    11.3 Showings Along the East Boundary of the Romanet Horst 46
    11.4 Showings in the Central Part of the Romanet Horst 48
12. Exploration 49
    12.1 Airborne Geophysical Surveying 49
    12.2 Prospecting and Grab Sampling 50
        12.2.1 Sampling Method and Approach 50
        12.2.2 Sample Preparation and Security 50
        12.2.3 Sample Analysis 51
13. Data Verification and interpretations 51
14. Thin Section Analysis 54
15. IOCG Alteration Analysis 56
    15.1 Description and classification of alteration facies 57
    15.2 Na alteration 59
    15.3 Ca-Fe (HT) 59
        15.3.1 Ca-Fe (HT;Amp-Mag) and Na-Ca±Fe (Ab-Amp±Mag) 59

15.4 K-Fe (HT) 60
15.4.1 K-Fe (HT;Bt-Mag) 60
15.4.2 K-Mg (HT;Bt) 60
15.5 K-Fe (LT) 61
15.5.1 K (LT; sericite) 61
15.5.2 K (K-feldspar) 61
15.5.3 K-Fe-Mg (Argillic) 61
15.5.4 K-Fe (LT; Ser-Hem, Cb-Hem±Qtz, Hem, Chl-Hem) 62
15.5.5 Mg-Fe (LT; chlorite) 62
15.5.6 K-Fe (LT; Kfs-Hem) 63
15.6 Dolomitisation 63
15.6.1 Si-Mg-Ca dolomitisation (White to whitish pink dolomitisation) 63
15.6.2 Mg-Mn±K-Fe (White dolomitisation) 64
15.6.3 Mg-Mn-Fe-K (Pink dolomitisation) 64
15.6.4 Mg-Mn-Fe (Reddish pink to red dolomitisation) 64
15.6.5 Mg-Fe (Pale green or brown sugar dolomitisation) 65
15.6.6 Mg (Talc alteration) 65
15.6.7 Ca (Calcite alteration) 65
15.7 Ca-Fe (LT; Ep) 65
15.8 Silicification 65
15.8.1 Quartz veins 66
15.9 Sulfate 66
15.10 Relative timing of formation of the hydrothermal alteration facies in the Sagar property 67
16. Drilling 68
17. Adjacent Properties 68
18. Mineral Processing and Metallurgical Testing 69
19. Mineral Resource and Mineral Reserve Estimates 69
20. Other Relevant Data and Information 69
21. Interpretation and Conclusions 69
22. Recommendations 72
23. References 74
Date and Signature Page 81
Additional Requirements for Technical Reports on Development Properties and Production 82

Tables

Table 6.1-1 – Claim blocks 100% under the responsibility of Energizer Resources Corp. 14
Table 6.1-2 –Registration information and subjected NSR on the claim blocks 100% under the responsibility of Energizer Resources Corp. 21
Table 8-1 – Summary of notable exploration work on Sagar Property. 33
Table 9.3-1: Table of formations on Sagar Property 39
Table 22-1: Budget 72

Figures

Figure 4-1: Sagar Property location. 10
Figure 6.1-1: Sagar Property claim configuration. 13
Figure 7.1-1: Sagar Property location map. 29
Figure 9.1-1: Outline of Labrador Trough thrust packages: Sketch modified after Clark (2005). The Archean Superior Province to the west still acts as a basement to Trough supracrustals unconformably overlying its complex gneissic packages. As one proceeds east, Trough units are successively detached from their basement. Large-igneous-province units have been emphasized on the figure as well. 36
Figure 10.2-1: Flow paths and hydrothermal features for alternative models of IOCG deposits from Barton and Johnson (2004). 43
Figure 11-1: Sagar Property mineral showings. 44
Figure 12.1-1: Flight path of the Sagar property area over a Google Earth image. 50
Figure 13.2-1: 2013 grab sample locations. 52
Figure 13.2-2: Copper-in-grab samples. 53
Figure 13.2-3: Cobalt-in-grab samples. 53
Figure 14.1-1 Map showing the distribution of the alteration facies from thin section and grab sample descriptions. 54
Figure 15.1-1 Main alteration facies identified in the Sagar Property 58
Figure 15.10-1 Preliminary paragenetic relationships between the some of the alteration facies observed at the Sagar Property 68
Figure 17.1-1 Properties adjacent to the Sagar Property 69

Maps

- Claims Location Map
- Showings Location Map
- Sample Location Map Compilation
- Copper Sample Map Compilation
- Cobalt Sample Map Compilation

Appendix A

1. Geological map of the Sagar property from the MRNF report ET 83 - 22

Appendix B

1. Analytical Results – Rock Grab + Summarized description
2. Actlabs Assay and Analytical Procedures

Appendix C

1. VTEMplus Suvey

Appendix D

1. Thin Section Analysis

Appendix E

1. List of Project Personnel

DVD-1

- Report Text and Figures
- All Raw Data

3. Summary

The Sagar Property comprises blocks of claims in the Territory of Nunavik, Province of Québec, Canada. Energizer Resources Inc. (Energizer) has a 100% undivided interest in the Sagar Property. The Sagar Property occurs in the Romanet Horst, a northwest-trending 40 by 12 kilometre uplifted structural block of sediments that is juxtaposed against younger surrounding metasedimentary rocks and igneous rocks within the Labrador Trough. As the metasedimentary rocks within the horst are less resistant than the surrounding sediments, the horst is a low-lying negative-relief feature, the Mistamisk Valley.

Gold, uranium, and copper showings were discovered within the boundaries of what is now the Sagar Property by various workers over the past 60 years. The most spectacular mineralization identified on the property was the discovery of the Mistamisk Boulder Field (a.k.a. Clandestine), which was identified in 1983 by Saarberg-Interplan. The Mistamisk Boulder Field is approximately 500 X 250 meters in size and contains many radioactive gold bearing albitized mudstone to sandstone boulders. In a Virginia Mines report, 70 boulders assayed an average of 64.9g/t Au and 1.3% U (with values up to 640 g/t Au and 4.11% U).

Although the grades are impressive over the Mistamisk Boulder Field, the source of this mineralization has yet to be discovered. An analysis of the geochemistry associated with the boulder filed in 2007 indicated that the mineralization may be associated with an Iron-Oxide-Copper-Gold (IOCG) mineralized system, and may therefore represent a small, surficially exposed portion of a much larger mineralized system. Energizer conducted two field exploration programs from February 14 through to March 17, and July 17 through to August 5, 2013 to ascertain if the Property as a whole had the potential to host a significant IOCG mineralized body.

The following work was completed on the Sagar Property during the 2013 exploration programs:

- 1114 line kilometres of helicopter-borne Versatile Time Domain Electromagnetic (VTEMplus) Horizontal Magnetic Gradiometer and Gamma-Ray Spectroscopy geophysical surveying
- Collection of 169 grab samples for geochemical analysisCollection of 54 samples for thin section analysis
- On-site hand-held XRF analysis of 623 grab and historic core samples to identify IOCG alteration mineral assemblages

Geochemical analsysis of prospecting samples collected during the course of the 2013 exploraiton program indicate that the IOCG metals copper and cobalt are found in highly anomalous concentrations along the boundaries of the Romanet Horst on the Property. Previous work identified anomalous gold, molybdenum and uranium in similar locations (i.e. along the horst boundaries).

Thin section analyses of 54 samples collected from ‘representative’ altered lithotypes found on the Property identified alteration minerals consistent with an IOCG alteration assemblage. Specifically, the alteration minerals albite, calcite, dolomite, quartz, hematite, biotite, actinolite, magnetite, titanite, white mica tourmaline and epidote were identified.

The alteration facies observed over the Sagar Property, comprising Na, magnetite-bearing Ca-Fe (HT) and K-Fe (HT) and specular hematite-bearing K-Fe (LT), indicate that the hydrothermal system contained in the Sagar Property has all the alteration facies expected in an IOAA system that may contain an important IOCG deposit (Hitzman et al., 1992; Williams et al., 2005; Corriveau et al., 2010; Groves et al., 2010). The characteristics of the hydrothermal system located in the Sagar Property include:

1. Extensive mantle and crustal melting related to the formation of the large igneous mafic province located on both sides of the horst and high to extreme paleogeothermal gradients that likely have resulted in major hydrothermal fluid convection cells and provided additional sulfur for deposit formation;
2. The presence of crustal scale structures, represented by the two bounding faults of the Romanet horst and the large E-W fault cutting the property in its center;
3. The likelihood that a large evaporitic sequence was formed in the pre-IOCG basin;
4. The inferred switch from a compressional regime to a transtensional tectonic regime in the Romanet Horst;
5. The preservation of the shallow section of the hydrothermal system as evidenced by the abundant low temperature hydrothermal alteration facies forming mineral assemblages comprised of hematite, chlorite, sericite and carbonate in the Sagar Property;
6. The presence of large-scale fluid conduits represented by the polymict breccia zones that could have channeled the sulfate-rich fluids to mixing zones with higher temperature and copper-bearing fluids; and
7. The presence of hydrothermal alteration facies containing combination of hematite, chlorite, sericite, carbonate, pyrite, chalcopyrite, P-bearing minerals and likely barite

The overall alteration package, the presence of crustal-scale structures, the switch from a compressive to transpressional tectonic regime and the abundance of low temperature alteration facies in the Sagar property answers most of the criteria stated by Skirrow (2010) for the recognition of geological environments likely to host polymetallic hematite-group or magnetite-group IOCG deposits according to the classification of Williams (2010).

The elements of typical IOCG districts that remain to be found in the Sagar system are the source of uranium and the location of the granitic magmatism. The presence of granite-sourced magmatic-hydrothermal fluids is partially evidenced by the thorium-rich uranium mineralization in the Kish and Eagle showings, localized rare earth element (REE) enrichments, and fluorine enrichment in the mineralized zones of the Taché showings. The uranium may have been partially sourced from the sedimentary rocks.

The following stages to fully characterize the hydrothermal alteration of the Sagar property include the completion of the light element XRF database for each alteration types, the characterization of the petrography of the main alteration facies and the treatment of whole-rock analyzes database that will be constructed as a result of this preliminary study.

Future exploration efforts should be focused on the discovery of potentially economic IOCG mineralization spatially associated with the boundaries of the Romanet Horst or the E-W lineament cutting the center of the property. This work should be conducted in a step-wise progression as follows:

- A robust geochemical analysis of all historical geochemical data should be conducted over the property with the prime focus of identifying geochemical vectors toward prospective IOCG targets
- Re-logging of available drill core should be completed. The objective is to document the alteration patterns, their cross-cutting relationships, and their possible geometry. This information will then be used to refine the geological model and to generating drill targets.
- A transient AMT (TAMT) tipper Internal Field Gradient (IFG) ground geophysical survey should be conducted over target areas identified by the geochemical vectoring
- A 3D compilation of all geophysical work completed over the Property should be performed over prospective target areas identified by the geochemical vectoring and the tipper/IFG ground geophysics in order to identify drill targets
- Targets identified by the geophysical compilation work should be drill tested with a diamond drill capable of depths to 500 metres

4. Introduction

This report was commissioned by Richard Schler, CEO of Energizer Resources Inc. (Energizer), to review the exploration activity on the Sagar Property, located in the Province of Québec, Canada (Figure 4-1). The report is intended as an internal report, and was requested by Energizer to be compliant with the guidelines set forth in National Instrument 43-101 (NI 43-101). Sections of two previous NI 43-101 compliant reports by Scherba (2008), and by Butler and Scherba (2006) have been used in a slightly modified form within. In particular, any sections not dealing directly with 2013 exploration are only slightly modified from the previous reports.

Energizer managed exploration activities on the Sagar Property. Craig Scherba, President of Energizer, or Quentin Yarie, Vice-President of Energizer, were involved in the design and implementation of the exploration programs conducted on Energizer's behalf from February 14 through to March 17, and July 17 through to August 5, 2013. Scherba and Yarie were on site from July 17 through to July 29, 2013.

In addition to personal observations and data collected by Energizer, the authours have used Scherba (2008), Butler and Scherba (2006), Setterfield *et al.* (2006), exploration data and internal reports from previous workers, geological maps and open file reports prepared by the Quebec and federal governments, and research in scientific journals for the preparation of this report.

The Sagar Property is an exploration property as there are no mineral reserves of any kind within its boundaries.

Universal Transverse Mercator (UTM) coordinates are used within this report, and are reported in UTM zone 19 N, NAD 83 datum.

The following work was completed on the Sagar Property during the 2013 exploration programs:

- 1114 line kilometres of helicopter-borne Versatile Time Domain Electromagnetic (VTEMplus) Horizontal Magnetic Gradiometer and Gamma-Ray Spectroscopy geophysical surveying
- Collection of 169 grab samples for geochemical analysisCollection of 54 samples for thin section analysis
- On-site hand-held XRF analysis of 623 grab and historic core samples to identify IOCG alteration mineral assemblages

Figure 4-1: Sagar Property location.

5. Reliance on Other Experts

C. Scherba, P. Geo., and Q. Yarie, P.Geo., supervised and conducted the exploration programs on which this report is based and have done so in accordance with normal industry practices. Property information in this report is sourced from official documents held by Energizer Resources Inc. For the purpose of this report, the authours assumed that Energizer Resources Inc. has appropriate right of title to the property area. The authors are not responsible however, for the accuracy of any property data and do not make any claim or state any opinion as to the validity of the property disposition described herein.

For the preparation of this report, the authors have relied upon maps, documents and electronic files generated by the exploration crew, contributing consultants and service providers working under their supervision. To the extent possible under the mandate of a National Instrument 43-101 review the authors have verified the material facts relating to the prospectiveness of the property reviewed in this report.

Considering the number of workers contributing to the project and the amount of information generated thereby, the authors take responsibility for work conducted under their supervision but can in no way be responsible for any inaccuracy, omission or misrepresentation of any historical, external or third party material used by them in preparation of this report.

6. Property Description and Location

6.1 Location

The Property comprises blocks of claims in the Territory of Nunavik, Province of Québec, Canada. The approximate center of exploration activity is 56°22' N latitude and 68° 00' W longitude. Details on the individual claims are given in Tables 6.1-1 and 6.1-2 and their location is shown on figure 6.1-1, based on information available on-line at the Government of Québec's Ministère des ressources naturelles, de la faune et des parcs GESTIM website (https://gestim.mines.gouv.qc.ca/MRN_GestimP_Presentation/ODM02201_menu_base.aspx).

6.2 Company Name Change

The Company changed its name to Energizer Resources in the spring of 2009. At the Special and Annual Shareholders' meeting held on December 9, 2009, the Company's shareholders approved a change of the Company's name from Uranium Star Corp. (trading symbol "URST" on the OTC BB, now ENZR) to Energizer Resources Inc. Energizer Resources Inc. also commenced its trading on the TSX Venture Exchange (TSX-V) on May 5, 2010, under the trading symbol "EGZ", and graduated to the TSX Exchange (TSX) on June 6, 2011.

6.3 Property Title and Tenure

The area of these claims is 15,502 hectares. Due dates are shown on Table 6. 1-11, and Energizer's tenure arrangement is described below. Claim outlines are predetermined by map staking. As a result, former staked claims are superimposed upon by the map-staking grid which results in some small parcels shown in the table below. There are no carried environmental liabilities on the Property. All surface work requires Provincial government permits including camp construction permits.

6.4 Terms of Option agreement on Sagar property

Energizer Resources, formely known as Uranium Star (changed to Energizer Resources, Spring 2009) and previously as Yukon Resources Corp. (changed to Uranium Star on December 22, 2006), entered into a joint venture agreement with Virgnia Mines Inc. (TSX-VGQ) and acquired a 100% interest in the claims forming the initial Sagar property in 2007 (see Figure 6.1-2; red colored claim block), indicated in a Uranium Star new release dated February 28, 2007 (see Scherba, 2008 for more details on the acquisition process). However Virginia Mines Inc. keeps a 1.5% NSR on the claims forming the initial Sagar Property acquired from the 2006 agreement as well as on any claims located within a 2 kilometers radius of the initial Sagar property. Some of the claims, initially owned by Jones & Poisson and acquired from the 2006 agreement, are also subjected to a 1% NSR or to a 0.5% NSR depending of the claims (see Table 6.2 and Figure 6.1-1). Energizer Resources has the right to buy back half of the 1% NSR (0.5%) for 200,000$ and half of the 0.5% NSR for 100,000$ (Table 6.2). From 2009-2013, Energizer Resources subseqently acquired new claims to complete the land holding to form an extended Sagar project. Some of the newly acquired claims are subjected to the 1.5% NSR to Virginia Mines Inc (Table 6.2-1).

From the 2006 agreement,

"Virginia also keeps a 51% back-in right in any gold discovery with a 43-101 indicated resources of no less than 500 000 ounces of contained gold equivalent (for all precious metals), Virginia will have, within 90 days of notice from Yukon of the discovery of a Gold Deposit of no less than 500,000 ounces, a one time right to back-in to re-acquire a 51% interest in the discovery by issuing a cash payment or a share certificate equivalent to an amount equal to 2.5 times the expenditure incurred by Yukon (now Energizer Resources) at such date. A joint venture would then be formed and Virginia would then become the operator".

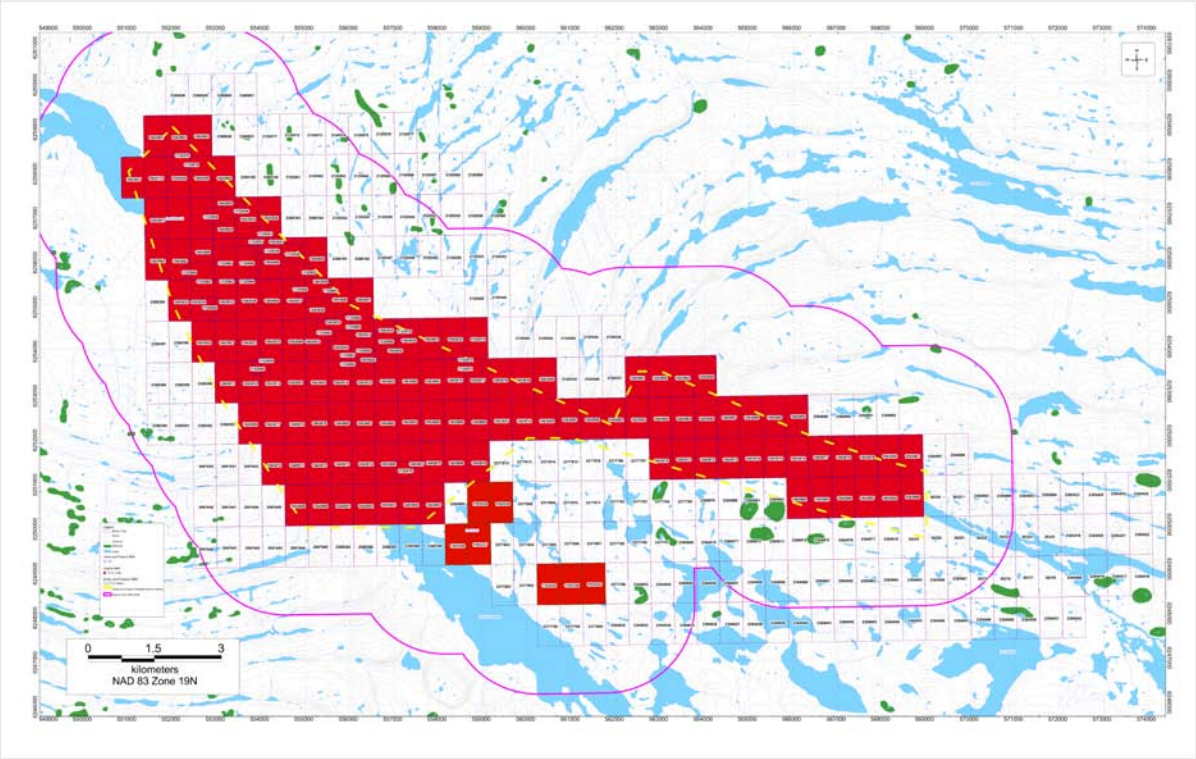

Figure 6.1-1: Sagar Property claim configuration.

Table 6.1-1 – Claim blocks 100% under the responsibility of Energizer Resources Corp.

NTS Sheet	Type of Title	Title No	Status	Date of Registration	[1]Expiry Date	# of Renewals	Area (Ha)	Excess Work ($)	Required Work ($)	Required Fees ($)
24B05	CDC	36315	Active	14/09/2004	13/09/2014	4	47.74	0.00	1,800.00	113.00
24B05	CDC	36316	Active	14/09/2004	13/09/2014	4	47.74	0.00	1,800.00	113.00
24B05	CDC	36317	Active	14/09/2004	13/09/2014	4	47.74	0.00	1,800.00	113.00
24B05	CDC	36318	Active	14/09/2004	13/09/2014	4	47.74	0.00	1,800.00	113.00
24B05	CDC	36319	Active	14/09/2004	13/09/2014	4	47.73	0.00	1,800.00	113.00
24B05	CDC	36320	Active	14/09/2004	13/09/2014	4	47.73	0.00	1,800.00	113.00
24B05	CDC	36321	Active	14/09/2004	13/09/2014	4	47.73	0.00	1,800.00	113.00
24B05	CDC	36322	Active	14/09/2004	13/09/2014	4	47.73	0.00	1,800.00	113.00
24B05	CDC	36323	Active	14/09/2004	13/09/2014	4	47.73	0.00	1,800.00	113.00
24B05	CDC	36324	Active	14/09/2004	13/09/2014	4	47.73	0.00	1,800.00	113.00
24B05	CDC	36325	Active	14/09/2004	13/09/2014	4	47.73	0.00	1,800.00	113.00
24B05	CDC	36326	Active	14/09/2004	13/09/2014	4	47.72	0.00	1,800.00	113.00
24B05	CDC	36327	Active	14/09/2004	13/09/2014	4	47.72	0.00	1,800.00	113.00
24C08	CDC	1043868	Active	15/01/2002	14/01/2016	6	47.72	0.00	2,500.00	113.00
24C08	CDC	1043869	Active	15/01/2002	14/01/2016	6	47.72	0.00	2,500.00	113.00
24C08	CDC	1043870	Active	15/01/2002	14/01/2016	6	47.71	0.00	2,500.00	113.00
24C08	CDC	1043871	Active	15/01/2002	14/01/2016	6	47.71	0.00	2,500.00	113.00
24C08	CDC	1043872	Active	15/01/2002	14/01/2016	6	47.71	0.00	2,500.00	113.00
24C08	CDC	1043873	Active	15/01/2002	14/01/2016	6	47.71	0.00	2,500.00	113.00
24C08	CDC	1043874	Active	15/01/2002	14/01/2016	6	47.71	0.00	2,500.00	113.00
24C08	CDC	1043875	Active	15/01/2002	14/01/2016	6	47.71	0.00	2,500.00	113.00
24C08	CDC	1043876	Active	15/01/2002	14/01/2016	6	47.71	0.00	2,500.00	113.00
24C08	CDC	1043877	Active	15/01/2002	14/01/2016	6	47.70	0.00	2,500.00	113.00
24C08	CDC	1043878	Active	15/01/2002	14/01/2016	6	47.70	0.00	2,500.00	113.00
24C08	CDC	1043879	Active	15/01/2002	14/01/2016	6	47.70	0.00	2,500.00	113.00
24C08	CDC	1043880	Active	15/01/2002	14/01/2016	6	47.70	0.00	2,500.00	113.00
24C08	CDC	1043881	Active	15/01/2002	14/01/2016	6	47.70	0.00	2,500.00	113.00
24C08	CDC	1043882	Active	15/01/2002	14/01/2016	6	47.70	0.00	2,500.00	113.00
24C08	CDC	1043883	Active	15/01/2002	14/01/2016	6	47.70	0.00	2,500.00	113.00
24C08	CDC	1043884	Active	15/01/2002	14/01/2016	6	47.70	0.00	2,500.00	113.00
24C08	CDC	1043885	Active	15/01/2002	14/01/2016	6	47.70	0.00	2,500.00	113.00
24C08	CDC	1043886	Active	15/01/2002	14/01/2016	6	47.70	0.00	2,500.00	113.00
24C08	CDC	1043887	Active	15/01/2002	14/01/2016	6	47.70	0.00	2,500.00	113.00
24C08	CDC	1043888	Active	15/01/2002	14/01/2016	6	47.70	0.00	2,500.00	113.00
24C08	CDC	1043889	Active	15/01/2002	14/01/2016	6	47.70	0.00	2,500.00	113.00
24C08	CDC	1043890	Active	15/01/2002	14/01/2016	6	47.70	0.00	2,500.00	113.00
24C08	CDC	1043891	Active	15/01/2002	14/01/2016	6	47.69	0.00	2,500.00	113.00
24C08	CDC	1043892	Active	15/01/2002	14/01/2016	6	47.69	0.00	2,500.00	113.00
24C08	CDC	1043893	Active	15/01/2002	14/01/2016	6	47.69	0.00	2,500.00	113.00
24C08	CDC	1043894	Active	15/01/2002	14/01/2016	6	47.69	0.00	2,500.00	113.00
24C08	CDC	1043895	Active	15/01/2002	14/01/2016	6	47.69	0.00	2,500.00	113.00
24C08	CDC	1043896	Active	15/01/2002	14/01/2016	6	47.69	0.00	2,500.00	113.00
24C08	CDC	1043897	Active	15/01/2002	14/01/2016	6	47.68	0.00	2,500.00	113.00
24C08	CDC	1043898	Active	15/01/2002	14/01/2016	6	47.68	0.00	2,500.00	113.00
24C08	CDC	1043899	Active	15/01/2002	14/01/2016	6	47.66	0.00	2,500.00	113.00
24C08	CDC	1043900	Active	15/01/2002	14/01/2016	6	47.64	0.00	2,500.00	113.00
24C08	CDC	1043901	Active	15/01/2002	14/01/2016	6	47.72	0.00	2,500.00	113.00
24C08	CDC	1043902	Active	15/01/2002	14/01/2016	6	47.72	0.00	2,500.00	113.00
24C08	CDC	1043903	Active	15/01/2002	14/01/2016	6	47.72	0.00	2,500.00	113.00

NTS Sheet	Type of Title	Title No	Status	Date of Registration	[1]Expiry Date	# of Renewals	Area (Ha)	Excess Work ($)	Required Work ($)	Required Fees ($)
24C08	CDC	1043904	Active	15/01/2002	14/01/2016	6	47.72	0.00	2,500.00	113.00
24C08	CDC	1043905	Active	15/01/2002	14/01/2016	6	47.72	0.00	2,500.00	113.00
24C08	CDC	1043906	Active	15/01/2002	14/01/2016	6	42.97	0.00	2,500.00	101.00
24C08	CDC	1043907	Active	15/01/2002	14/01/2016	6	36.59	0.00	2,500.00	101.00
24C08	CDC	1043908	Active	15/01/2002	14/01/2016	6	47.71	0.00	2,500.00	113.00
24C08	CDC	1043909	Active	15/01/2002	14/01/2016	6	47.70	0.00	2,500.00	113.00
24C08	CDC	1043910	Active	15/01/2002	14/01/2016	6	47.70	0.00	2,500.00	113.00
24C08	CDC	1043911	Active	15/01/2002	14/01/2016	6	47.69	0.00	2,500.00	113.00
24C08	CDC	1043912	Active	15/01/2002	14/01/2016	6	42.41	0.00	2,500.00	101.00
24C08	CDC	1043913	Active	15/01/2002	14/01/2016	6	41.47	0.00	2,500.00	101.00
24C08	CDC	1043914	Active	15/01/2002	14/01/2016	6	44.60	0.00	2,500.00	101.00
24C08	CDC	1043915	Active	15/01/2002	14/01/2016	6	45.31	0.00	2,500.00	113.00
24C08	CDC	1043916	Active	15/01/2002	14/01/2016	6	46.38	0.00	2,500.00	113.00
24C08	CDC	1043917	Active	15/01/2002	14/01/2016	6	33.86	0.00	2,500.00	101.00
24C08	CDC	1043918	Active	15/01/2002	14/01/2016	6	47.69	0.00	2,500.00	113.00
24C08	CDC	1043919	Active	15/01/2002	14/01/2016	6	47.69	0.00	2,500.00	113.00
24C08	CDC	1043920	Active	15/01/2002	14/01/2016	6	47.68	0.00	2,500.00	113.00
24C08	CDC	1043921	Active	15/01/2002	14/01/2016	6	46.45	0.00	2,500.00	113.00
24C08	CDC	1043922	Active	15/01/2002	14/01/2016	6	46.32	0.00	2,500.00	113.00
24C08	CDC	1043923	Active	15/01/2002	14/01/2016	6	37.20	0.00	2,500.00	101.00
24C08	CDC	1043924	Active	15/01/2002	14/01/2016	6	24.59	522.72	1,000.00	28.00
24C08	CDC	1043925	Active	15/01/2002	14/01/2016	6	1.23	0.00	1,000.00	28.00
24C08	CDC	1043926	Active	15/01/2002	14/01/2016	6	1.65	0.00	1,000.00	28.00
24C08	CDC	1043927	Active	15/01/2002	14/01/2016	6	25.24	0.00	2,500.00	101.00
24C08	CDC	1043928	Active	15/01/2002	14/01/2016	6	14.13	0.00	1,000.00	28.00
24C08	CDC	1043929	Active	15/01/2002	14/01/2016	6	12.85	0.00	1,000.00	28.00
24C08	CDC	1043930	Active	15/01/2002	14/01/2016	6	36.65	0.00	2,500.00	101.00
24C08	CDC	1043931	Active	15/01/2002	14/01/2016	6	47.68	0.00	2,500.00	113.00
24C08	CDC	1043932	Active	15/01/2002	14/01/2016	6	47.60	0.00	2,500.00	113.00
24C08	CDC	1043933	Active	15/01/2002	14/01/2016	6	47.66	0.00	2,500.00	113.00
24C08	CDC	1043934	Active	15/01/2002	14/01/2016	6	37.00	0.00	2,500.00	101.00
24C08	CDC	1043935	Active	15/01/2002	14/01/2016	6	40.84	0.00	2,500.00	101.00
24C08	CDC	1043936	Active	15/01/2002	14/01/2016	6	46.22	0.00	2,500.00	113.00
24C08	CDC	1043937	Active	15/01/2002	14/01/2016	6	39.70	0.00	2,500.00	101.00
24C08	CDC	1043938	Active	15/01/2002	14/01/2016	6	24.43	0.00	1,000.00	28.00
24C08	CDC	1043939	Active	15/01/2002	14/01/2016	6	2.48	0.00	1,000.00	28.00
24C08	CDC	1043940	Active	15/01/2002	14/01/2016	6	39.07	0.00	2,500.00	101.00
24C08	CDC	1043941	Active	15/01/2002	14/01/2016	6	46.87	0.00	2,500.00	113.00
24C08	CDC	1043942	Active	15/01/2002	14/01/2016	6	47.65	0.00	2,500.00	113.00
24C08	CDC	1043943	Active	15/01/2002	14/01/2016	6	42.61	0.00	2,500.00	101.00
24C08	CDC	1043944	Active	15/01/2002	14/01/2016	6	28.37	0.00	2,500.00	101.00
24C08	CDC	1043945	Active	15/01/2002	14/01/2016	6	15.02	0.00	1,000.00	28.00
24C08	CDC	1043946	Active	15/01/2002	14/01/2016	6	12.20	0.00	1,000.00	28.00
24C08	CDC	1043947	Active	15/01/2002	14/01/2016	6	3.79	0.00	1,000.00	28.00
24C08	CDC	1043948	Active	15/01/2002	14/01/2016	6	24.15	0.00	1,000.00	28.00
24C08	CDC	1043949	Active	15/01/2002	14/01/2016	6	22.74	48.80	1,000.00	28.00
24C08	CDC	1043950	Active	15/01/2002	14/01/2016	6	43.15	0.00	2,500.00	101.00
24C08	CDC	1043951	Active	15/01/2002	14/01/2016	6	47.64	0.00	2,500.00	113.00
24C08	CDC	1043952	Active	15/01/2002	14/01/2016	6	43.21	0.00	2,500.00	101.00
24C08	CDC	1043953	Active	15/01/2002	14/01/2016	6	9.39	0.00	1,000.00	28.00
24C08	CDC	1043954	Active	15/01/2002	14/01/2016	6	18.90	0.00	1,000.00	28.00

NTS Sheet	Type of Title	Title No	Status	Date of Registration	[1]Expiry Date	# of Renewals	Area (Ha)	Excess Work ($)	Required Work ($)	Required Fees ($)
24C08	CDC	1043955	Active	15/01/2002	14/01/2016	6	35.77	0.00	2,500.00	101.00
24C08	CDC	1043956	Active	15/01/2002	14/01/2016	6	41.83	0.00	2,500.00	101.00
24C08	CDC	1043957	Active	15/01/2002	14/01/2016	6	47.63	0.00	2,500.00	113.00
24C08	CDC	1043958	Active	15/01/2002	14/01/2016	6	36.30	0.00	2,500.00	101.00
24C08	CDC	1043959	Active	15/01/2002	14/01/2016	6	46.36	0.00	2,500.00	113.00
24C08	CDC	1043960	Active	15/01/2002	14/01/2016	6	47.63	0.00	2,500.00	113.00
24C08	CDC	1043961	Active	15/01/2002	14/01/2016	6	47.62	0.00	2,500.00	113.00
24C08	CDC	1043962	Active	15/01/2002	14/01/2016	6	43.55	0.00	2,500.00	101.00
24C08	CDC	1043963	Active	15/01/2002	14/01/2016	6	47.12	0.00	2,500.00	113.00
24B05	CDC	1043964	Active	15/01/2002	14/01/2014	5	47.72	0.00	1,800.00	226.00
24B05	CDC	1043965	Active	15/01/2002	14/01/2014	5	47.72	133.02	1,800.00	226.00
24B05	CDC	1043966	Active	15/01/2002	14/01/2014	5	47.72	133.02	1,800.00	226.00
24B05	CDC	1043967	Active	15/01/2002	14/01/2014	5	47.72	0.00	1,800.00	226.00
24B05	CDC	1043968	Active	15/01/2002	14/01/2014	5	47.72	0.00	1,800.00	226.00
24B05	CDC	1043969	Active	15/01/2002	14/01/2014	5	47.72	0.00	1,800.00	226.00
24B05	CDC	1043970	Active	15/01/2002	14/01/2014	5	47.71	0.00	1,800.00	226.00
24B05	CDC	1043971	Active	15/01/2002	14/01/2014	5	47.71	0.00	1,800.00	226.00
24B05	CDC	1043972	Active	15/01/2002	14/01/2014	5	47.71	0.00	1,800.00	226.00
24B05	CDC	1043973	Active	15/01/2002	14/01/2014	5	47.71	836.01	1,800.00	226.00
24B05	CDC	1043974	Active	15/01/2002	14/01/2014	5	47.71	197.76	1,800.00	226.00
24B05	CDC	1043975	Active	15/01/2002	14/01/2014	5	47.71	197.76	1,800.00	226.00
24B05	CDC	1043976	Active	15/01/2002	14/01/2014	5	47.71	131.84	1,800.00	226.00
24B05	CDC	1043977	Active	15/01/2002	14/01/2014	5	47.71	131.84	1,800.00	226.00
24B05	CDC	1043978	Active	15/01/2002	14/01/2014	5	47.71	131.84	1,800.00	226.00
24B05	CDC	1043979	Active	15/01/2002	14/01/2014	5	47.71	131.84	1,800.00	226.00
24B05	CDC	1043980	Active	15/01/2002	14/01/2014	5	47.71	0.00	1,800.00	226.00
24B05	CDC	1043981	Active	15/01/2002	14/01/2014	5	47.71	0.00	1,800.00	226.00
24B05	CDC	1043982	Active	15/01/2002	14/01/2016	6	47.70	0.00	2,500.00	113.00
24B05	CDC	1043983	Active	15/01/2002	14/01/2016	6	47.70	0.00	2,500.00	113.00
24B05	CDC	1043984	Active	15/01/2002	14/01/2016	6	47.70	0.00	2,500.00	113.00
24B05	CDC	1043985	Active	15/01/2002	14/01/2014	5	47.70	261.30	1,800.00	226.00
24B05	CDC	1043986	Active	15/01/2002	14/01/2014	5	47.70	1,030.65	1,800.00	226.00
24B05	CDC	1043987	Active	15/01/2002	14/01/2014	5	47.70	197.16	1,800.00	226.00
24B05	CDC	1043988	Active	15/01/2002	14/01/2014	5	47.70	197.16	1,800.00	226.00
24B05	CDC	1043989	Active	15/01/2002	14/01/2014	5	47.70	263.67	1,800.00	226.00
24B05	CDC	1043990	Active	15/01/2002	14/01/2014	5	47.70	263.67	1,800.00	226.00
24B05	CDC	1043991	Active	15/01/2002	14/01/2016	6	47.69	0.00	2,500.00	113.00
24B05	CDC	1043992	Active	15/01/2002	14/01/2014	5	47.69	1,029.46	1,800.00	226.00
24B05	CDC	1043993	Active	15/01/2002	14/01/2014	5	47.69	1,030.46	1,800.00	226.00
24B05	CDC	1043994	Active	15/01/2002	14/01/2014	5	47.69	1,029.46	1,800.00	226.00
24C08	CDC	1044170	Active	15/01/2002	14/01/2016	6	47.63	0.00	2,500.00	113.00
24C08	CDC	1103333	Active	25/10/2002	24/10/2014	5	47.74	0.00	1,800.00	113.00
24C08	CDC	1103334	Active	25/10/2002	24/10/2014	5	47.74	0.00	1,800.00	113.00
24C08	CDC	1103335	Active	25/10/2002	24/10/2014	5	47.74	0.00	1,800.00	113.00
24C08	CDC	1103336	Active	25/10/2002	24/10/2014	5	47.73	0.00	1,800.00	113.00
24C08	CDC	1103337	Active	25/10/2002	24/10/2014	5	47.73	0.00	1,800.00	113.00
24C08	CDC	1103338	Active	25/10/2002	24/10/2014	5	47.72	0.00	1,800.00	113.00
24C08	CDC	1103339	Active	25/10/2002	24/10/2014	5	47.72	0.00	1,800.00	113.00
24C08	CDC	1132934	Active	06/06/2005	30/09/2014	4	4.43	16,401.09	640.00	28.00
24C08	CDC	1132935	Active	06/06/2005	30/09/2014	4	19.35	22,125.63	640.00	28.00
24C08	CDC	1132936	Active	06/06/2005	30/09/2014	4	8.25	31,371.60	640.00	28.00

NTS Sheet	Type of Title	Title No	Status	Date of Registration	[1]Expiry Date	# of Renewals	Area (Ha)	Excess Work ($)	Required Work ($)	Required Fees ($)
24C08	CDC	1132937	Active	06/06/2005	10/09/2014	4	2.20	4,795.95	640.00	28.00
24C08	CDC	1132938	Active	06/06/2005	10/09/2014	4	19.72	31,651.33	640.00	28.00
24C08	CDC	1132939	Active	06/06/2005	10/09/2014	4	16.94	30,760.78	640.00	28.00
24C08	CDC	1132940	Active	06/06/2005	10/09/2014	4	3.62	8,511.14	640.00	28.00
24C08	CDC	1132941	Active	06/06/2005	10/09/2014	4	5.81	14,240.93	640.00	28.00
24C08	CDC	1132942	Active	06/06/2005	04/09/2015	5	0.48	0.00	750.00	28.00
24C08	CDC	1132943	Active	06/06/2005	04/09/2015	5	1.13	0.00	750.00	28.00
24C08	CDC	1132944	Active	06/06/2005	04/09/2015	5	1.44	357.07	750.00	28.00
24C08	CDC	1132945	Active	06/06/2005	04/09/2015	5	5.04	5,249.74	750.00	28.00
24C08	CDC	1132946	Active	06/06/2005	04/09/2015	5	19.29	24,616.57	750.00	28.00
24C08	CDC	1132947	Active	06/06/2005	04/09/2015	5	32.63	40,346.65	1,800.00	101.00
24C08	CDC	1132948	Active	06/06/2005	04/09/2015	5	33.26	38,745.85	1,800.00	101.00
24C08	CDC	1132949	Active	06/06/2005	17/08/2014	4	7.96	29,738.69	640.00	28.00
24C08	CDC	1132950	Active	06/06/2005	17/08/2014	4	20.76	35,579.42	640.00	28.00
24C08	CDC	1132951	Active	06/06/2005	17/08/2014	4	4.05	14,659.31	640.00	28.00
24C08	CDC	1132952	Active	06/06/2005	17/08/2014	4	7.98	28,915.82	640.00	28.00
24C08	CDC	1132953	Active	06/06/2005	17/08/2014	4	4.50	16,394.79	640.00	28.00
24C08	CDC	1132954	Active	06/06/2005	04/09/2015	5	10.18	34,006.79	750.00	28.00
24C08	CDC	1132955	Active	06/06/2005	04/09/2015	5	5.70	19,271.05	750.00	28.00
24C08	CDC	1132956	Active	06/06/2005	04/09/2015	5	5.28	27,277.01	750.00	28.00
24C08	CDC	1132957	Active	06/06/2005	04/09/2015	5	6.21	26,196.33	750.00	28.00
24C08	CDC	1132958	Active	06/06/2005	04/09/2015	5	1.22	5,072.34	750.00	28.00
24C08	CDC	1132959	Active	06/06/2005	04/09/2015	5	1.35	5,783.33	750.00	28.00
24C08	CDC	1132960	Active	06/06/2005	31/08/2014	4	10.48	32,618.48	640.00	28.00
24C08	CDC	1132961	Active	06/06/2005	31/08/2014	4	16.03	38,400.55	640.00	28.00
24C08	CDC	1132962	Active	06/06/2005	31/08/2014	4	1.70	5,216.86	640.00	28.00
24C08	CDC	1132963	Active	06/06/2005	31/08/2014	4	4.55	15,572.17	640.00	28.00
24C08	CDC	1132964	Active	06/06/2005	31/08/2014	4	0.79	1,910.41	640.00	28.00
24C08	CDC	1132965	Active	06/06/2005	26/07/2014	4	3.09	7,619.99	640.00	28.00
24C08	CDC	1132966	Active	06/06/2005	26/07/2014	4	2.37	5,620.76	640.00	28.00
24C08	CDC	1132967	Active	06/06/2005	26/07/2014	4	5.83	15,228.13	640.00	28.00
24C08	CDC	1132968	Active	06/06/2005	26/07/2014	4	19.08	34,472.61	640.00	28.00
24C08	CDC	1132969	Active	06/06/2005	26/07/2014	4	20.70	34,445.16	640.00	28.00
24C08	CDC	1132970	Active	06/06/2005	26/07/2014	4	11.02	25,589.18	640.00	28.00
24C08	CDC	1132971	Active	06/06/2005	31/08/2014	4	1.30	2,682.95	640.00	28.00
24C08	CDC	1132972	Active	06/06/2005	31/08/2014	4	13.83	13,483.49	640.00	28.00
24C08	CDC	1132973	Active	06/06/2005	31/08/2014	4	0.08	0.00	640.00	28.00
24C08	CDC	1132974	Active	06/06/2005	31/08/2014	4	47.68	0.00	1,800.00	113.00
24C08	CDC	1132975	Active	06/06/2005	31/08/2014	4	4.73	11,910.97	640.00	28.00
24C08	CDC	1132976	Active	06/06/2005	31/08/2014	4	11.12	22,099.03	640.00	28.00
24C08	CDC	1132977	Active	06/06/2005	30/09/2014	4	11.33	43,799.73	640.00	28.00
24C08	CDC	1132978	Active	06/06/2005	30/09/2014	4	1.27	4,641.02	640.00	28.00
24C08	CDC	1132979	Active	06/06/2005	30/09/2014	4	4.07	16,989.72	640.00	28.00
24C08	CDC	1132980	Active	06/06/2005	30/09/2014	4	0.50	1,245.12	640.00	28.00
24C08	CDC	2097640	Active	28/06/2007	27/06/2015	3	47.73	0.00	1,350.00	113.00
24C08	CDC	2097641	Active	28/06/2007	27/06/2015	3	47.73	0.00	1,350.00	113.00
24C08	CDC	2097642	Active	28/06/2007	27/06/2015	3	47.73	0.00	1,350.00	113.00
24C08	CDC	2097643	Active	28/06/2007	27/06/2015	3	47.73	0.00	1,350.00	113.00
24C08	CDC	2097644	Active	28/06/2007	27/06/2015	3	47.73	0.00	1,350.00	113.00
24C08	CDC	2097645	Active	28/06/2007	27/06/2015	3	47.73	0.00	1,350.00	113.00
24C08	CDC	2097646	Active	28/06/2007	27/06/2015	3	47.72	0.00	1,350.00	113.00

NTS Sheet	Type of Title	Title No	Status	Date of Registration	[1]Expiry Date	# of Renewals	Area (Ha)	Excess Work ($)	Required Work ($)	Required Fees ($)
24C08	CDC	2097647	Active	28/06/2007	27/06/2015	3	47.72	0.00	1,350.00	113.00
24C08	CDC	2097648	Active	28/06/2007	27/06/2015	3	47.72	0.00	1,350.00	113.00
24C08	CDC	2097649	Active	28/06/2007	27/06/2015	3	47.72	0.00	1,350.00	113.00
24C08	CDC	2097650	Active	28/06/2007	27/06/2015	3	47.71	0.00	1,350.00	113.00
24C08	CDC	2097651	Active	28/06/2007	27/06/2015	3	47.71	0.00	1,350.00	113.00
24C08	CDC	2097652	Active	28/06/2007	27/06/2015	3	47.71	0.00	1,350.00	113.00
24B05	CDC	2120537	Active	07/09/2007	06/09/2015	3	47.69	0.00	1,350.00	113.00
24B05	CDC	2120538	Active	07/09/2007	06/09/2015	3	47.68	0.00	1,350.00	113.00
24C08	CDC	2120539	Active	07/09/2007	06/09/2015	3	47.69	0.00	1,350.00	113.00
24C08	CDC	2120540	Active	07/09/2007	06/09/2015	3	47.69	0.00	1,350.00	113.00
24C08	CDC	2120541	Active	07/09/2007	06/09/2015	3	47.68	0.00	1,350.00	113.00
24C08	CDC	2120542	Active	07/09/2007	06/09/2015	3	47.68	0.00	1,350.00	113.00
24C08	CDC	2120543	Active	07/09/2007	06/09/2015	3	47.68	0.00	1,350.00	113.00
24C08	CDC	2120544	Active	07/09/2007	06/09/2015	3	47.68	0.00	1,350.00	113.00
24C08	CDC	2120545	Active	07/09/2007	06/09/2015	3	47.67	0.00	1,350.00	113.00
24C08	CDC	2120546	Active	07/09/2007	06/09/2015	3	47.67	0.00	1,350.00	113.00
24C08	CDC	2120547	Active	07/09/2007	06/09/2015	3	47.65	0.00	1,350.00	113.00
24C08	CDC	2120548	Active	07/09/2007	06/09/2015	3	47.65	0.00	1,350.00	113.00
24C08	CDC	2120549	Active	07/09/2007	06/09/2015	3	47.65	0.00	1,350.00	113.00
24C08	CDC	2120550	Active	07/09/2007	06/09/2015	3	47.66	0.00	1,350.00	113.00
24C08	CDC	2120551	Active	07/09/2007	06/09/2015	3	47.65	0.00	1,350.00	113.00
24C08	CDC	2120552	Active	07/09/2007	06/09/2015	3	47.66	0.00	1,350.00	113.00
24C08	CDC	2120553	Active	07/09/2007	06/09/2015	3	47.64	0.00	1,350.00	113.00
24C08	CDC	2120554	Active	07/09/2007	06/09/2015	3	47.64	0.00	1,350.00	113.00
24C08	CDC	2120555	Active	07/09/2007	06/09/2015	3	47.64	0.00	1,350.00	113.00
24C08	CDC	2120556	Active	07/09/2007	06/09/2015	3	47.64	0.00	1,350.00	113.00
24C08	CDC	2120557	Active	07/09/2007	06/09/2015	3	47.64	0.00	1,350.00	113.00
24C08	CDC	2120558	Active	07/09/2007	06/09/2015	3	47.64	0.00	1,350.00	113.00
24C08	CDC	2120559	Active	07/09/2007	06/09/2015	3	47.64	0.00	1,350.00	113.00
24C08	CDC	2120560	Active	07/09/2007	06/09/2015	3	47.64	0.00	1,350.00	113.00
24C08	CDC	2120561	Active	07/09/2007	06/09/2015	3	47.63	0.00	1,350.00	113.00
24C08	CDC	2120562	Active	07/09/2007	06/09/2015	3	47.63	0.00	1,350.00	113.00
24C08	CDC	2120563	Active	07/09/2007	06/09/2015	3	47.63	0.00	1,350.00	113.00
24C08	CDC	2120564	Active	07/09/2007	06/09/2015	3	47.63	0.00	1,350.00	113.00
24C08	CDC	2120565	Active	07/09/2007	06/09/2015	3	47.63	0.00	1,350.00	113.00
24C08	CDC	2120566	Active	07/09/2007	06/09/2015	3	47.63	0.00	1,350.00	113.00
24C08	CDC	2120567	Active	07/09/2007	06/09/2015	3	47.63	0.00	1,350.00	113.00
24C08	CDC	2120568	Active	07/09/2007	06/09/2015	3	47.63	0.00	1,350.00	113.00
24C08	CDC	2120569	Active	07/09/2007	06/09/2015	3	47.63	0.00	1,350.00	113.00
24C08	CDC	2120571	Active	07/09/2007	06/09/2015	3	47.62	0.00	1,350.00	113.00
24C08	CDC	2120572	Active	07/09/2007	06/09/2015	3	47.62	0.00	1,350.00	113.00
24C08	CDC	2120573	Active	07/09/2007	06/09/2015	3	47.62	0.00	1,350.00	113.00
24C08	CDC	2120574	Active	07/09/2007	06/09/2015	3	47.62	0.00	1,350.00	113.00
24C08	CDC	2120575	Active	07/09/2007	06/09/2015	3	47.62	0.00	1,350.00	113.00
24C08	CDC	2120576	Active	07/09/2007	06/09/2015	3	47.62	0.00	1,350.00	113.00
24C08	CDC	2120577	Active	07/09/2007	06/09/2015	3	47.62	0.00	1,350.00	113.00
24B05	CDC	2377788	Active	07/02/2013	06/02/2015	0	47.74	0.00	135.00	113.00
24B05	CDC	2377789	Active	07/02/2013	06/02/2015	0	47.73	0.00	135.00	113.00
24B05	CDC	2377790	Active	07/02/2013	06/02/2015	0	47.73	0.00	135.00	113.00
24B05	CDC	2377791	Active	07/02/2013	06/02/2015	0	47.73	0.00	135.00	113.00
24B05	CDC	2377792	Active	07/02/2013	06/02/2015	0	47.72	0.00	135.00	113.00

NTS Sheet	Type of Title	Title No	Status	Date of Registration	[1]Expiry Date	# of Renewals	Area (Ha)	Excess Work ($)	Required Work ($)	Required Fees ($)
24B05	CDC	2377793	Active	07/02/2013	06/02/2015	0	47.72	0.00	135.00	113.00
24B05	CDC	2377794	Active	07/02/2013	06/02/2015	0	47.72	0.00	135.00	113.00
24B05	CDC	2377795	Active	07/02/2013	06/02/2015	0	47.72	0.00	135.00	113.00
24B05	CDC	2377796	Active	07/02/2013	06/02/2015	0	47.71	0.00	135.00	113.00
24B05	CDC	2377797	Active	07/02/2013	06/02/2015	0	47.71	0.00	135.00	113.00
24C08	CDC	2377798	Active	07/02/2013	06/02/2015	0	47.75	0.00	135.00	113.00
24C08	CDC	2377799	Active	07/02/2013	06/02/2015	0	47.75	0.00	135.00	113.00
24C08	CDC	2377800	Active	07/02/2013	06/02/2015	0	47.75	0.00	135.00	113.00
24C08	CDC	2377801	Active	07/02/2013	06/02/2015	0	47.74	0.00	135.00	113.00
24C08	CDC	2377802	Active	07/02/2013	06/02/2015	0	47.74	0.00	135.00	113.00
24C08	CDC	2377803	Active	07/02/2013	06/02/2015	0	47.73	0.00	135.00	113.00
24C08	CDC	2377804	Active	07/02/2013	06/02/2015	0	47.73	0.00	135.00	113.00
24C08	CDC	2377805	Active	07/02/2013	06/02/2015	0	47.73	0.00	135.00	113.00
24C08	CDC	2377806	Active	07/02/2013	06/02/2015	0	47.73	0.00	135.00	113.00
24C08	CDC	2377807	Active	07/02/2013	06/02/2015	0	47.73	0.00	135.00	113.00
24C08	CDC	2377808	Active	07/02/2013	06/02/2015	0	47.72	0.00	135.00	113.00
24C08	CDC	2377809	Active	07/02/2013	06/02/2015	0	47.72	0.00	135.00	113.00
24C08	CDC	2377810	Active	07/02/2013	06/02/2015	0	47.72	0.00	135.00	113.00
24C08	CDC	2377811	Active	07/02/2013	06/02/2015	0	47.72	0.00	135.00	113.00
24C08	CDC	2377812	Active	07/02/2013	06/02/2015	0	47.71	0.00	135.00	113.00
24C08	CDC	2377813	Active	07/02/2013	06/02/2015	0	47.71	0.00	135.00	113.00
24C08	CDC	2377814	Active	07/02/2013	06/02/2015	0	47.71	0.00	135.00	113.00
24C08	CDC	2377815	Active	07/02/2013	06/02/2015	0	47.71	0.00	135.00	113.00
24C08	CDC	2377816	Active	07/02/2013	06/02/2015	0	47.71	0.00	135.00	113.00
24B05	CDC	2384932	Active	08/05/2013	07/05/2015	0	47.75	0.00	135.00	113.00
24B05	CDC	2384933	Active	08/05/2013	07/05/2015	0	47.75	0.00	135.00	113.00
24B05	CDC	2384934	Active	08/05/2013	07/05/2015	0	47.75	0.00	135.00	113.00
24B05	CDC	2384935	Active	08/05/2013	07/05/2015	0	47.75	0.00	135.00	113.00
24B05	CDC	2384936	Active	08/05/2013	07/05/2015	0	47.75	0.00	135.00	113.00
24B05	CDC	2384937	Active	08/05/2013	07/05/2015	0	47.75	0.00	135.00	113.00
24B05	CDC	2384938	Active	08/05/2013	07/05/2015	0	47.75	0.00	135.00	113.00
24B05	CDC	2384939	Active	08/05/2013	07/05/2015	0	47.75	0.00	135.00	113.00
24B05	CDC	2384940	Active	08/05/2013	07/05/2015	0	47.75	0.00	135.00	113.00
24B05	CDC	2384941	Active	08/05/2013	07/05/2015	0	47.75	0.00	135.00	113.00
24B05	CDC	2384942	Active	08/05/2013	07/05/2015	0	47.75	0.00	135.00	113.00
24B05	CDC	2384943	Active	08/05/2013	07/05/2015	0	47.75	0.00	135.00	113.00
24B05	CDC	2384944	Active	08/05/2013	07/05/2015	0	47.75	0.00	135.00	113.00
24B05	CDC	2384945	Active	08/05/2013	07/05/2015	0	47.75	0.00	135.00	113.00
24B05	CDC	2384946	Active	08/05/2013	07/05/2015	0	47.75	0.00	135.00	113.00
24B05	CDC	2384947	Active	08/05/2013	07/05/2015	0	47.75	0.00	135.00	113.00
24B05	CDC	2384948	Active	08/05/2013	07/05/2015	0	47.75	0.00	135.00	113.00
24B05	CDC	2384949	Active	08/05/2013	07/05/2015	0	47.75	0.00	135.00	113.00
24B05	CDC	2384950	Active	08/05/2013	07/05/2015	0	47.75	0.00	135.00	113.00
24B05	CDC	2384951	Active	08/05/2013	07/05/2015	0	47.75	0.00	135.00	113.00
24B05	CDC	2384952	Active	08/05/2013	07/05/2015	0	47.75	0.00	135.00	113.00
24B05	CDC	2384953	Active	08/05/2013	07/05/2015	0	47.74	0.00	135.00	113.00
24B05	CDC	2384954	Active	08/05/2013	07/05/2015	0	47.74	0.00	135.00	113.00
24B05	CDC	2384955	Active	08/05/2013	07/05/2015	0	47.74	0.00	135.00	113.00
24B05	CDC	2384956	Active	08/05/2013	07/05/2015	0	47.74	0.00	135.00	113.00
24B05	CDC	2384957	Active	08/05/2013	07/05/2015	0	47.74	0.00	135.00	113.00
24B05	CDC	2384958	Active	08/05/2013	07/05/2015	0	47.74	0.00	135.00	113.00

NTS Sheet	Type of Title	Title No	Status	Date of Registration	[1]Expiry Date	# of Renewals	Area (Ha)	Excess Work ($)	Required Work ($)	Required Fees ($)
24B05	CDC	2384959	Active	08/05/2013	07/05/2015	0	47.74	0.00	135.00	113.00
24B05	CDC	2384960	Active	08/05/2013	07/05/2015	0	47.74	0.00	135.00	113.00
24B05	CDC	2384961	Active	08/05/2013	07/05/2015	0	47.74	0.00	135.00	113.00
24B05	CDC	2384962	Active	08/05/2013	07/05/2015	0	47.74	0.00	135.00	113.00
24B05	CDC	2384963	Active	08/05/2013	07/05/2015	0	47.74	0.00	135.00	113.00
24B05	CDC	2384964	Active	08/05/2013	07/05/2015	0	47.74	0.00	135.00	113.00
24B05	CDC	2384965	Active	08/05/2013	07/05/2015	0	47.74	0.00	135.00	113.00
24B05	CDC	2384966	Active	08/05/2013	07/05/2015	0	47.74	0.00	135.00	113.00
24B05	CDC	2384967	Active	08/05/2013	07/05/2015	0	47.74	0.00	135.00	113.00
24B05	CDC	2384968	Active	08/05/2013	07/05/2015	0	47.74	0.00	135.00	113.00
24B05	CDC	2384969	Active	08/05/2013	07/05/2015	0	47.73	0.00	135.00	113.00
24B05	CDC	2384970	Active	08/05/2013	07/05/2015	0	47.73	0.00	135.00	113.00
24B05	CDC	2384971	Active	08/05/2013	07/05/2015	0	47.73	0.00	135.00	113.00
24B05	CDC	2384972	Active	08/05/2013	07/05/2015	0	47.73	0.00	135.00	113.00
24B05	CDC	2384973	Active	08/05/2013	07/05/2015	0	47.73	0.00	135.00	113.00
24B05	CDC	2384974	Active	08/05/2013	07/05/2015	0	47.73	0.00	135.00	113.00
24B05	CDC	2384975	Active	08/05/2013	07/05/2015	0	47.73	0.00	135.00	113.00
24B05	CDC	2384976	Active	08/05/2013	07/05/2015	0	47.73	0.00	135.00	113.00
24B05	CDC	2384977	Active	08/05/2013	07/05/2015	0	47.73	0.00	135.00	113.00
24B05	CDC	2384978	Active	08/05/2013	07/05/2015	0	47.73	0.00	135.00	113.00
24B05	CDC	2384979	Active	08/05/2013	07/05/2015	0	47.72	0.00	135.00	113.00
24B05	CDC	2384980	Active	08/05/2013	07/05/2015	0	47.72	0.00	135.00	113.00
24B05	CDC	2384981	Active	08/05/2013	07/05/2015	0	47.72	0.00	135.00	113.00
24B05	CDC	2384982	Active	08/05/2013	07/05/2015	0	47.72	0.00	135.00	113.00
24B05	CDC	2384983	Active	08/05/2013	07/05/2015	0	47.72	0.00	135.00	113.00
24B05	CDC	2384984	Active	08/05/2013	07/05/2015	0	47.72	0.00	135.00	113.00
24B05	CDC	2384985	Active	08/05/2013	07/05/2015	0	47.72	0.00	135.00	113.00
24B05	CDC	2384986	Active	08/05/2013	07/05/2015	0	47.72	0.00	135.00	113.00
24B05	CDC	2384987	Active	08/05/2013	07/05/2015	0	47.71	0.00	135.00	113.00
24B05	CDC	2384988	Active	08/05/2013	07/05/2015	0	47.71	0.00	135.00	113.00
24B05	CDC	2384989	Active	08/05/2013	07/05/2015	0	47.70	0.00	135.00	113.00
24B05	CDC	2384990	Active	08/05/2013	07/05/2015	0	47.70	0.00	135.00	113.00
24B05	CDC	2384991	Active	08/05/2013	07/05/2015	0	47.70	0.00	135.00	113.00
24B05	CDC	2384992	Active	08/05/2013	07/05/2015	0	47.70	0.00	135.00	113.00
24C08	CDC	2384993	Active	08/05/2013	07/05/2015	0	47.72	0.00	135.00	113.00
24B05	CDC	2385416	Active	17/05/2013	16/05/2015	0	47.74	0.00	135.00	113.00
24B05	CDC	2385417	Active	17/05/2013	16/05/2015	0	47.74	0.00	135.00	113.00
24B05	CDC	2385418	Active	17/05/2013	16/05/2015	0	47.74	0.00	135.00	113.00
24B05	CDC	2385419	Active	17/05/2013	16/05/2015	0	47.73	0.00	135.00	113.00
24B05	CDC	2385420	Active	17/05/2013	16/05/2015	0	47.73	0.00	135.00	113.00
24B05	CDC	2385421	Active	17/05/2013	16/05/2015	0	47.73	0.00	135.00	113.00
24B05	CDC	2385422	Active	17/05/2013	16/05/2015	0	47.73	0.00	135.00	113.00
24B05	CDC	2385423	Active	17/05/2013	16/05/2015	0	47.72	0.00	135.00	113.00
24B05	CDC	2385424	Active	17/05/2013	16/05/2015	0	47.72	0.00	135.00	113.00
24B05	CDC	2385425	Active	17/05/2013	16/05/2015	0	47.72	0.00	135.00	113.00
24B05	CDC	2385426	Active	17/05/2013	16/05/2015	0	47.72	0.00	135.00	113.00
24C08	CDC	2386856	Active	19/06/2013	18/06/2015	0	47.62	0.00	135.00	113.00
24C08	CDC	2386857	Active	19/06/2013	18/06/2015	0	47.62	0.00	135.00	113.00
24C08	CDC	2386858	Active	19/06/2013	18/06/2015	0	47.61	0.00	135.00	113.00
24C08	CDC	2386859	Active	19/06/2013	18/06/2015	0	47.61	0.00	135.00	113.00
24C08	CDC	2386860	Active	19/06/2013	18/06/2015	0	47.61	0.00	135.00	113.00

NTS Sheet	Type of Title	Title No	Status	Date of Registration	[1]Expiry Date	# of Renewals	Area (Ha)	Excess Work ($)	Required Work ($)	Required Fees ($)
24C08	CDC	2386861	Active	19/06/2013	18/06/2015	0	47.61	0.00	135.00	113.00
24C08	CDC	2388385	Active	22/07/2013	21/07/2015	0	47.73	0.00	135.00	113.00
24C08	CDC	2388386	Active	22/07/2013	21/07/2015	0	47.73	0.00	135.00	113.00
24C08	CDC	2388387	Active	22/07/2013	21/07/2015	0	47.73	0.00	135.00	113.00
24C08	CDC	2388388	Active	22/07/2013	21/07/2015	0	47.73	0.00	135.00	113.00
24C08	CDC	2388389	Active	22/07/2013	21/07/2015	0	47.73	0.00	135.00	113.00
24C08	CDC	2388390	Active	22/07/2013	21/07/2015	0	47.70	0.00	135.00	113.00
24C08	CDC	2388391	Active	22/07/2013	21/07/2015	0	47.70	0.00	135.00	113.00
24C08	CDC	2388392	Active	22/07/2013	21/07/2015	0	47.70	0.00	135.00	113.00
24C08	CDC	2388393	Active	22/07/2013	21/07/2015	0	47.70	0.00	135.00	113.00
24C08	CDC	2388394	Active	22/07/2013	21/07/2015	0	47.69	0.00	135.00	113.00
24C08	CDC	2388395	Active	22/07/2013	21/07/2015	0	47.69	0.00	135.00	113.00
24C08	CDC	2388396	Active	22/07/2013	21/07/2015	0	47.69	0.00	135.00	113.00
24C08	CDC	2388397	Active	22/07/2013	21/07/2015	0	47.67	0.00	135.00	113.00
24C08	CDC	2388398	Active	22/07/2013	21/07/2015	0	47.67	0.00	135.00	113.00
24C08	CDC	2388399	Active	22/07/2013	21/07/2015	0	47.66	0.00	135.00	113.00
24C08	CDC	2389191	Active	20/08/2013	19/08/2015	0	47.65	0.00	135.00	113.00
24C08	CDC	2389192	Active	20/08/2013	19/08/2015	0	47.65	0.00	135.00	113.00
24C08	CDC	2389193	Active	20/08/2013	19/08/2015	0	47.64	0.00	135.00	113.00
24C08	CDC	2389194	Active	20/08/2013	19/08/2015	0	47.64	0.00	135.00	113.00
24C08	CDC	2389195	Active	20/08/2013	19/08/2015	0	47.63	0.00	135.00	113.00
24C08	CDC	2389196	Active	20/08/2013	19/08/2015	0	47.63	0.00	135.00	113.00

[1]All claims due in January 2014 have a renewal application submitted November 7, 2013 (request #1316050). Pending are the Quebec government updates to the claim status in GESTIM.

CDC stands for map designated claims

Table 6.1-2 –Registration information and subjected NSR on the claim blocks 100% under the responsibility of Energizer Resources Corp.

NTS Sheet	Title No	[1]Titleholder(s) (Name, Number and Percentage)	Virginia 1.5% NSR	Jones & Poisson 1% NSR	Jones & Poisson 0.5% NSR
24B05	1043964	Uranium Star Corp. (99720) 100 % (responsible)	Y	Y	N
24B05	1043965	Uranium Star Corp. (99720) 100 % (responsible)	Y	Y	N
24B05	1043966	Uranium Star Corp. (99720) 100 % (responsible)	Y	Y	N
24B05	1043967	Uranium Star Corp. (99720) 100 % (responsible)	Y	Y	N
24B05	1043968	Uranium Star Corp. (99720) 100 % (responsible)	Y	Y	N
24B05	1043969	Uranium Star Corp. (99720) 100 % (responsible)	Y	Y	N
24B05	1043970	Uranium Star Corp. (99720) 100 % (responsible)	Y	Y	N
24B05	1043971	Uranium Star Corp. (99720) 100 % (responsible)	Y	Y	N
24B05	1043972	Uranium Star Corp. (99720) 100 % (responsible)	Y	Y	N
24B05	1043973	Uranium Star Corp. (99720) 100 % (responsible)	Y	Y	N
24B05	1043974	Uranium Star Corp. (99720) 100 % (responsible)	Y	Y	N
24B05	1043975	Uranium Star Corp. (99720) 100 % (responsible)	Y	Y	N
24B05	1043976	Uranium Star Corp. (99720) 100 % (responsible)	Y	Y	N
24B05	1043977	Uranium Star Corp. (99720) 100 % (responsible)	Y	Y	N
24B05	1043978	Uranium Star Corp. (99720) 100 % (responsible)	Y	Y	N
24B05	1043979	Uranium Star Corp. (99720) 100 % (responsible)	Y	Y	N
24B05	1043980	Uranium Star Corp. (99720) 100 % (responsible)	Y	Y	N
24B05	1043981	Uranium Star Corp. (99720) 100 % (responsible)	Y	Y	N
24B05	1043985	Uranium Star Corp. (99720) 100 % (responsible)	Y	Y	N
24B05	1043986	Uranium Star Corp. (99720) 100 % (responsible)	Y	Y	N

NTS Sheet	Title No	[1]Titleholder(s) (Name, Number and Percentage)	Virginia 1.5% NSR	Jones & Poisson 1% NSR	Jones & Poisson 0.5% NSR
24B05	1043987	Uranium Star Corp. (99720) 100 % (responsible)	Y	Y	N
24B05	1043988	Uranium Star Corp. (99720) 100 % (responsible)	Y	Y	N
24B05	1043989	Uranium Star Corp. (99720) 100 % (responsible)	Y	Y	N
24B05	1043990	Uranium Star Corp. (99720) 100 % (responsible)	Y	Y	N
24B05	1043992	Uranium Star Corp. (99720) 100 % (responsible)	Y	Y	N
24B05	1043993	Uranium Star Corp. (99720) 100 % (responsible)	Y	Y	N
24B05	1043994	Uranium Star Corp. (99720) 100 % (responsible)	Y	Y	N
24C08	1132965	Uranium Star Corp. (99720) 100 % (responsible)	Y	Y	N
24C08	1132966	Uranium Star Corp. (99720) 100 % (responsible)	Y	Y	N
24C08	1132967	Uranium Star Corp. (99720) 100 % (responsible)	Y	Y	N
24C08	1132968	Uranium Star Corp. (99720) 100 % (responsible)	Y	Y	N
24C08	1132969	Uranium Star Corp. (99720) 100 % (responsible)	Y	Y	N
24C08	1132970	Uranium Star Corp. (99720) 100 % (responsible)	Y	Y	N
24C08	1132949	Uranium Star Corp. (99720) 100 % (responsible)	Y	Y	N
24C08	1132950	Uranium Star Corp. (99720) 100 % (responsible)	Y	Y	N
24C08	1132951	Uranium Star Corp. (99720) 100 % (responsible)	Y	Y	N
24C08	1132952	Uranium Star Corp. (99720) 100 % (responsible)	Y	Y	N
24C08	1132953	Uranium Star Corp. (99720) 100 % (responsible)	Y	Y	N
24C08	1132960	Uranium Star Corp. (99720) 100 % (responsible)	Y	Y	N
24C08	1132961	Uranium Star Corp. (99720) 100 % (responsible)	Y	Y	N
24C08	1132962	Uranium Star Corp. (99720) 100 % (responsible)	Y	Y	N
24C08	1132963	Uranium Star Corp. (99720) 100 % (responsible)	Y	Y	N
24C08	1132964	Uranium Star Corp. (99720) 100 % (responsible)	Y	Y	N
24C08	1132971	Uranium Star Corp. (99720) 100 % (responsible)	Y	Y	N
24C08	1132972	Uranium Star Corp. (99720) 100 % (responsible)	Y	Y	N
24C08	1132973	Uranium Star Corp. (99720) 100 % (responsible)	Y	Y	N
24C08	1132974	Uranium Star Corp. (99720) 100 % (responsible)	Y	Y	N
24C08	1132975	Uranium Star Corp. (99720) 100 % (responsible)	Y	Y	N
24C08	1132976	Uranium Star Corp. (99720) 100 % (responsible)	Y	Y	N
24C08	1132937	Uranium Star Corp. (99720) 100 % (responsible)	Y	Y	N
24C08	1132938	Uranium Star Corp. (99720) 100 % (responsible)	Y	Y	N
24C08	1132939	Uranium Star Corp. (99720) 100 % (responsible)	Y	Y	N
24C08	1132940	Uranium Star Corp. (99720) 100 % (responsible)	Y	Y	N
24C08	1132941	Uranium Star Corp. (99720) 100 % (responsible)	Y	Y	N
24B05	36315	Uranium Star Corp. (99720) 100 % (responsible)	Y	N	N
24B05	36316	Uranium Star Corp. (99720) 100 % (responsible)	Y	N	N
24B05	36317	Uranium Star Corp. (99720) 100 % (responsible)	N	N	N
24B05	36318	Uranium Star Corp. (99720) 100 % (responsible)	N	N	N
24B05	36319	Uranium Star Corp. (99720) 100 % (responsible)	Y	N	N
24B05	36320	Uranium Star Corp. (99720) 100 % (responsible)	Y	N	N
24B05	36321	Uranium Star Corp. (99720) 100 % (responsible)	Y	N	N
24B05	36322	Uranium Star Corp. (99720) 100 % (responsible)	Y	N	N
24B05	36323	Uranium Star Corp. (99720) 100 % (responsible)	Y	N	N
24B05	36324	Uranium Star Corp. (99720) 100 % (responsible)	Y	N	N
24B05	36325	Uranium Star Corp. (99720) 100 % (responsible)	N	N	N
24B05	36326	Uranium Star Corp. (99720) 100 % (responsible)	Y	N	N
24B05	36327	Uranium Star Corp. (99720) 100 % (responsible)	Y	N	N
24C08	1132934	Uranium Star Corp. (99720) 100 % (responsible)	Y	Y	N
24C08	1132935	Uranium Star Corp. (99720) 100 % (responsible)	Y	Y	N
24C08	1132936	Uranium Star Corp. (99720) 100 % (responsible)	Y	Y	N
24C08	1132977	Uranium Star Corp. (99720) 100 % (responsible)	Y	Y	N
24C08	1132978	Uranium Star Corp. (99720) 100 % (responsible)	Y	Y	N

NTS Sheet	Title No	[1]Titleholder(s) (Name, Number and Percentage)	Virginia 1.5% NSR	Jones & Poisson 1% NSR	Jones & Poisson 0.5% NSR
24C08	1132979	Uranium Star Corp. (99720) 100 % (responsible)	Y	Y	N
24C08	1132980	Uranium Star Corp. (99720) 100 % (responsible)	Y	Y	N
24C08	1103333	Uranium Star Corp. (99720) 100 % (responsible)	Y	N	Y
24C08	1103334	Uranium Star Corp. (99720) 100 % (responsible)	Y	N	Y
24C08	1103335	Uranium Star Corp. (99720) 100 % (responsible)	Y	N	Y
24C08	1103336	Uranium Star Corp. (99720) 100 % (responsible)	Y	N	Y
24C08	1103337	Uranium Star Corp. (99720) 100 % (responsible)	Y	N	Y
24C08	1103338	Uranium Star Corp. (99720) 100 % (responsible)	Y	N	Y
24C08	1103339	Uranium Star Corp. (99720) 100 % (responsible)	Y	N	Y
24B05	2377788	Uranium Star Corp. (99720) 100 % (responsible)	Y	N	N
24B05	2377789	Uranium Star Corp. (99720) 100 % (responsible)	Y	N	N
24B05	2377790	Uranium Star Corp. (99720) 100 % (responsible)	Y	N	N
24B05	2377791	Uranium Star Corp. (99720) 100 % (responsible)	Y	N	N
24B05	2377792	Uranium Star Corp. (99720) 100 % (responsible)	Y	N	N
24B05	2377793	Uranium Star Corp. (99720) 100 % (responsible)	Y	N	N
24B05	2377794	Uranium Star Corp. (99720) 100 % (responsible)	Y	N	N
24B05	2377795	Uranium Star Corp. (99720) 100 % (responsible)	Y	N	N
24B05	2377796	Uranium Star Corp. (99720) 100 % (responsible)	Y	N	N
24B05	2377797	Uranium Star Corp. (99720) 100 % (responsible)	Y	N	N
24C08	2377798	Uranium Star Corp. (99720) 100 % (responsible)	Y	N	N
24C08	2377799	Uranium Star Corp. (99720) 100 % (responsible)	Y	N	N
24C08	2377800	Uranium Star Corp. (99720) 100 % (responsible)	Y	N	N
24C08	2377801	Uranium Star Corp. (99720) 100 % (responsible)	Y	N	N
24C08	2377802	Uranium Star Corp. (99720) 100 % (responsible)	Y	N	N
24C08	2377803	Uranium Star Corp. (99720) 100 % (responsible)	Y	N	N
24C08	2377804	Uranium Star Corp. (99720) 100 % (responsible)	Y	N	N
24C08	2377805	Uranium Star Corp. (99720) 100 % (responsible)	Y	N	N
24C08	2377806	Uranium Star Corp. (99720) 100 % (responsible)	Y	N	N
24C08	2377807	Uranium Star Corp. (99720) 100 % (responsible)	Y	N	N
24C08	2377808	Uranium Star Corp. (99720) 100 % (responsible)	Y	N	N
24C08	2377809	Uranium Star Corp. (99720) 100 % (responsible)	Y	N	N
24C08	2377810	Uranium Star Corp. (99720) 100 % (responsible)	Y	N	N
24C08	2377811	Uranium Star Corp. (99720) 100 % (responsible)	Y	N	N
24C08	2377812	Uranium Star Corp. (99720) 100 % (responsible)	Y	N	N
24C08	2377813	Uranium Star Corp. (99720) 100 % (responsible)	Y	N	N
24C08	2377814	Uranium Star Corp. (99720) 100 % (responsible)	Y	N	N
24C08	2377815	Uranium Star Corp. (99720) 100 % (responsible)	Y	N	N
24C08	2377816	Uranium Star Corp. (99720) 100 % (responsible)	Y	N	N
24B05	2384932	Uranium Star Corp. (99720) 100 % (responsible)	Y	N	N
24B05	2384933	Uranium Star Corp. (99720) 100 % (responsible)	Y	N	N
24B05	2384934	Uranium Star Corp. (99720) 100 % (responsible)	Y	N	N
24B05	2384935	Uranium Star Corp. (99720) 100 % (responsible)	Y	N	N
24B05	2384936	Uranium Star Corp. (99720) 100 % (responsible)	N	N	N
24B05	2384937	Uranium Star Corp. (99720) 100 % (responsible)	N	N	N
24B05	2384938	Uranium Star Corp. (99720) 100 % (responsible)	Y	N	N
24B05	2384939	Uranium Star Corp. (99720) 100 % (responsible)	Y	N	N
24B05	2384940	Uranium Star Corp. (99720) 100 % (responsible)	Y	N	N
24B05	2384941	Uranium Star Corp. (99720) 100 % (responsible)	Y	N	N
24B05	2384942	Uranium Star Corp. (99720) 100 % (responsible)	Y	N	N
24B05	2384943	Uranium Star Corp. (99720) 100 % (responsible)	Y	N	N
24B05	2384944	Uranium Star Corp. (99720) 100 % (responsible)	Y	N	N
24B05	2384945	Uranium Star Corp. (99720) 100 % (responsible)	Y	N	N

NTS Sheet	Title No	[1]Titleholder(s) (Name, Number and Percentage)	Virginia 1.5% NSR	Jones & Poisson 1% NSR	Jones & Poisson 0.5% NSR
24B05	2384946	Uranium Star Corp. (99720) 100 % (responsible)	Y	N	N
24B05	2384947	Uranium Star Corp. (99720) 100 % (responsible)	Y	N	N
24B05	2384948	Uranium Star Corp. (99720) 100 % (responsible)	N	N	N
24B05	2384949	Uranium Star Corp. (99720) 100 % (responsible)	N	N	N
24B05	2384950	Uranium Star Corp. (99720) 100 % (responsible)	N	N	N
24B05	2384951	Uranium Star Corp. (99720) 100 % (responsible)	N	N	N
24B05	2384952	Uranium Star Corp. (99720) 100 % (responsible)	N	N	N
24B05	2384953	Uranium Star Corp. (99720) 100 % (responsible)	Y	N	N
24B05	2384954	Uranium Star Corp. (99720) 100 % (responsible)	Y	N	N
24B05	2384955	Uranium Star Corp. (99720) 100 % (responsible)	Y	N	N
24B05	2384956	Uranium Star Corp. (99720) 100 % (responsible)	Y	N	N
24B05	2384957	Uranium Star Corp. (99720) 100 % (responsible)	Y	N	N
24B05	2384958	Uranium Star Corp. (99720) 100 % (responsible)	Y	N	N
24B05	2384959	Uranium Star Corp. (99720) 100 % (responsible)	Y	N	N
24B05	2384960	Uranium Star Corp. (99720) 100 % (responsible)	Y	N	N
24B05	2384961	Uranium Star Corp. (99720) 100 % (responsible)	Y	N	N
24B05	2384962	Uranium Star Corp. (99720) 100 % (responsible)	Y	N	N
24B05	2384963	Uranium Star Corp. (99720) 100 % (responsible)	Y	N	N
24B05	2384964	Uranium Star Corp. (99720) 100 % (responsible)	Y	N	N
24B05	2384965	Uranium Star Corp. (99720) 100 % (responsible)	Y	N	N
24B05	2384966	Uranium Star Corp. (99720) 100 % (responsible)	Y	N	N
24B05	2384967	Uranium Star Corp. (99720) 100 % (responsible)	Y	N	N
24B05	2384968	Uranium Star Corp. (99720) 100 % (responsible)	N	N	N
24B05	2384969	Uranium Star Corp. (99720) 100 % (responsible)	Y	N	N
24B05	2384970	Uranium Star Corp. (99720) 100 % (responsible)	Y	N	N
24B05	2384971	Uranium Star Corp. (99720) 100 % (responsible)	Y	N	N
24B05	2384972	Uranium Star Corp. (99720) 100 % (responsible)	Y	N	N
24B05	2384973	Uranium Star Corp. (99720) 100 % (responsible)	Y	N	N
24B05	2384974	Uranium Star Corp. (99720) 100 % (responsible)	Y	N	N
24B05	2384975	Uranium Star Corp. (99720) 100 % (responsible)	Y	N	N
24B05	2384976	Uranium Star Corp. (99720) 100 % (responsible)	Y	N	N
24B05	2384977	Uranium Star Corp. (99720) 100 % (responsible)	Y	N	N
24B05	2384978	Uranium Star Corp. (99720) 100 % (responsible)	Y	N	N
24B05	2384979	Uranium Star Corp. (99720) 100 % (responsible)	Y	N	N
24B05	2384980	Uranium Star Corp. (99720) 100 % (responsible)	Y	N	N
24B05	2384981	Uranium Star Corp. (99720) 100 % (responsible)	Y	N	N
24B05	2384982	Uranium Star Corp. (99720) 100 % (responsible)	Y	N	N
24B05	2384983	Uranium Star Corp. (99720) 100 % (responsible)	Y	N	N
24B05	2384984	Uranium Star Corp. (99720) 100 % (responsible)	Y	N	N
24B05	2384985	Uranium Star Corp. (99720) 100 % (responsible)	N	N	N
24B05	2384986	Uranium Star Corp. (99720) 100 % (responsible)	N	N	N
24B05	2384987	Uranium Star Corp. (99720) 100 % (responsible)	Y	N	N
24B05	2384988	Uranium Star Corp. (99720) 100 % (responsible)	Y	N	N
24B05	2384989	Uranium Star Corp. (99720) 100 % (responsible)	Y	N	N
24B05	2384990	Uranium Star Corp. (99720) 100 % (responsible)	Y	N	N
24B05	2384991	Uranium Star Corp. (99720) 100 % (responsible)	Y	N	N
24B05	2384992	Uranium Star Corp. (99720) 100 % (responsible)	Y	N	N
24C08	2384993	Uranium Star Corp. (99720) 100 % (responsible)	Y	N	N
24B05	2385416	Uranium Star Corp. (99720) 100 % (responsible)	N	N	N
24B05	2385417	Uranium Star Corp. (99720) 100 % (responsible)	N	N	N
24B05	2385418	Uranium Star Corp. (99720) 100 % (responsible)	N	N	N
24B05	2385419	Uranium Star Corp. (99720) 100 % (responsible)	N	N	N

NTS Sheet	Title No	[1]Titleholder(s) (Name, Number and Percentage)	Virginia 1.5% NSR	Jones & Poisson 1% NSR	Jones & Poisson 0.5% NSR
24B05	2385420	Uranium Star Corp. (99720) 100 % (responsible)	N	N	N
24B05	2385421	Uranium Star Corp. (99720) 100 % (responsible)	N	N	N
24B05	2385422	Uranium Star Corp. (99720) 100 % (responsible)	N	N	N
24B05	2385423	Uranium Star Corp. (99720) 100 % (responsible)	N	N	N
24B05	2385424	Uranium Star Corp. (99720) 100 % (responsible)	N	N	N
24B05	2385425	Uranium Star Corp. (99720) 100 % (responsible)	N	N	N
24B05	2385426	Uranium Star Corp. (99720) 100 % (responsible)	N	N	N
24C08	2386856	Uranium Star Corp. (99720) 100 % (responsible)	Y	N	N
24C08	2386857	Uranium Star Corp. (99720) 100 % (responsible)	Y	N	N
24C08	2386858	Uranium Star Corp. (99720) 100 % (responsible)	Y	N	N
24C08	2386859	Uranium Star Corp. (99720) 100 % (responsible)	Y	N	N
24C08	2386860	Uranium Star Corp. (99720) 100 % (responsible)	Y	N	N
24C08	2386861	Uranium Star Corp. (99720) 100 % (responsible)	Y	N	N
24C08	2097640	Uranium Star Corp. (99720) 100 % (responsible)	Y	N	N
24C08	2097641	Uranium Star Corp. (99720) 100 % (responsible)	Y	N	N
24C08	2097642	Uranium Star Corp. (99720) 100 % (responsible)	Y	N	N
24C08	2097643	Uranium Star Corp. (99720) 100 % (responsible)	Y	N	N
24C08	2097644	Uranium Star Corp. (99720) 100 % (responsible)	Y	N	N
24C08	2097645	Uranium Star Corp. (99720) 100 % (responsible)	Y	N	N
24C08	2097646	Uranium Star Corp. (99720) 100 % (responsible)	Y	N	N
24C08	2097647	Uranium Star Corp. (99720) 100 % (responsible)	Y	N	N
24C08	2097648	Uranium Star Corp. (99720) 100 % (responsible)	Y	N	N
24C08	2097649	Uranium Star Corp. (99720) 100 % (responsible)	Y	N	N
24C08	2097650	Uranium Star Corp. (99720) 100 % (responsible)	Y	N	N
24C08	2097651	Uranium Star Corp. (99720) 100 % (responsible)	Y	N	N
24C08	2097652	Uranium Star Corp. (99720) 100 % (responsible)	Y	N	N
24C08	2388385	Uranium Star Corp. (99720) 100 % (responsible)	Y	N	N
24C08	2388386	Uranium Star Corp. (99720) 100 % (responsible)	Y	N	N
24C08	2388387	Uranium Star Corp. (99720) 100 % (responsible)	Y	N	N
24C08	2388388	Uranium Star Corp. (99720) 100 % (responsible)	Y	N	N
24C08	2388389	Uranium Star Corp. (99720) 100 % (responsible)	Y	N	N
24C08	2388390	Uranium Star Corp. (99720) 100 % (responsible)	Y	N	N
24C08	2388391	Uranium Star Corp. (99720) 100 % (responsible)	Y	N	N
24C08	2388392	Uranium Star Corp. (99720) 100 % (responsible)	Y	N	N
24C08	2388393	Uranium Star Corp. (99720) 100 % (responsible)	Y	N	N
24C08	2388394	Uranium Star Corp. (99720) 100 % (responsible)	Y	N	N
24C08	2388395	Uranium Star Corp. (99720) 100 % (responsible)	Y	N	N
24C08	2388396	Uranium Star Corp. (99720) 100 % (responsible)	Y	N	N
24C08	2388397	Uranium Star Corp. (99720) 100 % (responsible)	Y	N	N
24C08	2388398	Uranium Star Corp. (99720) 100 % (responsible)	Y	N	N
24C08	2388399	Uranium Star Corp. (99720) 100 % (responsible)	Y	N	N
24C08	2389191	Uranium Star Corp. (99720) 100 % (responsible)	Y	N	N
24C08	2389192	Uranium Star Corp. (99720) 100 % (responsible)	Y	N	N
24C08	2389193	Uranium Star Corp. (99720) 100 % (responsible)	Y	N	N
24C08	2389194	Uranium Star Corp. (99720) 100 % (responsible)	Y	N	N
24C08	2389195	Uranium Star Corp. (99720) 100 % (responsible)	Y	N	N
24C08	2389196	Uranium Star Corp. (99720) 100 % (responsible)	Y	N	N
24C08	1132942	Uranium Star Corp. (99720) 100 % (responsible)	Y	Y	N
24C08	1132943	Uranium Star Corp. (99720) 100 % (responsible)	Y	Y	N
24C08	1132944	Uranium Star Corp. (99720) 100 % (responsible)	Y	Y	N
24C08	1132945	Uranium Star Corp. (99720) 100 % (responsible)	Y	Y	N
24C08	1132946	Uranium Star Corp. (99720) 100 % (responsible)	Y	Y	N

NTS Sheet	Title No	[1]Titleholder(s) (Name, Number and Percentage)	Virginia 1.5% NSR	Jones & Poisson 1% NSR	Jones & Poisson 0.5% NSR
24C08	1132947	Uranium Star Corp. (99720) 100 % (responsible)	Y	Y	N
24C08	1132948	Uranium Star Corp. (99720) 100 % (responsible)	Y	Y	N
24C08	1132954	Uranium Star Corp. (99720) 100 % (responsible)	Y	Y	N
24C08	1132955	Uranium Star Corp. (99720) 100 % (responsible)	Y	Y	N
24C08	1132956	Uranium Star Corp. (99720) 100 % (responsible)	Y	Y	N
24C08	1132957	Uranium Star Corp. (99720) 100 % (responsible)	Y	Y	N
24C08	1132958	Uranium Star Corp. (99720) 100 % (responsible)	Y	Y	N
24C08	1132959	Uranium Star Corp. (99720) 100 % (responsible)	Y	Y	N
24B05	2120537	Uranium Star Corp. (99720) 100 % (responsible)	Y	N	N
24B05	2120538	Uranium Star Corp. (99720) 100 % (responsible)	Y	N	N
24C08	2120539	Uranium Star Corp. (99720) 100 % (responsible)	Y	N	N
24C08	2120540	Uranium Star Corp. (99720) 100 % (responsible)	Y	N	N
24C08	2120541	Uranium Star Corp. (99720) 100 % (responsible)	Y	N	N
24C08	2120542	Uranium Star Corp. (99720) 100 % (responsible)	Y	N	N
24C08	2120543	Uranium Star Corp. (99720) 100 % (responsible)	Y	N	N
24C08	2120544	Uranium Star Corp. (99720) 100 % (responsible)	Y	N	N
24C08	2120545	Uranium Star Corp. (99720) 100 % (responsible)	Y	N	N
24C08	2120546	Uranium Star Corp. (99720) 100 % (responsible)	Y	N	N
24C08	2120547	Uranium Star Corp. (99720) 100 % (responsible)	Y	N	N
24C08	2120548	Uranium Star Corp. (99720) 100 % (responsible)	Y	N	N
24C08	2120549	Uranium Star Corp. (99720) 100 % (responsible)	Y	N	N
24C08	2120550	Uranium Star Corp. (99720) 100 % (responsible)	Y	N	N
24C08	2120551	Uranium Star Corp. (99720) 100 % (responsible)	Y	N	N
24C08	2120552	Uranium Star Corp. (99720) 100 % (responsible)	Y	N	N
24C08	2120553	Uranium Star Corp. (99720) 100 % (responsible)	Y	N	N
24C08	2120554	Uranium Star Corp. (99720) 100 % (responsible)	Y	N	N
24C08	2120555	Uranium Star Corp. (99720) 100 % (responsible)	Y	N	N
24C08	2120556	Uranium Star Corp. (99720) 100 % (responsible)	Y	N	N
24C08	2120557	Uranium Star Corp. (99720) 100 % (responsible)	Y	N	N
24C08	2120558	Uranium Star Corp. (99720) 100 % (responsible)	Y	N	N
24C08	2120559	Uranium Star Corp. (99720) 100 % (responsible)	Y	N	N
24C08	2120560	Uranium Star Corp. (99720) 100 % (responsible)	Y	N	N
24C08	2120561	Uranium Star Corp. (99720) 100 % (responsible)	Y	N	N
24C08	2120562	Uranium Star Corp. (99720) 100 % (responsible)	Y	N	N
24C08	2120563	Uranium Star Corp. (99720) 100 % (responsible)	Y	N	N
24C08	2120564	Uranium Star Corp. (99720) 100 % (responsible)	Y	N	N
24C08	2120565	Uranium Star Corp. (99720) 100 % (responsible)	Y	N	N
24C08	2120566	Uranium Star Corp. (99720) 100 % (responsible)	Y	N	N
24C08	2120567	Uranium Star Corp. (99720) 100 % (responsible)	N	N	N
24C08	2120568	Uranium Star Corp. (99720) 100 % (responsible)	N	N	N
24C08	2120569	Uranium Star Corp. (99720) 100 % (responsible)	N	N	N
24C08	2120571	Uranium Star Corp. (99720) 100 % (responsible)	Y	N	N
24C08	2120572	Uranium Star Corp. (99720) 100 % (responsible)	Y	N	N
24C08	2120573	Uranium Star Corp. (99720) 100 % (responsible)	Y	N	N
24C08	2120574	Uranium Star Corp. (99720) 100 % (responsible)	Y	N	N
24C08	2120575	Uranium Star Corp. (99720) 100 % (responsible)	Y	N	N
24C08	2120576	Uranium Star Corp. (99720) 100 % (responsible)	N	N	N
24C08	2120577	Uranium Star Corp. (99720) 100 % (responsible)	N	N	N
24C08	1043868	Uranium Star Corp. (99720) 100 % (responsible)	Y	Y	N
24C08	1043869	Uranium Star Corp. (99720) 100 % (responsible)	Y	Y	N
24C08	1043870	Uranium Star Corp. (99720) 100 % (responsible)	Y	Y	N
24C08	1043871	Uranium Star Corp. (99720) 100 % (responsible)	Y	Y	N

NTS Sheet	Title No	[1]Titleholder(s) (Name, Number and Percentage)	Virginia 1.5% NSR	Jones & Poisson 1% NSR	Jones & Poisson 0.5% NSR
24C08	1043872	Uranium Star Corp. (99720) 100 % (responsible)	Y	Y	N
24C08	1043873	Uranium Star Corp. (99720) 100 % (responsible)	Y	Y	N
24C08	1043874	Uranium Star Corp. (99720) 100 % (responsible)	Y	Y	N
24C08	1043875	Uranium Star Corp. (99720) 100 % (responsible)	Y	Y	N
24C08	1043876	Uranium Star Corp. (99720) 100 % (responsible)	Y	Y	N
24C08	1043877	Uranium Star Corp. (99720) 100 % (responsible)	Y	Y	N
24C08	1043878	Uranium Star Corp. (99720) 100 % (responsible)	Y	Y	N
24C08	1043879	Uranium Star Corp. (99720) 100 % (responsible)	Y	Y	N
24C08	1043880	Uranium Star Corp. (99720) 100 % (responsible)	Y	Y	N
24C08	1043881	Uranium Star Corp. (99720) 100 % (responsible)	Y	Y	N
24C08	1043882	Uranium Star Corp. (99720) 100 % (responsible)	Y	Y	N
24C08	1043883	Uranium Star Corp. (99720) 100 % (responsible)	Y	Y	N
24C08	1043884	Uranium Star Corp. (99720) 100 % (responsible)	Y	Y	N
24C08	1043885	Uranium Star Corp. (99720) 100 % (responsible)	Y	Y	N
24C08	1043886	Uranium Star Corp. (99720) 100 % (responsible)	Y	Y	N
24C08	1043887	Uranium Star Corp. (99720) 100 % (responsible)	Y	Y	N
24C08	1043888	Uranium Star Corp. (99720) 100 % (responsible)	Y	Y	N
24C08	1043889	Uranium Star Corp. (99720) 100 % (responsible)	Y	Y	N
24C08	1043890	Uranium Star Corp. (99720) 100 % (responsible)	Y	Y	N
24C08	1043891	Uranium Star Corp. (99720) 100 % (responsible)	Y	Y	N
24C08	1043892	Uranium Star Corp. (99720) 100 % (responsible)	Y	Y	N
24C08	1043893	Uranium Star Corp. (99720) 100 % (responsible)	Y	Y	N
24C08	1043894	Uranium Star Corp. (99720) 100 % (responsible)	Y	Y	N
24C08	1043895	Uranium Star Corp. (99720) 100 % (responsible)	Y	Y	N
24C08	1043896	Uranium Star Corp. (99720) 100 % (responsible)	Y	Y	N
24C08	1043897	Uranium Star Corp. (99720) 100 % (responsible)	Y	Y	N
24C08	1043898	Uranium Star Corp. (99720) 100 % (responsible)	Y	Y	N
24C08	1043899	Uranium Star Corp. (99720) 100 % (responsible)	Y	Y	N
24C08	1043900	Uranium Star Corp. (99720) 100 % (responsible)	Y	Y	N
24C08	1043901	Uranium Star Corp. (99720) 100 % (responsible)	Y	Y	N
24C08	1043902	Uranium Star Corp. (99720) 100 % (responsible)	Y	Y	N
24C08	1043903	Uranium Star Corp. (99720) 100 % (responsible)	Y	Y	N
24C08	1043904	Uranium Star Corp. (99720) 100 % (responsible)	Y	Y	N
24C08	1043905	Uranium Star Corp. (99720) 100 % (responsible)	Y	Y	N
24C08	1043906	Uranium Star Corp. (99720) 100 % (responsible)	Y	Y	N
24C08	1043907	Uranium Star Corp. (99720) 100 % (responsible)	Y	Y	N
24C08	1043908	Uranium Star Corp. (99720) 100 % (responsible)	Y	Y	N
24C08	1043909	Uranium Star Corp. (99720) 100 % (responsible)	Y	Y	N
24C08	1043910	Uranium Star Corp. (99720) 100 % (responsible)	Y	Y	N
24C08	1043911	Uranium Star Corp. (99720) 100 % (responsible)	Y	Y	N
24C08	1043912	Uranium Star Corp. (99720) 100 % (responsible)	Y	Y	N
24C08	1043913	Uranium Star Corp. (99720) 100 % (responsible)	Y	Y	N
24C08	1043914	Uranium Star Corp. (99720) 100 % (responsible)	Y	Y	N
24C08	1043915	Uranium Star Corp. (99720) 100 % (responsible)	Y	Y	N
24C08	1043916	Uranium Star Corp. (99720) 100 % (responsible)	Y	Y	N
24C08	1043917	Uranium Star Corp. (99720) 100 % (responsible)	Y	Y	N
24C08	1043918	Uranium Star Corp. (99720) 100 % (responsible)	Y	Y	N
24C08	1043919	Uranium Star Corp. (99720) 100 % (responsible)	Y	Y	N
24C08	1043920	Uranium Star Corp. (99720) 100 % (responsible)	Y	Y	N
24C08	1043921	Uranium Star Corp. (99720) 100 % (responsible)	Y	Y	N
24C08	1043922	Uranium Star Corp. (99720) 100 % (responsible)	Y	Y	N
24C08	1043923	Uranium Star Corp. (99720) 100 % (responsible)	Y	Y	N

NTS Sheet	Title No	[1]Titleholder(s) (Name, Number and Percentage)	Virginia 1.5% NSR	Jones & Poisson 1% NSR	Jones & Poisson 0.5% NSR
24C08	1043924	Uranium Star Corp. (99720) 100 % (responsible)	Y	Y	N
24C08	1043925	Uranium Star Corp. (99720) 100 % (responsible)	Y	Y	N
24C08	1043926	Uranium Star Corp. (99720) 100 % (responsible)	Y	Y	N
24C08	1043927	Uranium Star Corp. (99720) 100 % (responsible)	Y	Y	N
24C08	1043928	Uranium Star Corp. (99720) 100 % (responsible)	Y	Y	N
24C08	1043929	Uranium Star Corp. (99720) 100 % (responsible)	Y	Y	N
24C08	1043930	Uranium Star Corp. (99720) 100 % (responsible)	Y	Y	N
24C08	1043931	Uranium Star Corp. (99720) 100 % (responsible)	Y	Y	N
24C08	1043932	Uranium Star Corp. (99720) 100 % (responsible)	Y	Y	N
24C08	1043933	Uranium Star Corp. (99720) 100 % (responsible)	Y	Y	N
24C08	1043934	Uranium Star Corp. (99720) 100 % (responsible)	Y	Y	N
24C08	1043935	Uranium Star Corp. (99720) 100 % (responsible)	Y	Y	N
24C08	1043936	Uranium Star Corp. (99720) 100 % (responsible)	Y	Y	N
24C08	1043937	Uranium Star Corp. (99720) 100 % (responsible)	Y	Y	N
24C08	1043938	Uranium Star Corp. (99720) 100 % (responsible)	Y	Y	N
24C08	1043939	Uranium Star Corp. (99720) 100 % (responsible)	Y	Y	N
24C08	1043940	Uranium Star Corp. (99720) 100 % (responsible)	Y	Y	N
24C08	1043941	Uranium Star Corp. (99720) 100 % (responsible)	Y	Y	N
24C08	1043942	Uranium Star Corp. (99720) 100 % (responsible)	Y	Y	N
24C08	1043943	Uranium Star Corp. (99720) 100 % (responsible)	Y	Y	N
24C08	1043944	Uranium Star Corp. (99720) 100 % (responsible)	Y	Y	N
24C08	1043945	Uranium Star Corp. (99720) 100 % (responsible)	Y	Y	N
24C08	1043946	Uranium Star Corp. (99720) 100 % (responsible)	Y	Y	N
24C08	1043947	Uranium Star Corp. (99720) 100 % (responsible)	Y	Y	N
24C08	1043948	Uranium Star Corp. (99720) 100 % (responsible)	Y	Y	N
24C08	1043949	Uranium Star Corp. (99720) 100 % (responsible)	Y	Y	N
24C08	1043950	Uranium Star Corp. (99720) 100 % (responsible)	Y	Y	N
24C08	1043951	Uranium Star Corp. (99720) 100 % (responsible)	Y	Y	N
24C08	1043952	Uranium Star Corp. (99720) 100 % (responsible)	Y	Y	N
24C08	1043953	Uranium Star Corp. (99720) 100 % (responsible)	Y	Y	N
24C08	1043954	Uranium Star Corp. (99720) 100 % (responsible)	Y	Y	N
24C08	1043955	Uranium Star Corp. (99720) 100 % (responsible)	Y	Y	N
24C08	1043956	Uranium Star Corp. (99720) 100 % (responsible)	Y	Y	N
24C08	1043957	Uranium Star Corp. (99720) 100 % (responsible)	Y	Y	N
24C08	1043958	Uranium Star Corp. (99720) 100 % (responsible)	Y	Y	N
24C08	1043959	Uranium Star Corp. (99720) 100 % (responsible)	Y	Y	N
24C08	1043960	Uranium Star Corp. (99720) 100 % (responsible)	Y	Y	N
24C08	1043961	Uranium Star Corp. (99720) 100 % (responsible)	Y	Y	N
24C08	1043962	Uranium Star Corp. (99720) 100 % (responsible)	Y	Y	N
24C08	1043963	Uranium Star Corp. (99720) 100 % (responsible)	Y	Y	N
24B05	1043982	Uranium Star Corp. (99720) 100 % (responsible)	Y	Y	N
24B05	1043983	Uranium Star Corp. (99720) 100 % (responsible)	Y	Y	N
24B05	1043984	Uranium Star Corp. (99720) 100 % (responsible)	Y	Y	N
24B05	1043991	Uranium Star Corp. (99720) 100 % (responsible)	Y	Y	N
24C08	1044170	Uranium Star Corp. (99720) 100 % (responsible)	Y	Y	N

[1] Uranium Star Corp. became Energizer Resources in Spring 2009 and Energizer Resources holds all the rights on the land positions detained by Uranium Star Corp.

7. Accessibility, Climate, Local Resources, Infrastructure and Physiography

Extracted and updated from the "Technical (Geological) Report On The Sagar Property" by Butler and Scherba, 2006.

7.1 Accessibility

The Sagar Property lies 190 km south of Kuujjuaq in the Territory of Nunavik, Québec, and 200 km NW of Schefferville, Québec (Figure 7.1-1). Defined as being north of the 55th parallel, Nunavik comprises the northern third of the Province of Québec covering an area of approximately 507,000 square km.

With the construction of two all weather air strips in the spring of 2007, the Sagar property is now accessible year-round by air.

Figure 7.1-1: Sagar Property location map.

7.2 Climate

The Sagar Property lies within the Subarctic to near-Arctic transition zone near the boundary of the Canadian "Middle North – Far North" (using Hamelin's "Nordicity" classification, 1979). Weather conditions across Nunavik are controlled by large-scale prevailing and synoptic winds crossing Hudson Bay to the west, Ungava Bay to the north and the Labrador Sea to the east. Sea ice usually develops on Ungava Bay in late October to early November and the sea may remain covered in pack ice until late July. Hudson Bay usually starts to freeze in late December.

Even during the present warming trend of mildly variable Holocene climate, true winter conditions here are long and cold, really extending from October to June. The warmest and coldest days are characterized by mean temperatures of >25°C and <-30°C. Mean annual precipitation is <0.45 m, which would normally classify the area as semi-arid, but the effects of low evaporation result in an abundance of surface water. Locally, break-up in the main rivers occurs in mid June, and freeze-up usually starts in September. The frost-free season is very brief, and is occasioned by clouds of very vigorous biting insects. First snow usually falls near the end of August. Strong "southerly" winds (20-30 knots) prevail during the frost-free season bringing in warm air masses. Lee wave turbulence and lenticular clouds can be observed in the atmosphere during this time. NW winds bring cold weather, and north and NE winds bring cold stormy weather off the Labrador Sea (winds in excess of 30 knots). Winter whiteout conditions can develop without warning and may last for several days. A low ceiling of stratus clouds makes whiteout conditions general, and movement across the ground then becomes difficult.

7.3 Local Resources

The limited land resources initially supported a transient hunting and gathering economy mostly near the coastline. This was followed by the Hudson Bay Company's commercial exploitation of the fur trade – Fort Mackenzie to the north was an interior Hudson Bay post. More recent provincial furbearer management strategies were created for desired economic sustainability, but have had a mixed success for isolated northern economies due to competition from artificial-fur alternatives as well as popular external "eco" causes quite unrelated to the realities of the region.

There are no true timber resources on the Sagar Property. Hill tops are generally barren and limited trees are located in valleys.

Most hunting and fishing is for local consumption, and restricted mainly to navigable rivers. Mineral exploration campaigns, an important potential source for local income, have been quite sporadic due to the nature of the business and the high-cost high-risk nature of exploring remote regions. Exploration and mining experts have to be contracted from outside the region.

7.4 Infrastructure and Physiography

No settlements are found within the vicinity. All field camps have to be self-contained and all supplies have to be flown in by float or ski-plane. Communication is facilitated by satellite

telephone. Lakes provide drinking water and float-plane access. Summer drainage may cause lake surfaces to drop from 0.5 to 1 m.

The Property occurs in the Romanet Horst which, because of differential weathering, forms the Mistamisk Valley. Valley bottom elevation varies from 275 m (NW) and up to 360 m (SE). A "ribbed" plateau to the north has elevations around 440-480 m, and a similar "ribbed" plateau to the south has elevations around 440-560 m with tops ~680 m. Topographic ribbing on the plateaux is caused by volcanic and sedimentary stratigraphy as broad folds clearly visible on drainage maps and satellite images. The Romanet River (Rivière Romanet) occupies the valley and drains NW into the Caniapiscau River (Rivière Caniapiscau) which then turns NW to join the Larch River (Rivière aux Mélèzes), both rivers becoming the Koksoak River draining past Kuujjuaq into Ungava Bay. The landscape was carved by Pleistocene ice sheets.

Local vegetation comprise lichens, mosses, sedges, perennial forbs, and dwarfed shrubs. Tundra vegetation is typically ground-hugging warmth-preserving forms including tussocky graminoids, mats or cushion plants, evergreen members of the heath family, and rosettes. Some dwarf shrubs are deciduous in habit. Trees occupy valleys and bowls. Spruce (*Picea glauca*) and tamarack (*Larix laricana*) are the most common trees, while poplar (*Populus tremuloides and P. balsamifera*) and birch (*Betula papyrifera*) occupy some sheltered spots. Alder (*Alnus sp.*) and willow thickets (*Salix sp.)* are common. The local fauna of note comprises caribou, bears, hares, wolves and waterfowl of various types, the latter especially in the short "summer" season.

8. Exploration History

Extracted and updated from the "Technical (Geological) Report On The Sagar Property" by Butler and Scherba, 2006.

No mine production has occurred on the Property, or anywhere within 150 km. There are, therefore, no carried mining environmental liabilities.

Regional geological mapping and descriptions of units in the Labrador Trough have been conducted from the 1960's to the 1980s (e.g., Baragar, 1960; Dimroth, 1964, 1969a, 1969b, 1970, 1978; Dressler, 1979); and geochemical investigations, including radioactivity, were conducted in the early 1980s (Kish *et al*. 1978, 1979; Kish and Cuney, 1981). Other reports on uranium showings were made about the same time (e.g., Masse, 1974; Ruzicka and Littlejohn, 1981). The area was mapped by Clark (1986) at a scale of 1:20,000 (for the Province of Québec), and metallogenic and geochemical studies were also carried out (Poisson, 1992a).

Regional reconnaissance exploration really commenced in the Labrador Trough from 1929 to the late 1940's. The Romanet Horst was covered by intense exploration in the period 1961 to 1966 leading to the discovery of Cu mineralization by Delhi-Pacific (with 12 diamond drill holes). The Taché Lake showing in the eastern portion of the Sagar Property was drilled by Riocanex in 1962 (5 diamond drill holes). Saucon Development Corp. examined the area between Eagle Lake and Lake Mistamisk in 1962. Bornite Copper Corp. examined ground west of Lac Du Chambon in 1962, and Conwest (St. Joe Syndicate) examined the area around Lac Plisse in 1963 (Béland, 1976).

During 1975, Canada Tungsten Mining Corp. re-examined gold-bearing radioactive albitite veins at the Eagle showing. Track-etch and emanometer surveys were carried out over a *circa* 1 square km grid, and 20 diamond drill holes totalling 2,907 m were completed with limited results. During 1978, Leslie Kish found another showing located about 1 km SE of the previous discovery – a showing comprised of Au-U-±Ni-bearing albite – chlorite − dolomite ± hematite - white mica veins. In 1979, Soquem optioned the property from Canada Tungsten, mapped radioactive boulders, made detailed geological maps and conducted an emanometer survey as extensions of the previous Canada Tungsten surveys. In 1983, Saarberg-Interplan (afterwards called Interuranium) identified the Mistamisk boulder field (a.k.a. "Clandestine") by ground follow-up of an airborne scintillometer survey. At that time, the boulder field was on the Canada Tungsten-Soquem ground so no work could be done (hence the name "Clandestine").

In 1986, La Fosse Platinum Group Inc. ("La Fosse") carried out preliminary sampling of all known showings, and 41 diamond drill holes for 1,585m (5,200 feet) were completed. The Mistamisk (Clandestine) radioactive boulder field was relocated and a limited drill program (21 drill holes totalling 1,636m or 5,367 feet) did not find the bedrock source. Further work narrowed targets down to 4 emanometer anomalies which were diamond drilled in 1990 (25 holes for a total of 1,117m or 3.664 feet), but again failed to trace the source of the mineralization. An unmineralized mudstone similar in appearance to the host of the radioactive boulders was intersected "up-ice" but yielded no mineralization results of note. Gamma ray logs were conducted down the drill holes.

In the winter of 1993, Virginia drilled 15 diamond holes for a total of 1,111.82 m with little success (Poisson, 1994a). In 1994 also, Hemlo Gold Inc. drilled 6 diamond drill holes for 1,081.9 m. Best results were 0.5% Cu over 0.5 m in hole SA-94-1, and 0.7% Cu over 2.9 m in hole SA-94-6 including 2.9% Cu over 0.5 m (Gariépy, 1994). In 1994, Kennecott Canada flew an airborne radiometric, electromagnetic and magnetic survey. In 1995, Kennecott drilled 7 holes for 1,390 m, but had limited results. Virginia renamed the Clandestine boulder field the Mistamisk boulder field. In 1997, Inmet drilled 6 diamond drill holes for 1,790 m, and the best assay was 0.5% Cu and 0.3 g/t Au over 1.5 m in hole SGR-02 (Tremblay and Gagnon, 1998). In 1998, Inmet drilled 21 diamond drill holes for a total of 6,074 m (Gagnon, 1998). Best intersections in the 1998 campaign were 3.31 g/t Au and 0.11% U over 0.6 m in hole SGR-09; 3.33 g/t Au and 0.15% U over 0.61 m in hole SGR-09 as well as 31.2 g/t Ag over 1.5 m. As in other drilling campaigns many small intervals with 0.1% to 0.4% Cu were also found.

In August of 2006, Yukon Resources Corp. retained GeoVector Management Inc. (GeoVector) to carry out reconnaissance exploration over the Sagar Property area (Setterfield *et al.*, 2006). This work included field prospecting and mapping; a low detection level water geochemical survey of small streams, ponds and seeps; and reassessment of the quaternary glacial direction. Structures were located in the field that were coincident with an east-west structure identified from the reinterpretation of Kennecott's Dighem airborne survey data. These structures were found to be mineralized with copper, and anomalously radiometric. The water survey identified an alteration anomaly associated with these structures, as well as several uranium anomalies south of Mistamisk Lake. The Quaternary study determined the dominant ice direction as being 009° +/- 10°.

Due to the positive results from the August exploration program, a follow-up program was executed in September, 2006. Work consisted of line cutting, ground geophysics, and prospecting. Line cutting was conducted over the Royal Montreal, Crow Bush, Red-Tail, Le Geant, and Osprey target areas, with all cut grids surveyed with radiometrics and magnetics. The Royal Montreal, Red-Tail, and Le Geant grids identified strong radiometric anomalies, with the Royal Montreal anomaly being proximal to water anomalies identified during the August program. Prospecting expanded the U-Au mineralized trend of boulders in the West Eagle area to a strike length of 1 km.

Based upon the results of the 2006 exploratio program, two exploration programs were conducted over the property from the months of February to April, and June to September, 2007. Work consisted of drilling 46 diamond drill holes (5610 metres), drilling of 164 reverse circulation holes (2624.5 metres), line cutting/grid placement over selected portions of the property area (169 total line kilometres), ground magnetometer surveying (240 total line kilometres), prospecting over selected target areas and the characterization of the the Mistamisk Boulder Field lithogeochemical signature. Table 8-1 summarizes exploration work conducted over the Sagar Property.

Table 8-1 – Summary of notable exploration work on Sagar Property.

Company	Year	Work Performed	Results Summary
Delhi-Pacific	1962	Geology, sampling, drilling	Delhi-Pacific Cu-Au showings found and drilled -12 holes for 1,635 m
Riocanex	1962	Geology, drilling	Taché Cu showing found and drilled – 5 holes for 89 m (results lost)

Company	Year	Work Performed	Results Summary
Canada Tungsten	1975	Geology, sampling, drilling	Kish U-Au showing – 20 holes for 2,907 m,* no significant mineralization discovered
Saarberg Interplan	1983	Airborne spectrometer survey	Discovery of "Clandestine" U-Au radioactive boulder field
Saarberg Interplan La Fosse Platinum	1986	Geology, Mag-VLF-IP, Powell tube scintillometer	Rediscovery of "Clandestine" U-Au boulder field – 21 holes for 1,636 m, no significant mineralization discovered
La Fosse Platinum	1989	Radon gas survey, pionjar drilling	Pionjar failed to test found anomalies due to poor drill penetration
La Fosse Platinum	1990	Drilling and trenching	Trenching did not reach bedrock - 25 holes for 1,117 m, no significant mineralization discovered
Virginia	1992	Geology, georadar, soil geochem in Clandestine boulder field	70 samples with average values of 65 g/t Au and 0.3% U; soil fines showed anomalous Au-U
Virginia	1993	Drilling in Clandestine boulder field	Source of boulders not found - 15 holes for 1,112 m
Hemlo Gold	1993	Quaternary study of Clandestine boulders	Clandestine boulder source was interpreted to be to the SW
Hemlo Gold	1993	Drilling	Boulder source not found - 6 holes for 1,082 m
Kennecott Canada	1994	Dighem airborne survey	Radiometric, AEM and magnetic anomalies were found. An unexplained anomaly was found at Lac Mistamisk
Kennecott Canada	1995	Drilling, prospecting	7 holes for 1,390 m
Virginia	1996	Quaternary study of Clandestine boulders	Boulders possibly due to mass flow from the NE
Inmet, Denison Mines	1997	Geology, prospecting, gravity survey	Viking Au-U showing discovered – 6 holes for 1,790 m
Inmet, Denison Mines	1998	Drilling	Small mineralized intersections during drilling – 21 holes for 6,094 m
Yukon Resources	2006	Geology, ground geophysics, water geochemistry	East-west structure bisecting property
Energizer Resources	2007	Drilling, ground geophysics, prospecting	46 diamond drill holes for 5,610 m; 164 reverse circulation drill holes for 2,624.5 m

9. Geological Setting

Extracted and updated from the "Technical (Geological) Report On The Sagar Property" by Butler and Scherba, 2006.

9.1 Regional Geology

Most of the surface of the Sagar Property is covered by unconsolidated material – the remains and reworked remains of Pleistocene till sheets. Poisson (1992b) estimates the area to have around 1% outcrop, mainly on the slopes bordering the Mistamisk Valley. Beneath the unconsolidated material, the claim groups are underlain by supracrustal units of the Labrador Trough (a.k.a. New Quebec Orogen), an Early Proterozoic continental margin sequence with remnants of large igneous provinces ("LIPs") back-thrust onto its former depositional basement (the Early Proterozoic-peneplained Superior Province).

Kearey (1976) observed that the Labrador Trough was a linear fold-belt partly marking the junction of the Superior and Churchill provinces - a NNW-SSE trending belt roughly 160 km wide by 1,200 km long (Figure 9.1-1). Gravity profiles show gently decreasing anomalies over the Superior Province to the west reaching a minimum beneath the Trough, and then increasing abruptly over the Churchill Province to the east (~15 mGal higher). Superimposed on this pattern are several broad gravity maxima parallel to the Trough, one corresponding to a zone of migmatites. Kearey interpreted this geophysical pattern in terms of a relatively elevated Conrad discontinuity beneath the eastern Churchill Province that was isostatically compensated by a thickened lower crust. The model is consistent with basement reactivation following the collision of the Superior and Churchill provinces which resulted in crustal thickening by ductile flow in the upper mantle and partial melting in the lower crust leading to a double-layered Churchillian crust (refractory lower portion and a more K-rich upper portion).

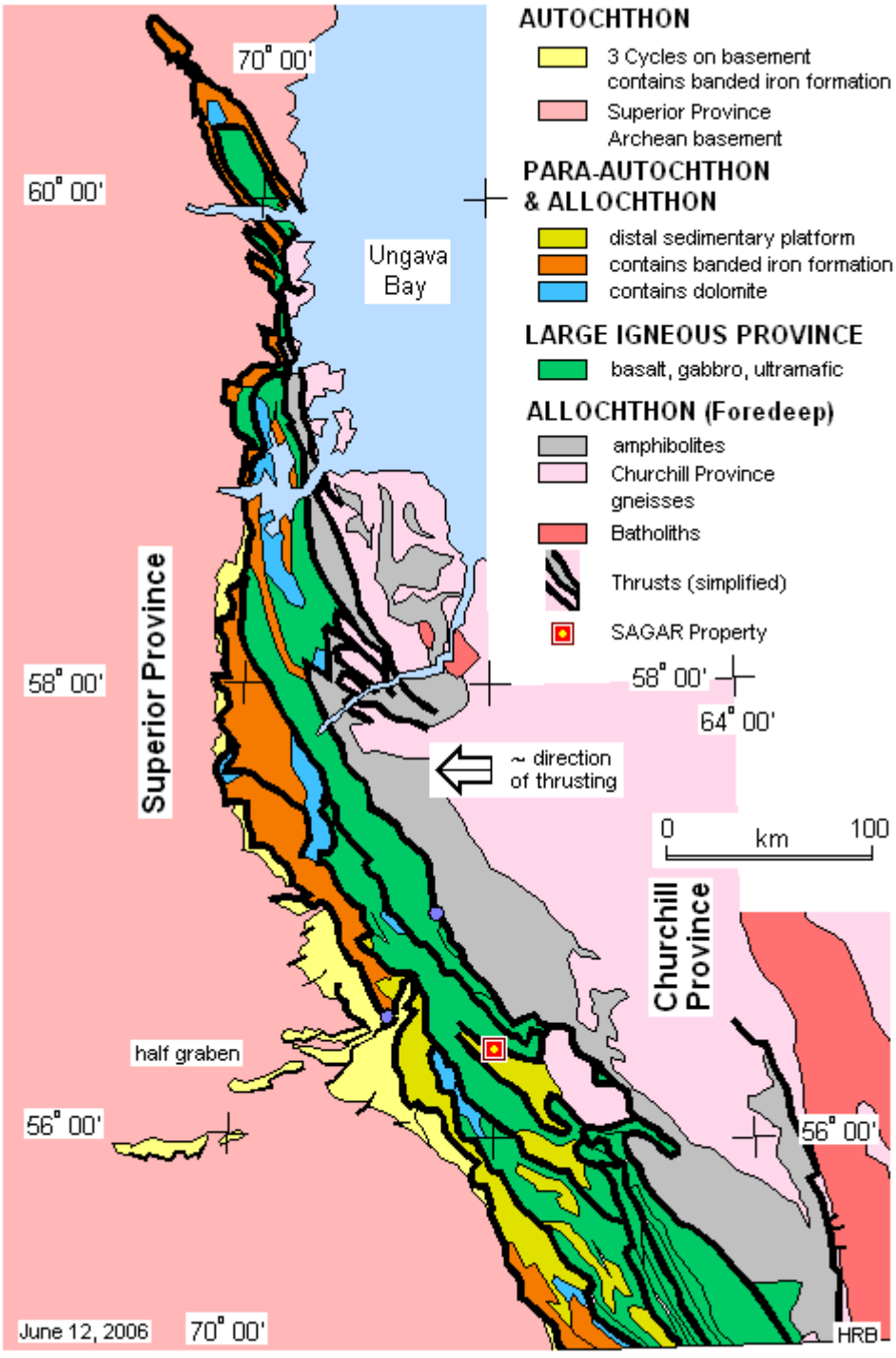

Figure 9.1-1: Outline of Labrador Trough thrust packages: Sketch modified after Clark (2005). The Archean Superior Province to the west still acts as a basement to Trough supracrustals unconformably overlying its complex gneissic packages. As one proceeds east, Trough units are successively detached from their basement. Large-igneous-province units have been emphasized on the figure as well.

In more detail, Goulet (2001) analyzed the timing of superimposed deformation in Ungava and observed both thin and thick-skinned tectonics in the Northern Labrador Trough ("N.L.T."). He noted that imbricated thrust slices, above a major decollement between the Trough's supracrustal

sequences and underlying Archean gneisses of the Superior Province, were part of a D1 nappe structure, that was transported more or less SE. Mylonitic schist developed above the basement and Archean gneisses were thrust over the supracrustals. Strong tectonite fabrics, oriented NNW-SSE, are pervasive to the east. Metamorphic facies vary between lower greenschist and middle amphibolite. Folding of the D1 nappe during a D2 event was oriented NE-SW and produced klippe at its northern end. A final D3 event produced open upright folds with plunges to the SE. To the east, strike-slip faults, oriented parallel to the Trough, have dextral and oblique SW-reverse movements associated with the late D3 folds.

9.2 Labrador Trough Stratigraphy

The Labrador Trough, the Torngat orogen, and the Cape Smith belt are composed of Early Proterozoic units, occupying a significant portion of Nunavik and Labrador. Between the Torngat orogen and the Labrador Trough lies a common hinterland called the "Core Zone" of the southeastern Churchill Province.[1] The Core Zone contains a significant Archean protolith and has also been called the Rae Province (James *et al*., 1996; Wardle *et al*., 2002).

The Trough comprises folded (SW-verging), faulted (strike-slip and/or thrust faults), and metamorphosed sedimentary and igneous supracrustal units belonging to the Kaniapiskau Supergroup. The Kaniapiskau has been subdivided into three cycles separated by erosional unconformities (Clark, 1994).[2] Lateral variations occur from west to east across the Trough. Zones to the west can consist of platform and marine basin sediments as well as fluviatile sediments. In the centre, zones may consist of volcanics and turbidites; to the east, zones comprise gneiss and schist.

9.3 Local Geology

Geological mapping in the Romanet Horst by Dimroth (1970), Chevé (1985) and Clark (1986) established the various units of Trough stratigraphy. The Montagnais Group gabbros on the table are

[1] Radiometric dating indicates that the Core Zone consists of reworked Archean gneisses subdivided into litho-tectonic domains separated by major shears. Northern Core Zone consists in part of amphibolite-grade pelitic gneiss, quartzite, and marble. The SE part contains high-grade, meta-plutonic and meta-volcanic sequences (Wardle *et al*., 2002). The western edge of the Core Zone contains the De Pas and Kuujjuaq batholiths (1.81 to 1.84 Ga) and the Kuujjuaq terrane (supracrustals, and tonalitic and granitic gneiss). The eastern part comprises several granulite domains, and the center consists of mafic to intermediate volcanics and intrusives, ultramafics, volcaniclastics, paragneisses, and leucogranites. The Torngat orogen farther east is bounded by Archean rocks of the Nain Province – a unit, itself subdivided by shear zones. Aswal *et al*. (1986) studied Sr, Nd and Pb isotopes of middle Proterozoic (1.4 to 1.65 Ga) magmas cutting Grenville, Churchillian and Archean units in Labrador, and argued that they were isotopically similar to the early Archean (>3.6 Ga) Uivak gneisses of Labrador or the Amitsoq gneisses of west Greenland." Such information may determine whether the crustal column beneath properties forms part of, or is separated from, adjacent metallogenic provinces - in this case, a metallogenic relationship to the uranium occurrences in the Central Labrador Mineral Belt ~300 km to the SE.

[2] In the southern Trough, the first cycle has conglomerates and red sandstones at its base (Chakonipau Formation) with intercalated (somewhat alkaline) lavas; succeeded by platformal dolomites, arenites, turbidites and tholeiitic basalts. The second cycle consists of basal quartz arenites overlain by cherts, pelitic units and iron formation capped by turbidites and tholeiitic basalts. The third cycle is marked by fluviatile sandstones and polymictic conglomerates.

not necessarily age-correlatives. Based on detailed mapping, Archer (Virginia internal report) believes that age correlation among the various gabbro sills in the Horst is inappropriate. At the present time, Montagnais magmatism has been dated in the interval 1.88-1.66 Ga, and is thought by some to belong to the Trough's second depositional cycle. From top to bottom, a summary of the various stratigraphic formations in the Romanet Horst is summarized in Table 9.3-1 and a detailed geology map can be found at appendix A.

Table 9.3-1: Table of formations on Sagar Property

Group*	Subgroup	Formation	Dominant Lithologies
Montagnais		Gabbro	Gabbro sills – differentiated and various
Knob Lake	intrusive contact		
		Mistamisk	Basalt, breccia, tuff, slate, greywacke, arkose
	Attikamagen	Bacchus	Basalt, slate, greywacke
	Swampy Bay	Romanet	Slate, greywacke, sandstone, basalt, congl
		Du Chambon	Slate, conglomerate, sandstone
	Pistolet	Uvé	Dolomite, sandstone mudstone, siltstone
		Alder	Dolomite, calcarenite, sandstone, chert
		Lace Lake	Mudstone, siltstone, dolomite
	Seward	Dunphy	Dolomite, minor chert, mudstone, dol-sandstone
		Chaponikau	Conglomerate, sandstone, mudstone, basalt

* Part of Kaniapiskau Supergroup; congl = conglomerate; dol-sandstone = dolomitic sandstone.

a) Mistamisk and Bacchus Formations: These units are quite similar and comprise massive and pillowed basaltic flows (from 10 to 20 m thick) interbedded with graphitic shale and gabbro sills. The Mistamisk Fm also contains tuffs. These units are present on the sides of the Horst.
b) Romanet Formation: This unit consists of distal grey to black graphitic slates along with pyritic greywacke, sandstone, pillowed basalt and conglomerate.
c) Du Chambon Formation: The unit occurs throughout the central part of the Horst. It consists mainly of grey to black shale that is frequently pyritiferous. Where it comes into contact with the Uvé Fm stratigraphically beneath, it is characterized by interbedded slates, dolomites and chert. Dimroth (1978) suggested that this unit was a facies correlative of the Romanet Fm. The Du Chambon Fm was the focus of local strain, and exhibits both strong folding and good cleavage.
d) Uvé Formation: Occurring throughout the central part of the Horst, around 60 m of non-stromatolitic dolomite is underlain by a similar thickness of interbedded mudstone, siltstone and dolomite.
e) Alder Formation: This unit also occurs in the central part of the Horst and consists of grey to white quartzitic sandstones, grey calc-arenites, calcareous siltstones, massive and stromatolitic dolomites, sandy dolomites, and dolomitic sandstones.
f) Lace Lake Formation: Occurring on the NW part of the Sagar Property, it is distinguished from the similar looking Dunphy Fm by the presence of ~50% mudstone. The mudstones are variegated purple, green, grey, black, and occasionally yellow and are laminated at the millimeter scale. North of Lac Romanet, greenish schists of possible volcanic origin are interbedded with the mudstones. Some sandstones and dolomite beds are also present.
g) Dunphy Formation: This unit comprises dolomite that is often laminated but rarely stromatolitic along with interbeds of laminated purple, green and grey mudstone – the mudstone content increases towards the top of the column.
h) Chaponikau Formation: Present throughout the Horst, it consists of conglomerate, sandstone, mudstone and basalt. A red conglomerate with arkosic sandstone interbeds occurs at the base, overlain by grey arkosic sandstones, arkoses, and black, grey, green and purple mudstones, as well as an upper massive grey or grayish green magnetic basalt unit.

Kuznetsov *et al*. (2003) note that dolomites of the Dunphy, Portage, Alder, and Uvé formations have the petrographic character of original limy units that were dolomitized immediately after the formation of early diagenetic calcite in unconsolidated units. Rb-Sr isotopic systematics suggest partial de-dolomitisation during regional metamorphism and summer 2013 work indicates many facies of epigenetic dolomotisation superimposed on the carbonaceous unit of the Dunphy formation. Such features might be used to determine whether Cu mineralization in dolomite in the SE part of the Property had a "syngenetic" or "epigenetic" origin and demonstrates its timing relation with regional metamorphism and IOAA-affiliated hydrothermal activity.

Outcropping intrusions are not common within the Horst, but some pegmatite dykes and rare granite dykes have been found. Small gabbro and microdioritic bodies have been mapped, most commonly to the SE (Gagnon, 1998). These gabbros are thought to be older than the Montagnais gabbros. Granite cobbles are abundant in the till to the N, but the source of the granite is not known. The abundance and uniformity of the cobbles lead Charbonneau (1996b, 1997) to postulate that the granite was derived from within the horst, as opposed to outside Archean terrains. A simplified structural cross-section is shown in Figure 9.3-1.

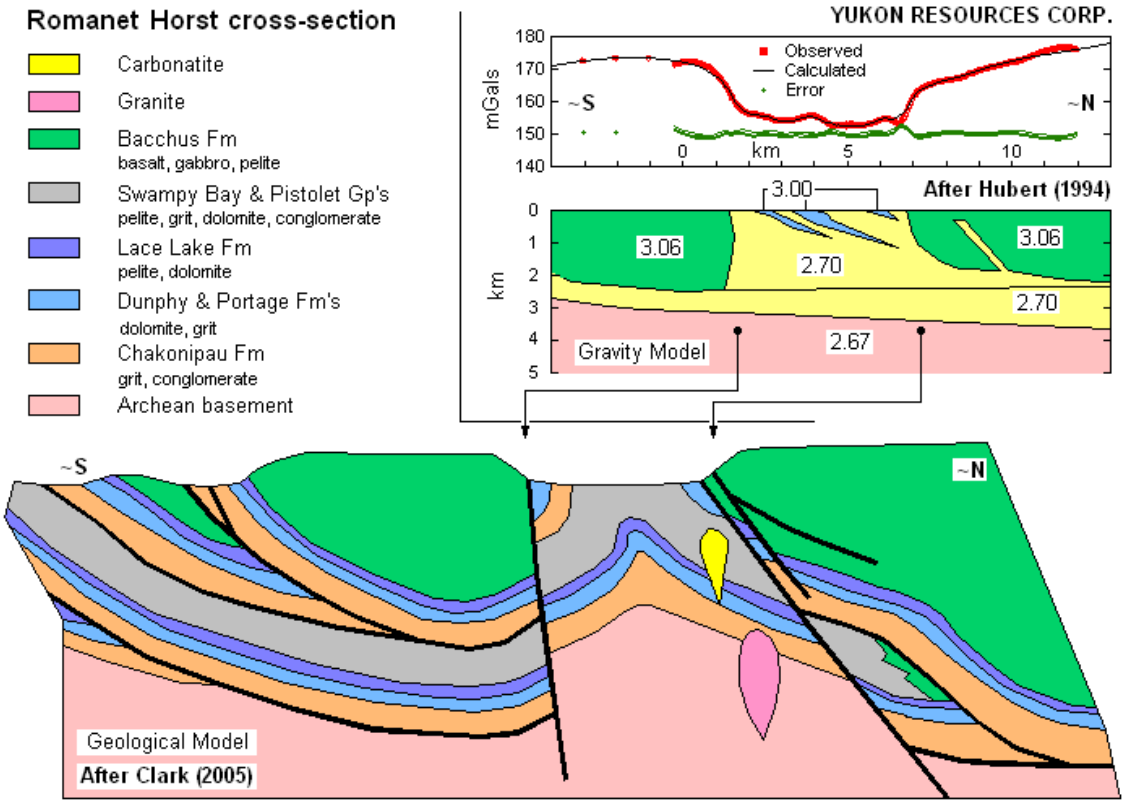

Figure 9.3-1: Gravity profile across the Romanet Horst; modified after Hubert, (1994).

9.4 Large Igneous Provinces (LIPs)

From time to time, Earth history is punctuated by periods when large volumes of mafic magma are erupted. These magmas are not generated at "normal" spreading ridges or above "normal" subduction zones and are termed Large Igneous Provinces (LIPs). In the Archean and Lower Proterozoic, komatiites (ultramafic lavas and sills) are common LIP units. Belts of LIP mafic-ultramafics surround the Superior Province including sequences in the Labrador Trough, the Cape Smith belt (northern Ungava), eastern Hudson Bay (Belcher Islands), the Thompson and Fox River belts (Manitoba and Ontario), and the Marquette Range Supergroup (USA). These belts represent a metallotect because of two known major Ni mining districts, the Thompson and the Raglan Nickel Belts.

During the period 2.19-2.17 Ga, the Payne River diabase dyke swarm cut northern Ungava (in the Cape Smith Belt), and the Cramolet Lake sills (as part of a Cycle 1 magmatic event) are found in the Labrador Trough. In the time interval 1.88 to 1.90 Ga, further LIPs are found surrounding the Archean Superior Province. This magmatism is present in the Labrador Trough (including the Montagnais sills belonging to a magmatic Cycle 2), and has been linked to rifting and possible separation of a micro-continent (St-Onge *et al*., 2000) in the NE-sector of the Superior Province.[3] Ni-Cu-PGE deposits are commonly associated with LIPs. Notable examples include the Siberian Traps and the Duluth Complex (Naldrett, 1999). Such deposits, however, are not expected to be found on the Sagar Property although small deposits of this type have been found in the Labrador Trough elsewhere (Clark, 2005).

LIP units on and beside the Sagar Property may explain the Cu-rich character of some drill intersections (e.g., Delhi-Pacific drill holes discussed below), since Cu deposits can occur in association with LIPs (e.g., on the Michigan Peninsula, and the Coppermine volcanics north of Yellowknife). Hydrothermal circulation of crustal fluids through the LIP basalts beside the Romanet Horst may have contributed Cu directly to the mineralization.

10. Deposit Types

Extracted and updated from the"Technical (Geological) Report On The Sagar Property" by Butler and Scherba, 2006.

10.1 Labrador Trough Deposit Types

[3] Baragar (1960) summarized geochemical data on one section of the Labrador Trough LIPs as follows, *quote*, "Basalts and sedimentary rocks in the eastern half of the Labrador Trough are profusely intruded by gabbro sills. In the Ahr Lake area, Quebec, where the igneous rocks were studied in detail, the gabbros are divided into normal gabbros, leopard rocks, and metagabbros. Metagabbros, which are confined to the eastern part of the area, are equivalent to normal gabbros except for two unusual varieties, leuco- and melano-metagabbros. Normal gabbro sills have differentiated into olivine-bearing lower and pegmatitic upper, portions. The pegmatite of one sill (albite gabbro pegmatite) has sodic plagioclase in contrast with andesine in other pegmatites and a mesostasis interpreted as devitrified glass. […] Normal gabbros are tholeiites which show an iron-rich trend similar to the Skaergaard trend but with negligible alkali enrichment. Basalts of the area are equivalent to the parent magma of the normal gabbros, and differentiation was in situ. Low K and Sr are characteristic of the province."

Explorationists were drawn to the Labrador Trough by large iron formations that have been mined since 1954. Direct shipping iron ores were mined at Schefferville from 1954 to 1982. Iron concentrate production began in 1961 in the SW Trough and in 2000, three mines were producing concentrate and pellets at a rate of 35 Mt per year (Neal, 2000). West and north of Schefferville, several billion metric tonnes have been outlined as fine-grained, cherty magnetite iron formation. Such targets have not been identified in the Romanet Horst.

According to Quebec's 2003 exploration overview, the economic potential of the Trough lies mainly in lithologies that host exhalative massive sulphides with Zn-Pb-Cu-Ag-Au, sediment-hosted stratiform Cu deposits, magmatic Cu-Ni-PGE deposits in picritic flows and sills, and lode Au deposits. According to this review, the Lac Romanet area constitutes a highly prospective area, especially in the Dunphy Formation, and offers promising potential for sedimentary Cu. Several Zn-Cu-Au-Ag sulphide deposits are known in sandy-pelitic units of the Trough's second cycle.

10.2 Iron-Oxide Copper Gold (IOCG) Deposit Model

According to Corriveau (2005), the Romanet Horst may be prospective for IOCG deposits. Deposits of this kind do not have unique lithological hosts or ages (Williams et al., 2005; Porter, 2010). Alteration zones associated with these deposits, however, have a primary Na-Ca±Fe regional alteration that is superimposed upon by focused potassic and K-Fe alteration. The deposits form at shallow to mid-crustal depths in transpressional to extensional continental and continental arc settings, and in the case of Olympic Dam in South Australia, at the junction of continental-scale lineaments (Reeve *et al*., 1990). As Figure 10.2-1 illustrates, IOCG deposit morphology is affected by the source of principal hydrothermal fluids, the host units of the ore zone and the main structures in the area (Barton and Johnson, 2004; Williams et al., 2005). The main ore minerals of IOCG deposits are iron oxides, Cu-Fe sulphides, U oxides, and/or REE-enriched minerals (Corriveau, 2007). Diagnostic element suites for geochemical exploration of IOCG deposits include Fe, Cu, Au, U, Ag, LREE and MREE (especially Ce, La, Nd, Pr, Sm, Gd), ±Nb, ±P, ±Co, ±F, ±B, ±Mo, ±Y, ±As, ±Bi, ±Te, ±Mn, ±Se, ±Ba, ±Pb, ±Ni, ±Zn (Corriveau, 2007).

In 1996, geologists working for Western Mining Corp. examined data on the Sagar Property, and speculated that the mineralization might be explained in terms of an iron oxide-copper-gold vein-breccia type model (Setterfield and Tykajlo, 2000). A hematite breccia has been found on an island in Mistamisk Lake, but its context has not yet been determined.

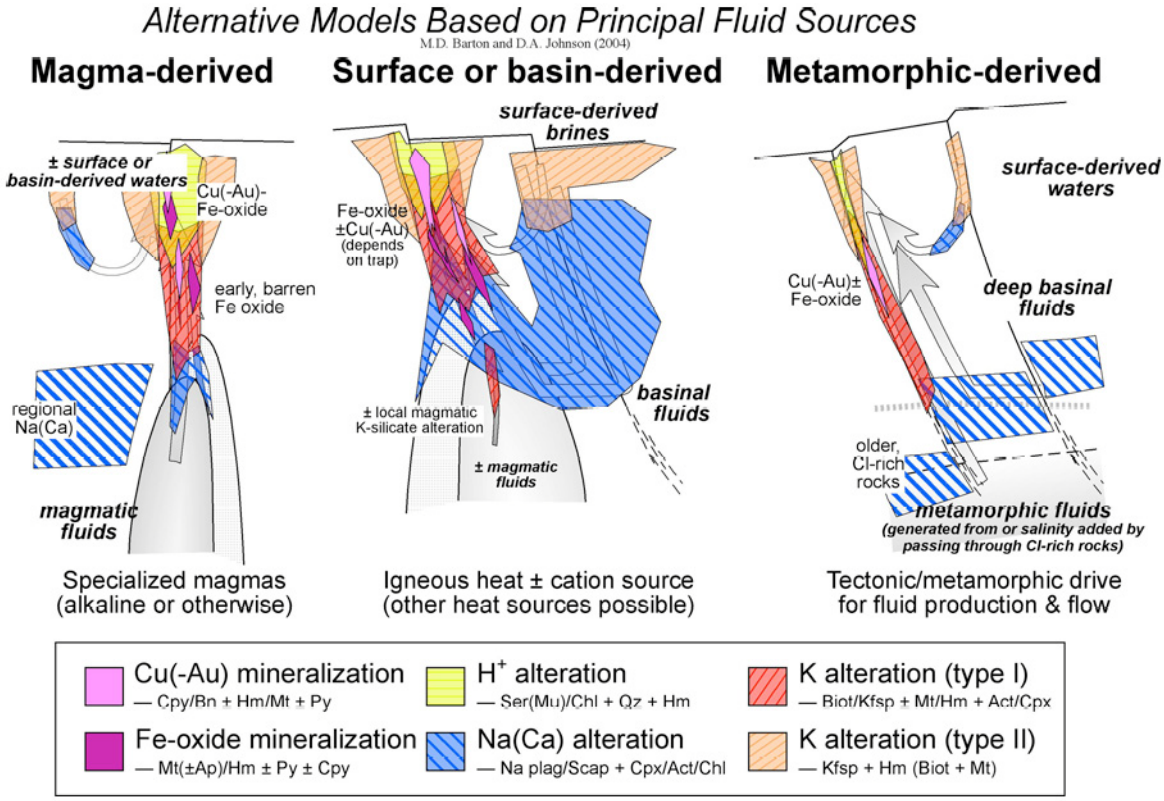

Figure 10.2-1: Flow paths and hydrothermal features for alternative models of IOCG deposits from Barton and Johnson (2004).

11. Mineralization

Extracted and updated from the "Report on work completed by GeoVector Management between June and October, 2006 on the Sagar property" by Setterfield, Chartrand, and Campbell, 2006.

The potentially economic interest of the Sagar property lies in its numerous metal-rich hydrothermal mineralization zones characterized by diversified metallic associations endowed in base and precious metals (e.g. Cu, Ni, Co, Mo, Zn, Au, Ag), rare earth elements (REE), high field strength elements (Th, Ta) and uranium. This association of a wide variety of metals in a spatially restricted area is a typical attribute of fertile iron oxide alkali-altered (IOAA; definition of Porter, 2010) systems in which iron oxide-copper-gold (IOCG) deposits can have been formed.

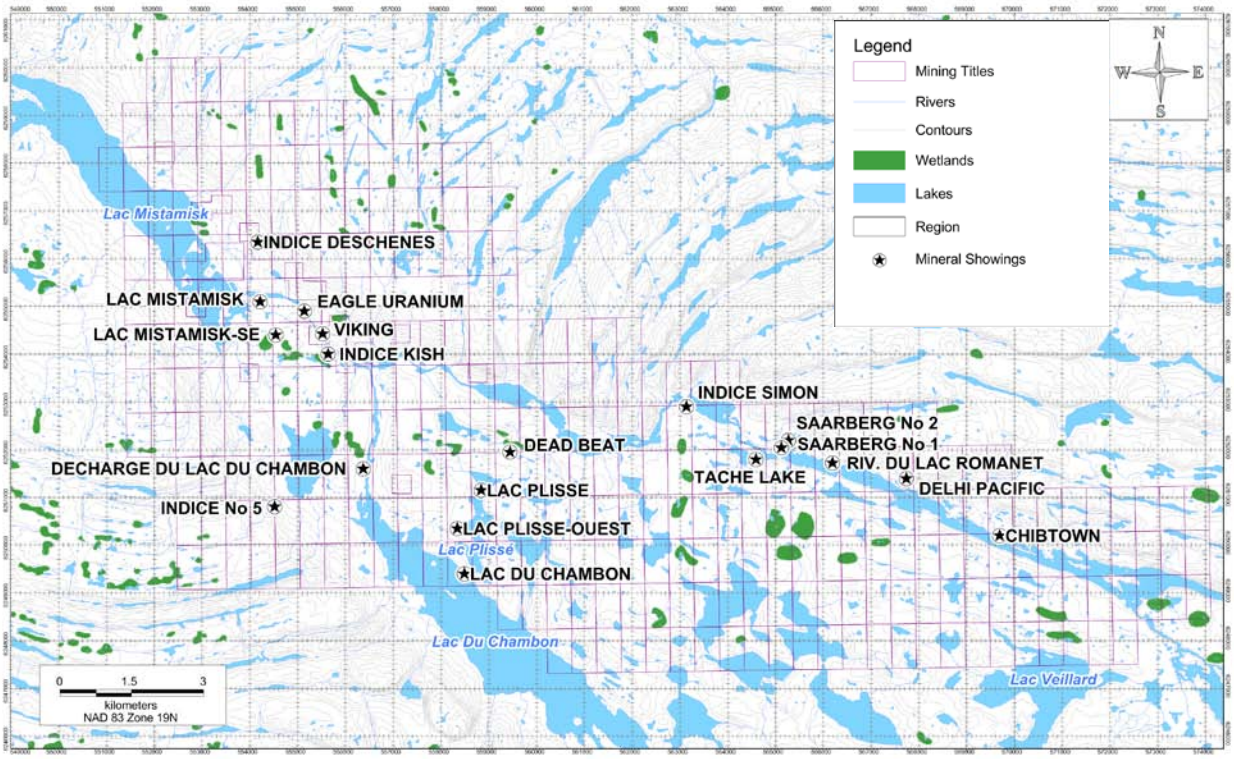

Figure 11-1: Sagar Property mineral showings.

11.1 Mistamisk Boulder Field

The Mistamisk Boulder Field was discovered following a radiometric survey in 1983, and first explored in 1986. The boulder field consists of on the order of 180 radioactive boulders in a 500 x 200 m area north of Lake Mistamisk. The boulder field was divided into six sub-fields by Charbonneau (1996a, b; 1997); collectively the boulders have a northerly trending long axis. GeoVector found two additional strongly radioactive boulder sites 1 km north-northwest of the main boulder field in 2006. The boulders are strongly albitized to a light beige to white colour, with

uranium-bearing minerals and minor hematite on fractures and less commonly associated with thin pegmatite veins (presumably composed of albite). When analysed with the XRF analyzer, some of the uraninum mineralization zones in the boulders exhibit weak to moderate potassium enrichments. Where gradations in alteration exist and the original rock type can be identified, the mineralized boulders are predominantly the green mudstone of the Lace Lake Formation, but some mineralized sandstone and dolostone boulders were also observed. A Virginia analytical study of 68 boulders returned up to 640.11 g/t Au and 4.11% U, with an average of 64.96 g/t Au and 1.26% U (Poisson, 1992b). Other companies have obtained similar high grade Au and U analyses from the boulder field. GeoVector collected two samples from the boulder field. The best sample taken ran 1.45% U, 43.4 g/t Au, 8.0 g/t Ag, 0.57% Pb and 0.10% Ni. A sample from GeoVector's newly discovered sites 1 km north of the main boulder field ran 1.89% U and 42.4 g/t Au.

11.2 Gold-Uranium Mineralization, Northern Part of the Romanet Horst

Three historical gold-uranium±nickel – copper showings occur in the northern part of the Romanet Horst, and may be related to a single northwest-trending structure. These are the Eagle, Kish and Viking showings (Figure 11-1).

Numerous strongly radioactive boulders occur northwest of the Eagle showing; at the present time the source of these boulders is not known. The Eagle showing consists of relatively flat-lying to open-folded green-grey to beige mudstone with subordinate dolostone interbeds cut by straight fractures and veins filled with red-stained carbonate, quartz and albite. The veins are locally radioactive, and host pitchblende, yellow uranium oxides, pyrite and chalcopyrite. They vary in width from several cm to 35 cm, typically thicken in fault jogs, and are oriented approximately 330/80 to 150/85. Veins both cross-cut the mudstone and are preferentially striking parallel to the bedding. Small vuggy cavities locally occur in the veins, suggesting open-space fill. The showing occurs in the transition zone between albitized carbonates of the Dunphy Lake Formation and albitized mudstone of the Lace Lake Formation, but the mineralized veins are preferentially developed in the mudstone. The best surface sample results are from Inmet's 1997 program, where 0.3 m @ 0.8% U and 5.4 g/t Au were reported (Archer, undated). Samples collected in 2006 ran up to 1.58% U, 0.96 g/t Au, 9.7 g/t Ag and 0.53% Cu.

The geology of the Kish showing is similar to that of the Eagle showing. Green-grey to beige, bedded mudstone is cut by thin radioactive veins and fractures filled with carbonate, chlorite and albite with minor specular hematite. The bulk of the veins trend 145 to 160° and dip at 74 to 78° southwest, although bedding parallel veins are also present. The host mudstone is albitized and altered to a pale reddish colour near the veins and fractures. Pitchblende and yellow uranium oxides are locally present in the veins along with melnite ($NiTe_2$), altaite (PbTe) and minor sulphides (chalcopyrite, pyrite and galena). Native gold in the veins occur as tiny grains (300-400 µm), mostly hosted by melonite and altaite (Kish and Cuney, 1981). Two veins have been trenched; small pieces of pitchblende were recovered from the trench rubble. Pyrite occurs as intergrowths within the pitchblende. Pink feldspar is more common at Kish than at the Eagle showing (i.e. pegmatitic veins are present). Inmet reported values of 1% U and 1.0 g/t Au at the Kish Showing (Archer, undated).

The Viking showing comprises thinly-bedded mudstone in contact with a bedded carbonate (dolostone) horizon several m thick. The mudstones are cut by straight, cm- to dm-thick veins oriented approximately 150/80° that are composed of redstained carbonate (dolomite), specular hematite, albite and quartz.
The veins occur at intervals of several m, and are locally weakly radioactive. Small cm-scale pods comprised of copper tellurides/selenides, nickel tellurides as well as galena and clays occur in jogs along an albite-quartz-carbonate vein that cuts the mudstone. Very high concentrations in Te, Hg, Ni and Se were also noted in the copper-rich jog. The host mudstone is variably albitized and sericitized near the veins and alteration typically increases in the proximity of the veins. A pervasive specular hematite alteration is also progressively superimposed in the carbonate unit with increasing proximity of to the vein and specular hematite, in the intense alteration zones, may compose 70-90% of the rocks. The carbonate unit is cut by fractures (000/80°) and minor veins that are locally radioactive (> 6000 cps). Disseminated chalcopyrite is present in some of the veins. The radioactive background of the dolostone is higher than that of the mudstone, indicating that the fluids carrying uranium also circulated in the dolomite unit. With its important specular hematite enrichments, the carbonate as the main host of the mineralized veins and localized copper-rich zones along the veins, the Viking showing is slightly different from the Kish and Eagle showings. Grab samples taken by Inmet have returned up to 223 g/t Au and 0.1% U (Archer, undated).

A number of radioactive boulders occur northwest of the Eagle showing and southeast of Lake Mistamisk. They are composed of green-grey to beige, finely-bedded, albitized mudstones similar to those hosting the Mistamisk boulder field mineralization and the Eagle and Kish showings. The mudstones are cut by thin veins of carbonate, quartz and albite, with local red hematite staining. The veins are radioactive, with scintillometer counts up to 5000 cps, but generally < 2000 cps. One of the boulders exhibited trace amounts of yellow uranium oxides and specular hematite. The host rock and the mineralization in the boulders are similar to those of the mineral showings nearby, and the mineralization is probably related to the same hydrothermal system/event. However the boulders are less intensely altered to hematite and albite, and are less fractured and mineralized than boulders in the Mistamisk field. At the present time it is not clear where these boulders may have been derived, but the preliminary interpretation is that these boulders do not have exactly the same source as those in the Mistamisk boulder field. GeoVector analyzed 30 of these boulders, with results up to 2.91% U, 213 g/t Au, 49 g/t Ag and 0.25% Cu.

11.3 Showings Along the East Boundary of the Romanet Horst

A number of showings with variable Au, Ag, Co Cu, Mo and U content occur over a strike length of 9 km along the fault which bounds the east side of the Romanet Horst (Fig. 11-1). These showings include Simon (renamed Red Tail), Taché Lake, Saarberg (two small showings), Rivière du Lac Romanet, Delhi Pacific, and Chibtown (renamed Le Geant). These showings are described briefly below.

The Simon (renamed Red Tail; also called Polar Ice in some reports) showing consists of several pinkish grey-coloured, massive felsic dikes up to 2 m wide, that transect dark green massive mafic lava or gabbro. The mafic rock is slightly carbonatized and exhibits < 10% medium-grained, disseminated carbonate crystals. The dikes, oriented at approximately 245/55°, are probably

composed largely of albite (an analysis from this showing ran 9.48% Na_2O; Clark, 1986) and carbonate. They locally exhibit reddish hematite staining, and disseminations and veinlets of specular hematite occur. Up to 3% molybdenite is locally present (Lawyer, 2006). The dikes are variably pegmatitic to aplitic. The radioactivity is irregular (up to 10,000 cps) but seems to be highest near the hematite and red staining. Although this showing has been known since the mid-1980's, it has not received the attention that it appears to merit. GeoVector collected five samples from this showing. Results ran up to 0.53% U, 159 g/t Au, 42.3 g/t Ag, 0.63% Cu, 0.39% Pb, 1.00% Se and 1.31% Mo.

Where seen by GeoVector and Energizer, the Taché Lake Co-Cu showing consists of semi-massive sulphide (pyrite-pyrrhotite-chalcopyrite) hosted in albitized mudstones. The mineralization is predominantly associated to an intense chlorite and subsequent white mica-quartz alteration. Pyrrhotite, presumably colbatian, and chalcopyrite are the main sulphides of the showing. Pyrrhotite is predominantly related to the chlorite stage alteration whereas chalcopyrite is predominantly related to the later white mica-quartz veins. Minor pentlandite, that may also be colbatian, is locally exsolved from the pyrrhotite crystals (Colombo, 2013). The mineralisation, enriched in fluorine, is located at the approximate contact between mudstone and dolomite. Clark (1986) took two high grade samples from this showing, which ran 30.8% and 21.2% Cu. Two trenches were sampled by GeoVector for a total of three samples. The best sample ran 11.3% Cu, 1.92 g/t Au and 0.27% Co; another sample had 0.81% Co.
The Saarberg 1 and 2 showings occur in black slates of the Lace Lake Formation, close to a gabbro intrusion (Lawyer, 2006).). The Saarberg 1 and 2 showings are charactetized by actinolite-chlorite-feldspar-chalcopyrite-pyrite with minor bornite cemented breccias comprising albitized rocks fragments as well as pervasive chlorite-quartz-carbonate-albite-chalcopyrite-pyrite replacement of the mudstone next to the breccia zone at Saarberg 2 (Clark, 1986). At Saarberg 2, the mineralized breccia zone is 3m wide whereas the mineralized replacement zone is 0.6m wide. As reported by Clark (1986), Lehto (1962c) reports low grade Cu (up to 1.11%), Au (up to 0.5 g/t) and Ag (up to approximately 3 g/t) associated with these showings. Similar results were obtained by GeoVector: five samples were collected, with assays ranging from 0.33-1.13% Cu, 1.0-3.8 g/t Ag and 86 to 337 ppb Au.

Rivière du Lac Romanet is a small showing which features a pegmatitic quartz vein cutting mafic intrusions near the margin of the horst. The vein trends 110° and dips 40°S, is 10 cm thick, and is very 'rusty'. Locally the vein contains semi-massive sulphide pods which have 3-5% chalcopyrite and pyrrhotite, with abundant malachite staining. This showing has received little previous attention, but the one sample collected by GeoVector ran 3.4% Cu, 16.6 g/t Ag and 367 ppb Au.

The Delhi Pacific showing occurs along the north escarpment of the horst, forming a rusty zone several tens of m thick and several hundred m long. Pyrite, pyrrhotite, chalcopyrite and bornite form disseminations, veinlets, and small semi-massive lenses at the faulted contact between schistose mafic intrusive and extrusive rocks, siltstones and mudstones interpreted to belong to the Bacchus Formation (Clark, 1986). Sulphides also occur as stockworks and in the matrix of altered breccia in which albitized fragments are cemented by an assemblage comprised of calcite-albite-pyrite-actinolite-biotite-chalcopyrite-titanite (Colombo, 2013). This breccia appears to form a horizon a few metres thick, and grades into the stockwork and veinlet mineralization in which the copper mineralization is related to the same hydrothermal mineral assemblages. Bedding is oriented

approximately 280/40°. The host rocks are carbonatized and albitized (Clark (1986) reports values between 7 and 11% Na_2O), producing a resemblance to felsic volcanics. Locally, structures are observed that are reminiscent of felsic lobes with massive centers and flow banding at the margins. In fact, given the intensity of alteration and the presence of shear and fault zones, the possibility that the rocks are altered felsic volcanic cannot be discarded. Delhi Pacific drilled 12 holes on the showing (see section 8), with a best result of 8 m @ 4.23% Cu and 13.7 g/t Ag. GeoVector's six samples returned maximum values of 17.8% Cu, 1.73 g/t Au, 35.0 g/t Ag, 0.14% Zn, 0.13% Pb and 0.21% U.

The Chibtown showing (renamed Le Geant by Yukon) is located at the contact between green mudstone of the Lace Lake Formation and Dunphy Formation dolomite. Mineralization consists of up to 25% chalcopyrite in a quartz-carbonate vein stockwork over an area of 15 m x 5 m in dolomite (Lawyer, 2006). Veining with disseminated chalcopyrite continues for up to 100 m from the stockwork zone. The mudstone at the contact is altered to a sericite schist which locally hosts near massive bands of chalcopyrite with minor bornite. Samples from this area have run up to 9% Cu and 3 g/t Ag (Archer, undated). Two samples taken by the Quebec government returned 2.25% Cu and 1.2 g/t Ag, and 1.76% Cu and 2.8 g/t Ag (Clark, 1986). GeoVector collected eight samples from the Le Geant showing. Assay results ranged from 2.96-13.1% Cu, 15-358 ppb Au and 3.4-15.3 g/t Ag.

11.4 Showings in the Central Part of the Romanet Horst

GeoVector targeted an easterly trending structure that cross-cuts the horst near the southern boundary of the main block of claims. This structure has the previously known Deadbeat and Decharge du Lac Chambon showings (Fig. 11-1).

The Deadbeat showing consists of pyrite, chalcopyrite and malachite in slates which are locally albitized. Prospecting by GeoVector resulted in the discovery of mineralized subcrops and locally derived mineralized boulders up to 150 m from the showing. GeoVector collected six samples in this area; best results were 5.53% Cu, 491 ppb Au and 1.4 g/t Ag.

The Decharge du Lac Chambon showing is a small zone of rusty slate with chalcopyrite, pyrite and malachite. GeoVector found a new showing 250 m northwest of Decharge du Lac Chambon. This is a small subcrop of bleached, rusty, vuggy and siliceous rock, with disseminated to massive chalcopyrite and pyrite on fresh faces. A sample collected by GeoVector from this showing ran >1% Cu and 0.62 g/t Au.

12. Exploration

Exploration activities conducted at Energizer's Sagar Property between the months of February to March, and July to August, 2013 consisted of the following:

- 1114 line kilometres of helicopter-borne Versatile Time Domain Electromagnetic (VTEMplus) Horizontal Magnetic Gradiometer and Gamma-Ray Spectroscopy geophysical surveying
- Collection of 169 grab samples for geochemical analysisCollection of 54 samples for thin section analysis
- On-site hand-held XRF analysis of 623 grab and historic core samples to identify IOCG alteration mineral assemblages

12.1 Airborne Geophysical Surveying

Energizer retained the services of Geotech Ltd. of Aurora, Ontario to conduct a helicopter-borne geophysical survey over the Sagar property between February 14 and March 17, 2013. The geophysical survey consisted of helicopter borne EM using the versatile time-domain electromagnetic (VTEMplus) system with Z and X component measurements and horizontal magnetic gradiometer using two cesium magnetometers and using RSI ARGS RSX-5 spectrometer system. A total of 1114 line-km of geophysical data were acquired during the survey. The complete Geotech report can be found in Appendix B.

The block was flown in a southwest to northeast (N 45° E azimuth) direction with traverse line spacing of 100 metres as depicted in Figure 12.1-1. Tie lines were flown perpendicular to the traverse lines at a spacing of 1000 metres.

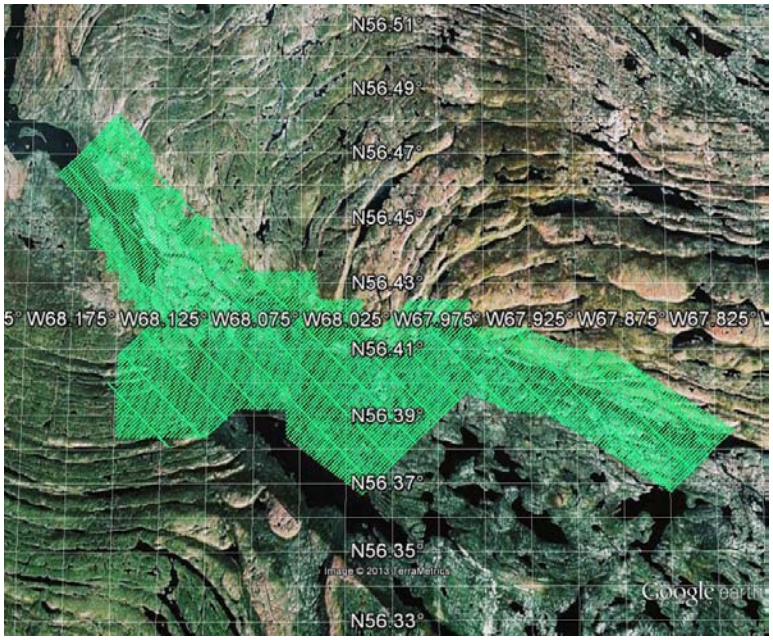

Figure 12.1-1: Flight path of the Sagar property area over a Google Earth image.

According to Prikhodko *et al.* (2013):

"Based on the geophysical results obtained, the area has conductors that can be considered as structural conductors and some as local targets. There is a correlation between TEM, magnetic and radiometric anomalies and features.

There are several linear conductors over the area. The long conductive structures are oriented NW-SE, and they are strongly associated with the magnetic anomalies. At the central and eastern part of the block, there are some structural conductors that are oriented SW-NE, and they are also associated with the magnetic anomalies. According to detail resistivity depth imaging, the top of the conductors varies in depth from near surface to about 50m.

If the conductors correspond to an exploration model on the area it is recommended picking anomalies with conductance grading and center localization of the targets, detail resistivity depth imaging and plate Maxwell modelling with test drillhole parameters prior to ground follow up and drill testing. Since the conductive zones are associated with magnetic anomalies, attendant inversion/modelling of the magnetic field is also recommended."

12.2 Prospecting and Grab Sampling

12.2.1 Sampling Method and Approach

With the assistance of a Bell 206 helicopter from Cochrane-based Expedition Helicopters, prospectors investigated historical showings and target areas generated from the 2013 airborne geophysical survey, and collected grab samples where prospective alteration mineralogy or sulphide mineralization was observed. In total, 169 grab samples were collected (Figure 12.2-1).

Composite grab samples of the mineralization were collected, with oxidized surfaces spalled off in order to provide samples with fresh faces. Composite samples were generally between 1 and 2 kg in size. Sample location and a brief description were recorded by prospectors in the field. Upon returning to camp, an Energizer geologist described each sample and recorded their observations in the sample summary table found in Appendix C.

12.2.2 Sample Preparation and Security

Each sample was double bagged with an assay tag number and sealed in 20 L pails with each pail holding approximately 4 to 8 samples. A sample submittal sheet with requested analyses and sample numbers was then placed in the pails. The pails were then secured with 3 security seals, and the numbers recorded. An Energizer geologist supervised the loading of samples on an Air Saguenay Single Otter flight out of the Sagar camp to Lac Pau. From Lac Pau, samples were transferred on to another Air Saguenay, and then on to Techni-Lab Abitibi Inc. (Sainte-Germaine-Boule, Quebec; subsidiary of ActLabs) to be crushed and pulverized. They were then delivered to Actalbs Ancaster

(Ontario) facility for analysis. Actlabs personnel personally received the samples to insure chain of custody for the samples.

12.2.3 Sample Analysis

Samples were analyzed by Actlabs of Ancaster, Ontario using a total digestions ICP and ICP/MS analytical package (Actalbs code *UT-6 Total Digestion ICP & ICP/MS*). Appendix C has descriptions, locations, and a summary of all elements analyzed.
The description below describes the analytical methodology as per Actlabs website (http://www.actlabs.com/page.aspx?page=510&app=226&cat1=549&tp=12&lk=no&menu=64):

> *Ultratrace 6 combines the 4-acid digestion (HF, HClO4, HNO3 and HCl) with analysis by ICP and ICP/MS. Resistate minerals are not digested.*
>
> ***Total Digestion - ICP Portion***
>
> *A 0.25 g sample is digested with four acids beginning with hydrofluoric, followed by a mixture of nitric and perchloric acids, heated using precise programmer controlled heating in several ramping and holdin gcycles which takes the samples to incipient dryness. After incipient dryness is attained, samples are brought back into solution using aqua regia.*
>
> *With this digestion, certain phases may be only partially solubilized. These phases include zircon, monazite, sphene, gahnite, chromite, cassiterite, rutile and barite. Ag greater than 100 ppm and Pb greater than 5000 ppm should be assayed as high levels may not be solubilized. Only sulphide sulfur will be solubilized.*
>
> *The samples are then analyzed using a Varian ICP. QC for the digestion is 14% for each batch, 5 method reagent blanks, 10 in-house controls (provided by Actlabs), 10 samples duplicates, and 8 certified reference materials. An additional 13% QC is performed as part of the instrumental analysis to ensure quality in the areas of instrumental drift.*

The authors are of the opinion that the chain of custody for all samples was maintained from sampling through to geochemical analysis. No problems have been identified with sample preparation or analytical procedures.

13. Data Verification and interpretations

All analytical results have been verified by the authors. The authors are also satisfied that the chain of custody for all samples has been maintained from collection through to analysis.

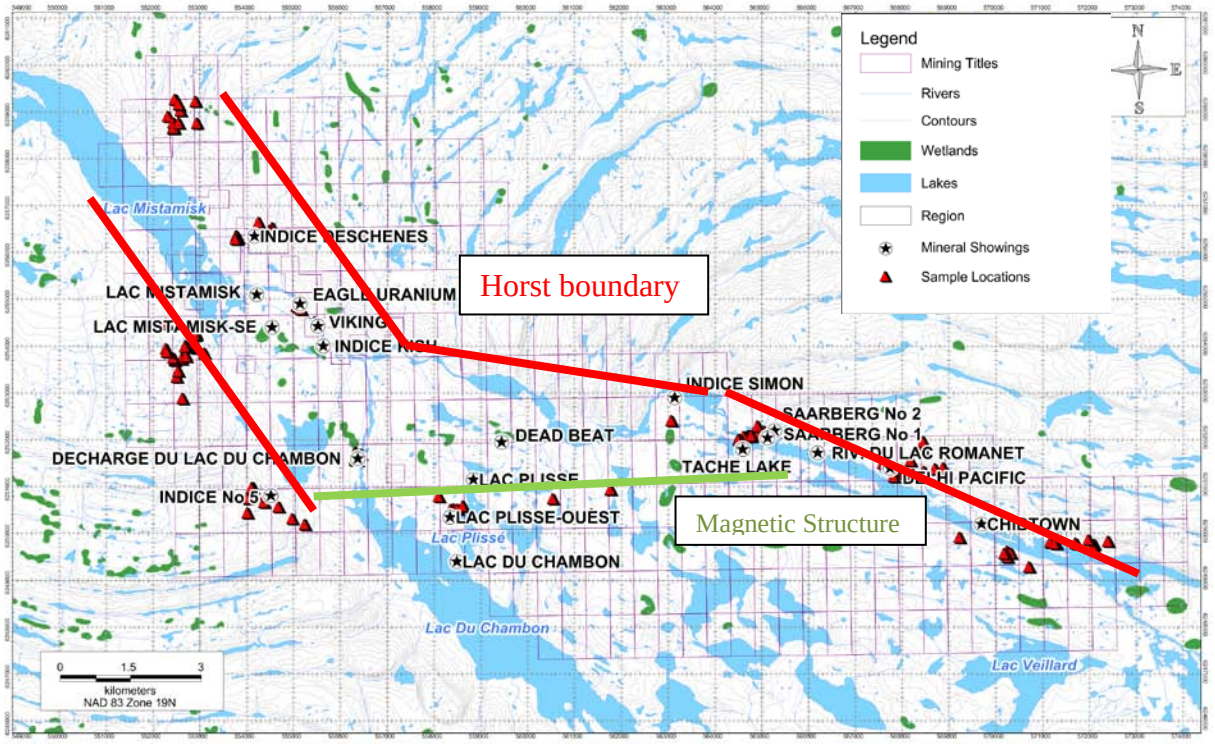

Figure 13.2-1: 2013 grab sample locations.

As illustrated in Figure 13.2-1, samples were concentrated over mineralized locations on the eastern and western boundaries of the horst, as well as along an east-west trending magnetic structure bisecting the horst.

Figures 13.2-2 and 13.2-3 identify anomalous copper and cobalt mineralization respectively. Copper mineralization is found on both the eastern and wester margins of the horst, with anomalous cobalt found along the eastern wall of the horst. In addition to anomalous copper and cobalt, the samples found along the margins of the horst were found predominantly in brecciated metasediments, or immediately adjacent to brecciated lithotypes. The presence of anomalous Cu and Co in brecciated rocks indicates that the margins of the horst are prospective as hosts for IOCG mineralization.

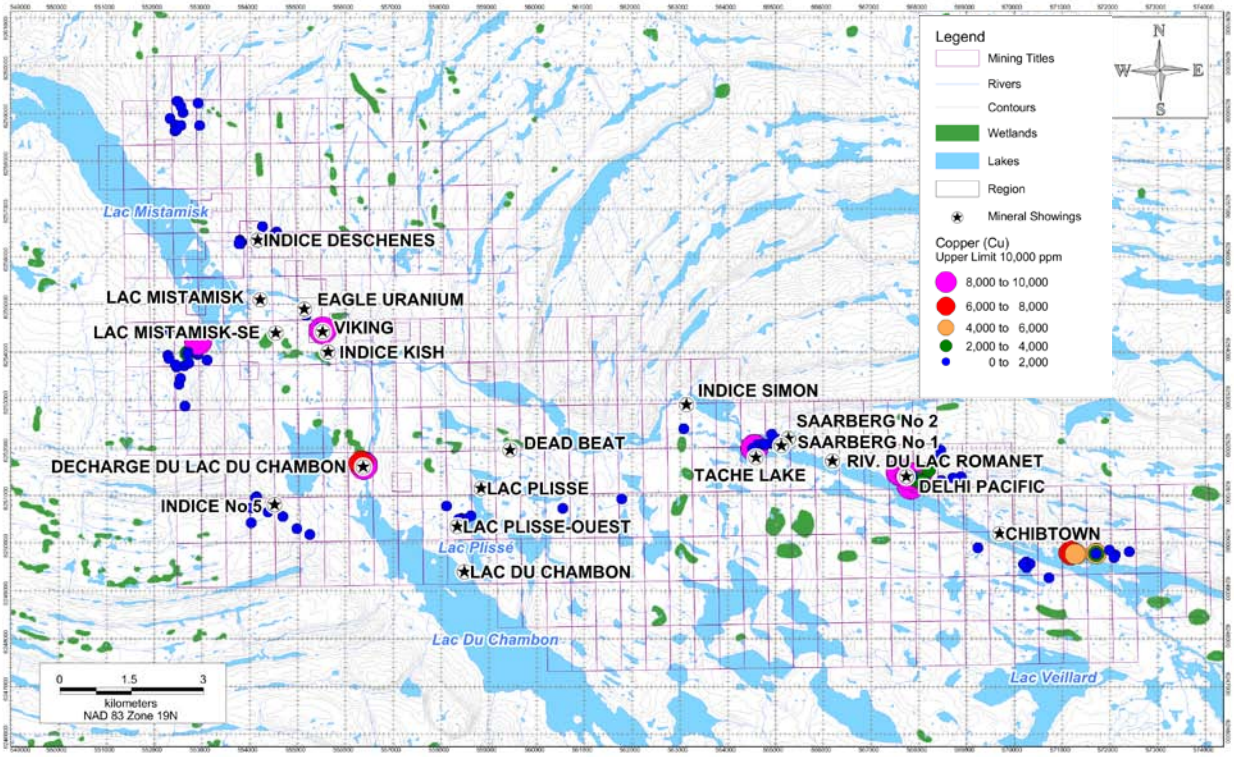

Figure 13.2-2: Copper-in-grab samples.

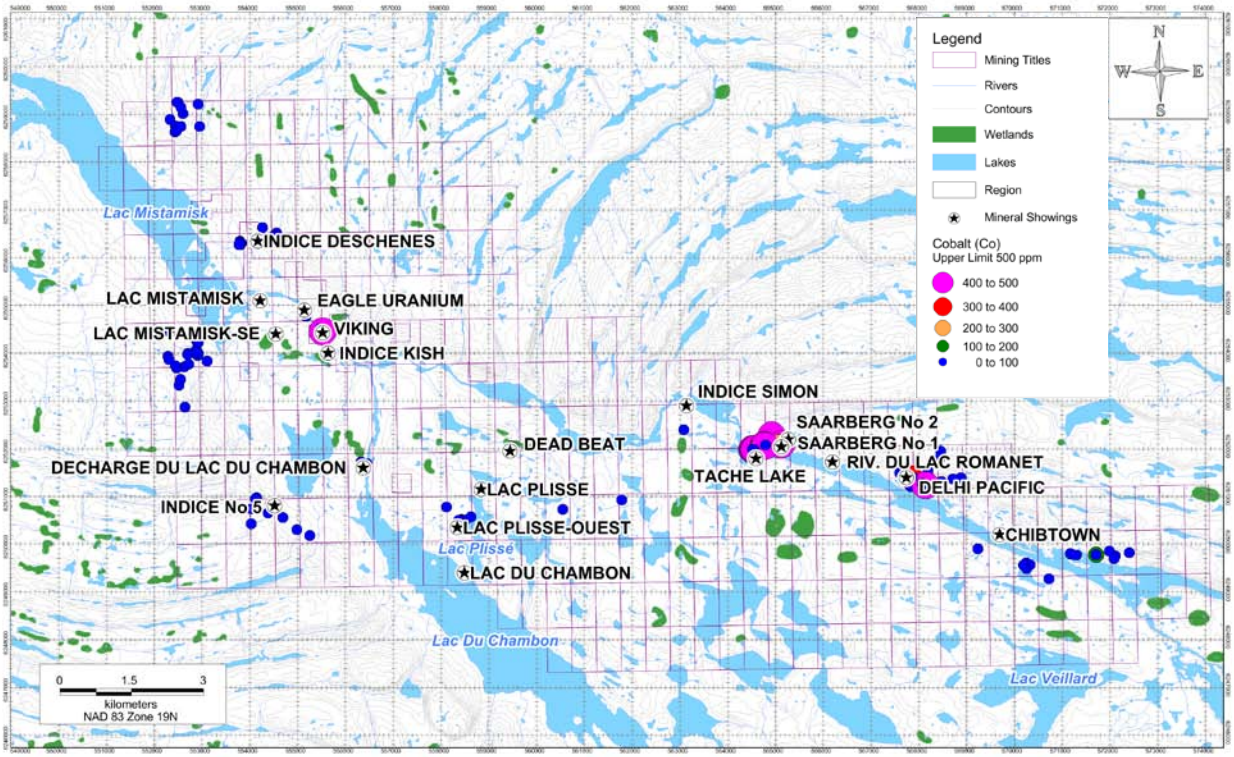

Figure 13.2-3: Cobalt-in-grab samples.

14. Thin Section Analysis

Energizer submitted 54 rock samples to Vancouver Petrographics Ltd. of Langley, British Columbia for petrographic analysis. Together with the samples, detailed sample descriptions and the reason for collecting each sample were provided.

The objective of the petrographic analysis was to determine the mineralogic composition of the samples, petrographically classify the rock types, describe the microstructure defined by the minerals, and to identify potential IOCG alteration assemblages.

The report describing each of the petrographic descriptions is provided in Appendix D. For each sample, the petrographic rock classification, a brief microstructural description, a table with the modal percentage and average grain size for each mineral, and a detailed description of the minerals in decreasing order of abundance were provided. The map of figure 14.1 shows the distribution of the alteration facies. It should be noted that the distribution of the alteration facies is strontly dependent on presence or absence of outcrops. Further drilling will provide additional information that may modify the distribution of the alteration facies.

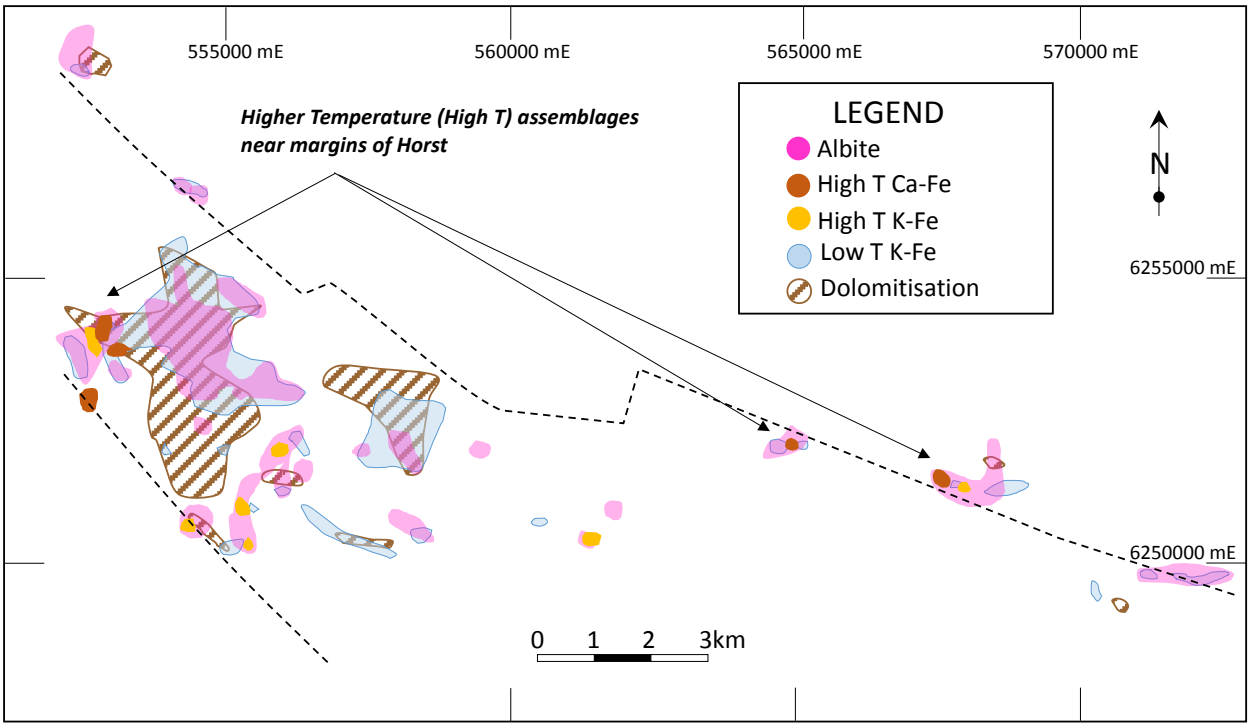

Figure 14.1-1 Map showing the distribution of the alteration facies from thin section and grab sample descriptions.

The following description from Colombo (2013) summarizes the results of the thin section analysis:

"Based on the mineral content, microstructural features, and sample description, five main suites were distinguished.

*The **first** suite (Samples **4**, **21**, **23**, and **28**) consists of metasedimentary rock ranging from very-fine-**sandstone** (Sample 4) to **mudstone** (Samples 21, 23, and 28). Quartz, plagioclase (albite), and white mica are the most abundant minerals within these samples. A sedimentary compositional layering is folded in Samples 4, 21, and 28. The alteration minerals include white mica, albite, quartz, chlorite, rutile, titanite, and tourmaline. The intensity of the alteration varies from weak to moderate (Sample 23). Sample 23 is crosscut by an albite dolomite/ankerite-iron oxide vein, and Sample 28 is crosscut by albite-quartz-chlorite veinlets.*

*The **second** suite (Samples **7**, **8**, **13**, **15**, **17**, **22**, **27**, **29**–**32**, **35**, **36**, **38**–**40**, **43**, **47**, and **48**) consists of metamorphic schists and granofels. Within the schist, the foliation is defined b white mica (Samples 7, 8, and 48), graphite (Sample 13), actinolite (Sample 15), albite ± dolomite ± chlorite ± quartz (Samples 27, 29, 30, 35, and 36). Within the granofels, the minerals (albite, tremolite, dolomite, chlorite, and hematite) are randomly oriented and do not define a foliation. Sulphides and oxides do not always occur within this suite (see details in the petrographic descriptions); however, significant amounts of hematite (Samples 7, 40, and 48), pyrrhotite (Samples 31 and 32), chalcopyrite (Samples 15, 30, and 32), pyrite (Samples 15, 17, and 30), and sphalerite (Sample 47) occur. In most cases, these were introduced as infill minerals.*

*The **third** suite (Samples **6**, **10**, **19**, **20**, **24**, **46**, **51**, **53,** and **54**) is a mixture of igneous rocks with intermediate composition. The different grain sizes of the primary minerals differentiate a **microdioritic** sub-suite (Sample 6 and 54). Sample 6 shows a sub-ophitic microstructure in which abundant actinolite and epidote moderately altered the magmatic rock. In Sample 54, slightly porphyritic plagioclase is immersed within a finer-grained plagioclase-rich groundmass. This sample was microbrecciated and filled in by fine-grained biotite and magnetite. Calcite-bornite-biotite-epidote-albite abundantly filled in the dioritic rock. The **basaltic** sub-suite (Samples 10, 19, 20, 24, 46, 51, and 53) is moderately to strongly altered (actinolite-albite-titanite-chlorite-epidote-calcite-magnetite) and crosscut by veins and veinlets that generally match the alteration assemblages.*

*The **fourth** suite (Samples **9**, **11**, **12**, **16**, **25**, and **26**) is characterized by brecciated microstructures. In most cases, the composition of the fragments indicates a sedimentary protolith (Samples 9, 11, and 12). Samples 16, 25, and 26 show metamorphic fragments. The fragments were filled in by albite ± quartz ± actinolite ± calcite ± white mica ± tourmaline ± epidote ± pyrrhotite ± pyrite ± chalcopyrite.*

*The **fifth** suite consists of **alteration**- and **mineralization-zone** (Samples **1**–**3**, **5**, **14**, **18**, **33**, **34**, **37**, **41**, **42**, **44**, **45**, **49**, **50**, and **52**). Within this group of samples, the intense alteration and replacement obliterated any structural and mineralogic relicts of the protolith. This suite is made up of heterogeneous mineral assemblages including dolomite ± clay ± quartz ± albite ± calcite ± tremolite ± actinolite ± clinozoisite ± rutile ± chlorite. The chalcocite is abundant in Samples 1 and 52. Abundant chalcopyrite occurs in Samples 14, 34, and 44. Tetrahedrite occurs as euhedral crystals in Sample 2.*

The detailed petrographic analysis, in some cases supported by short-wave infrared spectroscopic analysis, determined the mineral composition of the submitted samples, described the microstructural arrangement of the minerals, and indicated the magmatic, metamorphic, and alteration assemblages. The petrographic analysis indicates the occurrence of an ***albite-dolomite-quartz*** *alteration event that is associated in some cases with a brittle deformation event within in the fourth and fifth suites. The occurrence of* ***hematite*** *(Samples 7, 9, 33, 37–41, 46, and 48) indicates oxidizing conditions during the mineralization. On the other hand, the* ***pyrrhotite*** *(Samples 3, 12, 14, 25, 26, 31, and 32) indicates intermediate to reducing conditions, which probably pre-dated the main alteration/mineralization event. The* ***chalcopyrite*** *is the copper-bearing mineral that occurs most often. It occurs as infill mineral, as in the case of Samples 3 and 44, in which the chalcopyrite was precipitated in association with albite-pyrrhotite-quartz-calcite and dolomitepyrite-quartz, respectively. The chalcopyrite is more abundant (~10% of the polished thin section) within Samples 14 and 34; within these alteration-zones, the chalcopyrite is associated with clay-pyrrhotite and calcite-actinolite, respectively. In Sample 14, the mineralization probably overprinted a pre-existent albite-rich alteration event. In many instances, the chalcopyrite is associated with rutile. Within the magmatic suite, the chalcopyrite mostly occurs as an infill mineral (Samples 10, 19, and 51). Within Sample 10, the chalcopyrite is more abundant (~0.2%) and precipitated in association with calcite-Kfeldspar-albite(?)-biotite-pyrite.*

In the second suite, the chalcopyrite is mostly associated with the pyrite (Samples 15–17, 30, 31, 32, and 47). Among these metamorphic samples, the chalcopyrite is more abundant within actinolite schist and albite-dolomite-chlorite schist. The chalcopyrite is subordinate and probably replaced the pyrrhotite within the chlorite-pyrrhotite-quartz granofels. ***Sphalerite*** *occurs only as infill minerals associated with dolomite and subordinate pyrite within a brecciated dolomite-rich granofels (Sample 47).* ***Chalcocite*** *dominates the composition of Sample 1 and is associated with subordinate clay.* ***Tetrahedrite*** *forms euhedral crystals associated with abundant dolomite within Sample 2, and* ***bornite*** *is associated with calcite-biotite-epidote-albite and filled in a strongly altered (actinolite) microdiorite."*

Based on the descriptions provided above, the suite of rock samples that were submitted for petrographic analysis have mineralogy consistent with a fertile iron oxide alkali-altered (IOAA) IOCG system.

15. IOCG Alteration Analysis

Jean-François Montreuil was retained by Energizer to test the hypothesis that the Sagar Property may contain an IOAA system in which a potential IOCG deposit can have been formed. A three week fieldwork campaign was conducted between July 17th and August 5th with the support of Energizer geologists, prospectors, camp managers, other external consultants and researchers from the University of Manitoba, to test this hypothesis and better define the regional-scale hydrothermal system of the Sagar property.

The hydrothermal system of the Sagar Property and its affiliation with IOAA-type system and its prospectivity for IOCG mineralization was tested using the following methodology:

1- Recognition and description of the alteration zones related to some of the main showings of the Sagar property and identification of the alteration related to the various type of base and precious metals as well as other elements (e.g. rare earth elements) mineralization;
2- Identification of the various alteration zones in a selection of diamond drill holes (DDH) for the Mistamik Lake area;
3- Mapping in a selection of DDH the spatial distribution of the various alteration types identified in the Sagar Property;
4- Definition of the geochemical signatures of the various hydrothermal alteration zones with XRF analyzer and whole rock lithogeochemistry. A total of 623 spot analyses were done with the XRF analyzer to confirm the proper alteration mineralogy.

Other activities performed during fieldwork include:

1. Guidance for the sampling of the diverse alteration facies in the various alteration families by the researchers of the University of Manitoba;
2. Contribution to the definition of the problematic that needs to be solved to improve the understanding of the Sagar hydrothermal system and its IOCG potential;
3. Systematic analyses of the various alteration facies with a light element Niton XRF analyzer;
4. Targeted lithogeochemical sampling of the various alteration facies of the Sagar hydrothermal system to define their chemical signature; and
5. Targeted petrographic sampling for thin sections of the various alteration types of the Sagar hydrothermal system.

15.1 Description and classification of alteration facies

This section describes the main alteration facies observed in the Sagar Property and their relations to the mineralization zones of the system. The distribution of the various alteration facies observed on the Sagar Property is shown on figure 14.1.

An alteration facies, according to Schmid et al. (2007) and Zharikov et al. (2007), is defined by the presence of *very systematic sets of mineral assemblages, repeatedly associated in time and space and showing a regular relationship between their mineral composition and bulk chemical composition, such that different alteration facies appear to be related to different physico-chemical conditions, in particular temperature*. The alteration facies approach facilitates the grouping of similar alteration facies in large and simplified family of alteration in complex and polyphase hydrothermal systems and provides a conceptual framework to portray the chemical evolution of the

system. The name of each alteration facies defined in this report is established using diagnostic chemical elements which are, except for Na, routinely analyzed by the light element XRF analyzer. All the mineral abbreviations in this section follow Whitney and Evans (2010).

Eight families of alteration facies were defined in the Sagar Property based on the chemical and mineralogical signature as well as the estimation of the intrinsic characteristics of the hydrothermal fluids associated to each alteration facies.

The main alteration families are (Fig. 15.1-1):

1. Sodic alteration (Na)
2. Ca-Fe (HT)
3. K-Fe (HT)
4. K-Fe (LT)
5. Dolomitisation (Mg alteration)
6. Ca-Fe (LT)
7. Silicification
8. Sulfates (Ca-SO4)

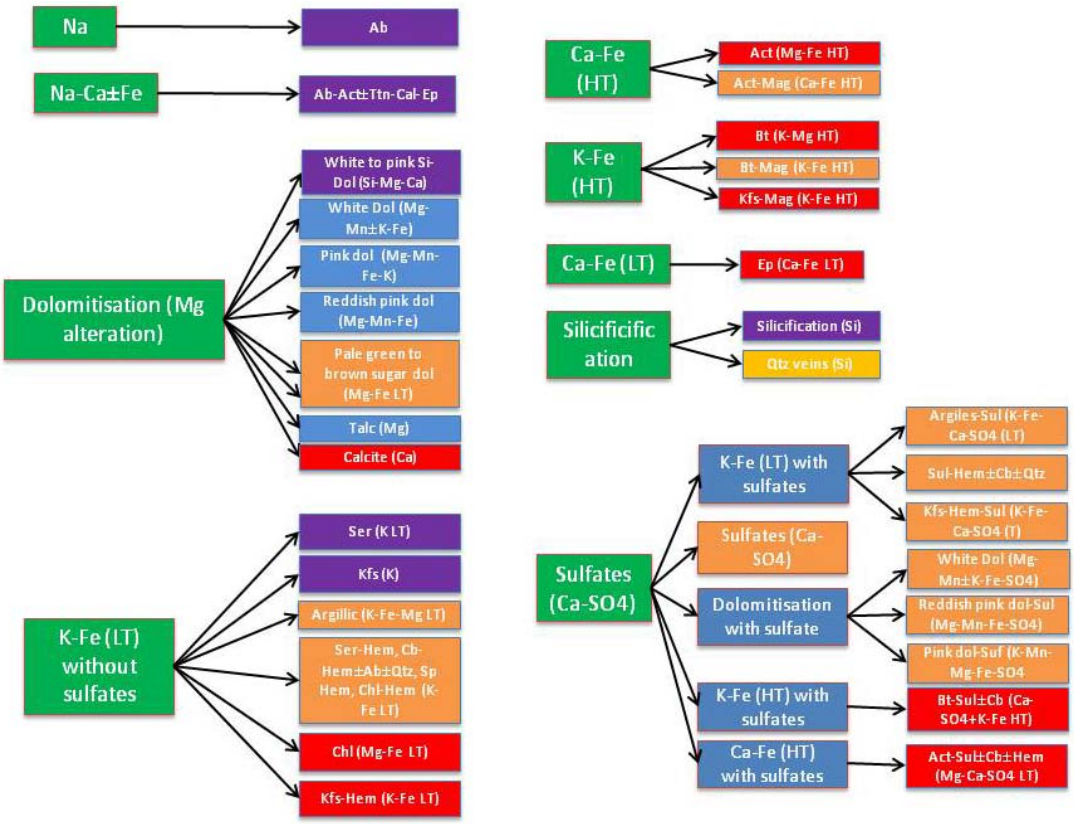

Figure 15.1-1 Main alteration facies identified in the Sagar Property

15.2 Na alteration

Two types of sodic alteration were observed. The first type appears to be the outer to proximal alteration halo of the hydrothermal system and the earliest alteration formed in many of the showings. It is regionnaly distributed as it is typical in most of the IOAA systems (Williams et al., 2005; Corriveau et al., 2010). This early sodic alteration typically occurs as pervasive replacement of the precursor sedimentary or basaltic rocks and its intensity grades from incipient to intense. Intense sodic alteration leads to the formation of albitites. Given the porous nature observed in many albitites (Engvik et al., 2008; Polito et al., 2010), the mechanical weakening of the albitites may have focused brecciation during tectonic deformation, like it was observed in the Delhi breccia zone where most of the breccia fragments are albitized. This spatially constrained brecciation within preferential unit is ideal to focus the flow of mineralizing fluids in favorable permeable windows in larger deformation zones (e.g. fault jogs).

The second type of albitization was observed in the uranium-mineralized samples of the boulder field as well as the Eagle uranium showing. It occurs as coarse-grained to pegmatitic albite veins and albite is associated with variable modal content of chlorite and hematite. In the Eagle showing, the veins are emplaced in late structures that cut the folded sedimentary rocks. This albite alteration event occurred in the late-stage development of the hydrothermal system and is likely not temporally related to the earlier regional albitization event. This coarse-grained to pegmatitic albitization is also more proximal and interpreted as genetically related to the uranium and gold mineralization of the Kish and Eagle uranium showings (c.f. Kish and Cuney, 1981; Kearvell and Clark, 1988). High thorium concentration measured in the Boulder field, Kish and Eagle uranium showings indicate a granitic or upper crustal component in the hydrothermal fluids to account for the high thorium content of the uranium mineralization.

15.3 Ca-Fe (HT)

This alteration family regroups the two observed amphibole±magnetite-bearing alteration facies that are typical alteration zones of IOAA systems.

15.3.1 Ca-Fe (HT;Amp-Mag) and Na-Ca±Fe (Ab-Amp±Mag)

This alteration forms at high temperature and is one of the primitive alteration zones associated to IOCG deposit, although it is not typically directly associated with the bulk of the base metal mineralization. It is also typically overprinted by more fertile alteration or exhibits potassium enrichment to form a Ca-Fe-K alteration, composed of actinolite-biotite or K-feldspar±magnetite. In the Sagar Property, the extent of this alteration facies is for now restricted to the basaltic units observed in the deeper sections of the DDH drilled by Virginia. Its presence is signaled by actinolite

crystallization in the basalt vesicles and variable magnetite enrichments in the basalt aphanitic groundmass, depending of the alteration intensity.

At surface in many mafic rocks, breccias zones and some sedimentary rocks of the Sagar property, a pervasive and weakly to extremely intense Na-Ca±Fe alteration is observed. This alteration is composed in variable modal proportions of albite and actinolite with accessory titanite-chlorite-epidote-magnetite. Actinolite veins are also commonly observed in the geological units altered by this pervasive Na-Ca±Fe alteration. For instance actinolite veins occurred in a strongly Na-Ca±Fe altered basalt below the Delhi Pacific copper showing and into a gabbroic unit located north of the Tache Lk. showing. This Na-Ca±Fe alteration is similar to the regional Na-Ca alteration described by Monteiro et al. (2008) that surrounds the IOCG deposits of Sequeihirino and Sossego in the Carajás IOCG district in Brasil. Localized copper enrichments were observed in this alteration zone, especially where Ca-Fe (LT) epidote and K-Mg (HT) alteration are superimposed.

15.4 K-Fe (HT)

This alteration family regroups the typical high temperature potassic-iron alteration facies characterized by the presence of magnetite with another potassic mineral that can be either biotite or K-feldspar. Actinolite can also be formed in the alteration facies of this family. Typically in the DDH, K-Fe (HT) alteration zones occur structurally above the Ca-Fe (HT) alteration facies. Base metal mineralization is also more common in alteration facies related to the K-Fe (HT) family.

15.4.1 K-Fe (HT;Bt-Mag)

This alteration facies, comprised of magnetite and biotite, was almost exclusively observed in the basalt in DDH where it is signaled by the formation of biotite in the vesicles that also locally include magnetite and the pervasive crystallization of magnetite in the generally albitized and fine-grained groundmass of the basalt. Outside the DDH in the Mistamik area, this alteration was observed in the Delhi showing where it forms thin veinlets composed of magnetite, biotite and sulfides that are emplaced parallel to the cleavage and locally form zones of microbrecciation in the albitized basalt. This alteration may also be formed in microdiorite units where it occurs as magnetite-biotite veins cementing albitized fragments of the microdiorite. This alteration facies is typically proximal to the base metal mineralization observed in the basalt, especially when it is overprinted or cut by sulfate-bearing alteration facies as well as K-Mg (HT; Bt), Mg-Fe (HT;Act) or Ca-Fe (LT; Ep) alteration.

15.4.2 K-Mg (HT;Bt)

This alteration facies occurs as veins, breccia filling or alteration fronts and was only observed in DDH. The K-Mg alteration fronts, where intense, transforms the basalt in biotitite. K-Mg (HT; Bt) alteration, when mingling with sulfate and sulfate-Cb veins, is directly associated with the copper

mineralization in the basalt. This mixing process likely represents one of the ore forming processes in the Mistamik area of the hydrothermal system. If it occurs massively in an extensive area favorable to fluid mixing, this sulfide precipitation process has the potential to form a large IOCG deposit as this reaction process leads to magnetite precipitation. Considering that magnetite is enriched in the vicinity and sometime into the reaction zones but that the largest reaction zones are demagnetized, the large base metal deposit may sit where there is a sharp transition from a magnetic high and a magnetic low.

15.5 K-Fe (LT)

This family of alteration facies regroups most of the hematite-bearing and low temperature Fe-rich and K-rich alteration facies formed after siliceous precursor rocks. Alteration facies of this family are widespread at surface and in DDH in the Sagar system and are typically proximal to or host to mineralization zones. Six different alteration facies were grouped to form this alteration family.

15.5.1 K (LT; sericite)

Pervasive sericite (white mica) replacement occurs as pale yellow and pervasive replacement of siliceous sedimentary precursor and as veins in dolomitisation zones. This alteration signals the ingress of potassium-rich and likely acidic fluids into the system. Intense sericitization with K concentration above 5% with the light element XRF analyzer, when spatially associated with Fe-rich K-Fe (LT) alteration facies (e.g. chloritic), is typically proximal to or host base metal mineralization whereas incipient but pervasive sericitization and sericite veins in dolomitisation can be distal to proximal to the intense K-Fe (LT) altered alteration and potential mineralization. This alteration is especially well developed in the northern boundary fault of the horst north of the Boulder field and is related to copper mineralization in the Taché Lk. showing.

15.5.2 K (K-feldspar)

Intense K-feldspar alteration without any Fe enrichment does not appears to be widespread in the Sagar Property and was only locally observed in DDH. The significance of this alteration is thus hard to establish until more observations can confirm its extent and role in the hydrothermal system. In other IOAA systems, intense potassic (Kfs) alteration form a regional and external alteration aureole of the IOCG deposit (Hitzman et al., 1992; Goad et al., 2000) or may mark the transition between the K-Fe (HT) and K-Fe (LT) alteration zones.

15.5.3 K-Fe-Mg (Argillic)

K-Fe-Mg argillic alteration is typically observed in siliceous rocks. In DDH in the Lac Mistamik area, itIt reaches its peak intensity in deformation zones in the immediate vicinity of the polymict breccia zones where it occurs in association with extensive sulfate-rich alteration. In this intense K-Fe-Mg alteration, Fe concentrations over 20% were measured with the light element XRF analyzer. This intense K-Fe-Mg alteration signals considerable fluid circulation in the deformation zone and important Fe ingress in the hydrothermal system. This alteration can be a low temperature equivalent of deeper and more fertile potassic-iron alteration zones that may host the bulk of IOCG mineralization. Less intense K-Fe-Mg alteration is also observed in siliceous precursor rocks in the dolomitisation zones where it may form the external K-Fe (LT) alteration halo of the hydrothermal system, similar to the Si-Mg-Ca dolomitisation. Considerable intensification of this K-Fe-Mg alteration, like the intensification of dolomitisation, may signal the proximity of a major fluid circulation pathway in which the ore-forming fluids can have circulated. According to petrographic descriptions, illite may be a predominant mineral in this alteration (Colombo, 2013).

15.5.4 K-Fe (LT; Ser-Hem, Cb-Hem±Qtz, Hem, Chl-Hem)

K-Fe (LT) alteration facies can be the external to proximal alteration halo of more fertile and structurally deeper potassic-iron alteration zones. This alteration facies forms pervasive replacements (Ser-Hem, Chl-Hem), veins (Hem, Hem-Cb±Qtz) and breccia cement (Hem, Hem-Cb±Qtz). The different mineral assemblages observed in this alteration facies may be partially controlled by the chemistry of the precursor rock but also to the chemistry of the fluid. Intensification of this alteration facies may signal the proximity to fertile and potentially mineralized alteration zones or to major fluid pathways, especially when it is sulfate-enriched. Intensification of LT K-Fe alteration can also be indicated by increasing abundance of specular hematite in the mineral paragenesis of the alteration or by very high potassium content content that can exceed 6% with the light element XRF analyzer. This is exemplified at the Viking showing where the Cb-Hem veins have a high modal content (> 25%) of specular hematite in the veins and where pervasive and intense specular hematite replacement, that locally evolve to pure specular hematite replacement zones, occurred in the dolomitisation zones that surround the veins.

15.5.5 Mg-Fe (LT; chlorite)

Mg-Fe (LT) alteration is one of the extensively mineralized alteration facies (Delhi, Tache Lk.) of the Sagar system. This alteration occurs as pervasive and extensive alteration fronts to localized replacement zones typically formed in reaction zones between a Fe-rich carbonate alteration and a siliceous rock. In the DDH in the Mistamik area, this reaction process forms chloritic alteration typically enriched in Ni at the contact between siliceous and carbonaceous beds. At Delhi, a reaction zone between the M-Fe (LT) and carbonaceous alteration also appears to be partially related to

copper sulfide precipitation whereas at Tache Lk. showing, the Co-mineralized Mg-Fe (LT) alteration is formed close to and likely at the contact between a partly albitized carbonaceous and an abitized siliceous precursor.
Mg-Fe (LT) alteration also occurred in the basalt at the contact with the polymict breccia zones and in this case, this alteration facies, typically enriched in sulfates, represents an alteration halo of the major fluid circulation pathway represented by the polymict breccia zones.

15.5.6 K-Fe (LT; Kfs-Hem)

This alteration facies primarily occurs as one of the main hydrothermal cements in the polymict breccia zones observed in the DDH in the Lac Mistamik area and as a selective and pervasive replacement formed in siliceous rocks in close association with Mg-Fe dolomitisation. In the polymict breccia zones, K-feldspar is either associated with earthy or earthy+specular hematite. Major increase of the specular hematite content in the polymict breccias can become a good vector towards the potentially more fertile and mineralized zones that can be associated with this alteration facies. When formed in association with Mg-Fe dolomitisation, increasing intensity of this alteration signals the proximity of the K-Fe-enriched zones of the hydrothermal system, which are the most likely host of base metal mineralization. K-Feldspar-hematite alteration was also observed in some of the boulder field mineralized samples where it can be related to a base metal overprint over the already formed uranium mineralization. In this case it may represent a distal manifestation of a fertile IOCG system.

15.6 Dolomitisation

Seven alteration facies were grouped in the dolomitisation family. All the alteration facies grouped in the dolomitisation family are characterized by substantial enrichment in either Mg or Ca and the formation of carbonates (dolomite or calcite) or talc. A subtype of dolomitisation that is not extensively described in this note, but may required more work, is the dolomitisation zone that shares some attributes (low Fe sphalerite) with Irish-type Zn-Pb deposit formed in carbonaceous sedimentary rocks.

15.6.1 Si-Mg-Ca dolomitisation (White to whitish pink dolomitisation)

This dolomitisation typically has a white to whitish pink color, completely replaced the precursor rocks (left only partially digestedsilificied fragments) and has a high Si content that gives it an elevated hardness, making this silica-rich dolomitisation easily confusable with either sodic alteration or silicification. This alteration facies, according to the observations made in the DDH, is interpreted to be an external dolomitisation halo in the Mistamik zone. It is likely to be found at surface and can signal the laterally or vertically distal parts of the hydrothermal system.

15.6.2 Mg-Mn±K-Fe (White dolomitisation)

This dolomitisation facies is characterized by low Si, but high Mg and Mn content, which discriminates it from the Si-Mg-Ca dolomitisation. It has an impure aspect illustrated by variations in its tints of white and grey, is typically cut by sericite veins, and is generally formed in the proximity of the Fe-enriched dolomitisation facies that are proximal to the most intensely altered zones of the hydrothermal system and the K-Fe (LT) alteration zones, especially when it becomes sulfatye-bearing. The apparition and intensification of this dolomitisation is an indication that the hydrothermal system is going in the right direction to the Fe-rich alteration types.

A subtype of this grayish white and Mn-rich dolomitisation, in the sulfate-bearing alteration zone, is also associated with chalcopyrite formation in the magnetite-altered basalts. . Another sub-type of this dolomitisation may be associated with the low-Fe sphalerite mineralisation with attributes to Irish-type Zn mineralisation (DDH SUS-07-15).

15.6.3 Mg-Mn-Fe-K (Pink dolomitisation)

This alteration forms pervasive pink dolomitisation fronts that are proximal to the major fluid conduits of the hydrothermal system (e.g. polymict breccia zones) and signal the proximity of intense K-Fe (LT) alteration zones, either in the polymict breccia zones or as pervasive replacement in siliceous precursor rocks. It occurs in close association with the Mg-Mn-Fe reddish pink dolomitisation, but has a higher K content and was not observed to formed hydrothermal breccias. It was only locally observed in the DDH.

15.6.4 Mg-Mn-Fe (Reddish pink to red dolomitisation)

This alteration type signals the first important ingress of Fe in the alteration facies of the dolomitisation familly and typically indicates intensification of hydrothermal alteration.. Hydrothermal brecciation, forming monomict crackle breccias after Si-Mg-Ca dolomitised or silicified fragments, typically appears with the apparition of this alteration. Hydrothermal brecciation can be extensive over few meters. With increasing lateral or vertical proximity to intense K-Fe (LT) alteration zones and even mineralization, specular hematite locally crystallizes in this alteration (e.g. incipient hematization of the dolomitisation in the vicinities of the Kish and Tache Lk. showings; localized enrichments of this alteration in Cu and Ni). When formed in the immediate vicinities of K-Fe (LT) alteration, it can also exhibit localized Zn enrichments. The apparition of this dolomitisation facies is thus a very good proximity indicator of major fluid conduit or potentially mineralized alteration facies.

15.6.5 Mg-Fe (Pale green or brown sugar dolomitisation)

Mg-Fe dolomitisation facies are the Fe-rich end-members of the dolomitisation family and typically occur in association with weak to strong K-Fe (LT) alteration developed in adjacent siliceous rocks. This dolomitisation facies is thus interpreted as being coeval with the K-Fe (LT) alteration stage and indicates that the Fe content of the hydrothermal fluid has substantially increased. The color of the dolomitisation, either white and green or brown sugar, is a direct function of the Fe content in the dolomitisation as indicated by XRF measurements. that is composed of disseminated chlorite, hematite, dolomite and potentially Fe-carbonates (ankerite or siderite; remain to be identified). The increasing abundance of brown dolomitisation is indicating increasing Fe content in the dolomitisation and increasing proximity to the Fe-rich zones of the system, which are the most likely to host the base metal mineralization.

15.6.6 Mg (Talc alteration)

This alteration is formed after siliceous rocks occurring into intense dolomitisation zones. Extensive talc formation typically signals the proximity of the Mg-Mn-Fe dolomitisation zones and closer proximity to a major fluid pathway.

15.6.7 Ca (Calcite alteration)

Pure calcite alteration locally occurs close to or is directly associated to base metal mineralization (Delhi Pacific showing). It is rare in the DDH of the Mistamik Lake area, but is abundant in the Delhi Pacific copper showing.

15.7 Ca-Fe (LT; Ep)

Epidote alteration was so far only observed in the basalt where it occurs as localized to pervasive alteration fronts highlighted by the crystallization of epidote in the basalt vesicles or by pervasive epidotization of the basalt matrix. This alteration also cements in situ hydrothermal breccia zones formed in the basalt that can extend over tens of centimeters. It may locallybe associated with localized Cu-mineralization. This alteration systematically overprints K-Fe (HT; Bt-Mag) and Ca-Fe (HT; Amp-Mag) alteration and typically destroys the magnetite formed during those alteration stages. This alteration can be regarded as proximal to the base metal mineralization in the basalt, especially where it forms extensive hydrothermal brecciation and is closely associated with sulfate-bearing alteration.

15.8 Silicification

Si alteration in the Sagar Property either occurs as pervasive silicification zones or as quartz veins. Both alteration facies can be mineralized in base metals.

Where it reaches its peak intensity, intense silicification is distal to the main mineralization zones of the Sagar system and formed a giant silicification zone that longitudinally extends over a kilometer? and laterally over a hundred meters. This silicification zone can be analog to the giant quartz vein systems observed in other IOAA district like the Great Lufillian Arc in Africa (Lobo-Guerrero, 2010) or the Great Bear magmatic zone in Canada (Mumin et al., 2010). Intense silicification also sporadically occurs in the dolomitisation zones where it overprints earlier K-Fe (LT) alteration but where it is almost completely overprinted by the Si-Mg-Ca dolomitisation and cut by the reddish pink dolomitisation. These zones of intense silicification are likely the distal alteration zone of a deeper IOCG system.

In the Eagle Lake zone, silicification, associated with sericitization, appears to be related to the copper-rich mineralization observed in SUS-07-16. This silicification, as it comes with sericite, is different from the pure and distal silicification which is almost exclusively composed of quartz and is closer associated to the K (LT; Ser) alteration facies.

15.8.1 Quartz veins

Mineralized and barren quartz veins are common in the Sagar Property and are generally formed in the vicinity or within some of the main showings of the hydrothermal system. The spatial and temporal relations between these mineralized quartz veins and potential IOCG mineralization remains to be established.

15.9 Sulfate

Sulfate-bearing alteration family comprises alteration facies from the dolomitisation, K-Fe (LT), Ca-Fe (HT) and K-Fe (HT) alteration families that have high S content with visible or invisible sulfate and devoid or very low modal content of sulfides. Sulfate-rich alteration facies are especially intense in DDH SGR-01, SGR-02 and SUS-07-30 in the vicinity and within the polymict breccia zones as well as in extensive deformation zones that may represent major fluid pathways. Pure sulfate veins are commonly formed in intense sulfate alteration zones and have low to high modal content of quartz, specular hematite and/or carbonate.

In the DDH SGR-01 and SGR-02, most of the base metal mineralization zones occur where sulfate alteration is mixed with K-Mg (HT) alteration veins. This mineralization process was also observed in the new copper showing discovered south Mistamik Lake.

The exact nature and the source of sulfur in these sulfate-rich alteration facies remain to be established, but very high chlorine, barium and strontium concentrations in somesulfate-rich alteration indicate a possible evaporitic source for the sulfates. If this hypothesis is verified, the

formation of the sulfate-rich alteration may indicate a regional remobilization of evaporitic sulphur during the build-up of the Sagar hydrothermal system. Channeling of the S-rich fluids in the polymict breccia zones to thebiotite-rich alteration zones (K-Fe HT) can be a process by which substantial IOCG mineralization may have been formed. The observation of large sulfate veins in the basalt down to 410 m in the Ca-Fe (HT)/K-Fe (HT)-altered zones indicate that the S-rich fluid percolated in the deeper part of the hydrothermal system to reached the magnetite-bearing Ca-Fe (HT) and K-Fe (HT) alteration zones. This mixing process is likely to have occurred in the most permeable zones of the hydrothermal systems where extensive tectono-hydrothermal brecciation has occurred.

In the Red Lake and Bannock zones, the interaction of this sulfate- and carbonate-rich fluid, that may also have high K and Fe content, may explain the observed and presumed hydrothermal graphite alteration enriched in K and Fe. . K- and Fe-rich graphitic alteration, superimposed over an earlier and pervasive albitization, may have been formed by reduction of C in the fluid. Coeval reduction of S may explain the high sulfide modal content of the graphitic alteration zones of the Sagar property and highlight the potential of these systems to host base metal mineralization that may reach high tonnage if an adequate trap is combined with important thickning of the reducing sedimentary unit (e.g. fold hinge, fault stacking).

15.10 Relative timing of formation of the hydrothermal alteration facies in the Sagar property

Field observations and thin section descriptions indicate that pervasive albitization is most likely the earliest hydrothermal alteration formed in the Sagar property (Fig. 15.10-1). Sodic alteration is then demonstably overprinted by Ca-Fe (HT) and K-Fe (HT) alteration in the Lac Mistamik area. Mixing reactions between K-Fe (HT) and sulfate-bearing alteration in the Lac Mistamik area indicate that some of the sulfate-rich alteration are contemporaneous with K-Fe (HT) alteration. LT Ca-Fe alteration overprints both the Ca-Fe (HT) and K-Fe (HT) alteration zones and destroyed the magnetite. LT K-Fe alteration, locally overprinting actinolite and biotite formed respectively at the Ca-Fe (HT) and K-Fe (HT) alteration stages, is probably occuring syn- to post- Ca-Fe (HT) and K-Fe (HT) alteration stages. The K-Fe (LT) alteration stage is also associated with the reapparition of albite, but accompanied by carbonates, chlorite and hematite, differentiating this sodium-rich K-Fe (LT) alteration from the early sodic alteration.

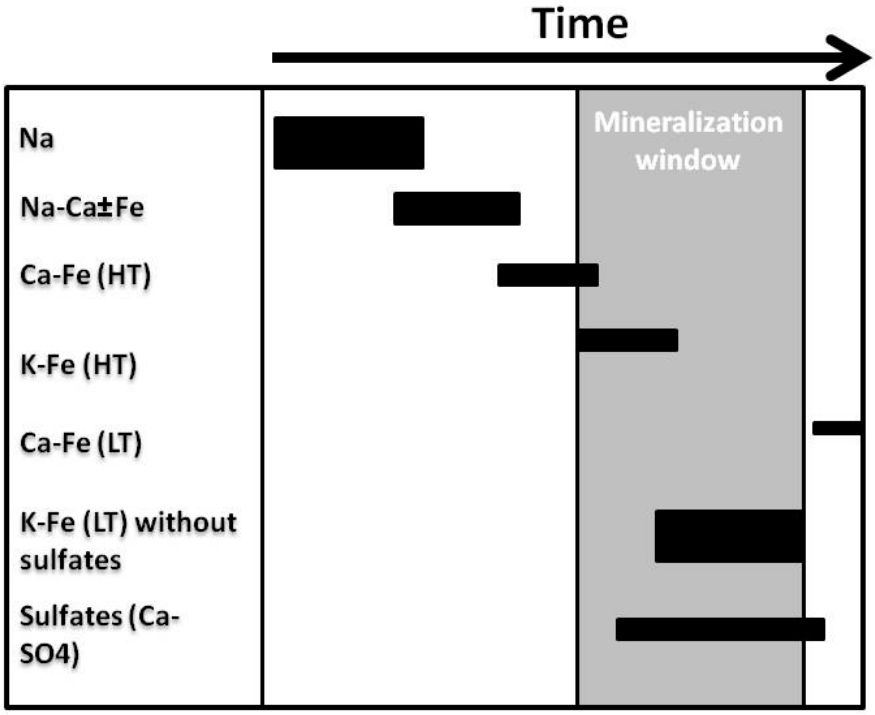

Figure 15.10-1 Preliminary paragenetic relationships between the some of the alteration facies observed at the Sagar Property

16. Drilling

No drilling was conducted during the course of the 2013 exploration program.

17. Adjacent Properties

Géologie C.Q. Inc. holds some parts of the ground to the immediate south of Energizer's Sagar Property. The author has not found any results for work performed by Géologie C.Q. Inc. since they acquired the property in 2006. To the Northwest 7987200 Canada inc. holds a claim, but no work wa reported by the company. Setterfield *et al.* (2006) report the Bacon-Ronsin horizon which is located 3 kilometres southeast of the Sagar Property in the claims of Géologie C.Q. Inc. contains a non-43-101 compliant mineral inventory of 18Mt at 0.5% Cu.

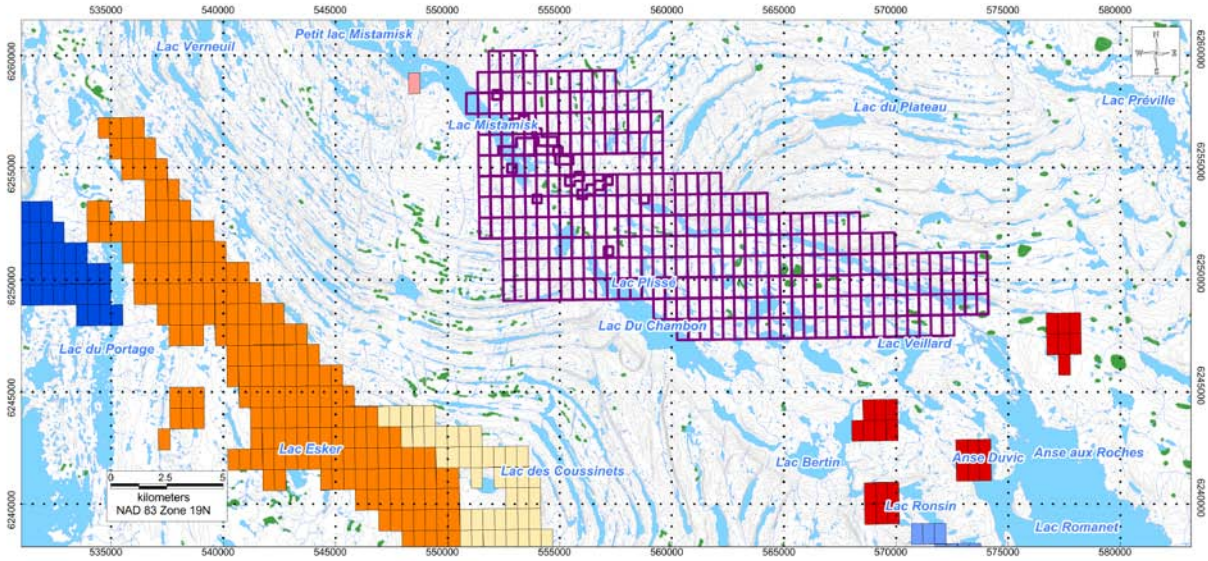

Figure 17.1-1 Properties adjacent to the Sagar Property

18. Mineral Processing and Metallurgical Testing

This item does not apply to the Sagar Property at the present time.

19. Mineral Resource and Mineral Reserve Estimates

This item does not apply to the Sagar Property at the present time.

20. Other Relevant Data and Information

This item does not apply to the Sagar Property at the present time.

21. Interpretation and Conclusions

Anomalous geochemistry (i.e. elevated Au, U, and Cu) identified during historic exploration programs was found to be structurally controlled, with mineralization restricted to small veinlets and breccia zones. Previous workers postulated that this mineralization was attributable to various mineralizing processes, including an IOCG-type of system. Although hypothesized the idea of a mineralized IOCG system was never rigorously tested until Energizer's work in the summer of 2013.

Geochemical analsyses of samples collected during the course of the 2013 exploration program indicate that the IOCG metals copper and cobalt, as well as REE locally, are found in highly anomalous concentrations along the boundaries of the Romanet Horst on the Property. Previous work identified anomalous gold, molybdenum and uranium in similar locations (i.e. along the horst boundaries).

Thin section analyses of 54 samples collected from 'representative' lithotypes found on the Property identified minerals consistent with an IOCG alteration assemblage. Specifically, the alteration minerals albite, calcite, dolomite, quartz, hematite, biotite, actinolite and epidote were identified.

The alteration facies observed over the Sagar Property, comprising Na, magnetite-bearing Ca-Fe (HT) and K-Fe (HT) and specular hematite-bearing K-Fe (LT), indicate that the hydrothermal system contained in the Sagar Property has all the alteration facies expected in an IOAA system that may contain an important IOCG deposit (Williams et al., 2005; Corriveau et al., 2010). The characteristics of the hydrothermal system located in the Sagar Property include:

1. Extensive mantle and crustal melting related to the formation of the large igneous mafic province located on both sides of the horst and high to extreme paleogeothermal gradients that likely have resulted in major hydrothermal fluid convection cells and provided additional sulfur for deposit formation;
2. The presence of crustal scale structures, represented by the two bounding faults of the Romanet horst and the large E-W fault cutting the property in its center;
3. The the likelihood that a large evaporitic sequence was formed in the pre-IOCG basin;
4. The inferred switch from a compressional regime to a transtensional tectonic regime in the Romanet Horst;
5. The preservation of the shallow sections of the hydrothermal system as evidenced by the abundant low temperature hydrothermal alteration facies in the Sagar Property;
6. The presence of large-scale fluid conduits represented by the polymict breccia zones that could have channeled the sulfate-rich fluids to mixing zones with higher temperature and copper-bearing fluids; and
7. The presence of hydrothermal alteration facies containing combination of hematite, chlorite, sericite, carbonate, pyrite, chalcopyrite, P-bearing minerals and likely barite

The overall alteration package, the presence of major crustal-scale structures, the switch from compression to transpression and the abundance of low temperature alteration facies in teh SAGAR property answers most of the criteria stated by Skirrow (2010) for the recognition of geological environments likely to host polymetallic hematite-group or magnetite-group IOCG deposits according to the classification of Williams (2010).

The elements of typical ICOG districts that remain to be found in the Sagar system are the source of uranium and the location of the granitic magmatism. The presence of granite-sourced magmatic-hydrothermal fluid is partially evidenced by thorium-rich uranium mineralization in the Kish and Eagle showings, localized REE enrichments in the hydrothermal system and fluorine enrichment in the mineralized zones of the Taché showings. The uranium may have been partially sourced from the sedimentary rocks.

The following stages to fully characterize the hydrothermal alteration of the Sagar property include the completion of the light element XRF database for each alteration types, the characterization of the petrography of the main alteration facies and the treatment of whole-rock analyzes database that will be constructed as a result of this preliminary study.

22. Recommendations

Exploration efforts should be focused on the discovery of potentially economic IOCG mineralization spatially associated with the boundaries of the Romanet Horst. This work should be conducted in a step-wise progression as follows:

- A robust geochemical analysis of all historical geochemical data should be conducted over the property with the prime focus of identifying geochemical vectors toward prospective IOCG targets;
- Additional examination of existing drill holes should be completed to properly identify the alteration facies in poorly outcropping areas and to confirm cross-cutting relationships. This will help upgrading the distribution of the alteration facies at the property-scale and to better define exploration targets;
- A transient AMT (TAMT) tipper Internal Field Gradient (IFG) ground geophysical survey should be conducted over target areas identified by the geochemical vectoring;
- A 3D compilation of all geophysical work completed over the Property should be performed over prospective target areas identified by the geochemical vectoring and the tipper/IFG ground geophysics in order to identify drill targets;
- Targets identified by the combination of geological work and geophysical compilation work should be drill tested with a diamond drill capable of depths to 500 metres.

A cost estimate for this proposed exploration work is presented in Table 22-1. The total recommended budget is on order of $8,665,000.

Table 22-1: Budget

Item	Proposed budget
Geochemical Vectoring	$35,000.00
Geophysics-DC-IP	$200,000.00
Geophysics mobilization-Charter's	$11,000.00
Geophyscial DeMobilization-Charter's	$11,000.00
Geophysics-Empulse	$225,000.00
Geophysics mobilization-Charter's	$11,000.00
Geophyscial DeMobilization-Charter's	$11,000.00
Helicopter Mob/De-Mobe	$16,400.00
Helicopter in Camp	$307,500.00
Camp support staff (3 at $500/day)	$180,000.00
Professional staff (4 at $750/day)	$90,000.00
Personnel mobilization	$24,000.00
Equipment mobilization	$325,000.00
Weekly camp support flights	$60,000.00
Drilling (10000m)	$6,000,000.00
Fuel	$150,000.00
Room & board	$15,000.00
Equipment rentals	$35,000.00

Disposable supplies	$30,000.00
Geochemical analyses	$60,000.00
Report writing	$40,000.00
Computer drafting	$20,000.00
Reproductions	$5,000.00
Telecommunications	$15,000.00
Subtotal	**$7,876,900.00**
Contingency (10%)	$787,690.00
Total	**$8,664,590.00**

23. References

23.1 References both cited and reviewed

Archer (current, undated): The Sagar Property, summary report prepared for Virginia Mines Inc., 18 p and 2 maps.

Ashwal, L. D., Wooden, J. L. and Emslie, R. F. (1986): Sr, Nd and Pb isotopes in Proterozoic intrusives astride the Grenville Front in Labrador: Implications for crustal contamination and basement mapping; *Geochimica et Cosmochimica Acta*, v. 50, Issue 12, pp.2571-2585.

Baragar, W.R.A. (1960): Petrology of basaltic rocks in part of the Labrador Trough; *Bull. Geol. Soc. America*, v. 71, pp.1598-1644.

Barton, M.D. and Johnson, D.A. (2004): Footprints of Fe-oxide (-Cu-Au) systems. SEG 2004: Predictive Mineral Discovery Under Cover. Centre for Global Metallogeny, Spec. Pub. 33, The University of Western Australia, pp 112-116.

Béland, R. (1976): The Eagle Permit Area (P598), Labrador Trough, Mistamisk Lake area, Geology of Copper and Uranium Sources.

Blake D.H., Etheridge M.A., Page R.W., Stewart A.J., Williams P.R., Wyborn L.A.I. (1990): Mt Isa Inlier - regional geology and mineralization; *in* Hughes F.E. (Ed); *Geology of the Mineral Deposits of Australia and Papua New Guinea*; The Aus.I.M.M. Melbourne, pp 915-925.

Butler, H.R. and Scherba, C.S. (2006)): Technical (geological) report on the Sagar Property: Yukon Resources Corp. Internal Report, 58p.

Charbonneau, R. (1996a): Traçage des blocs minéralisés au projet Sagar III: revue de l'étude du Quaternaire et offre de service; Mines d'Or Virginia Inc.

Charbonneau, R. (1996b): Glacial dispersal of U-Au-bearing boulders at the Sagar property, Labrador Trough, Québec; Virginia Gold Mines Inc.

Charbonneau, R. (1997): Tracing of U-Au mineralization at the Sagar property; Virginia Gold Mines Inc.

Chevé, S.R. (1985): Les indices minéralizés du Lac Romanet, Fosse du Labrador; Ministère de l'Énergie et des Ressources, Québec; ET83-13.

Clark, T. (1986): Géologie et minéralisations de la region du lac Mistamisk et de la rivière Romanet; MERQ, ET 83-22.

Clark, T. (1994): Géologie et gîtes de l'Orogène du Nouveau-Québec et de son arrière pays; *in*, *Géologie du Québec*; Ministère des Ressources naturelles, Québec; MM 94-01, pp. 47-65.

Clark, T. (2005): Les gîtes minéraux et l'évolution de la Fosse du Labrador: bien plus que du fer; Power-point presentation at *CIM Conference 2005-2006*; presentation on behalf of Ministère des Ressources naturelles et de la Faune, Québec.

Colombo, F. (2013) : Petrographic report on 54 samples from Sagar Property; Vancouver Petrographics Ltd., 133p.

Corriveau, L. (2005): Iron oxides copper-gold (±Ag ±Nb ±P ±REE ±U) deposits: a Canadian perspective; *Geological Survey of Canada*, open file report.

Corriveau, L. (2007): Iron oxide copper-gold deposits: a Canadian perspective; *in* Goodfellow, W.D., ed., Mineral Deposits of Canada: A Synthesis of Major Deposit-Types, District Metallogeny, the Evolution of Geological Provinces, and Exploration Methods: Geological Association of Canada, Mineral Deposits Division, Special Publication No. 5, p. 307-328.

Dimroth, E. (1964): Geology of the Romanet Lake Area, Quebec; Dept. Natural Resources, Preliminary Report 523.

Dimroth, E. (1969a): Geology of the Castignon Lake Area, Quebec; Dept. Natural Resources, Preliminary Report 571.

Dimroth, E. (1969b): Evolution of the Labrador Geosyncline; *Bull. Geol. Soc. America*, v.81, pp.2717-2741.

Dimroth, E. (1970): Cartes geologiques du Lac Romanet et du Lac Cramolet (Fosse du Labrador); 1 map at 1 inch to 1 mile.

Dimroth, E. (1978): Région de la Fosse du Labrador; MERQ, Quebec, RG-193.

Dressler, B. (1979): Region de la Fosse du Labrador – Labrador Trough Area; Ministère des Richesses Naturelles, Rapport Geologique, No. 195.

Fournier, D.A. (1988): Mistamisk Lake, permit 732, 1988 year end report: La Fosse Platinum Group Inc. report.

Gagnon, M. (1998): Rapport des forages 1998 sur la propriété Sagar, Fosse du Labrador, Québec; Corporation Minière Inmet and copy to Mines d'Or Virginia Inc.

Gariépy, L. (1994): Rapport sur la campagne de forage en 1994, propriété Sagar 3, Fosse du Labrador; Hemlo Gold Inc.

Gates, B.I. (1991): Sudbury Mineral Occurrence Study; Ontario Geological Survey Open File Report 5771.

Goulet, N. (2001): New similarities in the tectonic style of folding and fracturing between the Cape Smith and Labrador Trough fold belts, northern Quebec; in *Abstracts*, Tectonic Integration of Circum-Superior Orogens; *GAC-MAC Conference*, St. John's, 2001.

Groves, D.L., Bierlein, F.P., Meinert, L.D., and Hitzman, M.W. (2010) Iron oxide copper-gold (IOCG) deposits through Earth history: Implications for origin, lithospheric setting, and distinction from other epigenetic iron oxide deposits, Economic Geology, v. 105, pp. 641-654.

Hamelin, L.E. (1979): *Canadian Nordicity: It's Your North, Too*; Harvest House, Montreal.

Hitzman, M.W., Oreskes, N., and Einaudi, M.T. (1992) Geological characteristics and tectonic setting of Proterozoic iron oxide (Cu-U-Au-LREE) deposits, Precambrian Research, v. 58, pp. 241-287.

Hubert, J. (1994): Traitement de données et modélisation de données gravimétriques, projet Sagar; Corporation Minière Inmet and Denison Mines Ltd. – profile interpretations across the Romanet Horst and maps.

Jackson, R.G. (2006): Water geochemical anomalies on the Sagar property, NW Quebec; Yukon Resources Corp. Internal Report, 40p.

James, D.T., Connelly, J.N., Wasteneys, H.A. and Kilfoil, H.A. (1996): Paleoproterozoic litho-tectonic division of the southeastern Churchill Province, western Labrador; *Canadian Journal of Earth Sciences*, v.33, pp. 216-230.

Jefferson, C.W., Thomas, D.J., Gandhi, S.S., Ramaekers, P., Delaney, G, Brisbin, D, Cutts, C., Quirt, D., Portella, P., and Olson, R.A. (2007): Unconformity-associated uranium Deposits on the Athabasca Basin, Saskatchewan and Alberta; *in Mineral Deposits of Canada*: A Synthesis of Major Deposit-types, District Metallogeny, the Evolution of Geological Provinces, and Exploration Methods, published jointly by the *Geological Survey of Canada* and the Mineral Deposits Division of the *Geological Association of Canada*.

Kearey, P. (1976): A regional structural model of the Labrador Trough, northern Quebec, from gravity studies, and its relevance to continent collision in the Precambrian; *Earth and Planetary Science Letters*, v. 28, Issue 3, pp. 371-378.

Kish L, and Cuney M. (1981): Uraninite-albite veins from the Mistamisk Valley of the Labrador Trough, Québec. *Mineralogical Magazine*, v. 44, pp. 471-483.

Kish *et al*. (1978, 1979): Geochemistry and Radioactivity in the Labrador Trough – Preliminary reports on the 1976 and 1977-1978 projects, Ministère des Richesses Naturelles, DPV-567 (1978), DPV-666 (1979).

Kuznetsov, A.B., Melezhik, V.A., Gorokhov, I.M., Melnikov, N.N. and Fallick, A.E. (2003): Sr isotope composition in paleoproterozoic carbonates extremely enriched in ^{13}C: Kaniapiskau supergroup, the Labrador Trough of the Canadian Shield; *Stratigraphy and Geological Correlation*, v.11. No.3, pp. 209-219.

Lawyer, J.I. (2006): Sagar Property-Target 5: Field Assessment and Recommendations; Yukon Resources Corp. Internal Report, 23p.

Lulin, J.M. (2002): The Sagar Project (Au, U, Cu): Strategic review; Mines d'Or Virginia Inc. Internal Report, 49p.

Masse, J.P. (1974): L'Uranium au Québec; Ministère des Richesses Naturelles, Services des Gites Mineraux, unpublished report.

McDonough, W.F. and Sun, S.S. (1995): The composition of the Earth; *Chemical Geology*, v.120 No.3-4, pp. 223-253.

McMillan, R.H. (1996): "Classical" U Veins; in *Selected British Columbia Mineral Deposit Profiles, Volume 2 – Metallic Deposits, Lefebure, D.V. and Hoy, T. Editors, British Columbia Ministry of Employment and Investment, Open File 1996-12,* pp. 93-96.

McNeil, R. (1990): Drill logs Mistamisk Lake (PE – 732); La Fosse Platinum Group Inc.

McNeill, P. (2006): Sagar Project, QC; Yukon Resources Corp. Internal Report, 15p.

Miller, J.K. (1984): Model for clastic indicator trains in till; in *Prospecting in Areas of Glaciated Terrain*: Institution of Mining and Metallurgy, London, pp. 69-77.

Naldrett, A.J. (1999): World-class Ni-Cu-PGE deposits: key factors in their genesis; *Mineralium Deposita*, v. 34, pp. 227-240.

Neal, H.E. (2000): Iron Deposits of the Labrador Trough; *Exploration and Mining Geology*, v.2, pp.113-121.

Poisson, P. (1992a): Introduction Report on Sagar III project, Exploration Permit 904, Labrador Trough, Nouveau Québec; Mines d'Or Virginia Inc.

Poisson, P. (1992b): Propriété Sagar III; Permis d'exploration 904, Fosse du Labrador, Nouveau-Québec; Mines d'Or Virginia Inc.

Poisson, P. (1994a): Rapport sur la campagne de forage de l'hiver 1993, propriété Sagar III; Mines d'Or Virginia Inc.

Poisson, P. (1994b): Introductory Report on Exploration Permit 936, Romanet-Mistamisk Lakes Area, Labrador Trough; Mines d'Or Virginia Inc.

Porter TM (2010) Current understanding of iron oxide associated-alkali altered mineralised systems: Part 1 - An overview. In: Porter TM (ed) Hydrothermal iron oxide copper-gold and related deposits: A global perspective, volume 3, Advances in the understanding of IOCG deposits. PGC Publishing, Adelaide, pp 5–32.

Prikhodko, N., Venter, N. and Mokubung, N. (2013): Report on a helicopter-borne Versatile Time Domain Electromagnetic (VTEMplus) Horizontal Magnetic Gradiometer and Gamma-Ray Spectroscopy geophysical survey; Geotech Ltd., 68p.

Reeve, J.S., Cross, K.C., Smith, R.N., and Oreskes, N., (1990): The Olympic Dam copper-uranium-gold-silver deposit, South Australia, *in* Hughes, F., ed., *Geology of mineral deposits of Australia and Papua New Guinea*: Australian Institute of Mining and Metallurgy, Monograph 14, pp. 1009-1035.

Ruzicka, V. and Littlejohn, A.L. (1981): Studies on uranium in Canada 1980; in Current Research, Part A, *GSC Paper 81 -1A*, pp.133-144.

St-Onge, M.R., Scott, D.J. and Lucas, S.B. (2000): Early partitioning of Quebec: microcontinent formation in the Paleoproteozoic; *Geology*, v. 28, pp. 323-326.

Scherba, C.S. (2008): Exploration report on the Sagar Property; Uranium Star Corp. NI 43-101 Technical Report, 139p.

Schmid R., Fettes D., Harte B., Davis E., Desmons J. (2007). How to name a metamorphic rock. Recommendations by the IUGS Subcommission on the Systematics of Metamorphic Rocks: Web version 01/02/07 at www.bgs.ac.uk/scmr/home.html

Setterfield, T. and Tykajlo, R. (2000): Exploration for Au, Cu and U in the Sagar Property and Romanet Horst, Labrador Trough, Quebec, Description of an exploration opportunity (summary report).

Setterfield, T., Chartrand, F., and Campbell, J. (2006): Report on work completed by GeoVector Management between June and October, 2006; Yukon Resources Corp. Internal Report, 76p.

Skirrow, R.G. (2010) "Hematite-group" IOCG±U ore systems: tectonic settings, hydrothermal characteristics and Cu-Au and U mineralizing processes, *in* Corriveau, L., and Mumin, A.H.,

eds., Exploring for iron oxide copper-gold deposits: Canada and global analogues, Geological Association of Canada, Short Course Notes 20, pp. 37-56.

Thomas, R.D. (1993): Report on Quaternary geological investigations, Sagar III property, Lac Mistamisk Area; Hemlo Gold Inc.

Thompson, A.J.B. and Thompson ,J.F.H. (editors) (1996): Atlas of Alteration: a Field and Petrographic Guide to Hydrothermal Alteration Minerals. GAC Mineral Deposits Division, 119p.

Tremblay, N. and Gagnon, M. (1998): Propriété Sagar, rapport des forages, 1997; Corporation Minière Inmet.

Wardle, R.J., James, B., Scott, D.J., and Hall, J. (2002): The Southeastern Churchill Province: synthesis of a Paleoproterozoic transpressional orogen; *Canadian Journal of Earth Sciences*, v. 39, pp. 639-663.

Whitney DL, Evans BW (2010): Abbreviations for rock-forming minerals. Am Miner 95: pp. 185–187.

Skirrow, R.G. (2010) "Hematite-group" IOCG±U ore systems: tectonic settings, hydrothermal characteristics and Cu-Au and U mineralizing processes, *in* Corriveau, L., and Mumin, A.H., eds., Exploring for iron oxide copper-gold deposits: Canada and global analogues, Geological Association of Canada, Short Course Notes 20, pp. 37-56.

Zharikov VA, Pertsev FN, Rusinov VL, Callegari E, Fettes DJ (2007) 9. Metasomatism and metasomatic rocks. Recommendations by the IUGS Subcommission on the Systematics of Metamorphic Rocks: Web version 01.02.07 at www.bgs.ac.uk/scmr/home.html

23.2 Assessment Data and Reports filed in Québec City

GM 13537 (Anacon Lead Mines Ltd., 1962)
GM 13575 (Hogg, G.M., 4 drill holes, 1962)
GM 13575 (Hogg. G.M. further drilling, 1962)
GM 13577 (Grant, J., geology of Romanet west group, 1962)
GM 13578 (Armstrong, T., geological report west Romanet claim group, 1962)
GM 13579 (Russell, R.E., preliminary report, 1963)
GM 13580 (Hogg G.M., geophysical surveys, 1962)
GM 13649 (Polson, C., diamond drill logs, south of Lac Bertin, 1962)
GM 14051, 14052 (Baldwin, A.B., Satellite Metal Mines Ltd., reports 1963)
GM 15546 (Hogg, G.M., geochemical sampling reports, 1964)
GM 17310 (Love, H.D., 17 drill logs, 1965)
GM 17523 (Love, H.D., geochemical survey, 1965)

GM 32511 (Halladay, L.B., geophysics and geology for Dome Exploration Canada Ltd., 1976)
GM 33219 (Geisterfer, P.K., exploration report for Conwest Exploration Co. Ltd., 1978) GM 33344 (Wagner, W.R., geology and geochemistry for Conwest Exploration Co. Ltd., 1978)
GM 34788 (Smith, M., field program lake sampling, airborne spectrometer for Quebec Ungava Mining Co. Ltd., 1978)
GM 34921, 34922 (field program for Conwest Exploration Co. Ltd., 1978)
GM 36256 (field program, 1979)
GM 36328, 37130, 38517 (Projet 306, Cambrien campagne, 1979)
GM 41409 (Saarberg Interplan, 1983).

Date and Signature Page

I, Jean-Philippe Desrochers, Ph.D., Geo. #1060 (OGQ), do hereby certify that:

1. I am a consulting geologist residing at 176-B chemin Tour du Lac, Lac-Beauport, Québec.
2. I graduated with a B.Sc. in Geology from University of Montreal, Quebec in 1988.
3. I obtained my Ph.D. in geology from University of Montreal, Quebec in 1998.
4. I am a member of the Ordre des Géologues du Quebec (#1060).
5. I have worked as a geologist since 1994 across Canada and in South America for numerous exploration companies. My relevant experience for the purpose of the report is:
   - VP Exploration – Eagle Hill Exploration Corp, QC, 2013 to current
   - Chief Geologist – Eagle Hill Exploration Corp, QC, 2010 to 2013
   - VP Exploration – Murgor Resources Inc., ON, MB, SK, 2005 to 2010
   - Principal Geologist – SRK Consulting, ON, 2005
   - Senior Geologist – Aur Resources Chile Ltda, 1999 to 2004
   - Project Geologist – Aur Resources Inc., Qc, 1994 to 1998
6. I have read the definition of "qualified person" set out in National Instrument 43-101 ("NI 43-101") and certify that by reason of my education, affiliation with a professional association (as defined by NI 43-101) and past relevant work experience, I fulfill the requirements to be a "qualified person" for the purposes of NI 43-101.
7. I am not aware of any material fact or material change with respect to the subject matter of the Technical Report that is not reflected in the Technical Report, the omission to disclose which makes the Technical Report misleading.
8. I am classified as an 'insider' of the issuer (Energizer Resources Inc.) applying all of the tests in section 1.5 of National Instrument 43-101, but there were no circumstances that were or could be seen to interfere with my judgement in preparing the Technical Report.
9. I have read National Instrument 43-101 and the (updated) Form 43-101F1, and the Technical Report has been prepared in compliance with that instrument and that form.
10. I consent to the filing of the Technical Report with any stock exchange and other regulatory authority and any publication by them for regulatory purposes, including electronic publication in the public company files on their websites accessible by the public, of the Technical Report.

DATED at Lac-Beauport, Québec, this 5th day of March, 2014.

Respectfully submitted,

GÉOLOGUE / GEOLOGIST * JEAN-PHILIPPE DESROCHERS * QUÉBEC

Jean-Philippe Desrochers, Ph.D., Geo (#1060)

Additional Requirements for Technical Reports on Development Properties and Production

This Item does not apply to the Sagar Property at this time. The property has no known reserves and is exploratory in nature.

Appendix A

Geological map of the Sagar property from the MRNF report ET 83 - 22

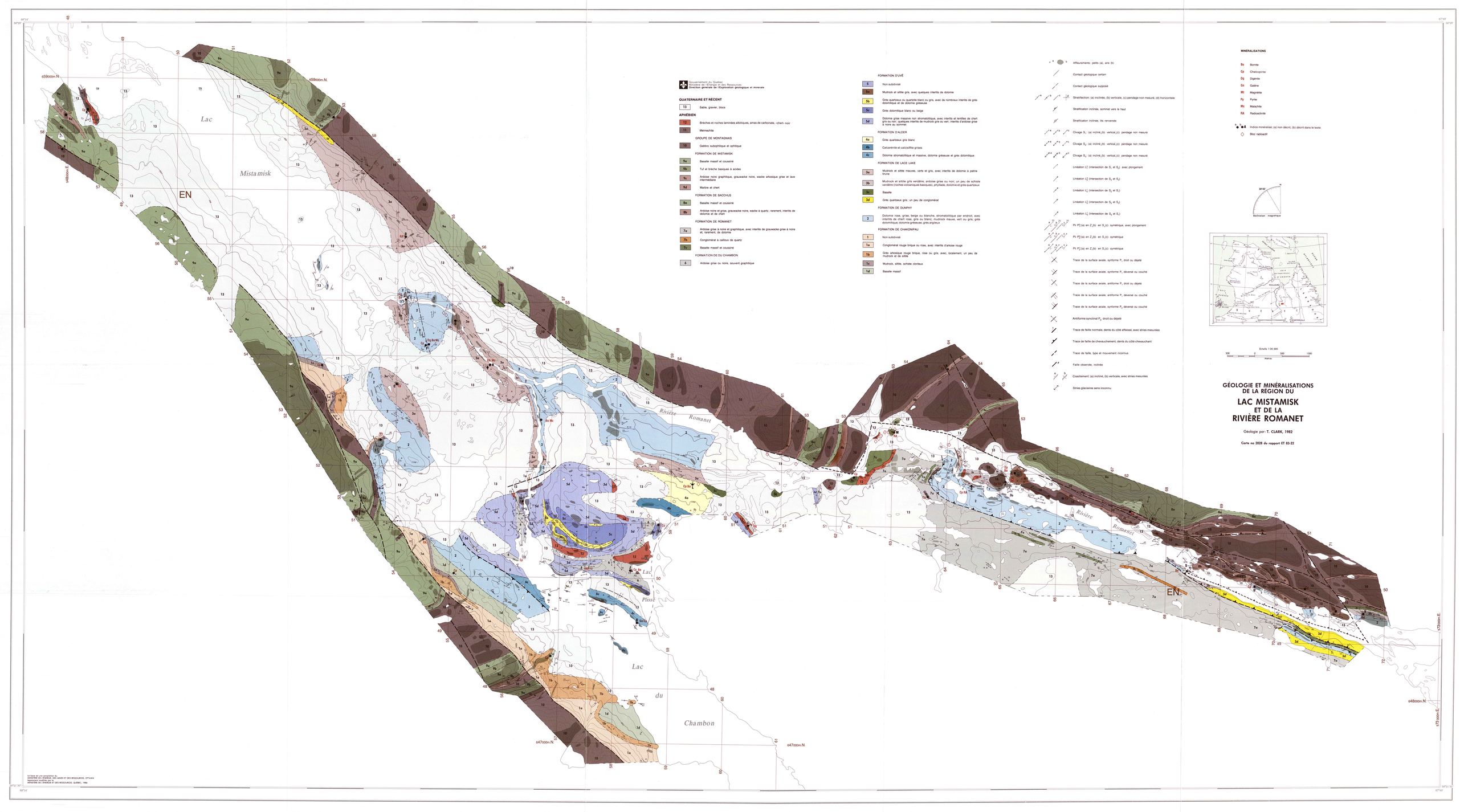

Gouvernement du Québec
Ministère de l'Énergie et des Ressources
Direction générale de l'Exploration géologique et minérale

QUATERNAIRE ET RÉCENT

13 Sable, gravier, blocs

APHÉBIEN

12 Brèches et roches laminées albitiques, amas de carbonate, «chert» noir

11 Méimechite

GROUPE DE MONTAGNAIS

10 Gabbro subophitique et ophitique

FORMATION DE MISTAMISK

9a Basalte massif et coussiné

9b Tuf et brèche basiques à acides

9c Ardoise noire graphitique, grauwacke noire, wacke arkosique grise et lave intermédiaire

9d Marbre et chert

FORMATION DE BACCHUS

8a Basalte massif et coussiné

8b Ardoise noire et grise, grauwacke noire, wacke à quartz ; rarement, interlits de dolomie et de chert

FORMATION DE ROMANET

7a Ardoise grise à noire et graphitique, avec interlits de grauwacke grise à noire et, rarement, de dolomie

7b Conglomérat à cailloux de quartz

7c Basalte massif et coussiné

FORMATION DE DU CHAMBON

6 Ardoise grise ou noire, souvent graphitique

FORMATION D'UVÉ

5 Non subdivisé

5a Mudrock et siltite gris, avec quelques interlits de dolomie

5b Grès quartzeux ou quartzite blanc ou gris, avec de nombreux interlits de grès dolomitique et de dolomie gréseuse

5c Grès dolomitique blanc ou beige

5d Dolomie grise massive non stromatolitique, avec interlits et lentilles de chert gris ou noir; quelques interlits de mudrock gris ou vert; interlits d'ardoise grise à noire au sommet

FORMATION D'ALDER

4a Grès quartzeux gris blanc

4b Calcarénite et calcisiltite grises

4c Dolomie stromatolitique et massive, dolomie gréseuse et grès dolomitique

FORMATION DE LACE LAKE

3a Mudrock et siltite mauves, verts et gris, avec interlits de dolomie à patine brune

3b Mudrock et siltite gris verdâtre; ardoise grise ou noir; un peu de schiste verdâtre (roches volcaniques basiques), phyllade, dolomie et grès quartzeux

3c Basalte

3d Grès quartzeux gris ; un peu de conglomérat

FORMATION DE DUNPHY

2 Dolomie rose, grise, beige ou blanche, stromatolitique par endroit, avec interlits de chert rose, gris ou blanc; mudrock mauve, vert ou gris; grès dolomitique, dolomie gréseuse, grès argileux

FORMATION DE CHACONPAU

1 Non subdivisé

1a Conglomérat rouge brique ou rose, avec interlits d'arkose rouge

1b Grès arkosique rouge brique, rose ou gris, avec, localement, un peu de mudrock et de siltite

1c Mudrock, siltite, schiste clorteux

1d Basalte massif

a Affleurements : petits (a), aire (b)

Contact géologique certain

Contact géologique supposé

Stratification: (a) inclinée, (b) verticale, (c) pendage non mesuré, (d) horizontale

Stratification inclinée, sommet vers le haut

Stratification inclinée, tête renversée

Clivage S_1 : (a) incliné,(b) vertical,(c) pendage non mesuré

Clivage S_2 : (a) incliné,(b) vertical,(c) pendage non mesuré

Clivage S_3 : (a) incliné,(b) vertical,(c) pendage non mesuré

Linéation L_1^2 (intersection de S_1 et S_2) avec plongement

Linéation L_2^3 (intersection de S_2 et S_3)

Linéation L_1^2 (intersection de S_1 et S_2)

Linéation L_2^3 (intersection de S_2 et S_3)

Linéation L_1^3 (intersection de S_1 et S_3)

Pli P_2[(a) en Z_2,(b) en S_2,(c) symétrique, avec plongement

Pli P_2[(a) en Z_2,(b) en S_2,(c) symétrique

Pli P_3[(a) en Z_3,(b) en S_3,(c) symétrique

Trace de la surface axiale, synforme P_1 droit ou déjeté

Trace de la surface axiale, synforme P_1 déversé ou couché

Trace de la surface axiale, antiforme P_1 droit ou déjeté

Trace de la surface axiale, antiforme P_1 déversé ou couché

Trace de la surface axiale, synforme P_2 déversé ou couché

Antiforme synclinal P_2, droit ou déjeté

Trace de faille normale, dents du côté affaissé, avec stries mesurées

Trace de faille de chevauchement, dents du côté chevauchant

Trace de faille, type et mouvement inconnus

Faille observée, inclinée

Cisaillement: (a) incliné, (b) verticale, avec stries mesurées

Stries glaciaires sens inconnu

MINÉRALISATIONS

Bo Bornite

Cp Chalcopyrite

Dg Digénite

Ga Galène

Mt Magnétite

Py Pyrite

Mc Malachite

RA Radioactivité

A Indice minéralisé: (a) non décrit, (b) décrit dans le texte

Bloc radioactif

30°02' Déclinaison magnétique

Échelle 1:20 000

500 0 500 1000

Mètres

GÉOLOGIE ET MINÉRALISATIONS DE LA RÉGION DU LAC MISTAMISK ET DE LA RIVIÈRE ROMANET

Géologie par: T. CLARK, 1982

Carte no 2028 du rapport ET 83-22

La base est une projection de
MINISTÈRE DES MINES ET DES RESSOURCES, OTTAWA
légèrement modifiée par le
MINISTÈRE DE L'ÉNERGIE ET DES RESSOURCES, QUÉBEC, 1984

Appendix B

Analytical Results – Rock Grab + Summarized description
Actlabs Assay and Analytical Procedures

Analyte Symbol	Certificate	UTMX_NAD83	UTMY_NAD83	Sample type	Rock type	Modifier	Alteration1	Alteration2	Li	Na	Mg	Al	K	Ca	Cd	V	Cr	Mn	Fe	Hf	Hg	Ni	Er	Be	Ho	Ag	Cs
Unit Symbol									ppm	%	%	%	%	%	ppm	ppm	ppm	ppm	%	ppm	ppb	ppm	ppm	ppm	ppm	ppm	ppm
Detection Limit									0.5	0.01	0.01	0.01	0.01	0.01	0.1	1	0.5	1	0.01	0.1	10	0.5	0.1	0.1	0.1	0.05	0.05
Analysis Method									TD-MS	TD-MS	TD-MS	TD-MS	TD-MS	TD-MS	TD-MS	TD-MS	TD-MS	TD-MS	TD-MS	TD-MS	TD-MS	TD-MS	TD-MS	TD-MS	TD-MS	TD-MS	TD-MS
1271851	A13-09848	567815	6251400	OTCP	SED	UNKN	Na	SIL	3.9	> 3.00	0.51	5.81	0.03	2.16	18.1	108	109	227	13.8	1.9	3600	89.1	0.8	0.4	0.3	24.9	< 0.05
1271852	A13-09848	567842	6251392	OTCP	SED	UNKN	Na	SIL	2.1	> 3.00	0.5	5.6	0.01	8.06	0.5	58	51.2	1410	7.33	1.6	1320	87.3	3.5	0.4	1.3	2.64	< 0.05
1271853	A13-09848	567896	6251362	OTCP	MAFINT	GAB	K-Fe (LT)		12.5	> 3.00	3.91	8.05	0.05	3.78	< 0.1	247	91.3	701	6.94	1.9	10	44	2.6	0.6	0.9	0.82	0.09
1271854	A13-09848	567773	6251395	OTCP	UNKN	UNKN	Na		1	> 3.00	0.08	9.82	0.06	0.97	< 0.1	41	76.1	32	0.31	0.8	< 10	4.8	3.5	0.9	1.3	0.29	< 0.05
1271855	A13-09848	567957	6251326	OTCP	SED	SILT	Na	DOL	1.4	> 3.00	0.08	5.96	0.05	6.62	0.1	78	85	574	7.29	2.9	200	92	1.9	0.5	0.7	0.36	0.84
1271856	A13-09848	567958	6251334	OTCP	BAS	VOL	Na	SIL	2.6	> 3.00	0.95	7.68	0.04	3.84	< 0.1	344	93.8	240	5.93	3	60	65.6	4.5	0.7	1.6	0.25	0.05
1271857	A13-09848	552697	6253973	OTCP	BAS	VOL	Na	K-Fe (HT)	53.1	> 3.00	2.72	7.97	1.57	1.42	< 0.1	77	57.8	621	11.4	1.7	< 10	53.2	2.8	1.9	1	0.16	1.47
1271858	A13-09848	552466	6253692	OTCP	BAS	VOL	Na	K-Fe (LT)	33.1	> 3.00	4.29	7.34	0.07	5.34	< 0.1	147	234	1050	8.93	0.5	< 10	90.8	2	0.4	0.7	0.08	0.38
1271859	A13-09848	552918	6259215	OTCP	BAS	VOL	SIL	Ca-Fe (LT)	2.6	0.25	3.78	4.92	0.2	11.2	< 0.1	308	433	1390	8.17	1.3	< 10	74.4	1.7	0.6	0.6	0.15	0.16
1271860	A13-09848	559465	6251998	OTCP	UNKN	UNKN	Na	SIL	1.9	> 3.00	0.22	5.4	0.31	0.77	< 0.1	67	252	82	3.05	2.5	< 10	46.9	0.5	0.8	0.2	0.17	0.18
1272001	A13-09848	567802	6251402	OTCP	BAS	VOL	Na	K-Fe (LT)	14.4	> 3.00	3.84	7.76	0.06	3.7	< 0.1	231	77.5	543	3.96	1.8	< 10	42.4	3.8	0.6	1.3	0.18	0.06
1272002	A13-09848	567816	6251398	OTCP	BAS	VOL	Na	K-Fe (LT)	15.8	> 3.00	3.12	7.15	0.18	2.96	0.7	253	137	660	10.9	1.7	70	126	2.4	0.5	0.8	1.7	0.92
1272003	A13-09848	567826	6251403	OTCP	BAS	VOL	Na	K-Fe (LT)	20.3	> 3.00	4.25	7.86	0.04	2.63	1.9	256	109	732	10.7	2	410	41.3	1.6	0.6	0.6	8.8	0.08
1272004	A13-09848	567862	6251402	OTCP	SED	UNKN	Na	K-Fe (LT)	1	> 3.00	0.08	9.15	0.04	2.61	< 0.1	56	60.5	190	0.58	2.4	110	9	1	0.8	0.4	1.16	< 0.05
1272005	A13-09848	567860	6251383	OTCP	BAS	VOL	Na	K-Fe (LT)	5.2	> 3.00	0.39	8.99	0.03	1.7	< 0.1	110	119	169	1.69	3.9	200	22.3	2.9	0.7	1.1	0.69	< 0.05
1272006	A13-09848	567825	6251206	OTCP	BAS	VOL	Na	DOL	1.5	> 3.00	0.19	7.22	0.03	5	0.4	84	121	453	5.16	2.4	180	85	2	0.4	0.7	0.76	0.07
1272007	A13-09848	567980	6251331	OTCP	BAS	VOL	Na	DOL	4.9	> 3.00	1.49	8.44	0.05	1.54	< 0.1	144	137	270	6.22	3.2	420	49.7	0.6	0.7	0.2	1.15	< 0.05
1272008	A13-09848	554262	6256631	OTCP	SED	MUD	Na	K-Fe (LT)	15.6	> 3.00	1.61	> 10.0	3.12	0.12	< 0.1	128	92.8	29	1.61	1.7	< 10	67.7	0.8	2.9	0.3	0.37	0.54
1272009	A13-09848	571300	6249772	OTCP	SED	UNKN	Na		13.8	> 3.00	0.8	8.57	0.95	0.75	0.5	36	161	181	3.03	3	< 10	24.1	1.2	1.1	0.4	8.52	0.63
1272010	A13-09848	571177	6249801	OTCP	BRX	UNKN	Na	K-Fe (LT)	20.1	> 3.00	1.19	5.66	0.71	0.47	0.7	41	184	200	4.64	2.9	< 10	76.9	0.6	0.9	0.2	8.33	0.4
1272011	A13-09848	571174	6249802	OTCP	SED	UNKN	Na	K-Fe (LT)	27.8	> 3.00	1.33	7.16	0.78	0.19	< 0.1	17	205	181	4.25	0.7	< 10	24.7	0.6	0.9	0.2	1.16	0.57
1272012	A13-09848	571174	6249802	OTCP	SED	UNKN	Na	SIL	31.3	2.51	1.46	7.03	1.23	0.09	< 0.1	21	191	200	4.95	0.7	< 10	13.1	0.3	1	0.1	0.56	0.86
1272013	A13-09848	571169	6249803	OTCP	SED	UNKN	Na	SIL	25.4	> 3.00	1.18	9.27	1.7	0.2	< 0.1	41	122	167	3.69	1.1	< 10	21.6	0.7	1.7	0.2	0.64	1.37
1272014	A13-09848	571268	6249775	OTCP	SED	UNKN	K-Fe (LT)	SIL	11.1	2.35	0.4	> 10.0	3.21	0.08	1.1	79	108	47	1.53	1.9	100	4.8	0.9	3.3	0.3	6.47	2.76
1272015	A13-09848	564560	6251994	OTCP	SED	UNKN	K-Fe (LT)	SIL	13.6	0.01	3.09	1.79	< 0.01	3.07	16.3	77	124	823	31	0.3	40	211	0.7	< 0.1	0.3	9.35	0.1
1272016	A13-09848	564560	6251994	OTCP	SED	UNKN	K-Fe (LT)		40.5	< 0.01	6.17	5.37	< 0.01	2.19	0.2	105	130	628	16	0.9	< 10	88.6	0.6	0.4	0.2	1.63	0.08
1272017	A13-09848	555526	6254457	OTCP	SED	DOL	DOL	K-Fe (LT)	2	0.92	10.1	1.13	0.06	18.3	0.1	9	33.9	2840	3.93	1.8	< 10	45.6	3.5	0.3	1.3	0.44	0.08
1272018	A13-09848	555522	6254457	OTCP	VN	UNKN	UNKN		5.3	0.15	0.43	0.54	0.01	1.19	0.2	7	125	177	23.4	< 0.1	2090	> 5000	5.7	0.8	2.4	12.1	0.06
1272019	A13-09848	556447	6251683	OTCP	BRX	UNKN	Na	SIL	1.2	> 3.00	2.37	5.99	0.07	4.85	< 0.1	78	224	667	2.64	1.7	10	78.9	1.1	0.9	0.3	1.03	0.14
1272020	A13-09848	556378	6251635	OTCP	BRX	UNKN	Na	SIL	1.4	> 3.00	1.04	4.69	0.09	1.88	0.1	111	203	375	3.57	3.9	360	60.4	0.5	1.1	0.1	0.52	0.1
1272021	A13-09848	552906	6253949	OTCP	SED	DOL	DOL		5	0.05	9.01	0.24	0.16	14.9	< 0.1	3	151	904	0.51	< 0.1	< 10	8.5	0.3	< 0.1	0.1	0.19	0.15
1272022	A13-09848	552921	6253987	OTCP	SED	DOL	DOL		4.3	0.03	12.9	0.13	0.08	24.3	< 0.1	2	14.1	2100	1.09	< 0.1	< 10	20.4	0.2	< 0.1	< 0.1	0.27	0.13
1272023	A13-09848	552928	6254254	OTCP	MAFINT	GAB	K-Fe (HT)		89.1	1.99	6.49	8.08	3.53	5.21	< 0.1	219	504	1110	9.17	0.7	< 10	184	1.4	0.6	0.5	0.17	7.98
1272024	A13-09848	552914	6254217	OTCP	QtzVein	UNKN	SIL		7.5	0.11	1.08	1.3	0.02	3.43	< 0.1	24	309	454	3.49	< 0.1	< 10	483	0.2	0.1	< 0.1	0.28	0.22
1272025	A13-09848	572402	6249822	OTCP	BAS	VOL	Na	K-Fe (LT)	10.1	> 3.00	1.03	4.89	0.28	0.34	< 0.1	37	257	187	3.37	2.6	< 10	84.6	0.6	0.5	0.2	0.21	0.52
1272026	A13-09848	572109	6249760	BLD	UNKN	UNKN	Na	SIL	14.2	> 3.00	0.77	6.29	0.77	0.73	0.4	48	162	189	2.86	2.9	< 10	57.3	1.5	1.2	0.6	0.81	0.5
1272027	A13-09848	572084	6249699	OTCP	SED	UNKN	Na	K-Fe (LT)	23.3	> 3.00	1.17	7.32	1.61	0.44	< 0.1	60	126	262	3.64	4.1	< 10	45.8	1.2	1.6	0.4	0.51	0.96
1272028	A13-09848	571722	6249771	OTCP	SED	UNKN	Na	K-Fe (LT)	7.3	> 3.00	3.65	8.92	1.73	7.37	< 0.1	31	51.7	799	1.01	2	< 10	18.6	3	1.9	1.1	2.17	1.33
1272029	A13-09848	571708	6249781	OTCP	SED	DOL	SIL	K-Fe (LT)	5.6	2.1	2.97	5.31	1.4	6.37	2.2	49	155	1320	3.12	0.9	< 10	42.5	0.9	1.5	0.3	5.16	1.05
1272030	A13-09848	571710	6249783	OTCP	SED	DOL	SIL	Na	2	1.77	1.23	2.68	0.33	2.77	0.3	10	235	363	2.7	0.3	< 10	47.7	0.6	0.4	0.2	2.18	0.29
1272031	A13-09848	571984	6249857	OTCP	MAFINT	GAB	Na	DOL	20.3	1.91	4.85	7.25	0.07	7.25	0.2	103	241	1410	7.98	0.2	< 10	162	1.8	0.3	0.6	0.56	0.22
1272032	A13-09848	571708	6249781	OTCP	BRX	UNKN	SIL		1	1.28	0.77	1.7	0.09	1.63	0.2	< 1	293	252	1.79	0.2	< 10	39.7	0.3	0.3	0.1	0.56	0.13
1272033	A13-09848	571708	6249781	OTCP	BRX	UNKN	SIL	Na	1.9	0.78	3.13	1.51	0.33	7.17	0.6	8	174	1630	2.55	0.2	< 10	47.1	0.6	0.3	0.2	0.74	0.33
1272034	A13-09848	552914	6254217	OTCP	BAS	VOL	Ca-Fe (HT)	K-Fe (LT)	1	< 0.01	0.18	0.05	0.02	0.73	< 0.1	14	104	5510	30.8	< 0.1	< 10	3.3	0.5	1.9	0.1	0.54	0.52
1272045	A13-09848	561783	6250926	BLD	SED	DOL	Na	SIL	4.8	> 3.00	0.69	4.98	0.26	0.98	< 0.1	31	142	155	8.39	1.8	< 10	178	0.6	0.3	0.2	0.24	0.45
1272051	A13-09848	554539	6250862	OTCP	SED	SILT	K-Fe (LT)	Na	33.4	2.11	1.24	7.12	3.23	0.85	< 0.1	46	200	377	4.62	2.5	< 10	16.8	0.5	1.8	0.2	0.19	1.89

Analyte Symbol	Certificate	UTMX_NAD83	UTMY_NAD83	Sample type	Rock type	Modifier	Alteration1	Alteration2	Li	Na	Mg	Al	K	Ca	Cd	V	Cr	Mn	Fe	Hf	Hg	Ni	Er	Be	Ho	Ag	Cs
Unit Symbol									ppm	%	%	%	%	%	ppm	ppm	ppm	ppm	%	ppm	ppb	ppm	ppm	ppm	ppm	ppm	ppm
Detection Limit									0.5	0.01	0.01	0.01	0.01	0.01	0.1	1	0.5	1	0.01	0.1	10	0.5	0.1	0.1	0.1	0.05	0.05
Analysis Method									TD-MS	TD-MS	TD-MS	TD-MS	TD-MS	TD-MS	TD-MS	TD-MS	TD-MS	TD-MS	TD-MS	TD-MS	TD-MS	TD-MS	TD-MS	TD-MS	TD-MS	TD-MS	TD-MS
1272052	A13-09848	554517	6250855	OTCP	SED	SILT	K-Fe (LT)	Ab	28.3	> 3.00	0.61	6.54	2.49	0.34	< 0.1	20	123	84	1	0.6	< 10	12.2	0.2	1.5	< 0.1	0.09	1.03
1272053	A13-09848	554376	6250659	OTCP	BAS	VOL	K-Fe (HT)	Ab	23.4	2.91	3.87	5.76	0.03	9.72	0.2	250	199	1690	7.62	1.5	< 10	86.8	2.1	0.6	0.7	0.26	0.09
1272054	A13-09848	554144	6250972	OTCP	BRX	UNKN	K-Fe (LT)		69.4	0.05	1.68	5.34	1.65	0.32	< 0.1	49	222	152	2.47	2.6	< 10	29.7	0.6	1.5	0.2	0.17	1.73
1272055	A13-09848	559464	6251988	OTCP	BAS	VOL	Na		4.2	> 3.00	1.05	6.33	0.09	2.24	0.2	33	162	566	2.01	3.7	< 10	33.1	0.9	0.7	0.3	0.16	0.14
1272056	A13-09848	559464	6251988	OTCP	UNKN	UNKN	Na	Si	2.3	> 3.00	0.79	4.57	0.19	1.99	< 0.1	46	219	333	1.52	1.6	< 10	31.6	0.6	0.7	0.2	0.13	0.13
1272101	A13-09848	564787	6252075	OTCP	BAS	VOL	SIL		15.4	0.23	2.49	2.86	< 0.01	0.02	0.4	128	235	279	11.1	1.1	< 10	261	0.1	0.3	< 0.1	0.48	0.09
1272102	A13-09848	564915	6252085	OTCP	MAFINT	GAB	Ca-Fe (HT)	Ab	1.7	> 3.00	1.06	5.24	0.04	2.67	< 0.1	348	108	290	19.5	4.3	< 10	36.2	4.8	1	1.5	0.22	0.07
1272103	A13-09848	564915	6252117	OTCP	QtzVein	UNKN	SIL		< 0.5	0.03	0.03	0.04	< 0.01	0.03	< 0.1	< 1	362	61	0.6	< 0.1	< 10	10	< 0.1	0.2	< 0.1	0.13	0.18
1272104	A13-09848	565061	6252174	OTCP	SED	SHL	Gr	Ab	10.4	1.54	0.82	8.85	4.03	0.12	< 0.1	91	154	51	5.55	3.6	< 10	32.6	1.3	2.3	0.5	0.29	2.36
1272106	A13-09848	564922	6252284	OTCP	SED	SHL	Na	Si	6	> 3.00	0.83	8.57	0.44	0.69	< 0.1	100	103	83	5.16	4	< 10	60.2	1	1.3	0.3	0.24	0.13
1272107	A13-09848	556320	6251720	OTCP	QtzVein	UNKN	SIL		0.9	1.17	1.29	1.4	0.08	2.92	0.1	< 1	313	404	0.83	0.1	< 10	16.9	0.5	0.4	0.2	0.1	0.26
1272108	A13-09848	556320	6251720	OTCP	SED	DOL	SIL		1.9	0.35	11.5	0.42	0.03	24.1	< 0.1	11	21.7	2460	2.1	0.1	< 10	14	1.1	0.5	0.4	0.06	0.09
1272109	A13-09848	556328	6251719	OTCP	QtzVein	UNKN	SIL		0.7	0.1	0.76	0.07	0.02	1.63	0.1	3	352	277	2.5	0.4	< 10	39.3	0.5	0.3	0.2	0.09	0.19
1272110	A13-09848	556328	6251719	OTCP	SED	DOL	SIL		1.9	0.77	6.09	0.93	0.09	16.9	< 0.1	31	135	1630	6.54	< 0.1	< 10	58.9	4.6	0.4	1.9	0.06	0.19
1272111	A13-09848	556374	6251681	OTCP	SED	SILT	Na		0.9	0.02	0.05	0.2	0.1	0.07	0.4	14	353	42	1.12	0.1	< 10	23.9	< 0.1	0.3	< 0.1	0.13	0.12
1272112	A13-09848	556383	6251640	OTCP	BRX	UNKN	Na		1.5	> 3.00	0.42	8.2	0.13	1.04	0.2	105	101	210	4.03	3.2	530	79.1	0.7	1.4	0.2	0.34	0.13
1272113	A13-09848	556382	6251623	OTCP	BRX	UNKN	Na		1.2	> 3.00	0.21	8.23	0.12	0.49	0.1	79	104	92	2.52	3.2	390	47.5	0.6	1.6	0.1	0.34	0.12
1272114	A13-09848	556370	6251544	OTCP	SED	SHL	Na	Gr	25	> 3.00	0.55	8.02	2.92	0.06	< 0.1	90	97.8	24	0.89	1.1	20	25.4	1.1	2.8	0.4	0.15	2.69
1272115	A13-09848	556316	6251554	OTCP	SED	UNKN	K-Fe (LT)		0.8	0.69	0.47	0.79	0.05	1.47	0.1	< 1	350	221	2.6	0.2	< 10	33.9	0.6	0.2	0.2	0.11	0.22
1272116	A13-09848	556312	6251603	OTCP	MS	UNKN	K-Fe (LT)		33.9	2.5	0.98	6.33	2.45	0.12	< 0.1	73	158	28	1.68	2.2	< 10	93.6	1.3	2.4	0.4	0.17	2.17
1272117	A13-09848	556327	6251679	OTCP	BAS	VOL	SIL		1.7	> 3.00	0.17	5.96	0.14	0.45	< 0.1	117	185	55	5.27	3.3	250	89	0.7	1.2	0.2	0.3	0.13
1272118	A13-09848	560547	6250727	OTCP	SED	SAND	K-Fe (LT)	Si	2.6	2.99	0.48	3.87	0.22	0.98	< 0.1	13	180	321	0.44	0.5	< 10	6.6	0.4	0.7	0.2	0.1	0.17
1272119	A13-09848	554426	6250828	OTCP	BAS	VOL	K-Fe (LT)	Ca	43.6	> 3.00	2.54	6.79	1.54	1.89	0.1	61	69.7	715	5.22	2.8	90	14.9	2	2	0.8	< 0.05	2.62
1272120	A13-09848	554445	6250790	OCTP	BAS	VOL	DOL	Ab	84.9	> 3.00	4.12	7.9	2.64	0.36	< 0.1	61	59	203	5.58	4	< 10	40.5	2.3	3	0.8	0.06	5.18
1272121	A13-09848	554690	6250558	OTCP	BAS	VOL	DOL		1.4	0.02	2.25	0.03	0.01	6.37	< 0.1	< 1	164	8820	19.2	< 0.1	60	4.1	0.1	0.7	< 0.1	< 0.05	0.12
1272122	A13-09848	554980	6250307	OTCP	BAS	VOL	DOL	K-Fe (LT)	38.3	> 3.00	1.86	7.23	1.42	0.17	< 0.1	50	143	113	3.81	2.8	< 10	20.8	0.3	1.7	0.1	0.07	1.22
1272123	A13-09848	555253	6250179	BLD	IF	UNKN	UNKN		1	0.02	1.59	0.03	0.01	4.53	< 0.1	< 1	209	6080	20.3	< 0.1	< 10	4.2	0.1	0.4	< 0.1	< 0.05	0.07
1272124	A13-09848	568440	6251804	OTCP	BAS	VOL	Na	Mg-Mn-Fe	15.7	1.86	4.81	7.75	0.21	8.66	< 0.1	269	237	1780	8.71	1.3	< 10	132	2.6	0.6	0.9	0.06	0.69
1272125	A13-09848	568187	6251541	OTCP	QtzVein	UNKN	UNKN		0.9	0.03	0.01	0.03	0.01	0.13	0.1	< 1	340	61	1.91	< 0.1	< 10	138	< 0.1	< 0.1	< 0.1	1.02	0.12
1272126	A13-09848	567598	6251489	OTCP	BAS	VOL	Na	Mag	16	> 3.00	4.14	7.17	0.04	3.68	0.8	332	93.6	678	9.07	2.3	10	38.7	4.5	0.8	1.6	2.49	0.05
1272127	A13-09848	567598	6251489	OTCP	BAS	VOL	Na	Si	2.7	> 3.00	0.24	5.38	0.05	0.56	1.3	71	139	99	4.95	2.9	< 10	40.3	1.1	0.8	0.4	3.44	< 0.05
1272201	A13-09848	567793	6251402	OCTP	BAS	VOL	K-Fe (LT)	Na	12.9	> 3.00	3.65	4.82	0.88	6.61	1	291	94.9	867	12.3	1.9	< 10	81.1	3	1.5	1.1	2.33	4.97
1272202	A13-09848	567793	6251402	OCTP	BAS	VOL	Na	K-Fe (LT)	14.3	> 3.00	3.73	6.8	0.14	5.91	0.2	184	36.1	1040	10.8	0.2	< 10	44.4	3.6	0.4	1.2	0.45	0.27
1272203	A13-09848	567793	6251402	OCTP	SED	UNKN	SIL	Na	2.4	> 3.00	0.11	6.49	0.04	0.65	21.3	109	62.1	72	11.4	2.2	< 10	103	0.3	0.4	0.1	19.9	< 0.05
1272204	A13-09848	567829	6251379	OCTP	BAS	VOL	K-Fe (HT)	K-Fe (LT)	11.6	> 3.00	3.45	5.69	0.05	9.87	< 0.1	302	43.2	683	8.73	1.9	< 10	73.3	3.1	0.8	1.1	1.46	0.06
1272205	A13-09848	567943	6251341	OCTP	SED	UNKN	Na	DOL	19.8	> 3.00	4.61	6.77	0.07	5.7	0.1	246	44.2	618	8.33	1.6	140	80.2	3.7	1.2	1.3	0.39	0.08
1272206	A13-09848	567949	6251338	OCTP	BAS	VOL	Na	K-Fe (HT)	2.4	> 3.00	2.34	4.46	0.03	18.3	< 0.1	294	57.1	872	5.15	1.6	30	61.1	2	1.1	0.7	0.33	< 0.05
1272207	A13-09848	555123	6254840	OCTP	SED	MUD	Na	DOL	2.5	> 3.00	2.08	9.03	0.56	4.44	0.1	38	43.8	312	0.5	3.8	< 10	59.9	1.2	0.7	0.5	0.19	0.15
1272208	A13-09848	555123	6254840	OCTP	SED	DOL	Na	K-Fe (LT)	13.7	> 3.00	1.19	9.44	0.45	4.74	< 0.1	4	14.7	340	1.47	0.9	180	23.9	4.1	1.2	1.7	0.13	0.13
1272209	A13-09848	565112	6252087	OCTP	MAFINT	GAB	Na	K-Fe (LT)	5.4	> 3.00	0.23	5.43	0.44	0.31	< 0.1	113	117	101	23.4	3.7	< 10	206	2.8	0.6	1.4	0.8	0.15
L307851	A13-09848	568457	6251950	OCTP	BAS	VOL	Na	SIL	18	0.63	3.05	4.07	0.06	3.27	< 0.1	141	192	958	7.01	0.5	50	56.6	0.9	0.3	0.3	0.24	0.13
L307852	A13-09848	568881	6251395	BLD	SED	SHL	Gr	K-Fe (LT)	119	0.91	2.87	7.39	1.41	0.17	< 0.1	66	122	160	4.1	1.7	20	49.9	0.4	1.9	0.2	0.16	2.72
L307853	A13-09848	568708	6251370	BLD	BAS	VOL	SIL		19.1	1.32	5.46	8.44	0.05	9.6	< 0.1	150	188	1400	8.64	0.5	< 10	193	2.2	0.6	0.7	0.08	0.2
L307854	A13-09848	568476	6251307	BLD	BAS	VOL	Na	K-Fe (LT)	14.5	> 3.00	0.78	7.01	1.36	1.37	< 0.1	63	77.9	209	2.63	3.8	< 10	32	1.3	0.9	0.5	0.2	2.9
L307855	A13-09848	568476	6251307	BLD	SED	SHL	Gr	K-Fe (LT)	42.6	1.97	1.36	9.62	2.8	1.03	0.1	85	121	241	3.73	3.4	< 10	11.7	1.4	2.3	0.5	0.11	3.35
L307856	A13-09848	568306	6241260	BLD	BAS	VOL	UNKN	Na	15	> 3.00	2.25	8.54	0.11	1.09	< 0.1	120	67.4	305	5.32	3.7	< 10	12.2	1.9	0.7	0.7	0.2	0.15

Analyte Symbol	Certificate	UTMX_NAD83	UTMY_NAD83	Sample type	Rock type	Modifier	Alteration1	Alteration2	Li	Na	Mg	Al	K	Ca	Cd	V	Cr	Mn	Fe	Hf	Hg	Ni	Er	Be	Ho	Ag	Cs
Unit Symbol									ppm	%	%	%	%	%	ppm	ppm	ppm	ppm	%	ppm	ppb	ppm	ppm	ppm	ppm	ppm	ppm
Detection Limit									0.5	0.01	0.01	0.01	0.01	0.01	0.1	1	0.5	1	0.01	0.1	10	0.5	0.1	0.1	0.1	0.05	0.05
Analysis Method									TD-MS	TD-MS	TD-MS	TD-MS	TD-MS	TD-MS	TD-MS	TD-MS	TD-MS	TD-MS	TD-MS	TD-MS	TD-MS	TD-MS	TD-MS	TD-MS	TD-MS	TD-MS	TD-MS
L307857	A13-09848	568240	6251257	OCTP	SED	SHL	Gr	Na	30.3	> 3.00	3.05	9.26	0.06	1.27	< 0.1	227	113	503	6.84	2.2	< 10	57.3	3.1	1.2	1	0.16	0.18
L307858	A13-09848	568189	6251226	OCTP	SED	SHL	Gr	Na	30.6	> 3.00	1.63	8.52	2.55	1.36	< 0.1	141	92.2	173	2.2	2.9	< 10	8.7	1.6	3.2	0.5	0.3	3.02
L307859	A13-09848	568139	6251239	OCTP	SED	SHL	Gr	Na	1.2	> 3.00	0.05	8.41	0.13	0.67	< 0.1	123	104	42	3.96	2.3	< 10	86	2.1	1	0.7	0.49	0.11
L307860	A13-09848	568128	6251236	BLD	SED	SHL	Gr	Na	0.8	> 3.00	0.12	8.83	0.07	0.52	0.1	135	113	33	1.15	4	50	2.1	1.4	1.1	0.5	3.61	0.06
1272151	A13-09848	564514	6251992	OTCP	SED	SAND	Ab	SIL	60.5	> 3.00	3.6	9.7	0.92	0.21	< 0.1	72	60.3	173	5.23	1.7	40	52.1	0.5	1.8	0.2	1.01	0.28
1272152	A13-09848	564510	6251985	OTCP	SED	DOL	DOL	SIL	1.3	0.29	0.43	0.46	0.06	1.12	0.2	4	23.6	265	9.57	0.1	< 10	113	0.2	0.2	0.1	0.72	0.08
1272153	A13-09848	564515	6251980	OTCP	UNKN	UNKN	DOL	SIL	44.3	0.03	9.75	3.97	0.04	9.99	0.1	105	48.1	1460	12.2	0.8	< 10	121	0.8	0.4	0.3	4.12	0.34
1272154	A13-09848	564518	6251988	OTCP	UNKN	UNKN	DOL	SIL	39.9	< 0.01	7.55	4.79	0.59	3.32	0.1	290	45.7	601	22.9	1.3	< 10	235	1.8	0.8	0.9	1.04	2.27
1272155	A13-09848	564542	6251983	OTCP	UNKN	UNKN	Ab	SIL	27.4	> 3.00	1.04	7.18	1.71	0.21	< 0.1	52	41.3	100	10.3	2.4	< 10	6.8	0.4	2.3	0.2	1.16	0.89
1272156	A13-09848	564558	6251990	OTCP	UNKN	UNKN	UNKN		24.2	0.02	2.82	2.51	< 0.01	0.56	0.5	53	15.9	219	18.8	0.4	20	14.1	0.2	< 0.1	< 0.1	5.21	0.07
1272128	A13-09934	567598	6251489	OTCP	BAS	VOL	Na	Ca	5.4	> 3.00	0.72	7.15	0.08	2	0.8	90	102	203	13.7	2.5	150	146	1.6	0.7	0.6	5.64	< 0.05
1272129	A13-09934	552911	6254216	OTCP	SED	DOL	DOL	K-Fe (LT)	8.1	0.04	15	0.59	0.03	16.5	< 0.1	14	23.2	1900	2.59	0.2	< 10	13.9	0.2	0.4	< 0.1	0.59	< 0.05
1272130	A13-09934	552883	6254261	OTCP	SED	DOL	DOL		8.7	0.03	11.7	0.7	0.03	15.5	< 0.1	10	146	2110	2.56	0.2	< 10	15.7	0.2	0.5	< 0.1	0.44	< 0.05
1272131	A13-09934	552921	6254266	OTCP	SED	DOL	DOL		22.4	0.05	9.29	0.81	0.04	25.4	< 0.1	25	31	3210	2.03	0.3	< 10	33.9	2.5	0.4	0.8	0.29	0.06
1272132	A13-09934	552872	6254062	OTCP	SED	DOL	DOL		3.3	0.02	3.68	0.06	0.05	13.6	< 0.1	< 1	194	1620	1.15	< 0.1	< 10	12.1	< 0.1	< 0.1	< 0.1	0.29	0.07
1272133	A13-09934	552836	6254005	OTCP	SED	DOL	DOL	Si	2.6	0.03	7.63	0.12	0.1	11.4	< 0.1	< 1	247	538	0.49	< 0.1	< 10	10.4	< 0.1	< 0.1	< 0.1	0.21	0.08
1272134	A13-09934	552871	6254059	OTCP	BAS	VOL	Ca-Fe (HT)	Ab	49.9	> 3.00	4.16	9.59	0.05	6.01	< 0.1	341	313	858	8.89	1.7	< 10	126	2.7	1.3	0.9	0.2	0.12
1272135	A13-09934	552915	6254224	OTCP	BAS	VOL	K-Fe (LT)	Ab	26.3	1.94	5.19	7.3	0.96	12	< 0.1	276	343	1540	7.82	1.1	50	93.1	2.8	0.8	1	0.57	1.78
1272136	A13-09934	570719	6249279	OTCP	SED	DOL	DOL		43.2	0.03	10.6	2.45	0.62	12.2	< 0.1	18	100	1620	1.58	0.2	< 10	17.1	0.5	0.5	0.2	0.23	0.43
1272137	A13-09934	570325	6249572	OTCP	UNKN	UNKN	SIL		9.1	0.08	0.34	3.57	1.32	0.2	< 0.1	76	296	79	1.56	0.1	< 10	16.6	1.2	0.7	0.4	0.33	1.16
1272138	A13-09934	570243	6249613	OTCP	SED	SILT			55.1	0.24	1.56	9.91	3.1	0.05	< 0.1	205	158	283	4.43	1.7	< 10	42.5	1.4	1.7	0.5	0.22	3.17
1272139	A13-09934	569232	6249905	OTCP	UNKN	UNKN	SIL		24	0.26	0.82	1.85	0.22	0.11	< 0.1	31	300	134	3.62	1.9	< 10	18.9	0.8	0.3	0.3	0.39	0.22
1272140	A13-09934	569232	6249905	OTCP	BAS	VOL	SIL		36.9	1.2	1.36	8.14	2.2	0.25	< 0.1	229	215	159	6.41	4.5	< 10	49.2	1.6	1.6	0.6	0.66	2.04
1272141	A13-09934	552437	6258635	OTCP	BAS	VOL	SIL		2.4	0.06	0.71	6.83	0.06	8.36	< 0.1	73	315	484	3.35	0.5	< 10	23.4	1.6	0.2	0.6	0.2	0.07
1272142	A13-09934	552553	6258742	OTCP	BAS	VOL	UNKN		1.6	1.47	1.72	6.92	0.07	7.97	< 0.1	151	261	657	4.84	0.6	< 10	82.3	1.7	0.4	0.6	0.21	0.05
1272143	A13-09934	549425	6236758	OTCP	SED	DOL	DOL	Si	5	0.06	11.9	0.28	0.12	19.9	0.3	10	118	1190	2.57	< 0.1	< 10	15.3	0.2	0.2	< 0.1	1.04	0.6
L307861	A13-09934	568128	6251236	BLD	BAS	VOL	Na		10.9	> 3.00	1.62	5.75	0.06	0.8	< 0.1	109	178	249	3.31	2.3	< 10	24.8	0.6	0.8	0.2	1.13	< 0.05
L307862	A13-09934	568069	6251266	OCTP	BAS	VOL	Na		14	> 3.00	3.24	8.59	0.06	2.52	0.1	265	159	484	6.45	1.8	< 10	30.5	1.9	0.7	0.6	1.49	0.08
L307863	A13-09934	565098	6252090	OCTP	BAS	VOL	Na	K-Fe (HT)	49.3	> 3.00	5.05	8.98	0.28	0.51	< 0.1	231	293	384	11.9	4.5	< 10	115	1.3	1.1	0.6	0.82	0.14
L307864	A13-09934	554503	6256462	BLD	BAS	VOL	Na	Na	2.3	> 3.00	0.46	> 10.0	0.08	0.58	< 0.1	47	49.3	143	0.39	1.6	< 10	14.8	0.5	1.6	0.2	0.25	0.08
L307865	A13-09934	554560	6256518	OCTP	BAS	VOL	Na	K-Fe (LT)	7.2	> 3.00	0.76	> 10.0	0.79	0.27	< 0.1	90	64.9	78	0.54	2	< 10	30.6	0.5	2.2	0.2	0.21	0.4
L307866	A13-09934	554503	6256462	OCTP	SED	DOL	Na	DOL	1.1	3	9.11	3.32	0.04	16.1	< 0.1	11	21.4	1350	1.84	2.6	< 10	16.6	1.2	0.3	0.4	0.23	< 0.05
L307867	A13-09934	552599	6259016	OCTP	BAS	VOL	DOL		4	0.69	3.39	6.76	0.08	11.7	< 0.1	247	229	1630	10.5	1	< 10	52.9	2.2	0.2	0.8	0.2	< 0.05
L307868	A13-09934	552502	6259241	OCTP	BAS	VOL	Na		13.9	2.15	4.87	7.79	0.14	8.29	< 0.1	312	230	1230	9.17	1	< 10	122	2.2	0.4	0.8	0.25	0.22
L307869	A13-09934	552473	6259249	OCTP	BAS	VOL	Na		10.8	2.47	4.76	7.77	0.14	8.37	< 0.1	324	235	1150	9.24	0.9	< 10	102	2.6	0.7	0.9	0.24	0.27
L307870	A13-09934	552554	6259146	OCTP	BAS	VOL	Na		11.9	1.54	4.78	8.12	0.07	9.65	< 0.1	304	239	1420	9.12	1.1	< 10	125	2.3	0.4	0.8	0.25	0.11
L307871	A13-09934	552324	6258897	OCTP	BAS	VOL	Na		12.1	2.8	4.24	7.58	0.26	7.05	< 0.1	264	235	1240	9.66	0.9	< 10	73.3	2.5	0.5	0.9	0.18	0.57
L307872	A13-09934	552443	6258755	OCTP	BAS	VOL	Na		10	1.92	4.78	7.85	0.14	8.97	< 0.1	288	322	1260	9.54	0.8	< 10	105	2.3	0.3	0.8	0.23	0.21
L307873	A13-09934	552457	6258648	OCTP	BAS	VOL	Na	K-Fe (LT)	24.8	> 3.00	5.22	7.55	1.87	4.68	< 0.1	249	256	897	9.49	0.6	< 10	115	1.6	0.7	0.5	0.15	4.09
L307874	A13-09934	552556	6258747	OTCP	BAS	VOL	Na	DOL	3.5	2.59	3.73	6.45	0.09	7.36	< 0.1	124	189	759	6.47	0.7	< 10	64	2	0.5	0.8	0.13	0.09
L307875	A13-09934	558109	6250777	OTCP	SED	DOL	Na		1.7	> 3.00	2.28	6.61	0.11	4.27	< 0.1	16	114	321	1.7	2.1	< 10	23.7	1.1	0.8	0.4	0.2	0.12
L307876	A13-09934	558420	6250516	OTCP	BAS	VOL	Na	K-Fe (LT)	34.2	> 3.00	3.69	8.1	1.69	1.15	< 0.1	65	56.5	355	9.66	1.7	< 10	43	2.3	1.3	0.9	0.16	2.95
L307877	A13-09934	558452	6250504	OTCP	SED	SILT	Na	K-Fe (LT)	32.5	> 3.00	3.62	8.26	1.38	2.53	< 0.1	150	74	425	1.45	3.1	< 10	44.5	0.6	1.4	0.2	0.2	2.05
L307878	A13-09934	558515	6250513	OTCP	SED	SILT	Na		7	> 3.00	2.13	8.41	0.27	3.38	< 0.1	50	108	658	1.15	2.9	< 10	20.4	1.3	1.1	0.4	0.12	0.41
L307879	A13-09934	552703	6253998	OTCP	BAS	VOL	Na	K-Fe (HT)	41.9	> 3.00	2.84	7.54	0.92	1.33	< 0.1	82	62.3	417	9.83	2.5	< 10	27	2.9	1.7	1.1	0.15	2.04
L307880	A13-09934	552697	6253976	OTCP	BAS	VOL	Na	K-Fe (HT)	49.8	> 3.00	2.84	6.97	1.11	1.14	< 0.1	87	49.5	404	10.7	1.5	< 10	50.9	2.4	1.6	0.9	0.14	1.29

Analyte Symbol	Certificate	UTMX_NAD83	UTMY_NAD83	Sample type	Rock type	Modifier	Alteration1	Alteration2	Li	Na	Mg	Al	K	Ca	Cd	V	Cr	Mn	Fe	Hf	Hg	Ni	Er	Be	Ho	Ag	Cs
Unit Symbol									ppm	%	%	%	%	%	ppm	ppm	ppm	ppm	%	ppm	ppb	ppm	ppm	ppm	ppm	ppm	ppm
Detection Limit									0.5	0.01	0.01	0.01	0.01	0.01	0.1	1	0.5	1	0.01	0.1	10	0.5	0.1	0.1	0.1	0.05	0.05
Analysis Method									TD-MS	TD-MS	TD-MS	TD-MS	TD-MS	TD-MS	TD-MS	TD-MS	TD-MS	TD-MS	TD-MS	TD-MS	TD-MS	TD-MS	TD-MS	TD-MS	TD-MS	TD-MS	TD-MS
L307881	A13-09934	552625	6253716	OTCP	BAS	VOL	DOL	SIL	16.6	0.05	4.85	1.36	0.62	7.77	0.2	9	310	685	0.62	< 0.1	< 10	14.3	0.5	0.3	0.1	0.11	0.58
L307882	A13-09934	552717	6253767	OTCP	BAS	VOL	K-Fe (HT)		97.8	0.06	2.67	5.89	2.58	6.2	< 0.1	111	331	1230	7.32	2.6	< 10	76.4	0.8	1.4	0.3	0.24	4.87
L307883	A13-09934	553106	6253833	OTCP	SED	DOL	DOL		4.6	0.05	14.4	0.36	0.22	21.6	< 0.1	3	49.2	880	0.63	< 0.1	< 10	15.4	0.7	< 0.1	0.3	0.08	0.19
L307884	A13-09934	553106	6253833	OTCP	SED	DOL	SIL	DOL	2.3	0.07	5.83	0.11	0.07	8.88	< 0.1	< 1	193	433	0.43	< 0.1	< 10	9.7	0.2	< 0.1	< 0.1	0.07	0.15
L307885	A13-09934	552634	6252872	OTCP	BAS	VOL	Ca-Fe (HT)		48.5	1.15	9.07	7.23	0.05	6	< 0.1	274	188	2470	14.3	0.8	< 10	156	1.4	0.3	0.5	0.1	0.22
L307886	A13-09934	552512	6253330	OTCP	BAS	VOL	Na	K-Fe (LT)	50.9	> 3.00	5.65	> 10.0	0.06	2.33	< 0.1	402	234	1470	10.3	2	< 10	35.4	2.3	0.7	0.8	0.28	0.09
L307887	A13-09934	552545	6253450	OTCP	MAFINT	GAB	Na		30.4	2.47	5.98	9	0.14	7.8	< 0.1	212	253	1520	8.9	1	< 10	170	2.1	0.4	0.7	0.16	0.15
L307888	A13-09934	552444	6253735	OTCP	BAS	VOL	Na		30.4	2.76	5.07	8.04	0.18	6.31	< 0.1	354	244	1420	10.5	1.2	< 10	97.9	2.5	0.5	0.9	0.19	0.88
L307889	A13-09934	552303	6253872	OTCP	BAS	VOL	Na	K-Fe (LT)	27.9	> 3.00	4.11	7.2	0.04	4.98	< 0.1	338	332	1450	8.92	1.1	< 10	99.9	2.3	0.6	0.8	0.18	< 0.05
L307890	A13-09934	552284	6253931	OTCP	BAS	VOL	Na		36.5	2.71	4.73	7.85	0.05	5.6	< 0.1	282	299	1760	9.62	1.2	< 10	120	2.1	0.5	0.7	0.22	0.14
L307891	A13-09934	552293	6254463	OTCP	SED	DOL	DOL		8.7	0.08	14.6	0.46	0.29	22.6	< 0.1	7	59.2	562	0.47	< 0.1	< 10	14	0.2	0.1	< 0.1	0.06	0.54
L307892	A13-09934	552288	6254473	OTCP	SED	DOL	DOL		1.7	0.02	6.99	0.12	0.08	10.8	< 0.1	< 1	160	312	0.36	< 0.1	< 10	9.1	0.1	< 0.1	< 0.1	0.11	0.08
L307893	A13-09934	552945	6258748	OTCP	BAS	VOL	DOL		2.2	0.1	5.12	7.84	0.06	14	< 0.1	232	188	1690	10	0.9	< 10	91.3	2.7	0.4	0.9	0.07	< 0.05
L307894	A13-09934	564754	6252081	UNKN	BAS	VOL	Na	K-Fe (LT)	20.6	> 3.00	2.67	7.79	0.99	0.14	0.2	189	228	277	7.56	2.8	< 10	37.1	0.2	1	0.1	0.66	0.41
L307895	A13-09934	564708	6252081	UNKN	BAS	VOL	SIL		44.2	0.02	5.64	5.53	0.03	0.08	2.5	267	371	392	10.6	1.7	< 10	61.6	0.2	0.3	< 0.1	0.34	0.06
L307896	A13-09934	564690	6252050	UNKN	BAS	VOL	Na	K-Fe (LT)	29.3	> 3.00	2.11	> 10.0	2.99	0.19	< 0.1	106	88.6	301	2.75	1.5	< 10	48.6	0.8	2.7	0.4	0.14	1.22
L307898	A13-09934	564626	6252066	UNKN	BAS	VOL	Na	K-Fe (LT)	22.4	> 3.00	0.98	> 10.0	3.73	0.11	< 0.1	502	188	78	2.56	5.2	< 10	7.8	0.3	3.3	0.1	0.36	1.3
L307899	A13-09934	564781	6252063	UNKN	BAS	VOL	K-Fe (HT)		18.7	0.63	0.77	9.92	3.59	0.11	0.3	240	203	50	7.96	3.8	< 10	111	0.6	2.8	0.3	0.35	1.25
L307900	A13-09934	564785	6252077	UNKN	QtzVein	UNKN	UNKN		1	0.05	0.11	0.14	0.04	0.04	< 0.1	< 1	398	70	0.56	< 0.1	< 10	7.1	< 0.1	< 0.1	< 0.1	0.11	0.22
1272213	A13-10175	552915	6254224	OCTP	BAS	VOL	Na	K-Fe (HT)	17.6	> 3.00	3.68	6.13	0.63	8.49	< 0.1	163	247	969	4.86	1.4	40	64.5	1.9	0.2	0.7	0.59	1.2
1272214	A13-10175	564560	6251992	OCTP	SED	MUD	Na	K-Fe (HT)	17.5	> 3.00	1.58	9.79	0.7	0.25	< 0.1	82	82.3	103	2.46	2.1	70	35	0.7	1.1	0.3	0.17	0.34
1272215	A13-10175	564560	6251992	OCTP	SED	MUD	K-Fe (LT)	SIL	79	0.03	9.87	9.33	0.02	0.17	< 0.1	196	110	339	14.8	2.5	110	28.3	0.4	0.2	0.2	0.37	0.12
1272216	A13-10175	564560	6251992	OCTP	MS	MS	K-Fe (LT)	SIL	0.7	0.02	0.04	0.08	0.01	< 0.01	< 0.1	4	17.7	18	> 50.0	< 0.1	150	557	< 0.1	< 0.1	< 0.1	1.71	< 0.05
1272217	A13-10175	555480	6254502	OCTP	SED	MUD	UNKN		25.8	1.91	1.37	6.01	1.91	0.2	0.1	201	179	41	5.12	3.4	130	102	0.4	3	0.1	0.54	6.31
1272218	A13-10175	564560	6251992	OCTP	SED	MUD	K-Fe (LT)	K-Fe (LT)	58	0.15	1.49	8.56	2.44	0.48	0.1	78	127	27	3.34	1.3	100	13.5	0.3	2.6	< 0.1	2.33	4.9
1272219	A13-10175	555510	6254462	OCTP	SED	DOL	DOL	K-Fe (LT)	1	1.6	4.29	1.93	0.04	8.48	< 0.1	381	101	1210	26.6	0.4	100	28.9	0.8	0.2	0.3	0.58	0.1
1272220	A13-10175	564560	6251992	OCTP	SED	DOL	Na	DOL	29.1	2.54	8.05	4.4	0.2	11	0.1	29	54	741	2.27	0.6	60	25.6	0.8	0.6	0.3	0.25	0.79
1272221	A13-10175	555461	6254516	OCTP	SED	MUD	Na	K-Fe (LT)	1.6	> 3.00	3.12	4.87	0.05	8.47	0.3	149	154	1260	15.6	2.7	70	37.8	1.7	0.4	0.7	0.25	0.15
1272222	A13-10175	555510	6254462	OCTP	SED	DOL	DOL	K-Fe (LT)	1.6	1.21	9.4	1.39	0.03	18.7	0.1	15	34.4	3160	2.94	1.6	50	37.8	2.7	< 0.1	1	0.17	0.05
1272223	A13-10175	570257	6249486	OCTP	SED	QTZE	K-Fe (LT)		56.4	0.02	7.81	4.93	0.02	0.33	0.1	63	186	219	6.68	4.7	60	17.9	0.8	0.4	0.3	0.17	< 0.05
1272228	A13-10175	555510	6254462	OCTP	SED	DOL	Na	DOL	0.6	0.92	8.75	1.05	0.01	16.6	< 0.1	3	53.5	1540	1.42	1.5	20	22.9	1.1	< 0.1	0.4	0.33	< 0.05

Co ppm 0.1 TD-MS	Eu ppm 0.05 TD-MS	Bi ppm 0.02 TD-MS	Se ppm 0.1 TD-MS	Zn ppm 0.2 TD-MS	Ga ppm 0.1 TD-MS	As ppm 0.1 TD-MS	Rb ppm 0.2 TD-MS	Y ppm 0.1 TD-MS	Sr ppm 0.2 TD-MS	Zr ppm 1 TD-MS	Nb ppm 0.1 TD-MS	Mo ppm 0.1 TD-MS	In ppm 0.1 TD-MS	Sn ppm 1 TD-MS	Sb ppm 0.1 TD-MS	Te ppm 0.1 TD-MS	Ba ppm 1 TD-MS	La ppm 0.1 TD-MS	Ce ppm 0.1 TD-MS	Pr ppm 0.1 TD-MS	Nd ppm 0.1 TD-MS	Sm ppm 0.1 TD-MS	Gd ppm 0.1 TD-MS	Tb ppm 0.1 TD-MS	Dy ppm 0.1 TD-MS	Cu ppm 0.2 TD-MS	Ge ppm 0.1 TD-MS	Tm ppm 0.1 TD-MS	Yb ppm 0.1 TD-MS	Lu ppm 0.1 TD-MS	Ta ppm 0.1 TD-MS	W ppm 0.1 TD-MS	Re ppm 0.001 TD-MS
71.3	0.18	0.48	8.6	851	12.8	18.5	< 0.2	8.3	32.6	73	5.4	28.1	0.1	< 1	0.2	1	9	3.3	7.9	1.1	4.7	1.3	1.3	0.2	1.4	> 10000	0.2	0.1	0.8	0.1	0.3	3.2	0.034
385	0.69	0.41	8.9	92.5	10.7	108	< 0.2	34.8	36.2	59	4.2	6.1	0.2	< 1	0.1	2	4	24.9	54	7.4	27.8	5.7	6.1	1	6.5	> 10000	0.2	0.5	2.9	0.4	0.1	0.9	0.015
10.3	0.54	0.03	2.3	29.3	18.5	2.2	< 0.2	24	45	61	1.5	1.6	< 0.1	< 1	< 0.1	0.1	10	3.7	10.8	1.8	8.9	3.1	3.8	0.7	4.7	1000	0.5	0.4	2	0.3	< 0.1	0.4	0.006
1	0.6	0.03	2.6	3.9	16.4	1	0.3	33.8	41.5	27	0.2	0.2	< 0.1	< 1	< 0.1	< 0.1	10	6.3	20.5	3.1	15.2	5	5.7	1	6.3	291	0.2	0.5	2.8	0.4	< 0.1	< 0.1	0.003
98.8	0.37	0.75	4.5	14.2	16.9	13.6	2.8	15.7	46.8	111	6.8	9	< 0.1	< 1	0.2	0.7	14	9.1	25.6	3.4	13.9	3.2	3.1	0.5	3.2	> 10000	0.2	0.3	1.6	0.2	0.3	1.6	0.024
38.4	0.9	0.25	7.5	< 0.2	15.7	18.7	< 0.2	42.6	37.3	106	7.9	2.6	< 0.1	1	0.2	0.2	7	2.2	9.4	2.5	15.6	6.3	7.3	1.3	8.2	414	0.2	0.6	3.6	0.5	0.2	0.7	0.004
54.3	1.41	0.16	3.2	51.7	25.5	1.8	80.4	26.2	37.2	71	1.1	0.4	0.2	< 1	< 0.1	< 0.1	302	13.4	32.2	4.2	16.9	4.2	4.5	0.8	5.1	2470	0.4	0.4	2.2	0.3	< 0.1	0.3	0.003
42	0.71	0.03	1.5	56.8	16.4	0.5	3.4	17.5	93.3	20	0.2	0.1	< 0.1	< 1	< 0.1	< 0.1	29	3.9	10	1.5	7	2.1	2.8	0.5	3.3	125	0.2	0.3	1.6	0.2	< 0.1	0.4	0.001
32.2	0.8	0.06	2	57.1	16.2	0.8	2.2	13.5	109	27	4.8	1.5	0.2	< 1	0.2	< 0.1	31	4.4	8.8	1.2	5	1.5	1.9	0.4	2.9	28	3.1	0.3	1.4	0.2	0.4	1	0.002
123	0.13	0.14	5.3	5.1	10.5	24	8.2	4.5	27	101	4.2	2.9	< 0.1	< 1	< 0.1	0.1	51	1.1	2.8	0.4	1.9	0.7	1	0.2	1.1	807	< 0.1	< 0.1	0.4	< 0.1	0.1	0.9	< 0.001
20.6	0.93	0.09	4.6	42.4	19.6	212	0.3	34.2	29.1	60	2.1	0.3	< 0.1	< 1	< 0.1	< 0.1	9	3.1	12.3	2.6	14.1	4.7	5.7	1	6.5	483	0.4	0.6	3.2	0.5	< 0.1	< 0.1	0.004
39.4	0.51	0.21	9.5	85.9	17.5	3.1	8.5	22.7	29.4	67	4.8	3.8	< 0.1	< 1	< 0.1	< 0.1	23	2.7	8.4	1.6	8.4	3.1	3.7	0.7	4.2	7670	0.2	0.3	1.9	0.3	0.1	0.8	0.015
14.9	0.38	0.11	11.5	136	24	7.9	< 0.2	15.5	25.4	74	5.4	6.8	0.1	< 1	< 0.1	0.3	6	3.4	11.3	2	9.8	2.7	2.7	0.4	2.8	> 10000	0.4	0.2	1.4	0.2	0.3	1.3	0.036
2.4	0.25	0.05	0.9	6.5	20.4	1.1	< 0.2	8.8	33.6	81	0.8	1.9	< 0.1	< 1	< 0.1	< 0.1	9	2.9	9.3	1.5	6.6	1.8	1.8	0.3	2	2830	0.2	0.1	0.8	0.1	< 0.1	< 0.1	0.006
38.3	0.53	0.05	2.2	4.1	19.3	7.2	< 0.2	29.3	43.3	142	7	7.3	< 0.1	< 1	< 0.1	< 0.1	7	5.5	16	2.7	13.7	4.8	5.1	0.9	5.6	2410	0.2	0.4	2.2	0.3	0.3	< 0.1	0.014
66.4	0.41	0.43	5.2	31.1	16.9	31.7	< 0.2	19.4	50.4	86	6	8	< 0.1	< 1	< 0.1	0.2	9	10.9	23.3	3.1	12.4	3.3	3.3	0.6	3.7	9330	0.1	0.3	1.5	0.2	0.3	0.3	0.01
17.4	0.15	0.18	8.5	17.2	16.2	24.4	< 0.2	6.2	27.4	122	7.2	10.1	< 0.1	< 1	< 0.1	0.7	10	2.2	4.9	0.7	3	1	1.1	0.2	1.1	9890	0.1	< 0.1	0.6	< 0.1	0.3	0.4	0.017
83	1.4	0.05	1.7	3.2	35.9	2.1	103	8	27	59	8.4	2.5	< 0.1	3	< 0.1	< 0.1	457	59	115	14	46.8	7.1	4.7	0.5	2.1	16.5	0.9	0.1	0.7	0.1	0.3	0.2	0.001
21.1	0.31	0.79	1.5	37.6	14.1	4	41.1	10.1	68.4	106	9.9	5.4	1	2	< 0.1	0.5	234	27.7	58.8	6.3	21.7	3.2	2.4	0.3	1.9	5600	0.3	0.2	1.1	0.2	0.5	0.4	< 0.001
69.1	0.1	0.8	3.7	51.9	14.7	3.3	13.9	4.4	38.4	104	9.6	4.9	0.8	2	< 0.1	0.5	153	2.4	6.1	0.6	2.2	0.4	0.5	< 0.1	0.8	6250	0.3	0.1	0.6	0.1	0.6	0.6	< 0.001
32.1	0.09	0.09	1	51.9	14.2	2.5	37.4	5.2	59.7	25	3.6	1.9	< 0.1	< 1	< 0.1	< 0.1	194	7.6	13.8	1.5	4.8	0.8	0.6	0.1	0.8	472	< 0.1	0.1	0.6	< 0.1	0.2	< 0.1	< 0.001
15.7	< 0.05	0.12	1.3	56.2	16.3	0.7	56.3	2.9	41.1	27	2.6	2.5	< 0.1	< 1	< 0.1	< 0.1	297	2.3	4	0.4	1.2	0.2	0.3	< 0.1	0.4	186	< 0.1	< 0.1	0.3	< 0.1	0.1	< 0.1	< 0.001
27.7	0.05	0.17	0.9	44.4	19.5	3.9	86.3	5.7	68	39	4.2	2.6	0.2	1	< 0.1	< 0.1	484	1.5	2.8	0.3	1.2	0.3	0.4	0.1	0.9	1040	< 0.1	0.1	0.6	< 0.1	0.3	0.1	< 0.001
5.7	0.14	0.27	1.3	46.1	34.9	1.4	153	8.2	63.6	69	8	2.6	1	2	0.2	0.1	946	10.3	22.6	2.6	8.4	1.4	1.2	0.2	1.4	4560	0.5	0.1	0.8	0.1	0.5	0.4	< 0.001
> 500	0.15	6.53	82.7	4830	7.6	1370	0.7	6.1	10.6	13	1.1	3.6	0.2	< 1	0.1	10.1	2	2.7	5.9	0.7	2.7	0.7	0.9	0.2	1.2	8560	0.5	0.1	0.8	0.1	< 0.1	2.9	0.005
> 500	0.14	0.1	45.7	99.1	17.4	58.7	< 0.2	4.9	7.5	30	0.6	3.1	< 0.1	2	< 0.1	0.5	< 1	1.4	3.7	0.6	2.5	0.9	1.1	0.2	1.1	1660	0.3	< 0.1	0.5	< 0.1	< 0.1	0.7	< 0.001
20.2	1.14	0.07	9.8	13	1.7	4.2	1	29.9	101	62	1.4	0.7	< 0.1	< 1	0.1	17.5	15	3.9	13.8	2.4	11.2	3.7	4.7	1	6.8	41.5	0.1	0.5	2.5	0.3	< 0.1	0.3	0.001
> 500	3.78	0.53	> 1000	9	1.3	8270	0.4	77.7	9.3	4	1.5	1.8	< 0.1	< 1	0.4	> 500	7	19.1	95.6	17.3	76.1	16.5	18.2	2.4	13	> 10000	392	0.6	2.8	0.4	< 0.1	5.7	< 0.001
24.3	0.17	0.07	409	11.5	13.6	45.5	1.4	9.4	67.1	61	4.3	1.6	< 0.1	< 1	0.1	5.6	30	1.2	3.2	0.5	2.2	0.7	1.1	0.2	1.5	434	1.5	0.2	1.1	0.2	0.2	1	0.003
6.8	0.06	0.13	60.6	15.6	17.6	12	< 0.2	3.8	35.6	135	10.1	6.2	0.8	1	0.2	1.5	25	0.4	1.5	0.2	0.9	0.3	0.4	< 0.1	0.6	> 10000	0.4	< 0.1	0.7	0.1	0.6	2.2	< 0.001
5.6	0.22	0.05	17.4	6.5	0.6	2.3	6	2.6	92	3	0.9	2.4	< 0.1	< 1	< 0.1	0.2	26	2.1	4.9	0.6	2.4	0.6	0.6	0.1	0.6	14.8	< 0.1	< 0.1	0.3	< 0.1	< 0.1	< 0.1	0.005
16.6	0.14	0.05	70.6	11.5	0.2	7.3	4	1.8	144	2	0.4	0.6	< 0.1	< 1	< 0.1	1.1	7	1.8	3.2	0.4	1.7	0.4	0.5	< 0.1	0.4	38	0.3	< 0.1	0.1	< 0.1	< 0.1	< 0.1	< 0.001
89.1	0.97	0.55	12.2	103	16.2	2	137	11.3	319	23	1.1	0.8	0.5	< 1	< 0.1	< 0.1	195	7.7	14.3	1.8	7.5	2	2.2	0.4	2.5	87.8	0.9	0.2	1.2	0.2	< 0.1	< 0.1	< 0.001
65.2	0.06	0.03	10.4	25.5	2.4	4.5	1.4	1.4	17.3	1	0.4	3.2	< 0.1	< 1	< 0.1	0.2	3	0.3	0.6	< 0.1	0.4	0.1	0.2	< 0.1	0.2	620	0.1	< 0.1	0.2	< 0.1	< 0.1	< 0.1	< 0.001
40.8	0.33	0.38	13	36.2	10	2.3	12.7	4.9	25.8	93	3.3	4.9	< 0.1	< 1	< 0.1	0.1	73	13.3	21.2	2.2	7.1	1.3	1	0.2	1	200	0.1	< 0.1	0.5	< 0.1	< 0.1	< 0.1	0.01
43.4	1.52	0.52	32.2	35.7	15	3.3	35.3	13.6	89.6	103	7.2	101	< 0.1	1	< 0.1	0.4	171	95.9	202	20.2	62.5	9.4	6.3	0.8	3.7	493	0.5	0.2	1.3	0.2	0.2	< 0.1	0.018
45.2	0.58	0.4	11.4	40.5	21.8	1.9	73.8	9.9	91	140	9.5	37.3	< 0.1	1	< 0.1	0.1	365	25.4	50.9	5.5	17.7	2.9	2.2	0.3	1.9	211	0.3	0.2	1.4	0.2	0.5	0.2	0.003
10.2	0.79	5.19	38.8	6.6	17	5.3	79	18.6	109	64	3.7	19.5	< 0.1	< 1	< 0.1	3.9	418	5.5	15.3	2.1	9.1	2.9	3.3	0.7	5.2	25.8	0.5	0.4	2.4	0.3	< 0.1	< 0.1	0.01
91.2	0.41	0.36	87.7	44	13.5	7.6	66	7.5	79.9	33	4.1	21.2	0.1	1	< 0.1	1.2	378	14.3	29.9	3.5	12.4	2.3	2.1	0.3	1.9	5570	0.4	0.1	0.8	0.1	0.2	< 0.1	0.003
109	0.13	0.24	115	19.2	4.8	14.1	15.6	5.2	41.4	13	1.9	21.9	< 0.1	< 1	< 0.1	1	88	4.2	8.9	1	3.8	0.8	0.9	0.1	0.9	2310	0.5	< 0.1	0.6	< 0.1	< 0.1	1	0.004
48.9	0.69	0.09	5	90.9	14.7	5.6	3.1	15.3	105	7	0.3	0.6	< 0.1	< 1	< 0.1	< 0.1	9	3.3	8.6	1.3	6.3	1.9	2.5	0.4	3	264	0.3	0.3	1.5	0.2	< 0.1	< 0.1	0.003
103	0.11	0.06	55.9	6.9	2.4	4	4.1	2.8	27.2	7	1.2	15.6	< 0.1	< 1	< 0.1	< 0.1	24	3.7	7.5	0.8	3	0.6	0.6	< 0.1	0.6	974	0.3	< 0.1	0.3	< 0.1	< 0.1	< 0.1	0.003
94.4	0.18	0.18	31.5	15.9	3.3	2.7	15.2	5	64.6	8	1.2	8.1	< 0.1	< 1	0.1	0.2	90	2.6	5.3	0.6	2.3	0.6	0.8	0.1	0.9	1020	0.2	< 0.1	0.5	< 0.1	< 0.1	< 0.1	0.006
4.9	0.22	0.25	4.1	6.4	1.2	9.6	1.5	4	4.4	7	1.8	1.5	< 0.1	< 1	0.5	< 0.1	15	1.4	3.2	0.3	1.4	0.3	0.5	< 0.1	0.6	6	0.3	< 0.1	0.4	< 0.1	< 0.1	2	0.013
76.3	0.52	0.23	17.8	11	11.8	30.2	15.9	6.1	21.5	65	1.7	3	< 0.1	< 1	0.2	< 0.1	19	15	29.7	3.4	11.8	1.9	1.6	0.2	1.3	38.9	0.3	< 0.1	0.5	< 0.1	< 0.1	0.3	< 0.001
6.1	0.52	0.11	2.9	6.4	18.6	1.3	126	5	32.1	85	2.9	2.5	< 0.1	1	0.1	0.1	252	16.8	31.8	3.6	12.6	2.1	1.8	0.2	1.1	14.2	0.3	< 0.1	0.5	< 0.1	0.1	< 0.1	0.005

Co	Eu	Bi	Se	Zn	Ga	As	Rb	Y	Sr	Zr	Nb	Mo	In	Sn	Sb	Te	Ba	La	Ce	Pr	Nd	Sm	Gd	Tb	Dy	Cu	Ge	Tm	Yb	Lu	Ta	W	Re
ppm	ppm	ppm	ppm	ppm	ppm	ppm	ppm	ppm	ppm	ppm	ppm	ppm	ppm	ppm	ppm	ppm	ppm	ppm	ppm	ppm	ppm	ppm	ppm	ppm	ppm	ppm	ppm	ppm	ppm	ppm	ppm	ppm	ppm
0.1	0.05	0.02	0.1	0.2	0.1	0.1	0.2	0.1	0.2	1	0.1	0.1	0.1	1	0.1	0.1	1	0.1	0.1	0.1	0.1	0.1	0.1	0.1	0.1	0.2	0.1	0.1	0.1	0.1	0.1	0.1	0.001
TD-MS	TD-MS	TD-MS	TD-MS	TD-MS	TD-MS	TD-MS	TD-MS	TD-MS	TD-MS	TD-MS	TD-MS	TD-MS	TD-MS	TD-MS	TD-MS	TD-MS	TD-MS	TD-MS	TD-MS	TD-MS	TD-MS	TD-MS	TD-MS	TD-MS	TD-MS	TD-MS	TD-MS	TD-MS	TD-MS	TD-MS	TD-MS	TD-MS	TD-MS
3.3	0.24	0.03	1.4	15.8	15.2	0.7	96.9	1.5	35.9	24	1	1.9	< 0.1	< 1	< 0.1	< 0.1	217	11.3	20.4	2.2	7.3	1.1	0.8	< 0.1	0.4	9.5	< 0.1	< 0.1	0.1	< 0.1	< 0.1	< 0.1	0.003
44	0.57	0.06	3.5	58.4	14	1.5	0.5	17.5	32	48	3.5	0.8	< 0.1	< 1	< 0.1	< 0.1	13	3.5	8.6	1.3	6.1	1.9	2.5	0.5	3.3	37	1.4	0.3	2	0.4	0.2	< 0.1	0.009
12.2	0.77	0.1	1.2	11.3	15.4	1.4	176	6.2	5.2	98	4.6	3.6	< 0.1	1	0.4	< 0.1	112	29.1	57	6.6	22.7	3.7	2.5	0.3	1.4	13	0.2	< 0.1	0.5	< 0.1	0.1	< 0.1	0.067
113	0.24	0.09	3.5	15.7	14.5	11.4	2.2	8.1	35.3	137	4.6	1.8	< 0.1	< 1	< 0.1	< 0.1	29	1.8	4.8	0.7	3.1	1.2	1.6	0.3	1.8	29.2	< 0.1	0.1	0.8	0.1	0.1	< 0.1	0.01
69.9	0.21	0.09	2.3	12	9.9	9.9	4.6	6.2	29.8	88	3.9	1.7	< 0.1	1	< 0.1	< 0.1	32	6.1	13	1.6	6.1	1.4	1.4	0.2	1.2	52.8	0.1	< 0.1	0.5	< 0.1	< 0.1	< 0.1	0.007
> 500	< 0.05	0.5	61.8	243	12.2	3640	0.3	1	1.8	43	0.8	4.2	< 0.1	< 1	0.1	2.1	3	0.4	0.9	0.1	0.4	0.1	0.1	< 0.1	0.2	1910	0.3	< 0.1	0.1	< 0.1	< 0.1	1.4	0.009
132	0.71	0.13	3.5	25.6	17.3	15.2	0.4	37.3	23.7	156	0.4	0.4	< 0.1	4	< 0.1	< 0.1	4	1.7	5.1	0.8	4.6	2	3.3	0.8	6.3	32.9	0.3	0.8	4.5	0.7	< 0.1	0.2	0.01
2.1	< 0.05	0.06	2.5	6.7	0.4	4.1	0.4	0.1	9.7	2	< 0.1	4.7	< 0.1	< 1	0.1	0.2	13	< 0.1	0.1	< 0.1	< 0.1	< 0.1	< 0.1	< 0.1	< 0.1	688	0.1	< 0.1	< 0.1	< 0.1	< 0.1	< 0.1	0.012
171	1.49	0.7	5.2	5.9	30.7	18.3	182	12.7	35.8	119	8	2.7	< 0.1	1	< 0.1	0.5	47	81	185	20.6	70.6	11.3	7.8	0.8	3.5	377	0.5	0.2	1.1	0.2	0.3	< 0.1	0.014
> 500	0.3	0.51	99.6	8.4	23.4	106	11.6	8.5	33.9	137	7.7	2.2	< 0.1	< 1	< 0.1	3.1	59	17.7	40.2	4.6	16.2	3	2.5	0.3	1.9	15.2	0.6	0.2	0.9	0.2	0.5	0.5	0.008
2	0.07	0.07	2.2	18.9	3.5	2.1	2.4	4.7	36.5	8	1.2	4.2	< 0.1	< 1	0.1	< 0.1	50	0.4	1.2	0.2	1	0.4	0.5	< 0.1	0.7	999	< 0.1	< 0.1	0.4	< 0.1	< 0.1	< 0.1	0.005
2.8	0.28	0.07	1.7	15.3	0.9	1.6	1	10.9	113	6	0.9	0.5	< 0.1	< 1	< 0.1	0.1	13	2.4	5.4	0.8	3.8	1.1	1.5	0.3	1.8	9.5	< 0.1	0.2	0.9	0.1	< 0.1	< 0.1	0.004
12.8	0.09	0.09	1.5	14.4	0.4	8.6	1	4.3	20.2	17	1.6	3.9	< 0.1	< 1	0.1	< 0.1	33	2.6	5.3	0.6	2.1	0.4	0.5	< 0.1	0.7	180	< 0.1	< 0.1	0.4	< 0.1	< 0.1	< 0.1	0.004
22.4	1.81	0.19	4	13.3	2.8	11	2.8	49.6	144	4	0.8	1.7	< 0.1	< 1	< 0.1	< 0.1	31	12.5	34.5	6	31.1	10.4	13.3	1.9	10.9	38.1	0.2	0.5	2.7	0.4	< 0.1	< 0.1	0.002
14.3	< 0.05	1.19	1.2	80.5	2.4	16.7	3.1	0.4	3.5	8	0.5	6	< 0.1	< 1	0.9	0.2	167	0.3	0.3	< 0.1	0.1	< 0.1	< 0.1	< 0.1	< 0.1	66.2	< 0.1	< 0.1	< 0.1	< 0.1	< 0.1	< 0.1	0.012
3	0.1	0.16	8.2	9.6	22.6	11.3	2.1	5.7	44.6	124	8.8	7.2	1.4	2	0.3	0.6	33	0.9	2.4	0.4	1.8	0.5	0.7	0.1	0.8	> 10000	0.1	0.1	0.8	0.2	0.4	1	0.011
2.8	0.06	0.09	4.1	5.4	24.2	6.3	1.5	4.2	46	116	9.1	2.8	1	1	0.2	0.3	35	0.6	1.6	0.2	0.9	0.3	0.4	< 0.1	0.6	> 10000	0.1	0.1	0.8	0.1	0.5	1	0.01
0.4	0.54	2.43	3.2	11.5	27.8	16.9	84.9	10.3	24.1	38	0.7	0.2	< 0.1	< 1	< 0.1	< 0.1	688	30.4	59.3	6.9	24.3	3.9	2.9	0.3	1.9	38.1	0.4	0.2	1	0.2	< 0.1	< 0.1	0.023
23.1	0.15	0.12	3.3	26.7	2.3	32.8	1.7	6.1	27.2	10	1.1	4.7	< 0.1	< 1	0.1	< 0.1	49	0.9	2.5	0.4	2.5	0.9	1.2	0.2	1.1	63.2	0.2	< 0.1	0.4	< 0.1	< 0.1	< 0.1	0.01
39.3	0.41	0.19	2.8	6.3	21.4	22.5	96.5	11.4	10	85	7.1	1.7	< 0.1	< 1	0.1	< 0.1	470	31.2	52.4	6.5	21.3	2.9	2.3	0.3	1.9	592	0.3	0.2	1.4	0.3	0.4	< 0.1	0.004
27.6	0.1	0.57	7.3	4.1	19.6	34.3	3.3	6.4	29.7	128	11.2	10.2	0.6	1	0.3	0.9	33	0.9	2.5	0.4	2	0.6	0.7	0.1	0.8	7680	0.2	0.1	0.9	0.2	0.7	1.8	0.019
1.4	0.76	0.11	0.6	9	6.8	1.3	5	4.2	17.2	16	1.4	5.7	< 0.1	< 1	< 0.1	0.2	18	21	38.5	4.3	14.6	2.2	1.5	0.2	0.9	62.9	0.1	< 0.1	0.4	< 0.1	< 0.1	< 0.1	0.012
42	3.34	0.06	2.3	70.8	23.2	1.3	96	18.7	47.1	97	0.3	0.2	< 0.1	2	< 0.1	< 0.1	104	107	247	29	110	18.8	11.8	1.2	4.9	85.9	0.8	0.3	1.8	0.3	< 0.1	< 0.1	0.102
58.9	1.44	0.03	1.8	31.9	27	0.8	170	19.7	31.2	153	1.2	< 0.1	< 0.1	< 1	< 0.1	< 0.1	107	22.7	51.5	6.7	27	6.1	5.5	0.8	4.5	22.6	0.4	0.3	1.9	0.3	< 0.1	< 0.1	0.044
5.2	0.09	0.07	1.1	5.5	0.4	3.8	1.5	1.5	17.6	4	0.3	2.2	< 0.1	< 1	0.2	0.1	14	1.3	3	0.3	1.2	0.2	0.3	< 0.1	0.2	9.8	0.2	< 0.1	< 0.1	< 0.1	< 0.1	0.2	0.082
28	0.21	0.05	1.4	10	17.9	1.6	66.7	3.2	23	106	3	1.9	< 0.1	< 1	< 0.1	< 0.1	76	6.4	13.4	1.5	5	0.9	0.8	0.1	0.7	6.8	0.2	< 0.1	0.3	< 0.1	0.1	< 0.1	0.007
4.8	0.07	0.03	0.5	5.7	0.3	3.1	0.9	1.2	11.6	3	0.4	1.8	< 0.1	< 1	< 0.1	< 0.1	16	1.1	2.5	0.2	1	0.2	0.2	< 0.1	0.2	11.5	0.2	< 0.1	< 0.1	< 0.1	< 0.1	0.2	0.007
45.4	0.84	0.06	2.1	91.8	19.5	4.8	8.9	21.8	115	29	2.6	1	< 0.1	< 1	< 0.1	< 0.1	27	4.7	12.4	1.9	9.3	2.8	3.5	0.6	4.2	50.3	0.7	0.4	2.2	0.3	0.1	< 0.1	0.007
36.9	< 0.05	0.02	2.9	9.5	0.2	1.6	0.7	0.1	3.8	< 1	0.2	5	< 0.1	< 1	< 0.1	0.2	10	0.1	0.2	< 0.1	< 0.1	< 0.1	< 0.1	< 0.1	< 0.1	3020	0.5	< 0.1	< 0.1	< 0.1	< 0.1	< 0.1	0.011
26.5	0.63	0.1	5.3	97.4	22.7	2.3	< 0.2	40.4	18.1	77	2	3.1	< 0.1	< 1	< 0.1	< 0.1	5	2.5	11.2	2.6	15.4	5.9	6.6	1.2	7.8	> 10000	0.4	0.7	3.5	0.5	< 0.1	< 0.1	0.018
35	0.2	0.08	7.6	88.8	22.4	1.3	< 0.2	9.9	21.4	98	7.1	9.8	0.2	< 1	< 0.1	0.4	9	1.1	4.7	0.7	3.6	1.4	1.6	0.3	2	> 10000	0.4	0.2	0.9	0.1	0.5	< 0.1	0.064
47.5	0.53	0.55	10.9	80.9	12.9	18.3	56.7	27.4	36.9	64	5.1	5.8	< 0.1	< 1	0.1	0.2	102	5.7	14.1	2.5	12.5	4.2	4.6	0.8	5.4	7480	0.2	0.4	2.2	0.3	0.2	0.6	0.035
48.5	1.24	0.05	2.2	73	22	1.8	2.5	29.3	28.6	7	0.4	< 0.1	< 0.1	< 1	< 0.1	< 0.1	11	5.8	15.7	2.4	11.7	3.6	4.6	0.8	5.9	131	0.4	0.5	2.8	0.4	< 0.1	< 0.1	0.009
62.1	0.13	0.34	13.3	1100	13.5	2.6	0.2	3.1	32.8	80	6.5	24.9	0.5	< 1	< 0.1	1.5	13	3	7.3	1	4	0.8	0.6	< 0.1	0.6	> 10000	0.1	< 0.1	0.4	< 0.1	0.4	1.4	0.059
52.2	0.72	0.15	5.7	18.1	15.4	12.2	< 0.2	27.1	35.9	62	2.3	1.9	< 0.1	< 1	< 0.1	< 0.1	7	2.7	7.9	1.6	9.4	4	4.9	0.8	5.4	2460	0.4	0.4	2.5	0.4	< 0.1	< 0.1	0.017
60.6	0.58	0.19	2.3	18.8	18	7.9	< 0.2	30.9	31	49	1.1	0.3	< 0.1	< 1	< 0.1	< 0.1	8	3.4	9.2	1.6	8.6	3.3	4.4	0.9	6.1	904	0.3	0.5	2.9	0.4	< 0.1	< 0.1	0.005
64.5	0.38	0.18	4.4	11.8	10	23.6	< 0.2	18.3	75.6	54	4	4.6	< 0.1	< 1	< 0.1	0.5	6	10.8	23	2.9	11.5	2.7	3	0.5	3.4	2560	0.2	0.3	1.7	0.3	0.2	< 0.1	0.026
3.4	0.78	0.08	18.2	7	12.7	1.8	16.2	10.2	40.9	134	1.8	12.4	< 0.1	< 1	< 0.1	68.3	65	27.1	52.5	6	20.7	3.7	3.1	0.4	2.6	35.3	0.6	0.2	0.9	0.1	< 0.1	< 0.1	0.016
2.7	1.36	0.05	13.4	12.2	13.5	2.8	4.6	36.7	44.4	29	1.1	1.3	< 0.1	< 1	< 0.1	11.2	47	3.9	9.5	2.4	12.5	5.2	6.2	1.3	8.6	27.1	0.6	0.4	1.5	0.2	< 0.1	< 0.1	0.008
> 500	9.2	0.84	46.3	4.1	14.4	29.8	15.8	28	35.5	136	7.2	0.5	< 0.1	1	< 0.1	1.2	41	511	976	96.2	319	46.8	27.8	2.6	10.4	554	1.9	0.3	1.5	0.2	< 0.1	0.4	0.006
29.5	0.33	0.04	2.2	64.1	9.2	1.2	0.8	7	44.6	12	2.4	0.4	< 0.1	< 1	< 0.1	0.3	22	2.2	5.4	0.8	3.4	1	1.2	0.2	1.4	105	0.5	0.1	0.8	0.1	0.1	< 0.1	0.003
15.9	0.59	0.05	0.5	93.7	18.4	0.2	93.6	3.7	25.4	60	4.3	0.2	< 0.1	< 1	< 0.1	0.2	537	17.6	48.9	4.4	15.4	2.7	2	0.2	1.2	28.2	0.7	< 0.1	0.4	< 0.1	0.2	< 0.1	< 0.001
58	0.9	0.03	0.8	89.5	18.4	3.2	1.3	16.8	141	14	0.3	0.2	< 0.1	< 1	< 0.1	< 0.1	11	3.7	10	1.5	7.4	2.2	2.9	0.5	3.5	56.9	0.4	0.3	1.8	0.3	< 0.1	< 0.1	0.007
9.2	1.46	0.08	0.8	23.4	12.6	0.8	71.9	11.4	207	130	4.3	0.2	< 0.1	< 1	< 0.1	< 0.1	325	37.1	67	7.5	25.6	4	3.1	0.4	2.3	20.3	0.4	0.2	1.1	0.2	< 0.1	< 0.1	0.003
5.2	0.94	0.12	1	36	21.6	0.6	123	11.4	88.1	106	1.1	0.2	< 0.1	< 1	< 0.1	< 0.1	1400	35	70	8	27.8	4.5	3.5	0.4	2.5	24.5	0.6	0.2	1.1	0.2	< 0.1	< 0.1	0.005
15.2	0.55	0.03	1.9	25.6	23.3	0.9	2.5	16.8	17.5	128	7.2	0.5	< 0.1	4	< 0.1	< 0.1	19	1.5	5.8	1.2	6.5	2.6	2.8	0.5	3.6	238	0.2	0.3	1.3	0.2	0.4	< 0.1	0.008

Co	Eu	Bi	Se	Zn	Ga	As	Rb	Y	Sr	Zr	Nb	Mo	In	Sn	Sb	Te	Ba	La	Ce	Pr	Nd	Sm	Gd	Tb	Dy	Cu	Ge	Tm	Yb	Lu	Ta	W	Re
ppm	ppm	ppm	ppm	ppm	ppm	ppm	ppm	ppm	ppm	ppm	ppm	ppm	ppm	ppm	ppm	ppm	ppm	ppm	ppm	ppm	ppm	ppm	ppm	ppm	ppm	ppm	ppm	ppm	ppm	ppm	ppm	ppm	ppm
0.1	0.05	0.02	0.1	0.2	0.1	0.1	0.2	0.1	0.2	1	0.1	0.1	0.1	1	0.1	0.1	1	0.1	0.1	0.1	0.1	0.1	0.1	0.1	0.1	0.2	0.1	0.1	0.1	0.1	0.1	0.1	0.001
TD-MS	TD-MS	TD-MS	TD-MS	TD-MS	TD-MS	TD-MS	TD-MS	TD-MS	TD-MS	TD-MS	TD-MS	TD-MS	TD-MS	TD-MS	TD-MS	TD-MS	TD-MS	TD-MS	TD-MS	TD-MS	TD-MS	TD-MS	TD-MS	TD-MS	TD-MS	TD-MS	TD-MS	TD-MS	TD-MS	TD-MS	TD-MS	TD-MS	TD-MS
33.5	1	0.16	10.3	52.5	23.5	6.6	0.9	26.6	37.9	65	3.1	0.8	< 0.1	< 1	< 0.1	0.2	8	19	41.4	4.9	18.1	4.1	4.4	0.8	5	284	0.5	0.5	2.7	0.4	< 0.1	< 0.1	0.022
3	0.58	0.21	4.2	19.1	27	2.6	101	13.6	66.5	101	3.1	1	< 0.1	< 1	0.4	0.1	552	12.2	27.6	3.3	12	2.6	2.1	0.4	2.4	107	0.6	0.2	1.3	0.2	< 0.1	< 0.1	0.023
> 500	0.24	0.74	11.6	1.8	21.1	> 10000	3.4	18.4	53.4	116	2	7.3	< 0.1	< 1	1.4	4.6	30	2.9	11.6	2.3	12.6	4	3.9	0.6	3.7	189	0.2	0.3	1.9	0.3	< 0.1	< 0.1	0.038
1.6	0.19	4.17	10.6	6.5	23.7	246	0.8	12.2	62.7	127	7	10.7	< 0.1	< 1	< 0.1	1	13	1.9	7.5	1.5	8.5	2.7	2.5	0.4	2.4	1910	0.4	0.2	1.3	0.2	0.1	< 0.1	0.048
131	1.07	0.99	7.2	28.2	27.7	96	34.3	5	23.6	49	7.1	1	0.2	2	< 0.1	0.5	173	52.8	108	12.8	45.7	7.4	4.6	0.5	1.9	1870	0.6	< 0.1	0.3	< 0.1	0.4	0.4	0.015
> 500	0.98	1.88	25.2	7.7	1.6	89.3	2.6	2.4	9.4	7	1	0.3	< 0.1	< 1	< 0.1	2.3	9	71.4	127	14.2	42	4.8	2.4	0.2	0.7	1920	0.4	< 0.1	0.2	< 0.1	< 0.1	< 0.1	0.003
> 500	1.18	2.89	23.5	73.6	17.6	338	4.2	7	43.4	23	0.9	0.9	0.8	< 1	0.2	3.5	2	97.4	169	20.3	66.6	10	6	0.5	2.3	7270	0.5	0.1	0.6	< 0.1	< 0.1	0.3	0.003
> 500	5.66	0.16	63	70.1	22.9	573	63.2	15.8	16.3	38	0.6	0.2	< 0.1	< 1	< 0.1	0.4	13	418	772	79.8	268	44	25.2	2.3	8	539	1.5	0.2	1.2	0.2	< 0.1	0.4	0.003
> 500	0.46	0.17	29.9	18.1	16.5	895	104	3.4	7.2	70	3.3	0.2	< 0.1	1	0.2	0.7	49	29.9	63.2	7.1	22.2	3.5	2.1	0.3	1.2	1870	0.3	< 0.1	0.4	< 0.1	0.2	2.1	0.002
> 500	0.07	0.98	95.5	78.8	9.1	1790	0.5	2.1	2.6	14	< 0.1	0.7	0.3	< 1	< 0.1	3.8	2	0.9	2	0.3	1.1	0.4	0.5	< 0.1	0.5	> 10000	0.5	< 0.1	0.2	< 0.1	< 0.1	< 0.1	< 0.001
74.6	0.29	0.1	12	70.8	19.4	1.5	< 0.2	14.5	23.6	96	6.8	16.7	< 0.1	< 1	0.1	0.4	11	3.2	9.1	1.5	7.3	2.5	2.9	0.5	2.9	> 10000	0.2	0.2	1.2	0.2	0.5	0.5	0.07
20.5	0.07	0.07	0.1	58.4	1.5	0.9	0.3	2.2	35.9	8	0.5	0.6	< 0.1	< 1	< 0.1	< 0.1	3	1.6	2.7	0.4	1.7	0.4	0.5	< 0.1	0.4	10	< 0.1	< 0.1	0.2	< 0.1	< 0.1	0.1	< 0.001
16.1	0.08	0.06	0.1	32.3	1.8	1	< 0.2	2.3	39.8	8	0.5	3.8	< 0.1	< 1	0.1	< 0.1	2	1.8	3.4	0.5	2.2	0.5	0.5	< 0.1	0.4	58.2	< 0.1	< 0.1	0.2	< 0.1	< 0.1	0.1	0.001
34.1	1.47	0.03	0.6	29.8	1.8	3	0.6	22.6	73.7	11	0.4	0.6	0.3	< 1	< 0.1	< 0.1	22	18.8	30.2	3.7	15.3	3.2	4.5	0.6	3.5	756	< 0.1	0.4	2	0.3	< 0.1	< 0.1	< 0.001
12.5	0.09	< 0.02	0.2	21.7	0.1	< 0.1	2	0.9	73.8	2	< 0.1	1.7	< 0.1	< 1	< 0.1	< 0.1	36	1	2.3	0.3	1.3	0.3	0.3	< 0.1	0.2	36.3	< 0.1	< 0.1	< 0.1	< 0.1	< 0.1	< 0.1	< 0.001
3	0.08	< 0.02	0.2	4.9	0.5	0.4	2.5	0.8	57.8	3	0.2	2.3	< 0.1	< 1	< 0.1	< 0.1	34	0.7	2	0.3	1	0.2	0.2	< 0.1	0.2	7	< 0.1	< 0.1	< 0.1	< 0.1	< 0.1	0.1	0.002
30.7	0.9	< 0.02	1.2	66.9	20.5	2	< 0.2	22.7	28.6	62	0.6	0.1	< 0.1	< 1	< 0.1	< 0.1	18	7.7	15	2.1	8.8	2.4	3.3	0.6	4.3	56.1	0.3	0.4	2.2	0.4	< 0.1	0.2	< 0.001
42.7	1.56	31.3	3.2	72.1	17.4	1.8	31.3	22.4	663	32	2.8	3.2	0.9	< 1	0.2	< 0.1	114	14.3	23.2	2.9	11.9	3.1	3.9	0.7	4.5	> 10000	0.3	0.4	2.1	0.3	0.2	1.8	0.003
5.5	0.22	0.36	< 0.1	31.7	5.7	< 0.1	15.4	4.6	65.2	19	0.5	1.6	< 0.1	< 1	< 0.1	< 0.1	74	2.4	6	0.7	2.8	0.7	0.8	0.1	0.8	17.4	< 0.1	< 0.1	0.3	< 0.1	< 0.1	0.2	< 0.001
23.7	0.29	0.26	3.5	10.4	8.5	26.2	44.3	11.2	6.8	12	2.3	4.5	< 0.1	< 1	0.3	< 0.1	345	9.5	20	2.4	9.1	1.7	2	0.3	2	66.6	0.1	0.2	0.9	0.1	< 0.1	0.5	0.006
0.3	0.52	0.22	6.2	44.8	21.5	4.4	106	12.2	19.4	73	0.2	0.9	< 0.1	< 1	< 0.1	< 0.1	1060	13	26.5	3.1	11	2.1	2.1	0.3	2.2	41.5	0.7	0.2	1.2	0.2	< 0.1	< 0.1	0.084
7.4	0.19	0.35	7.1	31.7	4.9	7.1	7.2	8.1	4.1	72	1.8	4.1	< 0.1	< 1	0.2	0.1	60	7.8	15.5	1.8	6.3	1.1	1.1	0.2	1.3	41.1	0.2	0.1	0.6	0.1	< 0.1	0.4	0.005
17.2	1.15	0.34	16	42.9	22.5	2.3	73.3	14.7	16.9	171	7.2	2.8	< 0.1	1	0.6	0.2	100	44.7	91	10.9	37.8	6.3	5.4	0.7	3.4	91.6	0.4	0.2	1.3	0.2	0.2	0.9	0.008
9.4	0.64	0.13	0.7	16.4	17.5	1	1.4	12.9	129	15	0.1	< 0.1	< 0.1	< 1	< 0.1	< 0.1	36	3	7.7	1.1	4.9	1.5	2.1	0.4	2.7	330	0.2	0.2	1.2	0.2	< 0.1	< 0.1	0.004
41.4	1.44	0.7	2.6	33.1	19.2	21.4	1	14.8	152	22	0.6	3.3	0.2	1	< 0.1	< 0.1	31	10.8	23.9	3.1	12.5	2.6	2.9	0.5	3	982	0.7	0.2	1.1	0.2	< 0.1	< 0.1	0.005
5.5	0.21	7.89	61.1	14.2	0.5	5.1	3.9	2.3	71.2	3	0.2	20.7	0.7	< 1	< 0.1	12.3	44	2.5	5.9	0.7	2.8	0.6	0.6	< 0.1	0.5	> 10000	0.3	< 0.1	0.1	< 0.1	< 0.1	0.1	0.038
3.5	0.16	0.1	4	21.3	19.9	11.3	< 0.2	5	31.3	84	7.1	3.4	< 0.1	< 1	< 0.1	0.4	6	2.8	8	0.9	3.7	1	1.1	0.2	1.1	705	1.3	< 0.1	0.6	< 0.1	0.4	0.4	0.003
8.3	0.35	0.04	2.7	52	19.7	1.3	0.3	15.7	46.3	73	5.6	9.4	< 0.1	< 1	< 0.1	< 0.1	7	6.1	13.8	1.9	7.9	2.2	2.6	0.5	3.1	2440	0.7	0.3	1.4	0.2	0.3	0.3	0.021
248	4.07	0.06	11.1	66.7	32.2	6.3	14	11.7	24.4	162	10.9	2.3	< 0.1	3	< 0.1	< 0.1	53	210	401	45.6	145	21.3	13.9	1.4	5	582	0.8	0.2	0.8	0.1	0.8	0.6	0.001
2.3	0.34	< 0.02	0.4	8.6	18.9	4.9	0.9	4.4	43	56	0.7	0.4	< 0.1	< 1	< 0.1	< 0.1	30	18.5	38	4.3	14.4	2.1	1.5	0.2	0.9	27.2	0.1	< 0.1	0.5	< 0.1	< 0.1	< 0.1	0.002
2.3	0.14	< 0.02	0.3	9.1	24.6	2	25.9	3.9	44.3	66	0.5	< 0.1	< 0.1	< 1	< 0.1	< 0.1	162	4.8	10.3	1.2	4	0.7	0.7	0.1	0.7	4.6	0.1	< 0.1	0.5	< 0.1	< 0.1	< 0.1	< 0.001
3.8	0.55	< 0.02	0.4	7	5.9	2.5	0.5	11.4	60.8	101	1.5	0.5	< 0.1	< 1	< 0.1	< 0.1	5	17.7	36.2	4.3	14.6	2.7	2.7	0.4	2.4	4	< 0.1	0.2	1	0.1	< 0.1	0.2	0.001
33.3	1.09	0.05	0.4	71	23.1	0.8	0.7	19.1	375	29	0.3	0.9	0.1	< 1	< 0.1	< 0.1	20	3.1	8.2	1.3	6.3	2	2.9	0.5	3.6	263	0.5	0.3	1.6	0.2	< 0.1	0.1	0.005
54.2	0.82	0.05	1	78.4	17.6	1.4	5.7	19.3	113	28	2.7	1.4	< 0.1	< 1	< 0.1	< 0.1	19	3.4	8.7	1.3	6.6	2	2.9	0.5	3.7	104	0.5	0.3	1.8	0.2	0.1	0.1	0.002
51.2	1.09	0.06	0.6	58	18.7	2.8	6	21.7	105	28	2.6	0.9	0.1	< 1	< 0.1	< 0.1	20	4.6	10.5	1.6	7.6	2.4	3.3	0.6	4.1	131	0.8	0.4	1.9	0.3	0.1	0.1	0.003
50.7	0.81	0.03	0.7	73.7	17.6	1.2	1.1	19.4	117	33	3	2.3	< 0.1	< 1	< 0.1	< 0.1	15	2.9	8	1.3	6.3	2	2.9	0.5	3.6	151	0.4	0.3	1.8	0.3	0.2	0.2	0.002
43.9	3.4	0.03	0.7	60	18.5	0.2	17.4	22	131	30	0.7	0.7	0.1	< 1	< 0.1	< 0.1	34	6.5	13.8	2	9.5	2.8	3.9	0.7	4.2	844	0.7	0.3	1.8	0.3	< 0.1	< 0.1	0.001
43.7	0.87	0.09	0.8	80.5	17.9	2.3	5.2	19.2	107	24	2.8	1.7	< 0.1	< 1	< 0.1	< 0.1	34	3.9	9.1	1.4	6.7	2.1	2.9	0.6	3.7	118	0.6	0.3	1.8	0.3	0.2	0.3	< 0.001
75.9	0.21	< 0.02	0.9	57.6	14.1	0.5	132	13	38.1	20	0.4	0.4	< 0.1	< 1	< 0.1	< 0.1	84	1.9	3.9	0.5	2.4	0.8	1.3	0.3	2.3	901	0.8	0.2	1.3	0.2	< 0.1	0.1	0.002
36.8	1.78	1.16	1	61.7	14.1	7	2.2	18.1	61.3	26	< 0.1	< 0.1	< 0.1	< 1	< 0.1	< 0.1	22	16.9	35.2	4.7	19.2	4.1	4.5	0.7	3.8	234	0.2	0.3	1.3	0.2	< 0.1	< 0.1	0.007
84.5	0.89	0.12	6.2	14	16.1	1.2	2.5	10.4	37.3	81	2.1	2.9	< 0.1	< 1	0.1	< 0.1	32	11.8	24.1	2.8	10.1	2	2	0.3	1.9	14.5	0.1	0.2	0.9	0.1	0.1	0.5	< 0.001
46.7	1.42	0.08	0.9	121	20.6	0.3	72	21	34.6	67	0.3	0.1	< 0.1	< 1	< 0.1	< 0.1	72	9.5	23.6	3.4	14.9	4.1	4.4	0.7	4.4	714	0.3	0.3	1.8	0.3	< 0.1	< 0.1	< 0.001
9.9	0.4	< 0.02	0.3	35.4	22.6	1	75	5.9	27.9	123	1.1	0.7	< 0.1	< 1	< 0.1	< 0.1	28	1.7	4	0.6	2.4	0.8	1	0.2	1	5.8	0.4	< 0.1	0.5	< 0.1	< 0.1	< 0.1	0.001
5.6	0.58	0.15	0.5	21.7	16.9	2.2	12.7	11	55.8	114	0.3	0.2	< 0.1	< 1	< 0.1	< 0.1	20	1.9	5.2	0.7	3.3	1	1.5	0.3	1.8	80.7	0.2	0.2	1.4	0.2	< 0.1	< 0.1	0.001
52.4	1.33	0.07	1.8	41.6	19.5	1.2	49.4	29.1	35.8	105	0.4	0.3	0.1	< 1	< 0.1	< 0.1	52	7.9	20	2.5	11.1	3.9	5.3	0.9	5.6	1450	0.3	0.4	2.1	0.3	< 0.1	< 0.1	0.003
45.3	1.49	0.2	1.1	37	19.2	0.3	56.7	22.4	29.3	67	< 0.1	< 0.1	0.1	< 1	< 0.1	< 0.1	323	17.9	38.7	4.9	19.8	4.2	4.6	0.7	4.4	1650	0.3	0.3	1.8	0.3	< 0.1	< 0.1	0.002

Co	Eu	Bi	Se	Zn	Ga	As	Rb	Y	Sr	Zr	Nb	Mo	In	Sn	Sb	Te	Ba	La	Ce	Pr	Nd	Sm	Gd	Tb	Dy	Cu	Ge	Tm	Yb	Lu	Ta	W	Re
ppm	ppm	ppm	ppm	ppm	ppm	ppm	ppm	ppm	ppm	ppm	ppm	ppm	ppm	ppm	ppm	ppm	ppm	ppm	ppm	ppm	ppm	ppm	ppm	ppm	ppm	ppm	ppm	ppm	ppm	ppm	ppm	ppm	ppm
0.1	0.05	0.02	0.1	0.2	0.1	0.1	0.2	0.1	0.2	1	0.1	0.1	0.1	1	0.1	0.1	1	0.1	0.1	0.1	0.1	0.1	0.1	0.1	0.1	0.2	0.1	0.1	0.1	0.1	0.1	0.1	0.001
TD-MS	TD-MS	TD-MS	TD-MS	TD-MS	TD-MS	TD-MS	TD-MS	TD-MS	TD-MS	TD-MS	TD-MS	TD-MS	TD-MS	TD-MS	TD-MS	TD-MS	TD-MS	TD-MS	TD-MS	TD-MS	TD-MS	TD-MS	TD-MS	TD-MS	TD-MS	TD-MS	TD-MS	TD-MS	TD-MS	TD-MS	TD-MS	TD-MS	TD-MS
3.4	0.09	0.02	0.2	19.8	2.8	1.2	16.1	3.7	36.4	5	0.6	3	< 0.1	< 1	< 0.1	< 0.1	136	2	4.4	0.4	1.5	0.3	0.4	< 0.1	0.6	16.8	< 0.1	< 0.1	0.5	< 0.1	< 0.1	< 0.1	< 0.001
41.1	1.04	0.04	0.3	14.2	15.8	0.2	137	7.7	16.2	101	1.7	4	0.2	1	< 0.1	0.1	216	35.4	60.4	6.8	22.6	3.7	3.2	0.4	1.8	13.7	0.4	0.1	0.7	0.1	< 0.1	0.2	0.001
6.7	0.34	< 0.02	0.2	6.5	0.7	0.5	6.3	6.7	98.2	3	0.3	1.5	< 0.1	< 1	< 0.1	< 0.1	20	1.6	5	0.8	3.5	1.1	1.3	0.2	1.5	5.8	< 0.1	< 0.1	0.5	< 0.1	< 0.1	< 0.1	< 0.001
3.2	0.12	< 0.02	< 0.1	16.5	0.3	0.5	1.8	2.4	43.2	2	0.1	3.1	< 0.1	< 1	< 0.1	< 0.1	18	0.8	2.3	0.3	1.4	0.4	0.5	< 0.1	0.5	15.8	< 0.1	< 0.1	0.2	< 0.1	< 0.1	< 0.1	< 0.001
64.5	0.25	< 0.02	0.3	176	9.5	0.2	1	11.9	21	19	0.7	0.4	< 0.1	< 1	< 0.1	< 0.1	13	1.2	3.6	0.6	3.3	1.2	1.8	0.3	2.4	4.2	0.2	0.2	1	0.1	< 0.1	0.2	< 0.001
20.1	0.59	0.02	0.6	125	17.8	0.2	0.4	18.7	86.5	72	3.4	0.6	< 0.1	< 1	< 0.1	< 0.1	40	1.8	4.9	0.8	4.2	1.7	2.5	0.5	3.6	55.4	0.4	0.4	2	0.3	0.2	0.2	< 0.001
52	0.77	< 0.02	0.4	94.7	17.7	0.3	3.4	18.4	206	39	2.4	1.5	< 0.1	< 1	< 0.1	< 0.1	100	2.9	7.8	1.2	5.8	1.8	2.5	0.5	3.3	51.6	0.6	0.3	1.8	0.3	0.1	0.2	0.001
53.1	1.09	< 0.02	1.6	73.9	18.2	2.1	10.2	22.6	141	41	3.3	1.1	< 0.1	< 1	0.1	< 0.1	58	4.7	11.5	1.7	7.8	2.3	3.3	0.6	4	244	0.4	0.4	2	0.3	0.2	0.2	0.001
35	0.55	< 0.02	0.5	105	17	0.6	< 0.2	15.5	80.2	36	4	1.2	< 0.1	< 1	0.1	< 0.1	25	1.5	4.8	0.8	4.1	1.5	2.4	0.5	3.4	17	1.7	0.3	1.7	0.2	0.2	0.3	0.001
59.7	0.57	0.03	1.7	100	18.6	0.6	0.4	18.2	76.2	45	2.8	1.5	< 0.1	< 1	< 0.1	< 0.1	21	2.7	7.4	1.2	5.6	1.8	2.6	0.5	3.4	305	0.3	0.3	1.6	0.2	0.1	0.3	0.001
4.1	0.16	0.02	0.1	13.9	0.9	1	11.7	2.2	83.3	5	0.3	0.8	< 0.1	< 1	< 0.1	< 0.1	68	2.5	6.4	0.8	3.1	0.6	0.6	< 0.1	0.4	8.3	< 0.1	< 0.1	0.2	< 0.1	< 0.1	0.1	< 0.001
2	0.08	< 0.02	< 0.1	3.7	0.4	< 0.1	2.2	1	36.3	2	0.1	2.3	< 0.1	< 1	< 0.1	< 0.1	16	0.7	2.2	0.3	1.3	0.3	0.3	< 0.1	0.2	4.1	< 0.1	< 0.1	< 0.1	< 0.1	< 0.1	< 0.1	< 0.001
45.9	1.01	< 0.02	0.5	68.4	18.8	0.7	1.5	24.2	183	25	0.2	0.1	< 0.1	< 1	< 0.1	< 0.1	10	3.8	9.6	1.5	7.5	2.4	3.5	0.7	4.4	35.4	0.3	0.4	2	0.3	< 0.1	0.1	< 0.001
> 500	0.31	0.38	61.9	105	22.3	3410	41.1	2.5	11.9	119	2	3.4	< 0.1	1	0.2	1.6	217	26.4	51.5	5.6	17.3	2.3	1.6	0.2	0.7	1840	0.4	< 0.1	0.2	< 0.1	0.1	3.9	0.001
97.5	< 0.05	0.22	6.8	1370	22.3	18.8	0.5	1.5	0.9	63	1	7.1	< 0.1	1	< 0.1	0.2	2	0.8	1.5	0.2	0.7	0.2	0.3	< 0.1	0.3	597	0.2	< 0.1	0.2	< 0.1	< 0.1	3.4	0.002
39	1.92	0.03	1.7	34.3	40.2	5.3	113	8.4	44.9	58	1	0.2	< 0.1	2	< 0.1	< 0.1	765	66.5	125	14.5	49.5	8	6	0.6	2.6	8.4	0.4	< 0.1	0.6	< 0.1	< 0.1	< 0.1	0.001
114	0.63	0.03	5.1	15.3	39.4	60.9	108	2.5	21	206	6.4	1.9	< 0.1	4	< 0.1	0.1	996	30	56.9	6.5	21.6	3.3	2.4	0.3	1	31.3	0.3	< 0.1	0.2	< 0.1	0.3	8.4	< 0.001
497	1.45	0.08	29.9	242	30.7	282	113	5.9	9.9	143	2.5	3.9	< 0.1	11	< 0.1	0.5	39	58	132	16.3	51.9	7.8	5	0.5	2.2	389	0.4	< 0.1	0.5	< 0.1	0.2	7.4	0.001
3.4	< 0.05	< 0.02	< 0.1	13.1	0.6	3.2	0.9	< 0.1	6.8	2	0.3	5	< 0.1	< 1	0.1	< 0.1	19	0.3	0.6	< 0.1	0.2	< 0.1	< 0.1	< 0.1	< 0.1	12.6	< 0.1	< 0.1	< 0.1	< 0.1	< 0.1	0.3	< 0.001
32.6	0.83	48.5	5.2	52.3	10.4	2.5	24.4	15.8	288	44	1.2	5.9	0.7	< 1	< 0.1	0.4	59	8	15.6	1.9	8.1	2	2.4	0.4	2.9	> 10000	0.6	0.3	1.8	0.3	< 0.1	< 0.1	0.015
18	1.67	2.23	1.6	23.2	18.9	8.2	35.2	7.2	45.1	87	0.4	0.3	< 0.1	< 1	< 0.1	0.2	146	79.9	152	17.1	58.5	8.9	5.7	0.6	2.3	58.2	0.3	0.1	0.6	0.1	< 0.1	< 0.1	0.008
> 500	0.21	0.84	8.8	145	30.5	1910	0.4	3.9	1.6	71	0.4	2.5	< 0.1	< 1	0.2	1	1	3.4	7.5	1	4	1.2	1.3	0.2	1	668	0.3	< 0.1	0.3	< 0.1	< 0.1	1.1	0.015
> 500	0.35	27.4	117	7.7	0.3	1360	0.5	0.5	0.5	4	0.1	0.8	< 0.1	< 1	0.4	30.4	2	26.1	53.5	5.7	17.5	2.5	1.3	0.1	0.4	624	0.9	< 0.1	< 0.1	< 0.1	< 0.1	0.2	0.029
19.1	0.12	1.14	2.5	7.6	33.8	13.9	76.6	1.6	31.3	126	11	0.9	< 0.1	2	0.3	1.6	918	1.6	4.2	0.5	2.2	0.5	0.5	< 0.1	0.5	9.8	0.8	< 0.1	0.5	< 0.1	0.7	1.1	0.025
5.8	0.35	0.46	1.1	8.8	24.7	7.2	190	2.2	6.9	63	7.9	0.9	< 0.1	2	0.6	0.5	749	33.3	62.3	6.4	20.3	2.4	1.3	0.1	0.5	5.8	0.4	< 0.1	0.3	< 0.1	0.5	1.1	0.014
10.7	0.33	0.41	2.8	11.8	7	2.7	2.2	6.8	36.2	23	1.7	1	< 0.1	4	< 0.1	1	7	3.1	7.1	0.9	4.2	1.2	1.3	0.2	1.4	5.7	0.4	0.1	0.6	< 0.1	< 0.1	5.6	0.023
11.2	0.65	0.2	0.9	36	12.4	6.7	17.1	7.8	53.5	30	3.1	0.9	< 0.1	< 1	0.1	0.4	9	27.5	53.1	5.7	19.6	3	2.3	0.3	1.5	5.4	0.4	0.1	0.7	0.1	0.2	0.4	0.019
8	1.68	0.21	1.6	9.4	12.1	4.7	1.8	18.7	43.4	140	3.3	1.5	< 0.1	< 1	< 0.1	0.6	18	58.8	112	12.6	45.3	7.9	6.9	0.9	4.3	4.4	0.5	0.2	1.2	0.2	< 0.1	0.3	0.017
19.9	0.73	0.15	7.6	10.1	2.1	2.3	0.9	22.8	93.2	73	1.8	1	< 0.1	< 1	0.1	4.5	8	3	8.6	1.3	6.3	2.4	3.3	0.7	4.8	12.6	0.1	0.4	2.1	0.3	< 0.1	0.3	0.017
11	0.39	0.39	1.1	75.3	14	1.4	0.2	7.2	6.6	191	2	3.2	< 0.1	< 1	0.1	0.7	8	4.1	8.2	1	4.1	1.2	1.4	0.2	1.5	5.2	0.2	0.1	0.7	0.1	0.1	< 0.1	0.016
8.9	0.45	1.48	2.5	6.4	1.5	1.6	0.3	10.6	70.2	36	1.2	1	< 0.1	< 1	< 0.1	< 0.1	2	11	21.7	2.5	9.3	1.8	2	0.3	2.1	224	0.2	0.2	1	0.2	0.1	0.2	0.001

Tl	Pb	Sc	Th	U	Ti	P	S
ppm	ppm	ppm	ppm	ppm	%	%	%
0.05	0.5	1	0.1	0.1	0.0005	0.001	0.01
TD-MS	TD-MS	TD-ICP	TD-MS	TD-MS	TD-ICP	TD-ICP	TD-ICP
< 0.05	3.2	9	4.6	1.3	0.362	0.071	11.4
< 0.05	5.1	15	3.2	0.9	0.246	0.072	5.3
< 0.05	1.3	52	2	0.8	0.583	0.046	0.34
< 0.05	2.2	4	2.3	1.2	0.117	0.007	0.05
0.06	3	4	8.9	1.9	0.362	0.054	4.32
< 0.05	2.4	87	0.9	1.4	1.15	0.054	3.95
0.31	1.4	9	6.8	1.6	0.263	0.06	0.16
< 0.05	0.8	43	0.3	< 0.1	0.151	0.021	0.05
< 0.05	5.1	44	0.2	0.2	0.761	0.03	0.06
< 0.05	4.1	9	5.3	2.4	0.288	0.128	1.99
< 0.05	1.5	61	0.9	1.1	0.571	0.05	0.77
0.06	1.9	37	1.9	0.8	0.66	0.039	4.04
< 0.05	2.4	25	4.7	1.7	0.47	0.052	3.52
< 0.05	1.5	4	8.5	4.6	0.119	0.003	0.14
< 0.05	2	3	8.6	2.2	0.481	0.038	0.74
< 0.05	4	13	3.9	1.3	0.481	0.041	3.12
< 0.05	3.1	21	2	0.6	0.577	0.031	2.47
0.23	2.1	18	16.1	1.6	0.361	0.022	0.43
0.18	3.3	7	14	2.7	0.312	0.031	0.49
0.17	3	5	2.8	1.4	0.322	0.037	1.33
0.19	4.7	4	6.4	1.4	0.108	0.022	0.27
0.28	7.2	4	5.2	0.7	0.0953	0.019	0.11
0.48	3.8	6	7.7	1.2	0.157	0.029	0.19
1	3.2	13	16.6	2.3	0.321	0.026	0.38
0.32	315	10	2.7	1.9	0.0217	0.038	19.2
< 0.05	32.5	15	9.2	3	0.0287	0.093	4.84
< 0.05	49	2	6.2	39.6	0.0766	0.046	0.1
0.26	47.2	9	> 200	422	0.25	0.045	0.08
< 0.05	3.7	15	5.5	1.8	0.504	0.022	1.19
< 0.05	4.4	5	5.4	9.7	0.713	0.025	2.68
< 0.05	1.9	< 1	0.6	0.2	0.0106	0.008	0.07
< 0.05	2.4	< 1	1.7	1	0.0093	0.038	0.1
1.19	1.8	40	1.5	2.7	0.293	0.007	0.03
0.07	1.9	5	0.1	< 0.1	0.0434	0.007	1.07
0.08	2.8	6	5.7	1	0.187	0.031	1.14
0.17	45.7	8	9.7	26.3	0.244	0.045	0.63
0.37	35.7	7	12	12.4	0.313	0.045	0.43
0.39	418	14	14.6	136	0.146	0.022	0.04
0.33	37.1	8	6.5	10.4	0.15	0.014	0.91
0.09	22.6	3	2.9	9.6	0.067	0.014	0.8
< 0.05	2.3	39	0.4	0.1	0.145	0.028	0.17
< 0.05	12.4	1	1.3	5.6	0.041	0.008	0.77
0.07	10.6	4	1	1.8	0.0436	0.003	0.41
< 0.05	0.9	< 1	0.1	< 0.1	0.0095	0.007	< 0.01
0.1	4.6	6	4.8	1.1	0.0847	0.056	7.15
0.3	3.7	7	6	1	0.173	0.039	0.02

Tl	Pb	Sc	Th	U	Ti	P	S
ppm	ppm	ppm	ppm	ppm	%	%	%
0.05	0.5	1	0.1	0.1	0.0005	0.001	0.01
TD-MS	TD-MS	TD-ICP	TD-MS	TD-MS	TD-ICP	TD-ICP	TD-ICP
0.18	1.1	2	1.3	0.3	0.0321	0.009	0.01
0.1	23.6	39	0.3	0.3	0.514	0.03	0.08
0.38	1.7	8	8.9	1.2	0.24	0.044	0.02
< 0.05	8.2	14	6.2	2.5	0.306	0.122	0.97
< 0.05	5.2	7	4.9	3.6	0.254	0.081	0.82
< 0.05	77.6	8	0.5	0.3	0.0772	0.001	5.23
< 0.05	1.5	47	0.8	1	0.461	0.093	0.95
< 0.05	3.8	< 1	< 0.1	0.1	0.0056	0.001	0.2
0.76	2.6	14	11	1.9	0.403	0.033	3.98
0.05	3.9	8	10.4	2.1	0.293	0.046	4.6
< 0.05	6.5	5	0.7	0.3	0.03	0.038	0.22
< 0.05	2.2	3	0.5	2.9	0.024	0.081	0.2
< 0.05	5.5	3	1.3	0.5	0.0852	0.012	1.94
< 0.05	4.4	10	1.3	1	0.068	1.83	3.68
0.22	152	< 1	0.4	0.2	0.0214	0.005	0.93
< 0.05	5.3	6	7.9	16.3	0.632	0.027	2.67
< 0.05	3.1	3	2.5	2.4	0.617	0.015	1.48
0.96	7	26	5.4	1.8	0.25	0.01	0.2
< 0.05	7.7	5	1.6	0.9	0.0443	0.187	1.5
0.64	2.8	19	8.8	1.7	0.386	0.041	1.1
< 0.05	2.9	3	9.6	5.7	0.527	0.085	4.33
< 0.05	1.9	2	2.5	0.4	0.105	0.029	0.02
0.57	2.1	8	9.7	2.8	0.228	0.085	0.03
0.89	3.5	8	12.5	41.7	0.217	0.093	0.01
< 0.05	< 0.5	< 1	0.1	0.1	0.0036	0.004	0.03
0.28	1.4	7	7.2	1.2	0.185	0.041	< 0.01
< 0.05	0.6	< 1	0.1	< 0.1	0.0016	0.003	0.02
0.07	7.7	47	0.5	0.1	0.617	0.034	0.1
< 0.05	2	< 1	< 0.1	0.1	0.0026	0.002	1.28
< 0.05	1.2	72	1	1.3	0.805	0.058	2.55
< 0.05	2.2	1	3.4	1.9	0.46	0.034	3.7
0.36	3.6	42	2.6	1.3	0.597	0.037	6.72
< 0.05	1	53	0.6	0.1	0.196	0.042	0.31
< 0.05	3.1	5	5.2	1.8	0.377	0.034	9.09
< 0.05	1.7	40	2.1	1.2	0.703	0.041	3.98
< 0.05	2.1	58	2.3	1.7	0.599	0.044	2.3
< 0.05	2.3	40	1.5	0.6	0.398	0.04	2.99
0.08	277	4	11.2	65.1	0.295	0.063	0.03
< 0.05	119	2	0.8	181	0.0482	0.014	0.03
0.05	5.7	30	61.5	4.9	0.292	0.036	14.1
< 0.05	1.9	16	0.6	0.1	0.299	0.021	0.06
0.7	3.5	13	7.9	0.6	0.303	0.034	0.02
< 0.05	3.6	37	0.4	0.1	0.275	0.019	0.1
0.4	2.9	8	8.1	0.8	0.28	0.05	0.18
0.73	3.1	14	13.8	1.3	0.285	0.049	0.18
< 0.05	1.3	13	6.5	1.2	0.385	0.068	0.42

Tl ppm 0.05 TD-MS	Pb ppm 0.5 TD-MS	Sc ppm 1 TD-ICP	Th ppm 0.1 TD-MS	U ppm 0.1 TD-MS	Ti % 0.0005 TD-ICP	P % 0.001 TD-ICP	S % 0.01 TD-ICP
< 0.05	4	31	2.2	3.5	0.705	0.034	0.82
0.47	4.9	14	11	3.1	0.349	0.032	0.11
< 0.05	18.6	4	11.8	4.9	0.345	0.037	1.79
< 0.05	760	4	10.8	4	0.52	0.014	0.38
0.13	4	10	11	1.2	0.287	0.025	1.25
< 0.05	2.2	< 1	0.9	0.3	0.0089	0.012	8.88
< 0.05	3.7	5	6.1	1.1	0.0723	0.041	5.09
0.39	2.9	28	9.3	1	0.142	0.016	13.3
0.38	2.9	4	6.7	1.3	0.155	0.061	8.02
< 0.05	18.1	5	3.8	1.3	0.0095	0.054	13.6
< 0.05	3	3	9.5	2.9	0.35	0.026	7.25
< 0.05	1	1	1.1	1.1	0.0176	0.018	0.06
< 0.05	1.3	2	0.8	1.2	0.0213	0.01	0.07
< 0.05	0.9	2	0.7	0.7	0.0246	0.011	0.15
< 0.05	1	< 1	0.1	0.6	0.0023	0.011	0.06
< 0.05	1.5	< 1	0.2	2.6	0.005	0.006	0.04
< 0.05	1.7	48	0.4	0.1	0.501	0.034	0.26
0.24	2.9	37	0.2	4.5	0.423	0.022	0.44
0.1	0.8	2	2.2	0.5	0.0283	0.019	0.04
0.57	1.8	9	3	1.5	0.204	0.067	0.43
1.64	4.3	24	4.4	2.3	0.119	0.016	0.04
0.14	34.8	3	2	0.5	0.119	0.034	1.13
1.14	30	20	11.4	1.9	0.502	0.133	1.58
< 0.05	4.3	30	0.7	0.4	0.069	0.019	0.06
0.05	5.3	17	1	0.5	0.256	0.018	0.32
0.06	16.4	< 1	0.5	4.3	0.0068	0.024	1.6
< 0.05	2.3	5	2.1	0.8	0.386	0.017	0.38
< 0.05	1.9	31	3.1	0.7	0.613	0.03	0.59
< 0.05	6.2	19	36.8	2.3	0.361	0.023	1.95
< 0.05	2.7	2	10.3	2	0.232	0.03	0.01
0.09	2.6	8	20.7	2.6	0.19	0.028	< 0.01
< 0.05	1.1	8	7.6	0.9	0.0582	0.053	0.05
< 0.05	1.1	43	0.7	< 0.1	0.346	0.021	0.07
< 0.05	4.4	44	0.4	< 0.1	0.554	0.023	0.15
< 0.05	2.3	45	0.3	< 0.1	0.558	0.025	0.07
< 0.05	0.8	41	0.3	< 0.1	0.542	0.024	0.19
0.05	1	42	0.9	0.2	0.451	0.023	0.13
0.05	1.1	41	0.3	0.1	0.526	0.024	0.1
0.39	0.6	38	0.2	0.5	0.399	0.018	0.09
0.08	4	30	1.4	0.8	0.155	0.014	0.23
< 0.05	2.5	8	4.5	0.4	0.0837	0.052	0.91
0.34	4.1	14	7	1.1	0.238	0.045	0.03
0.24	2	7	9.6	0.9	0.258	0.052	0.01
0.06	3.4	12	14.8	2.8	0.176	0.074	0.02
0.18	1.7	9	7.1	1.5	0.341	0.058	0.08
0.19	1.4	8	6.9	1.5	0.188	0.053	0.11

Tl ppm 0.05 TD-MS	Pb ppm 0.5 TD-MS	Sc ppm 1 TD-ICP	Th ppm 0.1 TD-MS	U ppm 0.1 TD-MS	Ti % 0.0005 TD-ICP	P % 0.001 TD-ICP	S % 0.01 TD-ICP
0.33	16.8	4	1	0.5	0.124	0.03	0.03
0.31	3	13	9.5	3.4	0.329	0.047	0.05
< 0.05	1.2	2	0.2	< 0.1	0.0115	0.01	0.06
< 0.05	3.1	< 1	0.1	0.8	0.0023	0.004	0.03
< 0.05	1.3	46	0.4	0.1	0.386	0.021	0.02
< 0.05	11	56	0.4	0.1	0.776	0.036	0.11
< 0.05	1.6	38	0.3	< 0.1	0.419	0.022	0.03
0.07	2.3	48	0.4	< 0.1	0.669	0.03	0.15
< 0.05	3.1	34	0.2	< 0.1	0.623	0.029	0.04
< 0.05	2.6	38	0.3	0.7	0.505	0.025	0.17
0.06	3	< 1	0.6	0.1	0.0157	0.009	0.07
< 0.05	0.9	< 1	< 0.1	1.3	0.0035	0.003	0.03
< 0.05	1.1	52	0.4	< 0.1	0.232	0.021	0.05
0.1	27.7	11	6.6	0.7	0.155	0.024	0.91
< 0.05	361	11	3.5	0.8	0.177	0.004	0.72
0.3	3.1	15	18.4	1.9	0.191	0.017	0.19
0.43	4.2	46	5.2	0.6	0.449	0.013	0.51
0.39	128	19	13.4	2.4	0.179	0.025	4.49
< 0.05	4.8	< 1	0.2	< 0.1	0.0162	< 0.001	0.01
0.21	2.3	40	6.4	2.3	0.378	0.026	0.83
0.13	3	14	21.7	1.3	0.349	0.022	0.01
< 0.05	6.2	15	37.9	5.2	0.0383	0.062	0.54
< 0.05	11.7	< 1	2.5	0.2	0.001	0.001	> 20.0
1.68	2.7	15	6.5	1.9	0.525	0.051	0.06
1.47	1.7	16	19.5	1	0.356	0.087	0.02
0.05	3.3	2	2.9	2.1	0.175	0.031	0.05
0.12	1.3	7	8.5	1.6	0.155	0.045	0.07
< 0.05	8.3	4	18.8	11.1	0.318	0.452	0.05
< 0.05	28.3	3	7.2	22	0.103	0.051	0.11
< 0.05	2	5	11.6	2	0.09	0.134	1.1
< 0.05	1.1	2	5.6	0.8	0.0398	0.024	0.09

Geochemical procedure - Ultratrace 6 - Total Digestion - ICP/MS

Sample decomposition - Combination of four acids
Analytical method - Inductively Coupled Plasma - Mass Spectrometry (ICP-MS)

A 0.25 g sample is digested with four acids beginning with hydrofluoric, followed by a mixture of nitric and perchloric acids, heated using precise programmer controlled heating in several ramping and holding cycles which takes the samples to dryness. After dryness is attained, samples are brought back into solution using hydrochloric and nitric acids. With this digestion, certain phases may be only partially solubilized. These phases include zircon, monazite, sphene, gahnite, chromite, cassiterite, rutile and barite. Ag greater than 100 ppm and Pb greater than 5000 ppm should be assayed as high levels may not be solubilized. Only sulphide sulfur will be solubilized.

The samples are then analyzed using a Varian ICP. QC for the digestion is 14% for each batch, 5 method reagent blanks, 10 in-house controls, 10 samples duplicates, and 8 certified reference materials. An additional 13% QC is performed as part of the instrumental analysis to ensure quality in the areas of instrumental drift.

Total Digestion – ICP/MS Portion

Additional elements are determined by ICP/MS on the multi-acid digest solution above. The samples are diluted and analyzed on a Perkin Elmer Sciex ELAN 6000, 6100 or 9000 ICP/MS. One blank is run for every 40 samples. In-house control is run every 20 samples. Digested standards are run every 80 samples. After every 15 samples, a digestion duplicate is analyzed. Instrument is recalibrated every 80 samples.

Code Ultratrace-6 - Elements and Detection Limits (**Concentration in ppm except where noted)**

Element	Detection Limit	Upper Limit	Reported By	Element	Detection Limit	Upper Limit	Reported By
Ag	0.05	50	ICP&ICP/MS	Na	0.001%	3%	ICP
Al	0.01%	10%	ICP	Nb	0.1	500	ICP/MS
As	0.1	10,000	ICP/MS	Nd	0.1	-	ICP/MS
Ba	1	6,000	ICP/MS	Ni	0.5	5,000	ICP/MS
Be	0.1	1,000	ICP/MS	P	0.001%	-	ICP
Bi	0.02	2,000	ICP/MS	Pb	0.5	5,000	ICP/MS
Ca	0.01%	50%	ICP	Pr	0.1	-	ICP/MS
Cd	0.1	-	ICP/MS	Rb	0.2	500	ICP/MS
Ce	0.1	10,000	ICP/MS	Re	0.001	100	ICP/MS
Co	0.1	500	ICP/MS	S	0.01%	20%	ICP
Cr	0.5	5,000	ICP/MS	Sb	0.1	500	ICP/MS
Cs	0.05	-	ICP/MS	Sc	1	-	ICP
Cu	0.2	10,000	ICP/MS	Se	0.1	1,000	ICP/MS
Dy	0.1	-	ICP/MS	Sm	0.1	100	ICP/MS
Er	0.1	-	ICP/MS	Sn	1	200	ICP/MS
Eu	0.05	100	ICP/MS	Sr	0.2	1,000	ICP/MS
Fe	0.01%	50%	ICP	Ta	0.1	50	ICP/MS
Ga	0.1	500	ICP/MS	Tb	0.1	100	ICP/MS
Ge	0.1	500	ICP/MS	Te	0.1	500	ICP/MS
Gd	0.1	-	ICP/MS	Th	0.1	200	ICP/MS
Hf	0.1	500	ICP/MS	Ti	0.0005%	-	ICP
Ho	0.1	-	ICP/MS	Tl	0.05	500	ICP/MS
In	0.1	100	ICP/MS	Tm	0.1	-	ICP/MS
K	0.01%	5%	ICP	U	0.1	10,000	ICP/MS
La	0.1	10,000	ICP/MS	V	1	1,000	ICP/MS
Li	0.5	-	ICP/MS	W	0.1	200	ICP/MS
Lu	0.1	100	ICP/MS	Y	0.1	-	ICP/MS
Mg	0.01%	50%	ICP	Yb	0.1	200	ICP/MS
Mn	1	10,000	ICP	Zn	0.2	10,000	ICP/MS
Mo	0.1	10,000	ICP/MS	Zr	1	5,000	ICP/MS

Quality Analysis ... *Innovative Technologies*

Date Submitted: 15-Aug-13
Invoice No.: A13-09934
Invoice Date: 30-Aug-13
Your Reference: 33693-33694

Techni-Lab Abitibi Inc.(Actlabs)
184 Rue Principale
Ste-Germaine-Boule Quebec J0Z 1M0
Canada

ATTN: Andre Caouette

CERTIFICATE OF ANALYSIS

97 Pulp samples were submitted for analysis.

The following analytical package was requested: Code UT-6 Total Digestion ICP & ICP/MS

REPORT **A13-09934**

This report may be reproduced without our consent. If only selected portions of the report are reproduced, permission must be obtained. If no instructions were given at time of sample submittal regarding excess material, it will be discarded within 90 days of this report. Our liability is limited solely to the analytical cost of these analyses. Test results are representative only of material submitted for analysis.

Notes:

CERTIFIED BY :

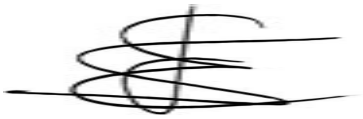

Emmanuel Eseme , Ph.D.
Quality Control

ISO/IEC 17025
SCC Accredited
LAB 266
LAB 266
Accrédité CCN

ACTIVATION LABORATORIES LTD.

1336 Sandhill Drive, Ancaster, Ontario Canada L9G 4V5 TELEPHONE +1.905.648.9611 or +1.888.228.5227 FAX +1.905.648.9613
E-MAIL Ancaster@actlabs.com ACTLABS GROUP WEBSITE www.actlabs.com

Analyte Symbol	Li	Na	Mg	Al	K	Ca	Cd	V	Cr	Mn	Fe	Hf	Hg	Ni	Er	Be	Ho	Ag	Cs	Co	Eu	Bi	Se	Zn
Unit Symbol	ppm	%	%	%	%	%	ppm	ppm	ppm	ppm	%	ppm	ppb	ppm	ppm	ppm	ppm	ppm	ppm	ppm	ppm	ppm	ppm	ppm
Detection Limit	0.5	0.01	0.01	0.01	0.01	0.01	0.1	1	0.5	1	0.01	0.1	10	0.5	0.1	0.1	0.1	0.05	0.05	0.1	0.05	0.02	0.1	0.2
Analysis Method	TD-MS	TD-MS	TD-MS	TD-MS	TD-MS	TD-MS	TD-MS	TD-MS	TD-MS	TD-MS	TD-MS	TD-MS	TD-MS	TD-MS	TD-MS	TD-MS	TD-MS	TD-MS	TD-MS	TD-MS	TD-MS	TD-MS	TD-MS	TD-MS
129051	17.4	> 3.00	3.25	5.67	0.93	3.76	< 0.1	114	72.1	607	5.02	2.0	40	189	1.9	1.3	0.7	0.34	1.16	62.5	0.94	0.53	10.5	15.8
129052	17.2	> 3.00	1.28	6.16	1.17	0.65	< 0.1	112	94.2	134	3.97	2.3	40	142	3.2	1.7	1.0	0.37	1.18	52.0	0.52	0.59	10.5	14.0
129053	21.7	> 3.00	1.15	7.07	1.36	0.18	< 0.1	131	109	71	0.95	2.7	20	123	2.6	2.1	0.8	0.11	1.74	3.8	0.57	0.04	2.0	9.9
129054	21.0	> 3.00	2.93	6.69	1.06	2.51	< 0.1	120	106	433	3.18	2.6	20	151	2.4	1.7	0.8	0.37	1.83	28.9	0.54	0.64	6.6	14.3
129055	22.7	> 3.00	1.74	7.18	1.46	0.49	< 0.1	149	94.0	100	2.12	2.9	< 10	159	2.7	1.8	0.9	0.38	2.53	27.5	1.50	0.26	5.3	13.5
129056	22.8	> 3.00	1.48	7.05	1.51	0.58	< 0.1	138	83.8	143	2.86	2.9	60	150	2.9	2.4	1.0	0.39	2.06	51.1	1.00	0.65	7.2	14.8
129057	23.2	> 3.00	1.35	6.70	1.46	0.44	< 0.1	134	93.0	116	2.82	2.6	80	164	3.0	2.4	1.0	0.37	1.91	32.8	1.36	0.49	7.5	14.8
129058	24.5	> 3.00	1.30	7.34	1.82	0.39	< 0.1	153	111	88	1.55	2.8	40	139	2.5	2.7	0.8	0.32	1.92	12.1	0.79	0.22	4.6	16.3
129059	20.2	> 3.00	1.83	5.32	1.14	0.73	< 0.1	125	151	175	1.55	3.0	30	125	1.8	1.6	0.6	0.37	1.58	13.0	0.58	0.14	2.8	9.6
129060	21.4	> 3.00	1.98	6.95	1.07	1.03	< 0.1	119	117	191	2.34	2.6	20	153	2.6	1.5	0.8	0.36	2.02	27.9	0.70	0.39	5.6	13.8
129061	21.1	> 3.00	1.83	7.55	1.65	1.33	< 0.1	127	138	283	2.00	2.6	< 10	133	2.8	2.0	0.9	0.35	1.90	27.5	0.71	0.20	4.1	12.6
129062	31.0	2.98	1.74	7.17	1.82	1.14	< 0.1	159	108	271	3.19	2.6	80	162	2.5	4.1	0.8	0.38	2.24	36.4	0.63	0.46	10.3	16.2
129063	9.4	1.83	7.43	3.01	0.55	13.5	< 0.1	60	62.5	3070	4.35	1.1	10	75.9	1.8	1.0	0.6	0.21	0.44	21.0	0.68	0.20	4.5	14.2
129064	3.8	1.00	10.1	1.44	0.20	19.2	< 0.1	31	35.3	4510	4.29	0.5	< 10	26.3	1.6	0.5	0.6	0.10	0.14	13.5	0.55	0.07	0.9	10.7
129065	20.9	2.46	4.43	5.22	1.49	7.23	< 0.1	104	68.6	1530	4.50	1.9	40	152	2.1	1.9	0.7	0.33	1.48	24.2	0.77	0.73	6.3	11.4
129066	29.1	> 3.00	1.51	6.45	2.16	0.76	< 0.1	143	91.1	157	4.80	2.6	90	173	3.2	2.5	1.0	0.42	2.21	73.1	1.13	1.08	8.7	11.1
129067	29.0	> 3.00	1.80	7.04	2.32	1.37	< 0.1	150	71.7	263	3.07	3.4	40	147	2.9	2.7	0.9	0.43	2.11	20.8	1.02	0.72	3.3	10.2
129068	27.9	> 3.00	1.56	7.03	2.28	1.00	< 0.1	123	70.3	214	2.34	2.8	70	106	2.3	2.9	0.8	0.40	1.98	19.2	1.07	0.57	2.3	7.1
129069	37.1	1.34	1.56	6.56	3.37	0.78	< 0.1	223	92.6	200	6.72	3.6	110	258	3.5	3.6	1.1	0.58	2.54	53.2	0.89	1.50	10.3	23.4
129070	29.7	2.96	1.73	5.30	1.81	1.01	< 0.1	139	126	250	2.18	3.4	50	101	1.7	2.6	0.5	0.45	2.32	14.6	0.78	0.44	2.7	9.2
129071	28.9	2.45	1.41	6.39	2.10	1.12	< 0.1	106	129	205	3.67	2.8	10	118	2.7	2.5	0.9	0.34	2.54	71.0	1.70	0.50	4.7	9.8
129072	29.4	2.72	1.62	6.88	1.86	1.37	< 0.1	114	120	230	2.07	2.9	< 10	78.5	2.8	2.5	0.9	0.29	2.50	23.2	1.03	0.19	2.4	8.5
129073	24.2	> 3.00	1.28	6.55	1.81	0.92	< 0.1	106	97.8	140	1.31	2.5	< 10	54.5	2.5	2.4	0.8	0.14	2.20	10.4	0.68	0.14	1.4	6.9
129074	27.9	2.66	1.59	6.53	2.09	1.24	< 0.1	108	90.8	224	2.60	2.3	20	118	2.6	2.4	0.9	0.32	2.48	28.8	0.89	0.41	4.4	11.0
129075	22.9	> 3.00	1.80	7.15	1.83	2.00	< 0.1	102	83.4	330	1.95	2.6	10	79.6	2.4	2.2	0.8	0.29	2.17	13.4	0.87	0.39	2.5	8.2
129076	21.8	2.96	1.21	5.56	1.78	0.73	< 0.1	101	133	124	3.99	2.7	40	139	2.8	2.1	1.0	0.33	2.05	38.4	1.10	0.85	9.9	9.8
129077	23.3	> 3.00	1.42	5.95	1.76	0.83	< 0.1	105	113	141	3.56	2.7	20	122	3.0	2.2	1.0	0.33	2.24	33.3	0.88	0.64	6.3	10.9
129078	15.2	> 3.00	1.59	6.72	1.04	1.92	< 0.1	114	106	322	1.86	2.8	< 10	80.9	2.4	1.6	0.8	0.32	1.54	27.5	0.44	0.25	2.5	8.2
129079	14.9	> 3.00	2.15	6.84	0.96	2.83	< 0.1	172	122	471	1.87	2.5	< 10	80.0	1.9	1.6	0.6	0.30	1.94	10.9	0.41	0.10	2.2	11.0
129080	13.0	> 3.00	1.89	7.43	0.88	2.16	< 0.1	125	80.3	275	1.59	2.1	30	58.5	2.0	1.3	0.7	0.18	2.08	19.7	0.31	0.10	2.0	11.9
129081	14.2	> 3.00	1.31	6.36	1.00	0.24	< 0.1	154	137	67	0.99	3.1	< 10	49.2	1.4	1.6	0.5	0.39	2.19	1.2	0.25	0.03	0.8	9.7
129082	19.5	> 3.00	1.80	7.40	0.88	0.79	< 0.1	140	88.4	146	1.49	2.5	< 10	74.9	1.4	1.7	0.4	0.24	2.07	9.3	0.22	< 0.02	1.6	15.7
129083	16.0	> 3.00	1.29	7.54	0.60	0.82	< 0.1	128	93.1	192	1.29	2.3	30	55.9	1.4	1.4	0.4	0.22	1.10	4.7	0.35	0.02	1.6	13.5
129084	2.7	0.04	8.13	0.23	0.12	14.0	< 0.1	3	12.5	670	0.87	< 0.1	< 10	10.6	0.1	< 0.1	< 0.1	< 0.05	0.05	0.7	0.07	< 0.02	0.1	20.4
129085	3.0	0.02	9.87	0.25	0.15	15.6	1.5	2	8.1	743	0.90	0.2	< 10	12.0	0.1	0.2	< 0.1	< 0.05	0.06	1.1	0.05	< 0.02	0.2	745
129086	3.4	0.01	9.56	0.30	0.18	15.8	5.0	3	9.4	824	1.27	0.3	80	13.0	0.1	0.1	< 0.1	0.06	0.06	1.7	< 0.05	< 0.02	0.3	2400
129087	2.8	0.01	10.0	0.24	0.15	15.9	1.1	2	8.7	778	0.98	0.1	< 10	11.5	< 0.1	0.2	< 0.1	< 0.05	< 0.05	0.9	< 0.05	< 0.02	0.3	570
129088	3.1	0.01	10.7	0.29	0.19	16.6	9.4	4	9.5	892	1.17	0.3	80	13.2	0.1	0.1	< 0.1	0.05	< 0.05	1.4	< 0.05	< 0.02	0.4	4130
129089	3.0	0.01	10.5	0.34	0.19	16.1	0.7	4	11.5	766	0.97	0.3	< 10	12.9	0.1	< 0.1	< 0.1	0.05	< 0.05	1.5	0.05	< 0.02	0.1	332
129090	2.8	0.01	9.00	0.31	0.19	14.3	2.4	3	10.6	660	0.88	0.2	< 10	11.0	0.2	0.2	< 0.1	0.10	< 0.05	1.3	0.06	< 0.02	0.2	1060
129091	3.3	0.01	9.53	0.43	0.24	14.6	< 0.1	2	9.4	684	1.04	< 0.1	< 10	10.8	0.1	< 0.1	< 0.1	< 0.05	0.06	1.0	0.06	< 0.02	< 0.1	33.8
129092	3.1	< 0.01	9.91	0.36	0.21	15.2	1.0	4	10.2	527	0.92	< 0.1	< 10	12.0	0.1	0.1	< 0.1	0.09	< 0.05	1.3	0.06	< 0.02	0.1	394
1272128	5.4	> 3.00	0.72	7.15	0.08	2.00	0.8	90	102	203	13.7	2.5	150	146	1.6	0.7	0.6	5.64	< 0.05	74.6	0.29	0.10	12.0	70.8
1272129	8.1	0.04	15.0	0.59	0.03	16.5	< 0.1	14	23.2	1900	2.59	0.2	< 10	13.9	0.2	0.4	< 0.1	0.59	< 0.05	20.5	0.07	0.07	0.1	58.4
1272130	8.7	0.03	11.7	0.70	0.03	15.5	< 0.1	10	146	2110	2.56	0.2	< 10	15.7	0.2	0.5	< 0.1	0.44	< 0.05	16.1	0.08	0.06	0.1	32.3
1272131	22.4	0.05	9.29	0.81	0.04	25.4	< 0.1	25	31.0	3210	2.03	0.3	< 10	33.9	2.5	0.4	0.8	0.29	0.06	34.1	1.47	0.03	0.6	29.8
1272132	3.3	0.02	3.68	0.06	0.05	13.6	< 0.1	< 1	194	1620	1.15	< 0.1	< 10	12.1	< 0.1	< 0.1	< 0.1	0.29	0.07	12.5	0.09	< 0.02	0.2	21.7
1272133	2.6	0.03	7.63	0.12	0.10	11.4	< 0.1	< 1	247	538	0.49	< 0.1	< 10	10.4	< 0.1	< 0.1	< 0.1	0.21	0.08	3.0	0.08	< 0.02	0.2	4.9
1272134	49.9	> 3.00	4.16	9.59	0.05	6.01	< 0.1	341	313	858	8.89	1.7	< 10	126	2.7	1.3	0.9	0.20	0.12	30.7	0.90	< 0.02	1.2	66.9
1272135	26.3	1.94	5.19	7.30	0.96	12.0	< 0.1	276	343	1540	7.82	1.1	50	93.1	2.8	0.8	1.0	0.57	1.78	42.7	1.56	31.3	3.2	72.1
1272136	43.2	0.03	10.6	2.45	0.62	12.2	< 0.1	18	100	1620	1.58	0.2	< 10	17.1	0.5	0.5	0.2	0.23	0.43	5.5	0.22	0.36	< 0.1	31.7
1272137	9.1	0.08	0.34	3.57	1.32	0.20	< 0.1	76	296	79	1.56	0.1	< 10	16.6	1.2	0.7	0.4	0.33	1.16	23.7	0.29	0.26	3.5	10.4

Analyte Symbol	Li	Na	Mg	Al	K	Ca	Cd	V	Cr	Mn	Fe	Hf	Hg	Ni	Er	Be	Ho	Ag	Cs	Co	Eu	Bi	Se	Zn
Unit Symbol	ppm	%	%	%	%	%	ppm	ppm	ppm	ppm	%	ppm	ppb	ppm	ppm	ppm	ppm	ppm	ppm	ppm	ppm	ppm	ppm	ppm
Detection Limit	0.5	0.01	0.01	0.01	0.01	0.01	0.1	1	0.5	1	0.01	0.1	10	0.5	0.1	0.1	0.1	0.05	0.05	0.1	0.05	0.02	0.1	0.2
Analysis Method	TD-MS	TD-MS	TD-MS	TD-MS	TD-MS	TD-MS	TD-MS	TD-MS	TD-MS	TD-MS	TD-MS	TD-MS	TD-MS	TD-MS	TD-MS	TD-MS	TD-MS	TD-MS	TD-MS	TD-MS	TD-MS	TD-MS	TD-MS	TD-MS
1272138	55.1	0.24	1.56	9.91	3.10	0.05	< 0.1	205	158	283	4.43	1.7	< 10	42.5	1.4	1.7	0.5	0.22	3.17	0.3	0.52	0.22	6.2	44.8
1272139	24.0	0.26	0.82	1.85	0.22	0.11	< 0.1	31	300	134	3.62	1.9	< 10	18.9	0.8	0.3	0.3	0.39	0.22	7.4	0.19	0.35	7.1	31.7
1272140	36.9	1.20	1.36	8.14	2.20	0.25	< 0.1	229	215	159	6.41	4.5	< 10	49.2	1.6	1.6	0.6	0.66	2.04	17.2	1.15	0.34	16.0	42.9
1272141	2.4	0.06	0.71	6.83	0.06	8.36	< 0.1	73	315	484	3.35	0.5	< 10	23.4	1.6	0.2	0.6	0.20	0.07	9.4	0.64	0.13	0.7	16.4
1272142	1.6	1.47	1.72	6.92	0.07	7.97	< 0.1	151	261	657	4.84	0.6	< 10	82.3	1.7	0.4	0.6	0.21	0.05	41.4	1.44	0.70	2.6	33.1
1272143	5.0	0.06	11.9	0.28	0.12	19.9	0.3	10	118	1190	2.57	< 0.1	< 10	15.3	0.2	0.2	< 0.1	1.04	0.60	5.5	0.21	7.89	61.1	14.2
L307861	10.9	> 3.00	1.62	5.75	0.06	0.80	< 0.1	109	178	249	3.31	2.3	< 10	24.8	0.6	0.8	0.2	1.13	< 0.05	3.5	0.16	0.10	4.0	21.3
L307862	14.0	> 3.00	3.24	8.59	0.06	2.52	0.1	265	159	484	6.45	1.8	< 10	30.5	1.9	0.7	0.6	1.49	0.08	8.3	0.35	0.04	2.7	52.0
L307863	49.3	> 3.00	5.05	8.98	0.28	0.51	< 0.1	231	293	384	11.9	4.5	< 10	115	1.3	1.1	0.6	0.82	0.14	248	4.07	0.06	11.1	66.7
L307864	2.3	> 3.00	0.46	> 10.0	0.08	0.58	< 0.1	47	49.3	143	0.39	1.6	< 10	14.8	0.5	1.6	0.2	0.25	0.08	2.3	0.34	< 0.02	0.4	8.6
L307865	7.2	> 3.00	0.76	> 10.0	0.79	0.27	< 0.1	90	64.9	78	0.54	2.0	< 10	30.6	0.5	2.2	0.2	0.21	0.40	2.3	0.14	< 0.02	0.3	9.1
L307866	1.1	3.00	9.11	3.32	0.04	16.1	< 0.1	11	21.4	1350	1.84	2.6	< 10	16.6	1.2	0.3	0.4	0.23	< 0.05	3.8	0.55	< 0.02	0.4	7.0
L307867	4.0	0.69	3.39	6.76	0.08	11.7	< 0.1	247	229	1630	10.5	1.0	< 10	52.9	2.2	0.2	0.8	0.20	< 0.05	33.3	1.09	0.05	0.4	71.0
L307868	13.9	2.15	4.87	7.79	0.14	8.29	< 0.1	312	230	1230	9.17	1.0	< 10	122	2.2	0.4	0.8	0.25	0.22	54.2	0.82	0.05	1.0	78.4
L307869	10.8	2.47	4.76	7.77	0.14	8.37	< 0.1	324	235	1150	9.24	0.9	< 10	102	2.6	0.7	0.9	0.24	0.27	51.2	1.09	0.06	0.6	58.0
L307870	11.9	1.54	4.78	8.12	0.07	9.65	< 0.1	304	239	1420	9.12	1.1	< 10	125	2.3	0.4	0.8	0.25	0.11	50.7	0.81	0.03	0.7	73.7
L307871	12.1	2.80	4.24	7.58	0.26	7.05	< 0.1	264	235	1240	9.66	0.9	< 10	73.3	2.5	0.5	0.9	0.18	0.57	43.9	3.40	0.03	0.7	60.0
L307872	10.0	1.92	4.78	7.85	0.14	8.97	< 0.1	288	322	1260	9.54	0.8	< 10	105	2.3	0.3	0.8	0.23	0.21	43.7	0.87	0.09	0.8	80.5
L307873	24.8	> 3.00	5.22	7.55	1.87	4.68	< 0.1	249	256	897	9.49	0.6	< 10	115	1.6	0.7	0.5	0.15	4.09	75.9	0.21	< 0.02	0.9	57.6
L307874	3.5	2.59	3.73	6.45	0.09	7.36	< 0.1	124	189	759	6.47	0.7	< 10	64.0	2.0	0.5	0.8	0.13	0.09	36.8	1.78	1.16	1.0	61.7
L307875	1.7	> 3.00	2.28	6.61	0.11	4.27	< 0.1	16	114	321	1.70	2.1	< 10	23.7	1.1	0.8	0.4	0.20	0.12	84.5	0.89	0.12	6.2	14.0
L307876	34.2	> 3.00	3.69	8.10	1.69	1.15	< 0.1	65	56.5	355	9.66	1.7	< 10	43.0	2.3	1.3	0.9	0.16	2.95	46.7	1.42	0.08	0.9	121
L307877	32.5	> 3.00	3.62	8.26	1.38	2.53	< 0.1	150	74.0	425	1.45	3.1	< 10	44.5	0.6	1.4	0.2	0.20	2.05	9.9	0.40	< 0.02	0.3	35.4
L307878	7.0	> 3.00	2.13	8.41	0.27	3.38	< 0.1	50	108	658	1.15	2.9	< 10	20.4	1.3	1.1	0.4	0.12	0.41	5.6	0.58	0.15	0.5	21.7
L307879	41.9	> 3.00	2.84	7.54	0.92	1.33	< 0.1	82	62.3	417	9.83	2.5	< 10	27.0	2.9	1.7	1.1	0.15	2.04	52.4	1.33	0.07	1.8	41.6
L307880	49.8	> 3.00	2.84	6.97	1.11	1.14	< 0.1	87	49.5	404	10.7	1.5	< 10	50.9	2.4	1.6	0.9	0.14	1.29	45.3	1.49	0.20	1.1	37.0
L307881	16.6	0.05	4.85	1.36	0.62	7.77	0.2	9	310	685	0.62	< 0.1	< 10	14.3	0.5	0.3	0.1	0.11	0.58	3.4	0.09	0.02	0.2	19.8
L307882	97.8	0.06	2.67	5.89	2.58	6.20	< 0.1	111	331	1230	7.32	2.6	< 10	76.4	0.8	1.4	0.3	0.24	4.87	41.1	1.04	0.04	0.3	14.2
L307883	4.6	0.05	14.4	0.36	0.22	21.6	< 0.1	3	49.2	880	0.63	< 0.1	< 10	15.4	0.7	< 0.1	0.3	0.08	0.19	6.7	0.34	< 0.02	0.2	6.5
L307884	2.3	0.07	5.83	0.11	0.07	8.88	< 0.1	< 1	193	433	0.43	< 0.1	< 10	9.7	0.2	< 0.1	< 0.1	0.07	0.15	3.2	0.12	< 0.02	< 0.1	16.5
L307885	48.5	1.15	9.07	7.23	0.05	6.00	< 0.1	274	188	2470	14.3	0.8	< 10	156	1.4	0.3	0.5	0.10	0.22	64.5	0.25	< 0.02	0.3	176
L307886	50.9	> 3.00	5.65	> 10.0	0.06	2.33	< 0.1	402	234	1470	10.3	2.0	< 10	35.4	2.3	0.7	0.8	0.28	0.09	20.1	0.59	0.02	0.6	125
L307887	30.4	2.47	5.98	9.00	0.14	7.80	< 0.1	212	253	1520	8.90	1.0	< 10	170	2.1	0.4	0.7	0.16	0.15	52.0	0.77	< 0.02	0.4	94.7
L307888	30.4	2.76	5.07	8.04	0.18	6.31	< 0.1	354	244	1420	10.5	1.2	< 10	97.9	2.5	0.5	0.9	0.19	0.88	53.1	1.09	< 0.02	1.6	73.9
L307889	27.9	> 3.00	4.11	7.20	0.04	4.98	< 0.1	338	332	1450	8.92	1.1	< 10	99.9	2.3	0.6	0.8	0.18	< 0.05	35.0	0.55	< 0.02	0.5	105
L307890	36.5	2.71	4.73	7.85	0.05	5.60	< 0.1	282	299	1760	9.62	1.2	< 10	120	2.1	0.5	0.7	0.22	0.14	59.7	0.57	0.03	1.7	100
L307891	8.7	0.08	14.6	0.46	0.29	22.6	< 0.1	7	59.2	562	0.47	< 0.1	< 10	14.0	0.2	0.1	< 0.1	0.06	0.54	4.1	0.16	0.02	0.1	13.9
L307892	1.7	0.02	6.99	0.12	0.08	10.8	< 0.1	< 1	160	312	0.36	< 0.1	< 10	9.1	0.1	< 0.1	< 0.1	0.11	0.08	2.0	0.08	< 0.02	< 0.1	3.7
L307893	2.2	0.10	5.12	7.84	0.06	14.0	< 0.1	232	188	1690	10.0	0.9	< 10	91.3	2.7	0.4	0.9	0.07	< 0.05	45.9	1.01	< 0.02	0.5	68.4
L307894	20.6	> 3.00	2.67	7.79	0.99	0.14	0.2	189	228	277	7.56	2.8	< 10	37.1	0.2	1.0	0.1	0.66	0.41	> 500	0.31	0.38	61.9	105
L307895	44.2	0.02	5.64	5.53	0.03	0.08	2.5	267	371	392	10.6	1.7	< 10	61.6	0.2	0.3	< 0.1	0.34	0.06	97.5	< 0.05	0.22	6.8	1370
L307896	29.3	> 3.00	2.11	> 10.0	2.99	0.19	< 0.1	106	88.6	301	2.75	1.5	< 10	48.6	0.8	2.7	0.4	0.14	1.22	39.0	1.92	0.03	1.7	34.3
L307898	22.4	> 3.00	0.98	> 10.0	3.73	0.11	< 0.1	502	188	78	2.56	5.2	< 10	7.8	0.3	3.3	0.1	0.36	1.30	114	0.63	0.03	5.1	15.3
L307899	18.7	0.63	0.77	9.92	3.59	0.11	0.3	240	203	50	7.96	3.8	< 10	111	0.6	2.8	0.3	0.35	1.25	497	1.45	0.08	29.9	242
L307900	1.0	0.05	0.11	0.14	0.04	0.04	< 0.1	< 1	398	70	0.56	< 0.1	< 10	7.1	< 0.1	< 0.1	< 0.1	0.11	0.22	3.4	< 0.05	< 0.02	< 0.1	13.1

Analyte Symbol	Ga	As	Rb	Y	Sr	Zr	Nb	Mo	In	Sn	Sb	Te	Ba	La	Ce	Pr	Nd	Sm	Gd	Tb	Dy	Cu	Ge	Tm
Unit Symbol	ppm	ppm	ppm	ppm	ppm	ppm	ppm	ppm	ppm	ppm	ppm	ppm	ppm	ppm	ppm	ppm	ppm	ppm	ppm	ppm	ppm	ppm	ppm	ppm
Detection Limit	0.1	0.1	0.2	0.1	0.2	1	0.1	0.1	0.1	1	0.1	0.1	1	0.1	0.1	0.1	0.1	0.1	0.1	0.1	0.1	0.2	0.1	0.1
Analysis Method	TD-MS	TD-MS	TD-MS	TD-MS	TD-MS	TD-MS	TD-MS	TD-MS	TD-MS	TD-MS	TD-MS	TD-MS	TD-MS	TD-MS	TD-MS	TD-MS	TD-MS	TD-MS	TD-MS	TD-MS	TD-MS	TD-MS	TD-MS	TD-MS
129051	14.3	77.2	48.9	19.0	35.8	85	7.4	1.8	< 0.1	< 1	0.5	0.3	81	59.6	105	13.7	49.1	7.8	6.6	0.7	3.7	1350	0.3	0.3
129052	15.7	60.1	52.2	31.4	18.3	98	8.3	2.5	< 0.1	< 1	0.6	0.3	112	22.0	39.0	5.2	18.5	3.4	3.9	0.7	4.6	754	0.2	0.5
129053	19.3	5.1	62.5	24.1	16.8	109	1.6	0.3	< 0.1	< 1	< 0.1	< 0.1	179	24.2	41.7	5.5	19.6	3.5	3.5	0.6	3.6	131	0.6	0.4
129054	17.8	35.8	55.6	23.2	25.7	107	8.8	2.9	< 0.1	< 1	0.5	0.6	111	21.1	36.9	4.9	18.0	3.5	3.7	0.6	3.5	255	0.3	0.4
129055	19.4	19.3	77.1	26.2	17.6	120	9.8	1.1	< 0.1	< 1	0.4	0.2	140	72.3	122	17.0	61.8	10.5	8.3	0.9	4.7	206	0.4	0.4
129056	20.0	39.2	71.0	27.8	17.1	120	10.1	3.6	< 0.1	< 1	0.6	0.6	178	41.0	70.2	9.4	34.3	6.2	5.7	0.8	4.6	243	0.2	0.4
129057	19.4	31.4	68.0	29.0	16.9	112	9.8	1.4	< 0.1	< 1	0.6	0.6	170	57.4	99.5	13.5	49.8	9.0	7.4	0.9	5.0	292	0.3	0.5
129058	20.5	15.4	75.4	24.2	18.4	117	8.5	1.7	< 0.1	1	0.4	0.2	307	33.1	56.8	7.6	28.1	5.1	4.5	0.6	3.9	152	0.4	0.4
129059	17.5	12.2	39.1	15.7	18.8	116	10.3	0.8	< 0.1	< 1	0.4	0.1	107	22.7	44.2	6.1	23.3	4.3	3.7	0.5	2.8	54.3	2.7	0.3
129060	16.9	25.9	58.7	25.1	21.9	108	8.9	1.3	< 0.1	< 1	0.5	0.3	98	31.8	54.6	7.3	26.7	4.9	4.6	0.6	3.8	85.1	0.3	0.4
129061	17.9	18.0	70.8	26.7	22.8	112	9.5	2.2	< 0.1	< 1	0.4	0.2	201	31.0	53.0	7.2	26.4	5.0	4.7	0.7	4.1	253	0.3	0.4
129062	25.6	34.7	80.6	24.1	18.9	112	9.1	3.1	< 0.1	1	0.7	0.4	114	25.2	45.3	6.1	23.0	4.3	4.2	0.6	3.8	858	0.3	0.4
129063	7.3	14.7	21.2	18.2	85.2	46	4.3	1.2	< 0.1	< 1	0.3	0.1	116	19.3	33.6	4.5	16.8	3.5	3.9	0.6	3.2	245	0.1	0.3
129064	2.8	5.0	6.8	16.1	116	22	2.0	0.7	< 0.1	< 1	< 0.1	< 0.1	48	6.0	11.0	1.6	6.3	1.9	2.9	0.5	3.0	28.4	< 0.1	0.2
129065	13.6	27.1	59.4	19.5	44.9	78	6.9	1.7	< 0.1	< 1	0.4	0.7	82	24.0	41.8	5.7	21.4	4.2	4.3	0.6	3.5	607	0.2	0.3
129066	20.2	41.2	87.0	29.0	14.5	106	9.2	4.1	< 0.1	1	0.5	1.1	56	39.5	71.7	9.8	36.7	6.8	6.2	0.9	5.0	862	0.3	0.5
129067	21.0	16.5	88.8	25.1	17.9	140	11.1	1.4	< 0.1	1	0.4	0.7	123	34.4	62.2	8.5	31.5	5.9	5.5	0.8	4.5	264	0.3	0.5
129068	19.9	11.9	84.1	19.9	16.5	114	10.4	1.0	< 0.1	1	0.3	0.5	254	36.4	64.3	8.8	32.3	5.9	5.4	0.7	3.7	196	0.3	0.4
129069	22.5	41.8	118	32.1	9.1	141	11.2	6.2	0.1	2	0.6	1.2	25	20.7	42.2	6.0	22.4	4.6	4.8	0.8	5.3	1270	0.3	0.6
129070	18.8	10.1	63.7	14.1	17.2	131	12.0	1.7	< 0.1	2	0.3	0.4	589	21.2	42.4	5.6	20.8	4.0	3.7	0.5	2.7	189	3.3	0.3
129071	18.3	20.9	80.5	26.0	16.1	112	8.5	2.1	< 0.1	1	0.4	0.2	52	51.7	92.3	13.0	46.9	8.2	7.2	1.0	5.0	494	0.3	0.4
129072	17.9	7.1	77.2	25.1	18.9	121	6.9	0.8	< 0.1	1	0.3	< 0.1	384	33.0	56.0	7.9	28.6	5.3	5.0	0.8	4.4	151	0.3	0.4
129073	17.2	3.4	69.9	22.1	17.8	116	3.1	0.7	< 0.1	< 1	0.2	< 0.1	517	21.0	36.4	5.1	18.9	3.7	3.9	0.6	3.6	64.5	0.3	0.4
129074	18.2	13.6	83.7	24.6	16.7	105	7.9	1.2	< 0.1	1	0.3	0.2	96	28.9	51.1	7.1	25.7	5.0	4.9	0.7	4.2	709	0.3	0.4
129075	18.1	7.7	72.6	23.1	23.9	110	7.0	0.9	< 0.1	< 1	0.2	0.2	427	30.6	54.7	7.2	26.3	5.0	5.2	0.7	4.1	207	0.3	0.4
129076	17.6	25.4	72.6	29.0	15.0	111	7.6	2.6	0.1	1	0.4	0.4	53	43.0	76.6	10.6	38.0	6.8	6.2	0.8	4.7	1610	0.3	0.4
129077	18.0	22.3	74.6	29.8	16.8	110	8.2	2.3	< 0.1	< 1	0.3	0.4	77	36.2	64.7	8.9	31.8	5.7	5.6	0.8	4.8	464	0.3	0.4
129078	16.5	9.7	47.4	22.3	25.9	116	8.0	1.1	< 0.1	< 1	0.2	0.3	202	18.8	33.3	4.6	17.1	3.3	3.6	0.6	3.6	153	0.3	0.4
129079	18.6	11.4	47.4	17.8	33.2	104	7.2	1.2	< 0.1	< 1	0.2	0.2	135	25.3	46.1	6.3	23.1	4.1	3.9	0.5	3.1	102	0.3	0.3
129080	19.4	15.3	44.1	18.0	40.2	95	3.0	1.2	< 0.1	< 1	0.2	0.1	101	5.5	11.5	1.7	7.2	2.1	3.0	0.5	3.3	111	0.2	0.3
129081	21.1	1.9	50.2	11.8	25.6	115	9.7	0.4	< 0.1	< 1	0.1	0.1	76	26.0	49.8	6.3	22.1	3.3	2.6	0.3	2.1	58.7	0.9	0.2
129082	21.2	16.0	46.6	12.2	30.6	100	6.0	0.5	< 0.1	< 1	< 0.1	< 0.1	122	15.3	29.1	3.7	13.4	2.3	2.2	0.3	2.0	129	0.6	0.2
129083	18.8	7.9	29.4	12.7	33.4	96	4.4	1.2	< 0.1	< 1	< 0.1	< 0.1	84	25.9	47.4	6.0	21.6	3.4	3.0	0.4	2.2	828	0.5	0.2
129084	0.5	0.9	2.9	1.4	34.8	2	0.2	0.4	< 0.1	< 1	< 0.1	< 0.1	16	1.1	2.3	0.3	1.1	0.2	0.2	< 0.1	0.2	7.1	< 0.1	< 0.1
129085	0.4	0.8	3.3	1.3	35.5	9	0.2	0.5	< 0.1	< 1	< 0.1	< 0.1	20	1.2	2.2	0.3	0.9	0.2	0.2	< 0.1	0.2	8.3	< 0.1	< 0.1
129086	0.5	2.0	4.1	1.3	33.5	13	0.3	0.4	< 0.1	< 1	< 0.1	< 0.1	21	1.3	2.3	0.3	1.0	0.2	0.2	< 0.1	0.2	11.8	< 0.1	< 0.1
129087	0.4	0.8	3.0	1.0	32.0	6	0.1	1.3	< 0.1	< 1	< 0.1	< 0.1	17	0.9	1.7	0.2	0.8	0.1	0.1	< 0.1	0.2	7.8	< 0.1	< 0.1
129088	0.5	1.3	3.7	1.3	34.0	13	0.2	2.3	< 0.1	< 1	< 0.1	< 0.1	26	1.0	2.0	0.2	0.9	0.2	0.2	< 0.1	0.2	9.4	< 0.1	< 0.1
129089	0.6	1.7	3.9	1.5	31.8	12	0.2	1.8	< 0.1	< 1	< 0.1	< 0.1	18	1.2	2.3	0.3	1.1	0.2	0.2	< 0.1	0.2	7.8	< 0.1	< 0.1
129090	0.5	2.4	3.9	1.4	29.8	9	0.2	1.5	< 0.1	< 1	0.1	< 0.1	18	1.0	2.2	0.3	1.0	0.2	0.2	< 0.1	0.2	4.7	< 0.1	< 0.1
129091	0.7	0.8	4.9	1.3	29.0	3	0.2	0.3	< 0.1	< 1	< 0.1	< 0.1	22	1.2	2.4	0.3	1.0	0.2	0.2	< 0.1	0.2	4.8	< 0.1	< 0.1
129092	0.6	0.8	4.3	1.4	28.8	2	0.1	0.6	< 0.1	< 1	< 0.1	< 0.1	19	1.3	2.5	0.3	1.0	0.2	0.2	< 0.1	0.2	5.3	< 0.1	< 0.1
1272128	19.4	1.5	< 0.2	14.5	23.6	96	6.8	16.7	< 0.1	< 1	0.1	0.4	11	3.2	9.1	1.5	7.3	2.5	2.9	0.5	2.9	> 10000	0.2	0.2
1272129	1.5	0.9	0.3	2.2	35.9	8	0.5	0.6	< 0.1	< 1	< 0.1	< 0.1	3	1.6	2.7	0.4	1.7	0.4	0.5	< 0.1	0.4	10.0	< 0.1	< 0.1
1272130	1.8	1.0	< 0.2	2.3	39.8	8	0.5	3.8	< 0.1	< 1	0.1	< 0.1	2	1.8	3.4	0.5	2.2	0.5	0.5	< 0.1	0.4	58.2	< 0.1	< 0.1
1272131	1.8	3.0	0.6	22.6	73.7	11	0.4	0.6	0.3	< 1	< 0.1	< 0.1	22	18.8	30.2	3.7	15.3	3.2	4.5	0.6	3.5	756	< 0.1	0.4
1272132	0.1	< 0.1	2.0	0.9	73.8	2	< 0.1	1.7	< 0.1	< 1	< 0.1	< 0.1	36	1.0	2.3	0.3	1.3	0.3	0.3	< 0.1	0.2	36.3	< 0.1	< 0.1
1272133	0.5	0.4	2.5	0.8	57.8	3	0.2	2.3	< 0.1	< 1	< 0.1	< 0.1	34	0.7	2.0	0.3	1.0	0.2	0.2	< 0.1	0.2	7.0	< 0.1	< 0.1
1272134	20.5	2.0	< 0.2	22.7	28.6	62	0.6	0.1	< 0.1	< 1	< 0.1	< 0.1	18	7.7	15.0	2.1	8.8	2.4	3.3	0.6	4.3	56.1	0.3	0.4
1272135	17.4	1.8	31.3	22.4	663	32	2.8	3.2	0.9	< 1	0.2	< 0.1	114	14.3	23.2	2.9	11.9	3.1	3.9	0.7	4.5	> 10000	0.3	0.4
1272136	5.7	< 0.1	15.4	4.6	65.2	19	0.5	1.6	< 0.1	< 1	< 0.1	< 0.1	74	2.4	6.0	0.7	2.8	0.7	0.8	0.1	0.8	17.4	< 0.1	< 0.1
1272137	8.5	26.2	44.3	11.2	6.8	12	2.3	4.5	< 0.1	< 1	0.3	< 0.1	345	9.5	20.0	2.4	9.1	1.7	2.0	0.3	2.0	66.6	0.1	0.2

Analyte Symbol	Ga	As	Rb	Y	Sr	Zr	Nb	Mo	In	Sn	Sb	Te	Ba	La	Ce	Pr	Nd	Sm	Gd	Tb	Dy	Cu	Ge	Tm
Unit Symbol	ppm	ppm	ppm	ppm	ppm	ppm	ppm	ppm	ppm	ppm	ppm	ppm	ppm	ppm	ppm	ppm	ppm	ppm	ppm	ppm	ppm	ppm	ppm	ppm
Detection Limit	0.1	0.1	0.2	0.1	0.2	1	0.1	0.1	0.1	1	0.1	0.1	1	0.1	0.1	0.1	0.1	0.1	0.1	0.1	0.1	0.2	0.1	0.1
Analysis Method	TD-MS	TD-MS	TD-MS	TD-MS	TD-MS	TD-MS	TD-MS	TD-MS	TD-MS	TD-MS	TD-MS	TD-MS	TD-MS	TD-MS	TD-MS	TD-MS	TD-MS	TD-MS	TD-MS	TD-MS	TD-MS	TD-MS	TD-MS	TD-MS
1272138	21.5	4.4	106	12.2	19.4	73	0.2	0.9	< 0.1	< 1	< 0.1	< 0.1	1060	13.0	26.5	3.1	11.0	2.1	2.1	0.3	2.2	41.5	0.7	0.2
1272139	4.9	7.1	7.2	8.1	4.1	72	1.8	4.1	< 0.1	< 1	0.2	0.1	60	7.8	15.5	1.8	6.3	1.1	1.1	0.2	1.3	41.1	0.2	0.1
1272140	22.5	2.3	73.3	14.7	16.9	171	7.2	2.8	< 0.1	1	0.6	0.2	100	44.7	91.0	10.9	37.8	6.3	5.4	0.7	3.4	91.6	0.4	0.2
1272141	17.5	1.0	1.4	12.9	129	15	0.1	< 0.1	< 0.1	< 1	< 0.1	< 0.1	36	3.0	7.7	1.1	4.9	1.5	2.1	0.4	2.7	330	0.2	0.2
1272142	19.2	21.4	1.0	14.8	152	22	0.6	3.3	0.2	1	< 0.1	< 0.1	31	10.8	23.9	3.1	12.5	2.6	2.9	0.5	3.0	982	0.7	0.2
1272143	0.5	5.1	3.9	2.3	71.2	3	0.2	20.7	0.7	< 1	< 0.1	12.3	44	2.5	5.9	0.7	2.8	0.6	0.6	< 0.1	0.5	> 10000	0.3	< 0.1
L307861	19.9	11.3	< 0.2	5.0	31.3	84	7.1	3.4	< 0.1	< 1	< 0.1	0.4	6	2.8	8.0	0.9	3.7	1.0	1.1	0.2	1.1	705	1.3	< 0.1
L307862	19.7	1.3	0.3	15.7	46.3	73	5.6	9.4	< 0.1	< 1	< 0.1	< 0.1	7	6.1	13.8	1.9	7.9	2.2	2.6	0.5	3.1	2440	0.7	0.3
L307863	32.2	6.3	14.0	11.7	24.4	162	10.9	2.3	< 0.1	3	< 0.1	< 0.1	53	210	401	45.6	145	21.3	13.9	1.4	5.0	582	0.8	0.2
L307864	18.9	4.9	0.9	4.4	43.0	56	0.7	0.4	< 0.1	< 1	< 0.1	< 0.1	30	18.5	38.0	4.3	14.4	2.1	1.5	0.2	0.9	27.2	0.1	< 0.1
L307865	24.6	2.0	25.9	3.9	44.3	66	0.5	< 0.1	< 0.1	< 1	< 0.1	< 0.1	162	4.8	10.3	1.2	4.0	0.7	0.7	0.1	0.7	4.6	0.1	< 0.1
L307866	5.9	2.5	0.5	11.4	60.8	101	1.5	0.5	< 0.1	< 1	< 0.1	< 0.1	5	17.7	36.2	4.3	14.6	2.7	2.7	0.4	2.4	4.0	< 0.1	0.2
L307867	23.1	0.8	0.7	19.1	375	29	0.3	0.9	0.1	< 1	< 0.1	< 0.1	20	3.1	8.2	1.3	6.3	2.0	2.9	0.5	3.6	263	0.5	0.3
L307868	17.6	1.4	5.7	19.3	113	28	2.7	1.4	< 0.1	< 1	< 0.1	< 0.1	19	3.4	8.7	1.3	6.6	2.0	2.9	0.5	3.7	104	0.5	0.3
L307869	18.7	2.8	6.0	21.7	105	28	2.6	0.9	0.1	< 1	< 0.1	< 0.1	20	4.6	10.5	1.6	7.6	2.4	3.3	0.6	4.1	131	0.8	0.4
L307870	17.6	1.2	1.1	19.4	117	33	3.0	2.3	< 0.1	< 1	< 0.1	< 0.1	15	2.9	8.0	1.3	6.3	2.0	2.9	0.5	3.6	151	0.4	0.3
L307871	18.5	0.2	17.4	22.0	131	30	0.7	0.7	0.1	< 1	< 0.1	< 0.1	34	6.5	13.8	2.0	9.5	2.8	3.9	0.7	4.2	844	0.7	0.3
L307872	17.9	2.3	5.2	19.2	107	24	2.8	1.7	< 0.1	< 1	< 0.1	< 0.1	34	3.9	9.1	1.4	6.7	2.1	2.9	0.6	3.7	118	0.6	0.3
L307873	14.1	0.5	132	13.0	38.1	20	0.4	0.4	< 0.1	< 1	< 0.1	< 0.1	84	1.9	3.9	0.5	2.4	0.8	1.3	0.3	2.3	901	0.8	0.2
L307874	14.1	7.0	2.2	18.1	61.3	26	< 0.1	< 0.1	< 0.1	< 1	< 0.1	< 0.1	22	16.9	35.2	4.7	19.2	4.1	4.5	0.7	3.8	234	0.2	0.3
L307875	16.1	1.2	2.5	10.4	37.3	81	2.1	2.9	< 0.1	< 1	0.1	< 0.1	32	11.8	24.1	2.8	10.1	2.0	2.0	0.3	1.9	14.5	0.1	0.2
L307876	20.6	0.3	72.0	21.0	34.6	67	0.3	0.1	< 0.1	< 1	< 0.1	< 0.1	72	9.5	23.6	3.4	14.9	4.1	4.4	0.7	4.4	714	0.3	0.3
L307877	22.6	1.0	75.0	5.9	27.9	123	1.1	0.7	< 0.1	< 1	< 0.1	< 0.1	28	1.7	4.0	0.6	2.4	0.8	1.0	0.2	1.0	5.8	0.4	< 0.1
L307878	16.9	2.2	12.7	11.0	55.8	114	0.3	0.2	< 0.1	< 1	< 0.1	< 0.1	20	1.9	5.2	0.7	3.3	1.0	1.5	0.3	1.8	80.7	0.2	0.2
L307879	19.5	1.2	49.4	29.1	35.8	105	0.4	0.3	0.1	< 1	< 0.1	< 0.1	52	7.9	20.0	2.5	11.1	3.9	5.3	0.9	5.6	1450	0.3	0.4
L307880	19.2	0.3	56.7	22.4	29.3	67	< 0.1	< 0.1	0.1	< 1	< 0.1	< 0.1	323	17.9	38.7	4.9	19.8	4.2	4.6	0.7	4.4	1650	0.3	0.3
L307881	2.8	1.2	16.1	3.7	36.4	5	0.6	3.0	< 0.1	< 1	< 0.1	< 0.1	136	2.0	4.4	0.4	1.5	0.3	0.4	< 0.1	0.6	16.8	< 0.1	< 0.1
L307882	15.8	0.2	137	7.7	16.2	101	1.7	4.0	0.2	1	< 0.1	0.1	216	35.4	60.4	6.8	22.6	3.7	3.2	0.4	1.8	13.7	0.4	0.1
L307883	0.7	0.5	6.3	6.7	98.2	3	0.3	1.5	< 0.1	< 1	< 0.1	< 0.1	20	1.6	5.0	0.8	3.5	1.1	1.3	0.2	1.5	5.8	< 0.1	< 0.1
L307884	0.3	0.5	1.8	2.4	43.2	2	0.1	3.1	< 0.1	< 1	< 0.1	< 0.1	18	0.8	2.3	0.3	1.4	0.4	0.5	< 0.1	0.5	15.8	< 0.1	< 0.1
L307885	9.5	0.2	1.0	11.9	21.0	19	0.7	0.4	< 0.1	< 1	< 0.1	< 0.1	13	1.2	3.6	0.6	3.3	1.2	1.8	0.3	2.4	4.2	0.2	0.2
L307886	17.8	0.2	0.4	18.7	86.5	72	3.4	0.6	< 0.1	< 1	< 0.1	< 0.1	40	1.8	4.9	0.8	4.2	1.7	2.5	0.5	3.6	55.4	0.4	0.4
L307887	17.7	0.3	3.4	18.4	206	39	2.4	1.5	< 0.1	< 1	< 0.1	< 0.1	100	2.9	7.8	1.2	5.8	1.8	2.5	0.5	3.3	51.6	0.6	0.3
L307888	18.2	2.1	10.2	22.6	141	41	3.3	1.1	< 0.1	< 1	0.1	< 0.1	58	4.7	11.5	1.7	7.8	2.3	3.3	0.6	4.0	244	0.4	0.4
L307889	17.0	0.6	< 0.2	15.5	80.2	36	4.0	1.2	< 0.1	< 1	0.1	< 0.1	25	1.5	4.8	0.8	4.1	1.5	2.4	0.5	3.4	17.0	1.7	0.3
L307890	18.6	0.6	0.4	18.2	76.2	45	2.8	1.5	< 0.1	< 1	< 0.1	< 0.1	21	2.7	7.4	1.2	5.6	1.8	2.6	0.5	3.4	305	0.3	0.3
L307891	0.9	1.0	11.7	2.2	83.3	5	0.3	0.8	< 0.1	< 1	< 0.1	< 0.1	68	2.5	6.4	0.8	3.1	0.6	0.6	< 0.1	0.4	8.3	< 0.1	< 0.1
L307892	0.4	< 0.1	2.2	1.0	36.3	2	0.1	2.3	< 0.1	< 1	< 0.1	< 0.1	16	0.7	2.2	0.3	1.3	0.3	0.3	< 0.1	0.2	4.1	< 0.1	< 0.1
L307893	18.8	0.7	1.5	24.2	183	25	0.2	0.1	< 0.1	< 1	< 0.1	< 0.1	10	3.8	9.6	1.5	7.5	2.4	3.5	0.7	4.4	35.4	0.3	0.4
L307894	22.3	3410	41.1	2.5	11.9	119	2.0	3.4	< 0.1	1	0.2	1.6	217	26.4	51.5	5.6	17.3	2.3	1.6	0.2	0.7	1840	0.4	< 0.1
L307895	22.3	18.8	0.5	1.5	0.9	63	1.0	7.1	< 0.1	1	< 0.1	0.2	2	0.8	1.5	0.2	0.7	0.2	0.3	< 0.1	0.3	597	0.2	< 0.1
L307896	40.2	5.3	113	8.4	44.9	58	1.0	0.2	< 0.1	2	< 0.1	< 0.1	765	66.5	125	14.5	49.5	8.0	6.0	0.6	2.6	8.4	0.4	< 0.1
L307898	39.4	60.9	108	2.5	21.0	206	6.4	1.9	< 0.1	4	< 0.1	0.1	996	30.0	56.9	6.5	21.6	3.3	2.4	0.3	1.0	31.3	0.3	< 0.1
L307899	30.7	282	113	5.9	9.9	143	2.5	3.9	< 0.1	11	< 0.1	0.5	39	58.0	132	16.3	51.9	7.8	5.0	0.5	2.2	389	0.4	< 0.1
L307900	0.6	3.2	0.9	< 0.1	6.8	2	0.3	5.0	< 0.1	< 1	0.1	< 0.1	19	0.3	0.6	< 0.1	0.2	< 0.1	< 0.1	< 0.1	< 0.1	12.6	< 0.1	< 0.1

Analyte Symbol	Yb	Lu	Ta	W	Re	Tl	Pb	Sc	Th	U	Ti	P	S
Unit Symbol	ppm	ppm	ppm	ppm	ppm	ppm	ppm	ppm	ppm	ppm	%	%	%
Detection Limit	0.1	0.1	0.1	0.1	0.001	0.05	0.5	1	0.1	0.1	0.0005	0.001	0.01
Analysis Method	TD-MS	TD-MS	TD-MS	TD-MS	TD-MS	TD-MS	TD-MS	TD-ICP	TD-MS	TD-MS	TD-ICP	TD-ICP	TD-ICP
129051	1.8	0.3	0.5	1.0	0.009	0.19	4.3	19	8.5	3.2	0.287	0.034	3.77
129052	2.7	0.5	0.5	0.8	0.015	0.24	5.7	14	9.2	3.7	0.329	0.043	3.21
129053	2.5	0.4	< 0.1	< 0.1	0.012	0.29	3.0	20	9.7	4.2	0.294	0.032	0.18
129054	2.3	0.4	0.6	1.0	0.009	0.28	3.0	18	9.2	2.9	0.339	0.039	1.63
129055	2.4	0.4	0.6	0.9	0.007	0.34	3.7	21	11.2	3.5	0.425	0.041	1.06
129056	2.7	0.5	0.7	1.0	0.010	0.38	5.6	19	10.8	3.9	0.384	0.040	1.84
129057	2.7	0.4	0.6	1.0	0.006	0.32	6.8	18	11.0	3.6	0.402	0.042	2.02
129058	2.4	0.4	0.5	1.0	0.008	0.33	4.5	20	10.8	4.4	0.426	0.042	0.75
129059	1.8	0.3	0.7	1.0	0.003	0.26	2.9	11	5.2	2.5	0.369	0.040	0.45
129060	2.3	0.4	0.6	0.9	0.010	0.27	3.2	15	9.2	3.1	0.348	0.050	1.17
129061	2.5	0.4	0.6	0.9	0.008	0.30	4.5	17	10.5	3.5	0.363	0.039	0.79
129062	2.4	0.4	0.6	1.2	0.009	0.40	5.5	21	7.9	3.5	0.369	0.052	1.98
129063	1.5	0.2	0.3	0.6	0.004	0.09	2.2	7	4.6	1.5	0.154	0.021	1.18
129064	1.2	0.2	0.1	0.4	0.003	< 0.05	0.9	4	1.9	0.8	0.0667	0.011	0.29
129065	1.9	0.3	0.5	1.3	0.006	0.26	4.3	13	7.1	2.2	0.248	0.029	2.38
129066	2.8	0.5	0.6	1.9	0.009	0.42	7.3	19	8.5	2.8	0.378	0.039	3.91
129067	2.8	0.5	0.7	2.3	0.007	0.39	3.5	21	8.7	2.7	0.416	0.044	1.98
129068	2.3	0.4	0.7	2.5	0.003	0.39	2.8	19	9.9	2.5	0.412	0.043	1.37
129069	3.2	0.6	0.7	2.5	0.014	0.54	8.6	19	6.1	3.6	0.417	0.047	5.51
129070	1.7	0.3	0.8	2.7	0.005	0.46	2.6	14	6.5	2.6	0.439	0.055	1.07
129071	2.3	0.4	0.5	1.5	0.004	0.45	3.7	15	9.8	2.2	0.343	0.138	2.57
129072	2.5	0.4	0.3	1.2	0.004	0.42	2.2	16	9.9	2.5	0.330	0.105	0.91
129073	2.3	0.4	< 0.1	0.7	0.002	0.35	1.6	15	9.8	2.5	0.268	0.084	0.43
129074	2.3	0.4	0.5	1.2	0.005	0.41	3.0	15	9.3	13.6	0.314	0.126	1.43
129075	2.1	0.4	0.3	1.4	0.004	0.34	2.7	15	10.4	2.3	0.347	0.171	0.82
129076	2.5	0.4	0.4	1.1	0.004	0.35	4.9	13	9.1	2.0	0.298	0.110	3.01
129077	2.6	0.4	0.5	1.1	0.007	0.35	4.0	14	8.3	2.5	0.309	0.116	2.53
129078	2.3	0.4	0.4	1.2	0.005	0.24	2.4	14	9.6	2.5	0.358	0.124	0.70
129079	1.9	0.3	0.3	1.1	0.009	0.22	2.4	17	8.9	2.9	0.356	0.113	0.48
129080	1.8	0.3	< 0.1	0.6	0.005	0.23	2.3	15	10.8	3.7	0.258	0.131	0.35
129081	1.6	0.3	0.6	0.8	0.001	0.25	1.5	16	8.7	2.5	0.472	0.043	0.04
129082	1.5	0.3	0.1	0.9	0.008	0.23	2.5	30	9.7	3.9	0.380	0.043	0.30
129083	1.3	0.2	< 0.1	0.5	0.006	0.12	3.4	15	9.9	3.9	0.364	0.046	0.25
129084	< 0.1	< 0.1	< 0.1	< 0.1	0.001	< 0.05	4.1	< 1	0.4	0.1	0.0088	0.027	0.10
129085	0.1	< 0.1	< 0.1	0.2	0.001	0.06	8.8	< 1	0.4	0.2	0.0105	0.023	0.16
129086	< 0.1	< 0.1	< 0.1	0.2	0.001	0.10	13.5	< 1	0.4	0.2	0.0126	0.025	0.43
129087	< 0.1	< 0.1	< 0.1	< 0.1	0.004	0.07	11.6	< 1	0.4	0.2	0.0091	0.023	0.14
129088	0.1	< 0.1	< 0.1	< 0.1	0.002	0.09	20.6	< 1	0.3	0.2	0.0124	0.024	0.35
129089	0.1	< 0.1	< 0.1	< 0.1	0.001	0.14	14.1	< 1	0.4	0.2	0.0120	0.030	0.20
129090	0.1	< 0.1	< 0.1	0.2	< 0.001	0.12	81.9	< 1	0.3	0.2	0.0092	0.030	0.19
129091	< 0.1	< 0.1	< 0.1	< 0.1	< 0.001	0.08	3.8	< 1	0.5	0.2	0.0114	0.032	0.09
129092	0.1	< 0.1	< 0.1	< 0.1	< 0.001	0.07	93.8	< 1	0.4	0.2	0.0113	0.028	0.12
1272128	1.2	0.2	0.5	0.5	0.070	< 0.05	3.0	3	9.5	2.9	0.350	0.026	7.25
1272129	0.2	< 0.1	< 0.1	0.1	< 0.001	< 0.05	1.0	1	1.1	1.1	0.0176	0.018	0.06
1272130	0.2	< 0.1	< 0.1	0.1	0.001	< 0.05	1.3	2	0.8	1.2	0.0213	0.010	0.07
1272131	2.0	0.3	< 0.1	< 0.1	< 0.001	< 0.05	0.9	2	0.7	0.7	0.0246	0.011	0.15
1272132	< 0.1	< 0.1	< 0.1	< 0.1	< 0.001	< 0.05	1.0	< 1	0.1	0.6	0.0023	0.011	0.06
1272133	< 0.1	< 0.1	< 0.1	0.1	0.002	< 0.05	1.5	< 1	0.2	2.6	0.0050	0.006	0.04
1272134	2.2	0.4	< 0.1	0.2	< 0.001	< 0.05	1.7	48	0.4	0.1	0.501	0.034	0.26
1272135	2.1	0.3	0.2	1.8	0.003	0.24	2.9	37	0.2	4.5	0.423	0.022	0.44
1272136	0.3	< 0.1	< 0.1	0.2	< 0.001	0.10	0.8	2	2.2	0.5	0.0283	0.019	0.04
1272137	0.9	0.1	< 0.1	0.5	0.006	0.57	1.8	9	3.0	1.5	0.204	0.067	0.43

Analyte Symbol	Yb	Lu	Ta	W	Re	Tl	Pb	Sc	Th	U	Ti	P	S
Unit Symbol	ppm	ppm	ppm	ppm	ppm	ppm	ppm	ppm	ppm	ppm	%	%	%
Detection Limit	0.1	0.1	0.1	0.1	0.001	0.05	0.5	1	0.1	0.1	0.0005	0.001	0.01
Analysis Method	TD-MS	TD-MS	TD-MS	TD-MS	TD-MS	TD-MS	TD-MS	TD-ICP	TD-MS	TD-MS	TD-ICP	TD-ICP	TD-ICP
1272138	1.2	0.2	< 0.1	< 0.1	0.084	1.64	4.3	24	4.4	2.3	0.119	0.016	0.04
1272139	0.6	0.1	< 0.1	0.4	0.005	0.14	34.8	3	2.0	0.5	0.119	0.034	1.13
1272140	1.3	0.2	0.2	0.9	0.008	1.14	30.0	20	11.4	1.9	0.502	0.133	1.58
1272141	1.2	0.2	< 0.1	< 0.1	0.004	< 0.05	4.3	30	0.7	0.4	0.0690	0.019	0.06
1272142	1.1	0.2	< 0.1	< 0.1	0.005	0.05	5.3	17	1.0	0.5	0.256	0.018	0.32
1272143	0.1	< 0.1	< 0.1	0.1	0.038	0.06	16.4	< 1	0.5	4.3	0.0068	0.024	1.60
L307861	0.6	< 0.1	0.4	0.4	0.003	< 0.05	2.3	5	2.1	0.8	0.386	0.017	0.38
L307862	1.4	0.2	0.3	0.3	0.021	< 0.05	1.9	31	3.1	0.7	0.613	0.030	0.59
L307863	0.8	0.1	0.8	0.6	0.001	< 0.05	6.2	19	36.8	2.3	0.361	0.023	1.95
L307864	0.5	< 0.1	< 0.1	< 0.1	0.002	< 0.05	2.7	2	10.3	2.0	0.232	0.030	0.01
L307865	0.5	< 0.1	< 0.1	< 0.1	< 0.001	0.09	2.6	8	20.7	2.6	0.190	0.028	< 0.01
L307866	1.0	0.1	< 0.1	0.2	0.001	< 0.05	1.1	8	7.6	0.9	0.0582	0.053	0.05
L307867	1.6	0.2	< 0.1	0.1	0.005	< 0.05	1.1	43	0.7	< 0.1	0.346	0.021	0.07
L307868	1.8	0.2	0.1	0.1	0.002	< 0.05	4.4	44	0.4	< 0.1	0.554	0.023	0.15
L307869	1.9	0.3	0.1	0.1	0.003	< 0.05	2.3	45	0.3	< 0.1	0.558	0.025	0.07
L307870	1.8	0.3	0.2	0.2	0.002	< 0.05	0.8	41	0.3	< 0.1	0.542	0.024	0.19
L307871	1.8	0.3	< 0.1	< 0.1	0.001	0.05	1.0	42	0.9	0.2	0.451	0.023	0.13
L307872	1.8	0.3	0.2	0.3	< 0.001	0.05	1.1	41	0.3	0.1	0.526	0.024	0.10
L307873	1.3	0.2	< 0.1	0.1	0.002	0.39	0.6	38	0.2	0.5	0.399	0.018	0.09
L307874	1.3	0.2	< 0.1	< 0.1	0.007	0.08	4.0	30	1.4	0.8	0.155	0.014	0.23
L307875	0.9	0.1	0.1	0.5	< 0.001	< 0.05	2.5	8	4.5	0.4	0.0837	0.052	0.91
L307876	1.8	0.3	< 0.1	< 0.1	< 0.001	0.34	4.1	14	7.0	1.1	0.238	0.045	0.03
L307877	0.5	< 0.1	< 0.1	< 0.1	0.001	0.24	2.0	7	9.6	0.9	0.258	0.052	0.01
L307878	1.4	0.2	< 0.1	< 0.1	0.001	0.06	3.4	12	14.8	2.8	0.176	0.074	0.02
L307879	2.1	0.3	< 0.1	< 0.1	0.003	0.18	1.7	9	7.1	1.5	0.341	0.058	0.08
L307880	1.8	0.3	< 0.1	< 0.1	0.002	0.19	1.4	8	6.9	1.5	0.188	0.053	0.11
L307881	0.5	< 0.1	< 0.1	< 0.1	< 0.001	0.33	16.8	4	1.0	0.5	0.124	0.030	0.03
L307882	0.7	0.1	< 0.1	0.2	0.001	0.31	3.0	13	9.5	3.4	0.329	0.047	0.05
L307883	0.5	< 0.1	< 0.1	< 0.1	< 0.001	< 0.05	1.2	2	0.2	< 0.1	0.0115	0.010	0.06
L307884	0.2	< 0.1	< 0.1	< 0.1	< 0.001	< 0.05	3.1	< 1	0.1	0.8	0.0023	0.004	0.03
L307885	1.0	0.1	< 0.1	0.2	< 0.001	< 0.05	1.3	46	0.4	0.1	0.386	0.021	0.02
L307886	2.0	0.3	0.2	0.2	< 0.001	< 0.05	11.0	56	0.4	0.1	0.776	0.036	0.11
L307887	1.8	0.3	0.1	0.2	0.001	< 0.05	1.6	38	0.3	< 0.1	0.419	0.022	0.03
L307888	2.0	0.3	0.2	0.2	0.001	0.07	2.3	48	0.4	< 0.1	0.669	0.030	0.15
L307889	1.7	0.2	0.2	0.3	0.001	< 0.05	3.1	34	0.2	< 0.1	0.623	0.029	0.04
L307890	1.6	0.2	0.1	0.3	0.001	< 0.05	2.6	38	0.3	0.7	0.505	0.025	0.17
L307891	0.2	< 0.1	< 0.1	0.1	< 0.001	0.06	3.0	< 1	0.6	0.1	0.0157	0.009	0.07
L307892	< 0.1	< 0.1	< 0.1	< 0.1	< 0.001	< 0.05	0.9	< 1	< 0.1	1.3	0.0035	0.003	0.03
L307893	2.0	0.3	< 0.1	0.1	< 0.001	< 0.05	1.1	52	0.4	< 0.1	0.232	0.021	0.05
L307894	0.2	< 0.1	0.1	3.9	0.001	0.10	27.7	11	6.6	0.7	0.155	0.024	0.91
L307895	0.2	< 0.1	< 0.1	3.4	0.002	< 0.05	361	11	3.5	0.8	0.177	0.004	0.72
L307896	0.6	< 0.1	< 0.1	< 0.1	0.001	0.30	3.1	15	18.4	1.9	0.191	0.017	0.19
L307898	0.2	< 0.1	0.3	8.4	< 0.001	0.43	4.2	46	5.2	0.6	0.449	0.013	0.51
L307899	0.5	< 0.1	0.2	7.4	0.001	0.39	128	19	13.4	2.4	0.179	0.025	4.49
L307900	< 0.1	< 0.1	< 0.1	0.3	< 0.001	< 0.05	4.8	< 1	0.2	< 0.1	0.0162	< 0.001	0.01

Quality Control

Analyte Symbol	Li	Na	Mg	Al	K	Ca	Cd	V	Cr	Mn	Fe	Hf	Hg	Ni	Er	Be	Ho	Ag	Cs	Co	Eu	Bi	Se	Zn
Unit Symbol	ppm	%	%	%	%	%	ppm	ppm	ppm	ppm	%	ppm	ppb	ppm	ppm	ppm	ppm	ppm	ppm	ppm	ppm	ppm	ppm	ppm
Detection Limit	0.5	0.01	0.01	0.01	0.01	0.01	0.1	1	0.5	1	0.01	0.1	10	0.5	0.1	0.1	0.1	0.05	0.05	0.1	0.05	0.02	0.1	0.2
Analysis Method	TD-MS	TD-MS	TD-MS	TD-MS	TD-MS	TD-MS	TD-MS	TD-MS	TD-MS	TD-MS	TD-MS	TD-MS	TD-MS	TD-MS	TD-MS	TD-MS	TD-MS	TD-MS	TD-MS	TD-MS	TD-MS	TD-MS	TD-MS	TD-MS
GXR-1 Meas	9.7	0.05	0.23	2.22	0.06	0.96	2.5	87	18.7	873	26.3	0.4	3240	43.5		1.1		37.7	2.82	8.6	0.66	1490	17.4	876
GXR-1 Cert	8.20	0.0520	0.217	3.52	0.050	0.960	3.30	80.0	12.0	852	23.6	0.960	3900	41.0		1.22		31.0	3.00	8.20	0.690	1380	16.6	760
DH-1a Meas																								
DH-1a Cert																								
GXR-4 Meas	14.2	0.64	1.92	7.38	2.93	1.19	< 0.1	95	51.1	165	3.33	1.2		44.8		2.5		3.92	2.66	15.7	1.51	19.0	6.8	83.5
GXR-4 Cert	11.1	0.564	1.66	7.20	4.01	1.01	0.860	87.0	64.0	155	3.09	6.30		42.0		1.90		4.00	2.80	14.6	1.63	19.0	5.60	73.0
SDC-1 Meas	45.3	1.92	1.15	8.80	2.03	1.25	< 0.1	59	51.4	908	5.38	1.1		41.8	4.0	3.6	1.4	0.13	4.05	20.2	1.65	0.29		128
SDC-1 Cert	34.00	1.52	1.02	8.34	2.72	1.00	0.0800	102.00	64.00	880.00	4.82	8.30		38.0	4.10	3.00	1.50	0.0410	4.00	18.0	1.70	2.60		103.00
GXR-6 Meas	45.8	0.12	0.70	> 10.0	2.13	0.22	< 0.1	161	62.3	1070	6.17	2.2		28.4		1.5		0.43	4.41	15.4	0.68	0.19	0.8	155
GXR-6 Cert	32.0	0.104	0.609	17.7	1.87	0.180	1.00	186	96.0	1010	5.58	4.30		27.0		1.40		1.30	4.20	13.8	0.760	0.290	0.940	118
SAR-M (U.S.G.S.) Meas	37.1	1.48	0.56	6.79	3.10	0.71	5.0	63	81.4	5400	3.57			47.1		3.2		3.78		12.3		1.71	1.4	1060
SAR-M (U.S.G.S.) Cert	27.4	1.140	0.50	6.30	2.94	0.61	5.27	67.2	79.7	5220	2.99			41.5		2.20		3.64		10.70		1.94	0.39	930.0
DNC-1a Meas	6.3							171	165					310						65.9	0.66			80.8
DNC-1a Cert	5.20							148.00	270					247						57.0	0.59			70.0
SBC-1 Meas	214						0.4	243	88.2			3.1		99.9	4.1	4.1	1.4		8.56	26.1	2.05	0.73		235
SBC-1 Cert	163.0						0.40	220.0	109			3.7		82.8	3.80	3.20	1.40		8.2	22.7	1.98	0.70		186.0
129051 Orig	17.1	> 3.00	3.21	5.62	0.93	3.78	< 0.1	114	74.5	607	4.96	2.0	20	188	1.9	1.3	0.7	0.32	1.15	61.4	0.94	0.53	10.2	15.0
129051 Dup	17.6	> 3.00	3.30	5.71	0.93	3.74	< 0.1	114	69.8	607	5.09	2.1	60	189	1.9	1.3	0.7	0.35	1.16	63.7	0.94	0.54	10.8	16.6
129089 Orig	3.1	0.01	10.5	0.32	0.19	16.1	0.7	3	15.6	766	0.96	0.3	< 10	12.7	0.1	0.1	< 0.1	0.06	< 0.05	1.5	0.05	< 0.02	0.1	324
129089 Dup	3.0	0.01	10.4	0.35	0.19	16.1	0.7	4	7.4	765	0.97	0.3	< 10	13.0	0.1	< 0.1	< 0.1	0.05	< 0.05	1.5	0.05	< 0.02	0.2	339
129091 Orig	3.3	0.01	9.53	0.43	0.23	14.4	< 0.1	2	10.8	675	1.04	< 0.1	< 10	10.7	0.1	< 0.1	< 0.1	0.05	0.06	0.9	0.06	< 0.02	< 0.1	34.4
129091 Dup	3.3	0.01	9.52	0.43	0.24	14.9	< 0.1	2	8.1	693	1.03	< 0.1	< 10	10.8	0.1	< 0.1	< 0.1	< 0.05	0.06	1.0	0.06	< 0.02	0.4	33.1
L307879 Orig	41.9	> 3.00	2.81	7.32	0.94	1.31	< 0.1	74	59.9	417	9.74	2.3	< 10	27.0	2.9	1.7	1.1	0.13	2.03	52.2	1.31	0.07	1.7	40.1
L307879 Dup	41.9	> 3.00	2.87	7.75	0.91	1.34	< 0.1	90	64.7	417	9.92	2.8	< 10	27.0	2.9	1.7	1.1	0.17	2.04	52.6	1.35	0.07	2.0	43.2
L307883 Orig	4.6	0.05	14.0	0.35	0.22	21.4	< 0.1	3	50.7	873	0.63	< 0.1	< 10	15.1	0.7	< 0.1	0.3	0.08	0.19	6.6	0.35	< 0.02	0.2	7.2
L307883 Dup	4.6	0.05	14.8	0.37	0.22	21.8	< 0.1	4	47.8	886	0.63	< 0.1	< 10	15.6	0.7	< 0.1	0.3	0.08	0.19	6.7	0.34	< 0.02	0.1	5.9
Method Blank	< 0.5	< 0.01	< 0.01	< 0.01	< 0.01	< 0.01	< 0.1	< 1	< 0.5	< 1	< 0.01	< 0.1	< 10	< 0.5	< 0.1	< 0.1	< 0.1	< 0.05	< 0.05	< 0.1	< 0.05	< 0.02	< 0.1	< 0.2
Method Blank																								
Method Blank																								

Quality Control

Analyte Symbol	Ga	As	Rb	Y	Sr	Zr	Nb	Mo	In	Sn	Sb	Te	Ba	La	Ce	Pr	Nd	Sm	Gd	Tb	Dy	Cu	Ge	Tm
Unit Symbol	ppm	ppm	ppm	ppm	ppm	ppm	ppm	ppm	ppm	ppm	ppm	ppm	ppm	ppm	ppm	ppm	ppm	ppm	ppm	ppm	ppm	ppm	ppm	ppm
Detection Limit	0.1	0.1	0.2	0.1	0.2	1	0.1	0.1	0.1	1	0.1	0.1	1	0.1	0.1	0.1	0.1	0.1	0.1	0.1	0.1	0.2	0.1	0.1
Analysis Method	TD-MS	TD-MS	TD-MS	TD-MS	TD-MS	TD-MS	TD-MS	TD-MS	TD-MS	TD-MS	TD-MS	TD-MS	TD-MS	TD-MS	TD-MS	TD-MS	TD-MS	TD-MS	TD-MS	TD-MS	TD-MS	TD-MS	TD-MS	TD-MS
GXR-1 Meas	10.2	432	2.9	32.1	298	23	0.7	18.6	0.8	28	27.8	9.2	713	7.7	15.0		8.2	2.7	4.2	0.8	5.2	1180		0.4
GXR-1 Cert	13.8	427	14.0	32.0	275	38.0	0.800	18.0	0.770	54.0	122	13.0	750	7.50	17.0		18.0	2.70	4.20	0.830	4.30	1110		0.430
DH-1a Meas																								
DH-1a Cert																								
GXR-4 Meas	19.3	103	121	14.9	213	44	9.4	318	0.2	7	4.4	0.8	96	56.5	104		39.9	5.9	4.9	0.6	3.0	6650		0.2
GXR-4 Cert	20.0	98.0	160	14.0	221	186	10.0	310	0.270	5.60	4.80	0.970	1640	64.5	102		45.0	6.60	5.25	0.360	2.60	6520		0.210
SDC-1 Meas	24.2	0.5	104	36.0	180	44	0.3	< 0.1		< 1	< 0.1		645	41.7	86.4		39.3	7.5	7.3	1.1	6.9	33.1		0.6
SDC-1 Cert	21.00	0.220	127.00	40.0	180.00	290.00	21.00	0.250		3.00	0.54		630	42.00	93.00		40.00	8.20	7.00	1.20	6.70	30.00		0.65
GXR-6 Meas	29.7	272	85.1	13.8	38.9	84	1.5	1.1	< 0.1	< 1	1.2	< 0.1	1360	13.3	35.7		12.6	2.5	2.5	0.4	2.7	76.4		0.3
GXR-6 Cert	35.0	330	90.0	14.0	35.0	110	7.50	2.40	0.260	1.70	3.60	0.0180	1300	13.9	36.0		13.0	2.67	2.97	0.415	2.80	66.0		0.0320
SAR-M (U.S.G.S.) Meas	18.3	33.5	141	36.9	157		6.2	6.0	1.0	2	3.5	0.3	840	59.6	123							361		
SAR-M (U.S.G.S.) Cert	17	38.8	146	28.00	151		29.9	13.1	1.08	2.76	6.0	0.96	801	57.4	122.0							331		
DNC-1a Meas				18.5	147	42					0.6		117	4.0			5.0					110		
DNC-1a Cert				18.0	144.0	38.000					0.96		118	3.6			5.20					100.0		
SBC-1 Meas	28.1	26.8	152	35.8	186	125	12.6	3.2		3	1.0		753	51.3	105	12.9	47.5	9.2	8.6	1.3	7.2	34.0		0.6
SBC-1 Cert	27.0	25.7	147	36.5	178.0	134.0	15.3	2.40		3.3	1.01		788.0	52.5	108.0	12.6	49.2	9.6	8.5	1.20	7.10	31.0		0.56
129051 Orig	14.2	76.2	48.7	18.8	35.6	84	7.3	1.9	< 0.1	< 1	0.5	0.4	83	58.3	103	13.5	48.4	8.0	6.5	0.7	3.6	1330	0.3	0.3
129051 Dup	14.4	78.1	49.1	19.2	36.0	85	7.5	1.7	< 0.1	4	0.5	0.3	80	60.9	106	13.9	49.9	7.6	6.7	0.8	3.7	1370	0.3	0.3
129089 Orig	0.5	1.6	3.9	1.5	31.5	12	0.2	1.7	< 0.1	< 1	< 0.1	< 0.1	18	1.2	2.4	0.3	1.1	0.2	0.2	< 0.1	0.2	5.6	< 0.1	< 0.1
129089 Dup	0.6	1.9	3.9	1.5	32.0	12	0.2	1.8	< 0.1	< 1	< 0.1	< 0.1	18	1.1	2.3	0.3	1.0	0.2	0.2	< 0.1	0.2	10.1	< 0.1	< 0.1
129091 Orig	0.6	1.0	4.9	1.3	28.8	4	0.2	0.4	< 0.1	< 1	< 0.1	< 0.1	22	1.2	2.4	0.3	1.0	0.2	0.2	< 0.1	0.2	4.6	< 0.1	< 0.1
129091 Dup	0.7	0.6	5.0	1.3	29.1	2	0.1	0.3	< 0.1	< 1	< 0.1	< 0.1	22	1.2	2.4	0.3	1.0	0.2	0.2	< 0.1	0.2	5.1	< 0.1	< 0.1
L307879 Orig	19.0	1.1	48.9	28.8	35.5	93	0.3	0.2	0.1	< 1	< 0.1	< 0.1	52	7.7	19.8	2.4	10.9	3.9	5.2	0.9	5.6	1440	0.3	0.4
L307879 Dup	20.0	1.2	49.9	29.4	36.0	118	0.5	0.4	0.1	< 1	< 0.1	< 0.1	52	8.1	20.2	2.5	11.2	3.9	5.3	0.9	5.7	1460	0.3	0.4
L307883 Orig	0.7	0.5	6.4	6.7	98.0	3	0.3	1.6	< 0.1	< 1	< 0.1	< 0.1	20	1.6	5.0	0.8	3.6	1.1	1.3	0.2	1.5	5.7	< 0.1	0.1
L307883 Dup	0.7	0.4	6.2	6.8	98.4	4	0.3	1.5	< 0.1	< 1	< 0.1	< 0.1	19	1.6	4.9	0.8	3.4	1.1	1.4	0.2	1.5	5.8	< 0.1	< 0.1
Method Blank	< 0.1	< 0.1	< 0.2	< 0.1	< 0.2	< 1	< 0.1	< 0.1	< 0.1	< 1	< 0.1	< 0.1	< 1	< 0.1	< 0.1	< 0.1	< 0.1	< 0.1	< 0.1	< 0.1	< 0.1	< 0.2	< 0.1	< 0.1
Method Blank																								
Method Blank																								

Quality Control

Analyte Symbol	Yb	Lu	Ta	W	Re	Tl	Pb	Sc	Th	U	Ti	P	S
Unit Symbol	ppm	ppm	ppm	ppm	ppm	ppm	ppm	ppm	ppm	ppm	%	%	%
Detection Limit	0.1	0.1	0.1	0.1	0.001	0.05	0.5	1	0.1	0.1	0.0005	0.001	0.01
Analysis Method	TD-MS	TD-MS	TD-MS	TD-MS	TD-MS	TD-MS	TD-MS	TD-ICP	TD-MS	TD-MS	TD-ICP	TD-ICP	TD-ICP
GXR-1 Meas	2.1	0.3	< 0.1	135		0.45	718	1	3.4	33.2		0.058	0.25
GXR-1 Cert	1.90	0.280	0.175	164		0.390	730	1.58	2.44	34.9		0.0650	0.257
DH-1a Meas									> 200	2120			
DH-1a Cert									910	2629			
GXR-4 Meas	1.0	0.1	0.5	34.0		3.39	47.0	8	19.9	5.5		0.131	1.73
GXR-4 Cert	1.60	0.170	0.790	30.8		3.20	52.0	7.70	22.5	6.20		0.120	1.77
SDC-1 Meas	3.2		< 0.1	< 0.1		0.65	23.4	16	12.7	2.8	0.234	0.055	0.06
SDC-1 Cert	4.00		1.20	0.800		0.70	25.00	17.00	12.00	3.10	0.606	0.0690	0.0650
GXR-6 Meas	1.7	0.3	< 0.1	0.4		2.42	101	29	5.8	1.4		0.035	0.02
GXR-6 Cert	2.40	0.330	0.485	1.90		2.20	101	27.6	5.30	1.54		0.0350	0.0160
SAR-M (U.S.G.S.) Meas				1.2		2.95	915	10	19.8	4.2	0.279	0.062	
SAR-M (U.S.G.S.) Cert				9.78		2.7	982	7.83	17.2	3.57	0.38	0.07	
DNC-1a Meas	2.0							32					
DNC-1a Cert	2.0							31					
SBC-1 Meas	3.3	0.5	0.6	1.5		0.97	34.9	22	17.1	5.7			
SBC-1 Cert	3.64	0.54	1.10	1.60		0.89	35.0	20.0	15.8	5.76			
129051 Orig	1.8	0.3	0.5	0.9	0.007	0.20	4.2	19	8.4	3.2	0.287	0.034	3.77
129051 Dup	1.8	0.3	0.5	1.0	0.010	0.18	4.3	19	8.6	3.2	0.287	0.034	3.77
129089 Orig	0.1	< 0.1	< 0.1	< 0.1	0.001	0.13	13.7	< 1	0.4	0.2	0.0115	0.029	0.20
129089 Dup	0.1	< 0.1	< 0.1	< 0.1	0.001	0.14	14.4	< 1	0.4	0.2	0.0125	0.030	0.20
129091 Orig	0.1	< 0.1	< 0.1	0.1	< 0.001	0.08	3.8	< 1	0.4	0.2	0.0115	0.032	0.09
129091 Dup	< 0.1	< 0.1	< 0.1	< 0.1	< 0.001	0.08	3.8	< 1	0.6	0.2	0.0112	0.032	0.09
L307879 Orig	2.1	0.3	< 0.1	< 0.1	0.001	0.18	1.7	8	7.1	1.5	0.288	0.056	0.08
L307879 Dup	2.1	0.3	< 0.1	< 0.1	0.004	0.19	1.8	9	7.1	1.5	0.393	0.060	0.08
L307883 Orig	0.5	< 0.1	< 0.1	< 0.1	< 0.001	< 0.05	1.3	2	0.2	0.1	0.0114	0.010	0.06
L307883 Dup	0.5	< 0.1	< 0.1	< 0.1	< 0.001	< 0.05	1.2	2	0.2	< 0.1	0.0115	0.011	0.07
Method Blank	< 0.1	< 0.1	< 0.1	< 0.1	< 0.001	< 0.05	< 0.5	< 1	< 0.1	< 0.1	< 0.0005	< 0.001	< 0.01
Method Blank								< 1			< 0.0005	< 0.001	< 0.01
Method Blank								< 1			< 0.0005	< 0.001	< 0.01

Quality Analysis ... *Innovative Technologies*

Date Submitted: 20-Aug-13
Invoice No.: A13-09848
Invoice Date: 27-Aug-13
Your Reference:

Techni-Lab Abitibi Inc.(Actlabs)
184 Rue Principale
Ste-Germaine-Boule Quebec J0Z 1M0
Canada

ATTN: Andre Caouette

CERTIFICATE OF ANALYSIS

113 Pulp samples were submitted for analysis.

The following analytical package was requested: Code UT-6 Total Digestion ICP & ICP/MS

REPORT **A13-09848**

This report may be reproduced without our consent. If only selected portions of the report are reproduced, permission must be obtained. If no instructions were given at time of sample submittal regarding excess material, it will be discarded within 90 days of this report. Our liability is limited solely to the analytical cost of these analyses. Test results are representative only of material submitted for analysis.

Notes:

CERTIFIED BY :

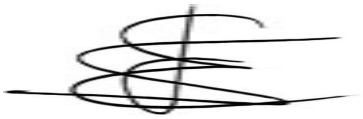

Emmanuel Eseme , Ph.D.
Quality Control

ISO/IEC 17025
SCC Accredited
LAB 266
LAB 266
Accrédité CCN

ACTIVATION LABORATORIES LTD.

1336 Sandhill Drive, Ancaster, Ontario Canada L9G 4V5 TELEPHONE +1.905.648.9611 or +1.888.228.5227 FAX +1.905.648.9613
E-MAIL Ancaster@actlabs.com ACTLABS GROUP WEBSITE www.actlabs.com

Analyte Symbol	Li	Na	Mg	Al	K	Ca	Cd	V	Cr	Mn	Fe	Hf	Hg	Ni	Er	Be	Ho	Ag	Cs	Co	Eu	Bi	Se	Zn
Unit Symbol	ppm	%	%	%	%	%	ppm	ppm	ppm	ppm	%	ppm	ppb	ppm	ppm	ppm	ppm	ppm	ppm	ppm	ppm	ppm	ppm	ppm
Detection Limit	0.5	0.01	0.01	0.01	0.01	0.01	0.1	1	0.5	1	0.01	0.1	10	0.5	0.1	0.1	0.1	0.05	0.05	0.1	0.05	0.02	0.1	0.2
Analysis Method	TD-MS	TD-MS	TD-MS	TD-MS	TD-MS	TD-MS	TD-MS	TD-MS	TD-MS	TD-MS	TD-MS	TD-MS	TD-MS	TD-MS	TD-MS	TD-MS	TD-MS	TD-MS	TD-MS	TD-MS	TD-MS	TD-MS	TD-MS	TD-MS
1271851	3.9	> 3.00	0.51	5.81	0.03	2.16	18.1	108	109	227	13.8	1.9	3600	89.1	0.8	0.4	0.3	24.9	< 0.05	71.3	0.18	0.48	8.6	851
1271852	2.1	> 3.00	0.50	5.60	0.01	8.06	0.5	58	51.2	1410	7.33	1.6	1320	87.3	3.5	0.4	1.3	2.64	< 0.05	385	0.69	0.41	8.9	92.5
1271853	12.5	> 3.00	3.91	8.05	0.05	3.78	< 0.1	247	91.3	701	6.94	1.9	10	44.0	2.6	0.6	0.9	0.82	0.09	10.3	0.54	0.03	2.3	29.3
1271854	1.0	> 3.00	0.08	9.82	0.06	0.97	< 0.1	41	76.1	32	0.31	0.8	< 10	4.8	3.5	0.9	1.3	0.29	< 0.05	1.0	0.60	0.03	2.6	3.9
1271855	1.4	> 3.00	0.08	5.96	0.05	6.62	0.1	78	85.0	574	7.29	2.9	200	92.0	1.9	0.5	0.7	0.36	0.84	98.8	0.37	0.75	4.5	14.2
1271856	2.6	> 3.00	0.95	7.68	0.04	3.84	< 0.1	344	93.8	240	5.93	3.0	60	65.6	4.5	0.7	1.6	0.25	0.05	38.4	0.90	0.25	7.5	< 0.2
1271857	53.1	> 3.00	2.72	7.97	1.57	1.42	< 0.1	77	57.8	621	11.4	1.7	< 10	53.2	2.8	1.9	1.0	0.16	1.47	54.3	1.41	0.16	3.2	51.7
1271858	33.1	> 3.00	4.29	7.34	0.07	5.34	< 0.1	147	234	1050	8.93	0.5	< 10	90.8	2.0	0.4	0.7	0.08	0.38	42.0	0.71	0.03	1.5	56.8
1271859	2.6	0.25	3.78	4.92	0.20	11.2	< 0.1	308	433	1390	8.17	1.3	< 10	74.4	1.7	0.6	0.6	0.15	0.16	32.2	0.80	0.06	2.0	57.1
1271860	1.9	> 3.00	0.22	5.40	0.31	0.77	< 0.1	67	252	82	3.05	2.5	< 10	46.9	0.5	0.8	0.2	0.17	0.18	123	0.13	0.14	5.3	5.1
1272001	14.4	> 3.00	3.84	7.76	0.06	3.70	< 0.1	231	77.5	543	3.96	1.8	< 10	42.4	3.8	0.6	1.3	0.18	0.06	20.6	0.93	0.09	4.6	42.4
1272002	15.8	> 3.00	3.12	7.15	0.18	2.96	0.7	253	137	660	10.9	1.7	70	126	2.4	0.5	0.8	1.70	0.92	39.4	0.51	0.21	9.5	85.9
1272003	20.3	> 3.00	4.25	7.86	0.04	2.63	1.9	256	109	732	10.7	2.0	410	41.3	1.6	0.6	0.6	8.80	0.08	14.9	0.38	0.11	11.5	136
1272004	1.0	> 3.00	0.08	9.15	0.04	2.61	< 0.1	56	60.5	190	0.58	2.4	110	9.0	1.0	0.8	0.4	1.16	< 0.05	2.4	0.25	0.05	0.9	6.5
1272005	5.2	> 3.00	0.39	8.99	0.03	1.70	< 0.1	110	119	169	1.69	3.9	200	22.3	2.9	0.7	1.1	0.69	< 0.05	38.3	0.53	0.05	2.2	4.1
1272006	1.5	> 3.00	0.19	7.22	0.03	5.00	0.4	84	121	453	5.16	2.4	180	85.0	2.0	0.4	0.7	0.76	0.07	66.4	0.41	0.43	5.2	31.1
1272007	4.9	> 3.00	1.49	8.44	0.05	1.54	< 0.1	144	137	270	6.22	3.2	420	49.7	0.6	0.7	0.2	1.15	< 0.05	17.4	0.15	0.18	8.5	17.2
1272008	15.6	> 3.00	1.61	> 10.0	3.12	0.12	< 0.1	128	92.8	29	1.61	1.7	< 10	67.7	0.8	2.9	0.3	0.37	0.54	83.0	1.40	0.05	1.7	3.2
1272009	13.8	> 3.00	0.80	8.57	0.95	0.75	0.5	36	161	181	3.03	3.0	< 10	24.1	1.2	1.1	0.4	8.52	0.63	21.1	0.31	0.79	1.5	37.6
1272010	20.1	> 3.00	1.19	5.66	0.71	0.47	0.7	41	184	200	4.64	2.9	< 10	76.9	0.6	0.9	0.2	8.33	0.40	69.1	0.10	0.80	3.7	51.9
1272011	27.8	> 3.00	1.33	7.16	0.78	0.19	< 0.1	17	205	181	4.25	0.7	< 10	24.7	0.6	0.9	0.2	1.16	0.57	32.1	0.09	0.09	1.0	51.9
1272012	31.3	2.51	1.46	7.03	1.23	0.09	< 0.1	21	191	200	4.95	0.7	< 10	13.1	0.3	1.0	0.1	0.56	0.86	15.7	< 0.05	0.12	1.3	56.2
1272013	25.4	> 3.00	1.18	9.27	1.70	0.20	< 0.1	41	122	167	3.69	1.1	< 10	21.6	0.7	1.7	0.2	0.64	1.37	27.7	0.05	0.17	0.9	44.4
1272014	11.1	2.35	0.40	> 10.0	3.21	0.08	1.1	79	108	47	1.53	1.9	100	4.8	0.9	3.3	0.3	6.47	2.76	5.7	0.14	0.27	1.3	46.1
1272015	13.6	0.01	3.09	1.79	< 0.01	3.07	16.3	77	124	823	31.0	0.3	40	211	0.7	< 0.1	0.3	9.35	0.10	> 500	0.15	6.53	82.7	4830
1272016	40.5	< 0.01	6.17	5.37	< 0.01	2.19	0.2	105	130	628	16.0	0.9	< 10	88.6	0.6	0.4	0.2	1.63	0.08	> 500	0.14	0.10	45.7	99.1
1272017	2.0	0.92	10.1	1.13	0.06	18.3	0.1	9	33.9	2840	3.93	1.8	< 10	45.6	3.5	0.3	1.3	0.44	0.08	20.2	1.14	0.07	9.8	13.0
1272018	5.3	0.15	0.43	0.54	0.01	1.19	0.2	7	125	177	23.4	< 0.1	2090	> 5000	5.7	0.8	2.4	12.1	0.06	> 500	3.78	0.53	> 1000	9.0
1272019	1.2	> 3.00	2.37	5.99	0.07	4.85	< 0.1	78	224	667	2.64	1.7	10	78.9	1.1	0.9	0.3	1.03	0.14	24.3	0.17	0.07	409	11.5
1272020	1.4	> 3.00	1.04	4.69	0.09	1.88	0.1	111	203	375	3.57	3.9	360	60.4	0.5	1.1	0.1	0.52	0.10	6.8	0.06	0.13	60.6	15.6
1272021	5.0	0.05	9.01	0.24	0.16	14.9	< 0.1	3	151	904	0.51	< 0.1	< 10	8.5	0.3	< 0.1	0.1	0.19	0.15	5.6	0.22	0.05	17.4	6.5
1272022	4.3	0.03	12.9	0.13	0.08	24.3	< 0.1	2	14.1	2100	1.09	< 0.1	< 10	20.4	0.2	< 0.1	< 0.1	0.27	0.13	16.6	0.14	0.05	70.6	11.5
1272023	89.1	1.99	6.49	8.08	3.53	5.21	< 0.1	219	504	1110	9.17	0.7	< 10	184	1.4	0.6	0.5	0.17	7.98	89.1	0.97	0.55	12.2	103
1272024	7.5	0.11	1.08	1.30	0.02	3.43	< 0.1	24	309	454	3.49	< 0.1	< 10	483	0.2	0.1	< 0.1	0.28	0.22	65.2	0.06	0.03	10.4	25.5
1272025	10.1	> 3.00	1.03	4.89	0.28	0.34	< 0.1	37	257	187	3.37	2.6	< 10	84.6	0.6	0.5	0.2	0.21	0.52	40.8	0.33	0.38	13.0	36.2
1272026	14.2	> 3.00	0.77	6.29	0.77	0.73	0.4	48	162	189	2.86	2.9	< 10	57.3	1.5	1.2	0.6	0.81	0.50	43.4	1.52	0.52	32.2	35.7
1272027	23.3	> 3.00	1.17	7.32	1.61	0.44	< 0.1	60	126	262	3.64	4.1	< 10	45.8	1.2	1.6	0.4	0.51	0.96	45.2	0.58	0.40	11.4	40.5
1272028	7.3	> 3.00	3.65	8.92	1.73	7.37	< 0.1	31	51.7	799	1.01	2.0	< 10	18.6	3.0	1.9	1.1	2.17	1.33	10.2	0.79	5.19	38.8	6.6
1272029	5.6	2.10	2.97	5.31	1.40	6.37	2.2	49	155	1320	3.12	0.9	< 10	42.5	0.9	1.5	0.3	5.16	1.05	91.2	0.41	0.36	87.7	44.0
1272030	2.0	1.77	1.23	2.68	0.33	2.77	0.3	10	235	363	2.70	0.3	< 10	47.7	0.6	0.4	0.2	2.18	0.29	109	0.13	0.24	115	19.2
1272031	20.3	1.91	4.85	7.25	0.07	7.25	0.2	103	241	1410	7.98	0.2	< 10	162	1.8	0.3	0.6	0.56	0.22	48.9	0.69	0.09	5.0	90.9
1272032	1.0	1.28	0.77	1.70	0.09	1.63	0.2	< 1	293	252	1.79	0.2	< 10	39.7	0.3	0.3	0.1	0.56	0.13	103	0.11	0.06	55.9	6.9
1272033	1.9	0.78	3.13	1.51	0.33	7.17	0.6	8	174	1630	2.55	0.2	< 10	47.1	0.6	0.3	0.2	0.74	0.33	94.4	0.18	0.18	31.5	15.9
1272034	1.0	< 0.01	0.18	0.05	0.02	0.73	< 0.1	14	104	5510	30.8	< 0.1	< 10	3.3	0.5	1.9	0.1	0.54	0.52	4.9	0.22	0.25	4.1	6.4
1272035	8.3	1.26	2.42	8.59	0.13	11.5	< 0.1	290	203	1300	11.0	0.7	< 10	68.3	2.3	0.5	0.8	0.19	0.32	117	1.30	0.71	3.7	30.0
1272036	9.1	0.05	13.2	0.72	0.04	14.0	0.5	33	20.1	506	0.95	0.3	< 10	30.6	0.3	1.2	< 0.1	6.90	0.17	17.2	0.10	19.8	21.5	123
1272037	8.4	0.04	10.2	0.81	0.02	8.33	3.0	26	28.8	403	0.82	< 0.1	< 10	29.9	0.1	0.7	< 0.1	3.76	0.11	14.6	< 0.05	37.9	203	105
1272038	8.1	0.03	10.1	0.75	0.02	7.97	3.0	22	14.8	390	0.89	< 0.1	< 10	28.6	0.1	0.6	< 0.1	3.99	0.12	14.5	< 0.05	67.3	236	102
1272039	6.4	0.01	22.6	0.88	0.02	4.51	1.8	35	12.3	506	2.83	< 0.1	< 10	44.0	0.2	0.2	< 0.1	2.45	0.41	21.4	0.08	21.0	4.4	160
1272040	1.9	< 0.01	18.2	0.37	< 0.01	14.7	< 0.1	21	11.0	640	1.72	< 0.1	< 10	17.3	0.2	0.3	< 0.1	2.95	0.20	14.9	0.10	0.67	2.5	106
1272041	1.6	0.05	8.52	0.09	0.02	15.0	0.3	4	67.2	844	5.68	< 0.1	20	8.3	0.1	< 0.1	< 0.1	0.97	0.17	5.2	0.16	17.9	225	12.0
1272042	5.0	0.06	12.0	0.19	0.04	20.5	0.3	10	41.2	967	1.46	< 0.1	< 10	11.8	0.2	0.2	< 0.1	0.66	0.25	5.2	0.21	1.24	33.5	13.3

Analyte Symbol	Li	Na	Mg	Al	K	Ca	Cd	V	Cr	Mn	Fe	Hf	Hg	Ni	Er	Be	Ho	Ag	Cs	Co	Eu	Bi	Se	Zn
Unit Symbol	ppm	%	%	%	%	%	ppm	ppm	ppm	ppm	%	ppm	ppb	ppm	ppm	ppm	ppm	ppm	ppm	ppm	ppm	ppm	ppm	ppm
Detection Limit	0.5	0.01	0.01	0.01	0.01	0.01	0.1	1	0.5	1	0.01	0.1	10	0.5	0.1	0.1	0.1	0.05	0.05	0.1	0.05	0.02	0.1	0.2
Analysis Method	TD-MS	TD-MS	TD-MS	TD-MS	TD-MS	TD-MS	TD-MS	TD-MS	TD-MS	TD-MS	TD-MS	TD-MS	TD-MS	TD-MS	TD-MS	TD-MS	TD-MS	TD-MS	TD-MS	TD-MS	TD-MS	TD-MS	TD-MS	TD-MS
1272043	10.4	0.09	13.4	0.41	0.07	21.5	0.3	12	18.7	995	0.84	< 0.1	< 10	11.7	0.2	< 0.1	< 0.1	0.28	0.30	5.4	0.20	0.43	6.5	15.0
1272044	5.5	0.08	12.0	0.24	0.04	19.9	0.2	9	22.1	930	1.42	< 0.1	< 10	9.4	0.2	< 0.1	< 0.1	0.25	0.23	5.1	0.19	1.52	30.7	11.9
1272045	4.8	> 3.00	0.69	4.98	0.26	0.98	< 0.1	31	142	155	8.39	1.8	< 10	178	0.6	0.3	0.2	0.24	0.45	76.3	0.52	0.23	17.8	11.0
1272051	33.4	2.11	1.24	7.12	3.23	0.85	< 0.1	46	200	377	4.62	2.5	< 10	16.8	0.5	1.8	0.2	0.19	1.89	6.1	0.52	0.11	2.9	6.4
1272052	28.3	> 3.00	0.61	6.54	2.49	0.34	< 0.1	20	123	84	1.00	0.6	< 10	12.2	0.2	1.5	< 0.1	0.09	1.03	3.3	0.24	0.03	1.4	15.8
1272053	23.4	2.91	3.87	5.76	0.03	9.72	0.2	250	199	1690	7.62	1.5	< 10	86.8	2.1	0.6	0.7	0.26	0.09	44.0	0.57	0.06	3.5	58.4
1272054	69.4	0.05	1.68	5.34	1.65	0.32	< 0.1	49	222	152	2.47	2.6	< 10	29.7	0.6	1.5	0.2	0.17	1.73	12.2	0.77	0.10	1.2	11.3
1272055	4.2	> 3.00	1.05	6.33	0.09	2.24	0.2	33	162	566	2.01	3.7	< 10	33.1	0.9	0.7	0.3	0.16	0.14	113	0.24	0.09	3.5	15.7
1272056	2.3	> 3.00	0.79	4.57	0.19	1.99	< 0.1	46	219	333	1.52	1.6	< 10	31.6	0.6	0.7	0.2	0.13	0.13	69.9	0.21	0.09	2.3	12.0
1272101	15.4	0.23	2.49	2.86	< 0.01	0.02	0.4	128	235	279	11.1	1.1	< 10	261	0.1	0.3	< 0.1	0.48	0.09	> 500	< 0.05	0.50	61.8	243
1272102	1.7	> 3.00	1.06	5.24	0.04	2.67	< 0.1	348	108	290	19.5	4.3	< 10	36.2	4.8	1.0	1.5	0.22	0.07	132	0.71	0.13	3.5	25.6
1272103	< 0.5	0.03	0.03	0.04	< 0.01	0.03	< 0.1	< 1	362	61	0.60	< 0.1	< 10	10.0	< 0.1	0.2	< 0.1	0.13	0.18	2.1	< 0.05	0.06	2.5	6.7
1272104	10.4	1.54	0.82	8.85	4.03	0.12	< 0.1	91	154	51	5.55	3.6	< 10	32.6	1.3	2.3	0.5	0.29	2.36	171	1.49	0.70	5.2	5.9
1272106	6.0	> 3.00	0.83	8.57	0.44	0.69	< 0.1	100	103	83	5.16	4.0	< 10	60.2	1.0	1.3	0.3	0.24	0.13	> 500	0.30	0.51	99.6	8.4
1272107	0.9	1.17	1.29	1.40	0.08	2.92	0.1	< 1	313	404	0.83	0.1	< 10	16.9	0.5	0.4	0.2	0.10	0.26	2.0	0.07	0.07	2.2	18.9
1272108	1.9	0.35	11.5	0.42	0.03	24.1	< 0.1	11	21.7	2460	2.10	0.1	< 10	14.0	1.1	0.5	0.4	0.06	0.09	2.8	0.28	0.07	1.7	15.3
1272109	0.7	0.10	0.76	0.07	0.02	1.63	0.1	3	352	277	2.50	0.4	< 10	39.3	0.5	0.3	0.2	0.09	0.19	12.8	0.09	0.09	1.5	14.4
1272110	1.9	0.77	6.09	0.93	0.09	16.9	< 0.1	31	135	1630	6.54	< 0.1	< 10	58.9	4.6	0.4	1.9	0.06	0.19	22.4	1.81	0.19	4.0	13.3
1272111	0.9	0.02	0.05	0.20	0.10	0.07	0.4	14	353	42	1.12	0.1	< 10	23.9	< 0.1	0.3	< 0.1	0.13	0.12	14.3	< 0.05	1.19	1.2	80.5
1272112	1.5	> 3.00	0.42	8.20	0.13	1.04	0.2	105	101	210	4.03	3.2	530	79.1	0.7	1.4	0.2	0.34	0.13	3.0	0.10	0.16	8.2	9.6
1272113	1.2	> 3.00	0.21	8.23	0.12	0.49	0.1	79	104	92	2.52	3.2	390	47.5	0.6	1.6	0.1	0.34	0.12	2.8	0.06	0.09	4.1	5.4
1272114	25.0	> 3.00	0.55	8.02	2.92	0.06	< 0.1	90	97.8	24	0.89	1.1	20	25.4	1.1	2.8	0.4	0.15	2.69	0.4	0.54	2.43	3.2	11.5
1272115	0.8	0.69	0.47	0.79	0.05	1.47	0.1	< 1	350	221	2.60	0.2	< 10	33.9	0.6	0.2	0.2	0.11	0.22	23.1	0.15	0.12	3.3	26.7
1272116	33.9	2.50	0.98	6.33	2.45	0.12	< 0.1	73	158	28	1.68	2.2	< 10	93.6	1.3	2.4	0.4	0.17	2.17	39.3	0.41	0.19	2.8	6.3
1272117	1.7	> 3.00	0.17	5.96	0.14	0.45	< 0.1	117	185	55	5.27	3.3	250	89.0	0.7	1.2	0.2	0.30	0.13	27.6	0.10	0.57	7.3	4.1
1272118	2.6	2.99	0.48	3.87	0.22	0.98	< 0.1	13	180	321	0.44	0.5	< 10	6.6	0.4	0.7	0.2	0.10	0.17	1.4	0.76	0.11	0.6	9.0
1272119	43.6	> 3.00	2.54	6.79	1.54	1.89	0.1	61	69.7	715	5.22	2.8	90	14.9	2.0	2.0	0.8	< 0.05	2.62	42.0	3.34	0.06	2.3	70.8
1272120	84.9	> 3.00	4.12	7.90	2.64	0.36	< 0.1	61	59.0	203	5.58	4.0	< 10	40.5	2.3	3.0	0.8	0.06	5.18	58.9	1.44	0.03	1.8	31.9
1272121	1.4	0.02	2.25	0.03	0.01	6.37	< 0.1	< 1	164	8820	19.2	< 0.1	60	4.1	0.1	0.7	< 0.1	< 0.05	0.12	5.2	0.09	0.07	1.1	5.5
1272122	38.3	> 3.00	1.86	7.23	1.42	0.17	< 0.1	50	143	113	3.81	2.8	< 10	20.8	0.3	1.7	0.1	0.07	1.22	28.0	0.21	0.05	1.4	10.0
1272123	1.0	0.02	1.59	0.03	0.01	4.53	< 0.1	< 1	209	6080	20.3	< 0.1	< 10	4.2	0.1	0.4	< 0.1	< 0.05	0.07	4.8	0.07	0.03	0.5	5.7
1272124	15.7	1.86	4.81	7.75	0.21	8.66	< 0.1	269	237	1780	8.71	1.3	< 10	132	2.6	0.6	0.9	0.06	0.69	45.4	0.84	0.06	2.1	91.8
1272125	0.9	0.03	0.01	0.03	0.01	0.13	0.1	< 1	340	61	1.91	< 0.1	< 10	138	< 0.1	< 0.1	< 0.1	1.02	0.12	36.9	< 0.05	0.02	2.9	9.5
1272126	16.0	> 3.00	4.14	7.17	0.04	3.68	0.8	332	93.6	678	9.07	2.3	10	38.7	4.5	0.8	1.6	2.49	0.05	26.5	0.63	0.10	5.3	97.4
1272127	2.7	> 3.00	0.24	5.38	0.05	0.56	1.3	71	139	99	4.95	2.9	< 10	40.3	1.1	0.8	0.4	3.44	< 0.05	35.0	0.20	0.08	7.6	88.8
1272144	2.3	0.03	5.11	0.09	0.03	9.59	0.3	5	27.0	595	1.15	< 0.1	< 10	5.1	0.2	< 0.1	< 0.1	1.97	0.40	2.7	0.13	0.12	9.6	11.0
1272201	12.9	> 3.00	3.65	4.82	0.88	6.61	1.0	291	94.9	867	12.3	1.9	< 10	81.1	3.0	1.5	1.1	2.33	4.97	47.5	0.53	0.55	10.9	80.9
1272202	14.3	> 3.00	3.73	6.80	0.14	5.91	0.2	184	36.1	1040	10.8	0.2	< 10	44.4	3.6	0.4	1.2	0.45	0.27	48.5	1.24	0.05	2.2	73.0
1272203	2.4	> 3.00	0.11	6.49	0.04	0.65	21.3	109	62.1	72	11.4	2.2	< 10	103	0.3	0.4	0.1	19.9	< 0.05	62.1	0.13	0.34	13.3	1100
1272204	11.6	> 3.00	3.45	5.69	0.05	9.87	< 0.1	302	43.2	683	8.73	1.9	< 10	73.3	3.1	0.8	1.1	1.46	0.06	52.2	0.72	0.15	5.7	18.1
1272205	19.8	> 3.00	4.61	6.77	0.07	5.70	0.1	246	44.2	618	8.33	1.6	140	80.2	3.7	1.2	1.3	0.39	0.08	60.6	0.58	0.19	2.3	18.8
1272206	2.4	> 3.00	2.34	4.46	0.03	18.3	< 0.1	294	57.1	872	5.15	1.6	30	61.1	2.0	1.1	0.7	0.33	< 0.05	64.5	0.38	0.18	4.4	11.8
1272207	2.5	> 3.00	2.08	9.03	0.56	4.44	0.1	38	43.8	312	0.50	3.8	< 10	59.9	1.2	0.7	0.5	0.19	0.15	3.4	0.78	0.08	18.2	7.0
1272208	13.7	> 3.00	1.19	9.44	0.45	4.74	< 0.1	4	14.7	340	1.47	0.9	180	23.9	4.1	1.2	1.7	0.13	0.13	2.7	1.36	0.05	13.4	12.2
1272209	5.4	> 3.00	0.23	5.43	0.44	0.31	< 0.1	113	117	101	23.4	3.7	< 10	206	2.8	0.6	1.4	0.80	0.15	> 500	9.20	0.84	46.3	4.1
L307851	18.0	0.63	3.05	4.07	0.06	3.27	< 0.1	141	192	958	7.01	0.5	50	56.6	0.9	0.3	0.3	0.24	0.13	29.5	0.33	0.04	2.2	64.1
L307852	119	0.91	2.87	7.39	1.41	0.17	< 0.1	66	122	160	4.10	1.7	20	49.9	0.4	1.9	0.2	0.16	2.72	15.9	0.59	0.05	0.5	93.7
L307853	19.1	1.32	5.46	8.44	0.05	9.60	< 0.1	150	188	1400	8.64	0.5	< 10	193	2.2	0.6	0.7	0.08	0.20	58.0	0.90	0.03	0.8	89.5
L307854	14.5	> 3.00	0.78	7.01	1.36	1.37	< 0.1	63	77.9	209	2.63	3.8	< 10	32.0	1.3	0.9	0.5	0.20	2.90	9.2	1.46	0.08	0.8	23.4
L307855	42.6	1.97	1.36	9.62	2.80	1.03	0.1	85	121	241	3.73	3.4	< 10	11.7	1.4	2.3	0.5	0.11	3.35	5.2	0.94	0.12	1.0	36.0
L307856	15.0	> 3.00	2.25	8.54	0.11	1.09	< 0.1	120	67.4	305	5.32	3.7	< 10	12.2	1.9	0.7	0.7	0.20	0.15	15.2	0.55	0.03	1.9	25.6
L307857	30.3	> 3.00	3.05	9.26	0.06	1.27	< 0.1	227	113	503	6.84	2.2	< 10	57.3	3.1	1.2	1.0	0.16	0.18	33.5	1.00	0.16	10.3	52.5

Analyte Symbol	Li	Na	Mg	Al	K	Ca	Cd	V	Cr	Mn	Fe	Hf	Hg	Ni	Er	Be	Ho	Ag	Cs	Co	Eu	Bi	Se	Zn
Unit Symbol	ppm	%	%	%	%	%	ppm	ppm	ppm	ppm	%	ppm	ppb	ppm	ppm	ppm	ppm	ppm	ppm	ppm	ppm	ppm	ppm	ppm
Detection Limit	0.5	0.01	0.01	0.01	0.01	0.01	0.1	1	0.5	1	0.01	0.1	10	0.5	0.1	0.1	0.1	0.05	0.05	0.1	0.05	0.02	0.1	0.2
Analysis Method	TD-MS	TD-MS	TD-MS	TD-MS	TD-MS	TD-MS	TD-MS	TD-MS	TD-MS	TD-MS	TD-MS	TD-MS	TD-MS	TD-MS	TD-MS	TD-MS	TD-MS	TD-MS	TD-MS	TD-MS	TD-MS	TD-MS	TD-MS	TD-MS
L307858	30.6	> 3.00	1.63	8.52	2.55	1.36	< 0.1	141	92.2	173	2.20	2.9	< 10	8.7	1.6	3.2	0.5	0.30	3.02	3.0	0.58	0.21	4.2	19.1
L307859	1.2	> 3.00	0.05	8.41	0.13	0.67	< 0.1	123	104	42	3.96	2.3	< 10	86.0	2.1	1.0	0.7	0.49	0.11	> 500	0.24	0.74	11.6	1.8
L307860	0.8	> 3.00	0.12	8.83	0.07	0.52	0.1	135	113	33	1.15	4.0	50	2.1	1.4	1.1	0.5	3.61	0.06	1.6	0.19	4.17	10.6	6.5
1272151	60.5	> 3.00	3.60	9.70	0.92	0.21	< 0.1	72	60.3	173	5.23	1.7	40	52.1	0.5	1.8	0.2	1.01	0.28	131	1.07	0.99	7.2	28.2
1272152	1.3	0.29	0.43	0.46	0.06	1.12	0.2	4	23.6	265	9.57	0.1	< 10	113	0.2	0.2	0.1	0.72	0.08	> 500	0.98	1.88	25.2	7.7
1272153	44.3	0.03	9.75	3.97	0.04	9.99	0.1	105	48.1	1460	12.2	0.8	< 10	121	0.8	0.4	0.3	4.12	0.34	> 500	1.18	2.89	23.5	73.6
1272154	39.9	< 0.01	7.55	4.79	0.59	3.32	0.1	290	45.7	601	22.9	1.3	< 10	235	1.8	0.8	0.9	1.04	2.27	> 500	5.66	0.16	63.0	70.1
1272155	27.4	> 3.00	1.04	7.18	1.71	0.21	< 0.1	52	41.3	100	10.3	2.4	< 10	6.8	0.4	2.3	0.2	1.16	0.89	> 500	0.46	0.17	29.9	18.1
1272156	24.2	0.02	2.82	2.51	< 0.01	0.56	0.5	53	15.9	219	18.8	0.4	20	14.1	0.2	< 0.1	< 0.1	5.21	0.07	> 500	0.07	0.98	95.5	78.8

Analyte Symbol	Ga	As	Rb	Y	Sr	Zr	Nb	Mo	In	Sn	Sb	Te	Ba	La	Ce	Pr	Nd	Sm	Gd	Tb	Dy	Cu	Ge	Tm
Unit Symbol	ppm	ppm	ppm	ppm	ppm	ppm	ppm	ppm	ppm	ppm	ppm	ppm	ppm	ppm	ppm	ppm	ppm	ppm	ppm	ppm	ppm	ppm	ppm	ppm
Detection Limit	0.1	0.1	0.2	0.1	0.2	1	0.1	0.1	0.1	1	0.1	0.1	1	0.1	0.1	0.1	0.1	0.1	0.1	0.1	0.1	0.2	0.1	0.1
Analysis Method	TD-MS	TD-MS	TD-MS	TD-MS	TD-MS	TD-MS	TD-MS	TD-MS	TD-MS	TD-MS	TD-MS	TD-MS	TD-MS	TD-MS	TD-MS	TD-MS	TD-MS	TD-MS	TD-MS	TD-MS	TD-MS	TD-MS	TD-MS	TD-MS
1271851	12.8	18.5	< 0.2	8.3	32.6	73	5.4	28.1	0.1	< 1	0.2	1.0	9	3.3	7.9	1.1	4.7	1.3	1.3	0.2	1.4	> 10000	0.2	0.1
1271852	10.7	108	< 0.2	34.8	36.2	59	4.2	6.1	0.2	< 1	0.1	2.0	4	24.9	54.0	7.4	27.8	5.7	6.1	1.0	6.5	> 10000	0.2	0.5
1271853	18.5	2.2	< 0.2	24.0	45.0	61	1.5	1.6	< 0.1	< 1	< 0.1	0.1	10	3.7	10.8	1.8	8.9	3.1	3.8	0.7	4.7	1000	0.5	0.4
1271854	16.4	1.0	0.3	33.8	41.5	27	0.2	0.2	< 0.1	< 1	< 0.1	< 0.1	10	6.3	20.5	3.1	15.2	5.0	5.7	1.0	6.3	291	0.2	0.5
1271855	16.9	13.6	2.8	15.7	46.8	111	6.8	9.0	< 0.1	< 1	0.2	0.7	14	9.1	25.6	3.4	13.9	3.2	3.1	0.5	3.2	> 10000	0.2	0.3
1271856	15.7	18.7	< 0.2	42.6	37.3	106	7.9	2.6	< 0.1	1	0.2	0.2	7	2.2	9.4	2.5	15.6	6.3	7.3	1.3	8.2	414	0.2	0.6
1271857	25.5	1.8	80.4	26.2	37.2	71	1.1	0.4	0.2	< 1	< 0.1	< 0.1	302	13.4	32.2	4.2	16.9	4.2	4.5	0.8	5.1	2470	0.4	0.4
1271858	16.4	0.5	3.4	17.5	93.3	20	0.2	0.1	< 0.1	< 1	< 0.1	< 0.1	29	3.9	10.0	1.5	7.0	2.1	2.8	0.5	3.3	125	0.2	0.3
1271859	16.2	0.8	2.2	13.5	109	27	4.8	1.5	0.2	< 1	0.2	< 0.1	31	4.4	8.8	1.2	5.0	1.5	1.9	0.4	2.9	28.0	3.1	0.3
1271860	10.5	24.0	8.2	4.5	27.0	101	4.2	2.9	< 0.1	< 1	< 0.1	0.1	51	1.1	2.8	0.4	1.9	0.7	1.0	0.2	1.1	807	< 0.1	< 0.1
1272001	19.6	212	0.3	34.2	29.1	60	2.1	0.3	< 0.1	< 1	< 0.1	< 0.1	9	3.1	12.3	2.6	14.1	4.7	5.7	1.0	6.5	483	0.4	0.6
1272002	17.5	3.1	8.5	22.7	29.4	67	4.8	3.8	< 0.1	< 1	< 0.1	< 0.1	23	2.7	8.4	1.6	8.4	3.1	3.7	0.7	4.2	7670	0.2	0.3
1272003	24.0	7.9	< 0.2	15.5	25.4	74	5.4	6.8	0.1	< 1	< 0.1	0.3	6	3.4	11.3	2.0	9.8	2.7	2.7	0.4	2.8	> 10000	0.4	0.2
1272004	20.4	1.1	< 0.2	8.8	33.6	81	0.8	1.9	< 0.1	< 1	< 0.1	< 0.1	9	2.9	9.3	1.5	6.6	1.8	1.8	0.3	2.0	2830	0.2	0.1
1272005	19.3	7.2	< 0.2	29.3	43.3	142	7.0	7.3	< 0.1	< 1	< 0.1	< 0.1	7	5.5	16.0	2.7	13.7	4.8	5.1	0.9	5.6	2410	0.2	0.4
1272006	16.9	31.7	< 0.2	19.4	50.4	86	6.0	8.0	< 0.1	< 1	< 0.1	0.2	9	10.9	23.3	3.1	12.4	3.3	3.3	0.6	3.7	9330	0.1	0.3
1272007	16.2	24.4	< 0.2	6.2	27.4	122	7.2	10.1	< 0.1	< 1	< 0.1	0.7	10	2.2	4.9	0.7	3.0	1.0	1.1	0.2	1.1	9890	0.1	< 0.1
1272008	35.9	2.1	103	8.0	27.0	59	8.4	2.5	< 0.1	3	< 0.1	< 0.1	457	59.0	115	14.0	46.8	7.1	4.7	0.5	2.1	16.5	0.9	0.1
1272009	14.1	4.0	41.1	10.1	68.4	106	9.9	5.4	1.0	2	< 0.1	0.5	234	27.7	58.8	6.3	21.7	3.2	2.4	0.3	1.9	5600	0.3	0.2
1272010	14.7	3.3	13.9	4.4	38.4	104	9.6	4.9	0.8	2	< 0.1	0.5	153	2.4	6.1	0.6	2.2	0.4	0.5	< 0.1	0.8	6250	0.3	0.1
1272011	14.2	2.5	37.4	5.2	59.7	25	3.6	1.9	< 0.1	< 1	< 0.1	< 0.1	194	7.6	13.8	1.5	4.8	0.8	0.6	0.1	0.8	472	< 0.1	0.1
1272012	16.3	0.7	56.3	2.9	41.1	27	2.6	2.5	< 0.1	< 1	< 0.1	< 0.1	297	2.3	4.0	0.4	1.2	0.2	0.3	< 0.1	0.4	186	< 0.1	< 0.1
1272013	19.5	3.9	86.3	5.7	68.0	39	4.2	2.6	0.2	1	< 0.1	< 0.1	484	1.5	2.8	0.3	1.2	0.3	0.4	0.1	0.9	1040	< 0.1	0.1
1272014	34.9	1.4	153	8.2	63.6	69	8.0	2.6	1.0	2	0.2	0.1	946	10.3	22.6	2.6	8.4	1.4	1.2	0.2	1.4	4560	0.5	0.1
1272015	7.6	1370	0.7	6.1	10.6	13	1.1	3.6	0.2	< 1	0.1	10.1	2	2.7	5.9	0.7	2.7	0.7	0.9	0.2	1.2	8560	0.5	0.1
1272016	17.4	58.7	< 0.2	4.9	7.5	30	0.6	3.1	< 0.1	2	< 0.1	0.5	< 1	1.4	3.7	0.6	2.5	0.9	1.1	0.2	1.1	1660	0.3	< 0.1
1272017	1.7	4.2	1.0	29.9	101	62	1.4	0.7	< 0.1	< 1	0.1	17.5	15	3.9	13.8	2.4	11.2	3.7	4.7	1.0	6.8	41.5	0.1	0.5
1272018	1.3	8270	0.4	77.7	9.3	4	1.5	1.8	< 0.1	< 1	0.4	> 500	7	19.1	95.6	17.3	76.1	16.5	18.2	2.4	13.0	> 10000	392	0.6
1272019	13.6	45.5	1.4	9.4	67.1	61	4.3	1.6	< 0.1	< 1	0.1	5.6	30	1.2	3.2	0.5	2.2	0.7	1.1	0.2	1.5	434	1.5	0.2
1272020	17.6	12.0	< 0.2	3.8	35.6	135	10.1	6.2	0.8	1	0.2	1.5	25	0.4	1.5	0.2	0.9	0.3	0.4	< 0.1	0.6	> 10000	0.4	< 0.1
1272021	0.6	2.3	6.0	2.6	92.0	3	0.9	2.4	< 0.1	< 1	< 0.1	0.2	26	2.1	4.9	0.6	2.4	0.6	0.6	0.1	0.6	14.8	< 0.1	< 0.1
1272022	0.2	7.3	4.0	1.8	144	2	0.4	0.6	< 0.1	< 1	< 0.1	1.1	7	1.8	3.2	0.4	1.7	0.4	0.5	< 0.1	0.4	38.0	0.3	< 0.1
1272023	16.2	2.0	137	11.3	319	23	1.1	0.8	0.5	< 1	< 0.1	< 0.1	195	7.7	14.3	1.8	7.5	2.0	2.2	0.4	2.5	87.8	0.9	0.2
1272024	2.4	4.5	1.4	1.4	17.3	1	0.4	3.2	< 0.1	< 1	< 0.1	0.2	3	0.3	0.6	< 0.1	0.4	0.1	0.2	< 0.1	0.2	620	0.1	< 0.1
1272025	10.0	2.3	12.7	4.9	25.8	93	3.3	4.9	< 0.1	< 1	< 0.1	0.1	73	13.3	21.2	2.2	7.1	1.3	1.0	0.2	1.0	200	0.1	< 0.1
1272026	15.0	3.3	35.3	13.6	89.6	103	7.2	101	< 0.1	1	< 0.1	0.4	171	95.9	202	20.2	62.5	9.4	6.3	0.8	3.7	493	0.5	0.2
1272027	21.8	1.9	73.8	9.9	91.0	140	9.5	37.3	< 0.1	1	< 0.1	0.1	365	25.4	50.9	5.5	17.7	2.9	2.2	0.3	1.9	211	0.3	0.2
1272028	17.0	5.3	79.0	18.6	109	64	3.7	19.5	< 0.1	< 1	< 0.1	3.9	418	5.5	15.3	2.1	9.1	2.9	3.3	0.7	5.2	25.8	0.5	0.4
1272029	13.5	7.6	66.0	7.5	79.9	33	4.1	21.2	0.1	1	< 0.1	1.2	378	14.3	29.9	3.5	12.4	2.3	2.1	0.3	1.9	5570	0.4	0.1
1272030	4.8	14.1	15.6	5.2	41.4	13	1.9	21.9	< 0.1	< 1	< 0.1	1.0	88	4.2	8.9	1.0	3.8	0.8	0.9	0.1	0.9	2310	0.5	< 0.1
1272031	14.7	5.6	3.1	15.3	105	7	0.3	0.6	< 0.1	< 1	< 0.1	< 0.1	9	3.3	8.6	1.3	6.3	1.9	2.5	0.4	3.0	264	0.3	0.3
1272032	2.4	4.0	4.1	2.8	27.2	7	1.2	15.6	< 0.1	< 1	< 0.1	< 0.1	24	3.7	7.5	0.8	3.0	0.6	0.6	< 0.1	0.6	974	0.3	< 0.1
1272033	3.3	2.7	15.2	5.0	64.6	8	1.2	8.1	< 0.1	< 1	0.1	0.2	90	2.6	5.3	0.6	2.3	0.6	0.8	0.1	0.9	1020	0.2	< 0.1
1272034	1.2	9.6	1.5	4.0	4.4	7	1.8	1.5	< 0.1	< 1	0.5	< 0.1	15	1.4	3.2	0.3	1.4	0.3	0.5	< 0.1	0.6	6.0	0.3	< 0.1
1272035	29.4	4.5	4.8	19.2	> 1000	21	1.8	1.1	0.7	< 1	0.3	< 0.1	20	4.4	10.2	1.5	7.0	2.1	2.9	0.5	3.6	436	0.2	0.3
1272036	2.3	2.9	1.7	2.5	39.6	10	0.6	0.9	< 0.1	< 1	0.5	0.8	6	2.9	6.2	0.7	2.7	0.5	0.5	< 0.1	0.5	4950	0.1	< 0.1
1272037	2.3	14.1	1.0	1.1	23.8	4	0.3	0.5	< 0.1	< 1	< 0.1	3.2	66	2.0	3.9	0.4	1.3	0.2	0.2	< 0.1	0.2	> 10000	0.8	< 0.1
1272038	2.2	15.6	1.2	1.1	20.5	4	0.3	1.1	< 0.1	4	< 0.1	3.2	56	2.0	3.7	0.4	1.5	0.3	0.3	< 0.1	0.2	> 10000	0.9	< 0.1
1272039	3.4	4.0	2.1	2.0	23.8	3	0.4	0.6	0.5	2	0.2	0.3	9	2.2	4.8	0.6	2.2	0.4	0.5	< 0.1	0.4	281	< 0.1	< 0.1
1272040	1.5	6.5	0.5	1.7	68.4	3	0.7	0.2	0.2	< 1	0.2	< 0.1	6	3.7	8.1	0.9	3.2	0.5	0.5	< 0.1	0.4	611	< 0.1	< 0.1
1272041	0.2	16.0	0.6	1.7	54.0	1	0.1	15.4	2.1	1	< 0.1	15.0	7	2.2	5.0	0.6	2.3	0.5	0.5	< 0.1	0.4	> 10000	0.9	< 0.1
1272042	0.4	2.4	1.5	2.1	77.7	2	0.1	3.8	0.3	< 1	< 0.1	2.3	17	2.7	6.3	0.8	3.1	0.7	0.6	< 0.1	0.5	7230	0.1	< 0.1

Analyte Symbol	Ga	As	Rb	Y	Sr	Zr	Nb	Mo	In	Sn	Sb	Te	Ba	La	Ce	Pr	Nd	Sm	Gd	Tb	Dy	Cu	Ge	Tm
Unit Symbol	ppm	ppm	ppm	ppm	ppm	ppm	ppm	ppm	ppm	ppm	ppm	ppm	ppm	ppm	ppm	ppm	ppm	ppm	ppm	ppm	ppm	ppm	ppm	ppm
Detection Limit	0.1	0.1	0.2	0.1	0.2	1	0.1	0.1	0.1	1	0.1	0.1	1	0.1	0.1	0.1	0.1	0.1	0.1	0.1	0.1	0.2	0.1	0.1
Analysis Method	TD-MS	TD-MS	TD-MS	TD-MS	TD-MS	TD-MS	TD-MS	TD-MS	TD-MS	TD-MS	TD-MS	TD-MS	TD-MS	TD-MS	TD-MS	TD-MS	TD-MS	TD-MS	TD-MS	TD-MS	TD-MS	TD-MS	TD-MS	TD-MS
1272043	0.8	0.4	2.7	2.1	89.0	4	0.3	0.4	< 0.1	< 1	< 0.1	0.2	28	3.3	7.4	0.9	3.5	0.7	0.6	< 0.1	0.4	869	< 0.1	< 0.1
1272044	0.4	1.6	1.5	1.9	75.7	2	0.1	3.4	0.3	< 1	< 0.1	1.7	17	2.7	6.3	0.8	2.9	0.6	0.6	< 0.1	0.4	7020	0.1	< 0.1
1272045	11.8	30.2	15.9	6.1	21.5	65	1.7	3.0	< 0.1	< 1	0.2	< 0.1	19	15.0	29.7	3.4	11.8	1.9	1.6	0.2	1.3	38.9	0.3	< 0.1
1272051	18.6	1.3	126	5.0	32.1	85	2.9	2.5	< 0.1	1	0.1	0.1	252	16.8	31.8	3.6	12.6	2.1	1.8	0.2	1.1	14.2	0.3	< 0.1
1272052	15.2	0.7	96.9	1.5	35.9	24	1.0	1.9	< 0.1	< 1	< 0.1	< 0.1	217	11.3	20.4	2.2	7.3	1.1	0.8	< 0.1	0.4	9.5	< 0.1	< 0.1
1272053	14.0	1.5	0.5	17.5	32.0	48	3.5	0.8	< 0.1	< 1	< 0.1	< 0.1	13	3.5	8.6	1.3	6.1	1.9	2.5	0.5	3.3	37.0	1.4	0.3
1272054	15.4	1.4	176	6.2	5.2	98	4.6	3.6	< 0.1	1	0.4	< 0.1	112	29.1	57.0	6.6	22.7	3.7	2.5	0.3	1.4	13.0	0.2	< 0.1
1272055	14.5	11.4	2.2	8.1	35.3	137	4.6	1.8	< 0.1	< 1	< 0.1	< 0.1	29	1.8	4.8	0.7	3.1	1.2	1.6	0.3	1.8	29.2	< 0.1	0.1
1272056	9.9	9.9	4.6	6.2	29.8	88	3.9	1.7	< 0.1	1	< 0.1	< 0.1	32	6.1	13.0	1.6	6.1	1.4	1.4	0.2	1.2	52.8	0.1	< 0.1
1272101	12.2	3640	0.3	1.0	1.8	43	0.8	4.2	< 0.1	< 1	0.1	2.1	3	0.4	0.9	0.1	0.4	0.1	0.1	< 0.1	0.2	1910	0.3	< 0.1
1272102	17.3	15.2	0.4	37.3	23.7	156	0.4	0.4	< 0.1	4	< 0.1	< 0.1	4	1.7	5.1	0.8	4.6	2.0	3.3	0.8	6.3	32.9	0.3	0.8
1272103	0.4	4.1	0.4	0.1	9.7	2	< 0.1	4.7	< 0.1	< 1	0.1	0.2	13	< 0.1	0.1	< 0.1	< 0.1	< 0.1	< 0.1	< 0.1	< 0.1	688	0.1	< 0.1
1272104	30.7	18.3	182	12.7	35.8	119	8.0	2.7	< 0.1	1	< 0.1	0.5	47	81.0	185	20.6	70.6	11.3	7.8	0.8	3.5	377	0.5	0.2
1272106	23.4	106	11.6	8.5	33.9	137	7.7	2.2	< 0.1	< 1	< 0.1	3.1	59	17.7	40.2	4.6	16.2	3.0	2.5	0.3	1.9	15.2	0.6	0.2
1272107	3.5	2.1	2.4	4.7	36.5	8	1.2	4.2	< 0.1	< 1	0.1	< 0.1	50	0.4	1.2	0.2	1.0	0.4	0.5	< 0.1	0.7	999	< 0.1	< 0.1
1272108	0.9	1.6	1.0	10.9	113	6	0.9	0.5	< 0.1	< 1	< 0.1	0.1	13	2.4	5.4	0.8	3.8	1.1	1.5	0.3	1.8	9.5	< 0.1	0.2
1272109	0.4	8.6	1.0	4.3	20.2	17	1.6	3.9	< 0.1	< 1	0.1	< 0.1	33	2.6	5.3	0.6	2.1	0.4	0.5	< 0.1	0.7	180	< 0.1	< 0.1
1272110	2.8	11.0	2.8	49.6	144	4	0.8	1.7	< 0.1	< 1	< 0.1	< 0.1	31	12.5	34.5	6.0	31.1	10.4	13.3	1.9	10.9	38.1	0.2	0.5
1272111	2.4	16.7	3.1	0.4	3.5	8	0.5	6.0	< 0.1	< 1	0.9	0.2	167	0.3	0.3	< 0.1	0.1	< 0.1	< 0.1	< 0.1	< 0.1	66.2	< 0.1	< 0.1
1272112	22.6	11.3	2.1	5.7	44.6	124	8.8	7.2	1.4	2	0.3	0.6	33	0.9	2.4	0.4	1.8	0.5	0.7	0.1	0.8	> 10000	0.1	0.1
1272113	24.2	6.3	1.5	4.2	46.0	116	9.1	2.8	1.0	1	0.2	0.3	35	0.6	1.6	0.2	0.9	0.3	0.4	< 0.1	0.6	> 10000	0.1	0.1
1272114	27.8	16.9	84.9	10.3	24.1	38	0.7	0.2	< 0.1	< 1	< 0.1	< 0.1	688	30.4	59.3	6.9	24.3	3.9	2.9	0.3	1.9	38.1	0.4	0.2
1272115	2.3	32.8	1.7	6.1	27.2	10	1.1	4.7	< 0.1	< 1	0.1	< 0.1	49	0.9	2.5	0.4	2.5	0.9	1.2	0.2	1.1	63.2	0.2	< 0.1
1272116	21.4	22.5	96.5	11.4	10.0	85	7.1	1.7	< 0.1	< 1	0.1	< 0.1	470	31.2	52.4	6.5	21.3	2.9	2.3	0.3	1.9	592	0.3	0.2
1272117	19.6	34.3	3.3	6.4	29.7	128	11.2	10.2	0.6	1	0.3	0.9	33	0.9	2.5	0.4	2.0	0.6	0.7	0.1	0.8	7680	0.2	0.1
1272118	6.8	1.3	5.0	4.2	17.2	16	1.4	5.7	< 0.1	< 1	< 0.1	0.2	18	21.0	38.5	4.3	14.6	2.2	1.5	0.2	0.9	62.9	0.1	< 0.1
1272119	23.2	1.3	96.0	18.7	47.1	97	0.3	0.2	< 0.1	2	< 0.1	< 0.1	104	107	247	29.0	110	18.8	11.8	1.2	4.9	85.9	0.8	0.3
1272120	27.0	0.8	170	19.7	31.2	153	1.2	< 0.1	< 0.1	< 1	< 0.1	< 0.1	107	22.7	51.5	6.7	27.0	6.1	5.5	0.8	4.5	22.6	0.4	0.3
1272121	0.4	3.8	1.5	1.5	17.6	4	0.3	2.2	< 0.1	< 1	0.2	0.1	14	1.3	3.0	0.3	1.2	0.2	0.3	< 0.1	0.2	9.8	0.2	< 0.1
1272122	17.9	1.6	66.7	3.2	23.0	106	3.0	1.9	< 0.1	< 1	< 0.1	< 0.1	76	6.4	13.4	1.5	5.0	0.9	0.8	0.1	0.7	6.8	0.2	< 0.1
1272123	0.3	3.1	0.9	1.2	11.6	3	0.4	1.8	< 0.1	< 1	< 0.1	< 0.1	16	1.1	2.5	0.2	1.0	0.2	0.2	< 0.1	0.2	11.5	0.2	< 0.1
1272124	19.5	4.8	8.9	21.8	115	29	2.6	1.0	< 0.1	< 1	< 0.1	< 0.1	27	4.7	12.4	1.9	9.3	2.8	3.5	0.6	4.2	50.3	0.7	0.4
1272125	0.2	1.6	0.7	0.1	3.8	< 1	0.2	5.0	< 0.1	< 1	< 0.1	0.2	10	0.1	0.2	< 0.1	< 0.1	< 0.1	< 0.1	< 0.1	< 0.1	3020	0.5	< 0.1
1272126	22.7	2.3	< 0.2	40.4	18.1	77	2.0	3.1	< 0.1	< 1	< 0.1	< 0.1	5	2.5	11.2	2.6	15.4	5.9	6.6	1.2	7.8	> 10000	0.4	0.7
1272127	22.4	1.3	< 0.2	9.9	21.4	98	7.1	9.8	0.2	< 1	< 0.1	0.4	9	1.1	4.7	0.7	3.6	1.4	1.6	0.3	2.0	> 10000	0.4	0.2
1272144	0.3	5.1	1.0	1.9	40.8	2	0.5	1.7	0.1	< 1	< 0.1	1.4	13	1.2	3.3	0.5	1.9	0.5	0.5	< 0.1	0.4	3260	< 0.1	< 0.1
1272201	12.9	18.3	56.7	27.4	36.9	64	5.1	5.8	< 0.1	< 1	0.1	0.2	102	5.7	14.1	2.5	12.5	4.2	4.6	0.8	5.4	7480	0.2	0.4
1272202	22.0	1.8	2.5	29.3	28.6	7	0.4	< 0.1	< 0.1	< 1	< 0.1	< 0.1	11	5.8	15.7	2.4	11.7	3.6	4.6	0.8	5.9	131	0.4	0.5
1272203	13.5	2.6	0.2	3.1	32.8	80	6.5	24.9	0.5	< 1	< 0.1	1.5	13	3.0	7.3	1.0	4.0	0.8	0.6	< 0.1	0.6	> 10000	0.1	< 0.1
1272204	15.4	12.2	< 0.2	27.1	35.9	62	2.3	1.9	< 0.1	< 1	< 0.1	< 0.1	7	2.7	7.9	1.6	9.4	4.0	4.9	0.8	5.4	2460	0.4	0.4
1272205	18.0	7.9	< 0.2	30.9	31.0	49	1.1	0.3	< 0.1	< 1	< 0.1	< 0.1	8	3.4	9.2	1.6	8.6	3.3	4.4	0.9	6.1	904	0.3	0.5
1272206	10.0	23.6	< 0.2	18.3	75.6	54	4.0	4.6	< 0.1	< 1	< 0.1	0.5	6	10.8	23.0	2.9	11.5	2.7	3.0	0.5	3.4	2560	0.2	0.3
1272207	12.7	1.8	16.2	10.2	40.9	134	1.8	12.4	< 0.1	< 1	< 0.1	68.3	65	27.1	52.5	6.0	20.7	3.7	3.1	0.4	2.6	35.3	0.6	0.2
1272208	13.5	2.8	4.6	36.7	44.4	29	1.1	1.3	< 0.1	< 1	< 0.1	11.2	47	3.9	9.5	2.4	12.5	5.2	6.2	1.3	8.6	27.1	0.6	0.4
1272209	14.4	29.8	15.8	28.0	35.5	136	7.2	0.5	< 0.1	1	< 0.1	1.2	41	511	976	96.2	319	46.8	27.8	2.6	10.4	554	1.9	0.3
L307851	9.2	1.2	0.8	7.0	44.6	12	2.4	0.4	< 0.1	< 1	< 0.1	0.3	22	2.2	5.4	0.8	3.4	1.0	1.2	0.2	1.4	105	0.5	0.1
L307852	18.4	0.2	93.6	3.7	25.4	60	4.3	0.2	< 0.1	< 1	< 0.1	0.2	537	17.6	48.9	4.4	15.4	2.7	2.0	0.2	1.2	28.2	0.7	< 0.1
L307853	18.4	3.2	1.3	16.8	141	14	0.3	0.2	< 0.1	< 1	< 0.1	< 0.1	11	3.7	10.0	1.5	7.4	2.2	2.9	0.5	3.5	56.9	0.4	0.3
L307854	12.6	0.8	71.9	11.4	207	130	4.3	0.2	< 0.1	< 1	< 0.1	< 0.1	325	37.1	67.0	7.5	25.6	4.0	3.1	0.4	2.3	20.3	0.4	0.2
L307855	21.6	0.6	123	11.4	88.1	106	1.1	0.2	< 0.1	< 1	< 0.1	< 0.1	1400	35.0	70.0	8.0	27.8	4.5	3.5	0.4	2.5	24.5	0.6	0.2
L307856	23.3	0.9	2.5	16.8	17.5	128	7.2	0.5	< 0.1	4	< 0.1	< 0.1	19	1.5	5.8	1.2	6.5	2.6	2.8	0.5	3.6	238	0.2	0.3
L307857	23.5	6.6	0.9	26.6	37.9	65	3.1	0.8	< 0.1	< 1	< 0.1	0.2	8	19.0	41.4	4.9	18.1	4.1	4.4	0.8	5.0	284	0.5	0.5

Analyte Symbol	Ga	As	Rb	Y	Sr	Zr	Nb	Mo	In	Sn	Sb	Te	Ba	La	Ce	Pr	Nd	Sm	Gd	Tb	Dy	Cu	Ge	Tm
Unit Symbol	ppm	ppm	ppm	ppm	ppm	ppm	ppm	ppm	ppm	ppm	ppm	ppm	ppm	ppm	ppm	ppm	ppm	ppm	ppm	ppm	ppm	ppm	ppm	ppm
Detection Limit	0.1	0.1	0.2	0.1	0.2	1	0.1	0.1	0.1	1	0.1	0.1	1	0.1	0.1	0.1	0.1	0.1	0.1	0.1	0.1	0.2	0.1	0.1
Analysis Method	TD-MS	TD-MS	TD-MS	TD-MS	TD-MS	TD-MS	TD-MS	TD-MS	TD-MS	TD-MS	TD-MS	TD-MS	TD-MS	TD-MS	TD-MS	TD-MS	TD-MS	TD-MS	TD-MS	TD-MS	TD-MS	TD-MS	TD-MS	TD-MS
L307858	27.0	2.6	101	13.6	66.5	101	3.1	1.0	< 0.1	< 1	0.4	0.1	552	12.2	27.6	3.3	12.0	2.6	2.1	0.4	2.4	107	0.6	0.2
L307859	21.1	> 10000	3.4	18.4	53.4	116	2.0	7.3	< 0.1	< 1	1.4	4.6	30	2.9	11.6	2.3	12.6	4.0	3.9	0.6	3.7	189	0.2	0.3
L307860	23.7	246	0.8	12.2	62.7	127	7.0	10.7	< 0.1	< 1	< 0.1	1.0	13	1.9	7.5	1.5	8.5	2.7	2.5	0.4	2.4	1910	0.4	0.2
1272151	27.7	96.0	34.3	5.0	23.6	49	7.1	1.0	0.2	2	< 0.1	0.5	173	52.8	108	12.8	45.7	7.4	4.6	0.5	1.9	1870	0.6	< 0.1
1272152	1.6	89.3	2.6	2.4	9.4	7	1.0	0.3	< 0.1	< 1	< 0.1	2.3	9	71.4	127	14.2	42.0	4.8	2.4	0.2	0.7	1920	0.4	< 0.1
1272153	17.6	338	4.2	7.0	43.4	23	0.9	0.9	0.8	< 1	0.2	3.5	2	97.4	169	20.3	66.6	10.0	6.0	0.5	2.3	7270	0.5	0.1
1272154	22.9	573	63.2	15.8	16.3	38	0.6	0.2	< 0.1	< 1	< 0.1	0.4	13	418	772	79.8	268	44.0	25.2	2.3	8.0	539	1.5	0.2
1272155	16.5	895	104	3.4	7.2	70	3.3	0.2	< 0.1	1	0.2	0.7	49	29.9	63.2	7.1	22.2	3.5	2.1	0.3	1.2	1870	0.3	< 0.1
1272156	9.1	1790	0.5	2.1	2.6	14	< 0.1	0.7	0.3	< 1	< 0.1	3.8	2	0.9	2.0	0.3	1.1	0.4	0.5	< 0.1	0.5	> 10000	0.5	< 0.1

Analyte Symbol	Yb	Lu	Ta	W	Re	Tl	Pb	Sc	Th	U	Ti	P	S
Unit Symbol	ppm	ppm	ppm	ppm	ppm	ppm	ppm	ppm	ppm	ppm	%	%	%
Detection Limit	0.1	0.1	0.1	0.1	0.001	0.05	0.5	1	0.1	0.1	0.0005	0.001	0.01
Analysis Method	TD-MS	TD-MS	TD-MS	TD-MS	TD-MS	TD-MS	TD-MS	TD-ICP	TD-MS	TD-MS	TD-ICP	TD-ICP	TD-ICP
1271851	0.8	0.1	0.3	3.2	0.034	< 0.05	3.2	9	4.6	1.3	0.362	0.071	11.4
1271852	2.9	0.4	0.1	0.9	0.015	< 0.05	5.1	15	3.2	0.9	0.246	0.072	5.30
1271853	2.0	0.3	< 0.1	0.4	0.006	< 0.05	1.3	52	2.0	0.8	0.583	0.046	0.34
1271854	2.8	0.4	< 0.1	< 0.1	0.003	< 0.05	2.2	4	2.3	1.2	0.117	0.007	0.05
1271855	1.6	0.2	0.3	1.6	0.024	0.06	3.0	4	8.9	1.9	0.362	0.054	4.32
1271856	3.6	0.5	0.2	0.7	0.004	< 0.05	2.4	87	0.9	1.4	1.15	0.054	3.95
1271857	2.2	0.3	< 0.1	0.3	0.003	0.31	1.4	9	6.8	1.6	0.263	0.060	0.16
1271858	1.6	0.2	< 0.1	0.4	0.001	< 0.05	0.8	43	0.3	< 0.1	0.151	0.021	0.05
1271859	1.4	0.2	0.4	1.0	0.002	< 0.05	5.1	44	0.2	0.2	0.761	0.030	0.06
1271860	0.4	< 0.1	0.1	0.9	< 0.001	< 0.05	4.1	9	5.3	2.4	0.288	0.128	1.99
1272001	3.2	0.5	< 0.1	< 0.1	0.004	< 0.05	1.5	61	0.9	1.1	0.571	0.050	0.77
1272002	1.9	0.3	0.1	0.8	0.015	0.06	1.9	37	1.9	0.8	0.660	0.039	4.04
1272003	1.4	0.2	0.3	1.3	0.036	< 0.05	2.4	25	4.7	1.7	0.470	0.052	3.52
1272004	0.8	0.1	< 0.1	< 0.1	0.006	< 0.05	1.5	4	8.5	4.6	0.119	0.003	0.14
1272005	2.2	0.3	0.3	< 0.1	0.014	< 0.05	2.0	3	8.6	2.2	0.481	0.038	0.74
1272006	1.5	0.2	0.3	0.3	0.010	< 0.05	4.0	13	3.9	1.3	0.481	0.041	3.12
1272007	0.6	< 0.1	0.3	0.4	0.017	< 0.05	3.1	21	2.0	0.6	0.577	0.031	2.47
1272008	0.7	0.1	0.3	0.2	0.001	0.23	2.1	18	16.1	1.6	0.361	0.022	0.43
1272009	1.1	0.2	0.5	0.4	< 0.001	0.18	3.3	7	14.0	2.7	0.312	0.031	0.49
1272010	0.6	0.1	0.6	0.6	< 0.001	0.17	3.0	5	2.8	1.4	0.322	0.037	1.33
1272011	0.6	< 0.1	0.2	< 0.1	< 0.001	0.19	4.7	4	6.4	1.4	0.108	0.022	0.27
1272012	0.3	< 0.1	0.1	< 0.1	< 0.001	0.28	7.2	4	5.2	0.7	0.0953	0.019	0.11
1272013	0.6	< 0.1	0.3	0.1	< 0.001	0.48	3.8	6	7.7	1.2	0.157	0.029	0.19
1272014	0.8	0.1	0.5	0.4	< 0.001	1.00	3.2	13	16.6	2.3	0.321	0.026	0.38
1272015	0.8	0.1	< 0.1	2.9	0.005	0.32	315	10	2.7	1.9	0.0217	0.038	19.2
1272016	0.5	< 0.1	< 0.1	0.7	< 0.001	< 0.05	32.5	15	9.2	3.0	0.0287	0.093	4.84
1272017	2.5	0.3	< 0.1	0.3	0.001	< 0.05	49.0	2	6.2	39.6	0.0766	0.046	0.10
1272018	2.8	0.4	< 0.1	5.7	< 0.001	0.26	47.2	9	> 200	422	0.250	0.045	0.08
1272019	1.1	0.2	0.2	1.0	0.003	< 0.05	3.7	15	5.5	1.8	0.504	0.022	1.19
1272020	0.7	0.1	0.6	2.2	< 0.001	< 0.05	4.4	5	5.4	9.7	0.713	0.025	2.68
1272021	0.3	< 0.1	< 0.1	< 0.1	0.005	< 0.05	1.9	< 1	0.6	0.2	0.0106	0.008	0.07
1272022	0.1	< 0.1	< 0.1	< 0.1	< 0.001	< 0.05	2.4	< 1	1.7	1.0	0.0093	0.038	0.10
1272023	1.2	0.2	< 0.1	< 0.1	< 0.001	1.19	1.8	40	1.5	2.7	0.293	0.007	0.03
1272024	0.2	< 0.1	< 0.1	< 0.1	< 0.001	0.07	1.9	5	0.1	< 0.1	0.0434	0.007	1.07
1272025	0.5	< 0.1	< 0.1	< 0.1	0.010	0.08	2.8	6	5.7	1.0	0.187	0.031	1.14
1272026	1.3	0.2	0.2	< 0.1	0.018	0.17	45.7	8	9.7	26.3	0.244	0.045	0.63
1272027	1.4	0.2	0.5	0.2	0.003	0.37	35.7	7	12.0	12.4	0.313	0.045	0.43
1272028	2.4	0.3	< 0.1	< 0.1	0.010	0.39	418	14	14.6	136	0.146	0.022	0.04
1272029	0.8	0.1	0.2	< 0.1	0.003	0.33	37.1	8	6.5	10.4	0.150	0.014	0.91
1272030	0.6	< 0.1	< 0.1	1.0	0.004	0.09	22.6	3	2.9	9.6	0.0670	0.014	0.80
1272031	1.5	0.2	< 0.1	< 0.1	0.003	< 0.05	2.3	39	0.4	0.1	0.145	0.028	0.17
1272032	0.3	< 0.1	< 0.1	< 0.1	0.003	< 0.05	12.4	1	1.3	5.6	0.0410	0.008	0.77
1272033	0.5	< 0.1	< 0.1	< 0.1	0.006	0.07	10.6	4	1.0	1.8	0.0436	0.003	0.41
1272034	0.4	< 0.1	< 0.1	2.0	0.013	< 0.05	0.9	< 1	0.1	< 0.1	0.0095	0.007	< 0.01
1272035	1.9	0.3	< 0.1	0.3	0.011	< 0.05	3.0	28	0.3	0.6	0.298	0.025	0.53
1272036	0.3	< 0.1	< 0.1	0.8	0.023	< 0.05	28.4	1	0.8	1.8	0.0234	0.025	0.16
1272037	0.1	< 0.1	< 0.1	< 0.1	0.020	< 0.05	15.9	< 1	0.5	2.5	0.0121	0.069	3.11
1272038	0.1	< 0.1	< 0.1	0.3	0.031	< 0.05	14.2	< 1	0.5	2.5	0.0117	0.066	3.66
1272039	0.2	< 0.1	< 0.1	< 0.1	0.007	< 0.05	6.9	1	0.7	6.3	0.0145	0.019	0.02
1272040	0.2	< 0.1	< 0.1	< 0.1	< 0.001	< 0.05	1.5	< 1	0.8	1.5	0.0157	0.048	0.06
1272041	< 0.1	< 0.1	< 0.1	0.2	0.067	< 0.05	35.6	< 1	0.7	6.0	0.0027	0.040	5.26
1272042	0.1	< 0.1	< 0.1	< 0.1	0.013	0.05	9.7	< 1	0.3	3.0	0.0065	0.021	0.83

Analyte Symbol	Yb	Lu	Ta	W	Re	Tl	Pb	Sc	Th	U	Ti	P	S
Unit Symbol	ppm	ppm	ppm	ppm	ppm	ppm	ppm	ppm	ppm	ppm	%	%	%
Detection Limit	0.1	0.1	0.1	0.1	0.001	0.05	0.5	1	0.1	0.1	0.0005	0.001	0.01
Analysis Method	TD-MS	TD-MS	TD-MS	TD-MS	TD-MS	TD-MS	TD-MS	TD-ICP	TD-MS	TD-MS	TD-ICP	TD-ICP	TD-ICP
1272043	0.1	< 0.1	< 0.1	< 0.1	< 0.001	< 0.05	4.2	< 1	0.4	0.6	0.0127	0.018	0.19
1272044	0.1	< 0.1	< 0.1	< 0.1	0.005	< 0.05	8.3	< 1	0.3	2.3	0.0070	0.021	0.83
1272045	0.5	< 0.1	< 0.1	0.3	< 0.001	0.10	4.6	6	4.8	1.1	0.0847	0.056	7.15
1272051	0.5	< 0.1	0.1	< 0.1	0.005	0.30	3.7	7	6.0	1.0	0.173	0.039	0.02
1272052	0.1	< 0.1	< 0.1	< 0.1	0.003	0.18	1.1	2	1.3	0.3	0.0321	0.009	0.01
1272053	2.0	0.4	0.2	< 0.1	0.009	0.10	23.6	39	0.3	0.3	0.514	0.030	0.08
1272054	0.5	< 0.1	0.1	< 0.1	0.067	0.38	1.7	8	8.9	1.2	0.240	0.044	0.02
1272055	0.8	0.1	0.1	< 0.1	0.010	< 0.05	8.2	14	6.2	2.5	0.306	0.122	0.97
1272056	0.5	< 0.1	< 0.1	< 0.1	0.007	< 0.05	5.2	7	4.9	3.6	0.254	0.081	0.82
1272101	0.1	< 0.1	< 0.1	1.4	0.009	< 0.05	77.6	8	0.5	0.3	0.0772	0.001	5.23
1272102	4.5	0.7	< 0.1	0.2	0.010	< 0.05	1.5	47	0.8	1.0	0.461	0.093	0.95
1272103	< 0.1	< 0.1	< 0.1	< 0.1	0.012	< 0.05	3.8	< 1	< 0.1	0.1	0.0056	0.001	0.20
1272104	1.1	0.2	0.3	< 0.1	0.014	0.76	2.6	14	11.0	1.9	0.403	0.033	3.98
1272106	0.9	0.2	0.5	0.5	0.008	0.05	3.9	8	10.4	2.1	0.293	0.046	4.60
1272107	0.4	< 0.1	< 0.1	< 0.1	0.005	< 0.05	6.5	5	0.7	0.3	0.0300	0.038	0.22
1272108	0.9	0.1	< 0.1	< 0.1	0.004	< 0.05	2.2	3	0.5	2.9	0.0240	0.081	0.20
1272109	0.4	< 0.1	< 0.1	< 0.1	0.004	< 0.05	5.5	3	1.3	0.5	0.0852	0.012	1.94
1272110	2.7	0.4	< 0.1	< 0.1	0.002	< 0.05	4.4	10	1.3	1.0	0.0680	1.83	3.68
1272111	< 0.1	< 0.1	< 0.1	< 0.1	0.012	0.22	152	< 1	0.4	0.2	0.0214	0.005	0.93
1272112	0.8	0.2	0.4	1.0	0.011	< 0.05	5.3	6	7.9	16.3	0.632	0.027	2.67
1272113	0.8	0.1	0.5	1.0	0.010	< 0.05	3.1	3	2.5	2.4	0.617	0.015	1.48
1272114	1.0	0.2	< 0.1	< 0.1	0.023	0.96	7.0	26	5.4	1.8	0.250	0.010	0.20
1272115	0.4	< 0.1	< 0.1	< 0.1	0.010	< 0.05	7.7	5	1.6	0.9	0.0443	0.187	1.50
1272116	1.4	0.3	0.4	< 0.1	0.004	0.64	2.8	19	8.8	1.7	0.386	0.041	1.10
1272117	0.9	0.2	0.7	1.8	0.019	< 0.05	2.9	3	9.6	5.7	0.527	0.085	4.33
1272118	0.4	< 0.1	< 0.1	< 0.1	0.012	< 0.05	1.9	2	2.5	0.4	0.105	0.029	0.02
1272119	1.8	0.3	< 0.1	< 0.1	0.102	0.57	2.1	8	9.7	2.8	0.228	0.085	0.03
1272120	1.9	0.3	< 0.1	< 0.1	0.044	0.89	3.5	8	12.5	41.7	0.217	0.093	0.01
1272121	< 0.1	< 0.1	< 0.1	0.2	0.082	< 0.05	< 0.5	< 1	0.1	0.1	0.0036	0.004	0.03
1272122	0.3	< 0.1	0.1	< 0.1	0.007	0.28	1.4	7	7.2	1.2	0.185	0.041	< 0.01
1272123	< 0.1	< 0.1	< 0.1	0.2	0.007	< 0.05	0.6	< 1	0.1	< 0.1	0.0016	0.003	0.02
1272124	2.2	0.3	0.1	< 0.1	0.007	0.07	7.7	47	0.5	0.1	0.617	0.034	0.10
1272125	< 0.1	< 0.1	< 0.1	< 0.1	0.011	< 0.05	2.0	< 1	< 0.1	0.1	0.0026	0.002	1.28
1272126	3.5	0.5	< 0.1	< 0.1	0.018	< 0.05	1.2	72	1.0	1.3	0.805	0.058	2.55
1272127	0.9	0.1	0.5	< 0.1	0.064	< 0.05	2.2	1	3.4	1.9	0.460	0.034	3.70
1272144	0.1	< 0.1	< 0.1	< 0.1	0.011	< 0.05	10.2	< 1	0.5	4.1	0.0056	0.024	0.36
1272201	2.2	0.3	0.2	0.6	0.035	0.36	3.6	42	2.6	1.3	0.597	0.037	6.72
1272202	2.8	0.4	< 0.1	< 0.1	0.009	< 0.05	1.0	53	0.6	0.1	0.196	0.042	0.31
1272203	0.4	< 0.1	0.4	1.4	0.059	< 0.05	3.1	5	5.2	1.8	0.377	0.034	9.09
1272204	2.5	0.4	< 0.1	< 0.1	0.017	< 0.05	1.7	40	2.1	1.2	0.703	0.041	3.98
1272205	2.9	0.4	< 0.1	< 0.1	0.005	< 0.05	2.1	58	2.3	1.7	0.599	0.044	2.30
1272206	1.7	0.3	0.2	< 0.1	0.026	< 0.05	2.3	40	1.5	0.6	0.398	0.040	2.99
1272207	0.9	0.1	< 0.1	< 0.1	0.016	0.08	277	4	11.2	65.1	0.295	0.063	0.03
1272208	1.5	0.2	< 0.1	< 0.1	0.008	< 0.05	119	2	0.8	181	0.0482	0.014	0.03
1272209	1.5	0.2	< 0.1	0.4	0.006	0.05	5.7	30	61.5	4.9	0.292	0.036	14.1
L307851	0.8	0.1	0.1	< 0.1	0.003	< 0.05	1.9	16	0.6	0.1	0.299	0.021	0.06
L307852	0.4	< 0.1	0.2	< 0.1	< 0.001	0.70	3.5	13	7.9	0.6	0.303	0.034	0.02
L307853	1.8	0.3	< 0.1	< 0.1	0.007	< 0.05	3.6	37	0.4	0.1	0.275	0.019	0.10
L307854	1.1	0.2	< 0.1	< 0.1	0.003	0.40	2.9	8	8.1	0.8	0.280	0.050	0.18
L307855	1.1	0.2	< 0.1	< 0.1	0.005	0.73	3.1	14	13.8	1.3	0.285	0.049	0.18
L307856	1.3	0.2	0.4	< 0.1	0.008	< 0.05	1.3	13	6.5	1.2	0.385	0.068	0.42
L307857	2.7	0.4	< 0.1	< 0.1	0.022	< 0.05	4.0	31	2.2	3.5	0.705	0.034	0.82

Analyte Symbol	Yb	Lu	Ta	W	Re	Tl	Pb	Sc	Th	U	Ti	P	S
Unit Symbol	ppm	ppm	ppm	ppm	ppm	ppm	ppm	ppm	ppm	ppm	%	%	%
Detection Limit	0.1	0.1	0.1	0.1	0.001	0.05	0.5	1	0.1	0.1	0.0005	0.001	0.01
Analysis Method	TD-MS	TD-MS	TD-MS	TD-MS	TD-MS	TD-MS	TD-MS	TD-ICP	TD-MS	TD-MS	TD-ICP	TD-ICP	TD-ICP
L307858	1.3	0.2	< 0.1	< 0.1	0.023	0.47	4.9	14	11.0	3.1	0.349	0.032	0.11
L307859	1.9	0.3	< 0.1	< 0.1	0.038	< 0.05	18.6	4	11.8	4.9	0.345	0.037	1.79
L307860	1.3	0.2	0.1	< 0.1	0.048	< 0.05	760	4	10.8	4.0	0.520	0.014	0.38
1272151	0.3	< 0.1	0.4	0.4	0.015	0.13	4.0	10	11.0	1.2	0.287	0.025	1.25
1272152	0.2	< 0.1	< 0.1	< 0.1	0.003	< 0.05	2.2	< 1	0.9	0.3	0.0089	0.012	8.88
1272153	0.6	< 0.1	< 0.1	0.3	0.003	< 0.05	3.7	5	6.1	1.1	0.0723	0.041	5.09
1272154	1.2	0.2	< 0.1	0.4	0.003	0.39	2.9	28	9.3	1.0	0.142	0.016	13.3
1272155	0.4	< 0.1	0.2	2.1	0.002	0.38	2.9	4	6.7	1.3	0.155	0.061	8.02
1272156	0.2	< 0.1	< 0.1	< 0.1	< 0.001	< 0.05	18.1	5	3.8	1.3	0.0095	0.054	13.6

Quality Control

Analyte Symbol	Li	Na	Mg	Al	K	Ca	Cd	V	Cr	Mn	Fe	Hf	Hg	Ni	Er	Be	Ho	Ag	Cs	Co	Eu	Bi	Se	Zn
Unit Symbol	ppm	%	%	%	%	%	ppm	ppm	ppm	ppm	%	ppm	ppb	ppm	ppm	ppm	ppm	ppm	ppm	ppm	ppm	ppm	ppm	ppm
Detection Limit	0.5	0.01	0.01	0.01	0.01	0.01	0.1	1	0.5	1	0.01	0.1	10	0.5	0.1	0.1	0.1	0.05	0.05	0.1	0.05	0.02	0.1	0.2
Analysis Method	TD-MS	TD-MS	TD-MS	TD-MS	TD-MS	TD-MS	TD-MS	TD-MS	TD-MS	TD-MS	TD-MS	TD-MS	TD-MS	TD-MS	TD-MS	TD-MS	TD-MS	TD-MS	TD-MS	TD-MS	TD-MS	TD-MS	TD-MS	TD-MS
GXR-1 Meas	9.3	0.04	0.21	2.20	0.04	0.91	2.4	77	26.5	805	23.8	0.4	2810	37.2		1.0		33.8	2.35	8.1	0.61	1700	16.2	752
GXR-1 Cert	8.20	0.0520	0.217	3.52	0.050	0.960	3.30	80.0	12.0	852	23.6	0.960	3900	41.0		1.22		31.0	3.00	8.20	0.690	1380	16.6	760
DH-1a Meas																								
DH-1a Cert																								
GXR-4 Meas	14.4	0.52	1.75	6.35	3.01	1.24	< 0.1	93	47.7	145	3.26	1.2		43.4		2.4		3.77	2.34	16.2	1.41	19.0	6.8	79.4
GXR-4 Cert	11.1	0.564	1.66	7.20	4.01	1.01	0.860	87.0	64.0	155	3.09	6.30		42.0		1.90		4.00	2.80	14.6	1.63	19.0	5.60	73.0
SDC-1 Meas	49.5	1.63	1.11	8.50	1.37	1.22	< 0.1	75	62.7	858	5.03	1.3		35.6	4.1	3.7	1.4	0.26	3.57	19.9	1.63	0.34		107
SDC-1 Cert	34.00	1.52	1.02	8.34	2.72	1.00	0.0800	102.00	64.00	880.00	4.82	8.30		38.0	4.10	3.00	1.50	0.0410	4.00	18.0	1.70	2.60		103.00
GXR-6 Meas	46.1	0.10	0.60	> 10.0	2.03	0.20	0.1	129	54.1	991	6.04	1.8		27.9		1.3		0.34	3.72	15.6	0.62	0.19	2.0	137
GXR-6 Cert	32.0	0.104	0.609	17.7	1.87	0.180	1.00	186	96.0	1010	5.58	4.30		27.0		1.40		1.30	4.20	13.8	0.760	0.290	0.940	118
SAR-M (U.S.G.S.) Meas	42.8	1.26	0.50	6.44	2.52	0.69	5.1	51	82.0	4940	3.41			43.5		3.8		2.97		12.0		1.94	0.9	969
SAR-M (U.S.G.S.) Cert	27.4	1.140	0.50	6.30	2.94	0.61	5.27	67.2	79.7	5220	2.99			41.5		2.20		3.64		10.70		1.94	0.39	930.0
DNC-1a Meas	5.7							141	277					289						65.5	0.58			68.7
DNC-1a Cert	5.20							148.00	270					247						57.0	0.59			70.0
SBC-1 Meas	200						0.4	223	86.7			3.0		91.5	3.9	3.8	1.4		7.46	24.9	1.95	0.77		202
SBC-1 Cert	163.0						0.40	220.0	109			3.7		82.8	3.80	3.20	1.40		8.2	22.7	1.98	0.70		186.0
1271851 Orig	3.7	> 3.00	0.49	5.62	0.03	2.03	17.6	108	106	202	13.2	1.9	3530	85.8	0.8	0.3	0.3	23.3	< 0.05	69.0	0.17	0.47	8.8	824
1271851 Dup	4.1	> 3.00	0.53	6.01	0.03	2.29	18.6	109	112	252	14.3	2.0	3670	92.3	0.8	0.5	0.3	26.5	< 0.05	73.5	0.19	0.50	8.4	877
1272029 Orig	5.8	2.11	3.01	5.36	1.50	6.36	2.4	51	162	1340	3.15	0.9	< 10	43.4	0.9	1.6	0.3	5.25	1.06	92.6	0.41	0.36	88.9	44.9
1272029 Dup	5.3	2.08	2.93	5.26	1.30	6.37	2.1	48	148	1310	3.09	0.9	< 10	41.7	0.9	1.5	0.3	5.07	1.05	89.8	0.41	0.35	86.5	43.0
1272031 Orig	20.6	1.97	5.04	7.51	0.07	7.39	0.2	105	245	1470	8.23	0.2	< 10	166	1.9	0.4	0.7	0.70	0.22	50.2	0.71	0.08	6.2	92.8
1272031 Dup	20.0	1.84	4.66	7.00	0.07	7.11	0.2	101	236	1360	7.74	0.2	< 10	158	1.8	0.3	0.6	0.42	0.21	47.6	0.67	0.09	3.9	89.0
1272117 Orig	1.5	> 3.00	0.17	5.96	0.15	0.45	< 0.1	120	199	52	5.38	3.5	230	90.2	0.7	1.3	0.2	0.30	0.14	27.9	0.10	0.57	7.6	4.1
1272117 Dup	1.9	> 3.00	0.16	5.96	0.14	0.45	0.1	113	172	59	5.16	3.2	260	87.8	0.7	1.1	0.2	0.31	0.12	27.3	0.09	0.57	7.0	4.2
1272122 Orig	35.7	> 3.00	1.82	7.06	1.24	0.16	< 0.1	48	142	109	3.78	2.9	< 10	20.1	0.3	1.5	0.1	0.08	1.20	27.4	0.21	0.04	1.4	9.9
1272122 Dup	40.9	> 3.00	1.90	7.41	1.60	0.17	< 0.1	53	144	116	3.84	2.8	< 10	21.6	0.3	1.9	0.1	0.07	1.24	28.6	0.21	0.06	1.4	10.1
1272156 Orig	25.1	0.02	2.86	2.54	< 0.01	0.57	0.6	54	15.3	225	19.0	0.4	20	14.1	0.2	< 0.1	< 0.1	4.82	0.08	> 500	0.07	1.00	95.9	78.3
1272156 Dup	23.2	0.02	2.77	2.48	< 0.01	0.55	0.5	52	16.5	213	18.5	0.4	30	14.1	0.2	< 0.1	< 0.1	5.61	0.06	> 500	0.07	0.97	95.2	79.3
Method Blank	< 0.5	< 0.01	< 0.01	< 0.01	< 0.01	< 0.01	< 0.1	< 1	< 0.5	< 1	< 0.01	< 0.1	< 10	< 0.5	< 0.1	< 0.1	< 0.1	< 0.05	< 0.05	< 0.1	< 0.05	< 0.02	< 0.1	< 0.2
Method Blank																								
Method Blank																								
Method Blank																								

Quality Control

Analyte Symbol	Ga	As	Rb	Y	Sr	Zr	Nb	Mo	In	Sn	Sb	Te	Ba	La	Ce	Pr	Nd	Sm	Gd	Tb	Dy	Cu	Ge	Tm
Unit Symbol	ppm	ppm	ppm	ppm	ppm	ppm	ppm	ppm	ppm	ppm	ppm	ppm	ppm	ppm	ppm	ppm	ppm	ppm	ppm	ppm	ppm	ppm	ppm	ppm
Detection Limit	0.1	0.1	0.2	0.1	0.2	1	0.1	0.1	0.1	1	0.1	0.1	1	0.1	0.1	0.1	0.1	0.1	0.1	0.1	0.1	0.2	0.1	0.1
Analysis Method	TD-MS	TD-MS	TD-MS	TD-MS	TD-MS	TD-MS	TD-MS	TD-MS	TD-MS	TD-MS	TD-MS	TD-MS	TD-MS	TD-MS	TD-MS	TD-MS	TD-MS	TD-MS	TD-MS	TD-MS	TD-MS	TD-MS	TD-MS	TD-MS
GXR-1 Meas	7.0	375	2.7	28.0	293	18	1.0	16.7	0.8	27	35.4	8.6	656	7.5	14.6		8.1	2.6	3.9	0.8	5.0	935		0.4
GXR-1 Cert	13.8	427	14.0	32.0	275	38.0	0.800	18.0	0.770	54.0	122	13.0	750	7.50	17.0		18.0	2.70	4.20	0.830	4.30	1110		0.430
DH-1a Meas																								
DH-1a Cert																								
GXR-4 Meas	19.9	101	135	14.0	233	40	8.9	318	0.2	7	4.4	0.9	203	59.9	108		42.1	6.4	4.4	0.6	2.9	6550		0.2
GXR-4 Cert	20.0	98.0	160	14.0	221	186	10.0	310	0.270	5.60	4.80	0.970	1640	64.5	102		45.0	6.60	5.25	0.360	2.60	6520		0.210
SDC-1 Meas	18.9	2.4	95.1	32.1	182	43	6.6	0.3		< 1	0.2		581	40.7	88.4		40.1	7.8	7.2	1.1	7.0	27.7		0.7
SDC-1 Cert	21.00	0.220	127.00	40.0	180.00	290.00	21.00	0.250		3.00	0.54		630	42.00	93.00		40.00	8.20	7.00	1.20	6.70	30.00		0.65
GXR-6 Meas	39.0	226	92.7	13.4	41.3	66	1.6	0.8	< 0.1	< 1	1.0	< 0.1	1070	13.6	36.5		12.8	2.6	2.3	0.4	2.5	66.8		0.3
GXR-6 Cert	35.0	330	90.0	14.0	35.0	110	7.50	2.40	0.260	1.70	3.60	0.0180	1300	13.9	36.0		13.0	2.67	2.97	0.415	2.80	66.0		0.0320
SAR-M (U.S.G.S.) Meas	11.7	30.3	130	33.4	159		7.5	6.1	1.0	2	4.7	0.2	786	58.6	118							304		
SAR-M (U.S.G.S.) Cert	17	38.8	146	28.00	151		29.9	13.1	1.08	2.76	6.0	0.96	801	57.4	122.0							331		
DNC-1a Meas				17.2	150	37					0.8		91	4.0			5.1					95.6		
DNC-1a Cert				18.0	144.0	38.000					0.96		118	3.6			5.20					100.0		
SBC-1 Meas	32.2	25.0	144	33.0	191	111	11.1	2.5		3	0.9		675	53.3	108	13.5	50.6	9.7	8.4	1.2	7.1	27.9		0.6
SBC-1 Cert	27.0	25.7	147	36.5	178.0	134.0	15.3	2.40		3.3	1.01		788.0	52.5	108.0	12.6	49.2	9.6	8.5	1.20	7.10	31.0		0.56
1271851 Orig	12.4	18.1	0.2	8.0	31.2	70	5.1	26.8	0.1	< 1	0.2	1.0	9	3.2	7.6	1.1	4.5	1.2	1.3	0.2	1.4	> 10000	0.2	0.1
1271851 Dup	13.1	18.8	< 0.2	8.6	34.0	77	5.7	29.4	0.1	1	0.2	1.0	10	3.4	8.2	1.1	4.9	1.3	1.4	0.2	1.4	> 10000	0.2	0.1
1272029 Orig	13.8	7.9	69.2	7.5	81.5	33	4.0	21.4	0.1	1	< 0.1	1.1	384	14.4	30.1	3.5	12.4	2.4	2.1	0.3	1.8	5630	0.4	0.1
1272029 Dup	13.1	7.3	62.8	7.4	78.3	33	4.1	21.0	0.1	1	< 0.1	1.3	373	14.3	29.7	3.5	12.3	2.3	2.1	0.3	1.9	5500	0.4	0.1
1272031 Orig	15.1	5.7	3.2	15.6	106	7	0.4	0.7	< 0.1	< 1	< 0.1	< 0.1	9	3.4	8.9	1.4	6.5	1.9	2.6	0.5	3.0	270	0.3	0.3
1272031 Dup	14.3	5.5	3.1	15.1	103	7	0.1	0.4	< 0.1	< 1	< 0.1	< 0.1	9	3.2	8.4	1.3	6.0	1.8	2.4	0.4	2.9	259	0.3	0.3
1272117 Orig	19.9	35.4	3.4	6.4	30.2	130	11.2	10.3	0.6	1	0.3	1.0	34	1.0	2.6	0.4	2.0	0.6	0.7	0.1	0.8	7840	0.1	0.1
1272117 Dup	19.3	33.2	3.1	6.3	29.3	125	11.2	10.1	0.6	1	0.3	0.9	33	0.9	2.5	0.4	2.0	0.6	0.7	0.1	0.8	7520	0.2	0.1
1272122 Orig	17.7	1.4	61.9	3.2	22.5	106	3.0	1.8	< 0.1	< 1	< 0.1	< 0.1	76	6.3	13.2	1.4	4.9	0.9	0.8	0.1	0.7	5.7	0.1	< 0.1
1272122 Dup	18.2	1.7	71.6	3.3	23.6	107	3.0	2.0	< 0.1	< 1	0.1	< 0.1	77	6.5	13.6	1.5	5.1	0.9	0.8	0.1	0.7	7.8	0.2	< 0.1
1272156 Orig	9.3	1810	0.6	2.1	2.6	15	0.3	1.1	0.3	< 1	< 0.1	3.8	2	0.8	1.9	0.3	1.1	0.4	0.5	< 0.1	0.5	> 10000	0.5	< 0.1
1272156 Dup	9.0	1780	0.4	2.1	2.7	14	< 0.1	0.2	0.3	< 1	< 0.1	3.8	2	0.9	2.1	0.3	1.1	0.4	0.5	< 0.1	0.5	> 10000	0.5	< 0.1
Method Blank	< 0.1	< 0.1	< 0.2	< 0.1	< 0.2	< 1	< 0.1	< 0.1	< 0.1	< 1	< 0.1	< 0.1	< 1	< 0.1	< 0.1	< 0.1	< 0.1	< 0.1	< 0.1	< 0.1	< 0.1	< 0.2	< 0.1	< 0.1
Method Blank																								
Method Blank																								
Method Blank																								

Quality Control

Analyte Symbol	Yb	Lu	Ta	W	Re	Tl	Pb	Sc	Th	U	Ti	P	S
Unit Symbol	ppm	ppm	ppm	ppm	ppm	ppm	ppm	ppm	ppm	ppm	%	%	%
Detection Limit	0.1	0.1	0.1	0.1	0.001	0.05	0.5	1	0.1	0.1	0.0005	0.001	0.01
Analysis Method	TD-MS	TD-MS	TD-MS	TD-MS	TD-MS	TD-MS	TD-MS	TD-ICP	TD-MS	TD-MS	TD-ICP	TD-ICP	TD-ICP
GXR-1 Meas	2.0	0.3	< 0.1	129		0.39	765	2	2.6	35.5		0.064	0.26
GXR-1 Cert	1.90	0.280	0.175	164		0.390	730	1.58	2.44	34.9		0.0650	0.257
DH-1a Meas									> 200	2190			
DH-1a Cert									910	2629			
GXR-4 Meas	1.0	0.1	0.5	33.6		3.49	51.1	9	18.8	5.6		0.137	1.75
GXR-4 Cert	1.60	0.170	0.790	30.8		3.20	52.0	7.70	22.5	6.20		0.120	1.77
SDC-1 Meas	3.3		0.3	< 0.1		0.76	27.2	17	12.9	3.1	0.452	0.060	0.07
SDC-1 Cert	4.00		1.20	0.800		0.70	25.00	17.00	12.00	3.10	0.606	0.0690	0.0650
GXR-6 Meas	1.6	0.3	< 0.1	< 0.1		2.40	101	30	5.1	1.4		0.035	0.01
GXR-6 Cert	2.40	0.330	0.485	1.90		2.20	101	27.6	5.30	1.54		0.0350	0.0160
SAR-M (U.S.G.S.) Meas				0.9		3.30	1120	10	21.0	4.9	0.261	0.063	
SAR-M (U.S.G.S.) Cert				9.78		2.7	982	7.83	17.2	3.57	0.38	0.07	
DNC-1a Meas	1.9							32					
DNC-1a Cert	2.0							31					
SBC-1 Meas	3.3	0.5	0.4	1.0		1.00	37.8	22	16.1	12.0			
SBC-1 Cert	3.64	0.54	1.10	1.60		0.89	35.0	20.0	15.8	5.76			
1271851 Orig	0.8	0.1	0.3	3.4	0.038	< 0.05	3.2	9	4.5	1.3	0.364	0.071	11.4
1271851 Dup	0.8	0.1	0.3	3.1	0.031	< 0.05	3.1	8	4.7	1.3	0.360	0.072	11.3
1272029 Orig	0.8	0.1	0.2	< 0.1	0.005	0.33	37.1	8	6.4	10.4	0.148	0.014	0.91
1272029 Dup	0.8	0.1	0.2	< 0.1	0.001	0.33	37.1	8	6.5	10.4	0.152	0.014	0.91
1272031 Orig	1.5	0.2	< 0.1	< 0.1	0.003	< 0.05	2.4	39	0.4	0.1	0.132	0.029	0.17
1272031 Dup	1.4	0.2	< 0.1	< 0.1	0.003	< 0.05	2.2	39	0.3	0.2	0.157	0.027	0.16
1272117 Orig	0.9	0.2	0.8	1.9	0.019	< 0.05	3.0	3	9.7	5.8	0.535	0.086	4.34
1272117 Dup	0.9	0.2	0.7	1.7	0.020	< 0.05	2.8	3	9.5	5.5	0.519	0.084	4.32
1272122 Orig	0.3	< 0.1	0.2	< 0.1	0.006	0.27	1.4	7	7.1	1.2	0.186	0.042	< 0.01
1272122 Dup	0.3	< 0.1	0.1	< 0.1	0.009	0.28	1.5	7	7.3	1.2	0.183	0.041	< 0.01
1272156 Orig	0.2	< 0.1	< 0.1	0.3	0.001	< 0.05	18.6	5	3.9	1.4	0.0098	0.056	13.6
1272156 Dup	0.2	< 0.1	< 0.1	< 0.1	< 0.001	< 0.05	17.6	5	3.8	1.3	0.0092	0.052	13.6
Method Blank	< 0.1	< 0.1	< 0.1	< 0.1	< 0.001	< 0.05	< 0.5	< 1	< 0.1	< 0.1	< 0.0005	< 0.001	< 0.01
Method Blank								< 1			0.0025	0.001	< 0.01
Method Blank								< 1			< 0.0005	< 0.001	< 0.01
Method Blank								< 1			< 0.0005	< 0.001	< 0.01

Quality Analysis ... *Innovative Technologies*

Date Submitted: 15-Aug-13
Invoice No.: A13-10175
Invoice Date: 04-Sep-13
Your Reference: 33695

Techni-Lab Abitibi Inc.(Actlabs)
184 Rue Principale
Ste-Germaine-Boule Quebec J0Z 1M0
Canada

ATTN: Andre Caouette

CERTIFICATE OF ANALYSIS

175 Pulp samples were submitted for analysis.

The following analytical package was requested: Code UT-6 Total Digestion ICP & ICP/MS

REPORT **A13-10175**

This report may be reproduced without our consent. If only selected portions of the report are reproduced, permission must be obtained. If no instructions were given at time of sample submittal regarding excess material, it will be discarded within 90 days of this report. Our liability is limited solely to the analytical cost of these analyses. Test results are representative only of material submitted for analysis.

Notes:

CERTIFIED BY :

Elitsa Hrischeva, Ph.D.
Quality Control

ISO/IEC 17025
SCC Accredited
LAB 266
LAB 266
Accrédité CCN

ACTIVATION LABORATORIES LTD.

1336 Sandhill Drive, Ancaster, Ontario Canada L9G 4V5 TELEPHONE +1.905.648.9611 or +1.888.228.5227 FAX +1.905.648.9613
E-MAIL Ancaster@actlabs.com ACTLABS GROUP WEBSITE www.actlabs.com

Analyte Symbol	Li	Na	Mg	Al	K	Ca	Cd	V	Cr	Mn	Fe	Hf	Hg	Ni	Er	Be	Ho	Ag	Cs	Co	Eu	Bi	Se	Zn
Unit Symbol	ppm	%	%	%	%	%	ppm	ppm	ppm	ppm	%	ppm	ppb	ppm	ppm	ppm	ppm	ppm	ppm	ppm	ppm	ppm	ppm	ppm
Detection Limit	0.5	0.01	0.01	0.01	0.01	0.01	0.1	1	0.5	1	0.01	0.1	10	0.5	0.1	0.1	0.1	0.05	0.05	0.1	0.05	0.02	0.1	0.2
Analysis Method	TD-MS	TD-MS	TD-MS	TD-MS	TD-MS	TD-MS	TD-MS	TD-MS	TD-MS	TD-MS	TD-MS	TD-MS	TD-MS	TD-MS	TD-MS	TD-MS	TD-MS	TD-MS	TD-MS	TD-MS	TD-MS	TD-MS	TD-MS	TD-MS
1272046	26.1	> 3.00	2.35	7.56	1.97	1.19	< 0.1	60	69.7	117	8.49	2.4	20	15.2	4.1	1.9	1.5	0.14	6.58	31.5	2.76	0.17	2.3	18.5
1272210	5.3	0.39	0.08	0.62	0.19	11.3	< 0.1	5	23.9	57	0.27	< 0.1	30	3.1	< 0.1	< 0.1	< 0.1	0.06	0.16	1.7	0.06	0.04	1.2	4.3
1272211	14.9	> 3.00	1.23	9.18	2.04	0.11	< 0.1	69	77.7	37	1.04	3.4	20	31.0	1.3	2.4	0.4	0.08	1.02	5.8	0.91	0.06	1.0	3.5
1272212	2.5	> 3.00	0.31	8.91	0.06	0.23	< 0.1	14	88.0	40	0.34	3.2	20	15.0	0.5	0.5	0.2	0.13	0.06	1.3	0.72	0.05	1.1	8.4
1272213	17.6	> 3.00	3.68	6.13	0.63	8.49	< 0.1	163	247	969	4.86	1.4	40	64.5	1.9	0.2	0.7	0.59	1.20	32.6	0.83	48.5	5.2	52.3
1272214	17.5	> 3.00	1.58	9.79	0.70	0.25	< 0.1	82	82.3	103	2.46	2.1	70	35.0	0.7	1.1	0.3	0.17	0.34	18.0	1.67	2.23	1.6	23.2
1272215	79.0	0.03	9.87	9.33	0.02	0.17	< 0.1	196	110	339	14.8	2.5	110	28.3	0.4	0.2	0.2	0.37	0.12	> 500	0.21	0.84	8.8	145
1272216	0.7	0.02	0.04	0.08	0.01	< 0.01	< 0.1	4	17.7	18	> 50.0	< 0.1	150	557	< 0.1	< 0.1	< 0.1	1.71	< 0.05	> 500	0.35	27.4	117	7.7
1272217	25.8	1.91	1.37	6.01	1.91	0.20	0.1	201	179	41	5.12	3.4	130	102	0.4	3.0	0.1	0.54	6.31	19.1	0.12	1.14	2.5	7.6
1272218	58.0	0.15	1.49	8.56	2.44	0.48	0.1	78	127	27	3.34	1.3	100	13.5	0.3	2.6	< 0.1	2.33	4.90	5.8	0.35	0.46	1.1	8.8
1272219	1.0	1.60	4.29	1.93	0.04	8.48	< 0.1	381	101	1210	26.6	0.4	100	28.9	0.8	0.2	0.3	0.58	0.10	10.7	0.33	0.41	2.8	11.8
1272220	29.1	2.54	8.05	4.40	0.20	11.0	0.1	29	54.0	741	2.27	0.6	60	25.6	0.8	0.6	0.3	0.25	0.79	11.2	0.65	0.20	0.9	36.0
1272221	1.6	> 3.00	3.12	4.87	0.05	8.47	0.3	149	154	1260	15.6	2.7	70	37.8	1.7	0.4	0.7	0.25	0.15	8.0	1.68	0.21	1.6	9.4
1272222	1.6	1.21	9.40	1.39	0.03	18.7	0.1	15	34.4	3160	2.94	1.6	50	37.8	2.7	< 0.1	1.0	0.17	0.05	19.9	0.73	0.15	7.6	10.1
1272223	56.4	0.02	7.81	4.93	0.02	0.33	0.1	63	186	219	6.68	4.7	60	17.9	0.8	0.4	0.3	0.17	< 0.05	11.0	0.39	0.39	1.1	75.3
1272224	1.3	0.03	5.64	0.66	0.01	31.0	0.1	10	8.7	982	0.80	< 0.1	< 10	12.5	0.6	< 0.1	0.2	0.09	0.09	5.3	0.21	0.87	0.7	33.1
1272225	2.3	0.01	17.9	0.49	0.01	9.91	0.1	31	10.3	514	1.61	< 0.1	< 10	26.5	0.2	< 0.1	< 0.1	7.43	0.27	16.3	0.09	7.70	5.0	143
1272226	18.6	0.04	9.97	0.17	0.02	19.1	0.2	6	5.0	795	0.68	< 0.1	< 10	12.6	0.2	1.0	< 0.1	2.66	0.08	11.4	0.09	18.0	7.4	92.3
1272227	5.1	0.05	9.02	0.47	0.02	16.2	0.2	23	13.6	612	1.26	< 0.1	< 10	25.7	0.4	0.3	0.1	1.01	< 0.05	19.4	0.10	19.1	113	161
1272228	0.6	0.92	8.75	1.05	0.01	16.6	< 0.1	3	53.5	1540	1.42	1.5	20	22.9	1.1	< 0.1	0.4	0.33	< 0.05	8.9	0.45	1.48	2.5	6.4
1272229	134	0.06	11.7	5.34	0.16	3.29	< 0.1	387	65.9	2710	9.99	0.6	40	147	131	0.3	45.2	0.39	0.95	44.3	57.4	6.40	37.8	424
1272230	36.9	0.55	2.15	8.10	1.62	0.16	< 0.1	53	170	168	6.91	2.2	< 10	114	1.8	1.3	0.7	0.26	0.82	58.8	0.92	0.77	0.5	17.7
1272231	21.7	2.03	1.01	> 10.0	3.59	0.12	< 0.1	65	64.4	31	1.06	1.7	< 10	31.1	1.2	5.0	0.4	0.13	1.62	21.4	0.57	0.32	0.6	4.5
1272232	9.8	1.38	4.41	7.12	0.23	8.30	< 0.1	185	215	1380	8.78	0.5	< 10	121	2.7	0.2	1.0	0.14	1.10	47.5	0.99	0.36	0.2	74.6
1272233	63.2	> 3.00	3.01	8.83	2.86	0.67	< 0.1	113	111	192	3.02	0.9	< 10	54.0	0.5	0.8	0.2	0.18	4.05	57.3	0.34	0.20	0.4	28.9
1272351	52.9	0.14	3.16	6.69	4.66	0.17	< 0.1	129	232	92	14.1	3.2	40	79.5	1.3	0.3	0.4	0.18	1.36	39.7	1.67	0.17	2.3	20.0
1272352	8.2	0.05	8.83	0.37	0.31	18.0	< 0.1	6	56.7	1860	1.17	< 0.1	< 10	6.8	0.3	< 0.1	0.1	0.07	0.23	7.7	0.32	0.10	< 0.1	11.9
1272353	37.7	0.12	0.87	6.22	4.75	0.15	< 0.1	49	135	57	2.18	1.3	< 10	16.9	0.5	0.4	0.1	0.09	1.40	9.4	0.37	0.14	0.9	10.1
1272354	40.8	0.07	1.54	2.84	1.68	0.76	< 0.1	36	309	164	1.52	< 0.1	< 10	37.5	0.2	0.2	< 0.1	0.08	0.88	21.2	0.77	0.15	0.1	14.0
1272355	11.0	0.07	0.15	2.83	2.92	0.24	< 0.1	23	232	58	0.80	0.7	< 10	5.9	0.2	< 0.1	< 0.1	0.08	0.66	1.9	0.19	0.11	0.4	5.0
1272356	37.7	0.72	1.05	6.43	2.56	0.12	< 0.1	68	220	73	1.50	1.4	< 10	16.3	0.3	1.3	0.1	0.09	2.22	9.9	0.58	0.09	< 0.1	11.5
1272357	37.9	1.83	0.99	6.27	1.88	0.21	< 0.1	56	198	95	2.61	2.1	< 10	16.6	0.6	0.8	0.2	0.06	1.71	10.3	0.53	0.09	0.3	8.1
1272358	14.3	0.08	0.35	3.72	2.70	0.35	< 0.1	23	314	130	1.42	< 0.1	< 10	9.4	0.5	< 0.1	0.2	0.08	0.63	3.4	0.30	0.09	< 0.1	4.0
1272359	35.9	1.55	0.79	6.19	2.49	0.12	< 0.1	56	241	62	2.45	1.8	< 10	16.1	0.5	0.6	0.2	0.06	1.57	8.3	0.41	0.08	0.6	6.2
1272360	19.1	0.42	0.54	3.73	2.09	0.88	< 0.1	18	372	139	2.33	< 0.1	< 10	11.6	0.7	0.1	0.3	0.06	1.45	4.1	1.46	0.07	2.0	4.2
1272361	31.9	0.03	1.98	4.22	2.09	2.46	< 0.1	57	262	836	1.91	1.0	< 10	12.7	0.7	0.5	0.2	0.27	1.23	10.3	0.64	0.08	3.5	14.5
1272362	1.7	0.02	7.48	0.17	0.10	13.2	0.2	3	100	191	0.31	< 0.1	< 10	7.2	< 0.1	< 0.1	< 0.1	0.08	0.12	2.0	0.06	0.05	< 0.1	18.3
1272363	48.6	0.07	4.65	6.25	2.28	3.73	< 0.1	61	117	120	3.38	3.2	< 10	26.2	0.7	0.9	0.2	0.16	4.03	5.6	0.56	0.10	0.8	23.5
1272364	4.4	0.02	11.4	0.22	0.17	19.6	0.2	6	59.8	1350	0.72	< 0.1	< 10	7.5	0.2	< 0.1	< 0.1	< 0.05	0.39	3.2	0.22	0.10	< 0.1	22.0
1272365	43.0	0.72	5.43	6.01	1.75	2.59	< 0.1	86	99.2	115	3.48	4.1	< 10	18.9	0.6	0.2	0.2	0.16	4.19	4.9	0.65	0.06	< 0.1	16.8
1272366	8.9	0.06	1.17	0.37	0.31	35.7	< 0.1	6	53.1	1180	0.50	< 0.1	< 10	10.2	0.2	< 0.1	< 0.1	0.06	0.95	2.2	0.18	0.10	0.7	7.0
1272367	31.7	1.24	4.97	4.53	2.10	12.2	< 0.1	47	87.1	1130	2.90	2.4	< 10	40.6	0.7	0.6	0.3	0.12	2.02	20.2	0.87	0.09	0.6	52.0
1272368	56.2	0.19	3.35	8.17	3.31	0.55	< 0.1	63	89.6	73	5.88	2.1	< 10	59.3	1.0	1.4	0.4	0.07	4.17	15.0	1.10	0.10	0.5	20.5
1272369	21.4	1.21	2.98	3.57	1.05	6.20	< 0.1	23	260	699	2.66	0.2	< 10	32.6	0.5	< 0.1	0.2	0.05	1.31	14.2	0.62	0.07	0.2	14.0
1272370	39.2	0.11	8.44	3.36	1.86	13.2	0.1	43	82.2	289	2.27	1.0	< 10	24.1	0.6	0.3	0.2	0.09	3.13	5.1	0.26	0.06	0.5	14.7
1272371	50.9	0.08	3.06	7.14	3.26	0.28	< 0.1	63	128	22	4.33	3.0	< 10	32.2	0.7	1.0	0.2	0.10	4.93	5.6	0.52	0.08	0.6	20.1
1272372	13.3	0.23	11.5	1.13	0.52	18.9	0.4	11	40.6	201	0.79	0.2	< 10	13.0	0.3	< 0.1	< 0.1	< 0.05	1.13	4.1	0.17	0.04	< 0.1	17.8
1272373	1.9	0.01	11.8	0.12	0.07	20.3	0.2	1	21.2	185	0.21	0.6	< 10	6.9	0.1	< 0.1	< 0.1	< 0.05	0.16	2.7	0.08	0.03	< 0.1	24.4
1272374	13.7	0.02	10.6	1.36	0.81	17.0	< 0.1	12	82.2	407	0.88	0.2	< 10	13.7	0.3	< 0.1	0.1	< 0.05	0.85	4.2	0.16	0.04	< 0.1	11.4
1272375	24.8	0.03	12.5	1.65	0.91	16.4	< 0.1	14	48.0	788	1.12	0.5	< 10	22.1	0.3	< 0.1	< 0.1	0.05	1.16	9.8	0.17	0.05	< 0.1	13.8
1272376	90.1	0.03	12.3	5.79	1.86	3.13	< 0.1	18	104	133	3.67	2.3	< 10	52.7	0.4	0.3	0.1	0.06	4.23	21.2	0.43	0.05	< 0.1	48.0
1272377	4.1	0.02	9.00	0.24	0.14	16.6	0.1	2	73.9	577	0.44	< 0.1	< 10	8.3	0.1	< 0.1	< 0.1	< 0.05	0.22	2.7	0.12	0.04	< 0.1	12.6

Analyte Symbol	Li	Na	Mg	Al	K	Ca	Cd	V	Cr	Mn	Fe	Hf	Hg	Ni	Er	Be	Ho	Ag	Cs	Co	Eu	Bi	Se	Zn
Unit Symbol	ppm	%	%	%	%	%	ppm	ppm	ppm	ppm	%	ppm	ppb	ppm	ppm	ppm	ppm	ppm	ppm	ppm	ppm	ppm	ppm	ppm
Detection Limit	0.5	0.01	0.01	0.01	0.01	0.01	0.1	1	0.5	1	0.01	0.1	10	0.5	0.1	0.1	0.1	0.05	0.05	0.1	0.05	0.02	0.1	0.2
Analysis Method	TD-MS	TD-MS	TD-MS	TD-MS	TD-MS	TD-MS	TD-MS	TD-MS	TD-MS	TD-MS	TD-MS	TD-MS	TD-MS	TD-MS	TD-MS	TD-MS	TD-MS	TD-MS	TD-MS	TD-MS	TD-MS	TD-MS	TD-MS	TD-MS
1272378	40.3	0.05	3.23	6.42	2.25	2.45	< 0.1	95	103	83	3.79	2.4	< 10	15.6	0.6	0.8	0.2	< 0.05	3.92	4.8	0.61	0.06	< 0.1	13.4
1272379	10.4	0.04	7.72	0.58	0.51	12.9	< 0.1	6	117	2100	1.04	< 0.1	< 10	22.8	0.1	< 0.1	< 0.1	< 0.05	0.59	12.5	0.12	0.04	< 0.1	171
1272380	15.4	0.02	11.2	0.77	0.57	17.7	< 0.1	9	45.6	1760	1.24	< 0.1	< 10	18.4	0.2	< 0.1	< 0.1	0.12	1.06	13.8	0.20	0.07	< 0.1	38.4
1272381	23.0	0.03	10.5	1.56	1.33	14.3	< 0.1	29	68.9	969	1.83	0.5	< 10	20.4	0.3	< 0.1	0.1	0.09	2.51	14.2	0.22	0.13	< 0.1	26.0
1272382	86.0	1.57	6.34	6.64	0.59	7.56	< 0.1	60	79.5	942	2.79	5.7	< 10	122	1.1	2.5	0.4	0.19	0.54	28.5	0.32	0.11	< 0.1	16.2
1272383	25.9	0.67	8.98	1.70	0.02	15.6	< 0.1	10	77.8	2050	2.83	2.2	< 10	64.4	1.1	< 0.1	0.4	0.08	< 0.05	18.9	0.34	0.04	< 0.1	11.3
1272384	13.0	0.39	9.57	0.86	< 0.01	18.0	< 0.1	4	65.0	2280	2.74	< 0.1	< 10	38.4	1.2	< 0.1	0.4	0.05	< 0.05	14.6	0.33	0.03	0.1	11.4
1272385	42.5	1.73	1.02	> 10.0	2.55	0.24	< 0.1	69	95.6	34	3.58	2.1	< 10	48.7	0.8	4.1	0.3	0.09	3.34	7.1	1.40	0.06	< 0.1	8.1
1272386	35.4	1.85	1.13	9.34	2.04	0.19	< 0.1	55	108	32	4.96	1.9	< 10	55.0	0.9	2.2	0.3	0.07	2.49	8.1	0.70	0.05	0.6	5.4
1272387	0.7	0.63	2.08	0.78	0.03	35.2	< 0.1	8	17.4	1390	0.79	< 0.1	< 10	10.6	1.1	< 0.1	0.4	0.05	0.05	3.3	0.39	0.04	0.9	3.7
1272388	1.1	1.20	10.0	1.37	0.01	20.1	< 0.1	16	21.8	2250	2.24	0.2	< 10	25.1	0.7	< 0.1	0.3	0.05	< 0.05	14.8	0.31	0.04	0.2	14.3
1272389	26.4	0.03	6.70	3.88	2.64	9.17	< 0.1	33	46.6	249	2.54	1.4	< 10	18.4	0.9	0.2	0.3	0.05	2.11	6.1	0.48	0.06	0.1	16.1
1272390	3.6	0.02	24.9	0.13	0.10	2.58	< 0.1	2	21.4	1150	0.67	< 0.1	< 10	15.0	0.1	< 0.1	< 0.1	< 0.05	0.26	10.5	0.06	0.05	< 0.1	553
1272391	8.6	0.02	10.0	0.31	0.24	16.3	< 0.1	5	74.1	1300	0.75	< 0.1	< 10	9.7	0.3	< 0.1	0.1	< 0.05	0.68	6.1	0.23	0.04	< 0.1	9.5
1272392	20.0	0.04	10.4	0.84	0.78	13.5	< 0.1	13	71.2	969	1.08	< 0.1	< 10	20.0	0.2	< 0.1	< 0.1	0.05	1.22	14.1	0.17	0.05	0.3	17.7
1272393	13.0	0.03	10.2	0.77	0.53	16.0	< 0.1	13	124	1690	1.43	< 0.1	< 10	26.7	0.2	< 0.1	0.1	< 0.05	0.60	15.9	0.36	0.03	0.6	12.4
1272394	12.7	> 3.00	1.24	3.44	2.09	0.44	< 0.1	40	197	51	2.32	2.9	< 10	15.6	0.2	< 0.1	< 0.1	0.11	1.61	3.7	0.23	0.05	< 0.1	2.9
1272395	48.5	0.17	3.54	7.19	2.65	2.35	< 0.1	135	153	371	4.68	2.5	< 10	40.9	0.8	1.2	0.3	0.07	2.98	12.8	0.85	0.06	< 0.1	7.9
1272396	55.3	0.58	4.16	7.75	2.75	1.00	< 0.1	114	179	163	4.21	5.2	< 10	51.2	0.9	1.3	0.3	0.09	2.34	16.2	1.17	0.05	< 0.1	7.8
1272397	84.4	0.56	5.11	7.01	3.13	4.81	0.3	68	142	274	4.66	2.2	< 10	80.4	0.7	1.6	0.3	< 0.05	3.49	30.7	0.99	0.06	< 0.1	53.1
1272398	68.4	0.09	2.80	6.47	3.07	2.54	< 0.1	109	259	419	5.55	2.5	< 10	55.9	0.8	0.9	0.3	0.83	4.10	23.8	1.07	0.08	1.8	9.1
1272399	7.6	0.03	11.0	0.23	0.17	20.1	< 0.1	5	64.6	4580	2.13	< 0.1	< 10	9.3	0.2	< 0.1	< 0.1	0.19	0.26	22.1	0.24	0.03	< 0.1	17.8
1272400	66.2	> 3.00	3.15	7.25	1.88	1.67	< 0.1	110	110	244	8.98	2.4	< 10	52.7	1.5	0.9	0.5	0.17	1.32	27.3	1.53	0.09	0.7	49.2
1272401	104	0.20	3.08	8.64	3.56	0.78	< 0.1	241	232	489	12.6	3.7	< 10	106	1.6	2.6	0.6	0.19	6.24	55.3	1.64	1.06	0.3	49.6
1272402	49.0	1.46	3.00	7.19	2.12	4.25	< 0.1	101	164	884	5.93	2.4	< 10	44.9	0.9	0.6	0.3	0.14	1.82	19.8	1.04	0.23	0.5	38.0
1272403	5.3	0.15	2.65	0.58	0.29	16.0	< 0.1	10	94.1	2030	1.37	< 0.1	< 10	8.4	0.7	< 0.1	0.2	< 0.05	0.23	7.2	0.51	0.06	0.6	17.2
1272404	68.4	0.05	2.74	5.44	2.23	6.45	< 0.1	122	298	374	9.16	2.2	< 10	75.2	0.8	1.2	0.3	0.27	4.15	32.1	1.19	0.37	0.8	38.2
1272405	50.8	0.50	6.45	1.26	0.86	17.0	< 0.1	34	93.0	1750	1.79	0.3	< 10	19.1	0.2	0.2	< 0.1	0.09	1.10	30.8	0.19	0.05	< 0.1	20.3
1272406	12.9	0.42	1.43	5.42	3.79	9.19	< 0.1	97	143	545	5.85	2.4	< 10	34.4	0.9	0.2	0.3	0.17	0.68	10.8	0.82	0.05	1.8	5.1
1272407	4.9	< 0.01	14.8	0.07	0.08	7.63	< 0.1	< 1	41.0	1010	0.63	< 0.1	< 10	5.1	< 0.1	< 0.1	< 0.1	0.06	0.14	8.1	< 0.05	0.04	< 0.1	11.8
1272408	82.8	0.68	2.56	5.24	2.52	7.49	< 0.1	89	164	409	4.99	2.2	< 10	52.3	0.8	0.8	0.3	0.25	2.80	23.4	1.06	0.07	1.8	11.3
1272409	72.0	> 3.00	5.03	7.48	1.78	0.43	< 0.1	187	151	352	9.95	4.3	< 10	51.1	1.9	1.9	0.6	0.17	3.17	105	0.78	0.06	0.6	34.3
1272410	58.3	> 3.00	4.26	6.85	1.33	1.17	< 0.1	87	91.2	443	9.14	1.7	< 10	42.1	2.4	0.8	0.9	0.10	1.45	60.2	1.47	0.05	1.3	27.1
1272411	41.5	> 3.00	2.73	7.50	1.17	2.96	< 0.1	57	123	587	9.83	1.0	< 10	45.2	2.8	1.4	1.0	0.06	0.86	56.9	1.54	0.29	1.2	38.9
1272412	13.4	> 3.00	2.48	5.14	0.39	1.71	< 0.1	149	76.4	318	3.74	3.7	< 10	24.3	1.9	0.7	0.7	0.24	0.28	34.1	0.65	0.06	0.9	27.1
1272413	129	2.78	5.51	7.49	2.64	1.72	< 0.1	122	59.5	878	9.32	2.1	< 10	96.6	2.3	1.6	0.8	0.08	2.34	147	1.16	0.04	1.2	65.6
1272414	174	0.40	7.76	6.50	4.22	1.12	< 0.1	254	32.5	1070	14.1	3.5	10	137	1.8	2.0	0.7	0.08	3.57	203	1.03	0.05	1.0	91.6
1272415	57.7	0.69	8.20	3.10	1.92	5.39	< 0.1	309	59.9	1370	9.09	1.2	< 10	105	0.8	2.8	0.3	0.07	0.99	130	1.43	0.04	1.1	128
1272416	16.9	> 3.00	1.55	7.58	0.63	1.78	< 0.1	60	71.2	247	9.21	1.7	< 10	33.0	2.8	1.6	1.0	0.06	0.48	37.5	1.37	0.09	1.7	22.5
1272417	24.5	> 3.00	2.43	7.15	0.94	2.28	< 0.1	76	54.1	433	10.1	2.3	< 10	45.2	2.6	1.7	1.0	0.06	0.66	55.6	1.74	0.09	0.7	31.6
1272418	76.5	2.93	4.84	7.09	2.28	4.43	< 0.1	293	236	778	8.97	1.7	< 10	107	2.4	1.3	0.8	0.09	3.55	88.1	1.07	0.16	0.5	45.2
1272419	63.9	0.20	2.07	4.32	2.90	5.79	< 0.1	86	135	438	4.68	2.1	< 10	51.5	0.6	0.7	0.3	0.12	4.06	32.7	0.86	0.07	0.7	10.9
1272420	68.3	0.09	2.62	4.47	2.59	10.7	< 0.1	95	132	926	4.95	2.0	< 10	46.5	1.0	1.0	0.4	0.18	3.47	29.5	1.00	0.06	3.9	12.0
1272421	8.7	0.02	6.45	0.23	0.22	20.6	< 0.1	3	78.4	2510	1.63	< 0.1	< 10	9.9	0.3	< 0.1	< 0.1	0.06	0.36	19.0	0.20	0.03	1.7	14.8
1272422	68.7	0.42	3.03	5.24	2.71	6.35	< 0.1	88	166	624	5.05	2.3	< 10	48.4	0.7	1.0	0.3	0.35	2.00	25.7	1.00	0.14	4.5	32.2
1272423	27.4	> 3.00	2.65	5.15	0.73	2.60	0.1	205	149	720	12.1	7.0	< 10	40.1	1.7	1.4	0.6	0.47	0.78	455	0.91	0.25	31.2	38.6
1272424	6.6	0.09	3.30	6.04	0.05	12.0	< 0.1	175	141	1120	9.16	1.8	< 10	39.7	5.1	1.1	2.2	0.11	0.06	32.2	8.36	0.28	3.7	41.3
1272425	16.1	> 3.00	2.69	5.43	0.91	3.37	0.1	50	110	636	4.32	1.3	< 10	37.7	1.6	1.2	0.5	0.13	0.35	30.5	0.61	0.09	1.5	60.6
1272426	33.7	> 3.00	2.23	6.56	1.28	2.69	< 0.1	113	70.7	750	10.7	1.4	< 10	44.4	2.0	1.3	0.8	0.10	1.02	52.8	1.19	0.08	1.9	73.5
1272427	46.1	> 3.00	2.06	5.85	1.00	2.62	< 0.1	91	54.0	698	8.89	1.3	< 10	40.2	1.7	0.9	0.6	0.09	1.58	42.2	0.83	0.06	1.0	74.0
1272428	34.9	> 3.00	2.89	7.61	1.32	4.49	< 0.1	80	57.0	1070	6.92	2.1	< 10	49.8	2.0	1.8	0.7	0.08	0.89	45.9	0.89	0.07	1.4	73.6
1272429	55.6	> 3.00	2.57	7.38	1.56	3.25	< 0.1	116	60.5	836	9.61	2.9	< 10	46.9	2.2	1.7	0.7	0.10	2.66	48.9	0.91	0.06	1.8	59.9

Analyte Symbol	Li	Na	Mg	Al	K	Ca	Cd	V	Cr	Mn	Fe	Hf	Hg	Ni	Er	Be	Ho	Ag	Cs	Co	Eu	Bi	Se	Zn
Unit Symbol	ppm	%	%	%	%	%	ppm	ppm	ppm	ppm	%	ppm	ppb	ppm	ppm	ppm	ppm	ppm	ppm	ppm	ppm	ppm	ppm	ppm
Detection Limit	0.5	0.01	0.01	0.01	0.01	0.01	0.1	1	0.5	1	0.01	0.1	10	0.5	0.1	0.1	0.1	0.05	0.05	0.1	0.05	0.02	0.1	0.2
Analysis Method	TD-MS	TD-MS	TD-MS	TD-MS	TD-MS	TD-MS	TD-MS	TD-MS	TD-MS	TD-MS	TD-MS	TD-MS	TD-MS	TD-MS	TD-MS	TD-MS	TD-MS	TD-MS	TD-MS	TD-MS	TD-MS	TD-MS	TD-MS	TD-MS
1272430	22.1	> 3.00	2.40	7.27	0.62	2.69	< 0.1	105	13.3	548	8.81	3.0	< 10	16.1	2.8	1.6	1.0	0.10	0.56	42.8	1.77	0.06	2.1	48.4
1272431	20.4	> 3.00	2.11	7.51	0.68	2.31	< 0.1	73	8.8	467	9.43	1.6	< 10	15.2	2.6	1.6	0.9	0.08	0.45	27.0	1.39	0.06	1.5	43.7
1272432	1.5	> 3.00	1.36	8.68	0.05	2.86	< 0.1	10	18.8	291	0.91	4.9	< 10	7.0	1.2	0.6	0.4	0.15	0.07	18.1	0.66	0.07	1.5	7.4
1272433	0.8	> 3.00	0.06	> 10.0	0.03	0.20	< 0.1	5	17.8	53	0.37	4.6	< 10	2.8	0.8	1.2	0.3	0.07	0.06	0.6	0.75	0.03	0.6	9.3
1272434	25.6	> 3.00	1.39	6.72	2.15	0.13	< 0.1	112	94.1	49	1.49	3.2	< 10	54.5	0.8	2.7	0.3	0.17	1.00	5.4	0.68	0.03	1.0	4.5
1272435	17.8	0.59	7.82	1.57	0.07	14.2	< 0.1	7	15.5	2320	3.38	0.3	< 10	52.9	1.1	< 0.1	0.5	0.05	0.07	9.2	2.36	0.06	1.4	6.6
1272436	28.7	1.41	1.48	9.39	2.87	0.32	< 0.1	40	66.8	73	4.29	1.7	< 10	66.8	1.0	2.7	0.3	0.07	1.97	6.2	0.42	0.05	1.0	5.5
1272437	3.1	1.66	9.67	2.18	0.05	17.3	< 0.1	19	19.6	1610	1.22	0.4	< 10	15.0	1.2	< 0.1	0.4	0.06	0.05	6.6	0.47	0.03	< 0.1	5.3
1272438	34.2	1.23	2.11	9.52	2.64	0.20	< 0.1	86	98.3	55	6.71	1.3	< 10	70.3	1.3	2.4	0.5	0.15	2.89	12.2	1.16	0.04	0.8	4.8
1272439	11.6	0.32	11.4	1.14	0.24	19.3	< 0.1	13	9.9	1700	1.09	0.3	< 10	11.1	0.6	< 0.1	0.2	0.05	0.18	5.8	0.38	0.05	< 0.1	9.3
1272440	36.7	1.39	2.99	7.94	1.56	0.20	< 0.1	37	61.9	135	5.77	4.1	< 10	62.8	0.8	1.6	0.3	0.08	1.11	16.6	0.49	0.04	0.6	10.7
1272441	3.7	> 3.00	0.30	> 10.0	0.03	0.20	< 0.1	6	7.6	46	0.48	< 0.1	< 10	10.3	< 0.1	1.6	< 0.1	< 0.05	0.10	1.3	< 0.05	0.03	0.5	6.3
1272442	86.8	0.80	3.01	9.33	1.19	0.17	< 0.1	56	81.0	153	8.02	2.2	< 10	106	1.0	1.6	0.4	0.12	0.60	28.2	0.67	0.03	0.8	9.8
1272443	63.7	1.53	1.16	> 10.0	1.93	0.09	< 0.1	69	62.2	68	3.07	1.6	< 10	49.3	1.1	3.0	0.4	0.25	1.10	9.9	0.45	0.05	0.3	9.4
1272444	70.8	0.08	3.31	6.08	2.13	2.90	< 0.1	107	111	578	6.41	1.5	< 10	52.0	0.8	1.4	0.3	0.20	2.05	25.4	1.04	0.22	1.9	34.3
1272445	83.7	2.59	5.31	6.60	0.29	2.44	< 0.1	271	170	1080	13.2	0.9	< 10	188	1.1	0.3	0.3	0.12	0.26	142	0.34	0.25	1.0	222
1272446	117	> 3.00	6.09	8.58	0.47	2.24	< 0.1	247	185	1250	9.48	1.3	< 10	269	1.5	0.6	0.5	0.10	1.62	69.1	0.53	0.09	1.4	352
1272447	48.6	0.14	1.46	5.65	2.10	2.52	< 0.1	71	44.0	389	3.88	0.6	< 10	33.6	0.7	1.0	0.2	0.12	1.02	10.3	0.98	0.06	0.4	27.5
1272448	67.6	0.10	3.55	6.51	4.16	1.89	< 0.1	100	76.3	363	5.10	3.4	< 10	71.9	1.1	0.9	0.4	0.18	1.88	48.1	2.41	0.05	0.7	36.8
1272449	25.9	0.16	1.94	5.92	4.80	5.12	< 0.1	87	113	629	8.30	3.2	< 10	63.5	1.7	0.2	0.6	0.54	0.78	27.0	2.58	0.26	1.5	19.0
1272450	50.4	> 3.00	3.04	6.58	1.51	1.21	< 0.1	81	5.4	458	9.39	2.4	< 10	40.3	3.0	1.1	1.1	0.18	2.55	32.9	2.00	0.10	1.1	29.2
1272451	23.4	> 3.00	2.90	7.06	0.08	1.04	< 0.1	60	25.3	130	7.69	3.5	< 10	17.6	3.2	1.6	1.2	0.08	0.29	19.6	1.83	0.10	1.7	9.4
1272452	36.1	> 3.00	3.02	7.23	0.72	0.83	< 0.1	58	10.2	309	10.3	1.2	< 10	28.2	2.3	1.7	0.8	0.09	2.08	50.3	1.57	0.07	1.3	27.8
1272453	36.0	> 3.00	3.66	6.95	0.70	0.78	< 0.1	71	8.7	274	10.2	1.2	< 10	21.8	2.3	1.7	0.9	0.10	3.51	55.2	1.46	0.09	1.0	30.1
1272454	37.5	> 3.00	3.28	6.82	1.80	0.90	< 0.1	79	8.9	377	8.50	1.6	< 10	23.8	2.5	1.8	0.9	0.12	4.38	55.9	1.34	0.10	1.0	31.2
1272455	63.3	> 3.00	2.86	7.47	1.90	0.28	< 0.1	198	16.0	170	10.9	4.3	< 10	22.6	1.5	2.4	0.5	0.12	2.84	69.4	0.90	0.08	1.5	28.6
1272456	61.0	> 3.00	2.70	7.35	1.74	0.28	0.1	160	19.4	167	9.98	4.7	< 10	23.1	2.0	2.0	0.7	0.13	2.86	62.4	2.64	0.08	1.5	27.4
1272457	30.1	0.02	1.32	0.65	0.29	31.4	< 0.1	10	11.2	3090	2.03	< 0.1	< 10	11.5	0.6	0.3	0.2	0.07	0.79	14.8	0.64	0.06	0.9	16.6
1272458	19.1	1.25	0.59	4.29	2.32	0.79	< 0.1	25	21.4	144	1.53	1.0	< 10	11.9	0.4	< 0.1	0.1	0.10	0.95	8.0	0.49	0.07	2.6	6.3
1272459	12.4	0.78	0.36	3.68	2.53	1.90	< 0.1	15	16.0	230	0.90	0.6	< 10	7.0	0.3	< 0.1	< 0.1	0.08	0.71	4.4	0.24	0.06	0.4	8.1
1272460	118	1.62	6.67	6.38	2.49	0.29	< 0.1	79	72.3	199	6.44	4.8	< 10	44.3	0.7	3.0	0.2	0.18	5.70	57.8	0.37	0.06	0.8	32.2
1272461	77.8	0.99	1.36	5.03	1.85	0.07	< 0.1	93	84.9	110	4.13	4.2	< 10	34.0	0.5	2.5	0.2	0.18	1.23	3.3	0.23	0.07	0.4	22.4
1272462	36.6	0.20	6.73	4.02	1.25	11.5	< 0.1	44	50.2	1770	4.02	3.0	< 10	51.2	1.2	0.4	0.4	0.12	0.95	10.6	0.46	0.03	0.6	13.4
1272463	38.6	1.14	1.69	9.37	2.39	0.45	< 0.1	73	70.8	115	4.66	2.3	< 10	68.7	0.9	3.4	0.4	< 0.05	3.44	11.2	1.30	0.03	< 0.1	8.0
1272464	49.7	2.54	2.84	8.94	1.92	1.46	< 0.1	71	56.0	342	2.40	2.6	< 10	111	1.3	2.0	0.4	0.09	1.79	18.2	1.32	0.19	1.2	11.4
1272465	15.6	0.52	8.39	1.87	0.17	14.1	< 0.1	22	24.2	4830	4.06	0.9	< 10	38.0	2.0	0.2	0.8	0.08	0.08	13.3	1.63	0.11	1.2	15.6
1272466	56.8	0.62	4.60	6.78	3.16	3.71	< 0.1	57	38.3	188	3.37	0.9	< 10	29.0	0.8	1.6	0.3	0.08	6.20	7.7	0.89	0.07	0.5	14.9
1272467	16.4	0.01	12.1	0.78	0.21	19.8	< 0.1	9	5.1	656	0.81	< 0.1	< 10	11.7	0.5	< 0.1	0.2	< 0.05	0.65	7.2	0.29	0.02	0.1	14.6
1272468	1.7	> 3.00	1.33	6.42	0.13	2.77	< 0.1	84	46.2	282	9.28	3.6	< 10	103	1.3	0.4	0.4	0.17	0.16	355	0.37	0.30	11.6	3.0
1272469	1.7	> 3.00	2.98	7.21	0.17	6.27	< 0.1	24	19.3	709	1.52	4.2	< 10	9.0	1.4	< 0.1	0.5	0.14	0.14	38.6	0.54	0.03	0.6	2.8
1272470	20.2	> 3.00	2.07	6.01	0.53	6.02	< 0.1	165	13.3	1450	9.81	4.1	< 10	35.2	2.3	0.8	0.8	0.34	1.27	26.8	0.75	0.07	7.1	18.2
1272471	8.9	0.02	9.33	0.43	0.01	15.9	< 0.1	16	8.2	1110	1.08	< 0.1	< 10	20.5	0.8	< 0.1	0.3	0.07	< 0.05	12.7	0.53	< 0.02	0.4	11.7
1272472	18.5	> 3.00	2.18	7.09	0.49	3.04	< 0.1	91	5.9	500	8.31	1.5	< 10	13.8	3.0	1.4	1.1	0.17	0.46	51.1	2.74	0.15	1.9	42.1
1272473	25.1	2.84	8.29	5.01	0.10	11.1	< 0.1	16	63.4	1390	1.82	1.1	< 10	98.7	1.0	0.4	0.3	0.11	0.10	10.6	0.53	0.03	< 0.1	5.8
1272474	57.8	0.06	2.64	7.78	2.50	0.92	< 0.1	25	59.8	43	4.17	1.0	< 10	24.1	0.4	1.4	0.1	0.07	7.05	4.4	0.48	0.10	< 0.1	8.7
1272475	4.3	0.04	6.42	0.28	0.17	11.7	< 0.1	4	9.8	940	0.99	< 0.1	< 10	5.6	0.5	< 0.1	0.2	0.07	0.22	4.2	0.31	0.05	< 0.1	8.6
1272476	3.8	0.01	12.9	0.32	0.24	21.7	< 0.1	3	5.6	610	0.58	< 0.1	< 10	10.6	0.2	< 0.1	< 0.1	< 0.05	0.37	5.2	0.14	0.05	0.2	4.7
1272477	14.0	0.04	6.99	1.07	0.76	10.1	< 0.1	11	14.4	824	1.18	< 0.1	< 10	17.6	0.8	< 0.1	0.3	0.09	0.73	9.3	0.49	0.06	< 0.1	13.5
1272478	2.3	0.03	12.3	0.06	0.06	20.9	< 0.1	< 1	< 0.5	2110	1.16	< 0.1	< 10	10.3	0.4	< 0.1	0.2	< 0.05	0.24	9.3	0.55	0.03	< 0.1	17.6
1272479	4.8	0.03	9.60	0.56	0.35	18.9	< 0.1	8	6.8	3230	1.93	< 0.1	< 10	14.1	0.5	< 0.1	0.2	< 0.05	0.13	13.7	0.63	0.05	< 0.1	10.6
1272480	47.2	0.35	2.06	2.85	1.67	0.15	< 0.1	147	76.3	55	4.62	2.5	< 10	44.8	0.3	0.5	0.1	0.10	1.40	10.1	0.25	0.04	< 0.1	13.7
1272481	1.8	0.01	1.23	0.17	0.10	16.0	< 0.1	4	9.9	256	0.71	< 0.1	< 10	4.5	0.4	< 0.1	0.2	< 0.05	0.08	1.7	0.37	0.02	< 0.1	3.4

Activation Laboratories Ltd. Report: A13-10175

Analyte Symbol	Li	Na	Mg	Al	K	Ca	Cd	V	Cr	Mn	Fe	Hf	Hg	Ni	Er	Be	Ho	Ag	Cs	Co	Eu	Bi	Se	Zn
Unit Symbol	ppm	%	%	%	%	%	ppm	ppm	ppm	ppm	%	ppm	ppb	ppm	ppm	ppm	ppm	ppm	ppm	ppm	ppm	ppm	ppm	ppm
Detection Limit	0.5	0.01	0.01	0.01	0.01	0.01	0.1	1	0.5	1	0.01	0.1	10	0.5	0.1	0.1	0.1	0.05	0.05	0.1	0.05	0.02	0.1	0.2
Analysis Method	TD-MS	TD-MS	TD-MS	TD-MS	TD-MS	TD-MS	TD-MS	TD-MS	TD-MS	TD-MS	TD-MS	TD-MS	TD-MS	TD-MS	TD-MS	TD-MS	TD-MS	TD-MS	TD-MS	TD-MS	TD-MS	TD-MS	TD-MS	TD-MS
1272482	65.3	1.73	2.62	5.30	2.20	5.47	< 0.1	81	53.0	343	4.53	2.4	< 10	50.4	0.7	1.1	0.3	0.21	2.24	21.6	1.03	0.12	2.5	11.9
1272483	17.6	0.02	6.79	0.59	0.49	17.6	< 0.1	11	14.9	1320	1.18	< 0.1	< 10	12.8	0.4	< 0.1	0.1	0.06	0.45	10.7	0.26	0.02	< 0.1	6.1
1272484	30.4	> 3.00	2.07	5.90	0.88	4.95	< 0.1	132	4.2	281	5.15	4.8	< 10	31.6	1.5	0.3	0.5	0.55	1.35	9.9	1.18	0.04	0.4	7.5
1272485	5.4	> 3.00	1.36	4.57	0.13	9.23	< 0.1	213	8.2	562	6.66	3.4	< 10	7.1	1.3	< 0.1	0.4	0.30	0.20	7.5	0.57	0.13	2.5	1.5
1272486	55.5	> 3.00	2.85	7.00	1.58	2.07	< 0.1	122	42.2	513	6.23	3.0	< 10	53.3	1.3	1.1	0.5	0.15	2.83	49.5	0.77	0.04	< 0.1	14.6
1272487	49.8	> 3.00	3.11	5.75	1.18	7.37	< 0.1	125	11.9	1580	3.57	3.4	< 10	41.8	1.4	0.3	0.5	0.40	0.99	24.2	1.36	0.15	2.0	13.7
1272488	162	1.48	7.31	7.42	> 5.00	0.09	< 0.1	315	146	983	10.9	2.3	< 10	125	0.3	1.6	< 0.1	0.17	5.70	138	< 0.05	0.04	< 0.1	105
1272489	17.8	> 3.00	1.00	7.53	0.77	1.73	< 0.1	56	24.1	288	8.85	1.6	< 10	17.8	4.5	0.5	1.6	0.08	0.69	26.6	2.08	0.08	1.4	20.8
1272490	43.5	> 3.00	4.32	6.03	1.42	3.36	< 0.1	113	23.4	632	6.76	1.8	< 10	40.2	3.0	1.5	1.1	0.06	1.26	52.8	2.06	0.04	0.2	36.6
1272491	115	1.01	5.72	3.35	2.41	3.48	< 0.1	183	24.7	1200	7.57	2.9	< 10	54.4	1.6	1.2	0.6	0.15	3.41	96.0	0.98	0.07	1.7	73.8
1272492	16.9	> 3.00	1.57	4.76	1.05	10.1	< 0.1	59	47.4	803	3.05	1.1	< 10	20.6	1.0	< 0.1	0.4	2.74	0.50	9.8	0.78	4.48	4.6	7.6
1272493	66.8	> 3.00	2.22	6.94	0.54	4.66	< 0.1	83	46.6	147	3.83	1.4	< 10	44.3	0.6	0.5	0.2	0.51	0.89	37.7	0.52	0.36	< 0.1	55.0
1272494	104	2.77	3.70	5.01	1.06	5.95	< 0.1	93	56.8	200	5.81	2.2	< 10	67.2	0.8	0.9	0.3	0.27	1.46	63.2	1.04	0.22	0.2	117
1272495	17.3	> 3.00	2.60	7.28	0.09	1.29	< 0.1	119	73.2	101	4.55	2.3	< 10	24.2	1.6	0.4	0.5	0.20	0.15	13.6	0.53	0.08	< 0.1	4.7
1272496	39.6	> 3.00	3.13	6.83	1.53	2.50	< 0.1	72	4.7	322	8.83	2.3	< 10	24.2	2.8	1.0	1.0	0.38	0.99	57.8	1.82	0.25	8.6	27.7
1272497	29.9	> 3.00	2.57	7.12	1.06	3.28	< 0.1	70	5.6	442	9.13	2.1	< 10	21.7	2.7	1.3	0.9	0.15	0.67	43.7	1.54	0.11	0.5	41.0
1272498	14.0	> 3.00	3.17	7.12	0.16	1.15	< 0.1	99	33.4	276	6.99	4.3	< 10	5.5	2.2	1.8	0.8	0.15	0.54	32.8	1.32	0.07	0.9	29.3
1272499	25.3	> 3.00	2.24	7.26	0.77	2.07	< 0.1	152	6.4	296	8.77	4.3	< 10	19.7	2.7	1.0	1.0	0.20	1.05	54.4	1.98	0.05	0.9	26.8
1272500	28.3	> 3.00	2.87	6.76	0.93	3.41	< 0.1	185	10.8	451	10.2	4.8	< 10	31.5	2.9	1.7	1.1	0.20	0.68	52.0	2.20	0.05	0.8	34.9

Analyte Symbol	Ga	As	Rb	Y	Sr	Zr	Nb	Mo	In	Sn	Sb	Te	Ba	La	Ce	Pr	Nd	Sm	Gd	Tb	Dy	Cu	Ge	Tm
Unit Symbol	ppm	ppm	ppm	ppm	ppm	ppm	ppm	ppm	ppm	ppm	ppm	ppm	ppm	ppm	ppm	ppm	ppm	ppm	ppm	ppm	ppm	ppm	ppm	ppm
Detection Limit	0.1	0.1	0.2	0.1	0.2	1	0.1	0.1	0.1	1	0.1	0.1	1	0.1	0.1	0.1	0.1	0.1	0.1	0.1	0.1	0.2	0.1	0.1
Analysis Method	TD-MS	TD-MS	TD-MS	TD-MS	TD-MS	TD-MS	TD-MS	TD-MS	TD-MS	TD-MS	TD-MS	TD-MS	TD-MS	TD-MS	TD-MS	TD-MS	TD-MS	TD-MS	TD-MS	TD-MS	TD-MS	TD-MS	TD-MS	TD-MS
1272046	21.4	2.5	185	37.9	45.4	110	0.2	2.8	< 0.1	< 1	< 0.1	0.3	59	30.1	65.8	8.5	35.7	8.3	8.3	1.3	7.8	10.8	0.3	0.6
1272210	1.4	1.4	6.7	0.4	> 1000	3	0.1	1.0	< 0.1	< 1	< 0.1	0.4	12	1.9	3.6	0.4	1.4	0.2	0.2	< 0.1	< 0.1	11.4	< 0.1	< 0.1
1272211	27.5	0.9	109	11.9	29.3	145	0.3	0.9	< 0.1	2	< 0.1	0.3	429	40.1	81.7	9.3	31.5	5.1	3.5	0.4	2.3	4.7	0.5	0.2
1272212	15.2	1.7	2.3	5.9	32.1	142	3.2	7.5	< 0.1	< 1	< 0.1	0.2	13	34.0	68.3	7.6	25.9	4.0	2.8	0.3	1.3	13.7	0.6	< 0.1
1272213	10.4	2.5	24.4	15.8	288	44	1.2	5.9	0.7	< 1	< 0.1	0.4	59	8.0	15.6	1.9	8.1	2.0	2.4	0.4	2.9	> 10000	0.6	0.3
1272214	18.9	8.2	35.2	7.2	45.1	87	0.4	0.3	< 0.1	< 1	< 0.1	0.2	146	79.9	152	17.1	58.5	8.9	5.7	0.6	2.3	58.2	0.3	0.1
1272215	30.5	1910	0.4	3.9	1.6	71	0.4	2.5	< 0.1	< 1	0.2	1.0	1	3.4	7.5	1.0	4.0	1.2	1.3	0.2	1.0	668	0.3	< 0.1
1272216	0.3	1360	0.5	0.5	0.5	4	0.1	0.8	< 0.1	< 1	0.4	30.4	2	26.1	53.5	5.7	17.5	2.5	1.3	0.1	0.4	624	0.9	< 0.1
1272217	33.8	13.9	76.6	1.6	31.3	126	11.0	0.9	< 0.1	2	0.3	1.6	918	1.6	4.2	0.5	2.2	0.5	0.5	< 0.1	0.5	9.8	0.8	< 0.1
1272218	24.7	7.2	190	2.2	6.9	63	7.9	0.9	< 0.1	2	0.6	0.5	749	33.3	62.3	6.4	20.3	2.4	1.3	0.1	0.5	5.8	0.4	< 0.1
1272219	7.0	2.7	2.2	6.8	36.2	23	1.7	1.0	< 0.1	4	< 0.1	1.0	7	3.1	7.1	0.9	4.2	1.2	1.3	0.2	1.4	5.7	0.4	0.1
1272220	12.4	6.7	17.1	7.8	53.5	30	3.1	0.9	< 0.1	< 1	0.1	0.4	9	27.5	53.1	5.7	19.6	3.0	2.3	0.3	1.5	5.4	0.4	0.1
1272221	12.1	4.7	1.8	18.7	43.4	140	3.3	1.5	< 0.1	< 1	< 0.1	0.6	18	58.8	112	12.6	45.3	7.9	6.9	0.9	4.3	4.4	0.5	0.2
1272222	2.1	2.3	0.9	22.8	93.2	73	1.8	1.0	< 0.1	< 1	0.1	4.5	8	3.0	8.6	1.3	6.3	2.4	3.3	0.7	4.8	12.6	0.1	0.4
1272223	14.0	1.4	0.2	7.2	6.6	191	2.0	3.2	< 0.1	< 1	0.1	0.7	8	4.1	8.2	1.0	4.1	1.2	1.4	0.2	1.5	5.2	0.2	0.1
1272224	1.8	3.4	0.4	5.2	152	8	0.7	0.1	0.1	< 1	< 0.1	0.3	3	3.7	9.7	1.3	5.2	1.1	1.2	0.2	1.0	168	< 0.1	< 0.1
1272225	2.1	3.5	0.5	1.9	43.8	4	0.4	0.4	0.5	< 1	< 0.1	0.3	4	2.9	7.1	0.9	3.3	0.6	0.5	< 0.1	0.4	7000	< 0.1	< 0.1
1272226	0.5	1.5	0.7	1.8	76.2	< 1	0.1	2.5	< 0.1	< 1	< 0.1	0.1	2	4.9	8.3	0.8	2.7	0.4	0.4	< 0.1	0.3	3130	< 0.1	< 0.1
1272227	1.4	9.2	0.5	3.1	63.5	1	0.2	0.6	0.2	< 1	< 0.1	3.5	4	23.1	26.7	1.7	4.2	0.5	0.6	< 0.1	0.5	> 10000	0.4	< 0.1
1272228	1.5	1.6	0.3	10.6	70.2	36	1.2	1.0	< 0.1	< 1	< 0.1	< 0.1	2	11.0	21.7	2.5	9.3	1.8	2.0	0.3	2.1	224	0.2	0.2
1272229	22.4	23.5	6.7	> 500	14.0	13	5.7	1.9	0.2	2	0.5	0.2	72	63.7	441	75.1	447	> 100	177	37.7	237	221	3.8	19.3
1272230	18.1	1.3	107	14.6	22.3	89	7.7	1.6	< 0.1	1	< 0.1	< 0.1	413	21.1	43.5	5.0	18.1	3.7	3.4	0.6	3.4	97.4	0.3	0.3
1272231	34.5	1.0	196	10.8	44.4	85	1.0	< 0.1	< 0.1	< 1	< 0.1	< 0.1	917	16.5	34.7	3.9	13.8	2.4	2.1	0.4	2.2	25.5	0.3	0.2
1272232	16.4	0.9	11.2	23.1	86.5	23	0.2	0.2	< 0.1	< 1	< 0.1	0.2	60	3.6	10.4	1.6	8.3	2.6	3.5	0.7	4.5	153	0.4	0.4
1272233	20.3	4.1	143	4.2	103	44	2.0	2.1	0.1	< 1	0.1	0.2	249	4.9	9.9	1.1	4.1	0.8	0.8	0.1	0.9	7.6	0.8	< 0.1
1272351	12.8	3.4	119	10.7	19.9	139	2.7	1.9	< 0.1	2	< 0.1	0.1	810	45.7	80.7	9.2	31.5	5.1	3.5	0.4	2.1	9.3	0.8	0.2
1272352	0.2	1.7	9.2	3.3	103	3	0.4	1.6	0.1	< 1	0.2	< 0.1	64	3.4	7.5	0.9	3.7	0.8	0.9	0.1	0.8	10.0	< 0.1	< 0.1
1272353	9.6	1.2	143	3.4	30.2	77	0.1	0.8	< 0.1	< 1	< 0.1	< 0.1	788	5.7	11.7	1.4	5.0	0.9	0.8	0.1	0.6	6.3	0.3	< 0.1
1272354	9.2	16.7	75.3	2.3	6.0	14	0.2	5.1	< 0.1	< 1	< 0.1	< 0.1	133	20.0	36.4	4.1	14.8	2.2	1.4	0.1	0.6	46.9	0.1	< 0.1
1272355	4.1	1.6	78.9	1.4	22.3	44	1.0	3.6	< 0.1	< 1	0.1	< 0.1	709	2.9	6.0	0.7	2.5	0.4	0.4	< 0.1	0.3	6.3	0.5	< 0.1
1272356	15.8	1.1	129	2.8	48.1	84	2.0	3.5	< 0.1	< 1	0.1	< 0.1	730	14.2	25.6	2.8	9.9	1.6	1.1	0.1	0.6	8.7	0.1	< 0.1
1272357	10.9	1.8	94.0	5.1	42.1	103	0.5	2.9	< 0.1	< 1	< 0.1	< 0.1	576	9.3	18.0	2.1	7.8	1.4	1.1	0.2	1.0	6.1	0.1	0.1
1272358	3.2	1.5	69.6	4.3	29.3	31	1.7	4.4	< 0.1	< 1	0.2	< 0.1	708	5.2	10.4	1.2	4.3	0.8	0.7	0.1	0.7	7.6	< 0.1	< 0.1
1272359	11.5	1.7	104	4.4	45.4	101	0.2	3.2	< 0.1	< 1	< 0.1	< 0.1	588	7.2	14.3	1.7	6.0	1.1	0.9	0.1	0.8	6.4	0.2	< 0.1
1272360	5.1	2.3	67.8	7.1	42.3	23	1.9	6.3	< 0.1	< 1	< 0.1	0.1	359	34.7	66.2	7.4	25.9	4.0	2.6	0.3	1.4	10.7	0.2	0.1
1272361	9.3	2.6	85.0	4.9	21.6	58	1.9	5.0	< 0.1	< 1	0.3	< 0.1	169	12.5	23.4	2.8	10.1	1.8	1.4	0.2	0.9	19.7	0.1	< 0.1
1272362	0.2	0.5	5.1	0.7	71.8	2	0.2	2.8	< 0.1	< 1	< 0.1	0.2	22	1.1	2.7	0.3	1.3	0.3	0.2	< 0.1	0.2	6.5	< 0.1	< 0.1
1272363	11.8	3.4	139	5.7	27.8	142	5.4	2.5	< 0.1	1	0.2	< 0.1	569	40.5	73.0	7.6	25.0	3.3	2.2	0.2	1.3	22.2	0.2	0.1
1272364	0.4	3.7	10.1	2.6	123	4	0.2	1.3	< 0.1	< 1	< 0.1	< 0.1	13	7.5	16.6	1.4	5.0	0.9	0.8	< 0.1	0.5	10.6	< 0.1	< 0.1
1272365	12.9	2.6	70.7	5.8	98.9	160	3.6	1.4	< 0.1	< 1	< 0.1	< 0.1	45	31.7	61.9	6.8	23.9	3.5	2.4	0.3	1.3	6.3	0.2	< 0.1
1272366	0.3	3.8	15.3	2.2	113	3	0.2	1.4	< 0.1	< 1	< 0.1	< 0.1	53	10.5	11.4	1.1	4.1	0.7	0.7	< 0.1	0.5	69.0	< 0.1	< 0.1
1272367	10.1	0.8	70.3	7.0	72.1	101	2.8	1.9	< 0.1	< 1	0.1	< 0.1	78	28.6	56.7	6.6	23.3	4.1	3.2	0.4	1.7	6.5	0.2	0.1
1272368	21.2	0.5	124	8.4	17.5	74	0.4	0.3	0.1	< 1	< 0.1	< 0.1	209	38.2	73.5	8.3	28.6	4.7	3.5	0.4	2.0	2.4	0.5	0.2
1272369	5.2	0.8	34.9	5.1	74.9	29	1.4	7.3	< 0.1	< 1	< 0.1	< 0.1	48	13.3	27.0	3.1	11.4	2.3	2.0	0.3	1.2	8.1	0.2	< 0.1
1272370	4.8	2.1	96.0	5.1	44.4	54	2.4	1.8	< 0.1	< 1	< 0.1	< 0.1	408	6.1	13.0	1.5	5.7	1.2	1.1	0.2	1.0	6.2	0.4	< 0.1
1272371	12.2	1.9	158	5.8	14.7	135	0.7	0.5	< 0.1	< 1	< 0.1	< 0.1	919	36.4	68.2	7.5	25.5	3.4	2.2	0.2	1.1	5.0	0.6	0.1
1272372	1.5	1.0	26.8	2.5	87.4	18	0.9	0.9	< 0.1	< 1	< 0.1	< 0.1	82	5.8	11.0	1.2	4.3	0.8	0.6	< 0.1	0.5	2.7	< 0.1	< 0.1
1272373	< 0.1	0.8	4.0	1.0	99.2	14	0.3	0.7	< 0.1	< 1	< 0.1	< 0.1	12	1.8	4.0	0.5	1.9	0.3	0.3	< 0.1	0.2	17.0	< 0.1	< 0.1
1272374	< 0.1	1.1	34.7	2.6	59.8	21	1.2	1.0	< 0.1	< 1	< 0.1	< 0.1	325	7.0	13.6	1.5	5.0	0.9	0.7	< 0.1	0.5	5.0	< 0.1	< 0.1
1272375	3.7	0.5	43.1	2.4	84.5	29	1.3	0.8	< 0.1	< 1	0.1	< 0.1	66	3.2	7.3	0.9	3.4	0.7	0.5	< 0.1	0.5	10.9	< 0.1	< 0.1
1272376	13.1	1.4	99.2	3.4	17.5	94	0.9	0.7	< 0.1	< 1	< 0.1	< 0.1	203	62.0	106	10.8	33.0	3.2	1.9	0.2	0.7	2.6	0.7	< 0.1
1272377	< 0.1	1.4	7.3	1.5	52.3	2	0.2	2.8	< 0.1	< 1	< 0.1	< 0.1	48	2.8	6.5	0.8	2.8	0.5	0.4	< 0.1	0.3	5.9	< 0.1	< 0.1

Analyte Symbol	Ga	As	Rb	Y	Sr	Zr	Nb	Mo	In	Sn	Sb	Te	Ba	La	Ce	Pr	Nd	Sm	Gd	Tb	Dy	Cu	Ge	Tm
Unit Symbol	ppm	ppm	ppm	ppm	ppm	ppm	ppm	ppm	ppm	ppm	ppm	ppm	ppm	ppm	ppm	ppm	ppm	ppm	ppm	ppm	ppm	ppm	ppm	ppm
Detection Limit	0.1	0.1	0.2	0.1	0.2	1	0.1	0.1	0.1	1	0.1	0.1	1	0.1	0.1	0.1	0.1	0.1	0.1	0.1	0.1	0.2	0.1	0.1
Analysis Method	TD-MS	TD-MS	TD-MS	TD-MS	TD-MS	TD-MS	TD-MS	TD-MS	TD-MS	TD-MS	TD-MS	TD-MS	TD-MS	TD-MS	TD-MS	TD-MS	TD-MS	TD-MS	TD-MS	TD-MS	TD-MS	TD-MS	TD-MS	TD-MS
1272378	11.3	0.9	135	5.0	20.1	112	0.3	0.4	< 0.1	< 1	< 0.1	< 0.1	644	39.6	72.9	7.9	27.1	3.3	2.2	0.2	1.1	3.9	0.3	< 0.1
1272379	1.1	2.3	29.4	1.3	78.2	6	0.2	2.3	< 0.1	< 1	< 0.1	< 0.1	24	1.9	3.5	0.4	1.8	0.4	0.4	< 0.1	0.3	30.4	< 0.1	< 0.1
1272380	1.9	2.3	33.7	2.5	72.4	13	0.6	2.0	< 0.1	< 1	< 0.1	< 0.1	17	4.9	9.4	1.1	4.2	0.8	0.7	< 0.1	0.5	5.8	< 0.1	< 0.1
1272381	3.7	2.2	65.2	2.6	76.4	27	1.4	2.7	< 0.1	< 1	0.1	< 0.1	55	7.5	15.0	1.7	5.8	1.0	0.8	0.1	0.6	3.2	0.2	< 0.1
1272382	15.7	11.9	34.3	10.7	130	223	6.1	1.0	< 0.1	1	0.1	< 0.1	159	4.0	8.9	1.1	4.4	1.3	1.7	0.3	1.9	2.6	0.2	0.2
1272383	3.6	0.8	1.7	10.7	51.9	58	1.9	1.1	< 0.1	< 1	< 0.1	< 0.1	6	8.8	17.5	2.0	7.4	1.5	1.6	0.3	1.9	1.7	0.2	0.2
1272384	1.8	0.3	0.6	11.2	58.6	7	0.5	0.9	< 0.1	< 1	< 0.1	< 0.1	1	7.1	14.2	1.6	6.0	1.2	1.5	0.3	1.9	3.0	< 0.1	0.2
1272385	20.0	0.7	174	6.9	123	103	2.4	0.3	< 0.1	< 1	< 0.1	< 0.1	1060	60.1	126	15.1	52.5	7.8	4.8	0.5	2.1	1.4	0.6	0.1
1272386	18.3	5.5	154	7.2	69.3	95	0.6	0.1	< 0.1	< 1	< 0.1	< 0.1	899	30.4	61.7	7.1	24.5	3.8	2.5	0.3	1.5	2.6	0.3	0.1
1272387	1.2	0.8	2.9	10.1	146	3	0.3	0.2	< 0.1	< 1	< 0.1	< 0.1	7	11.4	22.6	2.6	9.1	1.6	1.5	0.3	1.7	1.3	< 0.1	0.1
1272388	2.6	0.5	1.0	8.7	71.6	16	1.0	0.3	< 0.1	< 1	< 0.1	< 0.1	2	3.5	7.0	0.8	3.4	1.0	1.4	0.3	1.7	1.8	< 0.1	< 0.1
1272389	6.6	0.8	117	8.3	51.6	67	0.5	0.4	< 0.1	< 1	< 0.1	< 0.1	317	19.3	37.5	4.3	15.0	2.4	2.0	0.3	1.5	3.3	0.3	0.1
1272390	0.2	0.6	6.3	1.0	22.8	3	< 0.1	1.7	< 0.1	< 1	< 0.1	< 0.1	8	0.7	1.4	0.2	0.7	0.2	0.2	< 0.1	0.2	10.5	< 0.1	< 0.1
1272391	0.7	1.1	14.8	3.1	85.2	3	0.2	2.2	< 0.1	< 1	< 0.1	< 0.1	10	4.2	8.3	1.1	4.1	0.8	0.8	0.1	0.7	4.6	< 0.1	< 0.1
1272392	2.3	0.9	44.9	2.0	94.0	3	0.6	1.5	< 0.1	1	0.1	< 0.1	13	2.7	5.5	0.7	2.7	0.6	0.6	< 0.1	0.4	5.8	< 0.1	< 0.1
1272393	2.9	0.8	31.7	2.7	74.1	9	0.3	1.7	< 0.1	< 1	< 0.1	< 0.1	11	3.1	6.1	0.9	3.6	1.0	1.1	0.2	0.7	10.6	< 0.1	< 0.1
1272394	12.7	0.5	31.6	1.3	37.0	106	3.2	2.7	< 0.1	< 1	0.2	< 0.1	62	5.0	13.4	1.5	5.5	0.9	0.7	< 0.1	0.4	12.5	0.5	< 0.1
1272395	16.7	1.0	133	6.9	32.3	104	1.1	1.6	< 0.1	< 1	< 0.1	< 0.1	387	27.6	50.6	5.8	20.3	3.2	2.5	0.3	1.6	1.6	0.5	0.1
1272396	17.6	4.8	144	7.9	18.4	223	0.7	1.4	< 0.1	< 1	< 0.1	< 0.1	276	40.5	81.0	9.5	33.6	5.4	3.5	0.4	1.8	4.4	0.2	0.1
1272397	17.3	1.6	175	6.4	38.4	87	0.3	0.4	< 0.1	< 1	< 0.1	< 0.1	125	46.0	85.0	9.6	32.4	4.8	3.3	0.3	1.5	3.4	0.5	< 0.1
1272398	3.0	0.9	169	7.5	95.4	126	3.0	5.0	< 0.1	2	< 0.1	< 0.1	1300	38.6	67.6	7.5	26.2	4.1	3.0	0.4	1.7	3.9	0.2	0.1
1272399	< 0.1	2.3	10.9	1.8	83.1	5	0.2	1.0	< 0.1	< 1	< 0.1	< 0.1	216	1.5	3.5	0.5	2.3	0.6	0.7	0.1	0.5	3.4	< 0.1	< 0.1
1272400	20.7	0.8	82.2	13.3	57.2	101	< 0.1	0.1	< 0.1	< 1	< 0.1	< 0.1	52	37.3	80.2	10.0	39.2	7.5	5.3	0.7	3.1	14.3	0.3	0.2
1272401	23.0	13.0	196	13.8	65.9	143	4.9	4.9	0.6	3	< 0.1	< 0.1	432	62.2	107	11.9	40.3	6.4	5.0	0.6	2.9	6.1	0.9	0.2
1272402	17.5	5.0	110	7.7	235	98	4.8	3.4	0.2	2	0.3	< 0.1	111	21.3	44.9	5.2	18.8	3.2	2.4	0.3	1.6	3.2	0.2	0.1
1272403	0.2	0.6	12.1	6.7	> 1000	2	0.5	1.6	< 0.1	< 1	< 0.1	< 0.1	92	1.4	3.0	0.5	2.2	0.9	1.3	0.2	1.4	10.5	< 0.1	< 0.1
1272404	14.1	14.0	134	7.8	733	90	5.8	5.7	0.2	3	0.7	0.9	97	49.4	80.5	8.4	27.5	4.3	3.2	0.4	1.8	29.8	0.2	0.1
1272405	4.1	0.8	64.2	2.1	794	20	0.7	1.4	0.1	< 1	< 0.1	< 0.1	32	3.7	7.5	0.9	3.1	0.6	0.6	< 0.1	0.4	4.4	< 0.1	< 0.1
1272406	9.4	1.9	118	7.8	520	105	3.5	2.6	< 0.1	1	0.5	0.2	88	30.4	51.9	5.5	18.3	2.9	2.4	0.3	1.7	4.9	0.2	0.1
1272407	< 0.1	0.4	6.1	0.4	675	< 1	< 0.1	1.0	< 0.1	< 1	< 0.1	< 0.1	119	0.9	1.7	0.2	0.6	< 0.1	< 0.1	< 0.1	< 0.1	2.6	< 0.1	< 0.1
1272408	12.8	0.9	148	8.4	258	90	3.3	3.8	< 0.1	2	0.1	< 0.1	94	29.9	55.8	6.3	22.4	3.9	3.1	0.4	1.9	4.0	0.2	0.1
1272409	23.5	2.6	113	14.8	35.4	159	4.1	1.6	0.1	2	< 0.1	< 0.1	38	12.5	30.6	3.9	14.8	3.1	2.7	0.5	3.0	10.8	0.7	0.3
1272410	18.9	1.0	92.0	22.1	64.9	75	0.7	0.3	< 0.1	< 1	< 0.1	< 0.1	103	22.6	50.9	6.6	27.0	5.6	4.9	0.8	4.4	9.4	0.3	0.3
1272411	21.3	0.4	42.1	25.8	128	48	< 0.1	0.1	0.2	< 1	< 0.1	0.1	45	16.3	39.8	5.4	23.0	5.5	5.3	0.9	5.3	9.9	0.3	0.4
1272412	11.9	1.5	10.7	15.0	41.3	145	10.5	1.3	< 0.1	2	< 0.1	< 0.1	17	2.9	10.7	1.3	6.0	1.9	2.3	0.5	3.3	10.0	0.9	0.3
1272413	35.7	0.6	116	20.1	24.5	92	0.6	< 0.1	0.2	< 1	< 0.1	< 0.1	91	13.0	30.5	4.1	17.1	4.1	4.1	0.7	4.1	1.0	0.3	0.3
1272414	43.6	0.6	143	17.8	54.1	148	0.3	< 0.1	0.3	< 1	< 0.1	0.1	138	11.4	26.6	3.5	15.1	3.6	4.0	0.7	3.8	0.8	0.5	0.3
1272415	18.3	0.7	65.2	7.9	117	58	< 0.1	0.3	0.2	< 1	< 0.1	0.2	78	46.6	97.0	12.2	46.5	7.2	4.2	0.4	1.7	15.4	0.9	0.1
1272416	14.6	0.7	23.1	26.4	24.9	76	< 0.1	< 0.1	< 0.1	< 1	< 0.1	0.3	24	7.4	19.4	2.8	13.4	4.3	5.1	0.9	5.1	3.6	0.2	0.4
1272417	17.7	0.4	31.2	27.8	36.1	102	< 0.1	< 0.1	0.1	< 1	< 0.1	0.1	43	20.2	42.8	5.5	23.3	5.3	5.4	0.9	5.3	3.2	0.3	0.4
1272418	18.6	0.7	124	20.3	150	60	2.8	0.8	0.3	< 1	< 0.1	< 0.1	110	5.2	13.7	2.0	9.2	2.6	3.0	0.6	3.9	45.7	0.7	0.3
1272419	11.5	1.3	147	6.2	389	91	3.5	2.9	0.1	2	< 0.1	< 0.1	70	32.5	55.9	6.2	21.6	3.4	2.5	0.3	1.4	3.4	0.2	< 0.1
1272420	11.7	1.8	154	9.0	715	89	4.3	3.6	0.2	2	< 0.1	0.7	89	36.2	62.9	6.8	23.3	4.0	3.0	0.4	2.1	8.9	0.2	0.1
1272421	< 0.1	1.2	19.6	2.5	891	3	0.2	1.3	< 0.1	< 1	0.2	0.4	67	3.6	7.2	0.9	3.4	0.6	0.6	< 0.1	0.5	7.2	0.1	< 0.1
1272422	13.0	1.3	127	7.1	539	89	3.0	3.6	0.1	2	0.3	0.5	73	30.8	56.5	6.2	21.8	3.6	2.9	0.4	1.6	3.8	0.2	0.1
1272423	14.3	53.5	22.3	13.6	104	169	10.4	3.2	< 0.1	1	0.3	1.3	78	8.3	18.8	2.5	10.9	2.7	2.8	0.5	2.9	3960	1.0	0.3
1272424	47.1	1.5	< 0.2	55.5	> 1000	76	0.3	0.2	0.9	< 1	< 0.1	0.2	19	112	240	31.9	132	25.8	22.1	2.7	13.1	21.5	1.0	0.6
1272425	12.3	0.6	33.1	13.5	157	66	< 0.1	< 0.1	0.2	< 1	< 0.1	0.2	173	6.1	13.4	1.8	8.0	1.9	2.2	0.4	2.4	5.1	0.2	0.2
1272426	15.3	1.1	44.7	20.3	138	69	< 0.1	< 0.1	< 0.1	< 1	< 0.1	0.3	283	15.4	37.2	4.9	20.6	4.7	4.5	0.7	4.0	139	0.2	0.3
1272427	15.6	< 0.1	41.2	15.7	88.2	67	< 0.1	< 0.1	< 0.1	< 1	< 0.1	0.4	69	9.2	22.5	3.0	12.7	2.9	2.9	0.5	3.0	7.3	0.2	0.2
1272428	16.9	0.6	43.2	17.5	124	87	0.1	0.3	< 0.1	< 1	< 0.1	0.2	179	8.1	19.0	2.6	11.2	2.5	2.7	0.5	3.0	118	0.3	0.3
1272429	19.2	0.7	77.5	19.3	77.3	125	0.2	0.3	< 0.1	< 1	< 0.1	0.2	71	11.2	27.5	3.7	15.5	3.4	3.3	0.6	3.5	6.1	0.3	0.3

Analyte Symbol	Ga	As	Rb	Y	Sr	Zr	Nb	Mo	In	Sn	Sb	Te	Ba	La	Ce	Pr	Nd	Sm	Gd	Tb	Dy	Cu	Ge	Tm
Unit Symbol	ppm	ppm	ppm	ppm	ppm	ppm	ppm	ppm	ppm	ppm	ppm	ppm	ppm	ppm	ppm	ppm	ppm	ppm	ppm	ppm	ppm	ppm	ppm	ppm
Detection Limit	0.1	0.1	0.2	0.1	0.2	1	0.1	0.1	0.1	1	0.1	0.1	1	0.1	0.1	0.1	0.1	0.1	0.1	0.1	0.1	0.2	0.1	0.1
Analysis Method	TD-MS	TD-MS	TD-MS	TD-MS	TD-MS	TD-MS	TD-MS	TD-MS	TD-MS	TD-MS	TD-MS	TD-MS	TD-MS	TD-MS	TD-MS	TD-MS	TD-MS	TD-MS	TD-MS	TD-MS	TD-MS	TD-MS	TD-MS	TD-MS
1272430	21.2	2.8	26.4	26.8	68.5	123	0.4	0.1	< 0.1	< 1	< 0.1	0.1	47	16.8	39.6	5.2	22.5	5.8	5.9	1.0	5.4	289	0.5	0.4
1272431	20.3	0.5	26.1	24.3	92.2	73	0.2	0.3	< 0.1	< 1	< 0.1	0.2	127	12.4	30.1	4.0	17.1	4.6	4.7	0.8	4.7	204	0.4	0.4
1272432	13.6	1.0	1.6	11.7	45.7	202	2.3	1.1	< 0.1	< 1	< 0.1	0.3	18	21.5	42.5	4.8	17.1	3.0	2.7	0.4	2.2	8.0	0.4	0.2
1272433	17.4	0.9	0.8	8.5	46.8	183	0.1	< 0.1	< 0.1	< 1	< 0.1	0.2	14	25.6	49.6	5.7	20.4	3.4	2.5	0.3	1.4	11.4	0.3	0.1
1272434	26.3	0.9	113	6.1	35.1	96	9.6	0.1	< 0.1	2	< 0.1	< 0.1	435	23.8	52.7	6.0	22.4	3.6	2.4	0.3	1.4	< 0.2	1.2	0.1
1272435	2.8	0.7	4.7	12.7	56.7	20	1.1	0.1	< 0.1	< 1	< 0.1	< 0.1	13	95.0	179	21.4	75.1	11.5	8.0	0.9	3.5	1.2	0.3	0.2
1272436	21.3	0.7	187	9.0	45.7	81	0.5	< 0.1	< 0.1	< 1	< 0.1	< 0.1	719	14.9	29.9	3.4	12.3	2.2	1.8	0.3	1.6	1.3	0.4	0.2
1272437	4.3	1.1	4.0	12.1	80.0	25	1.4	0.1	< 0.1	< 1	< 0.1	< 0.1	10	10.6	22.3	2.6	9.9	2.0	2.1	0.3	2.1	2.3	0.1	0.2
1272438	21.3	0.9	159	12.6	43.4	63	5.6	0.1	< 0.1	1	< 0.1	< 0.1	736	45.8	90.4	10.4	35.9	5.7	4.3	0.6	2.6	3.0	1.1	0.2
1272439	2.5	1.5	9.0	7.0	88.0	21	0.7	< 0.1	< 0.1	< 1	< 0.1	< 0.1	7	8.5	18.7	2.3	8.4	1.6	1.6	0.2	1.3	1.8	< 0.1	< 0.1
1272440	29.6	1.0	110	7.0	16.4	173	0.5	< 0.1	< 0.1	< 1	< 0.1	< 0.1	348	19.5	41.9	4.9	17.4	2.9	2.1	0.3	1.4	5.4	0.4	0.1
1272441	19.8	0.6	2.4	0.4	51.6	9	0.4	0.4	< 0.1	14	< 0.1	0.7	15	0.6	1.2	0.1	0.5	< 0.1	< 0.1	< 0.1	< 0.1	171	0.1	< 0.1
1272442	26.6	0.1	72.8	9.8	48.4	88	0.5	< 0.1	< 0.1	< 1	< 0.1	< 0.1	224	29.1	56.5	6.3	21.5	3.4	2.5	0.4	1.9	2.8	0.8	0.2
1272443	26.3	2.6	143	10.4	100	66	6.8	1.4	< 0.1	1	< 0.1	0.1	456	11.0	21.6	2.5	9.1	1.7	2.0	0.3	1.9	0.6	1.3	0.2
1272444	1.6	2.1	117	9.1	85.1	117	2.5	1.3	0.1	1	< 0.1	0.2	3000	35.1	62.8	7.0	23.9	3.9	2.9	0.4	1.7	8.4	0.2	0.1
1272445	12.3	19.1	9.9	8.8	44.9	38	1.2	0.9	< 0.1	< 1	< 0.1	0.3	55	3.4	7.1	0.9	4.1	1.1	1.2	0.2	1.5	58.5	0.4	0.2
1272446	15.4	15.6	34.7	13.0	78.9	49	2.3	0.4	< 0.1	< 1	< 0.1	0.2	80	2.4	5.7	0.8	4.1	1.3	1.7	0.4	2.4	37.0	0.4	0.2
1272447	9.3	1.8	79.6	6.6	28.2	54	1.9	0.7	< 0.1	< 1	< 0.1	0.1	390	27.0	46.0	5.1	17.9	2.8	2.1	0.3	1.3	35.9	0.5	0.1
1272448	17.8	3.0	132	10.6	32.7	143	4.0	0.9	< 0.1	2	< 0.1	< 0.1	402	69.5	122	13.9	47.4	7.5	4.9	0.5	2.2	2.2	0.9	0.2
1272449	11.3	2.8	110	15.5	34.7	139	3.2	0.9	< 0.1	2	< 0.1	0.8	503	65.4	116	13.3	47.5	7.5	5.4	0.6	3.0	2.6	0.7	0.3
1272450	21.1	1.3	87.1	26.5	60.8	100	3.5	< 0.1	< 0.1	< 1	< 0.1	< 0.1	27	28.7	65.1	7.8	31.3	6.6	6.2	1.0	5.6	2.1	0.6	0.4
1272451	17.6	9.3	4.1	30.1	133	166	0.5	< 0.1	< 0.1	< 1	< 0.1	0.3	20	22.7	51.0	6.7	27.1	6.3	6.3	1.0	5.9	4.2	0.2	0.5
1272452	19.5	1.4	54.5	21.5	91.3	61	0.1	< 0.1	0.1	< 1	< 0.1	0.3	35	28.8	62.7	8.0	31.7	5.9	5.2	0.8	4.4	439	0.3	0.3
1272453	20.5	1.8	68.6	22.4	158	59	0.1	0.1	0.1	< 1	< 0.1	0.2	27	22.0	49.9	6.5	26.8	5.3	5.0	0.8	4.4	269	0.4	0.3
1272454	21.2	0.5	105	24.7	81.8	74	< 0.1	< 0.1	0.2	< 1	< 0.1	0.2	86	16.0	36.3	4.7	19.8	4.4	4.7	0.8	4.8	798	0.4	0.3
1272455	20.9	1.4	151	12.8	32.9	184	0.3	0.3	< 0.1	< 1	< 0.1	0.2	171	15.0	34.5	4.3	17.2	3.3	3.1	0.5	2.5	614	0.6	0.2
1272456	21.3	0.7	138	17.7	35.5	192	0.4	< 0.1	< 0.1	< 1	< 0.1	0.2	33	51.8	116	15.1	60.4	11.0	8.0	0.9	4.2	26.2	0.5	0.3
1272457	< 0.1	2.8	25.2	4.9	267	2	0.2	3.9	< 0.1	< 1	0.1	0.3	193	15.6	28.4	3.0	9.7	1.6	1.4	0.2	1.1	10.3	0.1	< 0.1
1272458	2.6	0.6	74.1	3.5	46.6	56	0.6	0.4	< 0.1	< 1	< 0.1	< 0.1	814	14.6	27.2	3.0	10.3	1.6	1.2	0.2	0.8	16.1	0.5	< 0.1
1272459	1.5	1.9	77.8	2.6	39.2	44	0.5	0.3	< 0.1	< 1	< 0.1	< 0.1	760	8.1	14.5	1.6	5.4	0.8	0.7	< 0.1	0.5	10.6	0.2	< 0.1
1272460	18.6	0.5	344	6.1	14.1	177	5.3	1.3	< 0.1	2	< 0.1	< 0.1	26	3.0	6.7	0.9	3.8	1.1	1.3	0.2	1.3	16.3	1.1	0.1
1272461	23.5	1.1	44.1	2.2	67.9	155	9.2	0.7	< 0.1	2	< 0.1	< 0.1	479	2.5	7.9	1.1	4.4	1.0	0.8	0.1	0.8	16.3	0.7	< 0.1
1272462	5.8	0.4	92.9	11.5	58.6	120	2.7	< 0.1	< 0.1	< 1	< 0.1	< 0.1	331	12.0	24.1	2.8	10.0	1.9	2.1	0.3	2.0	1.3	0.3	0.2
1272463	19.6	0.5	179	9.4	83.4	105	0.6	< 0.1	< 0.1	< 1	< 0.1	< 0.1	714	49.7	97.7	11.4	39.7	6.1	4.4	0.5	2.3	9.5	0.4	0.1
1272464	18.8	0.8	126	11.6	54.6	110	2.2	0.3	< 0.1	< 1	< 0.1	< 0.1	452	51.2	99.9	11.6	40.8	6.8	4.8	0.6	2.7	3.7	0.6	0.2
1272465	5.2	1.3	5.2	22.6	46.8	41	1.3	0.6	< 0.1	< 1	< 0.1	0.4	14	26.8	62.2	7.5	28.7	6.6	7.1	1.0	4.9	38.8	0.3	0.3
1272466	14.1	1.8	195	6.8	26.3	44	3.0	0.1	< 0.1	1	< 0.1	< 0.1	552	53.2	100	10.9	36.9	5.2	3.3	0.3	1.5	0.9	0.7	0.1
1272467	1.5	1.1	15.4	4.9	96.8	9	0.7	< 0.1	< 0.1	< 1	< 0.1	< 0.1	27	3.6	7.4	1.0	4.1	1.0	1.1	0.2	1.1	5.7	< 0.1	< 0.1
1272468	14.2	48.4	4.1	12.4	40.5	142	6.6	0.8	< 0.1	< 1	< 0.1	< 0.1	19	1.3	4.0	0.6	3.3	1.2	1.7	0.3	1.8	197	0.2	0.2
1272469	15.5	1.1	4.1	13.3	69.1	169	5.2	0.2	< 0.1	< 1	< 0.1	< 0.1	15	1.6	4.9	0.8	4.2	1.6	2.0	0.4	2.3	130	0.1	0.2
1272470	14.8	2.0	34.1	22.4	128	169	5.0	1.1	0.3	< 1	< 0.1	0.1	145	7.2	15.0	2.0	8.8	2.4	3.3	0.6	3.7	7090	0.3	0.4
1272471	1.2	0.9	1.0	7.5	767	7	0.5	2.7	< 0.1	< 1	< 0.1	< 0.1	22	4.5	9.6	1.3	5.3	1.4	1.7	0.3	1.7	10.5	< 0.1	< 0.1
1272472	21.4	3.8	21.5	30.1	130	55	0.3	1.1	< 0.1	1	< 0.1	< 0.1	49	41.9	92.1	12.1	49.2	9.6	8.9	1.2	6.3	1330	0.5	0.4
1272473	11.9	0.7	4.6	9.5	62.8	44	1.0	0.3	< 0.1	< 1	< 0.1	< 0.1	19	15.3	31.2	3.6	13.2	2.2	2.1	0.3	1.8	4.1	0.3	0.1
1272474	16.1	1.7	180	3.5	11.2	54	0.2	< 0.1	< 0.1	< 1	< 0.1	< 0.1	642	58.5	102	10.6	33.4	3.5	2.0	0.2	0.7	3.9	0.4	< 0.1
1272475	0.4	1.0	9.3	5.0	70.5	7	0.3	0.4	< 0.1	< 1	< 0.1	< 0.1	30	3.0	6.7	0.8	3.4	0.8	1.0	0.2	1.1	5.8	< 0.1	< 0.1
1272476	0.2	2.3	13.4	1.8	96.7	3	0.2	< 0.1	< 0.1	< 1	0.4	< 0.1	37	1.8	5.2	0.7	2.8	0.6	0.5	< 0.1	0.4	1.9	< 0.1	< 0.1
1272477	2.0	1.3	36.2	7.1	88.0	< 1	0.6	0.3	< 0.1	< 1	< 0.1	< 0.1	43	3.1	7.2	0.9	3.9	1.0	1.4	0.3	1.6	15.6	< 0.1	0.1
1272478	0.1	7.5	3.8	5.5	103	< 1	< 0.1	< 0.1	< 0.1	< 1	< 0.1	< 0.1	5	10.6	15.9	1.9	7.9	1.7	1.8	0.2	1.1	11.0	< 0.1	< 0.1
1272479	0.6	0.8	13.4	5.5	77.1	5	0.4	0.4	< 0.1	< 1	< 0.1	< 0.1	40	8.2	15.4	1.9	7.7	1.7	1.9	0.3	1.3	2.2	< 0.1	< 0.1
1272480	13.1	0.8	16.8	1.3	7.3	95	3.9	1.1	< 0.1	1	0.1	< 0.1	436	2.2	6.1	0.8	3.5	0.7	0.7	0.1	0.5	0.9	0.6	< 0.1
1272481	< 0.1	0.3	3.6	4.3	> 1000	< 1	0.2	0.6	< 0.1	< 1	< 0.1	< 0.1	74	1.3	3.2	0.5	2.3	0.8	1.1	0.2	0.9	3.3	< 0.1	< 0.1

Analyte Symbol	Ga	As	Rb	Y	Sr	Zr	Nb	Mo	In	Sn	Sb	Te	Ba	La	Ce	Pr	Nd	Sm	Gd	Tb	Dy	Cu	Ge	Tm
Unit Symbol	ppm	ppm	ppm	ppm	ppm	ppm	ppm	ppm	ppm	ppm	ppm	ppm	ppm	ppm	ppm	ppm	ppm	ppm	ppm	ppm	ppm	ppm	ppm	ppm
Detection Limit	0.1	0.1	0.2	0.1	0.2	1	0.1	0.1	0.1	1	0.1	0.1	1	0.1	0.1	0.1	0.1	0.1	0.1	0.1	0.1	0.2	0.1	0.1
Analysis Method	TD-MS	TD-MS	TD-MS	TD-MS	TD-MS	TD-MS	TD-MS	TD-MS	TD-MS	TD-MS	TD-MS	TD-MS	TD-MS	TD-MS	TD-MS	TD-MS	TD-MS	TD-MS	TD-MS	TD-MS	TD-MS	TD-MS	TD-MS	TD-MS
1272482	13.0	0.2	130	6.6	470	98	2.3	0.7	< 0.1	1	< 0.1	< 0.1	88	31.8	60.2	6.9	23.7	4.0	3.0	0.4	1.6	1.8	0.1	< 0.1
1272483	0.6	0.2	30.1	3.8	> 1000	7	0.4	0.2	< 0.1	< 1	< 0.1	< 0.1	69	2.4	5.6	0.7	3.1	0.7	0.8	0.1	0.8	9.2	< 0.1	< 0.1
1272484	16.3	0.6	70.0	13.4	110	192	3.3	0.5	< 0.1	< 1	< 0.1	< 0.1	21	18.6	41.0	5.3	21.1	4.3	3.9	0.5	2.9	0.8	0.1	0.2
1272485	8.7	0.7	8.0	12.2	479	145	4.7	4.0	< 0.1	< 1	0.1	< 0.1	101	3.6	9.5	1.4	6.3	1.8	2.2	0.4	2.1	8.0	< 0.1	0.2
1272486	21.8	0.4	120	12.0	63.9	115	0.4	0.1	< 0.1	< 1	< 0.1	< 0.1	66	14.4	29.9	3.7	14.5	2.9	2.9	0.4	2.5	4.4	0.4	0.2
1272487	10.2	4.9	64.4	17.0	256	136	3.9	1.3	< 0.1	< 1	0.6	0.1	128	16.9	39.5	5.3	21.9	4.8	4.7	0.6	3.1	1.1	0.1	0.2
1272488	21.3	0.2	245	1.8	13.4	81	2.9	0.4	0.2	< 1	< 0.1	< 0.1	305	0.6	1.5	0.2	0.9	0.2	0.2	< 0.1	0.2	0.8	1.1	< 0.1
1272489	12.1	0.7	42.4	43.4	56.9	73	0.7	< 0.1	< 0.1	< 1	< 0.1	< 0.1	59	12.5	30.6	4.4	20.8	6.3	7.4	1.4	8.4	43.5	0.3	0.6
1272490	13.2	0.2	70.8	28.0	76.8	77	0.1	0.2	0.2	< 1	< 0.1	< 0.1	88	5.5	18.1	3.4	18.7	5.8	6.0	1.0	5.7	2.6	0.5	0.4
1272491	13.7	1.0	63.1	12.2	135	114	5.2	0.6	0.2	< 1	< 0.1	< 0.1	448	10.4	29.9	3.9	15.7	3.7	3.3	0.5	3.1	528	1.3	0.2
1272492	8.5	0.6	39.5	10.8	506	55	1.0	0.3	< 0.1	< 1	< 0.1	0.8	103	10.6	20.7	2.5	10.1	2.3	2.6	0.4	2.1	22.3	0.1	0.1
1272493	13.8	0.3	39.8	5.7	91.0	61	1.1	0.2	< 0.1	< 1	< 0.1	< 0.1	153	10.8	19.4	2.2	8.1	1.4	1.4	0.2	1.2	15.7	< 0.1	< 0.1
1272494	16.5	0.9	83.0	8.5	301	95	3.2	0.2	< 0.1	2	< 0.1	< 0.1	86	27.7	50.6	5.6	19.2	3.1	2.7	0.4	1.8	81.8	0.2	0.1
1272495	12.9	0.5	4.5	12.5	70.5	96	4.1	0.2	< 0.1	< 1	< 0.1	< 0.1	12	3.2	7.4	1.0	4.1	1.2	1.7	0.4	2.7	1.4	0.2	0.2
1272496	21.6	0.9	80.4	26.9	59.5	88	0.8	< 0.1	0.1	1	< 0.1	< 0.1	59	21.8	50.2	6.5	26.7	5.6	5.8	0.9	5.3	3980	0.4	0.4
1272497	20.4	0.4	50.9	25.2	175	85	0.2	< 0.1	< 0.1	< 1	< 0.1	< 0.1	46	18.3	43.2	5.8	23.8	5.2	5.4	0.8	4.7	298	0.3	0.4
1272498	20.3	0.6	9.0	17.8	54.0	174	0.7	0.1	0.1	< 1	< 0.1	< 0.1	13	19.1	45.4	5.6	22.8	4.7	4.7	0.7	4.1	674	0.5	0.3
1272499	20.0	0.7	42.7	25.2	30.3	172	3.0	0.5	< 0.1	< 1	< 0.1	< 0.1	26	34.8	81.7	10.4	42.3	7.6	6.7	0.9	5.0	532	0.6	0.4
1272500	20.8	0.9	38.0	28.7	66.9	188	5.4	0.7	0.2	< 1	< 0.1	< 0.1	36	28.7	61.0	7.8	31.3	6.4	6.8	1.1	6.1	264	0.6	0.4

Analyte Symbol	Yb	Lu	Ta	W	Re	Tl	Pb	Sc	Th	U	Ti	P	S
Unit Symbol	ppm	ppm	ppm	ppm	ppm	ppm	ppm	ppm	ppm	ppm	%	%	%
Detection Limit	0.1	0.1	0.1	0.1	0.001	0.05	0.5	1	0.1	0.1	0.0005	0.001	0.01
Analysis Method	TD-MS	TD-MS	TD-MS	TD-MS	TD-MS	TD-MS	TD-MS	TD-ICP	TD-MS	TD-MS	TD-ICP	TD-ICP	TD-ICP
1272046	3.2	0.4	< 0.1	< 0.1	0.157	0.46	2.9	8	10.6	2.6	0.180	0.063	0.01
1272210	< 0.1	< 0.1	< 0.1	< 0.1	0.008	0.05	3.9	< 1	0.5	< 0.1	0.0191	0.002	10.1
1272211	1.1	0.2	< 0.1	< 0.1	0.005	0.47	2.4	12	24.0	4.2	0.318	0.020	0.09
1272212	0.5	< 0.1	< 0.1	0.4	0.010	< 0.05	2.9	< 1	15.6	5.9	0.320	0.040	0.02
1272213	1.8	0.3	< 0.1	< 0.1	0.015	0.21	2.3	40	6.4	2.3	0.378	0.026	0.83
1272214	0.6	0.1	< 0.1	< 0.1	0.008	0.13	3.0	14	21.7	1.3	0.349	0.022	0.01
1272215	0.3	< 0.1	< 0.1	1.1	0.015	< 0.05	6.2	15	37.9	5.2	0.0383	0.062	0.54
1272216	< 0.1	< 0.1	< 0.1	0.2	0.029	< 0.05	11.7	< 1	2.5	0.2	0.0010	0.001	> 20.0
1272217	0.5	< 0.1	0.7	1.1	0.025	1.68	2.7	15	6.5	1.9	0.525	0.051	0.06
1272218	0.3	< 0.1	0.5	1.1	0.014	1.47	1.7	16	19.5	1.0	0.356	0.087	0.02
1272219	0.6	< 0.1	< 0.1	5.6	0.023	0.05	3.3	2	2.9	2.1	0.175	0.031	0.05
1272220	0.7	0.1	0.2	0.4	0.019	0.12	1.3	7	8.5	1.6	0.155	0.045	0.07
1272221	1.2	0.2	< 0.1	0.3	0.017	< 0.05	8.3	4	18.8	11.1	0.318	0.452	0.05
1272222	2.1	0.3	< 0.1	0.3	0.017	< 0.05	28.3	3	7.2	22.0	0.103	0.051	0.11
1272223	0.7	0.1	0.1	< 0.1	0.016	< 0.05	2.0	5	11.6	2.0	0.0900	0.134	1.10
1272224	0.4	< 0.1	< 0.1	1.4	0.007	< 0.05	0.9	1	1.2	1.3	0.0340	0.015	0.18
1272225	0.2	< 0.1	< 0.1	0.2	0.012	< 0.05	2.2	< 1	1.1	5.5	0.0179	0.014	0.20
1272226	0.2	< 0.1	< 0.1	0.3	0.023	< 0.05	1.6	< 1	0.4	2.5	0.0052	0.006	0.20
1272227	0.3	< 0.1	< 0.1	0.1	0.019	< 0.05	10.5	< 1	0.6	0.9	0.0098	0.019	1.23
1272228	1.0	0.2	0.1	0.2	0.001	< 0.05	1.1	2	5.6	0.8	0.0398	0.024	0.09
1272229	109	13.1	< 0.1	< 0.1	< 0.001	0.08	> 5000	30	40.5	> 10000	0.0848	0.084	0.03
1272230	1.5	0.2	0.6	0.9	< 0.001	0.52	34.2	9	17.3	119	0.332	0.026	0.47
1272231	1.1	0.1	< 0.1	< 0.1	0.004	0.92	9.1	16	25.6	30.9	0.179	0.021	0.02
1272232	2.2	0.3	< 0.1	< 0.1	0.005	0.16	11.5	43	2.9	39.5	0.254	0.024	0.12
1272233	0.5	< 0.1	0.1	0.4	0.006	0.68	6.4	13	2.5	31.1	0.168	0.008	0.03
1272351	1.3	0.2	0.2	0.5	0.009	0.55	4.1	11	13.7	6.4	0.199	0.052	< 0.01
1272352	0.2	< 0.1	< 0.1	< 0.1	0.004	0.05	4.3	< 1	0.5	4.9	0.0152	0.008	0.11
1272353	0.4	< 0.1	< 0.1	< 0.1	0.007	0.55	4.9	6	2.7	4.7	0.143	0.021	0.02
1272354	0.2	< 0.1	< 0.1	0.1	0.002	0.23	2.2	2	3.3	5.2	0.0920	0.013	0.01
1272355	0.1	< 0.1	< 0.1	0.2	0.003	0.28	3.3	2	4.9	1.3	0.0677	0.013	< 0.01
1272356	0.3	< 0.1	0.1	0.1	< 0.001	0.49	4.7	6	3.5	1.3	0.164	0.021	< 0.01
1272357	0.6	< 0.1	< 0.1	< 0.1	0.002	0.45	4.9	5	3.8	3.9	0.255	0.024	0.01
1272358	0.4	< 0.1	< 0.1	0.2	0.004	0.30	3.5	2	2.0	1.5	0.155	0.018	0.02
1272359	0.5	< 0.1	< 0.1	< 0.1	0.003	0.41	4.6	4	3.5	2.4	0.245	0.025	0.01
1272360	0.6	< 0.1	< 0.1	0.1	< 0.001	0.22	3.8	2	2.6	2.6	0.177	0.021	0.03
1272361	0.4	< 0.1	< 0.1	0.2	0.010	0.33	1.2	5	2.8	1.3	0.158	0.020	0.05
1272362	< 0.1	< 0.1	< 0.1	< 0.1	0.007	< 0.05	1.6	< 1	0.5	1.1	0.0090	0.011	0.08
1272363	0.6	< 0.1	0.3	0.3	0.006	0.63	9.8	10	14.3	27.2	0.359	0.114	0.03
1272364	0.2	< 0.1	< 0.1	< 0.1	0.013	< 0.05	7.5	< 1	0.8	3.3	0.0116	0.015	0.12
1272365	0.6	< 0.1	0.1	0.2	0.002	0.19	4.7	6	15.7	3.6	0.283	0.070	0.02
1272366	0.2	< 0.1	< 0.1	< 0.1	0.007	0.09	5.3	< 1	0.7	15.3	0.0186	0.018	0.22
1272367	0.6	< 0.1	0.1	0.3	0.006	0.31	3.6	8	11.0	2.5	0.200	0.054	0.10
1272368	0.9	0.2	< 0.1	< 0.1	0.003	0.72	3.3	23	18.6	3.0	0.172	0.046	< 0.01
1272369	0.4	< 0.1	< 0.1	< 0.1	0.005	0.12	3.0	4	3.9	1.7	0.118	0.026	0.04
1272370	0.5	< 0.1	< 0.1	0.2	0.005	0.48	1.7	7	8.1	2.1	0.198	0.033	0.07
1272371	0.7	< 0.1	< 0.1	< 0.1	0.001	0.87	2.6	15	16.1	4.6	0.261	0.077	< 0.01
1272372	0.2	< 0.1	< 0.1	< 0.1	0.006	0.19	1.5	2	1.9	0.7	0.0661	0.021	0.10
1272373	< 0.1	< 0.1	< 0.1	< 0.1	0.006	< 0.05	1.7	< 1	2.5	0.2	0.0060	0.009	0.11
1272374	0.2	< 0.1	< 0.1	< 0.1	0.001	0.16	0.9	2	1.6	0.6	0.0689	0.018	0.09
1272375	0.2	< 0.1	< 0.1	0.3	< 0.001	0.20	1.2	2	2.6	1.8	0.0776	0.019	0.09
1272376	0.4	< 0.1	< 0.1	< 0.1	< 0.001	0.63	1.8	6	16.8	1.5	0.243	0.054	0.02
1272377	0.1	< 0.1	< 0.1	< 0.1	< 0.001	< 0.05	2.1	< 1	0.7	0.2	0.0105	0.017	0.09

Analyte Symbol	Yb	Lu	Ta	W	Re	Tl	Pb	Sc	Th	U	Ti	P	S
Unit Symbol	ppm	ppm	ppm	ppm	ppm	ppm	ppm	ppm	ppm	ppm	%	%	%
Detection Limit	0.1	0.1	0.1	0.1	0.001	0.05	0.5	1	0.1	0.1	0.0005	0.001	0.01
Analysis Method	TD-MS	TD-MS	TD-MS	TD-MS	TD-MS	TD-MS	TD-MS	TD-ICP	TD-MS	TD-MS	TD-ICP	TD-ICP	TD-ICP
1272378	0.5	< 0.1	< 0.1	< 0.1	< 0.001	0.77	2.8	13	13.9	3.4	0.247	0.064	0.02
1272379	0.1	< 0.1	< 0.1	< 0.1	0.002	0.11	2.2	1	1.4	1.3	0.0287	0.043	0.07
1272380	0.1	< 0.1	< 0.1	0.2	< 0.001	0.15	1.8	1	0.8	1.4	0.0365	0.018	0.10
1272381	0.3	< 0.1	< 0.1	0.2	0.005	0.28	1.4	4	2.3	1.1	0.115	0.021	0.09
1272382	0.9	0.1	0.4	1.1	0.001	0.19	1.9	4	24.3	3.1	0.346	0.125	0.05
1272383	0.8	0.1	0.1	0.3	0.026	< 0.05	0.5	3	8.4	0.6	0.0611	0.019	0.09
1272384	0.9	0.1	< 0.1	< 0.1	< 0.001	< 0.05	0.5	2	2.4	0.4	0.0273	0.015	0.10
1272385	0.7	< 0.1	0.1	0.6	< 0.001	1.26	2.2	16	22.9	2.4	0.215	0.032	< 0.01
1272386	0.9	0.1	< 0.1	< 0.1	0.002	0.94	1.4	16	16.9	1.8	0.224	0.033	< 0.01
1272387	0.8	< 0.1	< 0.1	< 0.1	0.007	< 0.05	0.7	2	3.7	0.7	0.0622	0.028	0.20
1272388	0.3	< 0.1	< 0.1	0.1	0.007	< 0.05	0.6	2	3.3	0.5	0.0647	0.024	0.11
1272389	0.8	0.1	< 0.1	< 0.1	< 0.001	0.39	2.2	9	7.6	1.5	0.201	0.043	0.05
1272390	0.1	< 0.1	< 0.1	0.1	0.003	< 0.05	0.9	< 1	0.7	0.5	0.0071	0.029	0.02
1272391	0.2	< 0.1	< 0.1	< 0.1	0.004	0.06	2.4	< 1	0.8	0.5	0.0159	0.014	0.10
1272392	0.2	< 0.1	< 0.1	1.1	0.003	0.15	1.2	2	1.2	0.4	0.0469	0.021	0.09
1272393	0.2	< 0.1	< 0.1	< 0.1	0.004	0.07	1.2	4	1.0	0.5	0.0389	0.012	0.09
1272394	0.2	< 0.1	0.2	0.3	0.003	0.09	1.8	3	4.1	0.4	0.226	0.045	0.01
1272395	0.7	0.1	< 0.1	0.1	< 0.001	0.42	1.8	16	11.8	1.9	0.356	0.045	0.02
1272396	0.8	0.1	< 0.1	< 0.1	< 0.001	0.45	2.6	13	18.7	2.3	0.356	0.061	0.02
1272397	0.6	0.1	< 0.1	< 0.1	0.002	0.49	2.5	11	18.4	2.1	0.166	0.062	0.03
1272398	0.5	< 0.1	0.2	0.6	0.001	0.44	6.6	11	14.8	2.9	0.249	0.049	0.05
1272399	0.1	< 0.1	< 0.1	< 0.1	0.002	< 0.05	0.9	< 1	0.8	0.2	0.0107	0.027	0.12
1272400	1.4	0.2	< 0.1	< 0.1	0.006	0.27	3.5	13	15.1	3.2	0.190	0.042	0.01
1272401	1.4	0.2	0.3	0.8	0.002	0.78	7.6	23	24.4	11.6	0.453	0.055	0.10
1272402	0.8	0.1	0.3	0.6	0.006	0.41	2.8	20	7.8	1.8	0.449	0.043	2.04
1272403	0.6	< 0.1	< 0.1	< 0.1	0.003	< 0.05	1.4	3	0.4	0.2	0.0315	0.004	10.1
1272404	0.8	0.1	0.4	1.5	0.004	0.52	4.0	12	11.9	5.4	0.338	0.054	4.31
1272405	0.1	< 0.1	< 0.1	< 0.1	0.002	0.18	0.8	2	1.4	0.6	0.0476	0.010	8.26
1272406	0.9	0.1	0.2	1.1	0.004	0.31	3.9	8	9.5	5.7	0.212	0.028	5.14
1272407	< 0.1	< 0.1	< 0.1	< 0.1	0.004	< 0.05	< 0.5	< 1	0.4	< 0.1	0.0031	0.016	6.82
1272408	0.6	< 0.1	0.2	0.7	0.003	0.33	3.8	9	8.8	4.2	0.228	0.045	3.58
1272409	1.7	0.3	0.1	< 0.1	0.007	0.36	1.1	14	10.6	2.5	0.716	0.062	0.22
1272410	1.8	0.3	< 0.1	< 0.1	0.008	0.23	1.4	13	8.0	0.9	0.261	0.049	0.14
1272411	2.1	0.3	< 0.1	< 0.1	0.006	0.17	2.1	13	8.8	1.3	0.167	0.045	0.03
1272412	1.5	0.2	0.7	0.4	0.005	0.07	1.7	7	3.3	1.4	0.863	0.037	0.02
1272413	1.9	0.3	< 0.1	< 0.1	0.005	0.55	1.3	9	7.6	2.6	0.249	0.054	0.02
1272414	1.4	0.2	< 0.1	< 0.1	0.008	0.71	0.7	14	7.7	2.4	0.298	0.060	0.02
1272415	0.7	0.1	< 0.1	< 0.1	0.014	0.23	1.1	19	6.5	1.5	0.221	0.011	0.06
1272416	2.1	0.3	< 0.1	< 0.1	0.010	0.10	2.8	10	7.9	2.9	0.185	0.030	0.01
1272417	1.9	0.3	< 0.1	< 0.1	0.009	0.14	4.0	14	8.4	3.5	0.243	0.042	0.02
1272418	1.9	0.3	0.1	< 0.1	0.003	0.50	0.6	45	1.4	0.7	0.649	0.024	0.05
1272419	0.5	< 0.1	0.2	0.5	0.005	0.30	1.3	9	7.0	6.4	0.264	0.038	3.76
1272420	0.9	0.1	0.3	0.9	0.002	0.31	8.5	9	8.4	18.3	0.276	0.038	6.49
1272421	0.2	< 0.1	< 0.1	0.5	0.016	0.08	2.1	1	1.1	5.6	0.0106	0.020	7.50
1272422	0.6	< 0.1	0.2	0.7	0.006	0.29	8.6	9	8.7	3.2	0.223	0.041	3.72
1272423	1.5	0.2	0.7	0.3	0.016	0.21	8.1	8	9.1	1.5	0.899	0.049	2.24
1272424	2.6	0.4	< 0.1	< 0.1	0.010	< 0.05	3.1	16	7.2	3.9	0.214	0.016	0.11
1272425	1.3	0.2	< 0.1	< 0.1	0.013	0.12	2.6	10	4.9	0.6	0.160	0.035	0.04
1272426	1.6	0.2	< 0.1	< 0.1	0.008	0.20	10.6	12	7.0	0.9	0.167	0.034	0.06
1272427	1.4	0.2	< 0.1	< 0.1	0.011	0.22	2.5	10	5.9	0.7	0.149	0.030	0.02
1272428	1.8	0.3	< 0.1	< 0.1	0.011	0.20	3.0	12	10.0	0.8	0.363	0.055	0.04
1272429	1.8	0.3	< 0.1	< 0.1	0.008	0.37	3.0	13	8.4	1.1	0.462	0.042	0.03

Analyte Symbol	Yb	Lu	Ta	W	Re	Tl	Pb	Sc	Th	U	Ti	P	S
Unit Symbol	ppm	ppm	ppm	ppm	ppm	ppm	ppm	ppm	ppm	ppm	%	%	%
Detection Limit	0.1	0.1	0.1	0.1	0.001	0.05	0.5	1	0.1	0.1	0.0005	0.001	0.01
Analysis Method	TD-MS	TD-MS	TD-MS	TD-MS	TD-MS	TD-MS	TD-MS	TD-ICP	TD-MS	TD-MS	TD-ICP	TD-ICP	TD-ICP
1272430	2.2	0.3	< 0.1	< 0.1	0.008	0.11	2.3	10	10.9	1.2	0.430	0.056	0.09
1272431	2.1	0.3	< 0.1	< 0.1	0.015	0.10	3.4	10	10.7	1.1	0.247	0.062	0.04
1272432	1.0	0.2	< 0.1	0.4	0.008	< 0.05	2.9	7	15.7	4.8	0.227	0.067	0.21
1272433	0.8	0.1	< 0.1	< 0.1	0.007	< 0.05	3.2	< 1	17.5	6.7	0.153	0.010	< 0.01
1272434	0.7	0.1	0.8	1.4	0.005	0.47	1.9	10	16.8	2.8	0.403	0.023	< 0.01
1272435	0.8	0.1	< 0.1	0.1	0.005	< 0.05	0.7	3	4.1	0.5	0.0457	0.014	0.08
1272436	0.9	0.1	< 0.1	< 0.1	0.006	0.88	2.0	15	20.0	2.6	0.145	0.035	< 0.01
1272437	1.0	0.1	< 0.1	0.1	0.002	< 0.05	0.8	5	5.0	0.7	0.0995	0.023	0.10
1272438	1.1	0.2	0.4	0.5	0.004	0.73	3.6	18	20.4	3.0	0.293	0.053	< 0.01
1272439	0.4	< 0.1	< 0.1	0.1	0.004	< 0.05	0.6	2	2.2	0.8	0.0404	0.026	0.11
1272440	0.8	0.1	< 0.1	< 0.1	0.001	0.35	2.3	16	14.5	2.4	0.143	0.014	0.03
1272441	< 0.1	< 0.1	< 0.1	0.2	0.002	< 0.05	2.8	< 1	2.0	0.5	0.0221	0.002	< 0.01
1272442	0.9	0.1	< 0.1	< 0.1	0.005	0.31	1.7	11	17.4	3.1	0.226	0.035	< 0.01
1272443	1.0	0.1	0.5	1.1	< 0.001	0.61	1.9	15	17.0	2.4	0.312	0.020	0.02
1272444	0.4	< 0.1	0.1	0.9	0.003	0.33	5.1	11	11.2	4.0	0.193	0.053	0.10
1272445	1.1	0.2	< 0.1	0.2	0.005	0.09	9.6	25	2.4	0.7	0.358	0.026	0.57
1272446	1.3	0.2	0.1	< 0.1	0.010	0.20	12.6	37	1.4	0.3	0.509	0.024	0.18
1272447	0.7	0.1	< 0.1	0.2	0.008	0.40	5.6	6	5.2	1.5	0.168	0.028	0.02
1272448	1.0	0.2	0.2	0.1	0.002	0.47	4.0	14	16.4	2.0	0.261	0.038	0.02
1272449	1.7	0.3	0.2	0.4	0.006	0.42	5.0	11	14.7	2.7	0.204	0.049	0.04
1272450	2.5	0.4	< 0.1	< 0.1	0.011	0.37	3.1	7	9.8	6.0	0.597	0.064	0.01
1272451	2.6	0.4	< 0.1	< 0.1	0.006	< 0.05	2.7	8	11.6	2.8	0.212	0.070	< 0.01
1272452	1.9	0.3	< 0.1	< 0.1	0.014	0.22	2.6	9	10.0	2.8	0.132	0.065	0.08
1272453	2.0	0.3	< 0.1	< 0.1	0.010	0.25	2.5	9	9.5	2.3	0.165	0.059	0.04
1272454	2.0	0.3	< 0.1	< 0.1	0.009	0.38	2.1	7	9.7	1.7	0.184	0.060	0.12
1272455	1.6	0.3	< 0.1	< 0.1	0.011	0.47	5.8	10	10.6	1.9	0.407	0.068	0.07
1272456	1.8	0.3	< 0.1	< 0.1	0.010	0.43	5.4	9	13.2	2.6	0.275	0.063	< 0.01
1272457	0.4	< 0.1	< 0.1	0.1	0.004	0.17	0.9	2	1.5	3.8	0.0296	0.086	0.20
1272458	0.3	< 0.1	< 0.1	< 0.1	0.006	0.24	2.1	3	3.3	1.6	0.0902	0.013	0.03
1272459	0.2	< 0.1	< 0.1	< 0.1	0.002	0.22	2.2	2	1.6	0.7	0.0501	0.010	0.03
1272460	0.7	0.1	0.4	0.1	0.010	0.90	2.4	10	15.9	2.0	0.308	0.056	0.01
1272461	0.5	< 0.1	0.8	1.2	< 0.001	0.88	2.0	7	4.5	2.7	0.348	0.032	0.05
1272462	1.0	0.1	0.2	0.1	0.003	0.49	0.8	6	11.0	1.2	0.198	0.035	0.06
1272463	0.8	0.1	< 0.1	0.1	0.002	1.27	1.9	15	20.2	1.6	0.249	0.036	< 0.01
1272464	1.2	0.2	0.1	0.2	0.005	0.77	1.5	14	16.8	1.9	0.243	0.050	0.01
1272465	1.7	0.3	< 0.1	0.1	0.003	< 0.05	1.8	4	5.1	9.0	0.0970	0.025	0.08
1272466	0.6	< 0.1	0.1	0.3	0.003	1.08	1.4	13	15.7	0.8	0.235	0.064	0.03
1272467	0.3	< 0.1	< 0.1	< 0.1	0.005	0.10	0.7	1	1.3	0.6	0.0340	0.023	0.11
1272468	1.4	0.3	0.5	2.7	0.006	< 0.05	2.4	5	7.1	3.6	0.497	0.074	9.64
1272469	1.4	0.2	0.3	1.6	0.006	< 0.05	1.2	4	15.1	6.5	0.194	0.081	0.43
1272470	2.2	0.4	0.2	< 0.1	0.016	0.14	2.6	7	7.7	3.2	0.480	0.069	1.09
1272471	0.5	< 0.1	< 0.1	< 0.1	0.005	< 0.05	< 0.5	2	0.7	< 0.1	0.0197	0.013	6.71
1272472	2.2	0.3	< 0.1	< 0.1	0.003	0.10	5.3	12	10.4	1.6	0.210	0.060	0.26
1272473	0.9	0.1	< 0.1	< 0.1	0.002	< 0.05	0.7	5	8.8	1.0	0.152	0.022	0.06
1272474	0.4	< 0.1	< 0.1	< 0.1	< 0.001	1.13	2.1	16	16.2	1.8	0.122	0.054	< 0.01
1272475	0.4	< 0.1	< 0.1	0.3	< 0.001	< 0.05	1.1	2	1.1	0.6	0.0196	0.005	0.07
1272476	0.1	< 0.1	< 0.1	< 0.1	< 0.001	0.07	0.7	< 1	0.6	0.1	0.0153	0.009	0.12
1272477	0.7	< 0.1	< 0.1	0.1	< 0.001	0.08	1.4	2	1.3	0.7	0.0649	0.036	0.06
1272478	0.3	< 0.1	< 0.1	< 0.1	< 0.001	< 0.05	1.4	< 1	0.5	0.3	0.0034	0.042	0.12
1272479	0.4	< 0.1	< 0.1	< 0.1	< 0.001	< 0.05	1.5	2	0.8	1.6	0.0256	0.014	0.11
1272480	0.3	< 0.1	0.3	0.5	< 0.001	0.47	2.4	11	2.9	1.8	0.373	0.027	< 0.01
1272481	0.3	< 0.1	< 0.1	< 0.1	< 0.001	< 0.05	< 0.5	1	0.2	< 0.1	0.0107	0.004	10.7

Analyte Symbol	Yb	Lu	Ta	W	Re	Tl	Pb	Sc	Th	U	Ti	P	S
Unit Symbol	ppm	ppm	ppm	ppm	ppm	ppm	ppm	ppm	ppm	ppm	%	%	%
Detection Limit	0.1	0.1	0.1	0.1	0.001	0.05	0.5	1	0.1	0.1	0.0005	0.001	0.01
Analysis Method	TD-MS	TD-MS	TD-MS	TD-MS	TD-MS	TD-MS	TD-MS	TD-ICP	TD-MS	TD-MS	TD-ICP	TD-ICP	TD-ICP
1272482	0.6	< 0.1	0.2	0.4	< 0.001	0.32	10.0	8	9.9	5.1	0.199	0.046	2.65
1272483	0.3	< 0.1	< 0.1	< 0.1	< 0.001	0.08	0.6	2	0.9	0.8	0.0317	0.012	6.15
1272484	1.5	0.2	0.3	0.4	< 0.001	0.16	2.0	6	9.1	3.9	0.389	0.074	2.45
1272485	1.2	0.2	0.5	0.7	0.025	< 0.05	1.8	6	5.9	6.4	0.643	0.055	5.18
1272486	1.2	0.2	< 0.1	0.5	< 0.001	0.29	1.3	15	9.0	2.9	0.312	0.046	0.11
1272487	1.2	0.2	0.3	0.7	0.003	0.19	2.6	8	5.2	5.2	0.474	0.049	2.60
1272488	0.5	0.1	0.2	< 0.1	< 0.001	1.11	< 0.5	24	1.1	0.3	0.601	0.007	0.01
1272489	3.2	0.4	< 0.1	1.9	< 0.001	0.14	2.8	7	6.4	1.4	0.235	0.054	0.02
1272490	2.2	0.3	< 0.1	< 0.1	< 0.001	0.23	1.4	11	4.7	1.5	0.360	0.048	0.12
1272491	1.1	0.2	0.4	< 0.1	< 0.001	0.72	0.7	9	2.6	1.8	0.646	0.042	1.07
1272492	0.6	< 0.1	< 0.1	0.5	< 0.001	0.08	1.6	8	2.4	1.7	0.145	0.036	5.89
1272493	0.5	< 0.1	0.2	0.4	< 0.001	0.08	0.9	10	2.4	1.5	0.209	0.032	3.18
1272494	0.7	0.1	0.2	< 0.1	< 0.001	0.14	1.2	8	10.6	2.3	0.292	0.047	4.32
1272495	1.3	0.2	0.2	< 0.1	< 0.001	< 0.05	1.1	15	4.3	1.2	0.403	0.034	0.60
1272496	2.2	0.3	< 0.1	< 0.1	0.002	0.16	5.7	8	9.8	1.8	0.420	0.067	0.53
1272497	2.1	0.3	< 0.1	< 0.1	< 0.001	0.11	1.8	9	10.0	1.2	0.260	0.057	0.07
1272498	2.1	0.3	< 0.1	< 0.1	0.003	< 0.05	3.7	7	13.7	1.6	0.517	0.079	0.12
1272499	2.2	0.3	< 0.1	< 0.1	0.004	0.10	18.8	11	10.7	1.4	0.666	0.069	0.15
1272500	2.0	0.3	0.2	< 0.1	0.001	0.09	2.4	9	11.2	1.6	0.704	0.058	0.10

Quality Control

Analyte Symbol	Li	Na	Mg	Al	K	Ca	Cd	V	Cr	Mn	Fe	Hf	Hg	Ni	Er	Be	Ho	Ag	Cs	Co	Eu	Bi	Se	Zn
Unit Symbol	ppm	%	%	%	%	%	ppm	ppm	ppm	ppm	%	ppm	ppb	ppm	ppm	ppm	ppm	ppm	ppm	ppm	ppm	ppm	ppm	ppm
Detection Limit	0.5	0.01	0.01	0.01	0.01	0.01	0.1	1	0.5	1	0.01	0.1	10	0.5	0.1	0.1	0.1	0.05	0.05	0.1	0.05	0.02	0.1	0.2
Analysis Method	TD-MS	TD-MS	TD-MS	TD-MS	TD-MS	TD-MS	TD-MS	TD-MS	TD-MS	TD-MS	TD-MS	TD-MS	TD-MS	TD-MS	TD-MS	TD-MS	TD-MS	TD-MS	TD-MS	TD-MS	TD-MS	TD-MS	TD-MS	TD-MS
GXR-1 Meas	9.8	0.05	0.23	2.32	0.04	0.91	2.5	83	13.7	806	24.2	< 0.1	2180	38.6		0.8		33.8	2.51	7.8	0.66	1650	17.2	885
GXR-1 Cert	8.20	0.0520	0.217	3.52	0.050	0.960	3.30	80.0	12.0	852	23.6	0.960	3900	41.0		1.22		31.0	3.00	8.20	0.690	1380	16.6	760
GXR-1 Meas																								
GXR-1 Cert																								
GXR-4 Meas	13.5	0.52	1.70	6.32	3.52	1.05	< 0.1	89	43.5	145	3.04	0.8		39.0		2.0		3.51	2.46	14.2	1.55	19.4	6.7	80.3
GXR-4 Cert	11.1	0.564	1.66	7.20	4.01	1.01	0.860	87.0	64.0	155	3.09	6.30		42.0		1.90		4.00	2.80	14.6	1.63	19.0	5.60	73.0
GXR-4 Meas																								
GXR-4 Cert																								
SDC-1 Meas	42.8	1.51	1.01	7.90	2.23	1.07	< 0.1	47	41.8	808	4.74	0.2		33.8	3.8	2.9	1.3	0.12	3.64	17.6	1.64	0.28		119
SDC-1 Cert	34.00	1.52	1.02	8.34	2.72	1.00	0.0800	102.00	64.00	880.00	4.82	8.30		38.0	4.10	3.00	1.50	0.0410	4.00	18.0	1.70	2.60		103.00
SDC-1 Meas																								
SDC-1 Cert																								
GXR-6 Meas	44.7	0.10	0.61	> 10.0	1.87	0.19	< 0.1	145	56.3	984	5.76	1.6		24.9		1.1		0.31	4.06	13.9	0.70	0.23	1.2	153
GXR-6 Cert	32.0	0.104	0.609	17.7	1.87	0.180	1.00	186	96.0	1010	5.58	4.30		27.0		1.40		1.30	4.20	13.8	0.760	0.290	0.940	118
GXR-6 Meas																								
GXR-6 Cert																								
SAR-M (U.S.G.S.) Meas	36.8	1.17	0.47	5.75	2.51	0.63	4.8	51	75.9	4610	3.20			41.9		3.0		3.08		10.5		1.79	1.3	1040
SAR-M (U.S.G.S.) Cert	27.4	1.140	0.50	6.30	2.94	0.61	5.27	67.2	79.7	5220	2.99			41.5		2.20		3.64		10.70		1.94	0.39	930.0
SAR-M (U.S.G.S.) Meas																								
SAR-M (U.S.G.S.) Cert																								
DNC-1a Meas	6.0							157	215					274						59.0	0.64			77.2
DNC-1a Cert	5.20							148.00	270					247						57.0	0.59			70.0
DNC-1a Meas																								
DNC-1a Cert																								
SBC-1 Meas	204						0.3	219	83.6			2.6		84.5	3.9	3.2	1.4		7.58	22.3	2.00	0.78		215
SBC-1 Cert	163.0						0.40	220.0	109			3.7		82.8	3.80	3.20	1.40		8.2	22.7	1.98	0.70		186.0
SBC-1 Meas																								
SBC-1 Cert																								
1272046 Orig	25.7	> 3.00	2.32	7.47	2.01	1.18	< 0.1	58	72.4	116	8.45	2.5	20	14.9	4.1	1.9	1.5	0.15	6.52	31.6	2.75	0.15	2.0	20.0
1272046 Dup	26.5	> 3.00	2.39	7.64	1.92	1.20	0.1	61	67.0	118	8.54	2.2	30	15.4	4.2	1.9	1.6	0.13	6.64	31.5	2.77	0.19	2.6	17.0
1272364 Orig	4.2	0.02	11.2	0.21	0.17	19.5	0.2	6	52.2	1320	0.71	< 0.1	< 10	7.5	0.2	< 0.1	< 0.1	0.05	0.39	3.1	0.22	0.06	< 0.1	21.1
1272364 Dup	4.6	0.02	11.5	0.22	0.17	19.7	0.3	7	67.4	1370	0.72	< 0.1	< 10	7.6	0.2	< 0.1	< 0.1	< 0.05	0.38	3.2	0.22	0.14	0.2	22.8
1272366 Orig	9.0	0.06	1.18	0.37	0.31	36.0	< 0.1	6	51.6	1190	0.50	< 0.1	< 10	10.3	0.2	< 0.1	< 0.1	0.06	0.94	2.2	0.18	0.10	1.1	6.0
1272366 Dup	8.7	0.06	1.17	0.36	0.31	35.4	< 0.1	6	54.5	1170	0.50	< 0.1	< 10	10.1	0.2	< 0.1	< 0.1	0.07	0.95	2.2	0.19	0.10	0.3	8.0
1272402 Orig	48.9	1.45	2.99	7.20	2.11	4.23	< 0.1	102	159	876	5.88	2.4	< 10	44.9	0.8	0.5	0.3	0.15	1.83	19.5	1.05	0.24	0.4	37.0
1272402 Dup	49.1	1.46	3.01	7.17	2.12	4.27	< 0.1	101	169	891	5.97	2.5	< 10	45.0	0.9	0.7	0.3	0.14	1.81	20.0	1.02	0.22	0.5	38.9
1272407 Orig	4.9	< 0.01	15.0	0.08	0.08	7.86	< 0.1	1	38.2	1000	0.64	< 0.1	< 10	5.3	< 0.1	< 0.1	< 0.1	0.06	0.14	8.2	< 0.05	0.04	< 0.1	11.9
1272407 Dup	4.9	< 0.01	14.7	0.07	0.08	7.40	< 0.1	< 1	43.7	1020	0.63	< 0.1	< 10	4.9	< 0.1	< 0.1	< 0.1	0.05	0.14	8.0	< 0.05	0.03	< 0.1	11.7
1272438 Orig	34.4	1.23	2.10	9.44	2.72	0.20	< 0.1	83	99.5	57	6.63	1.3	< 10	69.8	1.3	2.4	0.5	0.16	2.85	12.2	1.13	0.04	0.9	4.7
1272438 Dup	34.0	1.23	2.12	9.60	2.57	0.20	< 0.1	89	97.0	53	6.79	1.3	< 10	70.8	1.4	2.3	0.5	0.15	2.93	12.3	1.18	0.04	0.8	4.9
1272448 Orig	68.2	0.10	3.53	6.50	4.32	1.88	< 0.1	99	76.3	360	5.08	3.4	< 10	71.9	1.1	0.8	0.4	0.17	1.87	47.9	2.38	0.06	0.2	36.5
1272448 Dup	67.1	0.10	3.56	6.51	3.99	1.90	< 0.1	101	76.4	366	5.12	3.5	< 10	71.9	1.1	1.1	0.4	0.18	1.88	48.3	2.45	0.05	1.3	37.2
1272450 Orig	52.2	> 3.00	3.25	7.28	1.56	1.28	< 0.1	49	4.9	464	9.61	1.5	< 10	41.2	3.2	1.1	1.2	0.14	2.87	33.6	2.19	0.10	1.1	31.4
1272450 Dup	48.7	> 3.00	2.84	5.88	1.46	1.14	< 0.1	113	5.8	452	9.16	3.2	< 10	39.4	2.8	1.1	1.0	0.22	2.24	32.2	1.81	0.10	1.2	27.0
1272477 Orig	14.0	0.04	7.03	1.08	0.76	10.1	< 0.1	11	17.5	838	1.19	< 0.1	< 10	17.4	0.8	< 0.1	0.3	0.09	0.72	9.4	0.48	0.05	< 0.1	14.3
1272477 Dup	13.9	0.04	6.95	1.06	0.76	10.0	< 0.1	10	11.4	810	1.17	< 0.1	< 10	17.7	0.9	< 0.1	0.3	0.08	0.74	9.2	0.50	0.07	< 0.1	12.7
Method Blank	< 0.5	< 0.01	< 0.01	< 0.01	< 0.01	< 0.01	< 0.1	< 1	< 0.5	< 1	< 0.01	< 0.1	< 10	< 0.5	< 0.1	< 0.1	< 0.1	< 0.05	< 0.05	< 0.1	< 0.05	< 0.02	< 0.1	< 0.2
Method Blank																								
Method Blank																								
Method Blank																								
Method Blank																								

Quality Control

Analyte Symbol	Ga	As	Rb	Y	Sr	Zr	Nb	Mo	In	Sn	Sb	Te	Ba	La	Ce	Pr	Nd	Sm	Gd	Tb	Dy	Cu	Ge	Tm
Unit Symbol	ppm	ppm	ppm	ppm	ppm	ppm	ppm	ppm	ppm	ppm	ppm	ppm	ppm	ppm	ppm	ppm	ppm	ppm	ppm	ppm	ppm	ppm	ppm	ppm
Detection Limit	0.1	0.1	0.2	0.1	0.2	1	0.1	0.1	0.1	1	0.1	0.1	1	0.1	0.1	0.1	0.1	0.1	0.1	0.1	0.1	0.2	0.1	0.1
Analysis Method	TD-MS	TD-MS	TD-MS	TD-MS	TD-MS	TD-MS	TD-MS	TD-MS	TD-MS	TD-MS	TD-MS	TD-MS	TD-MS	TD-MS	TD-MS	TD-MS	TD-MS	TD-MS	TD-MS	TD-MS	TD-MS	TD-MS	TD-MS	TD-MS
GXR-1 Meas	7.6	433	3.1	30.4	296	18	0.9	17.7	0.8	27	41.4	10.2	716	7.7	15.2		8.7	2.8	4.1	0.8	5.0	1140		0.4
GXR-1 Cert	13.8	427	14.0	32.0	275	38.0	0.800	18.0	0.770	54.0	122	13.0	750	7.50	17.0		18.0	2.70	4.20	0.830	4.30	1110		0.430
GXR-1 Meas																								
GXR-1 Cert																								
GXR-4 Meas	15.8	111	167	14.8	224	37	8.1	308	0.2	7	4.5	1.0	187	58.5	107		41.8	6.3	4.8	0.6	3.1	6140		0.2
GXR-4 Cert	20.0	98.0	160	14.0	221	186	10.0	310	0.270	5.60	4.80	0.970	1640	64.5	102		45.0	6.60	5.25	0.360	2.60	6520		0.210
GXR-4 Meas																								
GXR-4 Cert																								
SDC-1 Meas	16.9	0.6	135	35.4	185	25	0.3	< 0.1		< 1	< 0.1		620	41.4	87.5		41.3	7.9	7.1	1.1	6.5	31.0		0.5
SDC-1 Cert	21.00	0.220	127.00	40.0	180.00	290.00	21.00	0.250		3.00	0.54		630	42.00	93.00		40.00	8.20	7.00	1.20	6.70	30.00		0.65
SDC-1 Meas																								
SDC-1 Cert																								
GXR-6 Meas	17.9	272	104	14.2	41.6	81	0.9	0.9	< 0.1	1	0.9	< 0.1	1320	13.8	37.1		13.6	2.8	2.5	0.4	2.7	75.0		0.3
GXR-6 Cert	35.0	330	90.0	14.0	35.0	110	7.50	2.40	0.260	1.70	3.60	0.0180	1300	13.9	36.0		13.0	2.67	2.97	0.415	2.80	66.0		0.0320
GXR-6 Meas																								
GXR-6 Cert																								
SAR-M (U.S.G.S.) Meas	11.3	32.0	151	36.9	160		2.8	5.8	1.0	2	4.2	0.3	776	59.6	122							318		
SAR-M (U.S.G.S.) Cert	17	38.8	146	28.00	151		29.9	13.1	1.08	2.76	6.0	0.96	801	57.4	122.0							331		
SAR-M (U.S.G.S.) Meas																								
SAR-M (U.S.G.S.) Cert																								
DNC-1a Meas				18.6	154	44					0.7		106	3.9			5.3					106		
DNC-1a Cert				18.0	144.0	38.000					0.96		118	3.6			5.20					100.0		
DNC-1a Meas																								
DNC-1a Cert																								
SBC-1 Meas	19.0	27.3	160	35.3	192	115	11.2	2.3		3	0.9		774	51.7	107	13.1	50.0	9.5	8.3	1.3	7.1	30.7		0.6
SBC-1 Cert	27.0	25.7	147	36.5	178.0	134.0	15.3	2.40		3.3	1.01		788.0	52.5	108.0	12.6	49.2	9.6	8.5	1.20	7.10	31.0		0.56
SBC-1 Meas																								
SBC-1 Cert																								
1272046 Orig	21.3	2.7	189	38.3	46.1	121	0.3	3.1	< 0.1	< 1	0.1	0.3	59	30.3	65.9	8.6	35.4	8.2	8.3	1.3	7.8	11.1	0.3	0.6
1272046 Dup	21.4	2.3	181	37.5	44.7	99	0.1	2.5	< 0.1	< 1	< 0.1	0.3	60	30.0	65.7	8.5	36.0	8.4	8.4	1.4	7.8	10.5	0.3	0.6
1272364 Orig	0.4	1.3	10.4	2.5	122	5	0.3	1.3	< 0.1	< 1	< 0.1	0.1	12	7.4	16.1	1.3	4.8	0.9	0.8	< 0.1	0.5	8.9	< 0.1	< 0.1
1272364 Dup	0.5	6.2	9.9	2.7	124	3	0.2	1.4	< 0.1	< 1	< 0.1	< 0.1	13	7.6	17.1	1.4	5.1	0.9	0.9	0.1	0.5	12.3	< 0.1	< 0.1
1272366 Orig	0.3	3.4	15.5	2.3	115	4	0.3	1.4	< 0.1	< 1	< 0.1	< 0.1	53	10.3	11.2	1.1	4.0	0.7	0.7	< 0.1	0.5	72.5	< 0.1	< 0.1
1272366 Dup	0.2	4.1	15.0	2.2	110	2	0.2	1.4	< 0.1	< 1	< 0.1	0.3	52	10.8	11.6	1.1	4.1	0.7	0.7	< 0.1	0.5	65.5	< 0.1	< 0.1
1272402 Orig	17.5	3.5	112	7.7	238	98	4.7	3.5	0.2	2	0.2	< 0.1	106	21.9	45.8	5.3	19.1	3.2	2.4	0.3	1.6	3.4	0.2	0.1
1272402 Dup	17.6	6.5	108	7.6	233	98	4.8	3.2	0.2	2	0.4	< 0.1	115	20.7	44.1	5.1	18.4	3.1	2.5	0.3	1.7	3.0	0.2	0.1
1272407 Orig	< 0.1	0.6	6.1	0.4	670	2	0.2	1.1	< 0.1	< 1	< 0.1	< 0.1	105	1.0	1.7	0.2	0.6	0.1	< 0.1	< 0.1	< 0.1	2.6	< 0.1	< 0.1
1272407 Dup	< 0.1	0.2	6.1	0.4	680	< 1	< 0.1	1.0	< 0.1	< 1	< 0.1	< 0.1	134	0.9	1.6	0.2	0.6	< 0.1	< 0.1	< 0.1	< 0.1	2.6	< 0.1	< 0.1
1272438 Orig	21.3	0.7	158	12.4	43.0	62	4.5	0.2	< 0.1	1	< 0.1	0.2	734	44.6	87.8	10.1	35.0	5.7	4.2	0.5	2.6	5.2	1.0	0.2
1272438 Dup	21.4	1.0	160	12.8	43.8	64	6.8	0.1	< 0.1	1	< 0.1	< 0.1	737	47.0	93.0	10.6	36.7	5.8	4.3	0.6	2.7	0.8	1.1	0.2
1272448 Orig	17.9	2.6	135	10.4	32.9	143	3.8	0.7	< 0.1	2	0.2	< 0.1	402	68.8	120	13.8	46.7	7.4	4.7	0.5	2.2	3.8	0.9	0.2
1272448 Dup	17.8	3.3	130	10.7	32.4	143	4.1	1.0	< 0.1	2	< 0.1	0.1	402	70.2	123	14.0	48.1	7.6	5.1	0.5	2.2	0.6	1.0	0.2
1272450 Orig	21.8	0.9	102	29.1	63.7	70	0.3	< 0.1	< 0.1	< 1	< 0.1	< 0.1	28	33.1	71.2	8.8	35.0	7.3	6.7	1.0	6.0	2.1	0.4	0.5
1272450 Dup	20.5	1.7	72.3	23.9	57.8	130	6.7	0.4	< 0.1	< 1	< 0.1	0.2	26	24.4	59.1	6.8	27.6	5.9	5.6	0.9	5.1	2.1	0.7	0.4
1272477 Orig	1.9	1.1	36.4	7.2	89.0	2	0.7	0.3	< 0.1	< 1	< 0.1	< 0.1	43	3.0	6.9	0.9	3.8	1.0	1.4	0.3	1.6	14.3	< 0.1	0.1
1272477 Dup	2.0	1.5	36.1	7.1	87.0	< 1	0.6	0.2	< 0.1	< 1	0.4	< 0.1	42	3.2	7.5	1.0	4.0	1.0	1.4	0.3	1.6	16.9	< 0.1	0.1
Method Blank	< 0.1	< 0.1	< 0.2	< 0.1	< 0.2	< 1	< 0.1	< 0.1	< 0.1	< 1	< 0.1	< 0.1	< 1	< 0.1	< 0.1	< 0.1	< 0.1	< 0.1	< 0.1	< 0.1	< 0.1	< 0.2	< 0.1	< 0.1
Method Blank																								
Method Blank																								
Method Blank																								
Method Blank																								

Quality Control

Analyte Symbol	Yb	Lu	Ta	W	Re	Tl	Pb	Sc	Th	U	Ti	P	S
Unit Symbol	ppm	ppm	ppm	ppm	ppm	ppm	ppm	ppm	ppm	ppm	%	%	%
Detection Limit	0.1	0.1	0.1	0.1	0.001	0.05	0.5	1	0.1	0.1	0.0005	0.001	0.01
Analysis Method	TD-MS	TD-MS	TD-MS	TD-MS	TD-MS	TD-MS	TD-MS	TD-ICP	TD-MS	TD-MS	TD-ICP	TD-ICP	TD-ICP
GXR-1 Meas	2.2	0.3	< 0.1	135		0.43	791	2		32.3		0.062	0.27
GXR-1 Cert	1.90	0.280	0.175	164		0.390	730	1.58		34.9		0.0650	0.257
GXR-1 Meas								1				0.059	0.26
GXR-1 Cert								1.58				0.0650	0.257
GXR-4 Meas	1.0	0.1	0.6	34.1		3.39	51.4	8	19.3	5.6		0.130	1.77
GXR-4 Cert	1.60	0.170	0.790	30.8		3.20	52.0	7.70	22.5	6.20		0.120	1.77
GXR-4 Meas								8				0.131	1.75
GXR-4 Cert								7.70				0.120	1.77
SDC-1 Meas	3.2		< 0.1	< 0.1		0.66	24.7	16	11.4	2.7	0.201	0.053	0.07
SDC-1 Cert	4.00		1.20	0.800		0.70	25.00	17.00	12.00	3.10	0.606	0.0690	0.0650
SDC-1 Meas								16			0.112	0.053	0.07
SDC-1 Cert								17.00			0.606	0.0690	0.0650
GXR-6 Meas	1.7	0.2	< 0.1	< 0.1		2.46	110	29	8.2	1.5		0.035	0.02
GXR-6 Cert	2.40	0.330	0.485	1.90		2.20	101	27.6	5.30	1.54		0.0350	0.0160
GXR-6 Meas								29				0.036	0.02
GXR-6 Cert								27.6				0.0350	0.0160
SAR-M (U.S.G.S.) Meas				0.8		2.93	950	9	18.4	4.2	0.256	0.058	
SAR-M (U.S.G.S.) Cert				9.78		2.7	982	7.83	17.2	3.57	0.38	0.07	
SAR-M (U.S.G.S.) Meas								9			0.281	0.063	
SAR-M (U.S.G.S.) Cert								7.83			0.38	0.07	
DNC-1a Meas	2.0							33					
DNC-1a Cert	2.0							31					
DNC-1a Meas								31					
DNC-1a Cert								31					
SBC-1 Meas	3.3	0.5	0.5	1.2		0.96	37.6	21	20.5	5.6			
SBC-1 Cert	3.64	0.54	1.10	1.60		0.89	35.0	20.0	15.8	5.76			
SBC-1 Meas								21					
SBC-1 Cert								20.0					
1272046 Orig	3.2	0.4	< 0.1	< 0.1	0.155	0.47	2.8	8	10.2	2.7	0.168	0.061	0.01
1272046 Dup	3.2	0.4	< 0.1	< 0.1	0.160	0.46	2.9	8	10.9	2.6	0.192	0.064	0.02
1272364 Orig	0.2	< 0.1	< 0.1	0.1	0.004	0.05	7.1	< 1	0.8	2.8	0.0119	0.015	0.12
1272364 Dup	0.2	< 0.1	< 0.1	< 0.1	0.022	< 0.05	8.0	< 1	0.9	3.8	0.0113	0.015	0.12
1272366 Orig	0.2	< 0.1	< 0.1	< 0.1	0.009	0.09	5.3	< 1	0.8	15.1	0.0184	0.018	0.22
1272366 Dup	0.2	< 0.1	< 0.1	< 0.1	0.004	0.09	5.4	< 1	0.7	15.4	0.0188	0.018	0.22
1272402 Orig	0.8	0.1	0.3	0.6	0.007	0.42	2.6	19	7.8	1.8	0.447	0.043	2.02
1272402 Dup	0.9	0.1	0.3	0.6	0.005	0.39	2.9	20	7.8	1.9	0.451	0.043	2.05
1272407 Orig	< 0.1	< 0.1	< 0.1	< 0.1	0.006	< 0.05	< 0.5	< 1	0.5	< 0.1	0.0032	0.017	6.90
1272407 Dup	< 0.1	< 0.1	< 0.1	< 0.1	0.003	< 0.05	< 0.5	< 1	0.3	< 0.1	0.0030	0.016	6.74
1272438 Orig	1.1	0.2	0.3	0.3	0.004	0.73	3.5	18	20.4	3.0	0.268	0.052	< 0.01
1272438 Dup	1.2	0.2	0.5	0.6	0.003	0.72	3.6	19	20.5	3.0	0.319	0.054	< 0.01
1272448 Orig	1.0	0.2	0.3	0.1	0.001	0.47	3.9	14	16.5	2.0	0.259	0.037	0.02
1272448 Dup	1.1	0.2	0.2	0.1	0.003	0.46	4.1	14	16.3	2.0	0.263	0.038	0.02
1272450 Orig	2.6	0.4	< 0.1	< 0.1	0.012	0.38	3.2	9	11.4	5.1	0.187	0.058	0.01
1272450 Dup	2.3	0.3	0.5	0.1	0.010	0.36	3.0	5	8.1	7.0	1.01	0.071	0.01
1272477 Orig	0.7	< 0.1	< 0.1	0.2	< 0.001	0.09	1.4	2	1.3	0.7	0.0651	0.036	0.06
1272477 Dup	0.7	0.1	< 0.1	0.1	< 0.001	0.08	1.5	2	1.4	0.7	0.0646	0.036	0.06
Method Blank	< 0.1	< 0.1	< 0.1	< 0.1	< 0.001	< 0.05	< 0.5	< 1	< 0.1	< 0.1	< 0.0005	< 0.001	< 0.01
Method Blank								< 1			< 0.0005	< 0.001	< 0.01
Method Blank								< 1			< 0.0005	< 0.001	< 0.01
Method Blank								< 1			< 0.0005	< 0.001	< 0.01
Method Blank								< 1			< 0.0005	< 0.001	< 0.01

Appendix C

VTEMplus Suvey

REPORT ON A HELICOPTER-BORNE VERSATILE TIME DOMAIN ELECTROMAGNETIC (VTEM^{plus}), HORIZONTAL MAGNETIC GRADIOMETER AND GAMMA-RAY SPECTROMETRY GEOPHYSICAL SURVEY

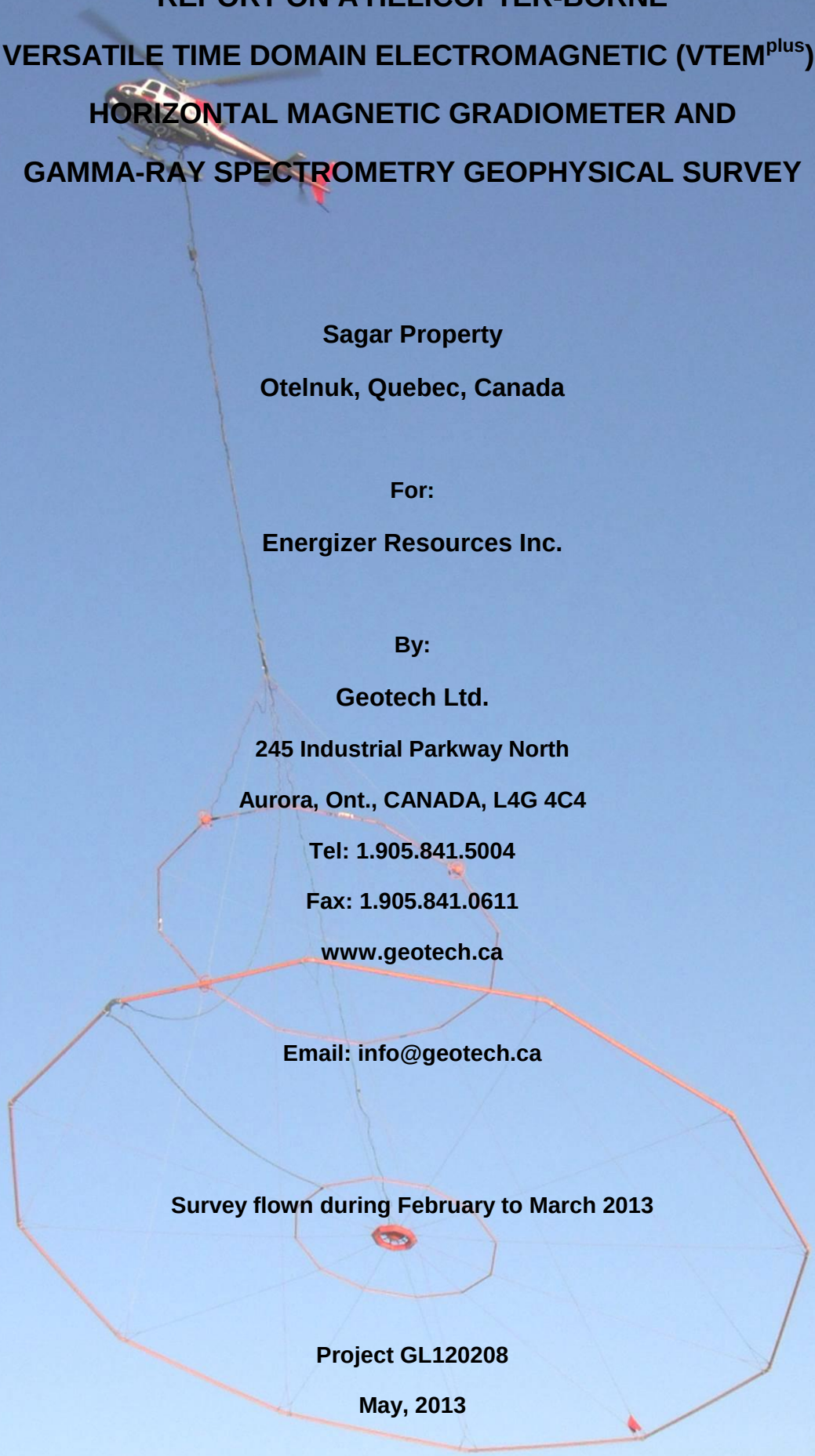

Sagar Property

Otelnuk, Quebec, Canada

For:

Energizer Resources Inc.

By:

Geotech Ltd.

245 Industrial Parkway North

Aurora, Ont., CANADA, L4G 4C4

Tel: 1.905.841.5004

Fax: 1.905.841.0611

www.geotech.ca

Email: info@geotech.ca

Survey flown during February to March 2013

Project GL120208

May, 2013

TABLE OF CONTENTS

EXECUTIVE SUMMARY ..... **iii**
1. INTRODUCTION **1**
1.1 General Considerations 1
1.2 Survey and System Specifications 2
1.3 Topographic Relief and Cultural Features 3
2. DATA ACQUISITION **4**
2.1 Survey Area 4
2.2 Survey Operations 4
2.3 Flight Specifications 5
2.4 Aircraft and Equipment 5
2.4.1 Survey Aircraft 5
2.4.2 Electromagnetic System 5
2.4.3 Horizontal Magnetic Gradiometer 9
2.4.4 Radar Altimeter 9
2.4.5 Airborne Gamma Ray Spectrometer 9
2.4.6 GPS Navigation System 9
2.4.7 Digital Acquisition System 9
2.5 Base Station 10
3. PERSONNEL **11**
4. DATA PROCESSING AND PRESENTATION **12**
4.1 Flight Path 12
4.2 Electromagnetic Data 12
4.3 Horizontal Magnetic Gradiometer Data 14
4.4 Gamma-ray Spectrometer Data 14
4.4.1 Aircraft and cosmic background corrections 14
4.4.2 Radon background correction 15
4.4.3 Compton stripping correction 15
4.4.4 Height Attenuation correction 16
4.4.5 Apparent Radioelement Concentrations 16
4.4.6 Radioelement Ratio, eTh/K 17
5. DELIVERABLES **18**
5.1 Survey Report 18
5.2 Maps 18
5.3 Digital Data 18
6. CONCLUSIONS AND RECOMMENDATIONS **24**

LIST OF FIGURES

Figure 1: Property Location. 1
Figure 2: Survey area location on Google Earth. 2
Figure 3: Flight path of the Sagar Property area over a Google Earth Image. 3
Figure 4: VTEM Waveform & Sample Times. 6
Figure 5: VTEMplus System Configuration. 8
Figure 6: Z, X and Fraser filtered X (FFx) components for “thin” target. 13

LIST OF TABLES

Table 1: Survey Specifications 4
Table 2: Survey schedule 4
Table 3: Off-Time Decay Sampling Scheme 7
Table 4: Acquisition Sampling Rates 10
Table 5: Geosoft GDB Data Format 19
Table 6: Geosoft GDB Spectrometer Data Format 21
Table 7: Geosoft Resistivity Depth Image GDB Data Format 22

APPENDICES

A. Survey location maps.....
B. Survey Block Coordinates.....
C. Geophysical Maps.....
D. Generalized Modelling Results of the VTEM System .....
E. TAU Analysis.....
F. TEM Resitivity Depth Imaging (RDI) .....

REPORT ON A HELICOPTER-BORNE VERSATILE TIME DOMAIN ELECTROMAGNETIC (VTEM^{plus}), HORIZONTAL MAGNETIC GRADIOMETER AND GAMMA-RAY SPECTROMETRY GEOPHYSICAL SURVEY

Sagar Property
Otelnuk, Quebec, Canada

EXECUTIVE SUMMARY

During February 14th to March 17th, 2013 Geotech Ltd. carried out a helicopter-borne geophysical survey over the Sagar Property area situated at Otelnuk, Quebec, Canada.

Principal geophysical sensors included a versatile time domain electromagnetic (VTEM^{plus}) system, horizontal magnetic gradiometer and RSI ARGS RSX-5 spectrometer and a cesium magnetometer. Ancillary equipment included a GPS navigation system and a radar altimeter. A total of 1114 line-kilometres of geophysical data were acquired during the survey.

In-field data quality assurance and preliminary processing were carried out on a daily basis during the acquisition phase. Preliminary and final data processing, including generation of final digital data and map products were undertaken from the office of Geotech Ltd. in Aurora, Ontario.

The processed survey results are presented as the following maps:

- Electromagnetic stacked profiles of the B-field Z Component,
- Electromagnetic stacked profiles of dB/dt Z Components,
- B-Field Z Component Channel grid
- Total Magnetic Intensity (TMI),
- dB/dt X Component Fraser Filter grid,
- Magnetic Total Horizontal Gradient of TMI
- Magnetic Tilt-Angle Derivative of TMI
- Calculated Time Constant (Tau) with contours of anomaly areas of the Calculated Vertical Derivative of TMI,
- Gamma-Ray Spectrometry products
- Resistivity Depth Images (RDI) sections are presented.

Digital data includes all electromagnetic and magnetic products, plus ancillary data including the waveform.

The survey report describes the procedures for data acquisition, processing, final image presentation and the specifications for the digital data set.

1. INTRODUCTION

1.1 General Considerations

Geotech Ltd. performed a helicopter-borne geophysical survey over the Sagar Property area situated at Otelnuk, Quebec, Canada (Figure 1 & Figure 2).

Quentin Yarie represented Energizer Resources Inc. during the data acquisition and data processing phases of this project.

The geophysical surveys consisted of helicopter borne EM using the versatile time-domain electromagnetic (VTEM^{plus}) system with Z and X component measurements and horizontal magnetic gradiometer using two cesium magnetometers and using RSI ARGS RSX-5 spectrometer system. A total of 1114 line-km of geophysical data were acquired during the survey.

The crew was based out of Otelnuk camp (Figure 2) in Quebec for the acquisition phase of the survey. Survey flying started on February 14th and was completed on March 17th, 2013.

Data quality control and quality assurance, and preliminary data processing were carried out on a daily basis during the acquisition phase of the project. Final data processing followed immediately after the end of the survey. Final reporting, data presentation and archiving were completed from the Aurora office of Geotech Ltd. in May, 2013.

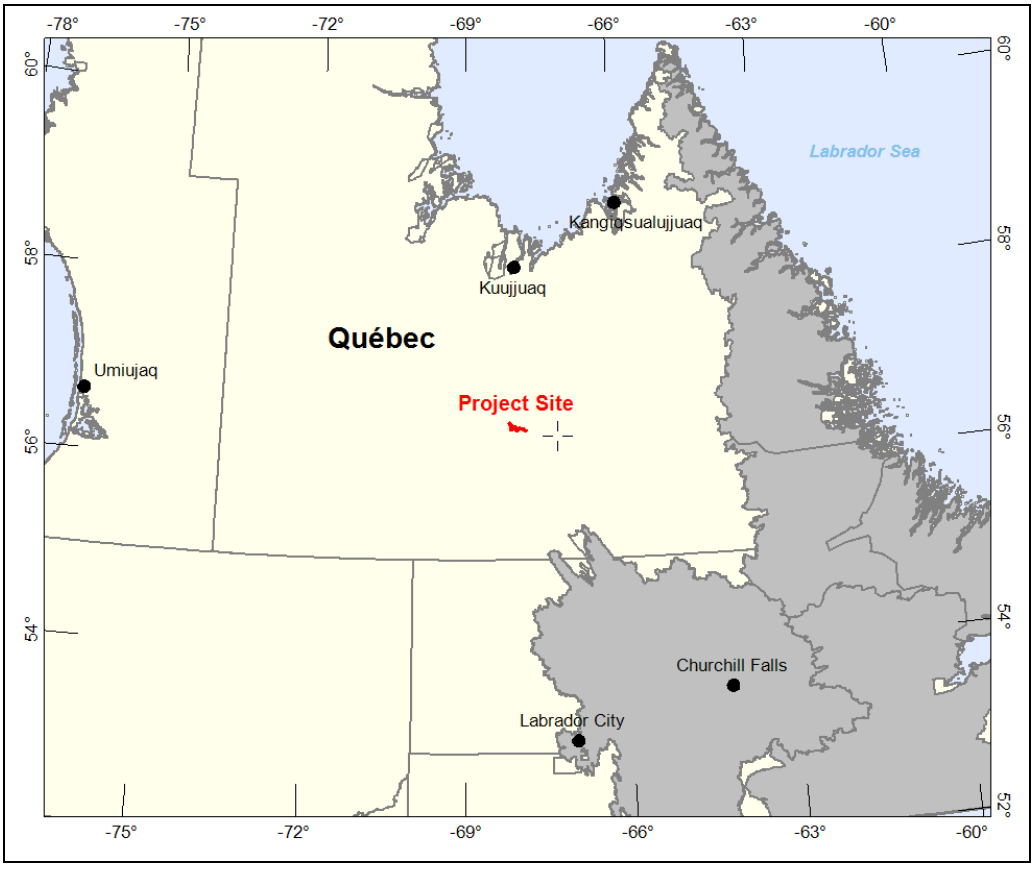

Figure 1: Property Location.

1.2 Survey and System Specifications

The Sagar Property area is situated at Otelnuk, Quebec, Canada (Figure 2).

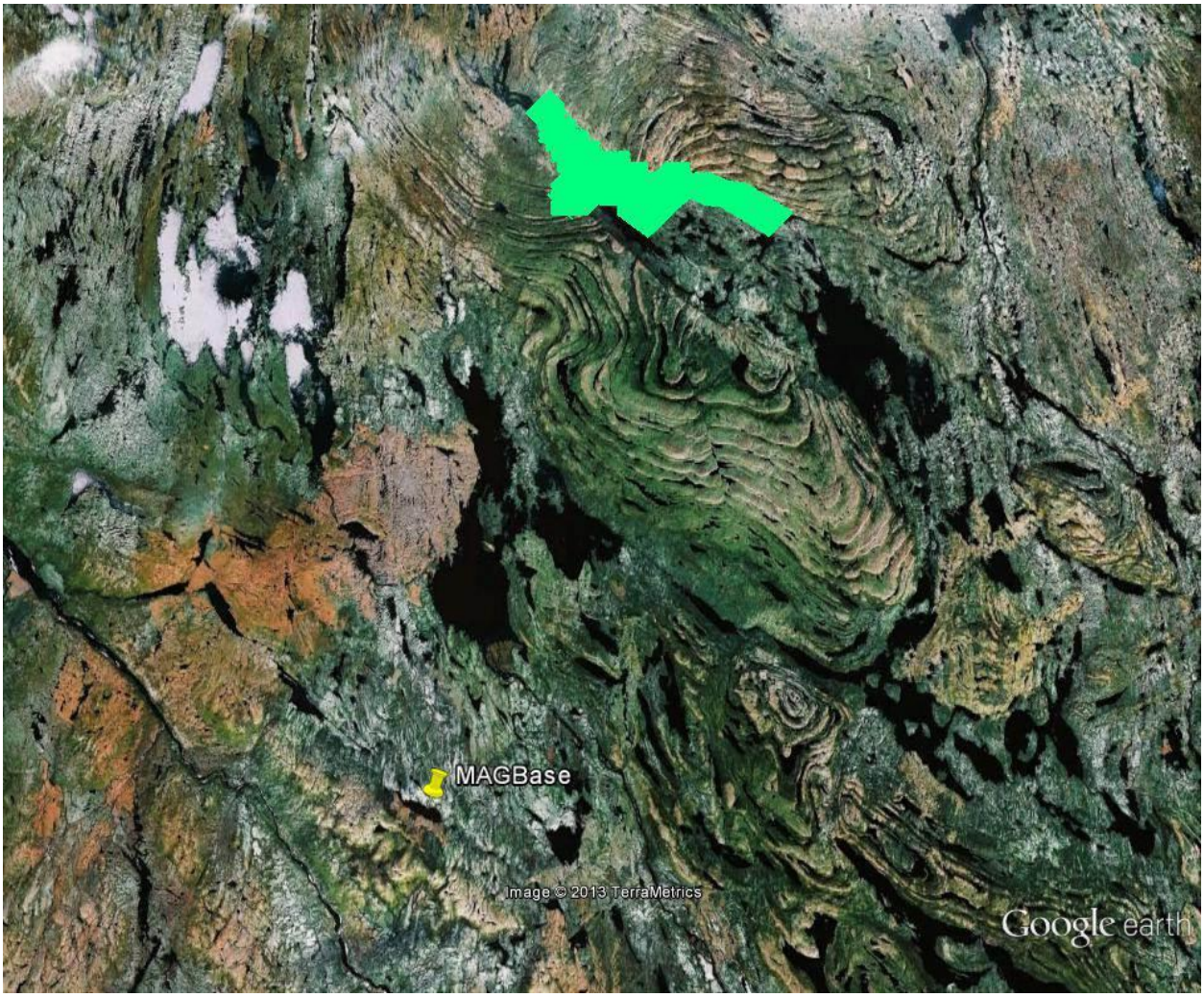

Figure 2: Survey area location on Google Earth.

The block was flown in a southwest to northeast (N 45° E azimuth) direction with traverse line spacing of 100 metres as depicted in Figure 3. Tie lines were flown perpendicular to the traverse lines at a spacing of 1000 metres. For more detailed information on the flight spacing and direction see Table 1.

1.3 Topographic Relief and Cultural Features

Topographically, the block exhibits an intermediately rugged relief with an elevation ranging from 260 to 518 metres above mean sea level over an area of 107 square kilometres (Figure 3).

There are various rivers and streams running through the survey area which connect to a series of lakes. There are no visible signs of culture located in the survey area. The survey area covers National Topographic System (NTS) sheets 024C08 and 024B05. There are also numerous mining claims located within the survey area.

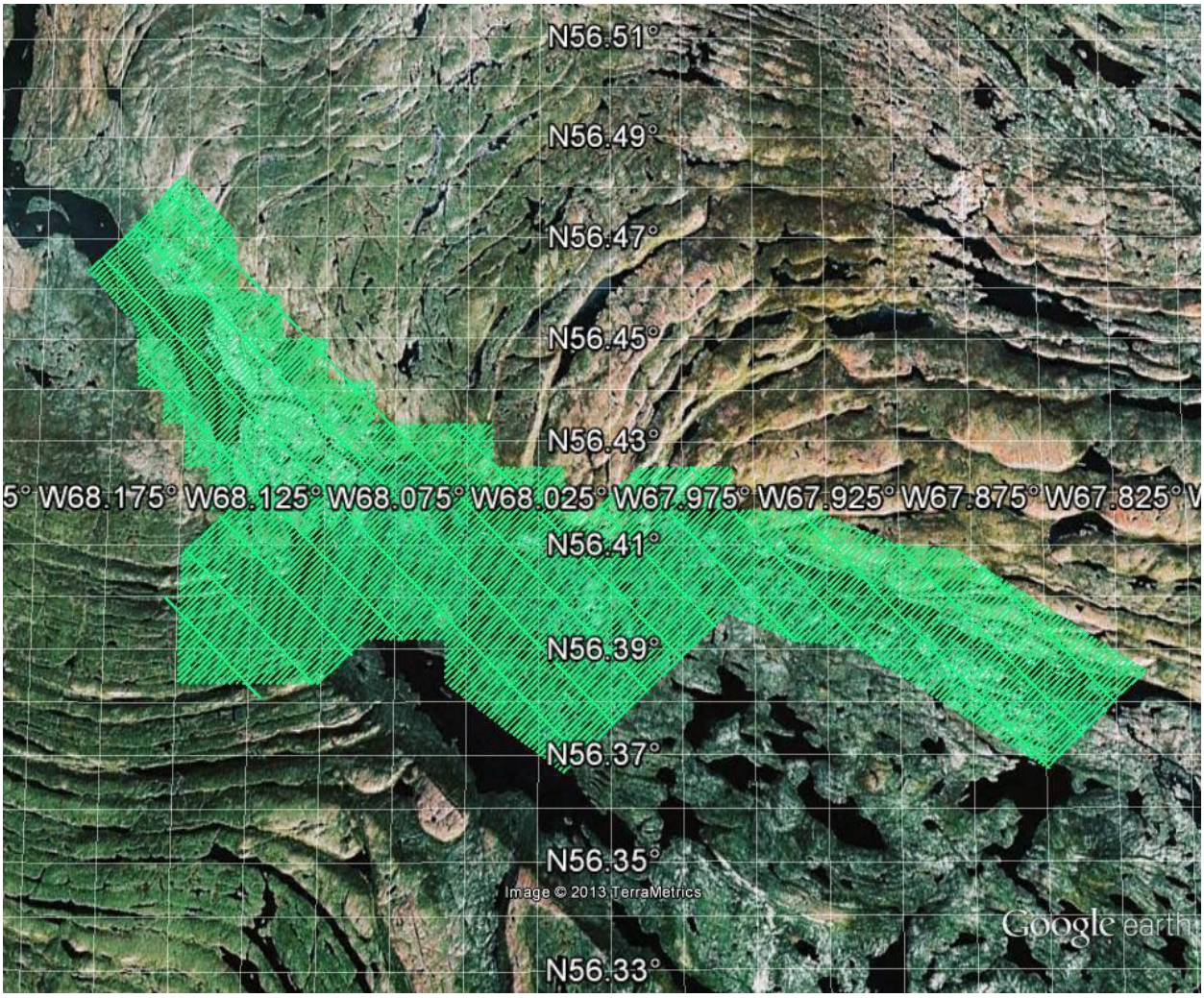

Figure 3: Flight path of the Sagar Property area over a Google Earth Image.

2. DATA ACQUISITION

2.1 Survey Area

The survey block (see Figure 3 and Appendix A) and general flight specifications are as follows:

Table 1: Survey Specifications

Survey block	Traverse Line spacing (m)	Area (Km^2)	Planned[1] Line-km	Actual Line-km	Flight direction	Line numbers
Sagar Property	Traverse: 100	107	1114	1058	N 45° E / N 225° E	L1000 – L3210
	Tie: 1000			108	N 135° E / N 315° E	T4000 – T4130
TOTAL		**107**	**1114**	**1166**		

Survey block boundaries co-ordinates are provided in Appendix B.

2.2 Survey Operations

Survey operations were based out of Otelnuk camp in Quebec from February 14th to March 17th, 2013. The following table shows the timing of the flying.

Table 2: Survey schedule

Date	Flight #	Flow km	Block	Crew location	Comments
14-Feb-2013				Otelnuk Camp,QC	Mobilization
15-Feb-2013				Otelnuk Camp,QC	Mobilization
16-Feb-2013				Otelnuk Camp,QC	Crew and equipment arrived in Sept Iles, QC
17-Feb-2013				Otelnuk Camp,QC	Local logistics
18-Feb-2013				Otelnuk Camp,QC	Prepared system for shipment
19-Feb-2013				Otelnuk Camp,QC	Arrived in Schefferville, QC
20-Feb-2013				Otelnuk Camp,QC	Arrived at Otelnuk Camp
21-Feb-2013				Otelnuk Camp,QC	System assembly
22-Feb-2013				Otelnuk Camp,QC	System assembly
23-Feb-2013				Otelnuk Camp,QC	Helicopter delayed due to weather
24-Feb-2013				Otelnuk Camp,QC	Helicopter delayed due to weather
25-Feb-2013				Otelnuk Camp,QC	Helicopter delayed due to weather
26-Feb-2013				Otelnuk Camp,QC	Helicopter arrived – Helicopter install completed
27-Feb-2013				Otelnuk Camp,QC	Ground testing completed
28-Feb-2013				Otelnuk Camp,QC	No test flights due to weather
1-Mar-2013				Otelnuk Camp,QC	No test flights due to weather
2-Mar-2013				Otelnuk Camp,QC	No test flights due to weather
3-Mar-2013				Otelnuk Camp,QC	No test flights due to weather
4-Mar-2013				Otelnuk Camp,QC	Test flights
5-Mar-2013				Otelnuk Camp,QC	Test flights
6-Mar-2013				Otelnuk Camp,QC	Flight aborted due to weather

[1] Note: Actual Line kilometres represent the total line kilometres in the final database. These line-km normally exceed the planned line-km, as indicated in the survey NAV files.

Date	Flight #	Flow km	Block	Crew location	Comments
7-Mar-2013	1,2	107		Otelnuk Camp,QC	107km flown
8-Mar-2013	3,4,5	244		Otelnuk Camp,QC	244km flown
9-Mar-2013	6,7	257		Otelnuk Camp,QC	257km flown
10-Mar-2013				Otelnuk Camp,QC	No production due to weather
11-Mar-2013				Otelnuk Camp,QC	No production due to weather
12-Mar-2013	8,9	210		Otelnuk Camp,QC	210km flown
13-Mar-2013				Otelnuk Camp,QC	No production due to weather
14-Mar-2013				Otelnuk Camp,QC	No production due to weather
15-Mar-2013				Otelnuk Camp,QC	No production due to weather
16-Mar-2013	10,11,12	296		Otelnuk Camp,QC	296km flown
17-Mar-2013				Otelnuk Camp,QC	Data review was preformed – flying complete

2.3 Flight Specifications

During the survey the helicopter was maintained at a mean altitude of 78 metres above the ground with an average survey speed of 80 km/hour. This allowed for an actual average EM bird terrain clearance of 44 metres and a magnetic sensor clearance of 54 metres.

The on board operator was responsible for monitoring the system integrity. He also maintained a detailed flight log during the survey, tracking the times of the flight as well as any unusual geophysical or topographic features.

On return of the aircrew to the base camp the survey data was transferred from a compact flash card (PCMCIA) to the data processing computer. The data were then uploaded via ftp to the Geotech office in Aurora for daily quality assurance and quality control by qualified personnel.

2.4 Aircraft and Equipment

2.4.1 Survey Aircraft

The survey was flown using a Eurocopter Aerospatiale A-star 350 B3 (C-GEOJ). The helicopter is owned and operated by Geotech Aviation. Installation of the geophysical and ancillary equipment was carried out by a Geotech Ltd crew.

2.4.2 Electromagnetic System

The electromagnetic system was a Geotech Time Domain EM (VTEM^{plus}) system. VTEM with the Serial number 22 had been used for the survey. The configuration is as indicated in Figure 5.

The VTEM Receiver and transmitter coils were in concentric-coplanar and Z-direction oriented configuration. The receiver system for the project also included a coincident-coaxial X-direction coil to measure the in-line dB/dt and calculate B-Field responses. The EM bird was towed at a mean distance of 34 metres below the aircraft as shown in Figure 5. The receiver decay recording scheme is shown diagrammatically in Figure 4.

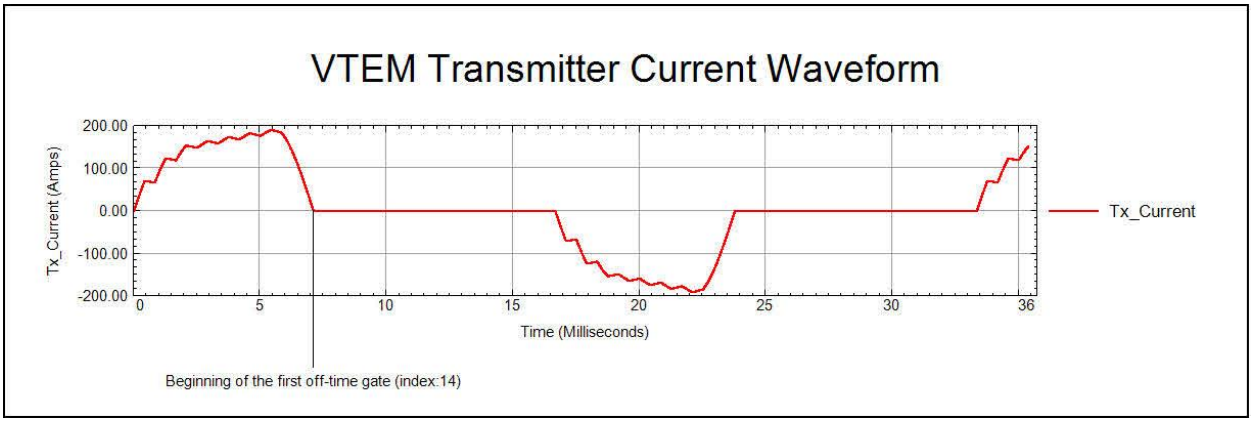

Figure 4: VTEM Waveform & Sample Times.

The VTEM decay sampling scheme is shown in Table 3 below. Thirty-two time measurement gates were used for the final data processing in the range from 0.096 to 7.036 msec.

Table 3: Off-Time Decay Sampling Scheme

VTEM Decay Sampling Scheme			
Index	**Middle**	**Start**	**End**
Milliseconds			
14	0.096	0.090	0.103
15	0.110	0.103	0.118
16	0.126	0.118	0.136
17	0.145	0.136	0.156
18	0.167	0.156	0.179
19	0.192	0.179	0.206
20	0.220	0.206	0.236
21	0.253	0.236	0.271
22	0.290	0.271	0.312
23	0.333	0.312	0.358
24	0.383	0.358	0.411
25	0.440	0.411	0.472
26	0.505	0.472	0.543
27	0.580	0.543	0.623
28	0.667	0.623	0.716
29	0.766	0.716	0.823
30	0.880	0.823	0.945
31	1.010	0.945	1.086
32	1.161	1.086	1.247
33	1.333	1.247	1.432
34	1.531	1.432	1.646
35	1.760	1.646	1.891
36	2.021	1.891	2.172
37	2.323	2.172	2.495
38	2.667	2.495	2.865
39	3.063	2.865	3.292
40	3.521	3.292	3.781
41	4.042	3.781	4.341
42	4.641	4.341	4.987
43	5.333	4.987	5.729
44	6.125	5.729	6.581
45	7.036	6.581	7.560

Z Component: 14-45 time gates
X Component: 20-45 time gates

VTEM system specifications:

Transmitter

- Transmitter coil diameter: 26 m
- Number of turns: 4
- Effective Transmitter coil area: 2123.7 m^2
- Transmitter base frequency: 30 Hz
- Peak current: 191 A
- Pulse width: 7.12 ms
- Wave form shape: Bi-polar trapezoid
- Peak dipole moment: 405,629 nIA
- Actual average EM Bird terrain clearance: 44 metres above the ground

Receiver

- X Coil diameter: 0.32 m
- Number of turns: 245
- Effective coil area: 19.69 m^2
- Z-Coil coil diameter: 1.2 m
- Number of turns: 100
- Effective coil area: 113.04 m^2

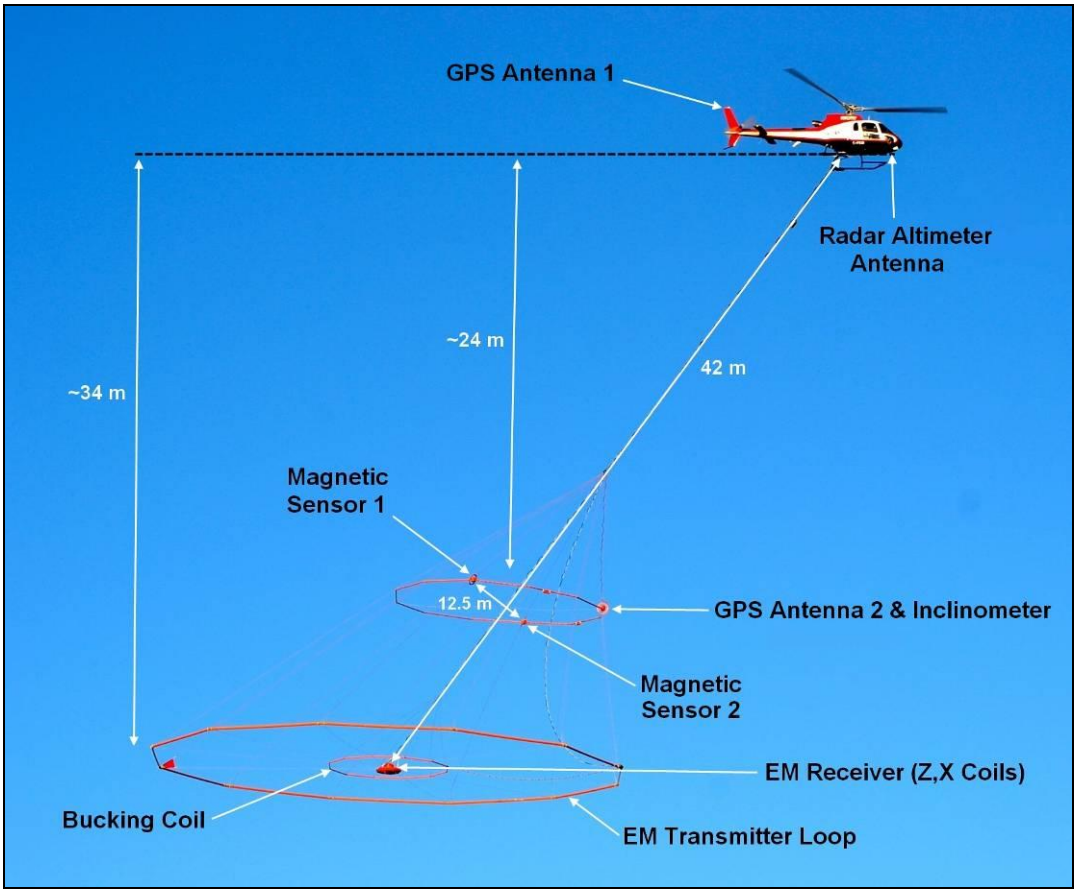

Figure 5: VTEM^{plus} System Configuration.

2.4.3 Horizontal Magnetic Gradiometer

The horizontal magnetic gradiometer consists of two Geometrics split-beam field magnetic sensors with a sampling interval of 0.1 seconds. These sensors are mounted 12.5 metres apart on a separate loop, 10 metres above the EM bird. A GPS antenna and Gyro Inclinometer is installed on the separate loop to accurately record the tilt and position of the magnetic gradiomag bird.

2.4.4 Radar Altimeter

A Terra TRA 3000/TRI 40 radar altimeter was used to record terrain clearance. The antenna was mounted beneath the bubble of the helicopter cockpit (Figure 5).

2.4.5 Airborne Gamma Ray Spectrometer

The Airborne gamma ray spectrometer utilized for the survey was an RSI ARGS RSX-5 (Radiation Solutions Inc. Airborne Gamma Ray Spectrometer 500), mounted on the interior floor of the helicopter cabin. A temperature and barometric pressure sensor is located on the outside of the helicopter and connected to the auxiliary port of the detector unit. The RSX-5 is equipped with four, 4.2 litre (1024cu in.) downward looking Nal (Sodium Iodide) crystals and one 4.2 litre (256cu in.) upward looking Nal crystal. The resolution of the crystals is <8.5%, with 1024 channels at a sampling interval of 1 second. Temperature and barometric pressure are also acquired at an interval of 1 second.

The gamma ray spectrometer data are acquired and stored in the internal memory of the RSX-5. Once the survey is completed the acquired data can then download onto a USB drive from the RSX-5 detector pack. The RSX-5 maintains the measured total counts, potassium, equivalent Thorium, and equivalent Uranium as counts per second in its internal memory. During the survey RadAssist Software (Radiation solutions Inc., 2008) is utilized by Geotech data acquisition system and displayed on the LCD screen. This allows the operator to monitor the integrity of the RSX-5 detector pack to ensure it is running properly.

2.4.6 GPS Navigation System

The navigation system used was a Geotech PC104 based navigation system utilizing a NovAtel's WAAS (Wide Area Augmentation System) enabled GPS receiver, Geotech navigate software, a full screen display with controls in front of the pilot to direct the flight and a NovAtel GPS antenna mounted on the helicopter tail (Figure 5). As many as 11 GPS and two WAAS satellites may be monitored at any one time. The positional accuracy or circular error probability (CEP) is 1.8 m, with WAAS active, it is 1.0 m. The co-ordinates of the block were set-up prior to the survey and the information was fed into the airborne navigation system. The second GPS antenna is installed on the additional magnetic loop together with Gyro Inclinometer.

2.4.7 Digital Acquisition System

A Geotech data acquisition system recorded the digital survey data on an internal compact flash card. Data is displayed on an LCD screen as traces to allow the operator to monitor the integrity of the system. The data type and sampling interval as provided in Table 4.

Table 4: Acquisition Sampling Rates

Data Type	Sampling
TDEM	0.1 sec
Magnetometer	0.1 sec
GPS Position	0.2 sec
Spectrometer	1 sec
Pressure and Temperature	1 sec
Radar Altimeter	0.2 sec
Inclinometer	0.1 sec

2.5 Base Station

A combined magnetometer/GPS base station was utilized on this project. A Geometrics Cesium vapour magnetometer was used as a magnetic sensor with a sensitivity of 0.001 nT. The base station was recording the magnetic field together with the GPS time at 1 Hz on a base station computer.

The base station magnetometer sensor was installed at the northeast side of the camp area (068° 18.5080' W, 055° 56.2389' N); away from electric transmission lines and moving ferrous objects such as motor vehicles. The base station data were backed-up to the data processing computer at the end of each survey day.

3. PERSONNEL

The following Geotech Ltd. personnel were involved in the project.

Field:	
Project Manager:	Adrian Sarmasag (Office)
Data QC:	Nick Venter (Office)
Crew chief:	Ioan Serbu Joseph Florjancic
Operator:	Juan Carlos Osorio Viktor Shevchenko

The survey pilot and the mechanical engineer were employed directly by the helicopter operator – Geotech Aviation

Pilot:	Claude Noel
Mechanical Engineer:	N/A
Office:	
Preliminary Data Processing:	Nick Venter
Final Data Processing:	Keeme Mokubung
Final Data QA/QC:	Alexander Prikhodko
Reporting/Mapping:	Karl Monje

Data acquisition phase was carried out under the supervision of Andrei Bagrianski, P. Geo, Chief Operating Officer. Processing and Interpretation phases were carried out under the supervision of Alexander Prikhodko, P. Geo, Senior Geophysicist, VTEM Interpretation Supervisor. The customer relations were looked after by Blair Walker.

4. DATA PROCESSING AND PRESENTATION

Data compilation and processing were carried out by the application of Geosoft OASIS Montaj and programs proprietary to Geotech Ltd.

4.1 Flight Path

The flight path, recorded by the acquisition program as WGS 84 latitude/longitude, was converted into the NAD83 Datum, UTM Zone 19 North coordinate system in Oasis Montaj.

The flight path was drawn using linear interpolation between x, y positions from the navigation system. Positions are updated every second and expressed as UTM easting's (x) and UTM northing's (y).

4.2 Electromagnetic Data

A three stage digital filtering process was used to reject major sferic events and to reduce noise levels. Local sferic activity can produce sharp, large amplitude events that cannot be removed by conventional filtering procedures. Smoothing or stacking will reduce their amplitude but leave a broader residual response that can be confused with geological phenomena. To avoid this possibility, a computer algorithm searches out and rejects the major sferic events.

The signal to noise ratio was further improved by the application of a low pass linear digital filter. This filter has zero phase shift which prevents any lag or peak displacement from occurring, and it suppresses only variations with a wavelength less than about 1 second or 15 metres. This filter is a symmetrical 1 sec linear filter.

The results are presented as stacked profiles of EM voltages for the time gates, in linear - logarithmic scale for the B-field Z component and dB/dt responses in the Z and X components. B-field Z component time channel recorded at 2.021 milliseconds after the termination of the impulse is also presented as a colour image. Fraser Filter X component is also presented as a colour image. Calculated Time Constant (TAU) with anomaly contours of Calculated Vertical Derivative of TMI is presented in Appendix C and E. Resistivity Depth Image (RDI) is also presented in Appendix E and F.

VTEM has two receiver coil orientations. Z-axis coil is oriented parallel to the transmitter coil axis and both are horizontal to the ground. The X-axis coil is oriented parallel to the ground and along the line-of-flight. This combined two coil configuration provides information on the position, depth, dip and thickness of a conductor. Generalized modeling results of VTEM data, are shown in Appendix D.

In general X-component data produce cross-over type anomalies: from "+ to – "in flight direction of flight for "thin" sub vertical targets and from "- to +" in direction of flight for "thick" targets. Z component data produce double peak type anomalies for "thin" sub vertical targets and single peak for "thick" targets.

The limits and change-over of "thin-thick" depends on dimensions of a TEM system (Appendix D, Figure D-16).

Because of X component polarity is under line-of-flight, convolution Fraser Filter (Figure 6) is applied to X component data to represent axes of conductors in the form of grid map. In this case positive FF anomalies always correspond to “plus-to-minus” X data crossovers independent of the flight direction.

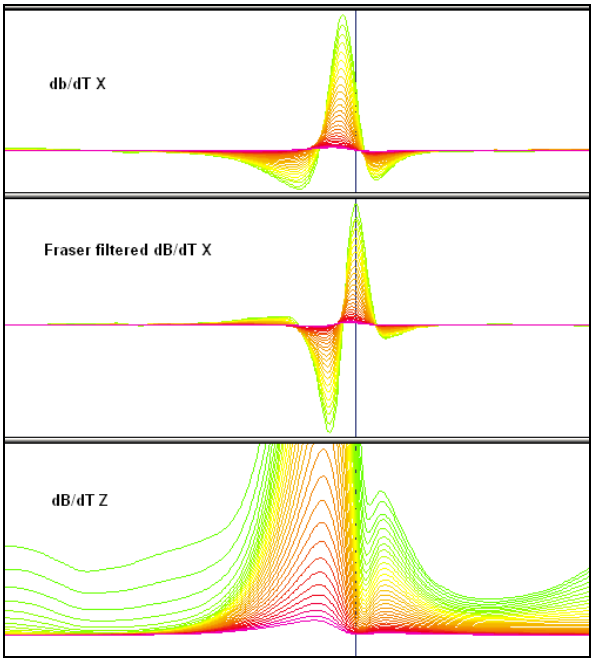

Figure 6: Z, X and Fraser filtered X (FFx) components for “thin” target.

4.3 Horizontal Magnetic Gradiometer Data

The horizontal gradients data from the VTEM^{plus} are measured by two magnetometers 12.5 m apart on an independent bird mounted10m above the VTEM loop. A GPS and a Gyro Inclinometer help to determine the positions and orientations of the magnetometers. The data from the two magnetometers are corrected for position and orientation variations, as well as for the diurnal variations using the base station data.

The position of the centre of the horizontal magnetic gradiometer bird is calculated from the GPS utilizing in-house processing tool in Geosoft. Following that total magnetic intensity is calculated at the center of the bird by calculating the mean values from both sensors. In addition to the total intensity advanced processing is done to calculate the in-line and cross-line (or lateral) horizontal gradient which enhance the understanding of magnetic targets. The in-line (longitudinal) horizontal gradient is calculated from the difference of two consecutive total magnetic field readings divided by the distance along the flight line direction, while the cross-line (lateral) horizontal magnetic gradient is calculated from the difference in the magnetic readings from both magnetic sensors divided by their horizontal separation.

Two advanced magnetic derivative products, the total horizontal derivative (THDR), and tilt angle derivative and are also created. The total horizontal derivative or gradient is also called the analytic signal, is defined as:

THDR = sqrt (Hx * Hx + Hy * Hy), where Hx and Hy are cross-line and in-line horizontal gradients.

The tilt angle derivative (TDR) is defined as:

TDR = arctan (Vz / THDR), where THDR is the total horizontal derivative, and Vz is the vertical derivative.

Measured cross-line gradients can help to enhance cross-line linear features during gridding.

4.4 Gamma-ray Spectrometer Data

The processing of the spectrometric data involved the transformation of the spectra into energy windows, corrections for aircraft and cosmic background, radon background correction, stripping corrections, height reducing to standard atmosphere using measured barometric pressure and temperature and to nominal height. The applied corrections were based on calibrations made before and during survey. The results of these calibrations and tests can be found on the digital archive.

4.4.1 Aircraft and cosmic background corrections

Cosmic and aircraft background expressions are determined for each spectral window. The general form of these expressions is N = a + bC, where N is the combined cosmic and aircraft background for each window; a is the aircraft background in the window; C is the cosmic channel count; and b is the cosmic stripping factor for the window.

The background correction coefficients were derived from the data from a calibration flight flown on 4th March, 2013 and are listed below.

Radioelement Window	a	b
TC	14.413	0.9595
K	3.6087	0.0542
U	0.0100	0.0434
Th	0.2542	0.0479
UpU	0.2288	0.0114

4.4.2 Radon background correction

The expression for the radon component in the downward looking uranium window is given by $Ur = (UpU – a_1U – a_2Th + a_2b_T – b_u)/(a_u – a_1 – a_2a_T)$, where Ur is the radon background detected in the downward U window; UpU is the measured count in the upward uranium window; U is the measured count in the downward uranium window; Th is the measured count in the downward thorium window; a_1, a_2, a_u and a_T are proportionality factors; and b_u and b_T are constants determined experimentally. The above equation can be simplified to an expression below:

$$Ur = 5.72*UpU – 0.407*U -0.094*Th.$$

The Radon background correction TCg, Kg, Ug and Thg channels can then be derived using the expressions below:

TCg = TC – 14*Ur,
Kg = K – 1.16*Ur,
Ug = U-Ur,
Thg = Th-0.051*Ur.

4.4.3 Compton stripping correction

Radar altimeter data are used in Compton stripping as well as height attenuation corrections. They are converted to effective height (STPA) at STP (Standard Temperature and Pressure) by the expression STPA = (radar * 273.15)/(T + 273.15)* (P/1013), where radar is the observed radar altitude, T is the temperature in degrees C, and P is the barometric pressure in mbars.

The stripping ratios α, β, γ, a, b and g are determined during tests over calibration pads. The principal ratios a, β and g should be adjusted for temperature, pressure and altitude (above ground) before stripping is carried out. These stripping ratios are used to remove the contribution in each of the three radioelement windows from higher energy sources, leaving only the contribution from potassium, uranium and thorium windows.

For the spectrometer used, a=0.045, b=-0.003 and g=0.001.

α = 0.271+0.00049*STPA,
β = 0.415+0.00065*STPA,
γ = 0.766+0.00069*STPA.

The Compton stripping corrected Thc, Uc and Kc channels are derived from the following expressions:

Thc = ((Thg*af7)+(Ug*af8)+(Kg*af9))/denom,
Uc = ((Thg*af4)+(Ug*af5)+(Kg*af6))/denom,
Kc = ((Thg*af1)+(Ug*af2)+(Kg*af3))/denom;

where:

af1=α*γ – β,
af2=a*β - γ,
af3=1.0 - a*α,
af4=-g*β - α,
af5=1.0 - b*β,
af6=b*α - g,
af7=1- g*γ,
af8=b*γ-a,
af9=ag - b,
af10=α-g*β,
af11=β-α*γ,
denom = 1-(g*γ)-(a*af10)-(b*af11)

4.4.4 Height Attenuation correction

The altitude attenuation correction corrects the data in each of the radioelement windows for the effects of altitude. The count rates decrease exponentially with altitude. They are corrected to a constant altimeter datum at the nominal height of 80m for all surveyed blocks.

A height attenuation calibration flight was flown on 4th March, 2013 for the survey. The height corrected radioelements, TCf, Kf, Uf and Thf, are computed using the following expressions:

TCf = TCg*exp -0.0064*(80-STPA)),
Kf = Kc*exp -0.0082*(80-STPA)),
Uf = Uc*exp -0.0051*(80-STPA)),
Thf = Thc*exp -0.0088*(80-STPA)).

Microlevelling procedures were applied to the data to remove minor residual noises.

4.4.5 Apparent Radioelement Concentrations

The corrected radioelement data can be converted to apparent ground concentrations of each of the three radioelements, potassium, uranium and thorium. The procedure assumes an infinite horizontal slab source with a uniform radioelement concentration. It also assumes radioactive equilibrium in the U and Th decay series. Therefore the U and Th concentrations are called equivalent concentrations using the nomenclature eU and eTh.

Percent K concentration, Kperc (%) = Kf/ 41.50458279,
Equivalent Uranium Concentraion, eU (ppm) = Uf/ 4.985937476,
Equivalent Thorium Concentraion, eTh (ppm) = Thf/ 2.42738625.

An estimate of the air absorbed dose rate, E, can be made from the apparent concentrations, K%, eU ppm and eTh ppm using the following formula:

Dose Rate E = 13.09*Kperc +5.68*eU + 2.49*eTh.

4.4.6 Radioelement Ratio, eTh/K

Standard radioelement ratio, eThppm/Kperc was computed from Kperc and eThppm channels. Data less than 0.1 was rejected for ratio calculations, so that there would be no extreme values in eTh/K.

The spectrometric data were processed and saved in a separate Geosoft GDB database because of different sampling rates to the VTEM plus magnetic data. Table 5 presents the database channels for the processed gamma-ray spectrometer data.

5. DELIVERABLES

5.1 Survey Report

The survey report describes the data acquisition, processing, and final presentation of the survey results. The survey report is provided in two paper copies and digitally in PDF format.

5.2 Maps

Final maps were produced at scale of 1:20,000 for best representation of the survey size and line spacing. The coordinate/projection system used was NAD83 Datum, UTM Zone 19 North. All maps show the mining claims, flight path trace and topographic data; latitude and longitude are also noted on maps.

The preliminary and final results of the survey are presented as EM profiles, a late-time gate gridded EM channel, and a colour magnetic TMI contour map. The following maps are presented on paper;

- VTEM dB/dt profiles Z Component, Time Gates 0.220 – 7.036 ms in linear – logarithmic scale.
- VTEM B-Field profiles Z Component, Time Gates 0.220 – 7.036 ms in linear – logarithmic scale.
- VTEM B-field late time Z Component colour image.
- VTEM dB/dt Calculated Time Constant (TAU) with contours of anomaly areas of the Calculated Vertical Derivative of TMI
- Fraser Filtered dB/dt X Component
- Total Magnetic Intensity (TMI) colour image and contours
- Magnetic Total Horizontal Gradient
- Magnetic Tilt-Angle Derivative
- Ternary Radiometric
- Gamma-Ray Spectrometer Potassium levels colour image.
- Gamma-Ray Spectrometer equivalent Uranium levels colour image.
- Gamma-Ray Spectrometer equivalent Thorium levels colour image.
- Gamma-Ray Spectrometer equivalent Thorium / Potassium ratio colour image
- Gamma-Ray Spectrometer Exposure Dose colour image.

5.3 Digital Data

Two copies of the data and maps on DVD were prepared to accompany the report. Each DVD contains a digital file of the line data in GDB Geosoft Montaj format as well as the maps in Geosoft Montaj Map and PDF format.

- DVD structure.

  Data contains databases, grids and maps, as described below.
  Report contains a copy of the report and appendices in PDF format.

  Databases in Geosoft GDB format, containing the channels listed in Table 5.

Table 5: Geosoft GDB Data Format

Channel name	Units	Description
X:	metres	UTM Easting NAD83 Zone 19 North
Y:	metres	UTM Northing NAD83 Zone 19 North
Longitude:	Decimal Degrees	WGS 84 Longitude data
Latitude:	Decimal Degrees	WGS 84 Latitude data
Z:	metres	GPS antenna elevation (above Geoid)
Radar:	metres	helicopter terrain clearance from radar altimeter
Radarb:	metres	Calculated EM bird terrain clearance from radar altimeter
DEM:	metres	Digital Elevation Model
Gtime:	Seconds of the day	GPS time
Mag1L:	nT	Measured Total Magnetic field data (left sensor)
Mag1R:	nT	Measured Total Magnetic field data (right sensor)
Basemag:	nT	Magnetic diurnal variation data
Mag2LZ	nT	Z corrected (w.r.t. loop center) and diurnal corrected magnetic field left mag
Mag2RZ	nT	Z corrected (w.r.t. loop center) and diurnal corrected magnetic field right mag
TMI2	nT	Calculated from diurnal corrected total magnetic field intensity of the centre of the loop
TMI3	nT	Microleveled total magnetic field intensity of the centre of the loop
CVG	nT/m	Calculated magnetic vertical gradient
Hgcxline		measured cross-line gradient
Hginline		Calculated in-line gradient
SFz[14]:	pV/(A*m^4)	Z dB/dt 0.096 millisecond time channel
SFz[15]:	pV/(A*m^4)	Z dB/dt 0.110 millisecond time channel
SFz[16]:	pV/(A*m^4)	Z dB/dt 0.126 millisecond time channel
SFz[17]:	pV/(A*m^4)	Z dB/dt 0.145 millisecond time channel
SFz[18]:	pV/(A*m^4)	Z dB/dt 0.167 millisecond time channel
SFz[19]:	pV/(A*m^4)	Z dB/dt 0.192 millisecond time channel
SFz[20]:	pV/(A*m^4)	Z dB/dt 0.220 millisecond time channel
SFz[21]:	pV/(A*m^4)	Z dB/dt 0.253 millisecond time channel
SFz[22]:	pV/(A*m^4)	Z dB/dt 0.290 millisecond time channel
SFz[23]:	pV/(A*m^4)	Z dB/dt 0.333 millisecond time channel
SFz[24]:	pV/(A*m^4)	Z dB/dt 0.383 millisecond time channel
SFz[25]:	pV/(A*m^4)	Z dB/dt 0.440 millisecond time channel
SFz[26]:	pV/(A*m^4)	Z dB/dt 0.505 millisecond time channel
SFz[27]:	pV/(A*m^4)	Z dB/dt 0.580 millisecond time channel
SFz[28]:	pV/(A*m^4)	Z dB/dt 0.667 millisecond time channel
SFz[29]:	pV/(A*m^4)	Z dB/dt 0.766 millisecond time channel
SFz[30]:	pV/(A*m^4)	Z dB/dt 0.880 millisecond time channel
SFz[31]:	pV/(A*m^4)	Z dB/dt 1.010 millisecond time channel
SFz[32]:	pV/(A*m^4)	Z dB/dt 1.161 millisecond time channel
SFz[33]:	pV/(A*m^4)	Z dB/dt 1.333 millisecond time channel
SFz[34]:	pV/(A*m^4)	Z dB/dt 1.531 millisecond time channel
SFz[35]:	pV/(A*m^4)	Z dB/dt 1.760 millisecond time channel
SFz[36]:	pV/(A*m^4)	Z dB/dt 2.021 millisecond time channel
SFz[37]:	pV/(A*m^4)	Z dB/dt 2.323 millisecond time channel
SFz[38]:	pV/(A*m^4)	Z dB/dt 2.667 millisecond time channel
SFz[39]:	pV/(A*m^4)	Z dB/dt 3.063 millisecond time channel
SFz[40]:	pV/(A*m^4)	Z dB/dt 3.521 millisecond time channel
SFz[41]:	pV/(A*m^4)	Z dB/dt 4.042 millisecond time channel

Channel name	Units	Description
SFz[42]:	pV/(A*m^4)	Z dB/dt 4.641 millisecond time channel
SFz[43]:	pV/(A*m^4)	Z dB/dt 5.333 millisecond time channel
SFz[44]:	pV/(A*m^4)	Z dB/dt 6.125 millisecond time channel
SFz[45]:	pV/(A*m^4)	Z dB/dt 7.036 millisecond time channel
SFx[20]:	pV/(A*m^4)	X dB/dt 0.220 millisecond time channel
SFx[21]:	pV/(A*m^4)	X dB/dt 0.253 millisecond time channel
SFx[22]:	pV/(A*m^4)	X dB/dt 0.290 millisecond time channel
SFx[23]:	pV/(A*m^4)	X dB/dt 0.333 millisecond time channel
SFx[24]:	pV/(A*m^4)	X dB/dt 0.383 millisecond time channel
SFx[25]:	pV/(A*m^4)	X dB/dt 0.440 millisecond time channel
SFx[26]:	pV/(A*m^4)	X dB/dt 0.505 millisecond time channel
SFx[27]:	pV/(A*m^4)	X dB/dt 0.580 millisecond time channel
SFx[28]:	pV/(A*m^4)	X dB/dt 0.667 millisecond time channel
SFx[29]:	pV/(A*m^4)	X dB/dt 0.766 millisecond time channel
SFx[30]:	pV/(A*m^4)	X dB/dt 0.880 millisecond time channel
SFx[31]:	pV/(A*m^4)	X dB/dt 1.010 millisecond time channel
SFx[32]:	pV/(A*m^4)	X dB/dt 1.161 millisecond time channel
SFx[33]:	pV/(A*m^4)	X dB/dt 1.333 millisecond time channel
SFx[34]:	pV/(A*m^4)	X dB/dt 1.531 millisecond time channel
SFx[35]:	pV/(A*m^4)	X dB/dt 1.760 millisecond time channel
SFx[36]:	pV/(A*m^4)	X dB/dt 2.021 millisecond time channel
SFx[37]:	pV/(A*m^4)	X dB/dt 2.323 millisecond time channel
SFx[38]:	pV/(A*m^4)	X dB/dt 2.667 millisecond time channel
SFx[39]:	pV/(A*m^4)	X dB/dt 3.063 millisecond time channel
SFx[40]:	pV/(A*m^4)	X dB/dt 3.521 millisecond time channel
SFx[41]:	pV/(A*m^4)	X dB/dt 4.042 millisecond time channel
SFx[42]:	pV/(A*m^4)	X dB/dt 4.641 millisecond time channel
SFx[43]:	pV/(A*m^4)	X dB/dt 5.333 millisecond time channel
SFx[44]:	pV/(A*m^4)	X dB/dt 6.125 millisecond time channel
SFx[45]:	pV/(A*m^4)	X dB/dt 7.036 millisecond time channel
BFz	(pV*ms)/(A*m^4)	Z B-Field data for time channels 13 to 48
BFx	(pV*ms)/(A*m^4)	X B-Field data for time channels 20 to 48
SFxFF	pV/(A*m^4)	Fraser Filtered X dB/dt
NchanBF		Latest time channels of TAU calculation
NchanSF		Latest time channels of TAU calculation
TauBF	ms	Time constant B-Field
TauSF	ms	Time constant dB/dt
PLM:		60 Hz power line monitor

Electromagnetic B-field and dB/dt Z component data is found in array channel format between indexes 14 - 45, and X component data from 20 - 45, as described above.

- Database of the gamma ray spectrometer data in Geosoft GDB format, containing the following channels:

Table 6: Geosoft GDB Spectrometer Data Format

Channel Name	Description
X	X positional data (meters – NAD83, UTM zone 19 North)
Y	Y positional data (meters – NAD83, UTM zone 19 North)
Z	GPS antenna elevation (meters - ASL)
Longitude	WGS 84 Longitude data (Decimal Degrees)
Latitude	WGS 84 Latitude data (Decimal Degrees)
gtime	UTC time in second past midnight
Radar	Aircraft (Spectrometer Pack) Terrain Clearance (meters)
DEM	Digital elevation model (m)
Pressure	Barometric Pressure (hPa)
Temperature	Outside air temperature in degrees Celsius
K_Raw	uncorrected Potassium Count (counts per sec) Downward looking
U_Raw	uncorrected Uranium Count (counts per sec) Downward looking
Th_Raw	uncorrected Thorium Count (counts per sec) Downward looking
TC_Raw	uncorrected Total Count (counts per sec) Downward looking
D_Cosmic	uncorrected Cosmic Count (counts per sec) Downward looking
UpU_Raw	uncorrected Uranium Count (counts per sec) Upward looking
Up_Cos	uncorrected Cosmic Count (counts per sec) Upward looking
Kfin	Corrected Potassium Count (counts per sec)
Ufin	Corrected Uranium count (counts per sec)
Thfin	Corrected Thorium Count (counts per sec)
TCfin	Corrected Total Count (counts per sec)
Kperc	Potassium (%)Concentrations (under calibration coefficients of the
eUppm	Uranium (ppm) Concentrations (under calibration coefficients of the
eThppm	Thorium (ppm) Concentrations (under calibration coefficients of the
Dose	Exposure Dose rate (nGy/h)
rThK	Thorium / Potassium Ratio

- Database of the VTEM Resistivity Depth Images in Geosoft GDB format, contains the following channels:

Table 7: Geosoft Resistivity Depth Image GDB Data Format

Channel name	Units	Description
Xg:	metres	UTM Easting NAD83 Zone 19 North
Yg:	metres	UTM Northing NAD83 Zone 19 North
Dist:	meters	Distance from the beginning of the line
Depth:	meters	array channel, depth from the surface
Z:	meters	array channel, depth from sea level
AppRes:	Ohm-m	array channel, Apparent Resistivity
TR:	meters	EM system height from sea level
Topo:	meters	digital elevation model
Radarb:	metres	Calculated EM bird terrain clearance from radar altimeter
CVG	nT/m	Calculated Magnetic Vertical Gradient of Pseudo RTP of TMI
SFz:	pV/(A*m^4)	array channel, dB/dT
DOI	Meters	Depth of Investigation; a measure of VTEM depth effectiveness

- Database of the VTEM Waveform "GL120208_Waveform_Final.gdb" in Geosoft GDB and XYZ format, containing the following channels:

  Time: Sampling rate interval, 5.2083 milliseconds
  Tx_Current: Output current of the transmitter (Amp)
  Rx_Volt: Output voltage of the receiver coil (Volt)

- Grids in Geosoft GRD and GeoTIFF format, as follows:

  BFz36: B-Field Z Component Channel 36 (Time Gate 2.021 ms)
  DEM: Digital Elevation Model (metres)
  TMI3: Total Magnetic Intensity (nT)
  Hgcxline: Measured Cross-Line Gradient (nT/m)
  Hginline: Measured In-Line Gradient (nT/m)
  SFxFF20: Fraser Filtered dB/dt X Component Channel 20 (Time Gate 0.220 ms)
  TauBF: B-Field Z Component, Calculated Time Constant (ms)
  TauSF: dB/dt Z Component, Calculated Time Constant (ms)
  TMI: Total Magnetic Intensity (nT)
  Tot_HGrad: Magnetic Total Horizontal Gradient (nT/m)
  TiltDrv: Magnetic Tilt derivative (radians)
  SFz20: dB/dt Z Component Channel 20 (Time Gate 0.220 ms)
  SFz30: dB/dt Z Component Channel 30 (Time Gate 0.880 ms)
  SFz40: dB/dt Z Component Channel 40 (Time Gate 3.521 ms)
  Dose: Exposure Dose (nGy/h)
  eThppm: Equivalent Thorium (eTh)
  eUppm: Uranium Equivalent Concentration (eU)
  Kperc: Potassium Levels (K)
  rThK: Thorium/Potassium Ratio

  A Geosoft .GRD file has a .GI metadata file associated with it, containing grid projection information. A grid cell size of 25 metres was used.

- Maps at 1:20,000 scale in Geosoft MAP format, as follows:

GL120208_20k_dBdt:	dB/dt profiles Z Component, Time Gates 0.220 – 7.036 ms in linear – logarithmic scale.
GL120208_20k_Bfield:	B-field profiles Z Component, Time Gates 0.220 – 7.036 ms in linear – logarithmic scale.
GL120208_20k_BFz36:	B-field late time Z Component Channel 36, Time Gate 2.021 ms colour image.
GL120208_20k_TMI:	Total Magnetic Intensity (TMI) colour image and contours.
GL120208_20k_TauSF:	dB/dt Calculated Time Constant (Tau) with contours of anomaly areas of the Calculated Vertical Derivative of TMI
GL120208_20k_SFxFF20:	Fraser Filtered X Component dB/dt, Channel 20, Time Gate 0.220 ms.
GL120208_20k_TotHGrad:	Magnetic Total Horizontal Gradient colour image.
GL120208_20k_TiltDrv:	Magnetic Tilt-Angle Derivative of TMI colour image.
GL120208_20k_Ternary:	Ternary Radiometric colour image
GL120208_20k_Kperc:	Gamma Ray Spectrometer Percent Potassium levels colour image.
GL120208_20k_eUppm:	Gamma Ray Spectrometer equivalent Uranium levels colour image.
GL120208_20k_eThppm:	Gamma Ray Spectrometer equivalent Thorium levels colour image.
GL120208_20k_rThK:	Gamma Ray Spectrometer equivalent Thorium / Potassium ratio colour image.
GL120208_20k_Dose:	Gamma Ray Spectrometer Expose Dose colour image.

  Maps are also presented in PDF format.

- The topographic data base was derived from DIVA-GIS at 1:1,000,000 scale (http://www.diva-gis.org/gdata)

- A Google Earth file *GL120208_FP.kml* showing the flight path of the block is included. Free versions of Google Earth software from: http://earth.google.com/download-earth.html

6. CONCLUSIONS AND RECOMMENDATIONS

A helicopter-borne versatile time domain electromagnetic (VTEM^{plus}), horizontal magnetic gradiometer and gamma-ray spectrometry geophysical survey has been completed over the Sagar Property situated at Otelnuk, Quebec, Canada.

The total area coverage is 107 km^2. Total survey line coverage is 1114 line kilometres. The principal sensors included a Time Domain EM system and horizontal magnetic gradiometer using two cesium magnetometers and using RSI ARGS RSX-5 spectrometer system. Results have been presented as stacked profiles, and contour colour images at a scale of 1:20,000. A formal Interpretation has not been included or requested.

Based on the geophysical results obtained, the area has conductors that can be considered as structural conductors and some as local targets *(See Appendix C RDI).* There is a correlation between TEM, magnetic and radiometric anomalies and features.

There are several linear conductors over the area. The long conductive structures are oriented NW-SE, and they are strongly associated with the magnetic anomalies. At the central and eastern part of the block, there are some structural conductors that are oriented SW-NE, and they are also associated with the magnetic anomalies. According to detail resistivity depth imaging, the top of the conductors varies in depth from near surface to about 50m *(See Appendix C RDI L1870, L2430 and L2970)*.

If the conductors correspond to an exploration model on the area it is recommended picking anomalies with conductance grading and center localization of the targets, detail resistivity depth imaging and plate Maxwell modelling with test drillhole parameters prior to ground follow up and drill testing. Since the conductive zones are associated with magnetic anomalies, attendant inversion/modelling of the magnetic field is also recommended.

Respectfully submitted[2],

Nick Venter
Geotech Ltd.

Keeme Mokubung
Geotech Ltd.

Alexander Prikhodko, P.Geo., PhD (OGQ#262)
VTEM Interpretation Supervisor
Geotech Ltd.

May, 2013

[2] Final data processing of the EM, magnetic, and spectrometry data were carried out by Keeme Mokubung from the office of Geotech Ltd. in Aurora, Ontario, under the supervision of Alexander Prikhodko, P.Geo., PhD, Senior Geophysicist, VTEM Interpretation Supervisor.

APPENDIX A

SURVEY BLOCK LOCATION MAP

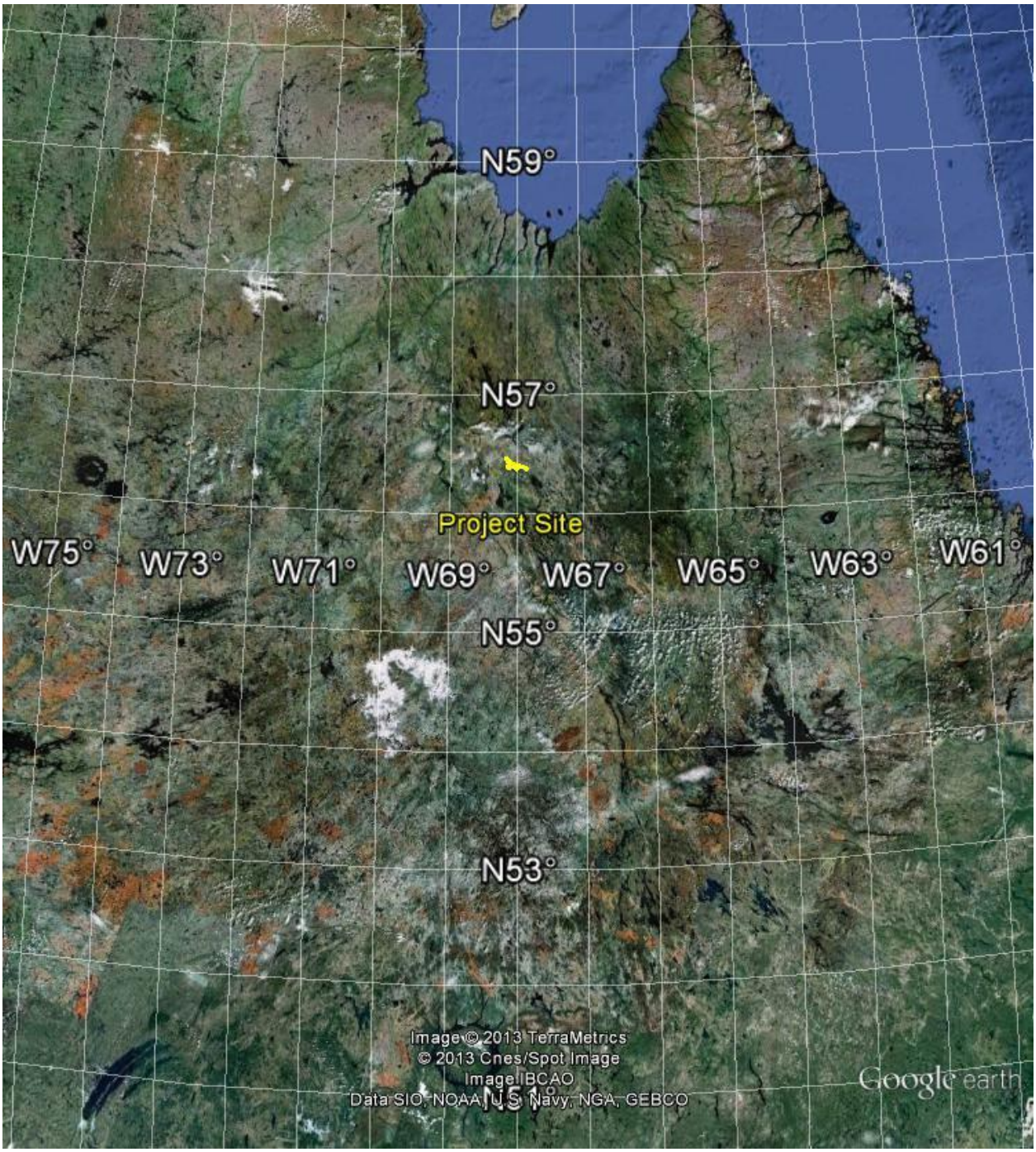

Survey Overview of the Survey Area

APPENDIX B

SURVEY BLOCK COORDINATES
(WGS 84, UTM Zone 19 North)

Sagar Property

X	Y
552300.9	6260084.9
550179.6	6257963.5
551209	6256857
551269	6256777
551351	6256293
551379.8	6255470.7
551941	6255327
551945	6254765
551946	6254643.1
552375.6	6254646.9
552455	6254427
552471.4	6253721.8
552985.3	6253728.2
552996.9	6252800.7
553417	6252804.9
552494.3	6251866.8
552528.7	6249084.2
555613.8	6249117.4
556550	6250064.6
558176.4	6250085.5
558189	6249158
560761.5	6247300
564259.1	6250730.5
565682	6250161
566962.9	6250060.3
571100.7	6247522.7

X	Y
573222	6249644
569084.2	6252181.6
567789.1	6252283.8
566380.4	6252851.9
566364.3	6252988.7
564307.7	6252957
564293.7	6253884.5
562237.6	6253853.8
561407.6	6252926.3
560708.8	6252904
560695.6	6253831.5
559153.4	6253809.7
559140.5	6254737.3
556571.1	6254702.3
556558.6	6255629.8
555531.2	6255616.2
555518.9	6256543.7
554578.4	6256541.9
554501	6256756
554479.6	6257458
554062.3	6257465.3
553501	6257594
553473	6258414
553387.3	6258917.1
552300.9	6260084.9

APPENDIX C
GEOPHYSICAL MAPS[1]

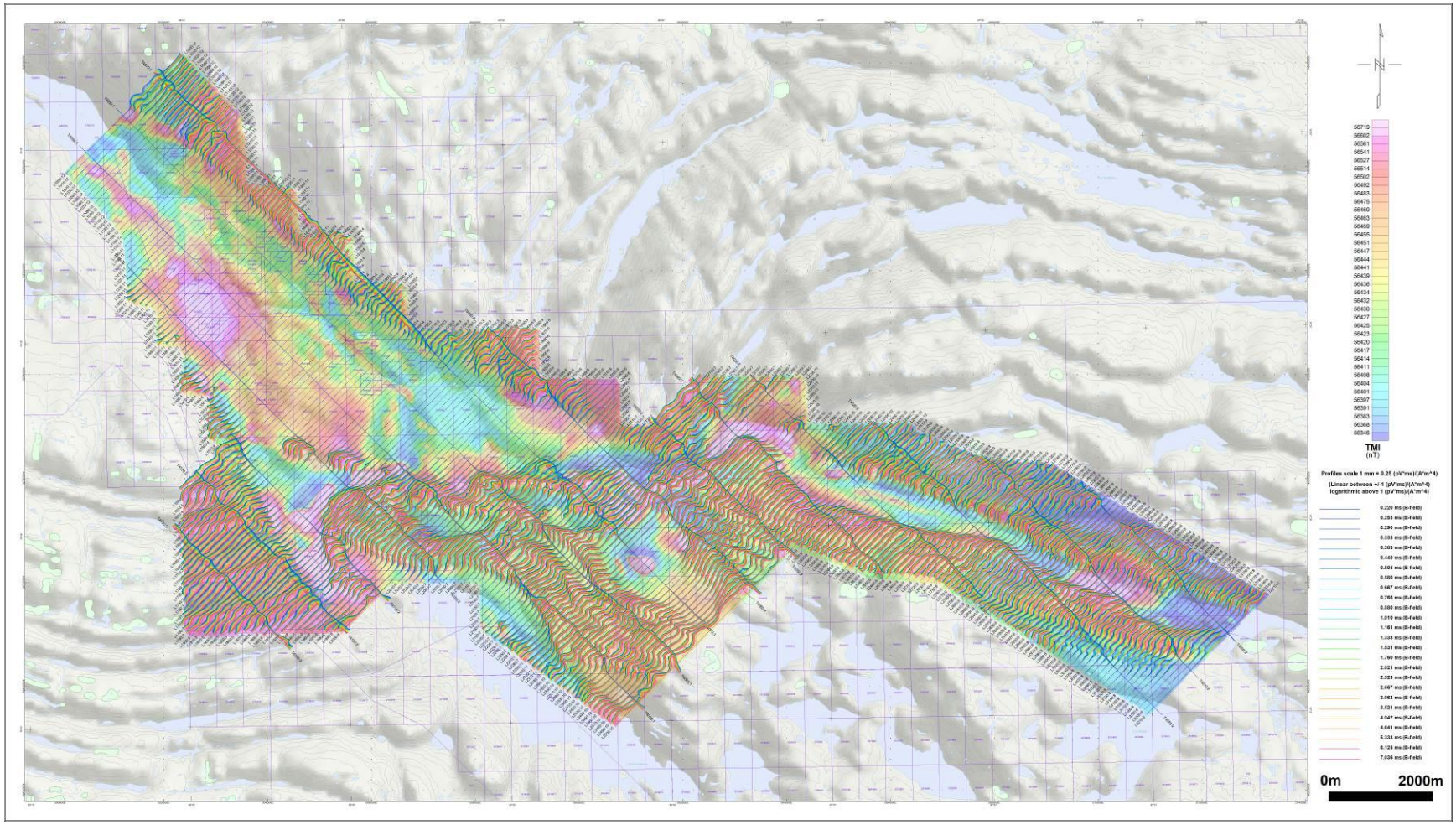

VTEM B-Field Z Component Profiles – Time Gates 0.220 – 7.036 ms – Over Total Magnetic Intensity Grid

[1] Full size geophysical maps are also available in PDF format on the final DVD

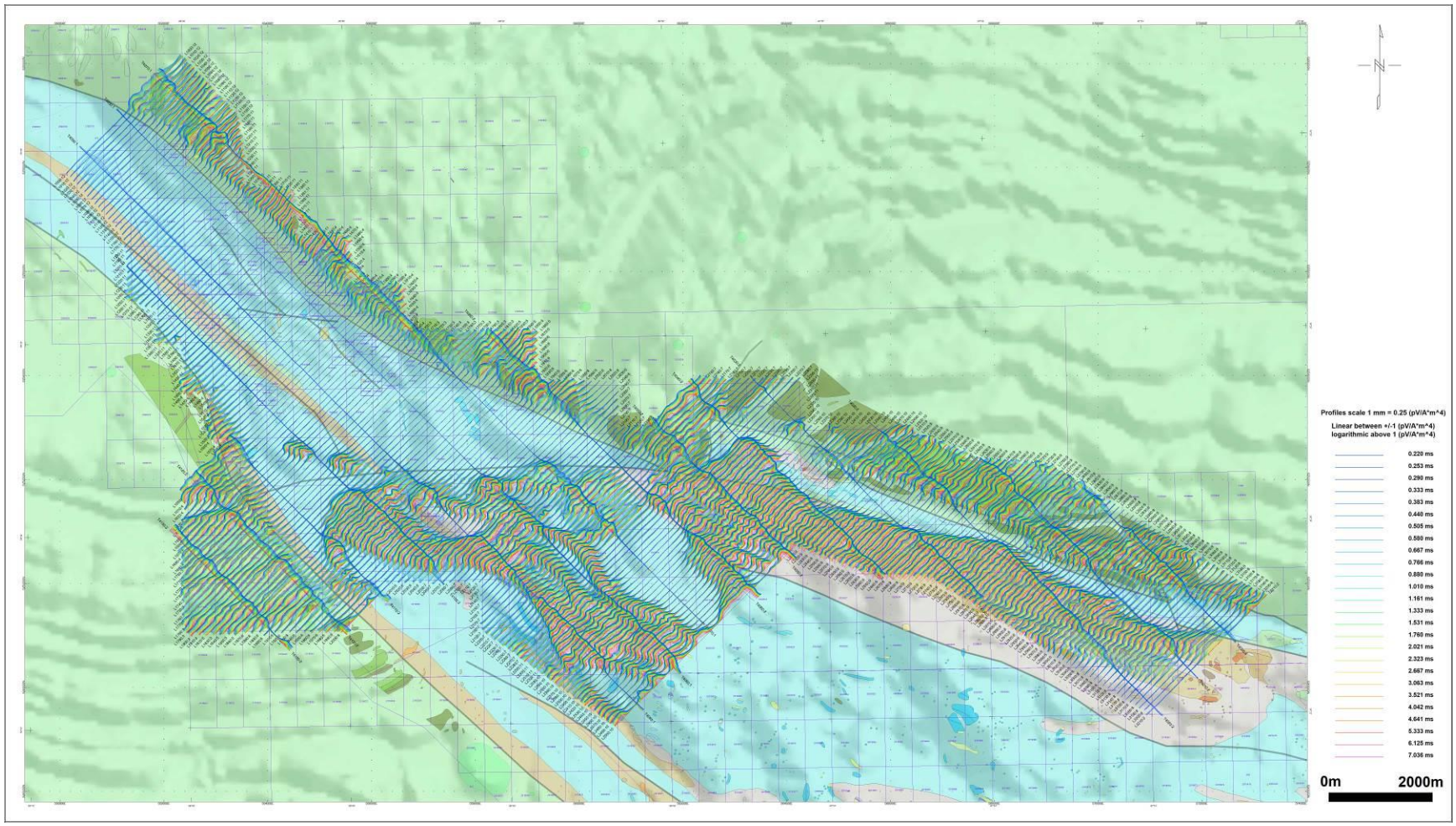

VTEM dB/dt Z Component Profiles – Time Gates 0.220 – 7.036 ms – Over Regional Geology Grid

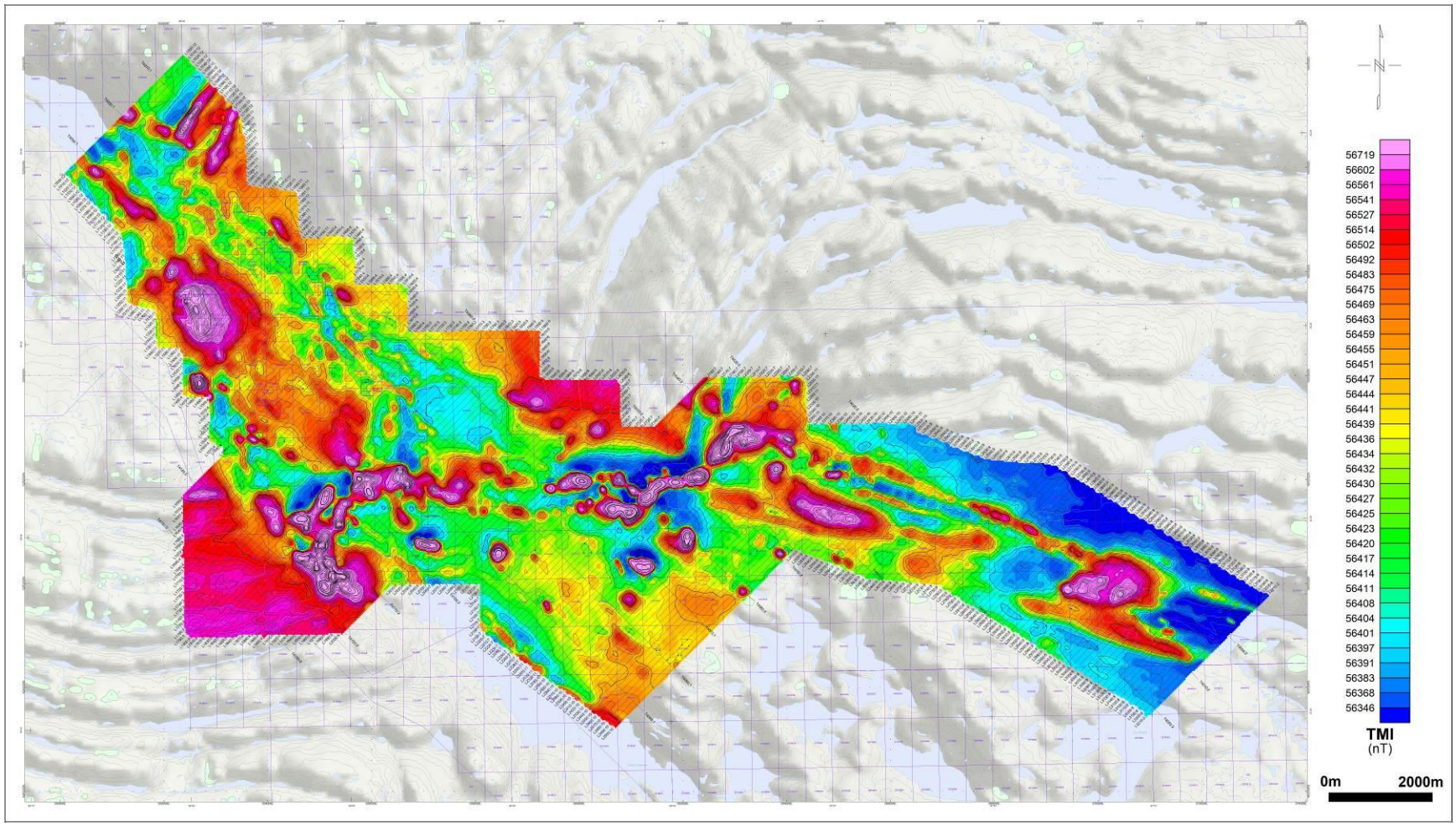

Total Magnetic Intensity (TMI)

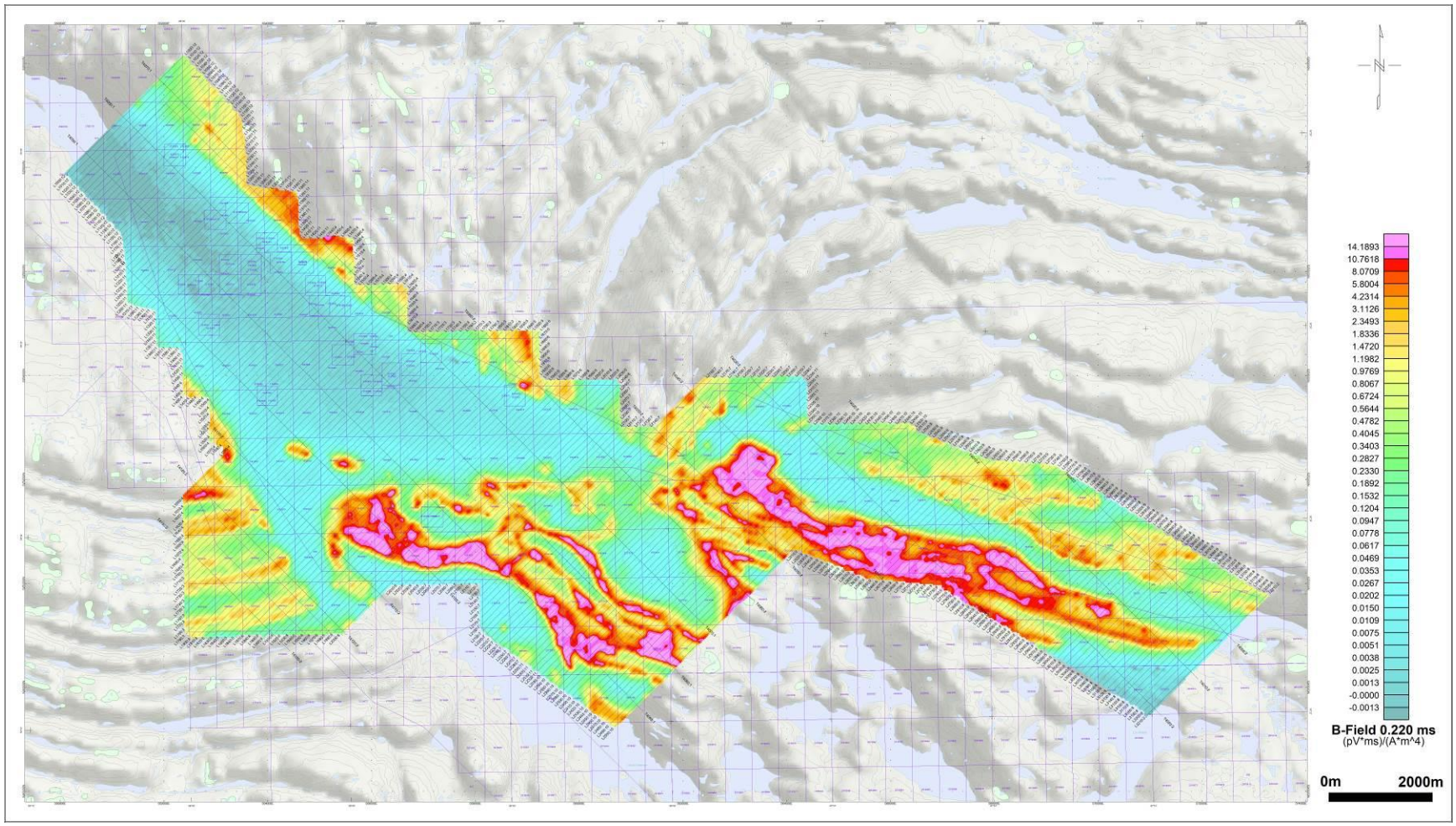

VTEM B-Field Z Component – Channel 20 – Time Gate 0.220 ms

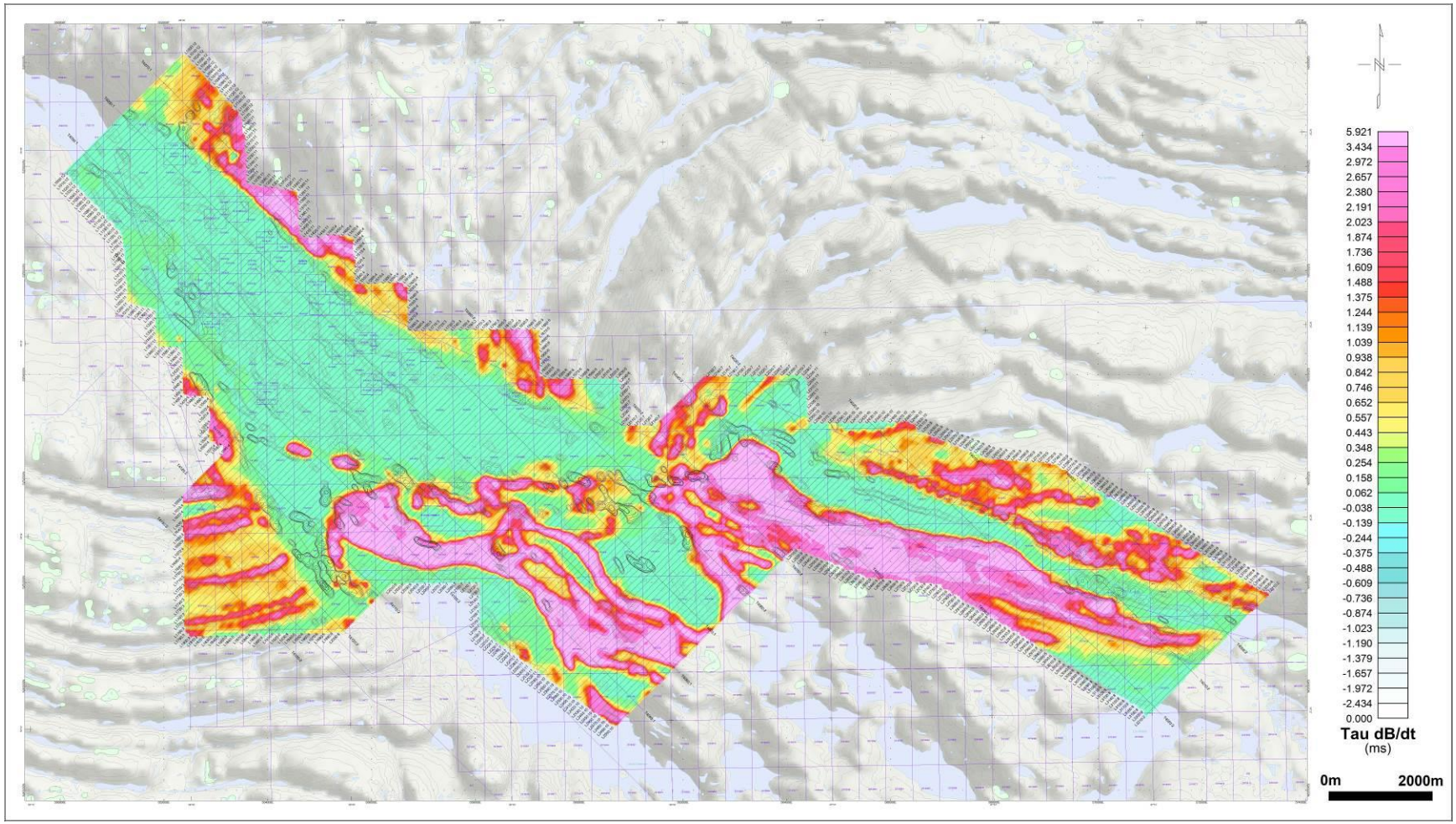

dB/dt Calculated Time Constant (Tau) with contours of anomaly areas of the Calculated Vertical Derivative of TMI

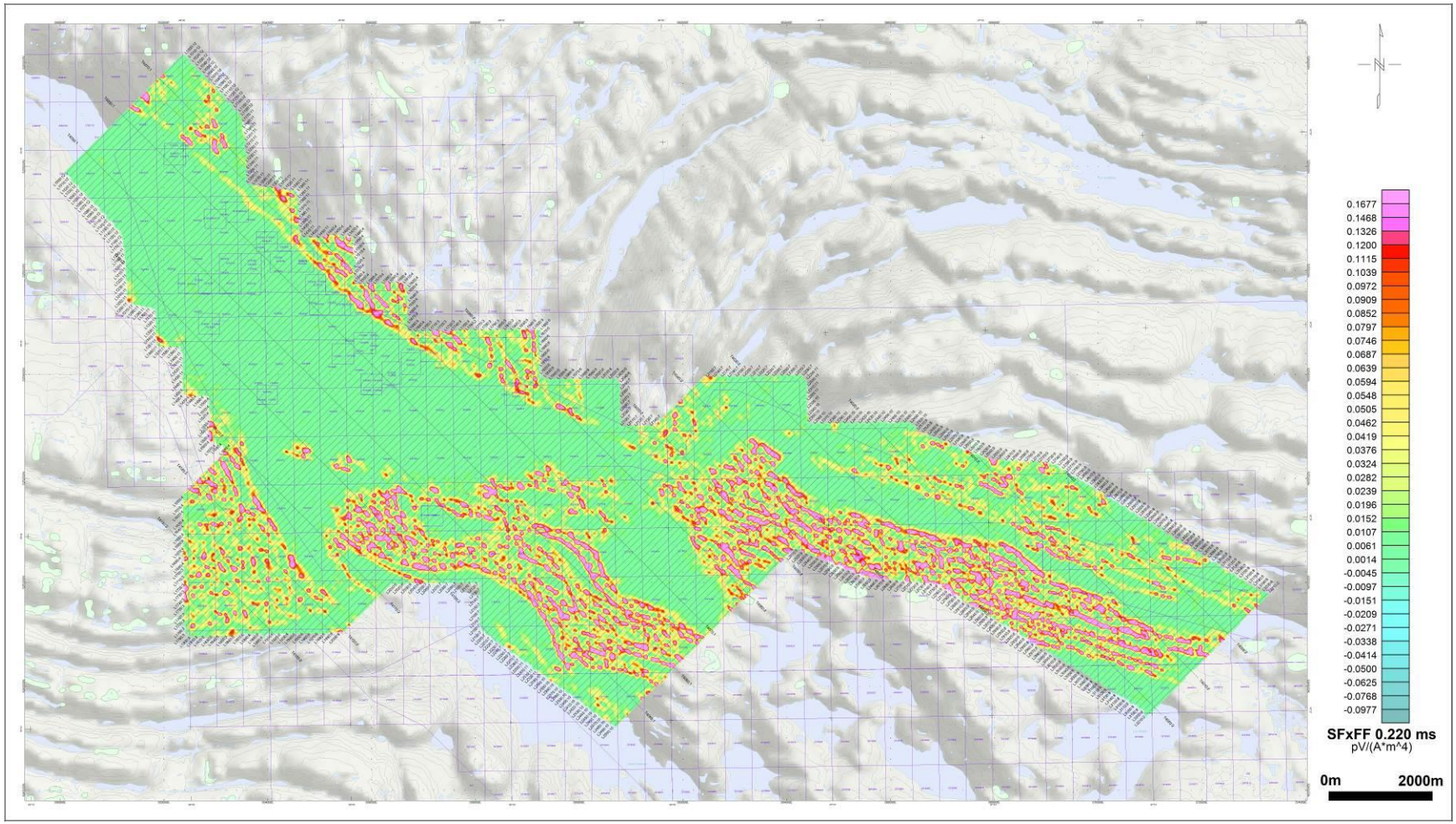

Fraser Filtered dB/dt X Component – Channel 20 – Time Gate 0.220 ms

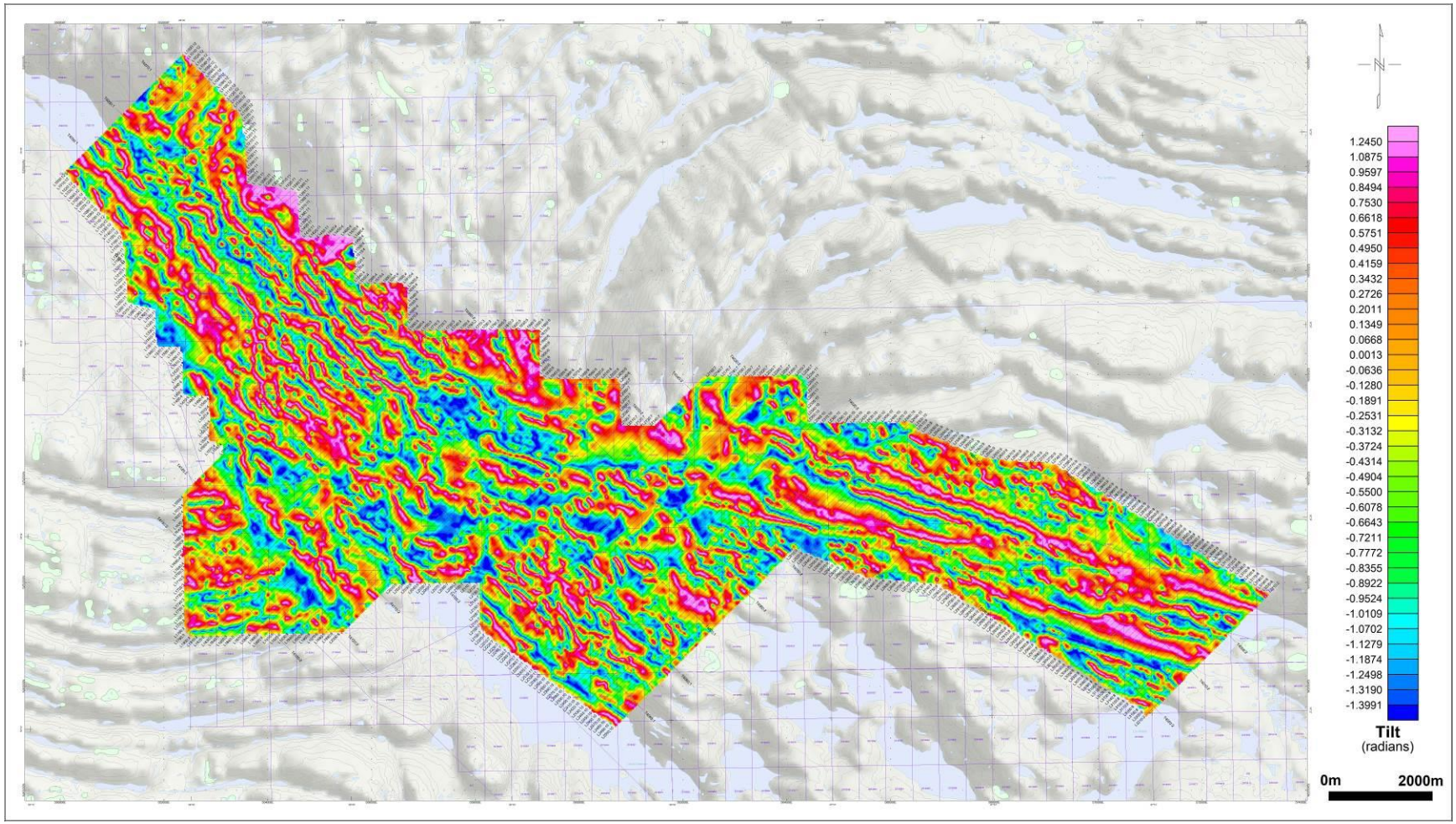

Magnetic Tilt-Angle Derivative of TMI

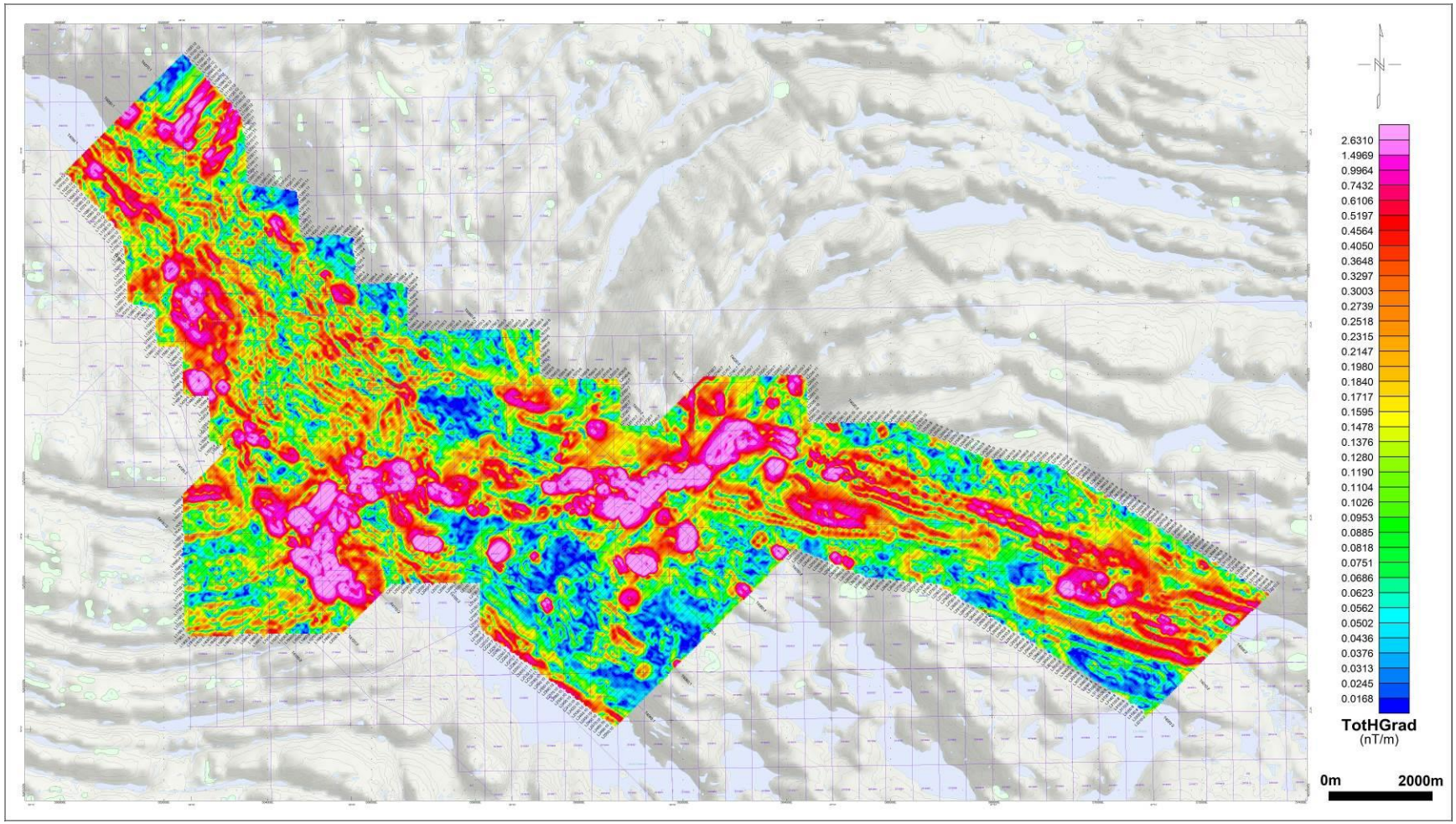

Magnetic Total Horizontal Gradient of TMI

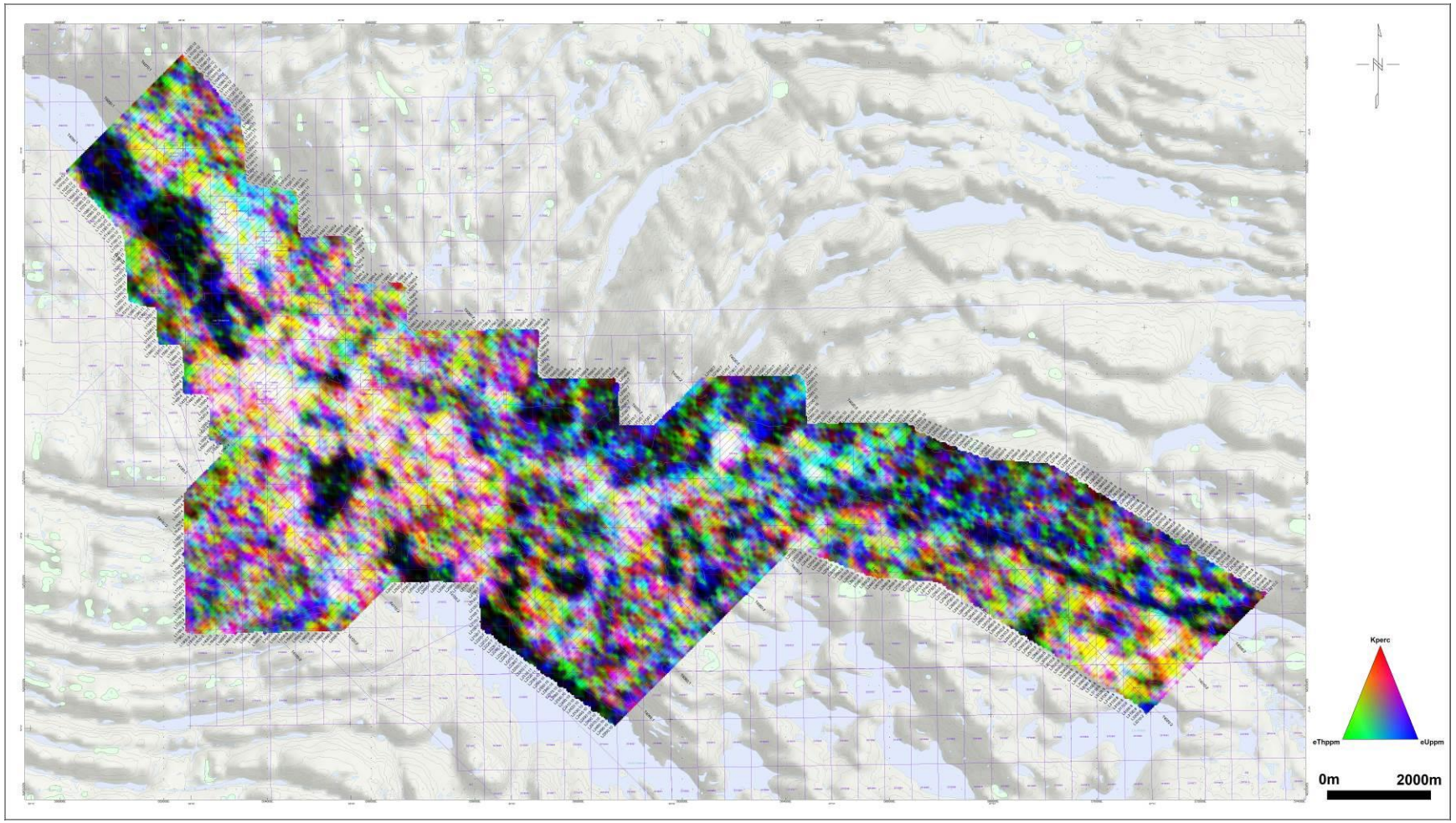

Gamma-Ray Spectrometer Ternary Map

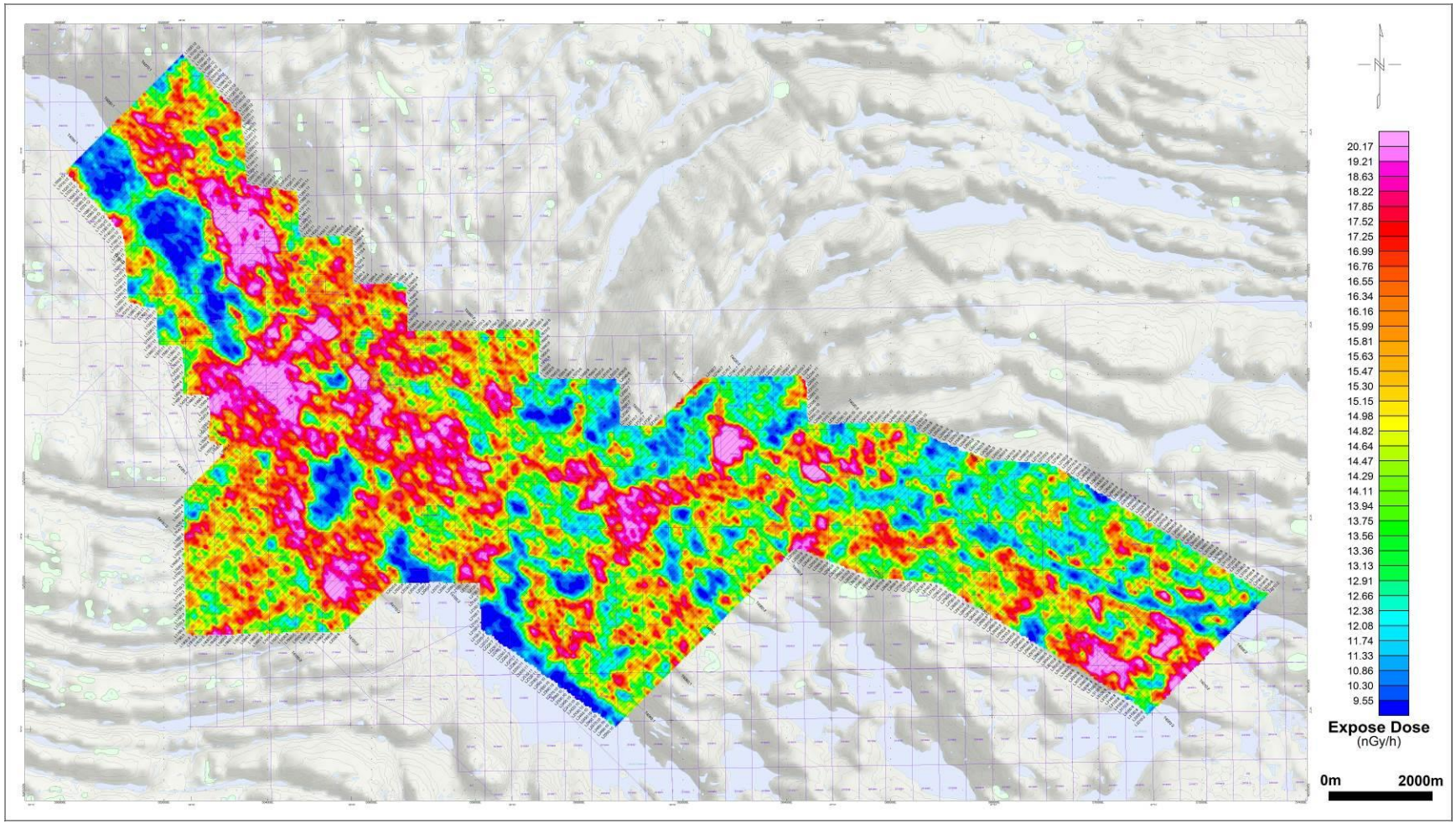

Gamma-Ray Spectrometer Expose Dose

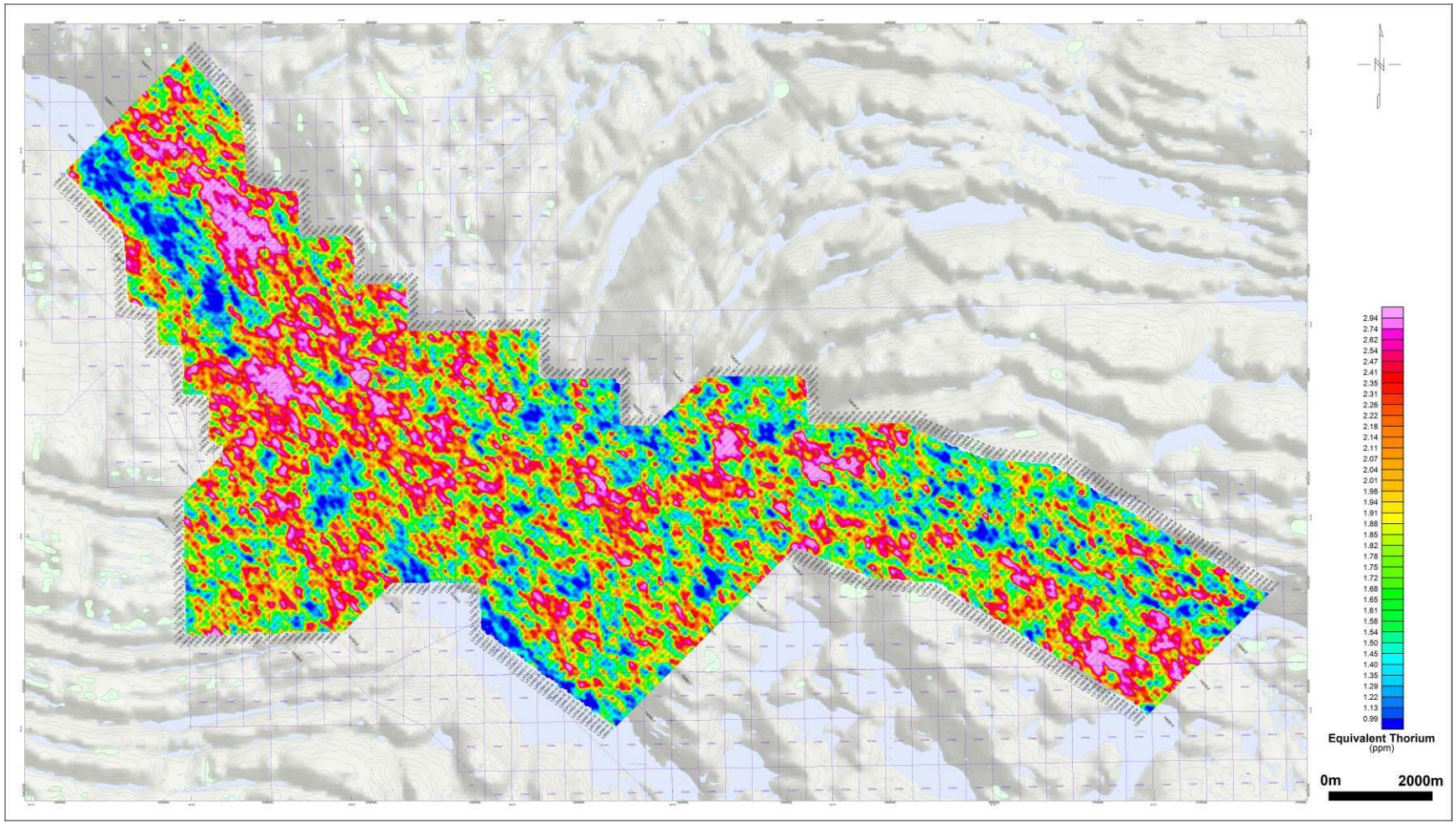

Gamma-Ray Spectrometer Equivalent Thorium Levels

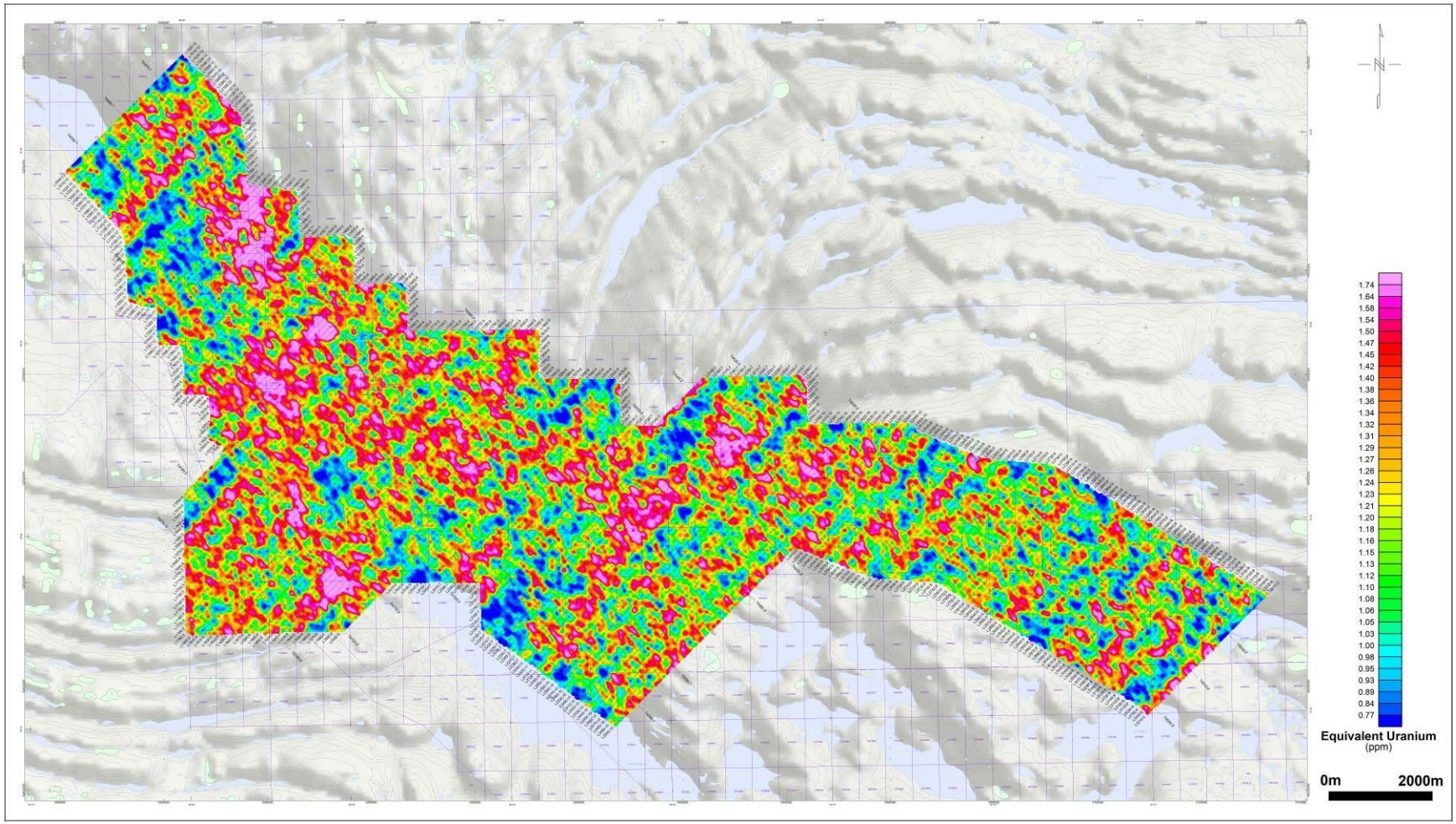

Gamma-Ray Spectrometer Equivalent Uranium Levels

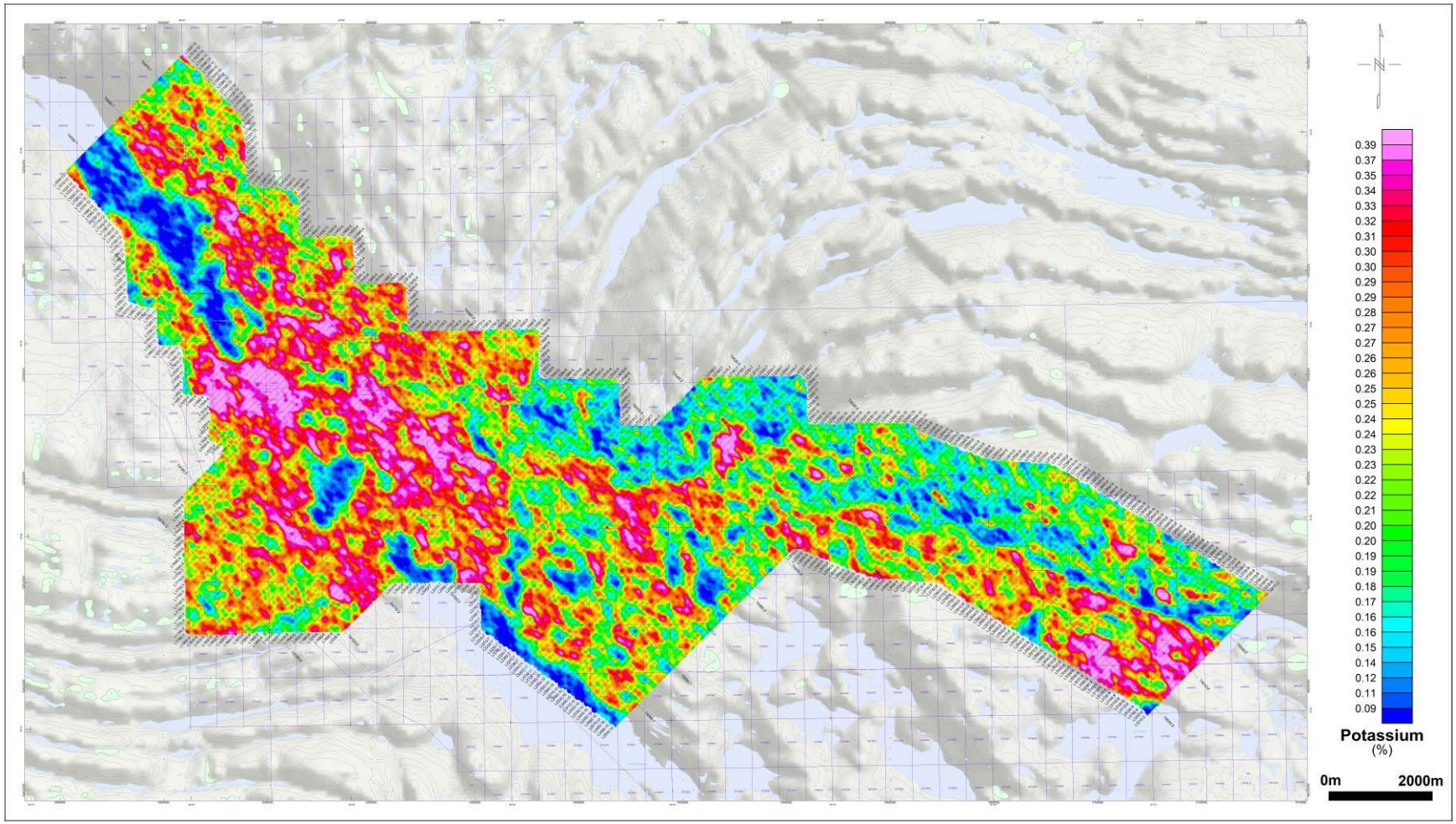

Gamma-Ray Spectrometer Percent Potassium Levels

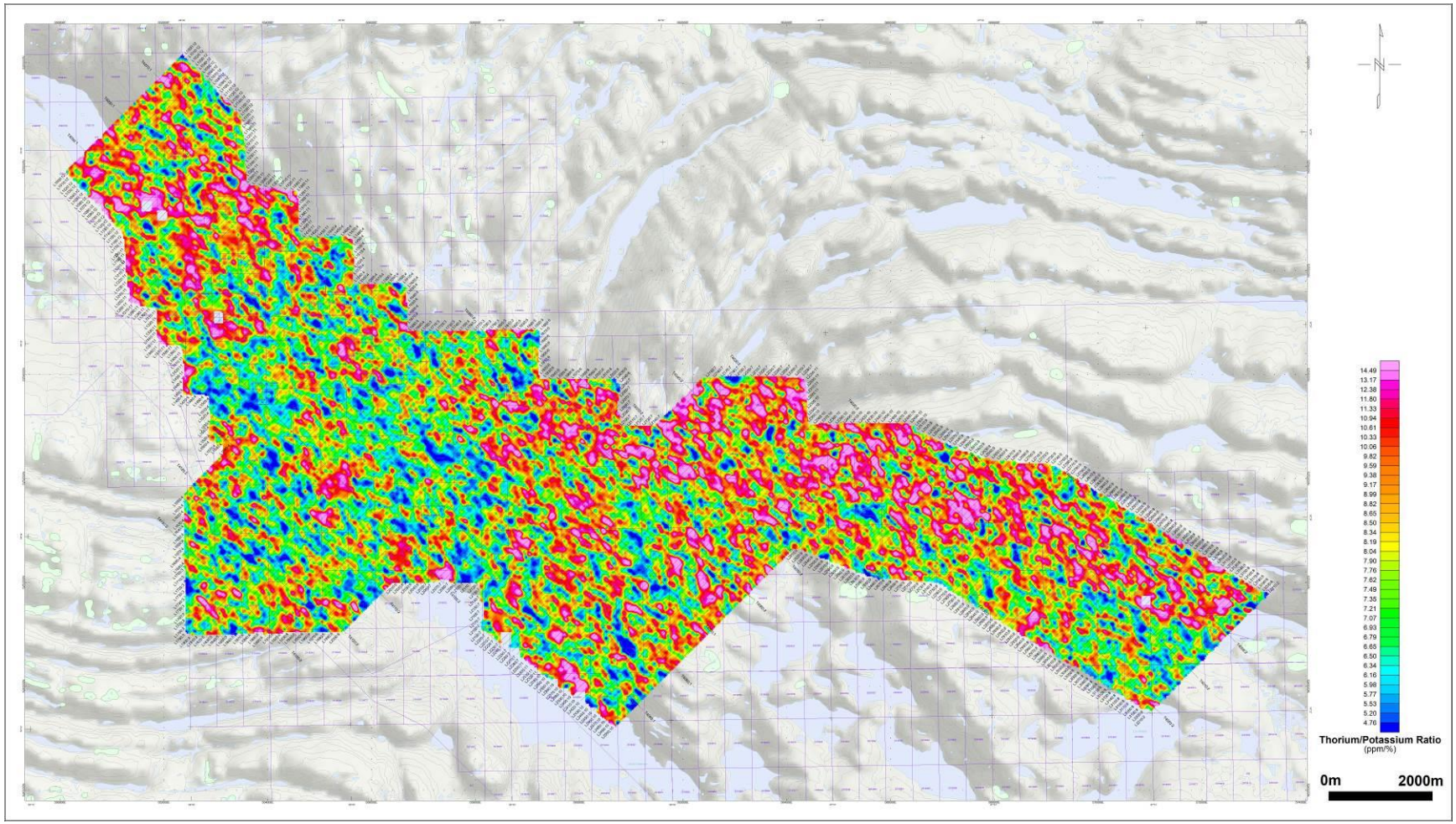

Gamma-Ray Spectrometer Thorium/Potassium Ratio

RESISTIVITY DEPTH IMAGE (RDI) MAPS

3D Resistivity-Depth Image (RDI)

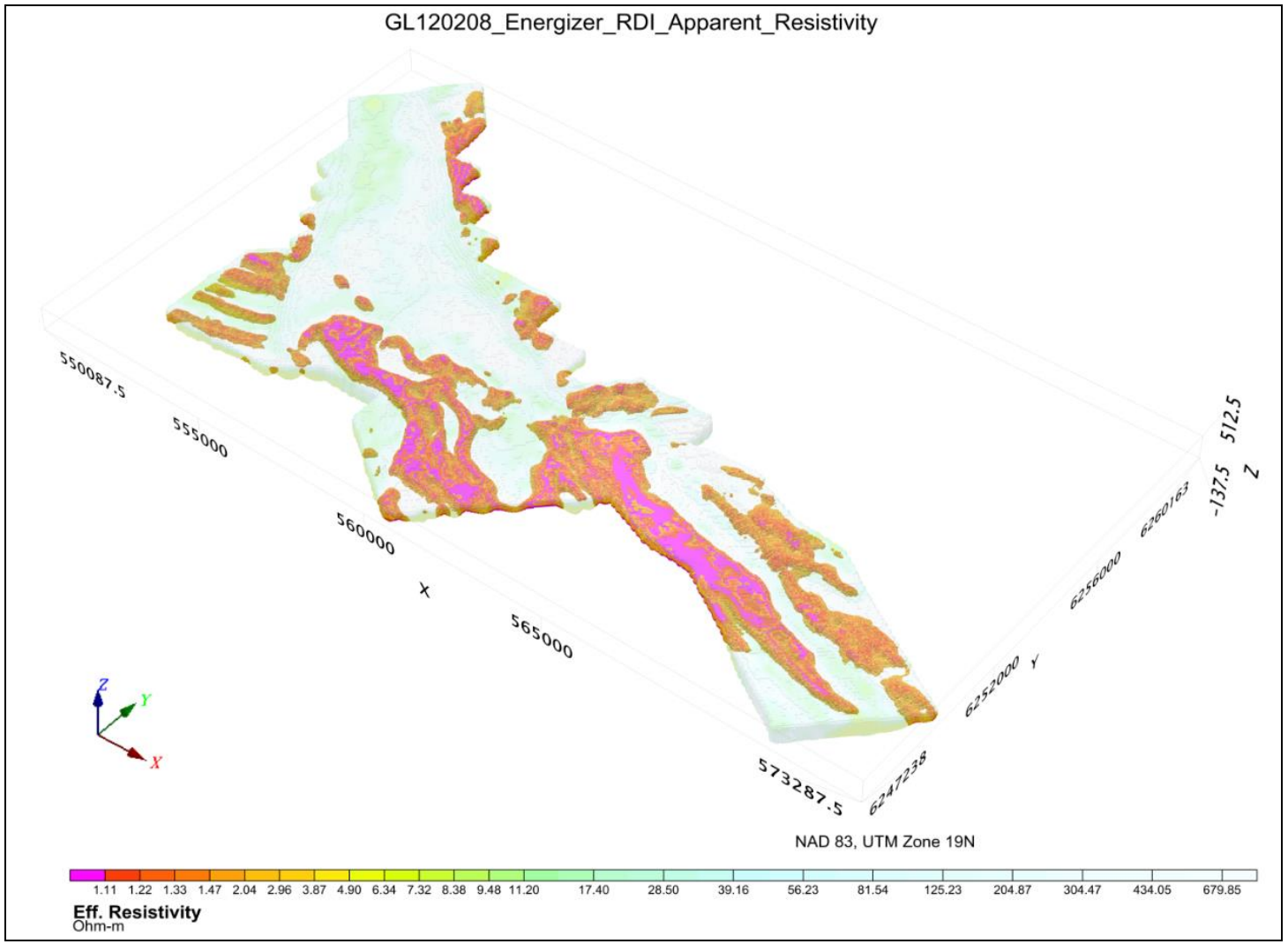

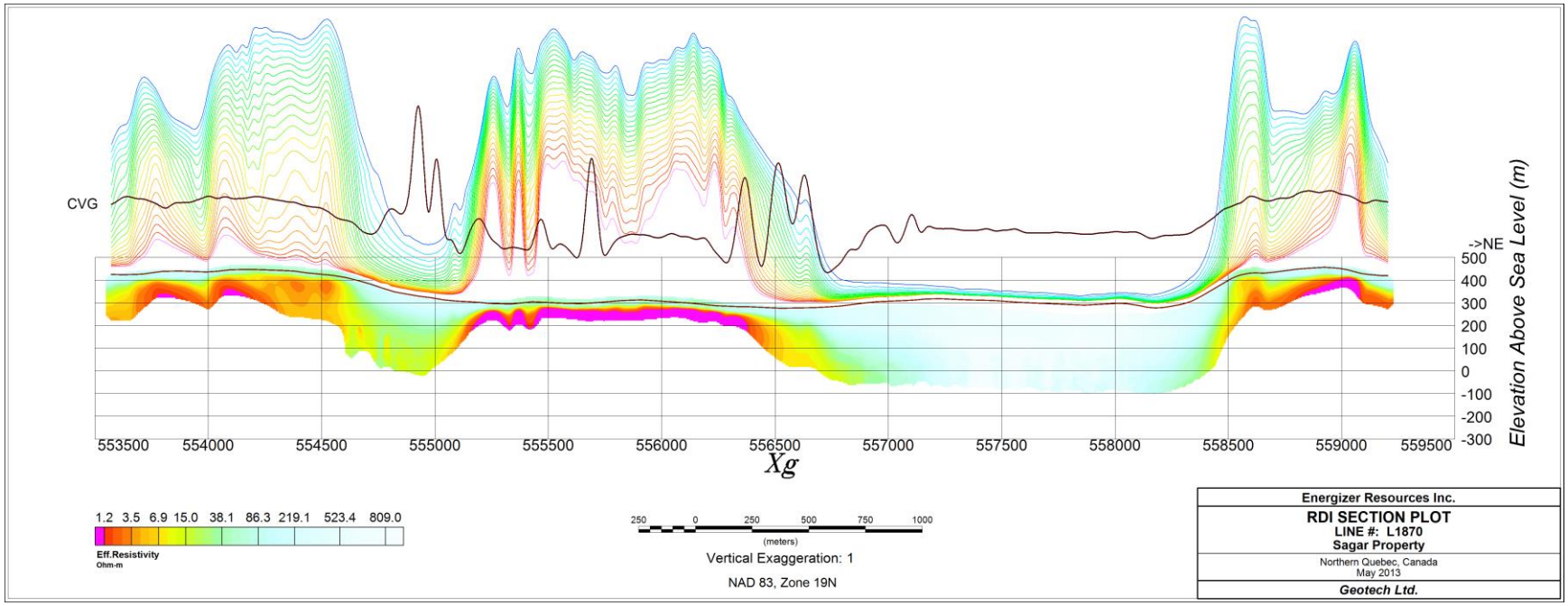
CVG
->NE
500
400
300
200
100
0
-100
-200
-300
Elevation Above Sea Level (m)
553500
554000
554500
555000
555500
556000
556500
557000
557500
558000
558500
559000
559500
Xg
1.2 3.5 6.9 15.0 38.1 86.3 219.1 523.4 809.0
Eff.Resistivity
Ohm-m
250 0 250 500 750 1000
(meters)
Vertical Exaggeration: 1
NAD 83, Zone 19N
Energizer Resources Inc.
RDI SECTION PLOT
LINE #: L1870
Sagar Property
Northern Quebec, Canada
May 2013
Geotech Ltd.

RDI – L1870

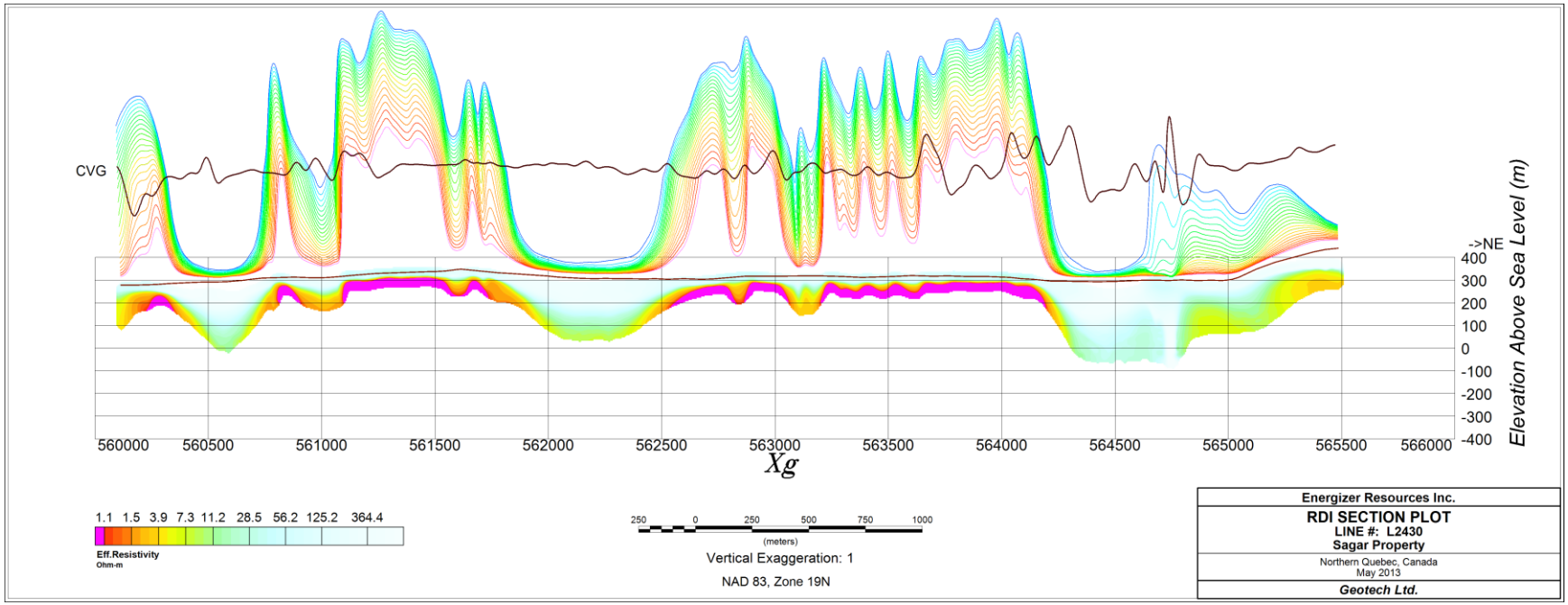
CVG
->NE
400
300
200
100
0
-100
-200
-300
-400
Elevation Above Sea Level (m)
560000
560500
561000
561500
562000
562500
563000
563500
564000
564500
565000
565500
566000
Xg
1.1 1.5 3.9 7.3 11.2 28.5 56.2 125.2 364.4
Eff.Resistivity
Ohm-m
250 0 250 500 750 1000
(meters)
Vertical Exaggeration: 1
NAD 83, Zone 19N
Energizer Resources Inc.
RDI SECTION PLOT
LINE #: L2430
Sagar Property
Northern Quebec, Canada
May 2013
Geotech Ltd.

RDI – L2430

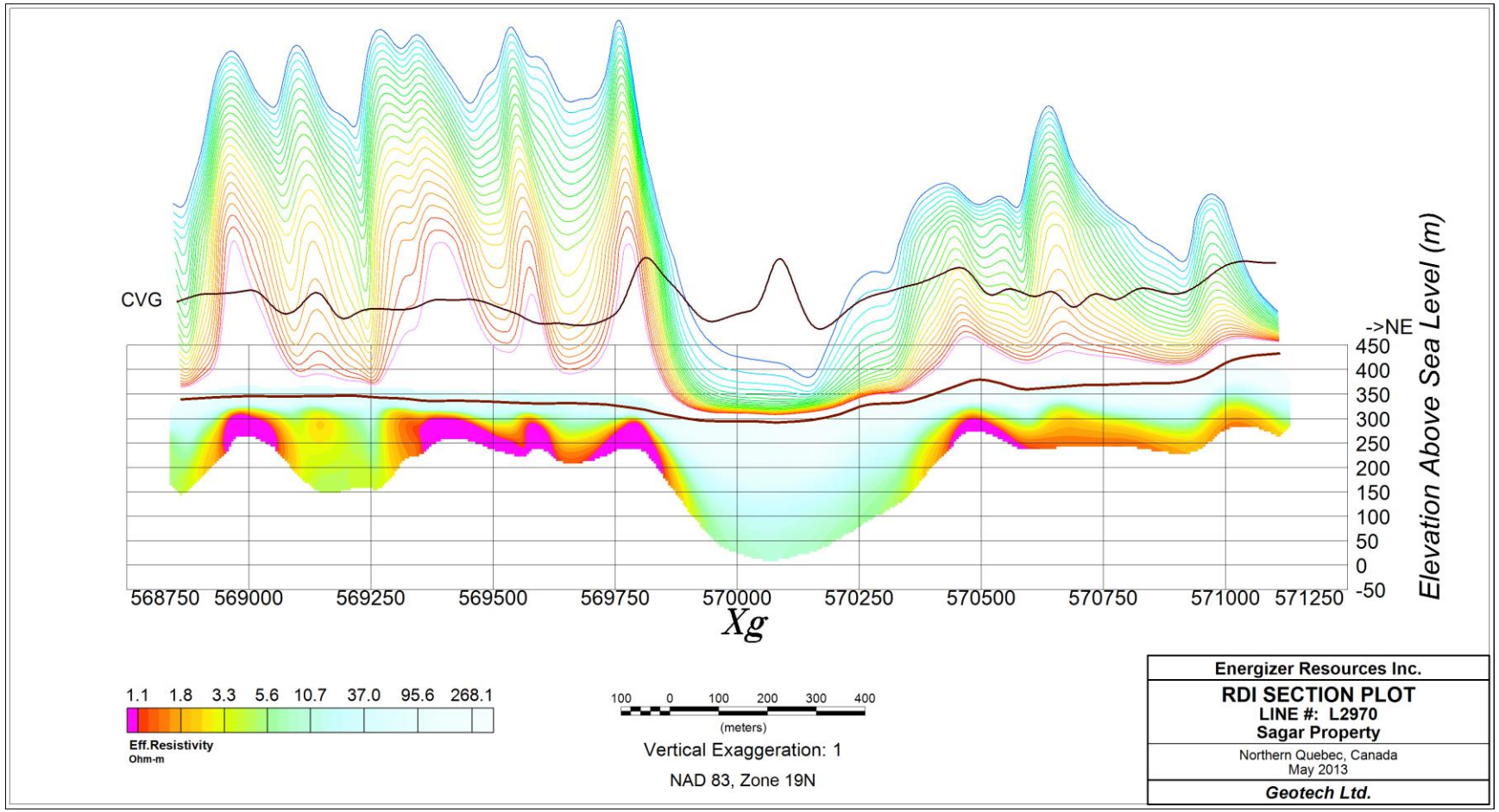
CVG
->NE
450
400
350
300
250
200
150
100
50
0
-50
Elevation Above Sea Level (m)
568750 569000 569250 569500 569750 570000 570250 570500 570750 571000 571250
Xg
1.1 1.8 3.3 5.6 10.7 37.0 95.6 268.1
Eff.Resistivity
Ohm-m
100 0 100 200 300 400
(meters)
Vertical Exaggeration: 1
NAD 83, Zone 19N
Energizer Resources Inc.
RDI SECTION PLOT
LINE #: L2970
Sagar Property
Northern Quebec, Canada
May 2013
Geotech Ltd.

RDI – L2970

APPENDIX D

GENERALIZED MODELING RESULTS OF THE VTEM SYSTEM

Introduction

The VTEM system is based on a concentric or central loop design, whereby, the receiver is positioned at the centre of a transmitter loop that produces a primary field. The wave form is a bi-polar, modified square wave with a turn-on and turn-off at each end.

During turn-on and turn-off, a time varying field is produced (dB/dt) and an electro-motive force (emf) is created as a finite impulse response. A current ring around the transmitter loop moves outward and downward as time progresses. When conductive rocks and mineralization are encountered, a secondary field is created by mutual induction and measured by the receiver at the centre of the transmitter loop.

Efficient modeling of the results can be carried out on regularly shaped geometries, thus yielding close approximations to the parameters of the measured targets. The following is a description of a series of common models made for the purpose of promoting a general understanding of the measured results.

A set of models has been produced for the Geotech VTEM® system dB/dT Z and X components (see models D1 to D15). The Maxwell ^{TM} modeling program (EMIT Technology Pty. Ltd. Midland, WA, AU) used to generate the following responses assumes a resistive half-space. The reader is encouraged to review these models, so as to get a general understanding of the responses as they apply to survey results. While these models do not begin to cover all possibilities, they give a general perspective on the simple and most commonly encountered anomalies.

As the plate dips and departs from the vertical position, the peaks become asymmetrical.

As the dip increases, the aspect ratio (Min/Max) decreases and this aspect ratio can be used as an empirical guide to dip angles from near 90º to about 30º. The method is not sensitive enough where dips are less than about 30º.

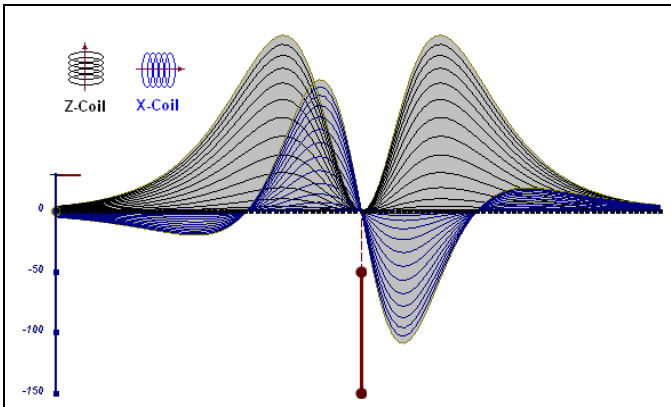

Figure D-1: vertical thin plate

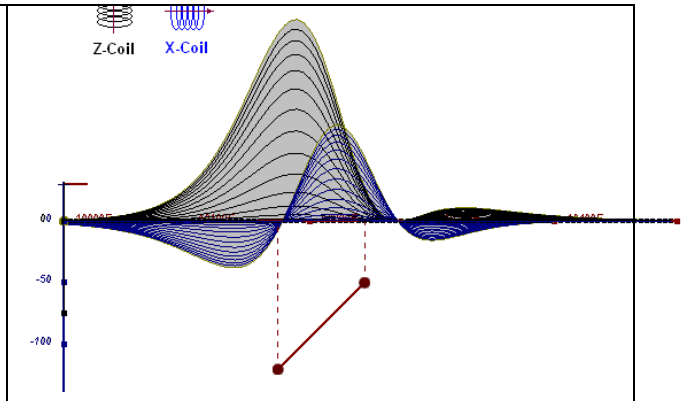

Figure D-2: inclined thin plate

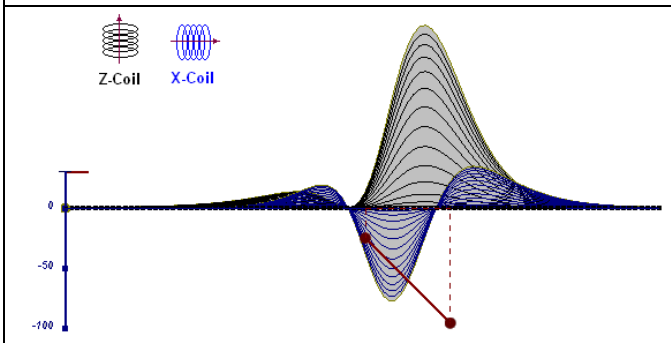

Figure D-3: inclined thin plate

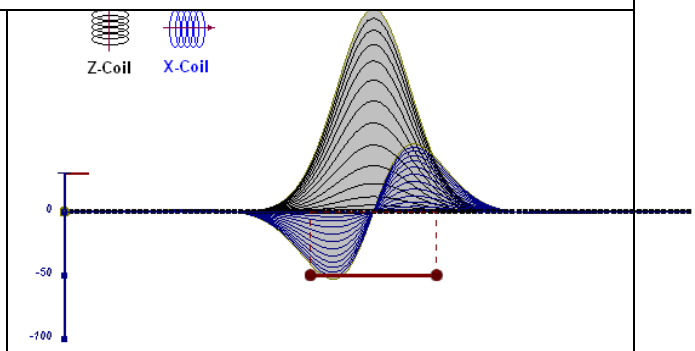

Figure D-4: horizontal thin plate

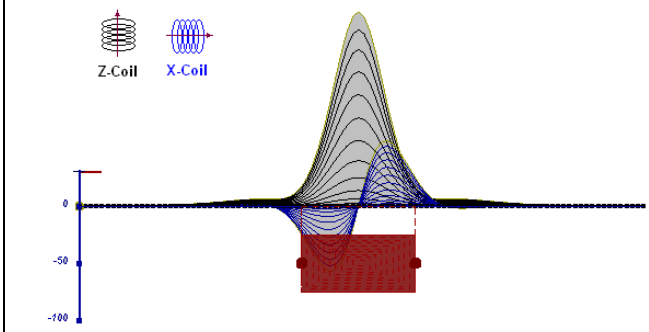

Figure D-5: horizontal thick plate (linear scale of the response)

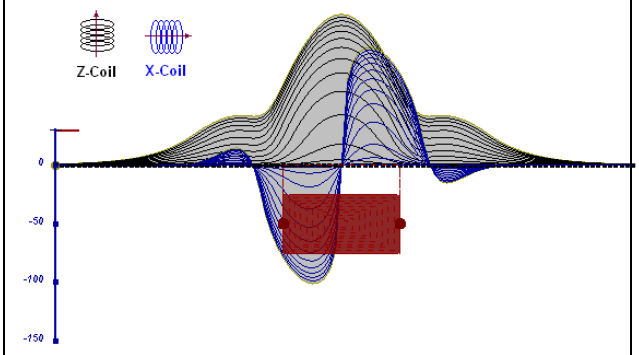

Figure D-6: horizontal thick plate (log scale of the response)

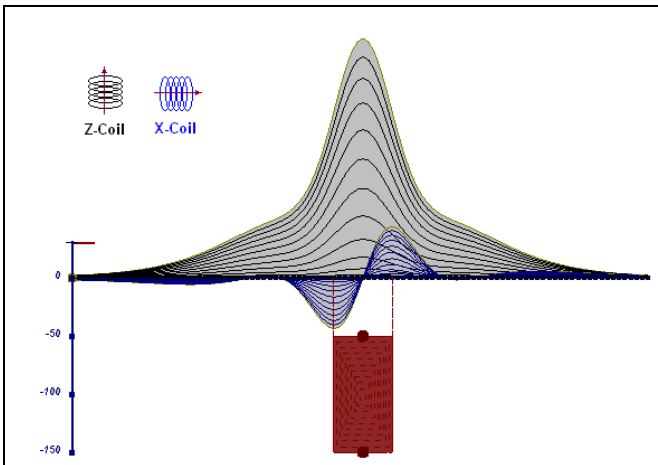

Figure D-7: vertical thick plate (linear scale of the response). 50 m depth

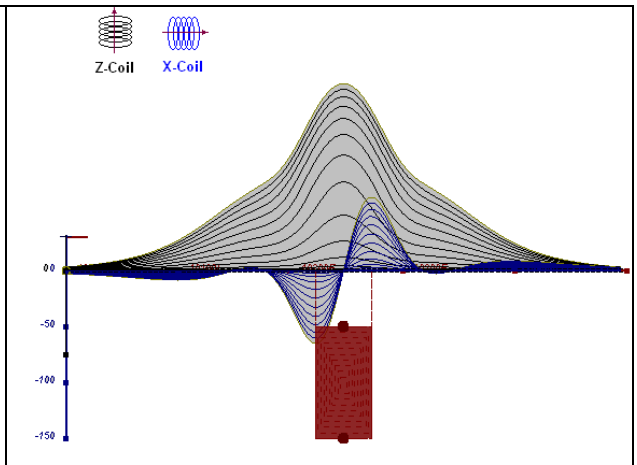

Figure D-8: vertical thick plate (log scale of the response). 50 m depth

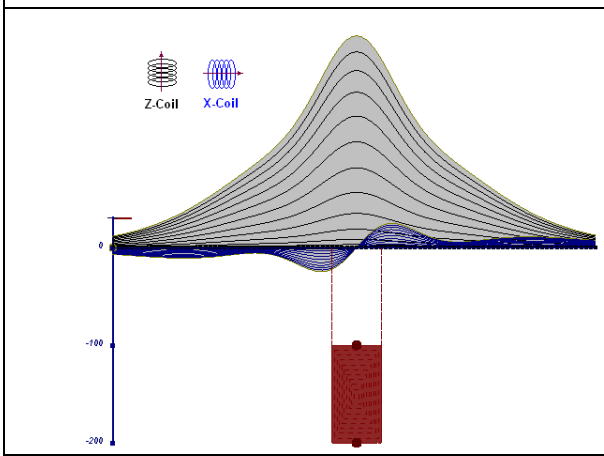

Figure D-9: vertical thick plate (linear scale of the response). 100 m depth

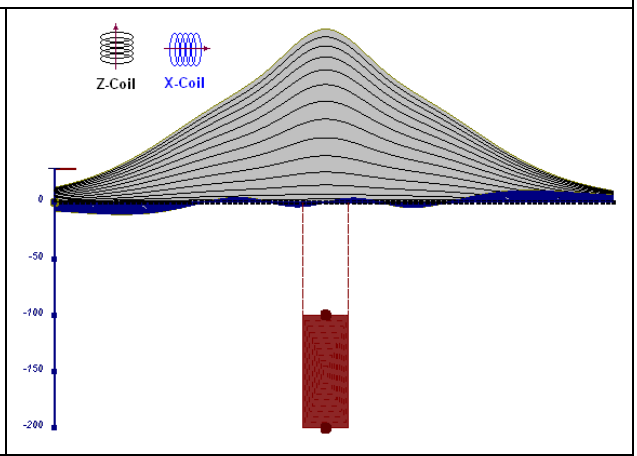

Figure D-10: vertical thick plate (linear scale of the response). Depth / horizontal thickness=2.5

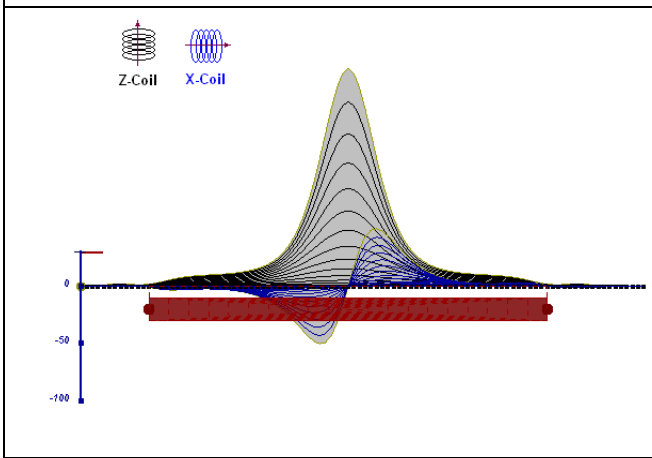

Figure D-10: horizontal thick plate (linear scale of the response)

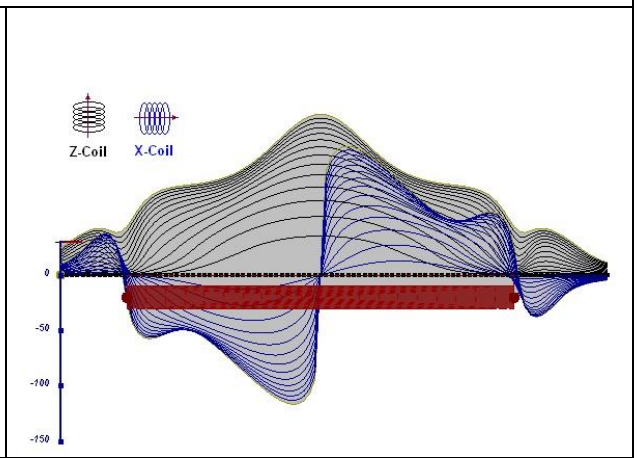

Figure D-11: horizontal thick plate (log scale of the response)

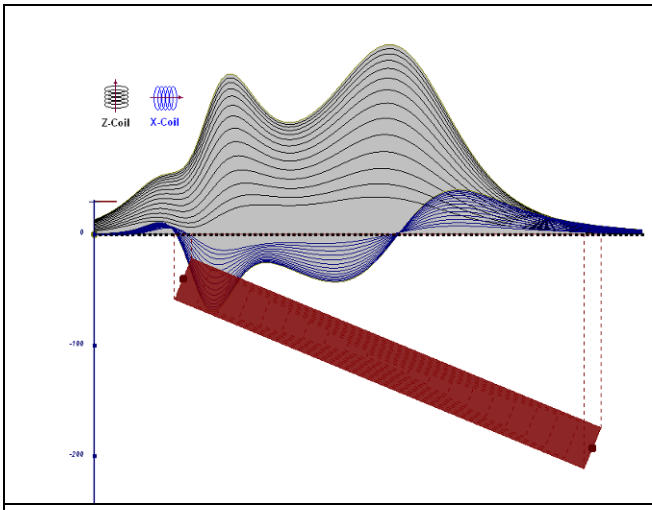

Figure D-12: inclined long thick plate

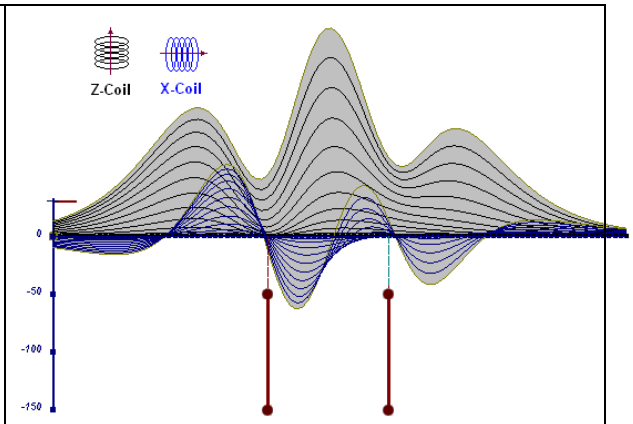

Figure D-13: two vertical thin plates

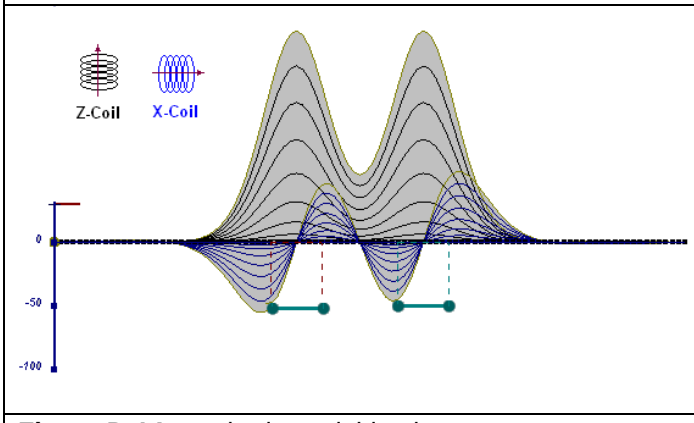

Figure D-14: two horizontal thin plates

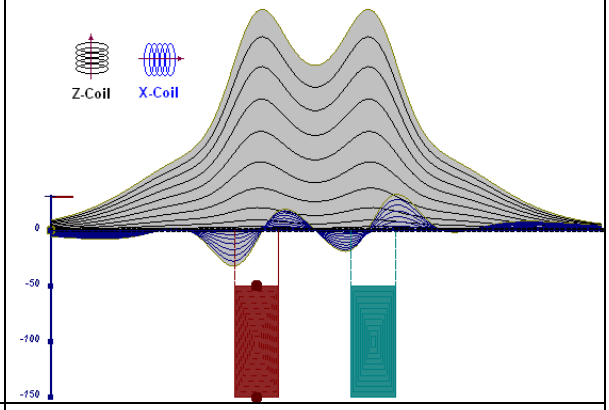

Figure D-15: two vertical thick plates

The same type of target but with different thickness, for example, creates different form of the response:

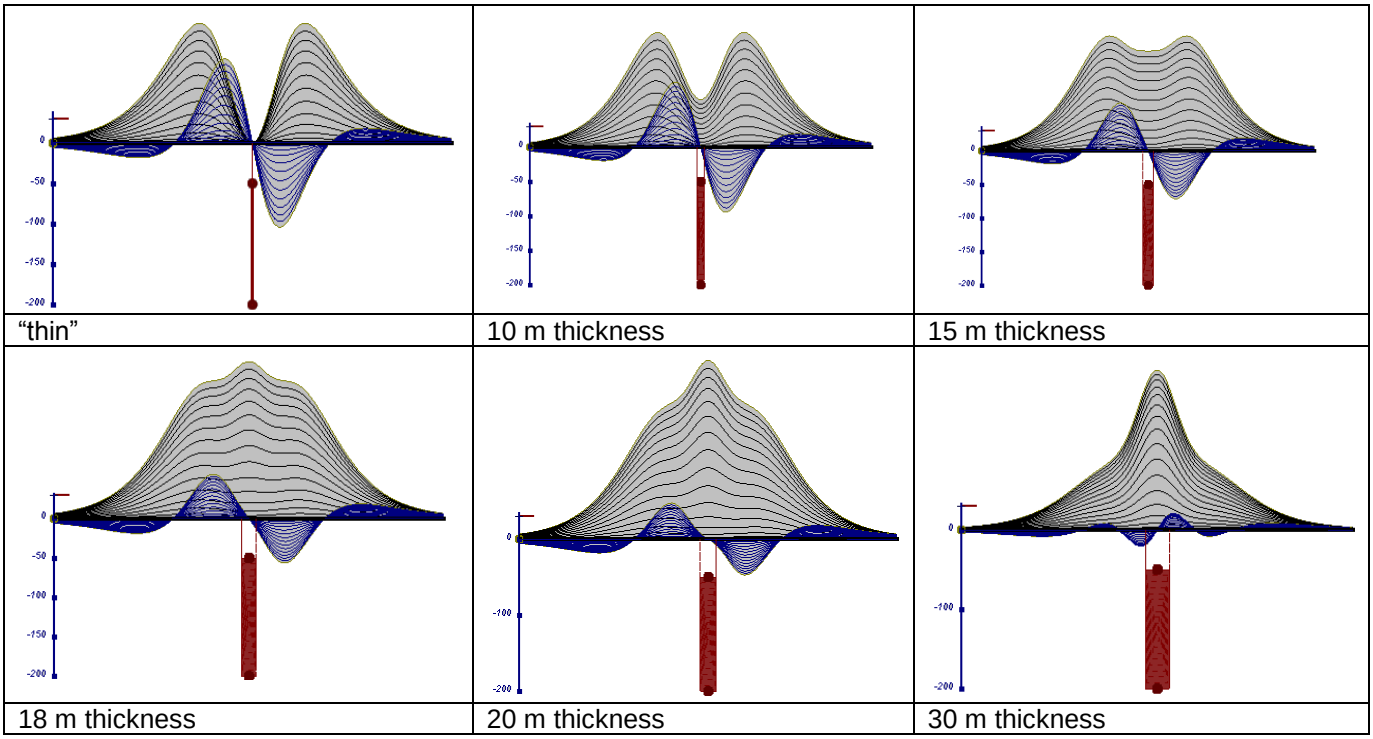

Figure D-16: Conductive vertical plate, depth 50 m, strike length 200 m, depth extends 150 m.

Alexander Prikhodko, PhD, P.Geo
Geotech Ltd.

September 2010

APPENDIX E

EM TIME CONSTANT (TAU) ANALYSIS

Estimation of time constant parameter[1] in transient electromagnetic method is one of the steps toward the extraction of the information about conductance's beneath the surface from TEM measurements.

The most reliable method to discriminate or rank conductors from overburden, background or one and other is by calculating the EM field decay time constant (TAU parameter), which directly depends on conductance despite their depth and accordingly amplitude of the response.

Theory

As established in electromagnetic theory, the magnitude of the electro-motive force (emf) induced is proportional to the time rate of change of primary magnetic field at the conductor. This emf causes eddy currents to flow in the conductor with a characteristic transient decay, whose Time Constant (Tau) is a function of the conductance of the survey target or conductivity and geometry (including dimensions) of the target. The decaying currents generate a proportional secondary magnetic field, the time rate of change of which is measured by the receiver coil as induced voltage during the Off time.

The receiver coil output voltage ($\mathbf{e_0}$) is proportional to the time rate of change of the secondary magnetic field and has the form,

$$e_0 \alpha (1 / \tau) e^{-(t/\tau)}$$

Where,
τ = L/R is the characteristic time constant of the target (TAU)
R = resistance
L = inductance

From the expression, conductive targets that have small value of resistance and hence large value of τ yield signals with small initial amplitude that decays relatively slowly with progress of time. Conversely, signals from poorly conducting targets that have large resistance value and small τ, have high initial amplitude but decay rapidly with time[1] (Fig. E1).

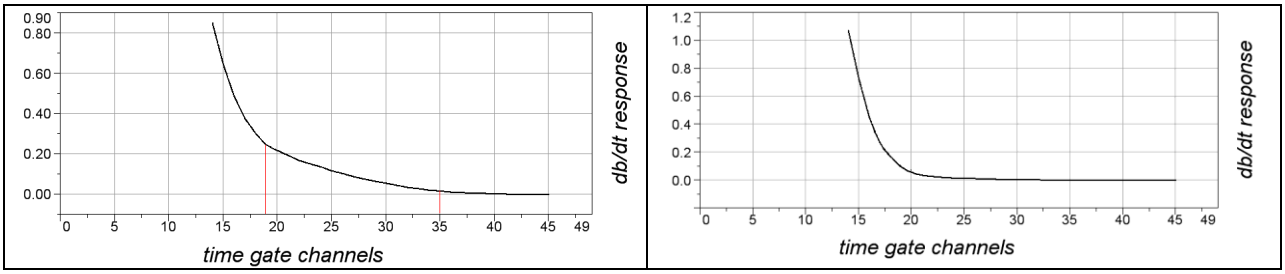

Figure E-1: Left – presence of good conductor, right – poor conductor.

[1] McNeill, JD, 1980, "Applications of Transient Electromagnetic Techniques", Technical Note TN-7 page 5, Geonics Limited, Mississauga, Ontario.

EM Time Constant (Tau) Calculation

The EM Time-Constant (TAU) is a general measure of the speed of decay of the electromagnetic response and indicates the presence of eddy currents in conductive sources as well as reflecting the "conductance quality" of a source. Although TAU can be calculated using either the measured dB/dt decay or the calculated B-field decay, dB/dt is commonly preferred due to better stability (S/N) relating to signal noise. Generally, TAU calculated on base of early time response reflects both near surface overburden and poor conductors whereas, in the late ranges of time, deep and more conductive sources, respectively. For example early time TAU distribution in an area that indicates conductive overburden is shown in Figure 2.

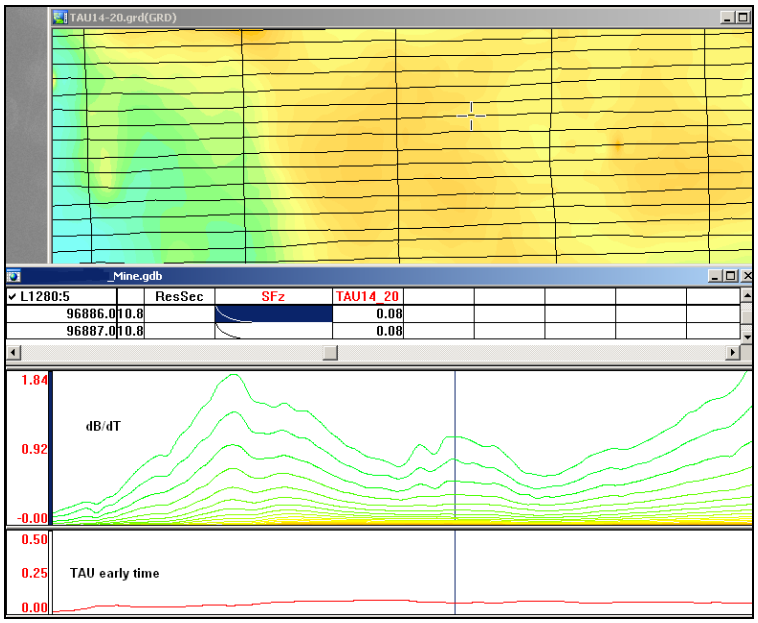

Figure E-2: Map of early time TAU. Area with overburden conductive layer and local sources.

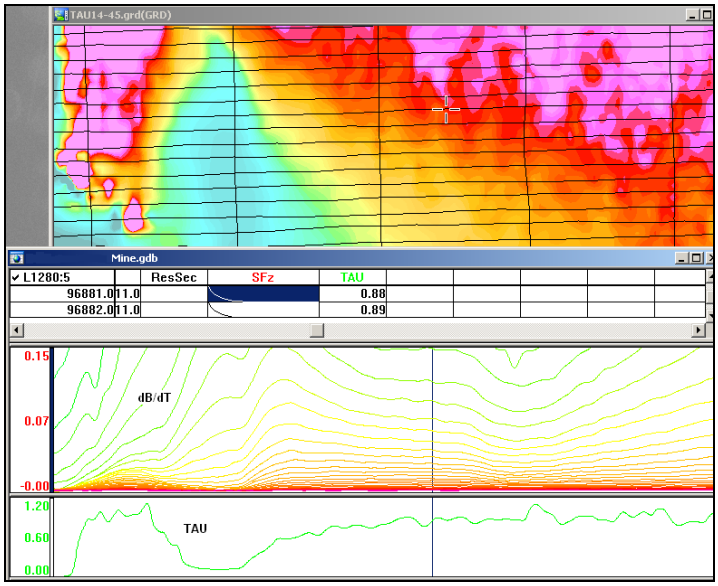

Figure E-3: Map of full time range TAU with EM anomaly due to deep highly conductive target.

There are many advantages of TAU maps:

- TAU depends only on one parameter (conductance) in contrast to response magnitude;
- TAU is integral parameter, which covers time range and all conductive zones and targets are displayed independently of their depth and conductivity on a single map.
- Very good differential resolution in complex conductive places with many sources with different conductivity.
- Signs of the presence of good conductive targets are amplified and emphasized independently of their depth and level of response accordingly.

In the example shown in Figure 4 and 5, three local targets are defined, each of them with a different depth of burial, as indicated on the resistivity depth image (RDI). All are very good conductors but the deeper target (number 2) has a relatively weak dB/dt signal yet also features the strongest total TAU (Figure 4). This example highlights the benefit of TAU analysis in terms of an additional target discrimination tool.

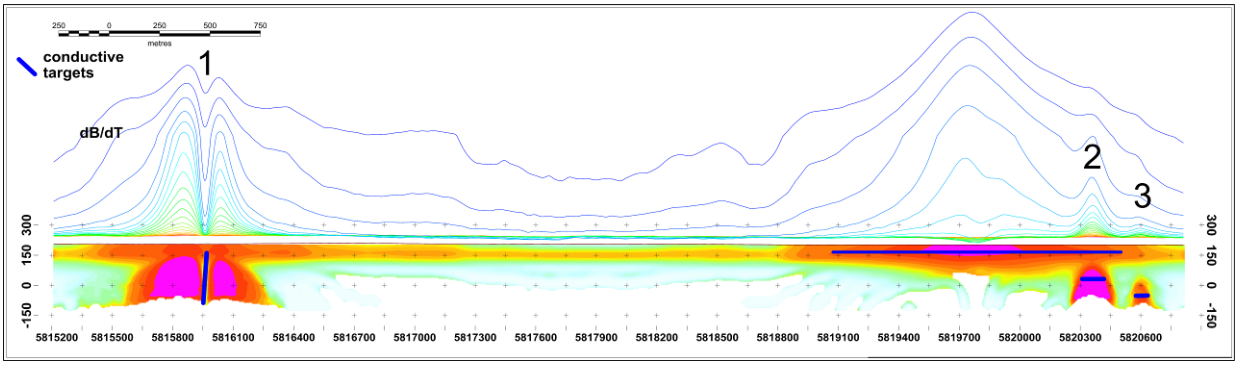

Figure E-4: dB/dt profile and RDI with different depths of targets.

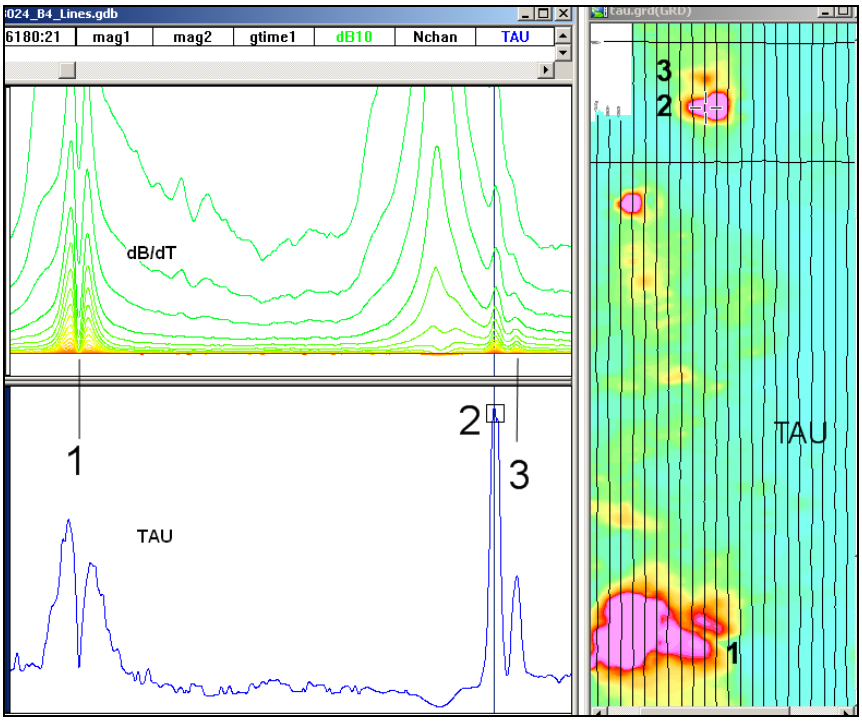

Figure E-5: Map of total TAU and dB/dt profile.

The EM Time Constants for dB/dt and B-field were calculated using the "sliding Tau" in-house program developed at Geotech2. The principle of the calculation is based on using of time window (4 time channels) which is sliding along the curve decay and looking for latest time channels which have a response above the level of noise and decay. The EM decays are obtained from all available decay channels, starting at the latest channel. Time constants are taken from a least square fit of a straight-line (log/linear space) over the last 4 gates above a pre-set signal threshold level (Figure F6). Threshold settings are pointed in the "label" property of TAU database channels. The sliding Tau method determines that, as the amplitudes increase, the time-constant is taken at progressively later times in the EM decay. Conversely, as the amplitudes decrease, Tau is taken at progressively earlier times in the decay. If the maximum signal amplitude falls below the threshold, or becomes negative for any of the 4 time gates, then Tau is not calculated and is assigned a value of "dummy" by default.

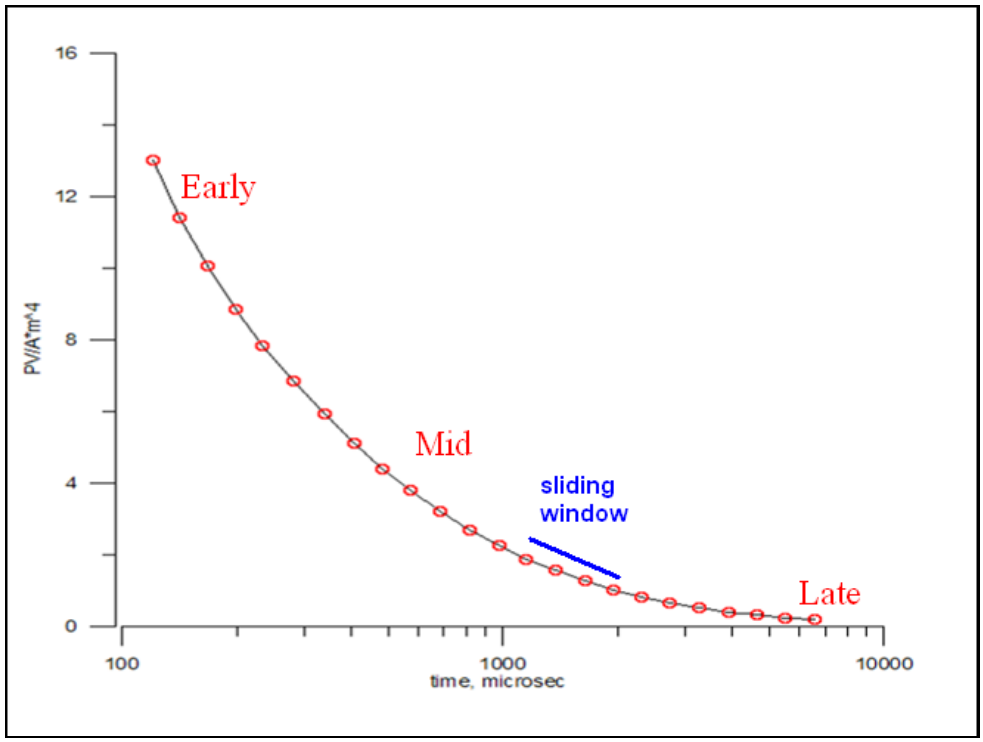

Figure E-6: Typical dB/dt decays of VTEM data

Alexander Prikhodko, PhD, P.Geo
Geotech Ltd.

September 2010

[2] by A.Prikhodko

APPENDIX F

TEM RESISTIVITY DEPTH IMAGING (RDI)

Resistivity depth imaging (RDI) is technique used to rapidly convert EM profile decay data into an equivalent resistivity versus depth cross-section, by deconvolving the measured TEM data.
The used RDI algorithm of Resistivity-Depth transformation is based on scheme of the apparent resistivity transform of Maxwell A.Meju (1998)[1] and TEM response from conductive half-space. The program is developed by Alexander Prikhodko and depth calibrated based on forward plate modeling for VTEM system configuration (Fig. 1-10).

RDIs provide reasonable indications of conductor relative depth and vertical extent, as well as accurate 1D layered-earth apparent conductivity/resistivity structure across VTEM flight lines. Approximate depth of investigation of a TEM system, image of secondary field distribution in half space, effective resistivity, initial geometry and position of conductive targets is the information obtained on base of the RDIs.

Maxwell forward modeling with RDI sections from the synthetic responses (VTEM system)

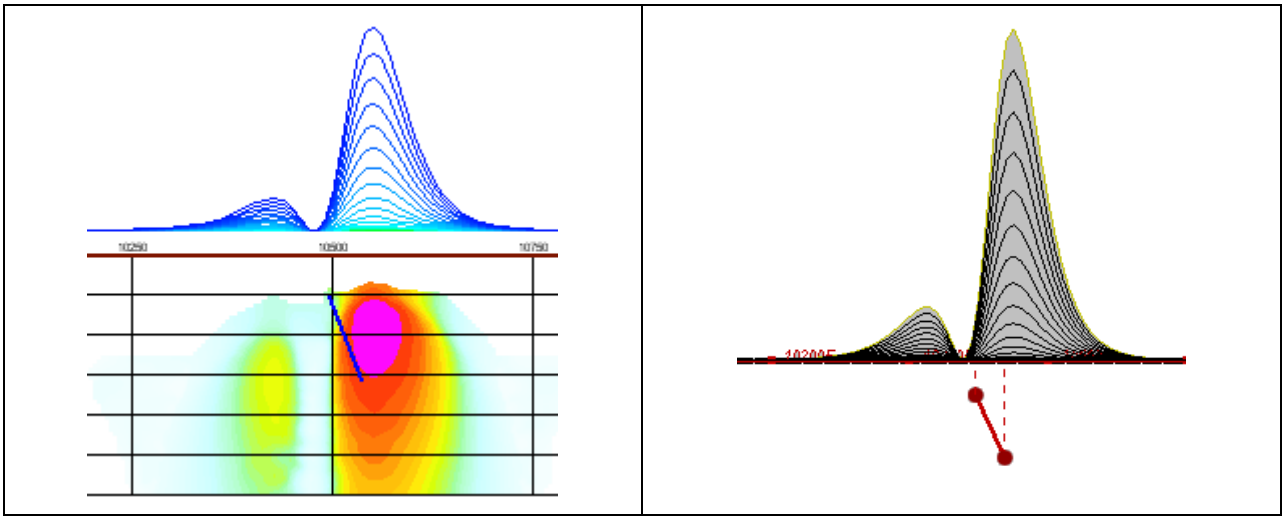

Figure F-1: Maxwell plate model and RDI from the calculated response for conductive “thin” plate (depth 50 m, dip 65 degree, depth extend 100 m).

[1] Maxwell A.Meju, 1998, Short Note: A simple method of transient electromagnetic data analysis, Geophysics, **63**, 405–410.

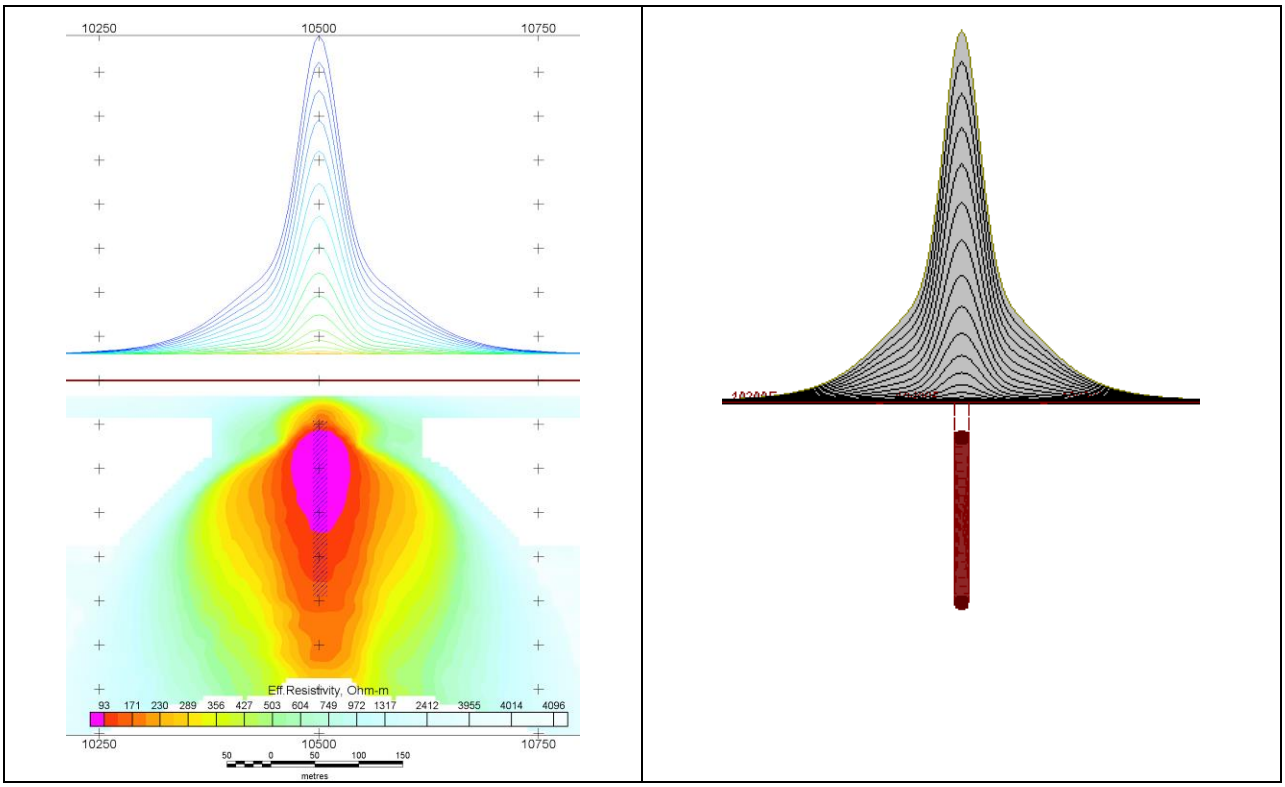

Figure F-2: Maxwell plate model and RDI from the calculated response for "thick" plate 18 m thickness, depth 50 m, depth extend 200 m).

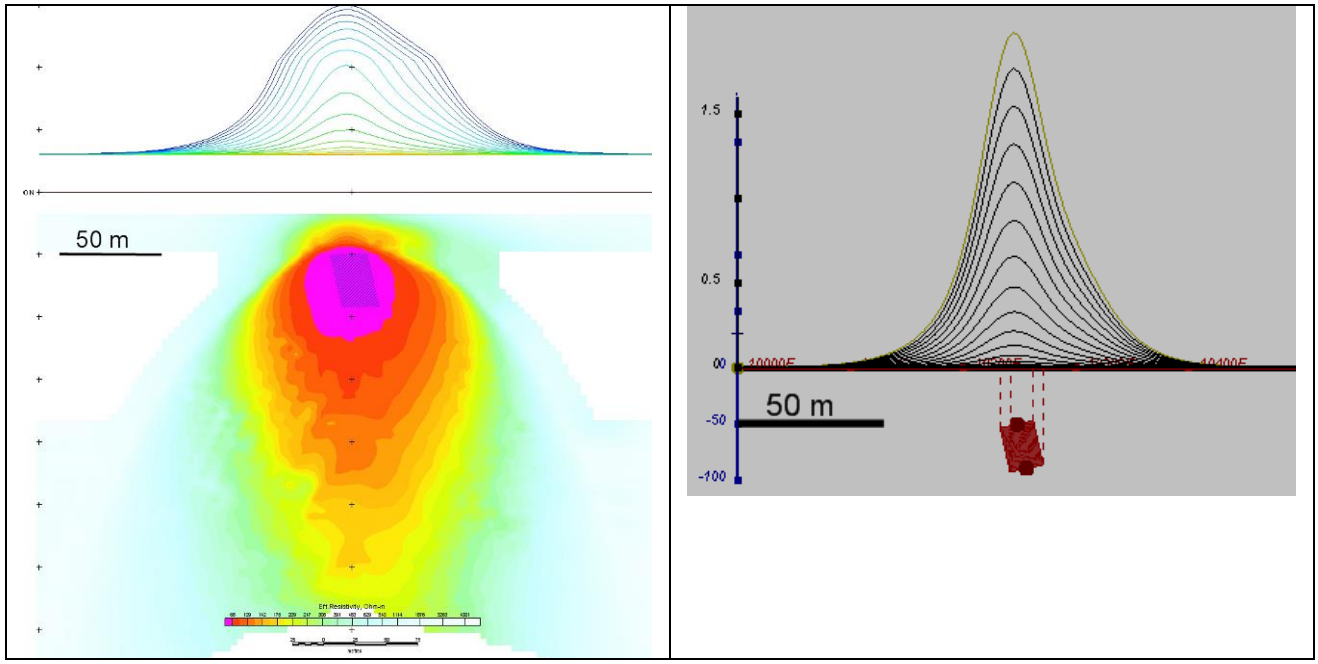

Figure F-3: Maxwell plate model and RDI from the calculated response for bulk ("thick") 100 m length, 40 m depth extend, 30 m thickness

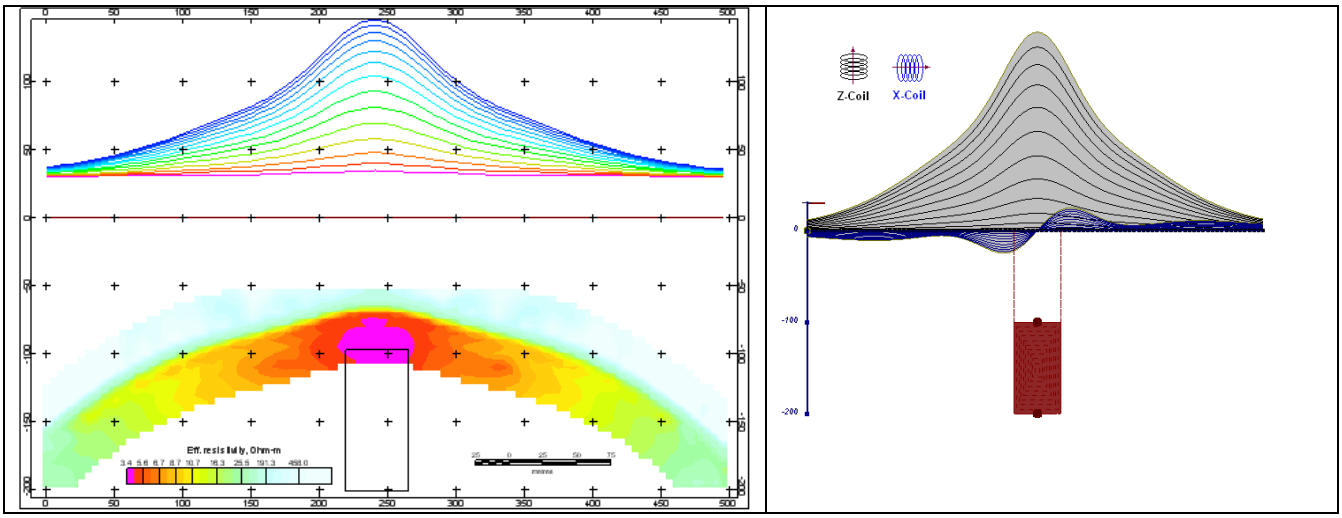

Figure F-4: Maxwell plate model and RDI from the calculated response for "thick" vertical target (depth 100 m, depth extend 100 m). 19-44 chan.

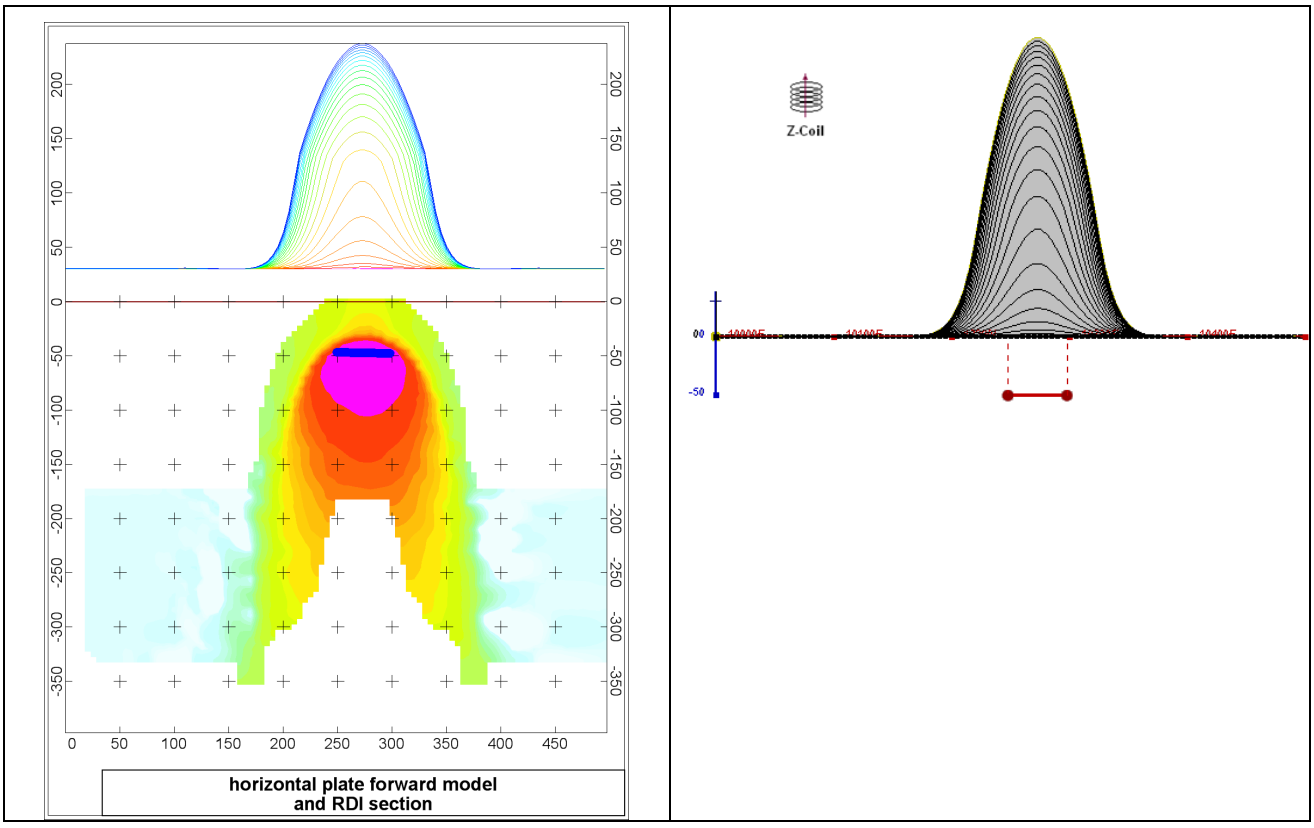

Figure F-5: Maxwell plate model and RDI from the calculated response for horizontal thin plate (depth 50 m, dim 50x100 m). 15-44 chan.

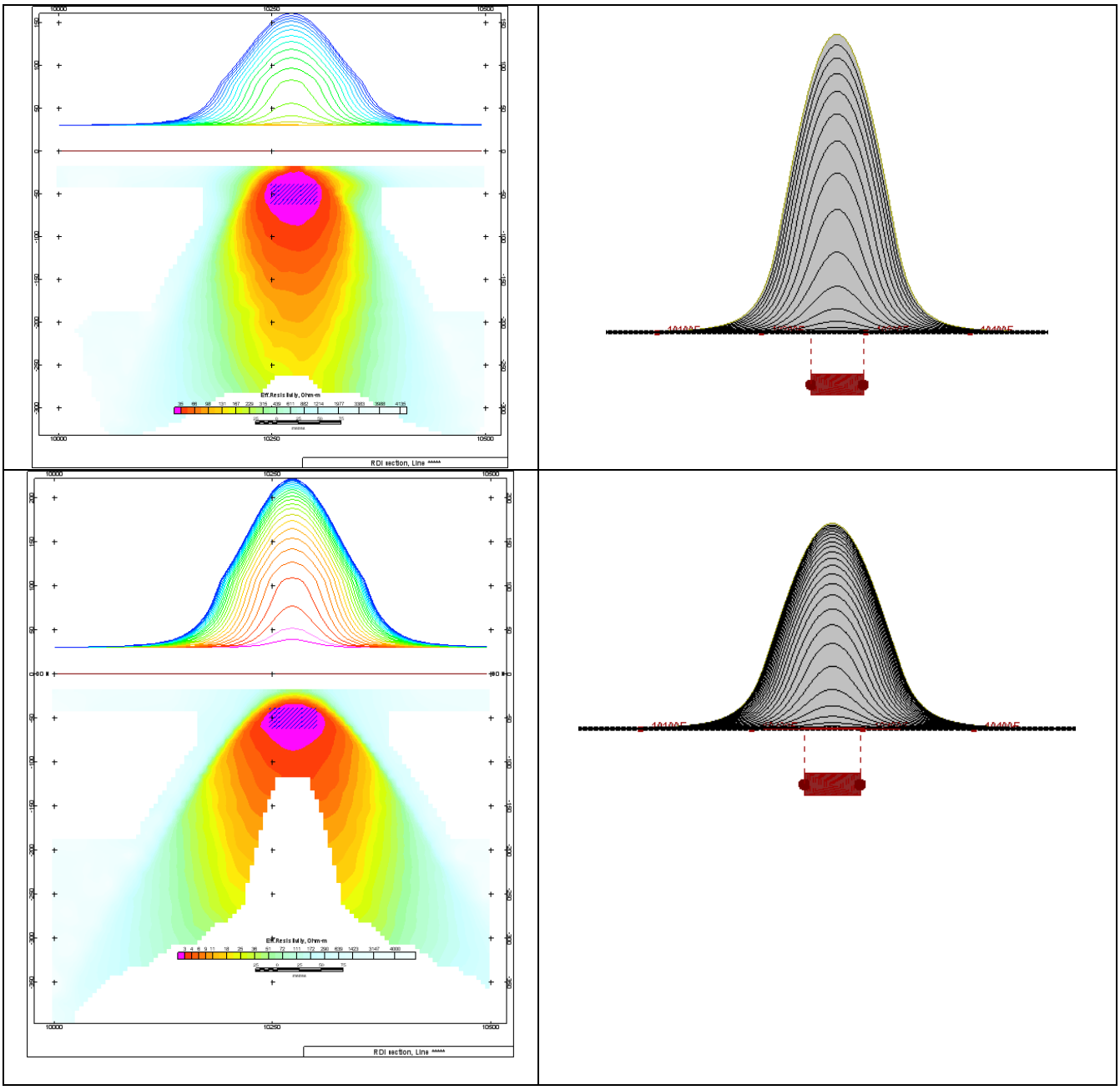

Figure F-6: Maxwell plate model and RDI from the calculated response for horizontal thick (20m) plate – less conductive (on the top), more conductive (below)

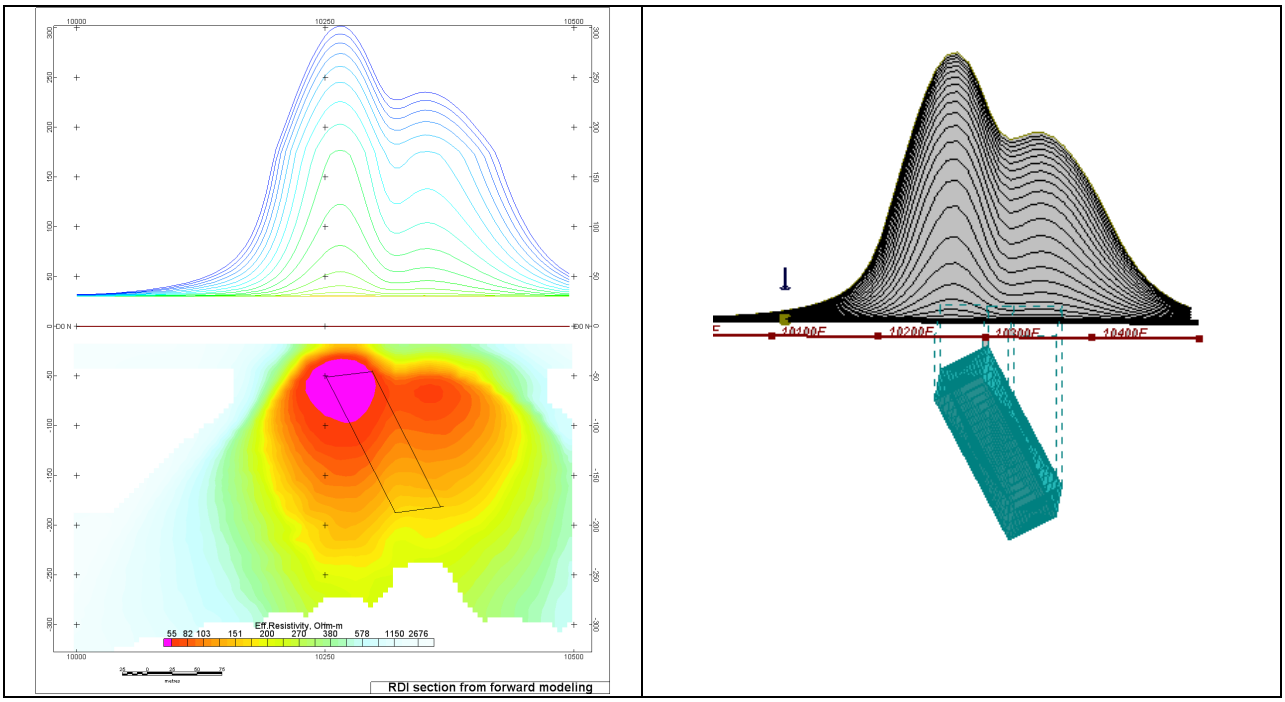

Figure F-7: Maxwell plate model and RDI from the calculated response for inclined thick (50m) plate. Depth extends 150 m, depth to the target 50 m.

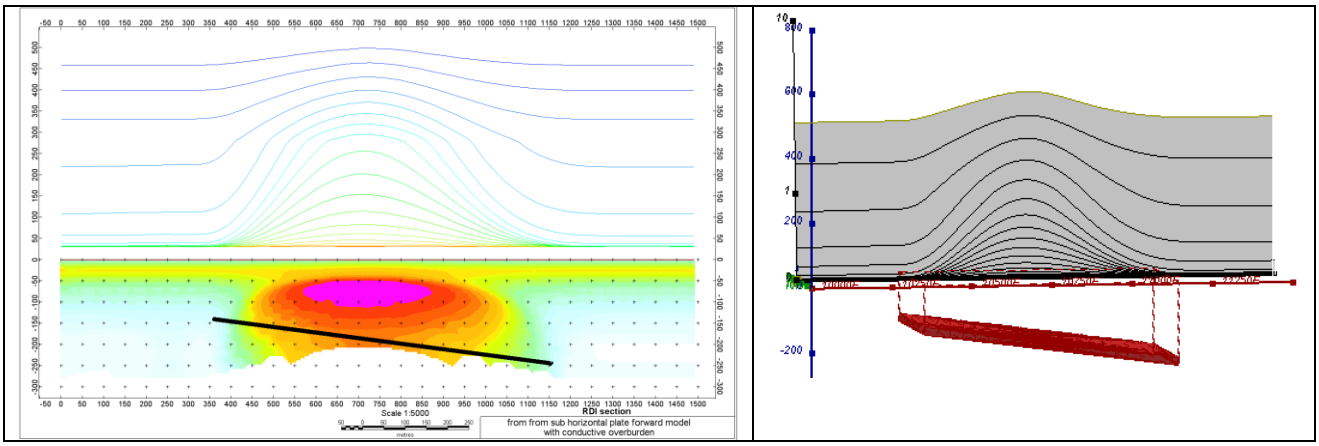

Figure F-8: Maxwell plate model and RDI from the calculated response for the long, wide and deep sub horizontal plate (depth 140 m, dim 25x500x800 m) with conductive overburden.

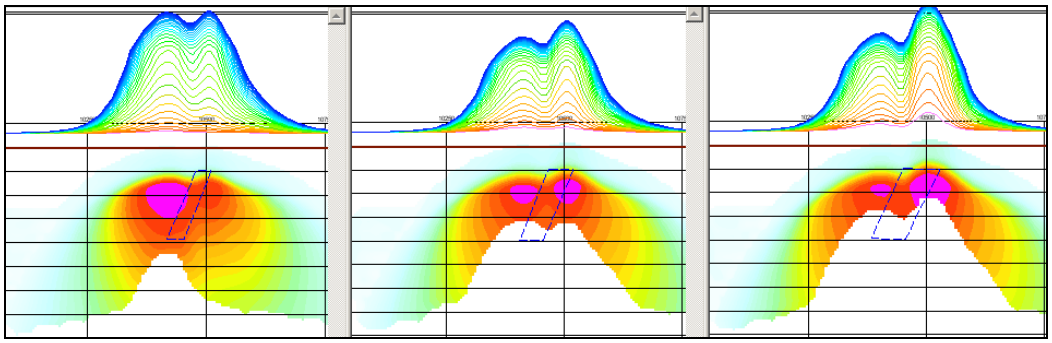

Figure F-9: Maxwell plate models and RDIs from the calculated response for “thick” dipping plates (35, 50, 75 m thickness), depth 50 m, conductivity 2.5 S/m.

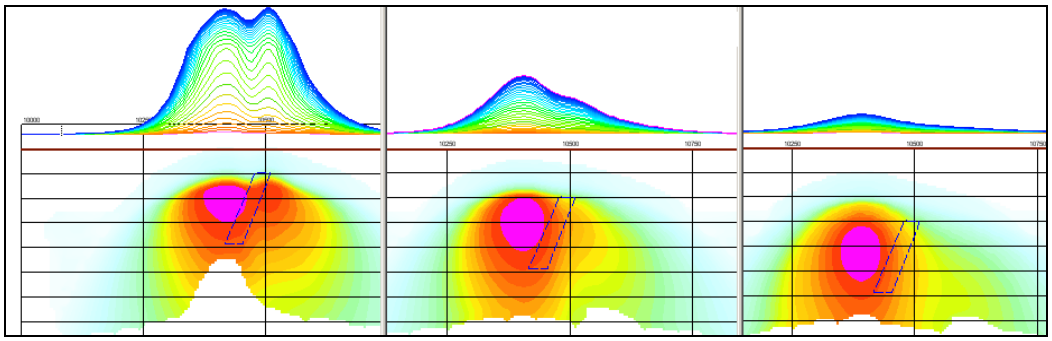

Figure F-10: Maxwell plate models and RDIs from the calculated response for “thick” (35 m thickness) dipping plate on different depth (50, 100, 150 m), conductivity 2.5 S/m.

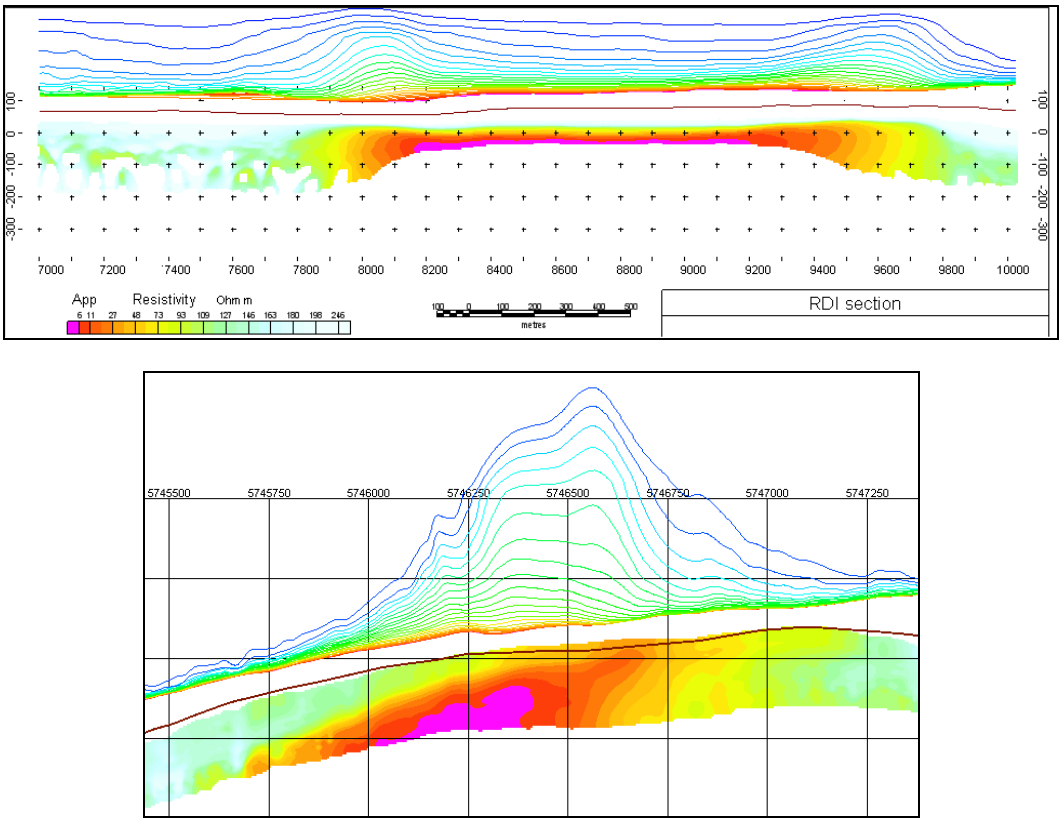

Figure F-11: RDI section for the real horizontal and slightly dipping conductive layers

FORMS OF RDI PRESENTATION

Presentation of series of lines

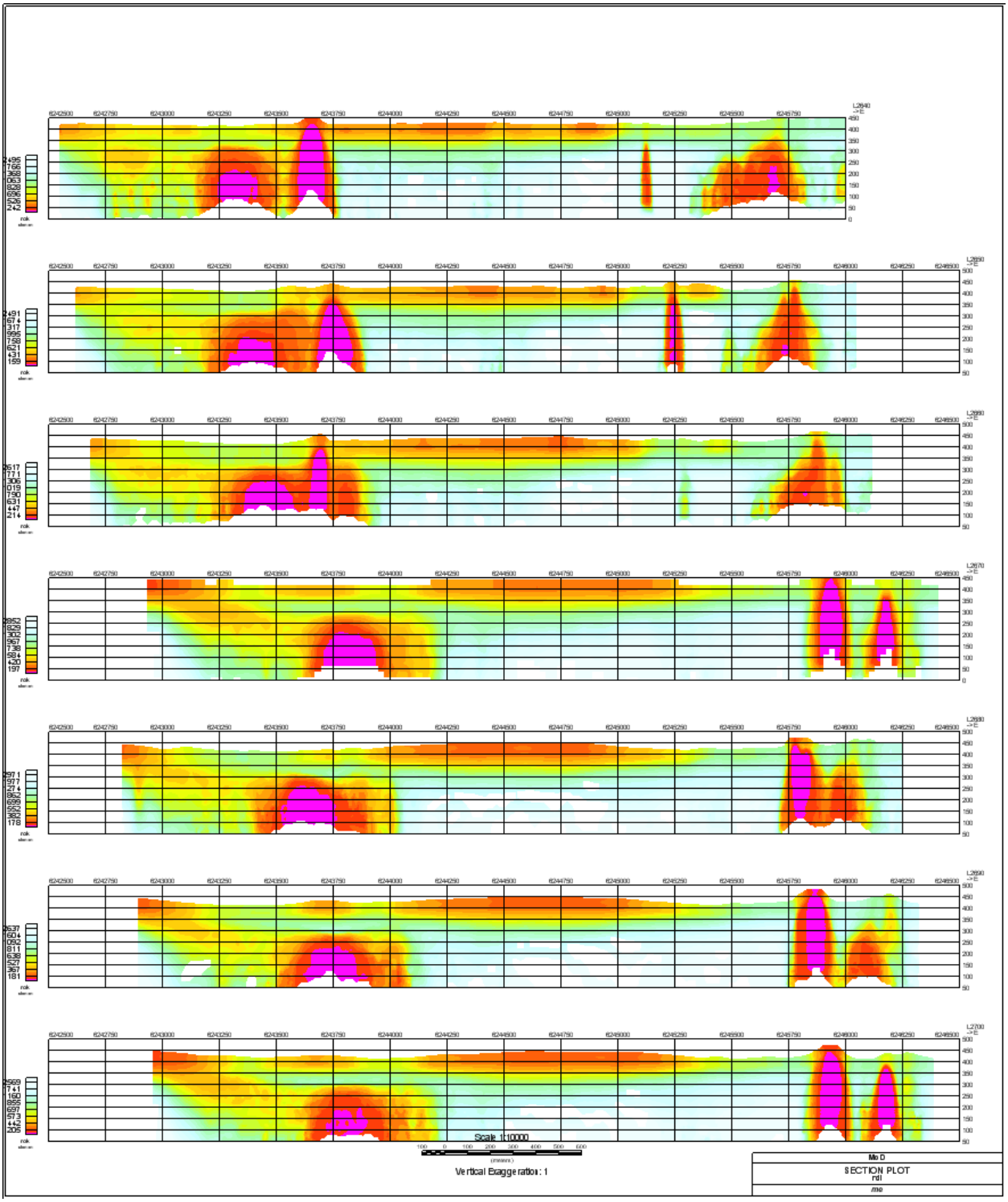

3d presentation of RDIs

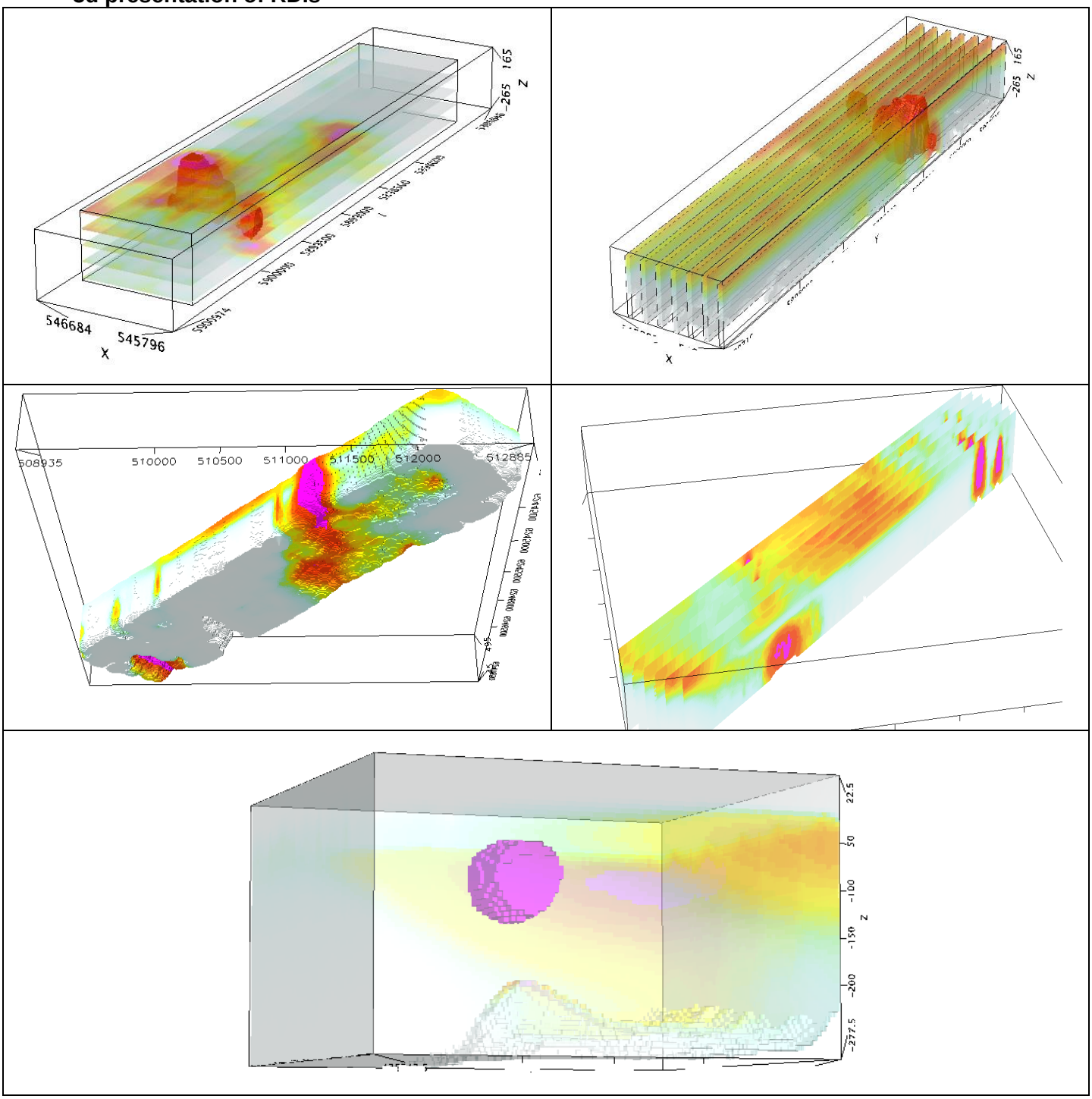

Apparent Resistivity Depth Slices plans:

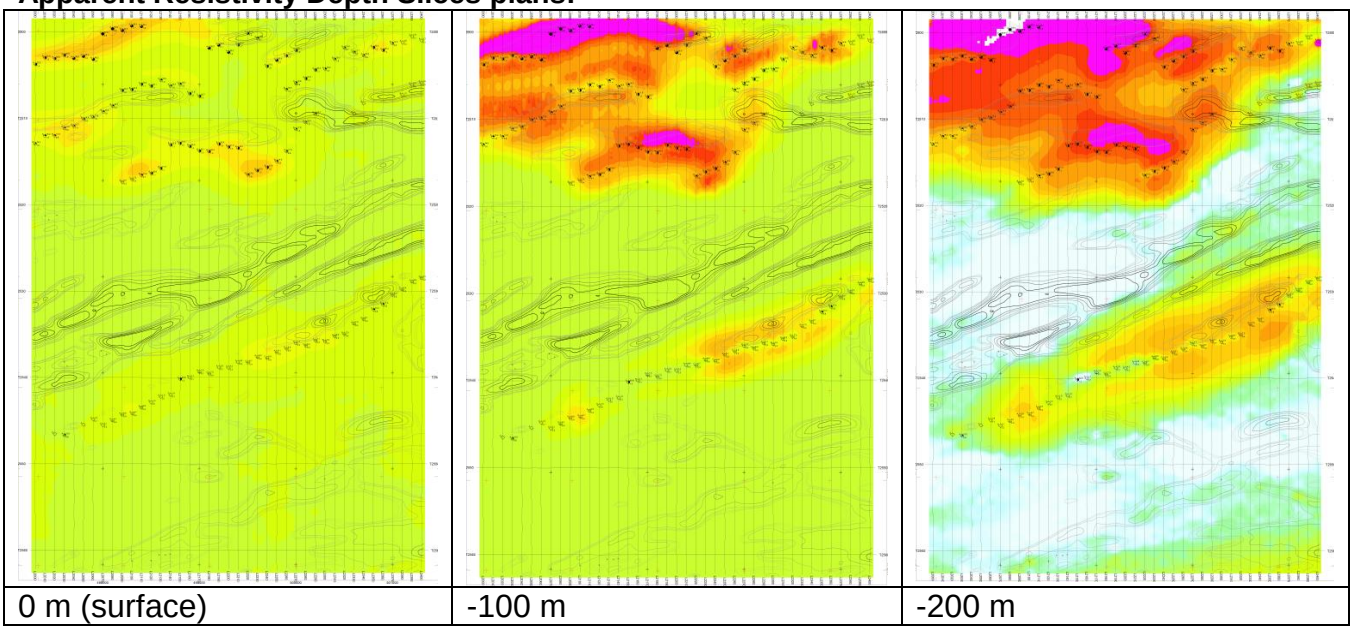

0 m (surface)	-100 m	-200 m

3d views of apparent resistivity depth slices:

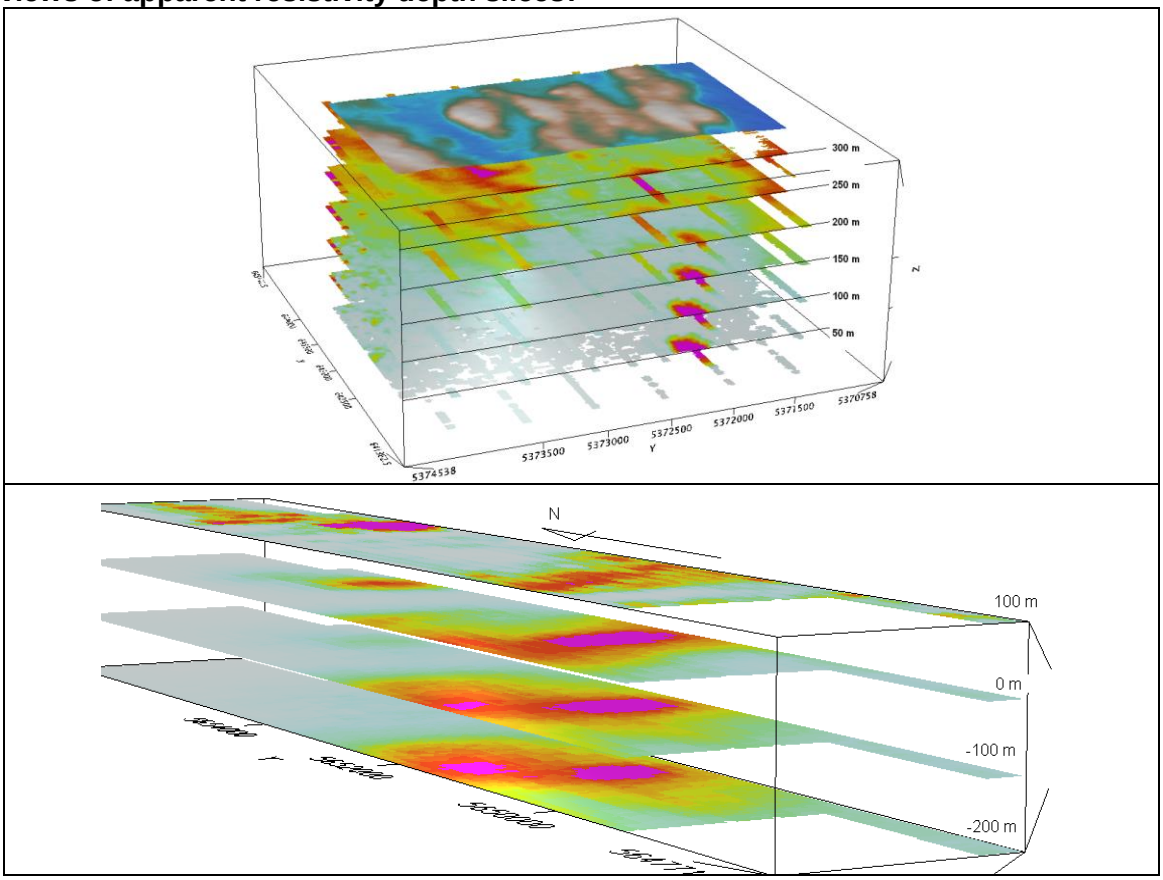

Real base metal targets in comparison with RDIs:

RDI section of the line over Caber deposit (“thin” sub vertical plate target and conductive overburden.

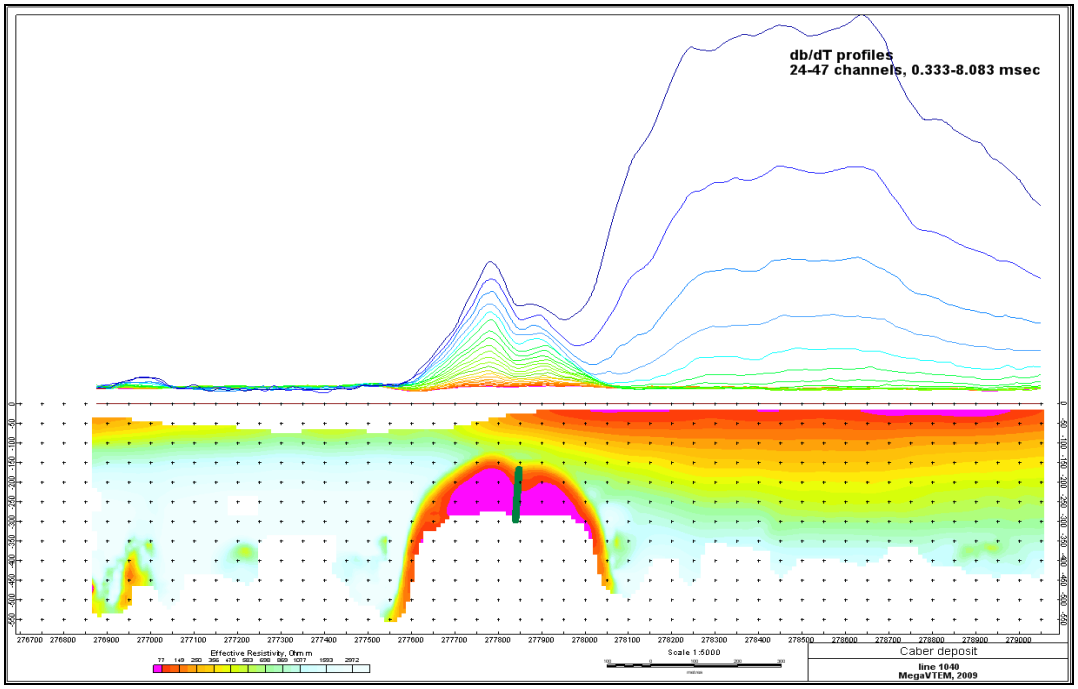

3d RDI voxels with base metals ore bodies (Middle East):

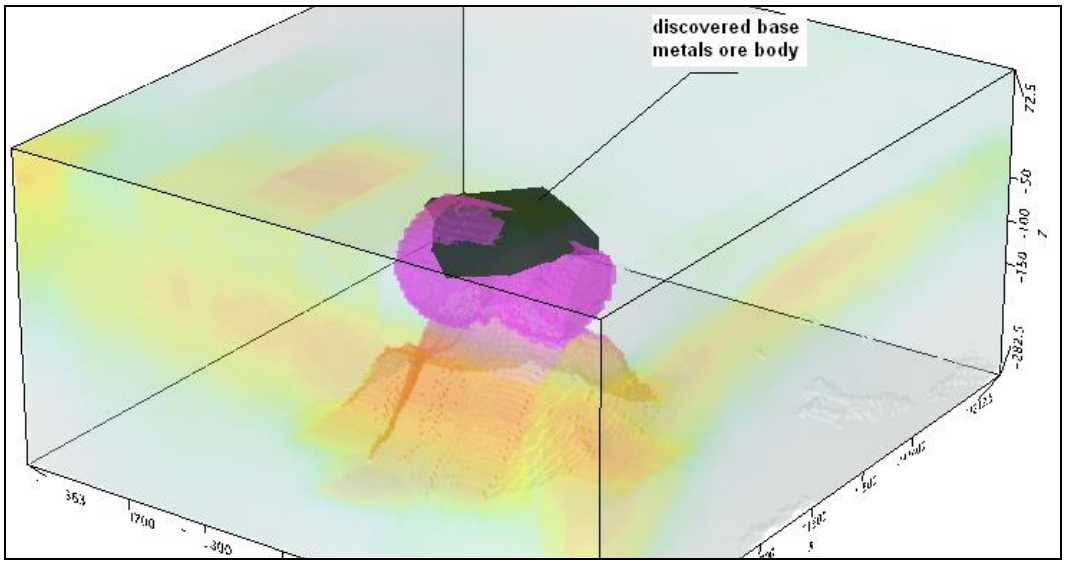

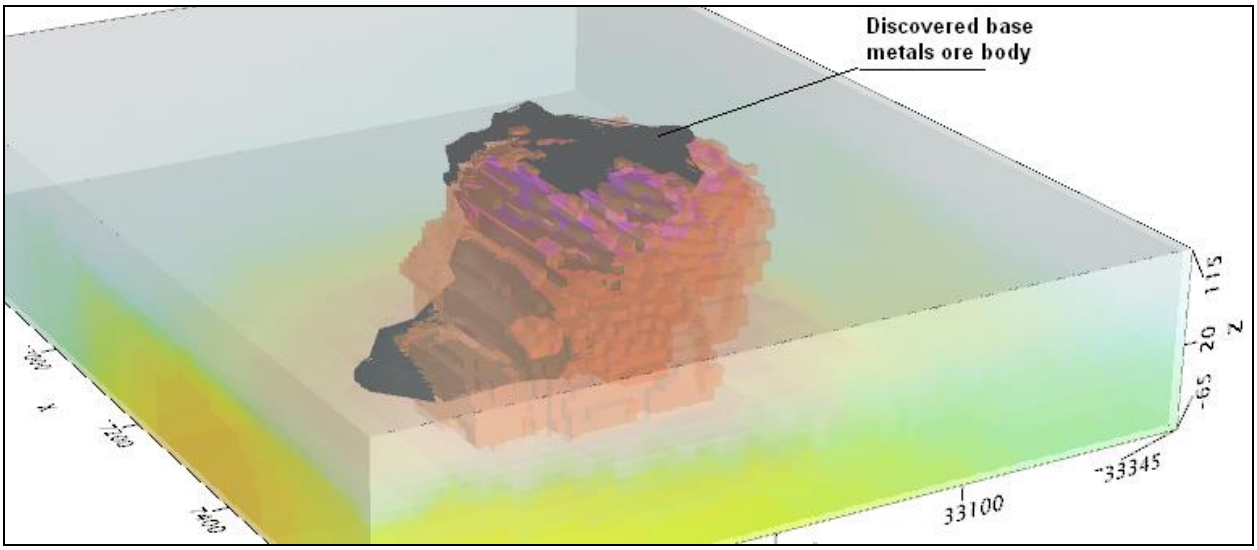

Alexander Prikhodko, PhD, P.Geo
Geotech Ltd.
April 2011

Appendix D

Thin Section Analysis

Vancouver Petrographics Ltd.
8080 GLOVER ROAD, LANGLEY, B.C. V1M 3S3
PHONE: 604-888-1323 • FAX: 604-888-3642
email: vanpetro@vanpetro.com
Website: www.vanpetro.com

Report for: Energizer Resources Inc.
141 Adelaide Street West Suite 520
Toronto, Ontario, Canada, M5H 3L5

Sent to: Craig Scherba <cscherba@energizerresources.com>
Jean-François Montreuil <montreuil.jean.francois@gmail.com>
Quentin Yarie <qyarie@macdonaldmines.com>

Report 130645

October 9, 2013

Petrographic Report on 54 Samples from Sagar Property Part 1 (Samples 1–30)

Fabrizio Colombo, Ph.D., P.Geo.

Table of Contents (Part 1)

1. Introduction....3
2. Results....3
3. Discussion....7
4. Reference List....8
5. Petrographic Descriptions....10
Sample 1: 1272018....10
Sample 2: 1272028....12
Sample 3: 1272033....14
Sample 4: 1272211....16
Sample 5: 1272212....18
Sample 6: 1272213....20
Sample 7: 1272438 23
Sample 8: 1272474....25
Sample 9: 1272475....27
Sample 10: 1307873....29
Sample 11: Boulder field, K-Fe front....32
Sample 12: Delhi breccia zone....35
Sample 13: JFM006-1....38
Sample 14: JFM008....40
Sample 15: JFM009....43
Sample 16: JFM009-1....46
Sample 17: JFM010-1....48
Sample 18: JFM016-1....50
Sample 19: JFM019....52
Sample 20: JFM020-1....54
Sample 21: JFM022-1....56
Sample 22: JFM022-2....59
Sample 23: JFM023-1....61
Sample 24: JFM028-1....64
Sample 25: JFM031-1....66
Sample 26: JFM032....69
Sample 27: JFM033-1....72
Sample 28: JFM033-1.5....74
Sample 29: JFM033-2a....76
Sample 30: JFM033-2b....78

1. Introduction

Mr. Scherba of Energizer Resources Inc. submitted 54 rock samples to Vancouver Petrographics for petrographic analysis. Together with the samples, the client provided detailed sample descriptions and the reason for collecting each sample.

The objective of the petrographic analysis is to determine the mineralogic composition of the samples, petrographically classify the rock types, describe the microstructure defined by the minerals, and recognize the alteration assemblages.

The attached “Petrographic Descriptions” section provides the following for each sample: the petrographic rock classification; a brief microstructural description; a table with the modal percentage and average grain size for each mineral; and a detailed description of the minerals in decreasing order of abundance.

Samples 1–54 (see Table 1) were cut and prepared as ~20 × 40 mm polished thin sections (see the image on the first page of each description).

The petrographic classification follows the recommendations of Gillespie and Styles (1999), Gillespie et al. (2011), and Robertson (1999).

The microstructural terminology used in this report follows the recommendations and definitions of Vernon (2004), Passchier and Trouw (1998), and Ramdohr (1980).

2. Results

Based on the mineral content, microstructural features, and sample description, five main suites were distinguished.

The **first** suite (Samples **4**, **21**, **23**, and **28**) consists of metasedimentary rock ranging from very-fine-**sandstone** (Sample 4) to **mudstone** (Samples 21, 23, and 28). Quartz, plagioclase (albite), and white mica are the most abundant minerals within these samples. A sedimentary compositional layering is folded in Samples 4, 21, and 28. The alteration minerals include white mica, albite, quartz, chlorite, rutile, titanite, and tourmaline. The intensity of the alteration varies from weak to moderate (Sample 23). Sample 23 is crosscut by an albite-dolomite/ankerite-iron oxide vein, and Sample 28 is crosscut by albite-quartz-chlorite veinlets.

The **second** suite (Samples **7**, **8**, **13**, **15**, **17**, **22**, **27**, **29**–**32**, **35**, **36**, **38**–**40**, **43**, **47**, and **48**) consists of metamorphic schists and granofels. Within the schist, the foliation is defined by white mica (Samples 7, 8, and 48), graphite (Sample 13), actinolite (Sample 15), albite ± dolomite ± chlorite ± quartz (Samples 27, 29, 30, 35, and 36). Within the granofels, the minerals (albite, tremolite, dolomite, chlorite, and hematite) are randomly oriented and do not define a foliation. Sulphides and oxides do not always occur within this suite (see details in the petrographic descriptions); however, significant amounts of hematite (Samples 7, 40, and 48), pyrrhotite (Samples 31 and 32), chalcopyrite (Samples 15, 30, and 32), pyrite (Samples

15, 17, and 30), and sphalerite (Sample 47) occur. In most cases, these were introduced as infill minerals.

The **third** suite (Samples **6**, **10**, **19**, **20**, **24**, **46**, **51**, **53,** and **54**) is a mixture of igneous rocks with intermediate composition. The different grain sizes of the primary minerals differentiate a **microdioritic** sub-suite (Sample 6 and 54). Sample 6 shows a sub-ophitic microstructure in which abundant actinolite and epidote moderately altered the magmatic rock. In Sample 54, slightly porphyritic plagioclase is immersed within a finer-grained plagioclase-rich groundmass. This sample was microbrecciated and filled in by fine-grained biotite and magnetite. Calcite-bornite-biotite-epidote-albite abundantly filled in the dioritic rock. The **basaltic** sub-suite (Samples 10, 19, 20, 24, 46, 51, and 53) is moderately to strongly altered (actinolite-albite-titanite-chlorite-epidote-calcite-magnetite) and crosscut by veins and veinlets that generally match the alteration assemblages.

The **fourth** suite (Samples **9**, **11**, **12**, **16**, **25**, and **26**) is characterized by brecciated microstructures. In most cases, the composition of the fragments indicates a sedimentary protolith (Samples 9, 11, and 12). Samples 16, 25, and 26 show metamorphic fragments. The fragments were filled in by albite ± quartz ± actinolite ± calcite ± white mica ± tourmaline ± epidote ± pyrrhotite ± pyrite ± chalcopyrite.

The **fifth** suite consists of **alteration**- and **mineralization**-**zone** (Samples **1**–**3**, **5**, **14**, **18**, **33**, **34**, **37**, **41**, **42**, **44**, **45**, **49**, **50**, and **52**). Within this group of samples, the intense alteration and replacement obliterated any structural and mineralogic relicts of the protolith. This suite is made up of heterogeneous mineral assemblages including dolomite ± clay ± quartz ± albite ± calcite ± tremolite ± actinolite ± clinozoisite ± rutile ± chlorite. The chalcocite is abundant in Samples 1 and 52. Abundant chalcopyrite occurs in Samples 14, 34, and 44. Tetrahedrite occurs as euhedral crystals in Sample 2.

The magnetic susceptibility (see Table 1) was measured with a hand-held KT Magnetic Susceptibility Meter, and is intended to provide only an approximate estimate of the relative content of magnetic minerals within the sample.

Table 1: List of samples with their magnetic susceptibility and petrographic classification.[1]

Sample No.	Sample ID	Magnetic Susceptibility ($\cdot 10^{-3}$)	Rock Type
1	1272018	0.367	Chalcocite-galena-covellite mineralization-zone
2	1272028	0.082	Dolomite-tetrahedrite alteration-zone
3	1272033	0.280	Strongly silicified rock/Quartz infill; Albite-pyrrhotite-quartz-calcite-chalcopyrite infill
4	1272211	0.010	Metasandstone
5	1272212	0.001	Albite-quartz-chlorite alteration-zone
6	1272213	0.100	Micro-diorite; Calcite-bornite-biotite-epidote-albite infill
7	1272438	0.060	White mica schist
8	1272474	0.014	White mica-quartz-dolomite schist
9	1272475	0.003	Dolomite-quartz breccia
10	1307873	16.700	Basalt; Calcite-K-feldsdpar-albite(?)-biotite-chalcopyrite-pyrite infill
11	Boulder field, K-Fe front	0.065	Clay-plagioclase-Mg-chlorite breccia
12	Delhi breccia zone	0.480	Calcite-albite-pyrite-actinolite-biotite breccia
13	JFM006-1	0.017	Graphitic schist
14	JFM008	1.600	Clay-chalcopyrite-pyrrhotite alteration-zone
15	JFM009	0.085	Actinolite schist; Calcite-actinolite-chlorite-pyrite-chalcopyrite infill
16	JFM009-1	0.099	Brecciated actinolite schist; Actinolite-calcite-chlorite-pyrite-chalcopyrite infill
17	JFM010-1	0.003	Albite-tremolite-pyrite granofels
18	JFM016-1	0.012	Calcite-actinolite-chalcopyrite infill/alteration-zone
19	JFM019	0.096	Basalt; Alteration: strong–actinolite-titanite-epidote-Mg-chlorite; Actinolite-epidote-chlorite-calcite veinlets
20	JFM020-1	0.148	Basalt; Alteration: strong–actinolite-epidote-Mg-chlorite-titanite; Actinolite-epidote-quartz-Mg-chlorite-calcite veins
21	JFM022-1	0.008	Metamudstone
22	JFM022-2	0.022	Albite-dolomite granofels
23	JFM023-1	0.010	Metamudstone; Alteration: moderate — white mica-albite; Albite-dolomite/ankerite-iron oxides vein
24	JFM028-1	0.085	Basalt; Alteration: strong— albite-actinolite-rutile-chlorite
25	JFM031-1	2.400	Brecciated (mosaic-breccia) albite-rich alteration-zone; Pyrrhotite-quartz-white mica-pyrite-tourmaline-chalcopyrite infill

1 Rock classification after Gillespie et al. 2011, Gillespie and Styles 1999, and Robertson 1999.

Sample No.	Sample ID	Magnetic Susceptibility ($\cdot 10^{-3}$)	Rock Type
26	JFM032	0.089	Brecciated albite-quartz-biotite granofels; Chlorite-quartz-calcite-albite-titanite infill
27	JFM033-1	0.076	Albite schist; Actinolite-albite-chlorite-chalcopyrite-pyrite infill
28	JFM033-1.5	0.016	Metamudstone; Albite-quartz-chlorite veinlets
29	JFM033-2a	0.010	Albite-dolomite-chlorite schist
30	JFM033-2b	0.018	Quartz-albite-chlorite schist; Chalcopyrite-quartz-white mica-chlorite-pyrite infill
31	JFM033-3	1.000	Chlorite granofels
32	JFM033-5	3.580	Chlorite-pyrrhotite-quartz granofels
33	JFM033-6	0.002	Clay-quartz-hematite(?) alteration-zone
34	JFM033-7	0.108	Dolomite-chalcopyrite-quartz vein
35	JFM035-1	0.008	Dolomite-quartz-white mica schist
36	JFM037	0.000	Quartz-chlorite schist
37	JFM039-1	0.263	Hematite-dolomite-quartz-albite vein
38	JFM039-2	0.020	Dolomite-albite granofels
39	JFM042-1	0.004	Dolomite-albite granofels
40	JFM042-2	0.130	Dolomite-hematite-albite granofels
41	JFM042-3	0.063	Dolomite-albite-hematite alteration-zone
42	JFM042-5	0.011	Albite-illite alteration-zone
43	JFM043-2	0.024	Dolomite-albite granofels; Quartz vein
44	JFM044-1	0.007	Brecciated clay-rutile alteration-zone; Dolomite-chalcopyrite-pyrite-quartz infill
45	JFM049	0.059	Quartz-rutile-calcite alteration-zone
46	SGR-02-440m	24.900	Basalt; Alteration: moderate—magnetite-actinolite-titanite-epidote-chlorite
47	SUS-07-15-275'	0.000	Brecciated(?) dolomite granofels; Quartz-dolomite infill(?); Dolomite-sphalerite-pyrite infill
48	SUS-07-44-234'	0.004	Layered dolomite-white mica-albite schist
49	WP-253	0.008	Dolomite-chlorite-tremolite alteration-zone
50	WP282	0.117	Actinolite-clinozoisite alteration-zone
51	WP284	0.142	Basalt(?); Alteration: strong—actinolite-epidote-titanite(?)-calcite
52	1272227	0.014	Tremolite-calcite-chalcocite alteration-zone
53	WP-292	0.191	Basalt(?); Alteration: strong—actinolite-clinozoisite-chlorite-titanite(?)-albite
54	WP535-CaRB-3	34.700	Micro-brecciated plagioclase-phyric microdiorite; Alteration: moderate—biotite-magnetite-titanite-dolomite(?)

The minerals distinguished by short-wave infrared spectroscopy (TerraSpec) are listed in Table 2. This analytical method is only suitable for light-coloured rocks; therefore, only some of the offcut were selected and analyzed with this method.

Table 1: List of minerals distinguished by short-wave infrared spectroscopy (TerraSpec).

Sample No.	Sample ID	Mineral
2	1272028	dolomite
4	1272211	muscovite
9	1272475	dolomite
18	JFM016-1	calcite
21	JFM022-1	muscovite
23	JFM023-1	muscovite
24	JFM028-1	chlorite
27	JFM033-1	actinolite
28	JFM033-1.5	chlorite
29	JFM033-2a	chlorite
34	JFM033-7	dolomite
35	JFM035-1	dolomite
37	JFM039-1	dolomite
38	JFM039-2	dolomite
39	JFM042-1	dolomite
41	JFM042-3	dolomite
42	JFM042-5	illite
43	JFM043-2	dolomite

3. Discussion

The detailed petrographic analysis, in some cases supported by short-wave infrared spectroscopic analysis, determined the mineral composition of the submitted samples, described the microstructural arrangement of the minerals, and indicated the magmatic, metamorphic, and alteration assemblages. The petrographic analysis indicates the occurrence of an **albite-dolomite-quartz** alteration event that is associated in some cases with a brittle deformation event within in the fourth and fifth suites. The occurrence of **hematite** (Samples 7, 9, 33, 37–41, 46, and 48) indicates oxidizing conditions during the mineralization. On the other hand, the **pyrrhotite** (Samples 3, 12, 14, 25, 26, 31, and 32) indicates intermediate to reducing conditions, which probably pre-dated the main

alteration/mineralization event. The **chalcopyrite** is the copper-bearing mineral that occurs most often. It occurs as infill mineral, as in the case of Samples 3 and 44, in which the chalcopyrite was precipitated in association with albite-pyrrhotite-quartz-calcite and dolomite-pyrite-quartz, respectively. The chalcopyrite is more abundant (~10% of the polished thin section) within Samples 14 and 34; within these alteration-zones, the chalcopyrite is associated with clay-pyrrhotite and calcite-actinolite, respectively. In Sample 14, the mineralization probably overprinted a pre-existent albite-rich alteration event. In many instances, the chalcopyrite is associated with rutile. Within the magmatic suite, the chalcopyrite mostly occurs as an infill mineral (Samples 10, 19, and 51). Within Sample 10, the chalcopyrite is more abundant (~0.2%) and precipitated in association with calcite-K-feldspar-albite(?)-biotite-pyrite.

In the second suite, the chalcopyrite is mostly associated with the pyrite (Samples 15–17, 30, 31, 32, and 47). Among these metamorphic samples, the chalcopyrite is more abundant within actinolite schist and albite-dolomite-chlorite schist. The chalcopyrite is subordinate and probably replaced the pyrrhotite within the chlorite-pyrrhotite-quartz granofels.

Sphalerite occurs only as infill minerals associated with dolomite and subordinate pyrite within a brecciated dolomite-rich granofels (Sample 47). **Chalcocite** dominates the composition of Sample 1 and is associated with subordinate clay. **Tetrahedrite** forms euhedral crystals associated with abundant dolomite within Sample 2, and **bornite** is associated with calcite-biotite-epidote-albite and filled in a strongly altered (actinolite) micro-diorite.

4. Reference List

Delvigne, J.E., 1998, Atlas of Micromorphology of Mineral Alteration and Weathering: The Canadian Mineralogist Special Publication No. 3. Mineralogical Association of Canada, 494 p.

Gillespie, M.R., and Styles, M.T, 1999, British Geological Survey Rock Classification Scheme Volume 2 Classification of Igneous Rocks: British Geological Survey Research Report (2nd edition), RR/99–06, 52 p.

Gillespie, M.R., Barnes, R.P., and Milodowski, A., 2011, British Geological Survey Scheme for Classifying Discontinuities and Fillings: British Geological Survey Research Report, RR/10–05, 56 p.

Passchier, C.W., and Trouw, R.A.J., 1998, Microtectonics: Springer, 289 p.

Robertson, S., 1999, British Geological Survey Rock Classification Scheme Volume 2 Classification of Metamorphic Rocks: British Geological Survey Research Report, RR/92–02, 24 p.

Ramdohr, P., 1980, The Ore Minerals and Their Intergrowths, 2nd edition, Vol. 1 and 2: Pergamon Press, 1207 p.

Tröger, W.E., 1979, Optical Determination of Rock-Forming Minerals. Part 1, Determinative

Tables: E. Schweizerbart'sche Verlagsbuchhandlung (Nägele u. Obermiller), 188 p.

Vernon, R.H., 2004, A Practical Guide to Rock Microstructure: Cambridge University Press, 594 p.

Signed by
F. Colombo, Ph.D., P.Geo.
E-mail: fab.petrologic@gmail.com
Web: www.petrographically.com

5. Petrographic Descriptions

Sample 1: 1272018

Chalcocite-galena-covellite mineralization-zone

Massive chalcocite dominates the composition of this polished thin section. The chalcocite hosts interstitial aggregates of clay, medium-grained anhedral galena, and anhedral replacement patches of covellite.

Mineral	*Modal %*	*Main Size Range (mm)*
chalcocite	95 – 98	massive
galena	1 – 1.5	up to 1
covellite	1	up to 0.05
clay	1	up to 0.05

Chalcocite forms a massive aggregate characterized by abundant fine-grained inclusions of covellite, which impart a porous aspect to the aggregate. The chalcocite is associated with fine-grained interstitial aggregates of **clay**. The chalcocite is distinguished by its medium reflectance, bluish colour, and distinct pleochroism.

Galena occurs as medium-grained (up to 1 mm) anhedral crystals immersed within and partially replaced by chalcocite. The galena is distinguished by its bright white colour, strong reflectance, perfect cleavage (see Photomicrograph 1b), and softness when polished. Some of the galena crystals show the triangular pits typical of this mineral, and most of the crystals are fractured. Fine-grained galena is dispersed within the fine-grained aggregates of covellite.

Covellite forms fine-grained aggregates, which define anhedral to interstitial pseudomorphs (Photomicrograph 1b) after a completely replaced copper-rich mineral. The covellite is distinguished by its softness, medium reflectance, and strong pleochroism with bluish to blue-violet tints. Fine-grained covellite is dispersed within the chalcocite. In some cases, the covellite aggregate mantles the anhedral galena.

Fine-grained aggregates of **clay** form interstitial domains and are heterogeneously dispersed within the chalcocite.

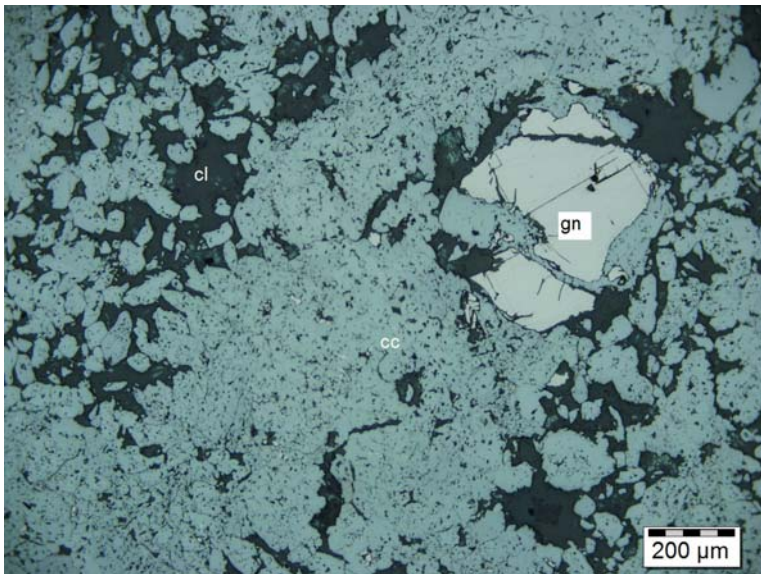

***Photomicrograph 1a**: Massive chalcocite (cc) is intergrown with interstitial clay (cl) and subordinate anhedral crystals of galena (gn). Plane-polarized reflected light.*

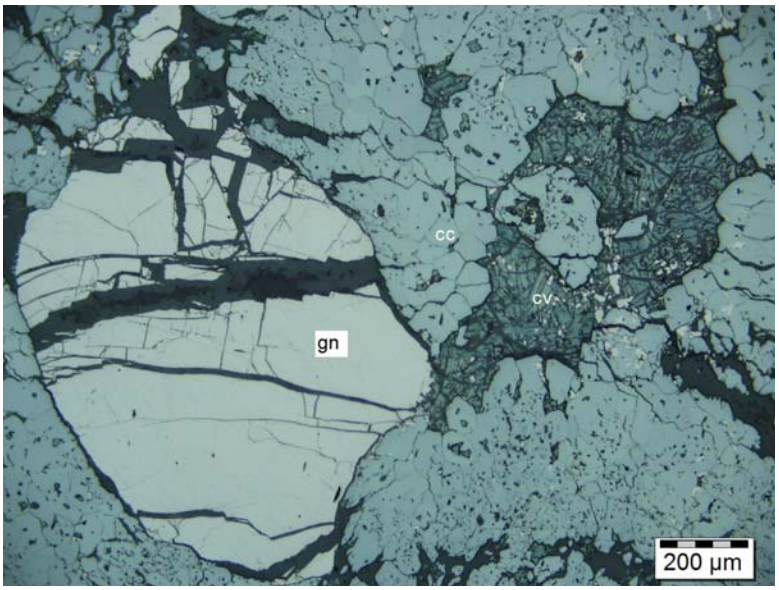

***Photomicrograph 1b**: An anhedral crystal of galena (gn) shows perfect perpendicular cleavagesystems. The galena is immersed within a massive aggregate of chalcocite (cc) that hosts anhedral pseudomorphs of fine-grained covellite (cv) and subordinate galena. The covellite is dispersed as fine-grained inclusions within the chalcocite. Plane-polarized reflected light.*

Sample 2: 1272028

Dolomite-tetrahedrite alteration-zone

Medium-grained euhedral crystals of tetrahedrite are immersed within an inequigranular subhedral to anhedral aggregate of dolomite, which dominates the composition of this polished thin section. The interstices between the dolomite are occupied by fine-grained calcite and rare white mica flakes.

Mineral	*Modal %*	*Main Size Range (mm)*
dolomite	96 – 99	up to 3
tetrahedrite	1.5 – 2	up to 2.5
calcite	1	up to 0.2
white mica	tr	up to 1 × 0.2
quartz	tr	4 × 1
galena	tr	up to 0.1
covellite?	tr	up to 0.04

Dolomite forms inequigranular crystals (up to 3 mm) that in most cases show anhedral shapes and moderate to strong undulose extinction. The shape of the dolomitic grains varies from interlobate to straight, and in some cases, the interstices are occupied by fine-grained interlobate crystals. The medium-grained dolomite is distinguished by its slow reaction to cold dilute (10%) HCl; the fine-grained interstitial carbonate is mostly **calcite**, as shown by its brisk reaction to the acid.

Medium-grained (up to 2.5 mm) euhedral to subhedral crystals of **tetrahedrite** are dispersed within the dolomite-rich aggregate. The tetrahedrite shows pseudo-cubic and tetrahedral shapes. The crystals are weakly fractured and the fractures are filled in by **galena**, which in some cases occupies the interstices between the tetrahedrite and the dolomite, and the interstices between the dolomite in association with calcite. The tetrahedrite is distinguished by its medium reflectance, grey colour, and isotropic nature. Very rare flakes of probable **covellite** occur near the tetrahedrite crystals.

Fine- to medium-grained **white mica** flakes occupy the interstices between the medium-grained dolomite. They occur as bent lamellae with moderate to strong undulose extinction.

Quartz is rare. It occurs as an interlobate crystal (4 × 1 mm) that is intergrown with the

dolomite and shows a strong undulose extinction.

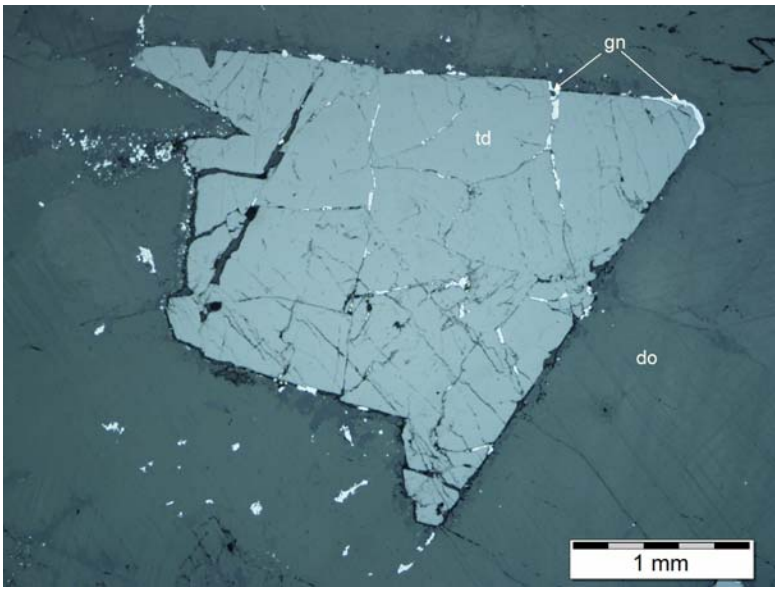

***Photomicrograph 2**: A subhedral crystal of tetrahedrite (td) is fractured, filled in by interstitial galena (gn), and immersed within a medium-grained aggregate of dolomite (do). Plane-polarized reflected light.*

Sample 3: 1272033

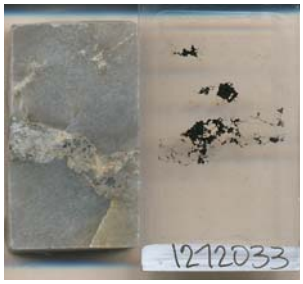

Strongly silicified rock/Quartz infill

Albite-pyrrhotite-quartz-calcite-chalcopyrite infill

An inequigranular interlobate aggregate of quartz and subordinate albite dominates the composition of this polished thin section, which was filled in by fine-grained quartz, albite, pyrrhotite, calcite, chalcopyrite, and rare pyrite.

Mineral	*Modal %*	*Main Size Range (mm)*
quartz	90 – 93	up to 1
pyrrhotite	5 – 5.5	up to 3
albite	1.5 – 2	up to 1
calcite	1 – 2	up to 1
chalcopyrite	0.1 0.2	up to 1
pyrite	tr	up to 0.2
rutile	tr	up to 0.1
pentlandite	tr	up to 0.02

Quartz forms an inequigranular (up to 1 mm) and interlobate aggregate in which the crystals show moderate to strong undulose extinction. The boundaries between the quartz crystals are finely interlobate and were produced by the recrystallization during a brittle-ductile deformation event, which probably triggered the emplacement of a vein-like domain and irregular infill domains made up of quartz, albite, pyrrhotite, calcite, chalcopyrite, and rare pyrite. The quartz within the infill domain shows weak to moderate undulose extinction. It is associated with fine-grained albite and his hosted as fine-grained and rounded inclusions within the pyrrhotite.

Albite is concentrated within the infill domains in association with fine-grained quartz as inequigranular anhedral, fractured crystals. The albite is distinguished by its typical albite twinning and its lower refractive indexes than those of quartz. Some of the crystals of albite are ductilely deformed and show a strong undulose extinction. Rare albite crystals are also dispersed within the strained quartz-rich aggregate.

Pyrrhotite occurs as anhedral to amoeboid crystals of up to 3 mm (see Photomicrograph 3)

that are concentrated along the irregular vein-like domain and are irregularly dispersed within the quartz-rich aggregates. Because of their spatial association within the infill domains, I interpret the pyrrhotite as having crystallized during the infill stage. The pyrrhotite is characterized by its strong reflectance, creamy pinkish-brown colour, and very distinct bireflectance. The pyrrhotite is intergrown with subordinate and amoeboid crystals (up to 1 mm) of **chalcopyrite**.

Calcite forms anhedral to amoeboid crystals that are concentrated around the pyrrhotite and form irregular infill domains, in association with subordinate albite, as medium-grained (up to 1 mm) interlobate aggregates. The calcite was distinguished by its high relief, extreme birefringence colours, and brisk reaction to cold dilute (10%) HCl.

Rare **pyrite** forms fine-grained (up to 0.2 mm) subhedral crystals that are immersed within the fine-grained aggregate of calcite that in some cases mantles the pyrrhotite-chalcopyrite intergrowths.

Very rare, very fine-grained **pentlandite** forms flame-like exsolutions within the pyrrhotite.

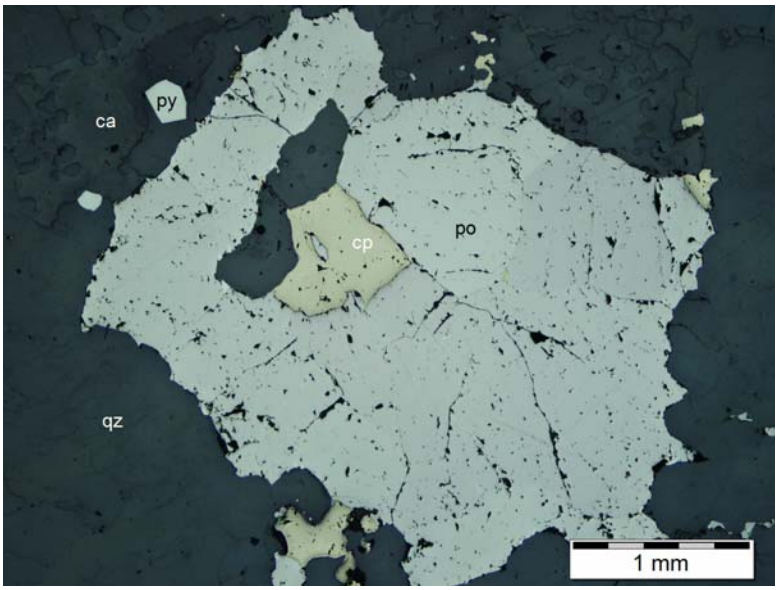

***Photomicrograph 3**: Anhedral to amoeboid pyrrhotite (po) is intergrown with subordinate chalcopyrite (cp) and immersed within the quartz-rich aggregate (qz). Some of the pyrrhotite crystals are rimmed by calcite (ca), which in some cases hosts fine-grained pyrite (py). Plane-polarized reflected light.*

Sample 4: 1272211

Metasandstone

This sample is made up of fine-grained quartz, white mica, and plagioclase. Different amounts of the above-mentioned minerals define a compositional layering that is gently curved (see image in the upper right part of this page). Within the different layers, the quartzofeldspathic grains are relatively well sorted and define a matrix-supported microstructure within the white mica-rich layers and a clast-supported microstructure within the quartzofeldspathic layers.

Mineral	*Modal %*	*Main Size Range (mm)*
quartz	47 – 50	up to 0.1
muscovite (and clay?)	43 – 45	up to 0.02
albite	5 – 6	up to 0.1
rutile	tr	up to 0.05
tourmaline?	tr	up to 0.05

Quartz forms fine-grained anhedral crystals immersed within a very fine-grained matrix of white mica and probable clay. Subtle differences in the relative amount of quartz and white mica as well as a coarser grain size (up to 0.1 mm) within the quartz-richer layers define a gently curved compositional layering.

Muscovite[1] (and probable clay) is very fine grained. The randomly oriented flakes form most of the matrix, which includes the quartzofeldspathic clasts. Due to the very fine grain size of the phyllosilicates, their mineralogy would be better resolved by short-wave infrared spectroscopy; however, the abundant crystals with very high birefringence suggest the presence of white mica among the phyllosilicates.

Albite is fine grained and anhedral to amoeboid. It is preferentially associated with the quartz-rich layers. The albite is distinguished by its typical albite twinning and lower refractive indexes than those of quartz.

Fine- to very fine-grained columnar and prismatic crystals show high relief and are transparent in plane-polarized transmitted light. In some cases, their moderate reflectance suggests they are probably **rutile**; however, in some other cases, their nature remains unresolved.

Rare fine-grained (up to 0.05 mm) crystals of **tourmaline** are dispersed within the quartzofeldspathic aggregate. They are distinguished by their strong pleochroism with brown

1 Determined by SWIR Spectroscopy. See Table 2.

tints and by a stronger absorption when the elongate crystals are oriented perpendicular to the polarization direction.

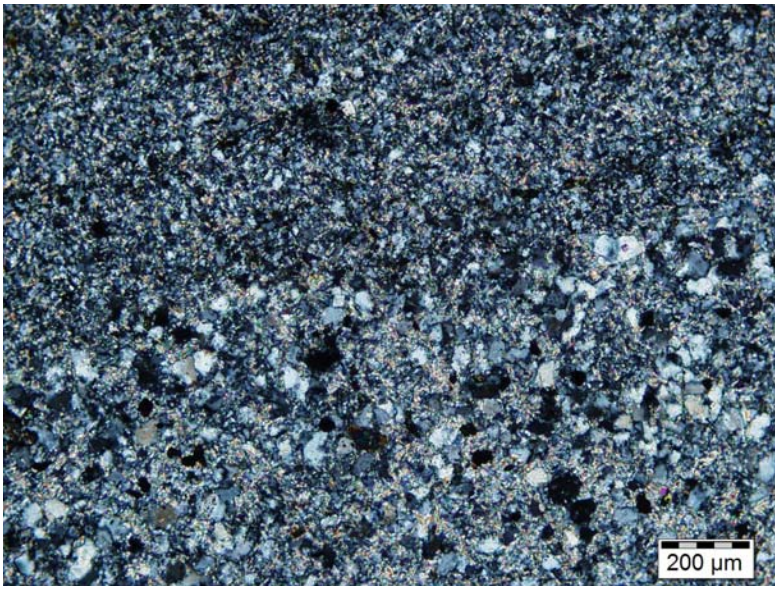

***Photomicrograph 4**: The compositional layering is defined by layers richer in white mica (very fine-grained and with high birefringence in the upper part of the photomicrograph) and layers with more abundant quartz and albite (grey-and-white grains), and subordinate white mica (in the lower part of the photomicrograph). Crossed Nicols transmitted light.*

Sample 5: 1272212

Albite-quartz-chlorite alteration-zone

Medium-grained subhedral poikilitic crystals of quartz are associated with subordinate chlorite and are immersed within a fine-grained interlobate aggregate of albite and quartz. Rare very fine-grained rutile crystals are dispersed within the quartzofeldspathic aggregate. The fine-grained albite-rich aggregate is slightly brecciated and filled in by quartz and albite.

Mineral	*Modal %*	*Main Size Range (mm)*
albite	80 – 90	up to 0.1
quartz	15 – 20	up to 2.5
Mg-chlorite	0.1	up to 0.5 × 0.2
rutile	tr	up to 0.05
apatite	tr	up to 0.1
iron oxides	tr	cryptocrystalline
pyrite	tr	up to 0.02

Albite occurs as fine-grained interlobate crystal aggregates that dominate the composition of this sample. The fine-grained albite is intergrown with subordinate fine-grained quartz, from which it is distinguished by its albite twinning and lower refractive indexes than those of quartz.

Quartz forms inequigranular (up to 2.5 mm) subhedral poikilitic crystals that are immersed within a fine-grained aggregate of albite and subordinate quartz. The quartz finally filled in the interstices and the triangular microstructures between the slightly brecciated albite-rich aggregate. In this case, the quartz occupies the interstices between fine-grained and subhedral albite. Because of the subhedral shape, poikilitic nature, and spatial association with tabular chlorite, I interpret the medium-grained quartz-chlorite as an overprinting assemblage, which post-dated the albite-rich replacement. The subhedral poikilitic quartz crystals host abundant fine-grained inclusions of albite, chlorite, rutile, apatite, and a very fine-grained unresolved material.

Mg-chlorite forms medium-grained tabular crystals that are preferentially associated and intergrown with the medium-grained subhedral quartz crystals. Chlorite shows negative elongation, which indicates a magnesium-rich composition of the chlorite.

Fine- to very fine-grained dispersions of **rutile** are irregularly dispersed within the albite-rich aggregates and in some cases form irregular, slightly curved, discontinuous clusters.

Very rare, very fine-grained pyrite is dispersed within the albite-rich aggregates and is surrounded by very rare dispersions of iron oxides.

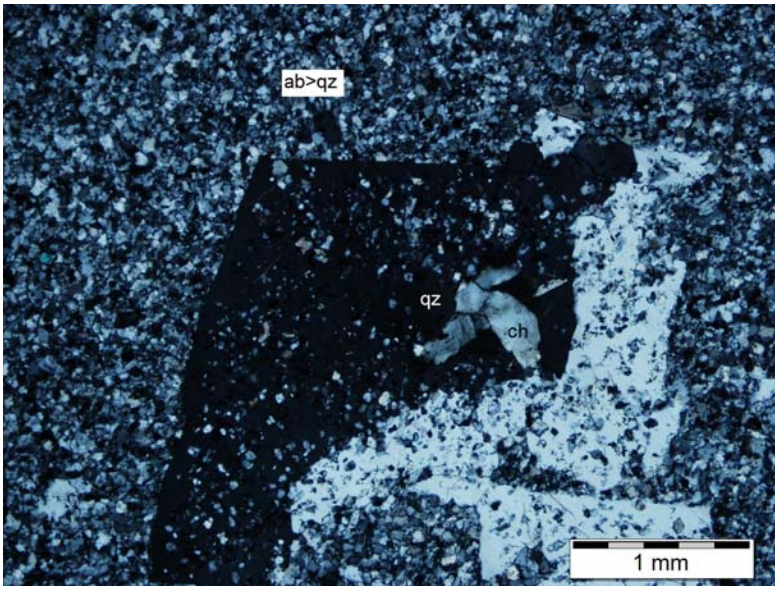

***Photomicrograph 5a**: Subhedral poikilitic quartz (qz) is intergrown with subordinate chlorite (ch) and overprinted the fine-grained aggregate of albite and subordinate quartz (ab>qz). Crossed Nicols transmitted light.*

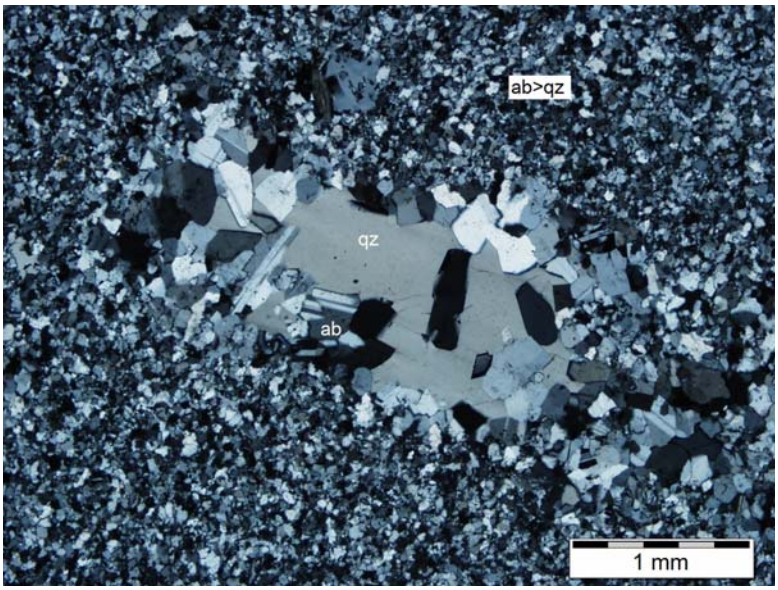

***Photomicrograph 5b**: Fine-grained subhedral albite (ab) and interstitial quartz (qz) filled in the interstices between the slightly brecciated aggregate of fine-grained albite and subordinate quartz (ab>qz). Crossed Nicols transmitted light.*

Sample 6: 1272213

Microdiorite

Calcite-bornite-biotite-epidote-albite infill

Medium-grained elongate laths of plagioclase are randomly oriented and define a sub-ophitic microstructure in association with medium-grained anhedral actinolite, which replaces a magmatic pyroxene. The medium-grained isotropic aggregate is crosscut by thin intersecting veins and veinlets of calcite-bornite-biotite-epidote-albite.

Mineral	*Modal %*	*Main Size Range (mm)*
micro-gabbro (80% of PTS)		
actinolite	38 – 42	up to 1
plagioclase	33 – 38	up to 0.5 × 0.2
epidote	4 – 5	up to 0.15
titanite	1	up to 0.5
biotite	tr	up to 0.15
calcite-bornite-biotite-epidote-albite infill (20% of PTS)		
calcite	10	up to 3.5
bornite	5	up to 10
biotite	2	up to 3
epidote	1	up to 0.3
albite	1	up to 0.25
covellite	tr	up to 0.2
chlorite(?)	tr	up to 0.1

Plagioclase occurs as medium-grained elongate laths that are randomly oriented and intergrown with the medium-grained actinolite within the host rock. The plagioclase-actinolite association defines a microstructural relict in which only the plagioclase represents a mineralogic relict from the magmatic rock. The plagioclase is characterized by albite twinning and is subtly to weakly altered by fine- to very fine-grained dispersions of epidote and probable calcite. In some cases, the plagioclase laths show a continuous growth zoning,

which is more evidence in favour of a magmatic origin. Less altered blocky to anhedral crystals of plagioclase occur at the vein walls, and in this case, I attribute the plagioclase to the infill phase, during which it probably crystallized in equilibrium with the calcite, bornite, and epidote.

Actinolite forms subidioblastic to xenoblastic crystals that completely replaced a probable magmatic pyroxene. The actinolite is characterized by distinct pleochroism (X: green; Y: green; Z: bluish green) and extinction angles (c:Z) up to 15°. In some cases, the actinolite is overprinted by fine-grained xenoblastic **biotite**. Fine-grained **titanite** is dispersed within the pseudomorphic aggregate after the pre-existent pyroxene.

Titanite is preferentially intergrown with the actinolite and the plagioclase and forms xenoblastic crystals of up to 0.5 mm.

Epidote forms fine- to medium-grained xenoblastic crystals that are concentrated within the infill and heterogeneously overprinted the host rock. In some cases, the epidote forms monomineralic veinlets.

Calcite is concentrated within the infill where it forms interlobate to granoblastic crystals of up to 3.5 mm. The calcite is distinguished by its high relief, extreme birefringence, and brisk reaction to cold dilute (10%) HCl. Within that infill, the calcite is intergrown with anhedral **bornite** (up to 10 mm), sub-tabular biotite (up to 3 mm long), and fine-grained albite, which is preferentially concentrated at the vein walls. The bornite also occurs as fine-grained dispersions within the host rock. It is weakly altered and partially replaced by fine-grained aggregates of covellite, which is distinguished by its typical lamellar fabric and distinct pleochroism with indigo to violet tints (see Photomicrograph 6b).

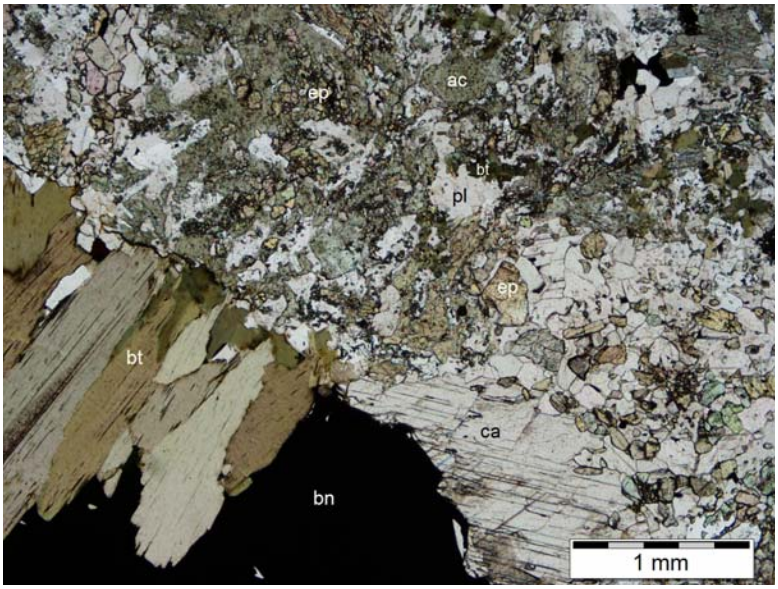

***Photomicrograph 6a**: A medium-grained aggregate of plagioclase (pl) and actinolite (ac) is overprinted by heterogeneously distributed epidote (ep) and biotite (bt in the upper part of the photomicrograph) and is filled in by medium- to coarse-grained calcite (ca), bornite (bn), and biotite. Plane-polarized transmitted light.*

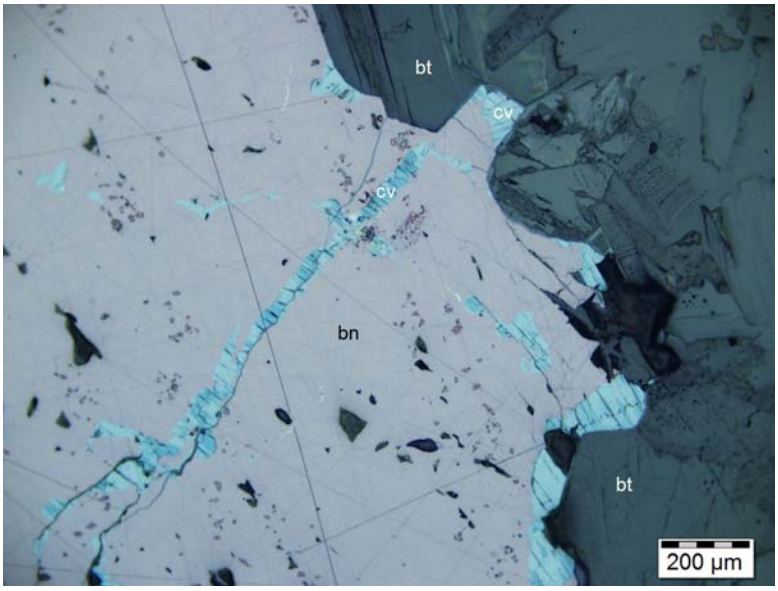

***Photomicrograph 6b**: Coarse-grained bornite (bn) crystallized within an infill domain and is intergrown with biotite (bt). Fine- to medium-grained covellite (cv) partially replaces the bornite. Plane-polarized reflectant light.*

Sample 7: 1272438

White mica schist

Very fine-grained and parallel crystals of white mica define a continuous cleavage. Very fine-grained ilmenite defines a compositional layering parallel to the cleavage. An irregular quartz veinlet crosscuts the cleavage.

Mineral	*Modal %*	*Main Size Range (mm)*
white mica	90 – 95	up to 0.02
ilmenite(?)	8 – 10	up to 0.02
quartz	tr	up to 0.1

White mica is very fine grained (up to 0.02 mm) and defines a continuous cleavage (as defined in Passchier and Trouw 1998). The white mica is distinguished by its moderate relief, lamellar habit, straight extinction, and high birefringence. Most of the white mica crystals host very fine-grained (less than 0.001 mm) inclusions of unresolved material; some of the material is transparent and prismatic and can tentatively be attributed to rutile and/or zircon. In some parts of the polished thin section, very fine-grained white mica overprinted the parallel crystals of white mica as randomly oriented (decussate) flakes.

I**lmenite** is very fine grained (up to 0.02 mm), and the sub-tabular crystals show a preferred dimensional orientation. The ilmenite is concentrated within parallel layers (up to 0.5 mm thick) and is dispersed within the white mica. The ilmenite was distinguished by its sub-tabular shape, low reflectivity, grey colour, and anisotropy under crossed Nicols reflected light.

Very rare fine-grained clasts of **quartz** are elongate parallel to the cleavage and show a moderate to strong undulose extinction. The quartz filled in an irregular veinlet that crosscut the cleavage at ~50° and was transposed by the cleavage (see Photomicrograph 7). The quartz veinlet shows “boudinage” microstructures, which are typical of a ductile style of deformation.

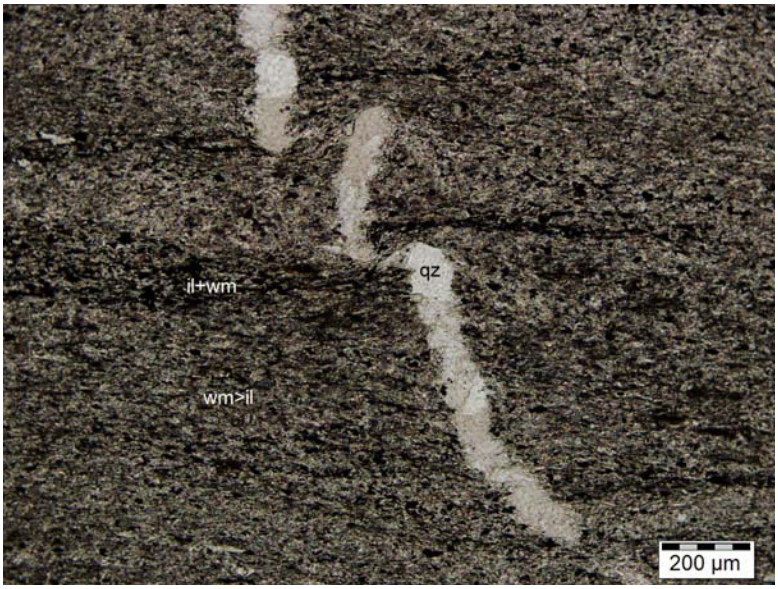

***Photomicrograph 7**: A compositional layering is defined by prevailing white mica and subordinate ilmenite (wm>il) and parallel layers with abundant ilmenite and white mica (il+wm). The compositional layering is crosscut by a boudinaged quartz veinlet. Plane-polarized transmitted light.*

Sample 8: 1272474

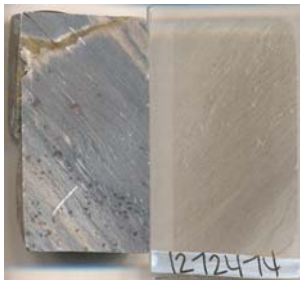

White mica-quartz-dolomite schist

Medium-grained porphyroclasts of quartz are wrapped by cleavage domains of white mica and are immersed within a spaced foliation defined by microlithons of fine-grained quartz, dolomite, and white mica, as well as white mica-rich cleavage domains.

Mineral	*Modal %*	*Main Size Range (mm)*
white mica	58 – 62	up to 0.02; rare up to 0.2
quartz	25 – 27	up to 1
dolomite	19 – 21	up to 0.2
ilmenite	3 – 4	up to 0.05
zircon	tr	up to 0.05

White mica is very fine grained (up to 0.02 mm) and is concentrated within spaced cleavage domains, in which it is dimensionally iso-oriented. The cleavage domains are anastomosing and mantle the quartz porphyroclasts. Very fine-grained white mica also crystallized within the quartz-dolomite microlithons and within the quartz strain shadows as randomly oriented flakes. Rare tabular crystals of white mica reach 0.2 mm and are oriented parallel to the schistosity. The subordinate amount of white mica within some of the microlithons and the asymmetric strain shadows around the quartz are reliable indicators of the shear sense. Oriented samples of this rock type would provide useful data about the structural and metamorphic evolution.

Quartz forms inequigranular (up to 1 mm) sub-rounded to amoeboid porphyroclasts that are mantled by the white mica cleavage domains. The quartz is associated with blocky to elongate crystals of dolomite and define fine-grained microlithons that are wrapped by the cleavage domains and define δ-type mantled porphyroclasts (see Passchier and Trouw, 1998, for a detailed discussion on the significance of these microstructures). The composition of this polished thin section varies from the upper left, where the quartz porphyroclasts are more abundant, to the lower right, where the volume percentage of the cleavage domains increases and reaches ~70%. The presence of porphyroclasts triggers the crystallization of strain shadows rich in dolomite, quartz, and in some cases, white mica.

Dolomite is fine grained (up to 0.2 mm) and is concentrated within the microlithons and within the strain shadows around the quartz porphyroclasts. The dolomite was distinguished by its high relief, extreme birefringence, and very slow reaction to cold dilute (10%) HCl.

Ilmenite is very fine to fine grained (up to 0.05 mm) and forms sub-tabular crystals that are preferentially associated with and dimensionally iso-oriented within the white mica cleavage domains. The ilmenite shows low reflectivity and a grey colour, and it is anisotropic under crossed Nicols reflected light.

Very rare **zircon** forms rare elongate crystals of up to 0.05 mm with rounded edges. The crystals are dispersed within the cleavage domains.

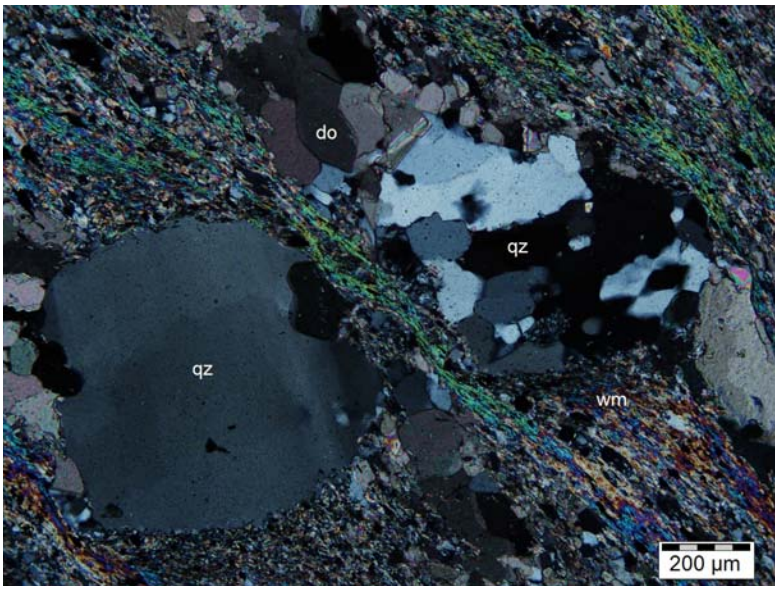

***Photomicrograph 8**: Quartz porphyroclasts (qz) are wrapped by cleavage domains of white mica (wm) and are surrounded by δ-type strain shadows of dolomite (do) and subordinate quartz. Plane-polarized transmitted light.*

Sample 9: 1272475

Dolomite-quartz breccia

Fractured fragments of medium- to coarse-grained quartz aggregates and fragments of fine-grained dolomite are filled in by fine- to medium-grained dolomite, quartz, white mica, and subordinate calcite.

Mineral	*Modal %*	*Main Size Range (mm)*
dolomite	70 – 74	up to 0.2
quartz	25 – 27	0.05–5
calcite	1 – 2	up to 0.2
white mica	tr	up to 0.25
hematite(?)	tr	up to 0.05

Dolomite forms fine-grained monomineralic aggregates with angular shapes (up to to 6 mm). The fine-grained dolomitic aggregates are associated with more abundant quartz aggregates and are filled in by an inequigranular matrix made up of blocky crystals of dolomite, quartz, and white mica. **Calcite** forms fine-grained (up to 0.2 mm) idioblastic crystals that coat the partially filled cavities. I interpret the calcite as post-dating the crystallization of the infill and the brittle deformation. The calcite was distinguished by its brisk reaction to cold dilute (10%) HCl.

Quartz forms medium- to coarse-grained crystal aggregates that are fractured and show moderate to strong undulose extinction. In some cases, the quartz aggregates are crosscut by thin (up to 0.2 mm) intersecting subgrain boundaries. The quartz aggregates define irregular, angular shapes and are filled in by carbonate-rich infill domains. Fine-grained blocky crystals of quartz are dispersed within the infill domains.

Rare fine-grained flakes of **white mica** are randomly dispersed within the carbonate-rich infill domains and in some cases show strong undulose extinction and bent lamellae.

Very rare fine-grained sub-lamellar **hematite** is heterogeneously dispersed within the carbonate-rich infill domains.

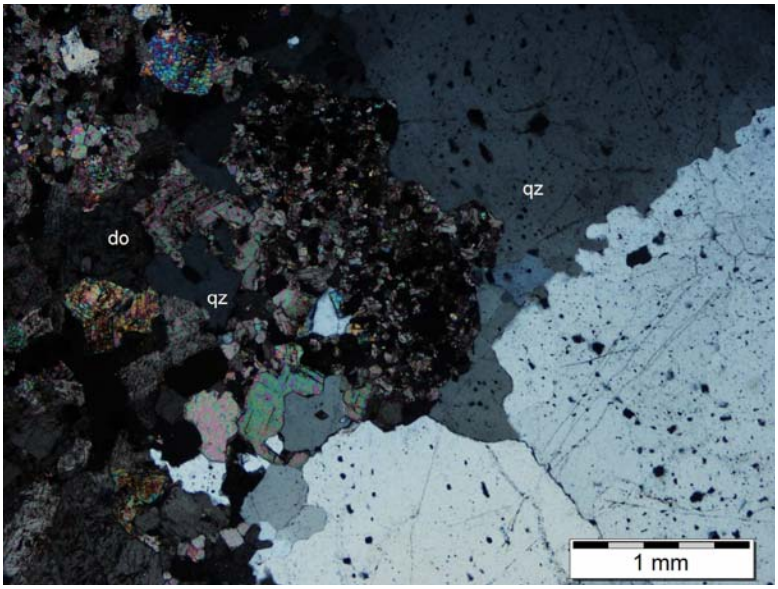

***Photomicrograph 9**: A medium- to coarse-grained domain of quartz is deformed and filled in by a dolomite-rich infill domain (do). Testing with HCl indicates that the calcite coats the partially filled cavities that crosscut the dolomitic infill domain. Plane-polarized transmitted light.*

Sample 10: 1307873

Basalt

Calcite-K-feldspar-albite(?)-biotite-chalcopyrite-pyrite infill

Fine-grained subhedral to anhedral crystals of plagioclase are randomly oriented and are associated with fine-grained subhedral magnetite and anhedral biotite. The granular and isotropic microstructure is crosscut by infill domains of calcite-K-feldspar-albite(?)-biotite-chalcopyrite-pyrite.

Mineral	*Modal %*	*Main Size Range (mm)*
basalt (97% of PTS)		
plagioclase (albite-oligoclase)	58 – 60	up to 0.25; rare prisms up to 1.2 mm long
magnetite	20 – 22	up to 0.05
biotite	17 – 19	up to 0.1
hematite	tr	up to 0.02
chalcopyrite	tr	up to 0.02
calcite-K-feldsdpar-albite(?)-biotite-chalcopyrite-pyrite infill (3% of PTS)		
calcite	1.5 – 1.7	up to 0.3
K-feldspar	0.5 – 0.7	up to 0.3
biotite	0.2 – 0.4	up to 0.2
plagioclase (albite?)	0.2 – 0.3	up to 0.2
chalcopyrite	0.1 – 0.2	up to 0.5
pyrite	tr	up to 0.2
rutile	tr	up to 0.02
apatite	tr	up to 0.2

Plagioclase (albite) is fine grained (up to 0.25 mm; rare prisms up to 1.2 mm long), subhedral to anhedral, and randomly oriented. The crystals show albite twinning and are subtly altered by very fine-grained and unresolved dispersions with high relief. The extinction angles between adjacent albite twins [a′:(010)=15°] indicates an albitic-oligoclasic

composition of the plagioclase. I interpret the subhedral shape of the plagioclase as the result of magmatic crystallization accompanied by the crystallization of fine-grained subhedral crystals of **magnetite** and fine-grained anhedral crystals of **biotite**. The colour index of the rock is ~45; therefore the rock is a basalt.

Hematite weakly altered the magnetite.

The fine-grained plagioclase-magnetite-biotite aggregate is weakly brecciated (crackle breccia) and filled in by irregular infill domains and discontinuous vein-like domains of calcite-K-feldspar-albite(?)-biotite-chalcopyrite-pyrite.

Calcite prevails within the infill domains as anhedral to amoeboid crystals of up to 0.3 mm. The calcite is intergrown with interstitial crystals of **K-feldspar**, which is distinguished by its low relief and low birefringence (up to first-order white). On the offcut, the K-feldspar is distinguished by the yellow staining, which indicates that the K-feldspar is exclusively crystallized within the infill domains.

Chalcopyrite forms anhedral to amoeboid crystals of up to 0.5 mm. The chalcopyrite is concentrated within the infill and forms very rare, very fine-grained (up to 0.02 mm) dispersions within the host rock. Chalcopyrite occurs within biotite-rich (see Photomicrograph 10b) and calcite-K-feldspar-rich segments of the infill domains.

Pyrite occurs as euhedral crystals up to 0.2 mm within the infill domains.

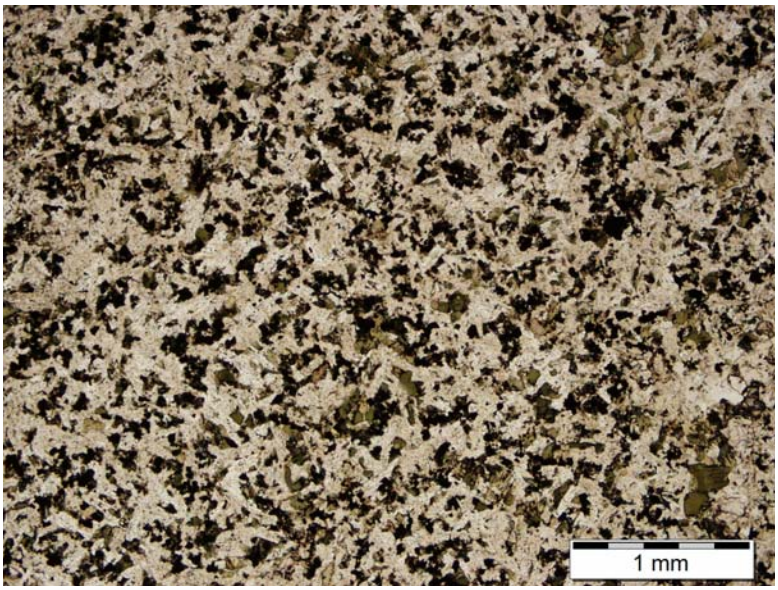

***Photomicrograph 10a**: The basalt is characterized by a colour index of ~45 and is made up of plagioclase (white), magnetite (opaque), and biotite (brown). Plane-polarized transmitted light.*

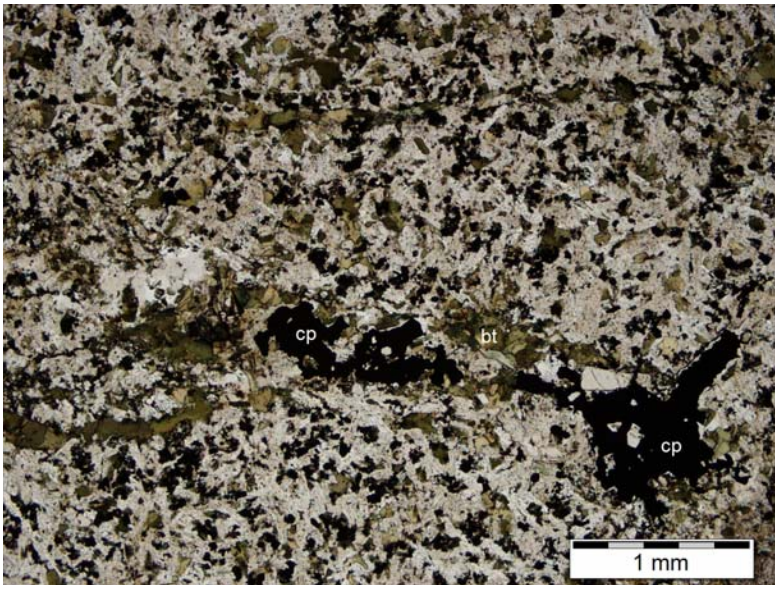

***Photomicrograph 10b**: Chalcopyrite (cp) forms amoeboid crystals associated with the biotite (bt) within the infill domains that crosscut a fine-grained basalt. Plane-polarized transmitted light.*

Sample 11: Boulder field, K-Fe front

Clay-plagioclase-Mg-chlorite breccia

Angular fragments (up to 24 × 7 mm) of a very fine-grained aggregate of clay (kaolinite?) are brecciated and filled in by an inequigranular heterogeneous infill made up of subhedral crystals of plagioclase, calcite, Mg-chlorite, and rare chalcopyrite, sphalerite, and probable arsenopyrite. The angular fragments are irregularly oxidized along their rims and around the fractures.

Mineral	*Modal %*	*Main Size Range (mm)*
altered (kaolinite?) and brecciated fragments (~75% of PTS)		
clay (kaolinite?)	55	up to 0.01
infill domain (~25% of PTS)		
plagioclase (albite)	20	up to 1.5
Mg-Chlorite	3	up to 1
calcite	1	up to 0.5
iron oxides (including goethite)	tr	cryptocrystalline
biotite/phlogopite(?)	tr	up to 0.05
chalcopyrite	tr	up to 0.1
arsenopyrite?	tr	up to 0.03

Clay (kaolinite?) is very fine grained and forms angular fragments that are fractured, rotated, and filled in by a plagioclase-rich infill domain (cl1 in Photomicrograph 11a). The deposition of cryptocrystalline iron oxides progressively oxidized the angular fragments and defined an oxidation front that completely overprinted the smaller fragments and penetrated up to 2 mm into the coarser fragments. A second generation of clay (cl2 in Photomicrograph 11a) was crystallized within the infill domain and is characterized by a brown colour under plane-polarized transmitted light. I tentatively interpret this as a potassium-bearing clay because of its yellow colour.

Plagioclase (albite) forms inequigranular (up to 1.5 mm) to subhedral crystals that in some cases are ductilely deformed and are immersed within a fine-grained aggregate of quartz and plagioclase. The plagioclase shows albite twinning, and measurement of the extinction angle

between the adjacent twinning lamellae [a′: (010)= 10°] indicates an albitic composition. The plagioclase is intergrown with subordinate anhedral crystals of **calcite**, which is distinguished by its high relief, extreme birefringence, and brisk reaction to cold dilute (10%) HCl. The calcite hosts abundant cryptocrystalline inclusions of iron oxides, which in some cases give it an earthy appearance.

Mg-chlorite occurs as deformed and bent lamellae of up to 1 mm long. The ubiquitous signs of deformation, which also include kink bands and undulose extinction, indicate that the chlorite crystallized during the same deformation event that fractured the fragments and deformed the plagioclase within the infill domain. The chlorite shows negative elongation and therefore is magnesium rich.

Iron oxides completely replaced inequigranular crystals (up to 0.3 mm) and are heterogeneously dispersed within the interstitial infill domain. I attribute rare lamellar shapes to oxidized chlorite as suggested by the low reflectance of the oxidized aggregate. Very rare **chalcopyrite** is partially replaced by **goethite** and only occurs within the infill domain.

Very rare **arsenopyrite**(?) forms a clustered aggregate of fine-grained crystals within the calcite in the infill domain.

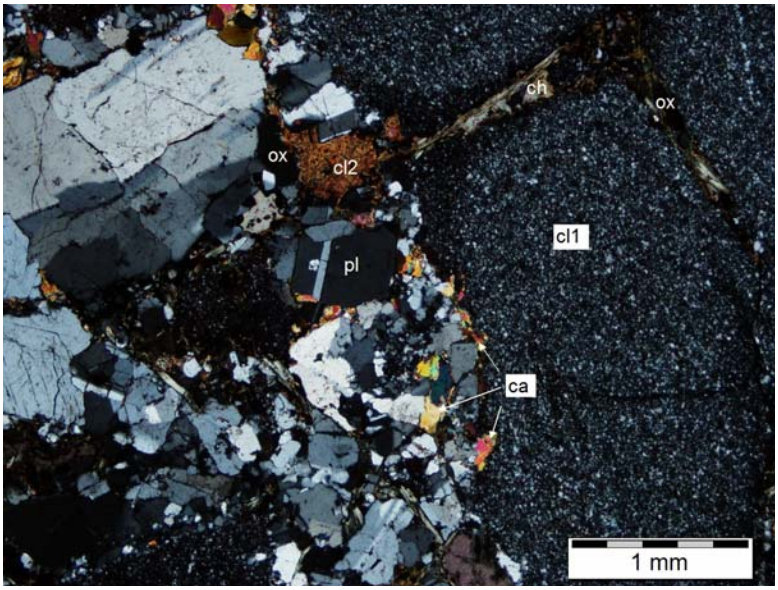

***Photomicrograph 11a**: Fractured fragments are made up of clay, probably kaolinite. This first generation of clay (cl1) pre-dated the brittle deformation and the infill of plagioclase (pl), calcite (ca), Mg-chlorite (ch), iron oxides (ox), and a second generation of clay (cl2). Crossed Nicols transmitted light.*

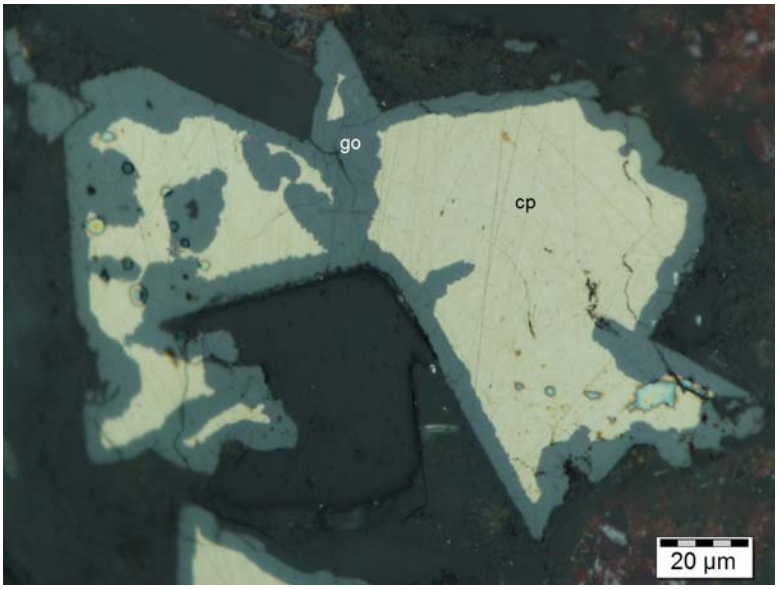

***Photomicrograph 11b**: Anhedral chalcopyrite (cp) is partially replaced by goethite (go). Plane-polarized transmitted light.*

Sample 12: Delhi breccia zone

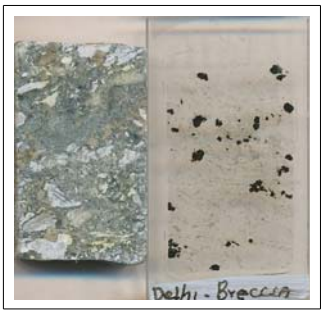

Calcite-albite-pyrite-actinolite-biotite breccia

Irregular sub-angular fragments (up to 8 × 3 mm) made up of a very fine-grained aggregate of clay (kaolinite?) and subordinate albite are immersed within an inequigranular matrix of calcite, albite, pyrite, biotite, actinolite, chalcopyrite, pyrrhotite, and titanite. The sub-angular, elongate shape of the clay-rich fragments indicates a low amount of mechanical wearing. The absence of undulose extinction within the calcite, which dominates the composition of the matrix, suggests that the matrix was not further deformed after the infill stage. These microstructural features do not allow me to determine whether hydrothermal or tectonic processes dominated during the brecciation process.

Mineral	*Modal %*	*Main Size Range (mm)*
fragments (~25% of PTS)		
clay	22 – 24	up to 0.02
plagioclase (albite)	1 – 2	up to 0.1
epidote/piemontite(?)	tr	up to 0.05
matrix (~75% of PTS)		
calcite	40 – 42	up to 1.2
plagioclase (albite)	25 – 27	up to 0.5
pyrite	3.5 – 4	up to 2.5
actinolite	1.5 – 2	up to 0.5 × 0.05
biotite	0.5 – 1	up to 0.8 × 0.2
chalcopyrite	tr	up to 0.50
pyrrhotite	tr	up to 0.15
titanite	tr	up to 0.7
zircon	tr	up to 0.002

Calcite forms xenoblastic and inequigranular crystals of up to 1.2 mm that prevail in the composition of the matrix, in which it forms interlobate crystal aggregates that are associated and intergrown with xenoblastic to subidioblastic crystals and crystal aggregates of albite,

xenoblastic pyrite, tabular crystals of biotite**,** randomly oriented actinolite, and rare chalcopyrite, pyrrhotite, and titanite. The calcite was distinguished by its high relief, extreme birefringence, and brisk reaction to cold dilute (10%) HCl.

The sub-angular and in some cases elongate fragments are made up of a very fine-grained aggregate of **clay** (probably kaolinite) and subordinate fine-grained albite. Some of these fragments show an internal foliation defined by the iso-orientation of very fine-grained clusters of unresolved minerals and fine-grained prismatic crystals with high relief, very high birefringence, and distinct pleochroism with dark-red to brown colours (possible zircon or epidote/piemontite). The clay-rich fragments are immersed within a heterogeneous, inequigranular matrix of calcite, albite, pyrite, biotite, tremolite/actinolite, chalcopyrite, pyrrhotite, and titanite.

Plagioclase (albite) forms inequigranular interlobate crystal aggregates that occupy the matrix. Fine-grained plagioclase forms vein-like domains and irregular replacement patches within the clay-rich fragments. The plagioclase shows albite twinning with relatively low (~10°) angles between the adjacent twinning lamellae, and I interpret its composition as albitic. Fine-grained and interlobate crystal aggregates of albite form irregular domains that I interpret as a sodium-rich infill phase that was associated with the actinolite crystallization and probably pre-dated the calcite-rich stage of the infill. This interpretation envisages a scenario in which the composition of the infill changed from a sodium-rich (albite, and albite-tremolite) earlier stage to a calcium-rich (calcite) final stage.

Pyrite forms medium-grained (up to 2.5 mm) subidioblastic crystals that are dispersed within the matrix and are intergrown with subordinate **pyrrhotite** and **chalcopyrite** (see Photomicrograph 12b). The pyrrhotite shows a moderate alteration, and based on microstructural interpretation, I interpret its crystallization as earlier than the pyrite, which was then followed and partially replaced by rare chalcopyrite.

Biotite is dispersed within the matrix as randomly oriented medium-grained (up to 0.8 × 0.2 mm) lamellae that host abundant very fine-grained inclusions of zircon. The biotite is spatially associated with the pyrite.

Actinolite form fine-grained prismatic to acicular crystals that are finely intergrown with subordinate albite and are characterized by a distinct pleochroism with green colours. The tremolite/actinolite shows oblique extinction (c:Z up to 13°).

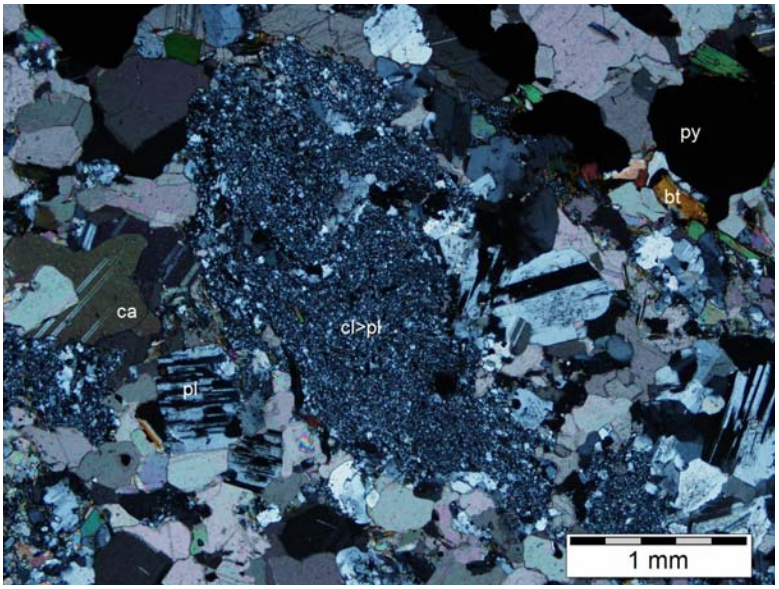

***Photomicrograph 12a**: Irregular fragments of very fine-grained clay and subordinate plagioclase (cl>pl) are immersed within a matrix of calcite (ca), plagioclase (pl), pyrite (py), and biotite (bt). Crossed Nicols transmitted light.*

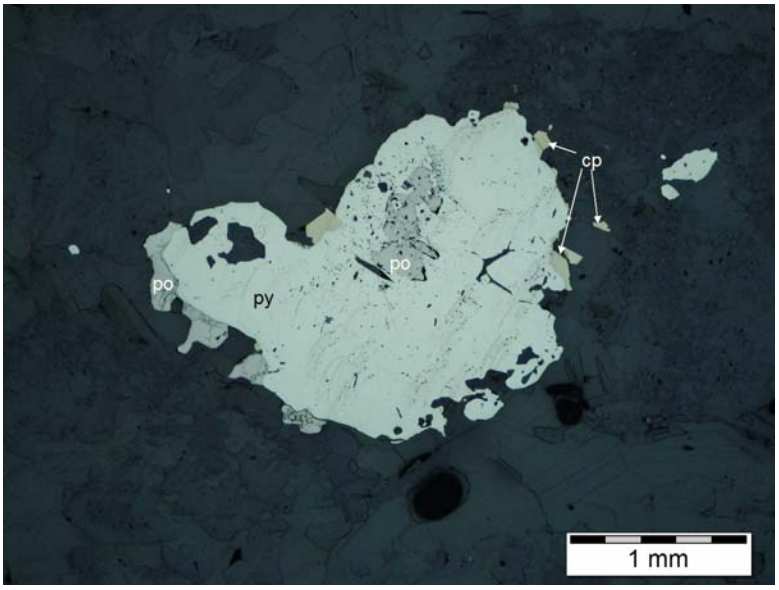

***Photomicrograph 12b**: Anhedral pyrite (py) is intergrown with and probably partially replaced pyrrhotite (po), and is partially replaced by rare chalcopyrite (cp). Plane-polarized reflected light.*

Sample 13: JFM006-1

Graphitic schist

Very fine-grained graphite is intergrown with very fine-grained quartz and/or albite and define a continuous foliation. During the ductile deformation the foliation was folded (see Photomicrograph 13a) and overprinted by inequigranular (0.01–0.1 mm) aggregate of albite.

Mineral	*Modal %*	*Main Size Range (mm)*
graphite	55 – 57	up to 0.02
plagioclase (albite)	40 – 44	0.01–0.1
quartz(?)	2 – 5	up to 0.02
titanite(?)	0.1 – 0.2	up to 1.5 mm long
tourmaline	tr	up to 0.2 mm long

Graphite is very fine grained and dominates the composition of the foliated and folded domains. The graphite is probably associated with subordinate and very fine-grained quartz and/or albite.

Fine-grained (up to 0.1 mm) **plagioclase (albite)** defines irregular lenticular and vein-like domains that crosscut the continuous foliation. The plagioclase hosts very fine-grained dispersions of graphite and prismatic crystals of unresolved minerals. The plagioclase shows albite twinning and in most cases forms inequigranular (0.01–0.1 mm) interlobate crystal aggregates.

Fine- to medium-grained prisms up to 1.5 mm long and xenoblastic crystals of probable titanite are aligned parallel to the foliation and in some cases (Photomicrograph 13b) overprinted the foliation. The prismatic crystals show very high relief, extreme birefringence colours, and distinct pleochroism with pale-brown to reddish colours.

Rare fine-grained (up to 0.2 mm long) prisms of **tourmaline** are preferentially crystallized within their albite-rich domains and are distinguished by their weak pleochroism (pale green) with stronger absorption when the prisms are oriented perpendicular to the direction of polarization.

Dilation jogs were formed along the foliation and were filled in by albite and probable K-feldspar, which is now moderately altered by a potassium-bearing clay, as suggested by the yellow staining on the offcut.

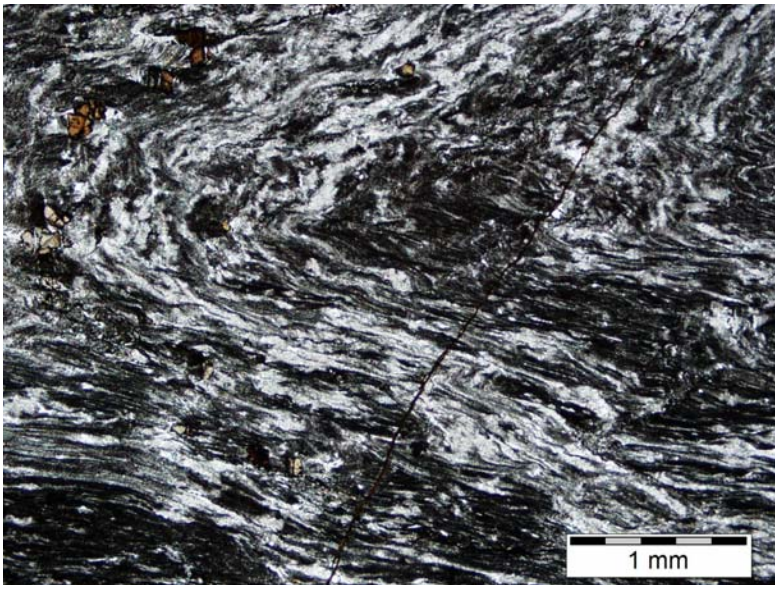

***Photomicrograph 13a**: The cryptocrystalline aggregates of graphite (opaque domains) alternate with fine-grained aggregates of albite (white domains) and are ductilely folded. Plane-polarized transmitted light.*

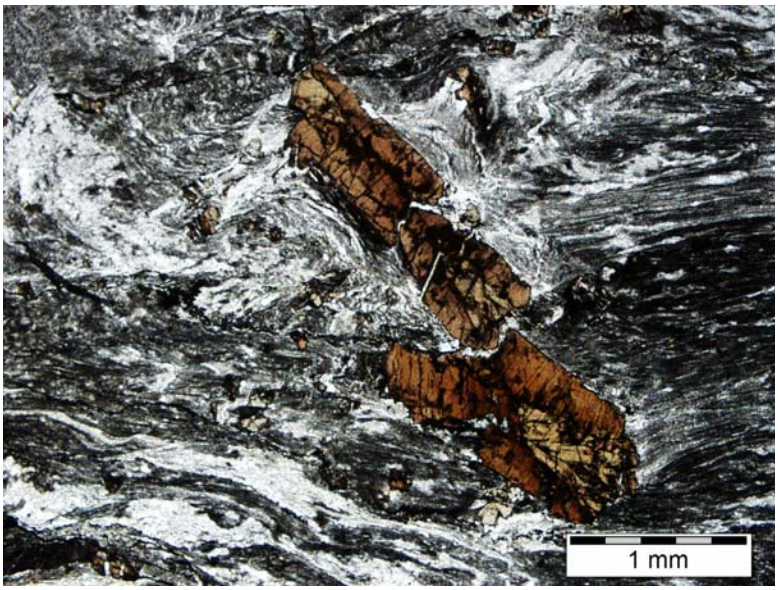

***Photomicrograph 13b**: Prismatic crystals of probable titanite show high relief and moderate pleochroism (pale-brown to reddish). They overprinted the chaotically folded and layered aggregates of albite (white) and graphite (opaque). Plane-polarized transmitted light.*

Sample 14: JFM008

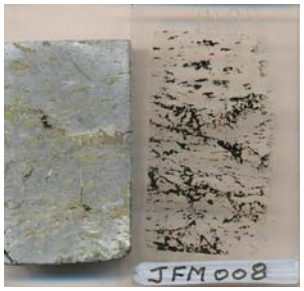

Clay-chalcopyrite-pyrrhotite alteration-zone

A very fine-grained aggregate of clay is intergrown with anastomosing and amoeboid aggregates of fine-grained plagioclase (albite), chalcopyrite, pyrrhotite, sphalerite, as well as very rare titanite(?) and white mica.

Mineral	*Modal %*	*Main Size Range (mm)*
clay	70 – 72	up to 0.02
plagioclase (albite)	10 – 14	up to 0.15
chalcopyrite	10 – 12	massive; up to 3 × 1
pyrrhotite	4 – 5	massive; up to 3 × 1
sphalerite	1 – 2	up to 0.5
titanite	tr	up to 0.2
white mica	tr	

Clay forms very fine-grained interlobate aggregates that are intergrown with anastomosing domains of chalcopyrite, plagioclase, pyrrhotite, lesser sphalerite, and rare titanite and white mica. The clay-rich aggregates host subordinate very fine- to fine-grained crystals of albite. This microstructural feature, together with the presence of subordinate and very fine-grained clay dispersed within the plagioclase-rich domains, suggests that the clay may have overprinted and progressively replaced the albite.

Plagioclase (**albite**) forms fine-grained and inequigranular-interlobate aggregates. The albite-rich domains are partially to completely overprinted by very fine-grained clay. The plagioclase shows albite twinning, and the relatively low angle between adjacent twinning lamellae [a′: (010) less than 15°] indicates an albitic composition of the plagioclase.

Chalcopyrite forms anastomosing and amoeboid domains that probably precipitated as infill within the fractured and progressively more altered aggregates of fine-grained albite. The chalcopyrite is associated and intergrown with anhedral domains of **pyrrhotite** and subordinate **sphalerite**.

Rare fine-grained **titanite** is preferentially intergrown with the chalcopyrite-rich aggregates, and I attribute this spatial association as a consequence of the crystallization of titanite during the sulphide precipitation event.

White mica is fine grained, and the lamellae are preferentially enclosed within the chalcopyrite. The association of white mica and chalcopyrite further supports the

interpretation of an earlier equilibrium of chalcopyrite-albite and white mica, which were filled in by chalcopyrite-pyrrhotite-sphalerite and overprinted by clay alteration. Spectroscopic analysis of the clay is highly recommended as the nature of the clay may further constrain the thermal evolution of this sample and the mineralizing event.

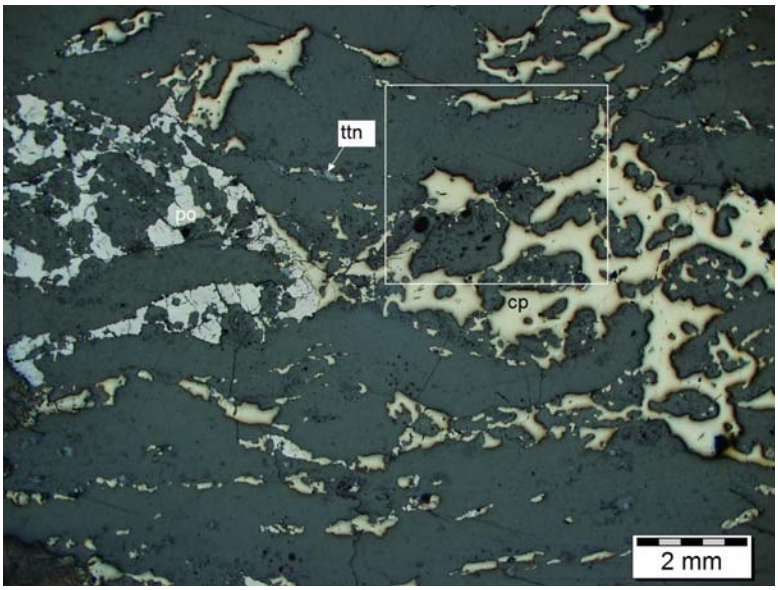

***Photomicrograph 14a**: Anastomosing sulphide-rich domains are made up of chalcopyrite (cp) and pyrrhotite (po). Rare titanite is preferentially intergrown with chalcopyrite. The composition of the gangue material (in the box) is shown in Photomicrograph 14b. Plane-polarized reflected light.*

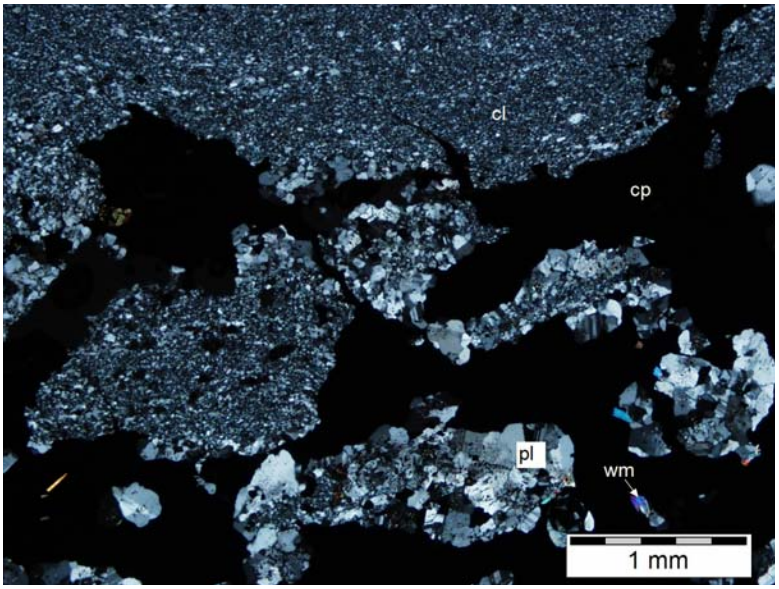

***Photomicrograph 14b**: Detail of the area in the box of Photomicrograph 14a. Very fine-grained clay (cl) overprinted fine-grained plagioclase (pl). Rare fine-grained lamellae of white mica (wm) are preferentially associated with the chalcopyrite. This microstructural feature indicates that the white mica pre-dated the clay alteration. Crossed Nicols transmitted light.*

Sample 15: JFM009

Actinolite schist

Calcite-actinolite-chlorite-pyrite-chalcopyrite infill

An irregular folded compositional layering is defined by fine-grained domains of clay-actinolite-quartz(?) and monomineralic domains of actinolite. Subhedral pyrite and amoeboid chalcopyrite overprinted the layered domains. They are mantled by Mg-chlorite strain shadows and are associated with calcite. The layered domains are crosscut by a calcite-rich vein-like domain that hosts fine-grained actinolite, chalcopyrite, pyrite, biotite, and irregular domains of albite.

Mineral	***Modal %***	***Main Size Range (mm)***
calcite	35 – 37	up to 1.2
clay	30 – 33	up to 0.02
actinolite	25 – 27	up to 1 mm long
pyrite	3 – 3.5	up to 1.5
chlorite	2 – 2.5	up to 0.5 mm long
chalcopyrite	1	up to 1
biotite	tr	up to 0.4 mm long
plagioclase	tr	up to 0.2
quartz(?)	tr	up to 0.05

Calcite forms inequigranular interlobate crystal aggregates that occupy the median part of the polished thin section. The calcite domain probably crosscut the layered clay-rich and actinolite domains and hosts fine-grained dispersions of acicular actinolite, anhedral chalcopyrite, subhedral pyrite, biotite, and irregular crystal aggregates of **albite**. Similarly with what was described in Sample 14, the albite-rich aggregates are interpreted as the less altered counterparts of the clay-altered domains.

Clay forms irregular to elongate domains that are interlayered and folded together with the actinolite domain. The clay is very fine grained and is associated with very fine- to fine-grained actinolite and probable albite and/or quartz.

Actinolite is fine grained. It is concentrated within irregular monomineralic domains in which the prismatic to acicular crystals are randomly oriented and characterized by a distinct green pleochroism (X: pale green; Y: light green; Z: light bluish green) and extinction angles (c:Z)

smaller than 15°. Fine-grained actinolite is dispersed within the calcite-rich domain together with elongate lamellae of Mg-chlorite and rare **biotite**. The actinolite domains preferentially host anhedral **chalcopyrite** and subhedral **pyrite** (up to 1.5 mm). In many instances, the pyrite is surrounded by an irregular strain shadow of fine-grained **Mg-chlorite**. The chalcopyrite preferentially crystallized around the pyrite, which it probably partially replaces within the calcite-rich domains.

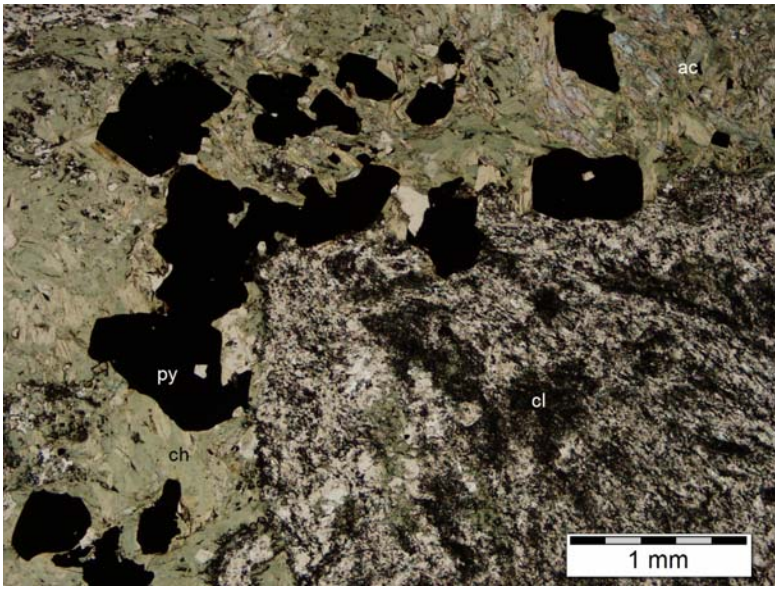

***Photomicrograph 15a**: Pyrite (py) is rimmed by chlorite (ch) and preferentially crystallized within the actinolite domains (ac) that alternate with clay-rich domains (cl). Plane-polarized transmitted light.*

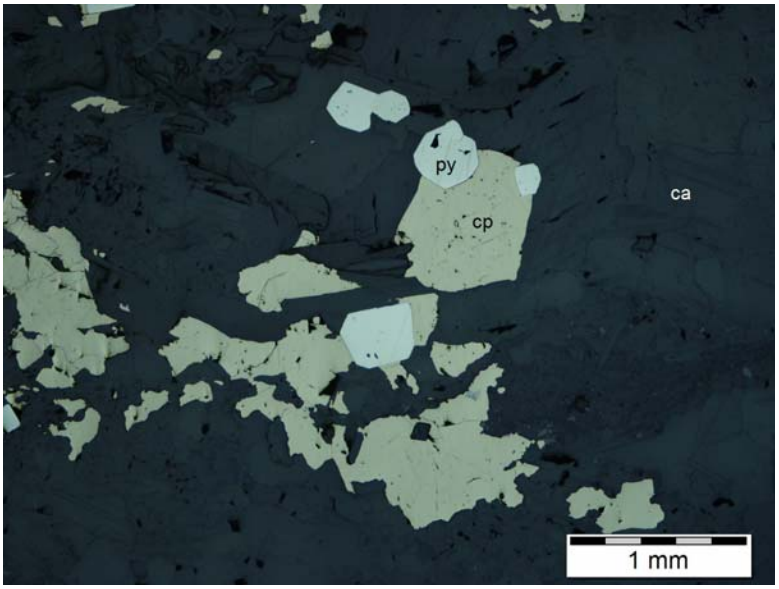

***Photomicrograph 15b**: Subhedral pyrite (py) is mantled and partially replaced by chalcopyrite (cp) within the calcite-rich (ca) infill domain. Plane-polarized reflected light.*

Sample 16: JFM009-1

Brecciated actinolite schist

Actinolite-calcite-chlorite-pyrite-chalcopyrite infill

This polished thin section contains the same type of mineral aggregates described in Sample 15; however, the relative abundance of the minerals is different. Very fine-grained replacement aggregates of clay define an anastomosing foliation and were filled in by actinolite-chlorite vein-like domains during a brittle-ductile deformation event. Medium-grained calcite preferentially filled in the strain shadows surrounding the sub-tabular clay-rich fragments. Pyrite and subordinate chalcopyrite preferentially occur within the actinolite-chlorite and calcite domains.

Mineral	***Modal %***	***Main Size Range (mm)***
clay	60 – 62	up to 0.02
actinolite	18 – 20	up to 0.2
calcite	11 – 12	up to 1
Mg-chlorite	5 – 6	up to 0.5
pyrite	2.5 – 3	up to 1
plagioclase (albite)	tr	up to 0.15
chalcopyrite	tr	up to 0.4

Clay forms very fine-grained replacement aggregates that are associated with varying amount of very fine-grained actinolite and an undetermined high-relief material (titanite?). The high-relief dispersions occur as subparallel clusters that define anastomosing cleavage domains within the clay-rich aggregates. The clay-rich aggregates are fragmented, and the fragments show sub-tabular shapes, with the longest dimension coincident with the cleavage domains. The interstices between the fragments are filled in by actinolite-chlorite. The strain shadows generated by the brittle-ductile deformation around the fragments are preferentially filled in by calcite.

Fine-grained and xenoblastic crystals of **actinolite** are concentrated within vein-like domains sub-parallel to the foliation and irregular infills that crosscut the foliation of the clay-actinolite fragments (Photomicrograph 16a). The microstructural features indicate that the actinolite crystallization occurred during and after the brittle-ductile deformation episode. Rare **plagioclase (albite)** forms fine-grained crystal aggregates within the actinolite-rich infill domains.

Mg-chlorite is fine grained and is preferentially intergrown with and probably partially replaces the actinolite-rich domains. The chlorite lamellae (up to 0.5 mm) show negative elongation; therefore, the chlorite is magnesium rich.

Calcite forms medium-grained (up to 1 mm) interlobate crystal aggregates that preferentially filled in the strain shadows around the sub-tabular clay-rich fragments.

Pyrite occurs as medium-grained (up to 1 mm) subidioblastic crystals that are preferentially crystallized within the actinolite-chlorite and calcite domains. In many cases, the pyrite crystals are characterized by irregularly shaped inclusion-rich cores, indicating multiple crystallization episodes and/or different growth velocity of the crystals.

Rare and xenoblastic **chalcopyrite** (up to 0.4 mm) preferentially occurs within the calcite, in which it mantles and partially replaces the pyrite.

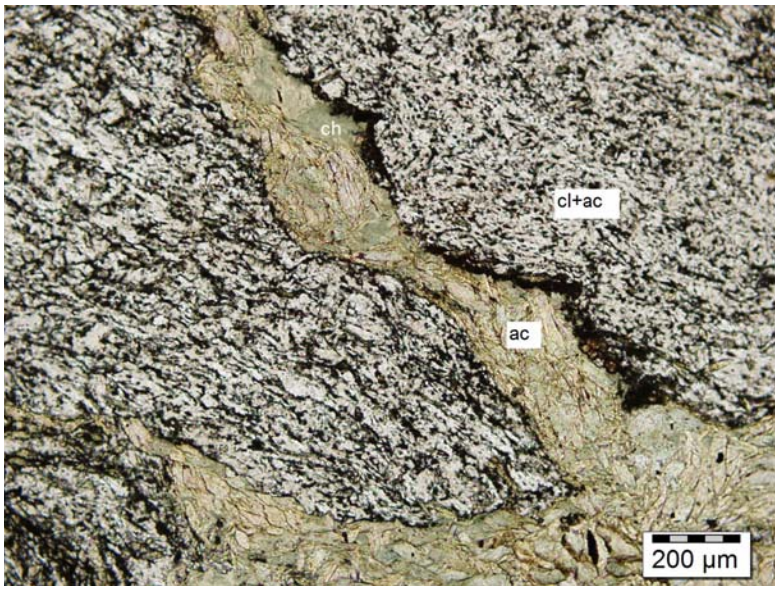

***Photomicrograph 16**: A fine-grained aggregate of actinolite (ac) and subordinate chlorite (ch) filled in a very fine-grained aggregate of clay, actinolite, and an unresolved high-relief material (cl+ac). Plane-polarized transmitted light.*

Sample 17: JFM010-1

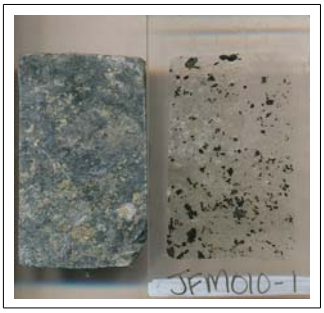

Albite-tremolite-pyrite granofels

A heterogeneous, xenoblastic inequigranular aggregate of fine- to medium-grained plagioclase, randomly oriented acicular actinolite, and xenoblastic pyrite. Subordinate amounts of Mg-chlorite, calcite, and anhydrite heterogeneously overprinted this sample.

Mineral	*Modal %*	*Main Size Range (mm)*
plagioclase (albite)	53 – 55	0.02–0.5 mm
tremolite	30 – 33	up to 1 mm long
pyrite (and marcasite?)	7.5 – 8	up to 2
calcite	5 – 6	up to 1
Mg-chlorite	0.2 – 0.5	up to 0.3
clay	tr	up to 0.02
chalcopyrite	tr	up to 0.2
iron oxides (including goethite)	tr	cryptocrystalline

Plagioclase (albite) forms inequigranular (0.02–0.5 mm) and interlobate crystal aggregates. The plagioclase shows albite twinning and the composition is albitic, as indicated by the low (less than 10°) extinction angle [a′:(010) in zone perpendicular to the (010)] in some of its crystals. In some areas of the polished thin section, the plagioclase is weakly to moderately altered by very fine-grained **clay**. The plagioclase aggregates in some cases form sub-rounded fragments that were filled in by the locally abundant calcite and anhydrite aggregate. In most of the polished thin section, the plagioclase is intergrown with tremolite.

Tremolite is fine to medium grained and forms elongate to acicular prisms that are randomly oriented and intergrown with the plagioclase. The tremolite is distinguished by its very weak to absent pleochroism, moderate to high relief, and extinction angles (c:Z) up to 18°. Some of the medium-grained acicular prisms (up to 1 mm long) show undulose extinction and are bent.

Pyrite is heterogeneously dispersed within the polished thin section as inequigranular and xenoblastic crystals (up to 2 mm). In some cases, the pyrite is associated and in contact with slightly less reflective pinkish-white crystals that I tentatively interpret as marcasite despite the absence of visible anisotropy. Alternatively, the slightly more pink mineral can be interpreted as a second generation of pyrite with a different composition. The pyrite and the pyrite-

marcasite(?) intergrowths are mantled by subordinate **chalcopyrite**. The pyrite and marcasite(?) are subtly altered by **iron oxides** and **goethite**.

Mg-chlorite forms interstitial and inequigranular (up to 1 mm) domains of calcite, distinguished by their high relief, extreme birefringence, and brisk reaction to cold dilute (10%) HCL.

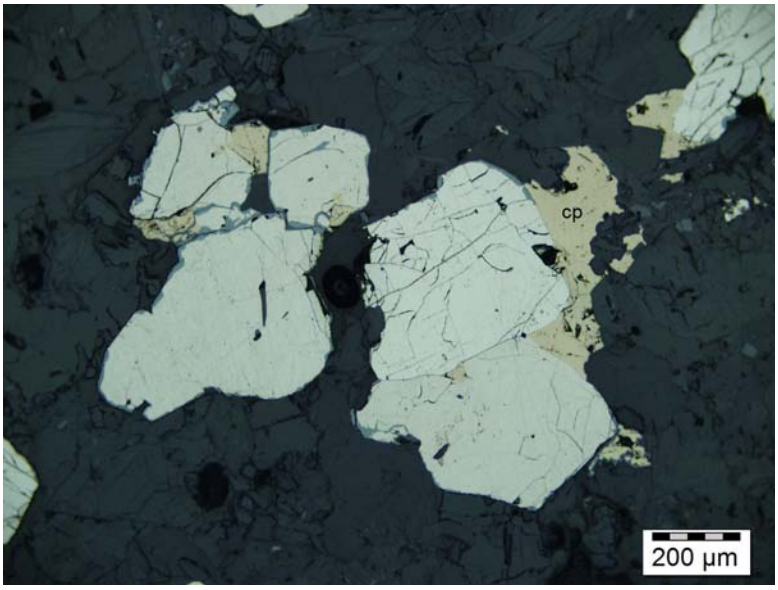

***Photomicrograph 17**: Anhedral pyrite (white crystal) is associated with slightly less reflective crystals (creamy-white) of marcasite(?). Chalcopyrite (cp) and iron oxides (ox) partially replace the pyrite and marcasite(?). Plane-polarized reflected light.*

Sample 18: JFM016-1

Calcite-actinolite-chalcopyrite infill/alteration-zone

Irregular fragments of very fine-grained clay are immersed within a medium-grained aggregate of calcite. Fine-grained actinolite, xenoblastic chalcopyrite, and idioblastic pyrite are concentrated around the clay-rich fragments and dispersed within the calcite.

Mineral	*Modal %*	*Main Size Range (mm)*
calcite	82 – 84	up to 4
clay	10 – 12	up to 0.02
actinolite	4 – 5	up to 1 mm long
chalcopyrite	1 – 1.2	up to 1
pyrite	0.8 – 1	up to 1.2

Calcite dominates the composition of this sample as inequigranular (up to 4 mm) and interlobate crystal aggregates containing irregularly shaped to sub-angular fragments of very fine-grained **clay**. The calcite crystals host fine-grained (up to 0.5 mm long; rarely up to 1 mm) needle-like crystals of **actinolite**, which are concentrated within fine-grained domains between the interstices and fractures within the calcite and form irregular coronae around some of the clay-rich fragments. The actinolite occurs as elongate prisms, columnar to acicular crystals with high aspect ratio (50:1 and higher). Actinolite shows a distinct deep green colour and a subtle pleochroism with extinction angles (c:Z) up to 15°.

Xenoblastic to amoeboid **chalcopyrite** and idioblastic **pyrite** preferentially crystallized within the actinolite-rich domains and at the boundaries between the actinolite-rich domains and the calcite. The chalcopyrite mantles and partially replaces the pyrite.

The microstructural position of the actinolite indicates that its crystallization occurred during the brittle-ductile deformation of the intensely altered clay-rich fragments.

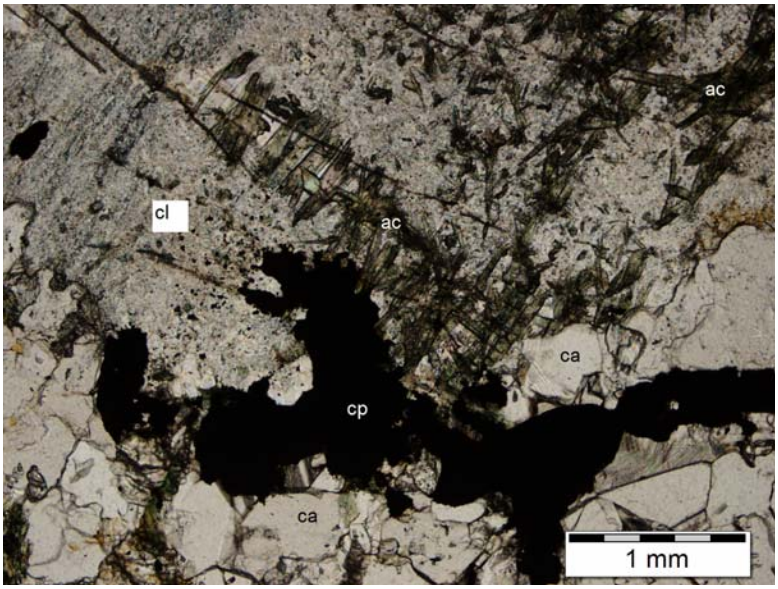

***Photomicrograph 18**: An intensely altered fragment is completely replaced by very fine-grained clay (cl). Columnar to acicular prisms of actinolite (ac) overprinted the clay and filled in the fractured clay-rich domain that is immersed within calcite (ca). Chalcopyrite (cp) preferentially crystallized around the clay-rich fragment. Plane-polarized transmitted light.*

Sample 19: JFM019

Basalt

Alteration: strong–actinolite-titanite-epidote-Mg-chlorite

Actinolite-epidote-chlorite-calcite veinlets

Fine-grained laths of plagioclase are randomly oriented and define an intergranular microstructure in which fine-grained and xenoblastic actinolite and subordinate titanite replaced the magmatic ferromagnesian minerals that were associated with the plagioclase. Irregular veinlets filled in by fine-grained actinolite crosscut the strongly altered basaltic rock and are associated with rare epidote and chlorite and very rare calcite.

Mineral	***Modal %***	***Main Size Range (mm)***
actinolite	55 – 58	up to 0.25
plagioclase (albite)	40 – 44	up to 0.5; up to 1.2 mm long prisms
titanite	1.5 – 2	up to 0.05
epidote	1	up to 0.1
Mg-chlorite	1 – 1.5	up to 0.25
calcite	tr	up to 0.15
chalcopyrite	tr	up to 0.03
iron oxides	tr	cryptocrystalline
galena(?)	tr	up to 0.01

Actinolite occurs as fine-grained xenoblastic to sub-prismatic crystals that replaced the ferromagnesian mineral that occupied the interstices between the plagioclase laths. The actinolite is distinguished by its distinct pleochroism (X: pale yellow green; Y: light green; Z: light bluish green) and by its oblique extinction up to 15°. The actinolite is associated with fine-grained xenoblastic crystals and crystal clusters of **titanite**. Finer-grained fibrous actinolite dominates the composition of irregular veinlets that crosscut the strongly altered sample. The actinolite is associated with rare fine-grained **epidote** and **chlorite** and very rare **calcite** within the veinlets.

Plagioclase forms elongated subhedral prisms (up to 1.2 mm long and with aspect ratios up to 25:1) and fine-grained prisms up to 0.5 mm. The plagioclase is relatively fresh and is subtly

altered by very fine-grained dispersions of a high-relief mineral, probably epidote. The low extinction angle [a′:(010) in zone perpendicular to the (010)=14°] indicates an albite-rich composition of the plagioclase.

Very rare, very fine-grained **chalcopyrite** is hosted within the fine-grained anhedral epidote, the plagioclase, and the actinolite, and is partially replaced by **iron oxides.** Very rare probable **galena** is spatially associated with the chalcopyrite.

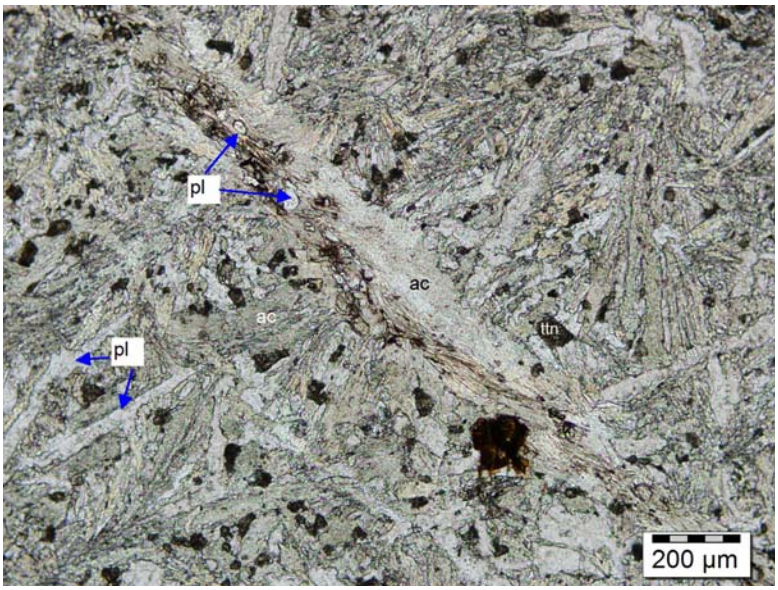

Photomicrograph 19*: Fine-grained actinolite (ac) and subordinate epidote (ep) and chlorite (ch) crosscut a strongly altered intergranular microstructure. Fine-grained actinolite (ac) completely replaced the ferromagnesian mineral(s) within the interstices between the elongated and randomly oriented laths of plagioclase (pl). Plane-polarized transmitted light.*

Sample 20: JFM020-1

Basalt

Alteration: strong–actinolite-epidote-Mg-chlorite-titanite

Actinolite-epidote-quartz-Mg-chlorite-calcite veins

This polished thin section is strongly altered by fine-grained actinolite, which in turn is partially replaced by chlorite and epidote. The actinolite is intergrown with plagioclase, which I interpret as the only mineralogic and microstructural relict of a primary mineral. Actinolite-quartz-clinozoisite/epidote veins (~2.5 mm and 1.2 mm thick) are subparallel and crosscut the strongly altered magmatic rock.

Mineral	*Modal %*	*Main Size Range (mm)*
meta-basalt (89% of PTS)		
actinolite	50 – 53	up to 0.5
plagioclase	30 – 35	up to 0.5
titanite	2.5 – 3	up to 0.4
Mg-chlorite	2	up to 0.1
epidote	1	up to 0.1
actinolite-quartz-clinozoisite/epidote veins (11% of PTS)		
actinolite	9 – 10	up to 1 mm long
quartz	1 – 1.5	up to 0.5
clinozoisite/epidote	0.5 – 0.6	up to 0.3
chlorite		
pyrite	tr	up to 0.02

Actinolite occurs as inequigranular (up to 0.5 × 0.2 mm) xenoblastic to sub-prismatic crystals that overprinted the plagioclase-bearing magmatic rock. Compared with Sample 19, the magmatic microstructure is less preserved in this sample, probably because a more extensive actinolite crystallization outgrew the magmatic interstitial ferromagnesian minerals. The actinolite is characterized by a distinct pleochroism (X: pale yellow green; Y: light green; Z: light brownish green) and extinction angle of up to 15°. The actinolite is partially replaced by

fine-grained **Mg-chlorite** and **epidote**. Within the actinolite-rich veins, elongated prisms (up to 1 mm long) of actinolite are oriented at high angle to the vein walls and show a more bluish colour along the Z optical indicatrix. The actinolite within the vein is associated with subordinate interstitial **quartz**, fine-grained blocky prisms of **clinozoisite (**distinguished by its anomalous interference colours), **epidote,** and **Mg-Chlorite**.
Plagioclase forms subhedral to anhedral crystals of up to 0.7 mm. The plagioclase is weakly altered by very fine-grained dispersions of actinolite, epidote, and probable clay. In some cases, it is recrystallized; however, in most cases, the albite twinning and the continuous growth zoning indicate the magmatic origin of the crystals. In some of the appropriately oriented crystals, the low extinction angle (10°–15°) between the adjacent twinned lamellae indicate an albite-rich composition of the plagioclase.
Fine- to medium-grained (up to 0.4 mm) crystals of **titanite** are dispersed within the actinolite-plagioclase aggregate and probably derived from the alteration of the primary ferromagnesian minerals.
Very rare **pyrite** (two grains up of 0.02 mm) is intergrown with the epidote at the actinolite-rich vein wall.

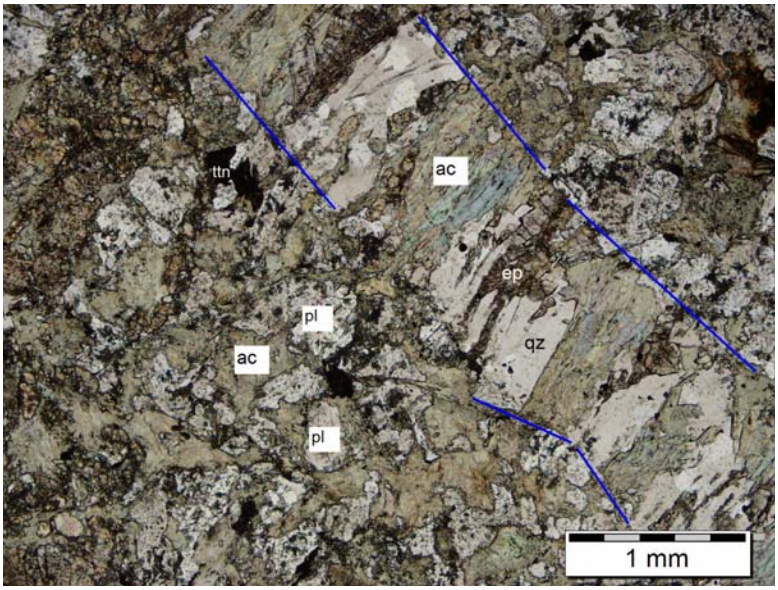

***Photomicrograph 20**: Xenoblastic actinolite (ac) and titanite (ttn) completely replaced the ferromagnesian minerals that were intergrown with the subhedral plagioclase (pl) in this strongly altered magmatic rock. Actinolite (ac), quartz (qz), and epidote (ep) filled in a vein (blue dashed lines) that crosscut the magmatic rock. Plane-polarized transmitted light.*

Sample 21: JFM022-1

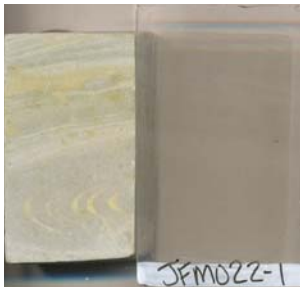

Metamudstone

This polished thin section was cut almost perpendicularly to the axial plane of a fold. In the upper part of the section, the fold limbs are highlighted by a subparallel compositional layering defined by alternating layers of fine-grained inequigranular interlobate aggregates of albite and subordinate dolomite and very fine-grained layers of white mica(?), albite, and subordinate dolomite. The hinge zone is characterized by fine-grained albite-dolomite aggregates that filled in the interlayer volume generated during the buckling. The fold is cylindrical and can be classified as a divergent isogon fold (class 3, Ramsay 1967).

Mineral	*Modal %*	*Main Size Range (mm)*
plagioclase (albite)	80 – 84	0.02–0.1
quartz	10 – 15	0.02–0.1
muscovite	4 – 6	up to 0.04
dolomite	1 – 2	up to 0.1
rutile	tr	up to 0.02

Plagioclase (albite) forms fine-grained interlobate crystals that are intergrown with lesser **quartz**. The plagioclase shows albite twinning and lower refractive indexes than those of quartz; therefore it is albitic. The quartzofeldspathic aggregate dominates the composition of this sample. Differences in the average grain size of the aggregate, which varies from 0.02 mm to 0.1 mm and is inversely proportional to the amount of intergrown clay, define a folded sub-parallel compositional layering. Within the hinge zone, in the lower part of this polished thin section, the composition is more homogeneous, and the grain size of the albite-quartz and subordinate calcite aggregate ranges from 0.02 mm to 0.1 mm. The layering is interrupted by the fine-grained aggregate of albite and dolomite, which filled in the volume between the buckled layers (see Photomicrograph 21b).

Dolomite is fine grained and is associated with the albite within the infill within the folded interlayer domains, and overprinted the quartzofeldspathic aggregate as fine-grained (up to 0.1 mm) amoeboid crystals. The dolomite is distinguished by its high relief and extreme birefringence and by the absence of a brisk reaction to cold dilute (10%) HCl.

Muscovite[1] forms very fine-grained crystals that are intergrown with the very fine-grained aggregate of albite and probable quartz. The very fine-grained flakes show high birefringence;

1 Determined by SWIR Spectroscopy. See Table 2.

however, the distinction of muscovite was confirmed by spectroscopic analysis.
Rare, very fine-grained **rutile** crystals are dispersed within the quartzofeldspathic aggregate.

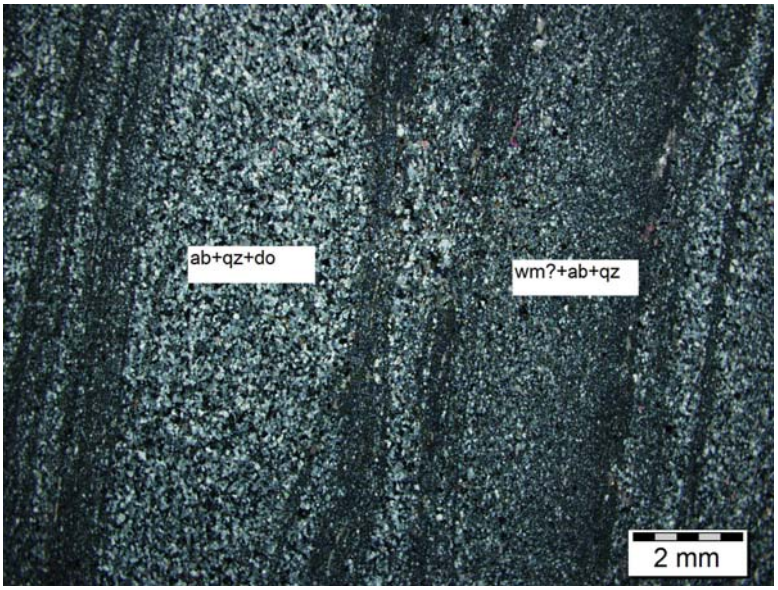

***Photomicrograph 21a**: The limb of the fold is characterized by a subparallel compositional layering in which coarser-grained domains are made up of albite, quartz, and subordinate dolomite (ab+qz+do), and very fine-grained layers are made up of very fine-grained white mica(?), albite, and probable quartz (wm? +ab+qz). Crossed Nicols transmitted light.*

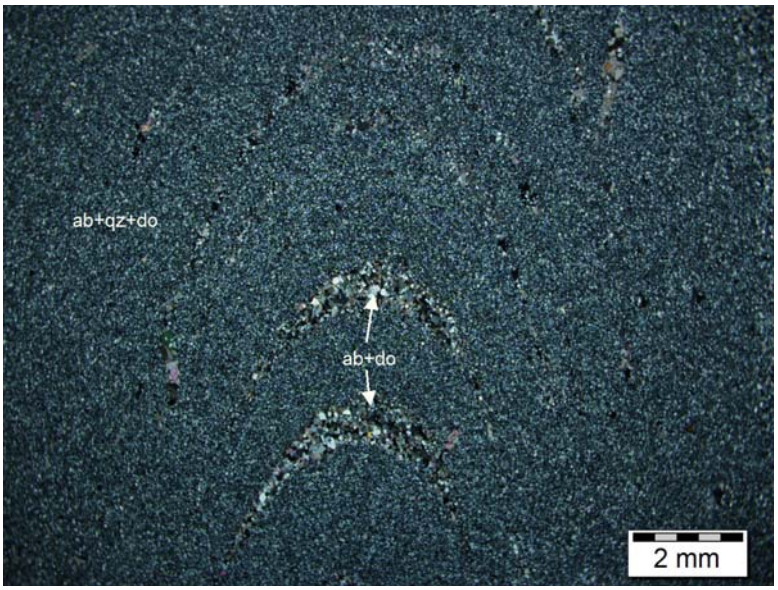

***Photomicrograph 21b**: Within the hinge zone, a very fine-grained aggregate of albite, quartz, and subordinate dolomite (ab+qz+do) is filled in by fine-grained albite and dolomite (ab+do). Crossed Nicols transmitted light.*

Sample 22: JFM022-2

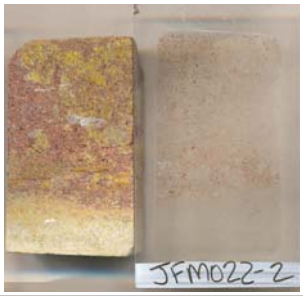

Albite-dolomite granofels

This polished thin section is made up of inequigranular (up to 1 mm) blocky and anhedral crystals of plagioclase and rare poikilitic crystals of dolomite. In the lower part of the polished thin section, the albite is fine grained (up to 0.2 mm) and is intergrown with fine-grained dolomite.

Mineral	*Modal %*	*Main Size Range (mm)*
plagioclase (albite)	93 – 95	up to 1
dolomite	4 – 5	up to 8
iron oxides and limonite	1 – 2	cryptocrystalline

Plagioclase (albite) forms blocky to anhedral crystals that define a medium-grained (up to 1 mm) inequigranular granoblastic aggregate that dominates the composition of this polished thin section. The plagioclase shows albite twinning with small angles (less than 10°) between the adjacent twinning lamellae, indicating its albitic composition. The grain size of the plagioclase progressively decreases in the lower part of the polished thin section, where the average grain size is around 0.2 mm.

Dolomite forms rare crystals with amoeboid and poikiloblastic shapes of up to 8 mm. The dolomite is fine grained within the lower part of the polished thin section. It is distinguished by its high relief, extreme birefringence, and slow reaction to cold dilute (10%) HCl. The presence of ankerite should be investigated by spectroscopic analysis. In some crystals, the dolomite is also distinguished by the presence of twinning parallel to the short diagonals of the cleavage rhombs.

Cryptocrystalline dispersions of **iron oxides** and **limonitic** stains occupy the interstices between the plagioclase and dolomite and are dispersed within some of the plagioclase crystals within the medium-grained domain.

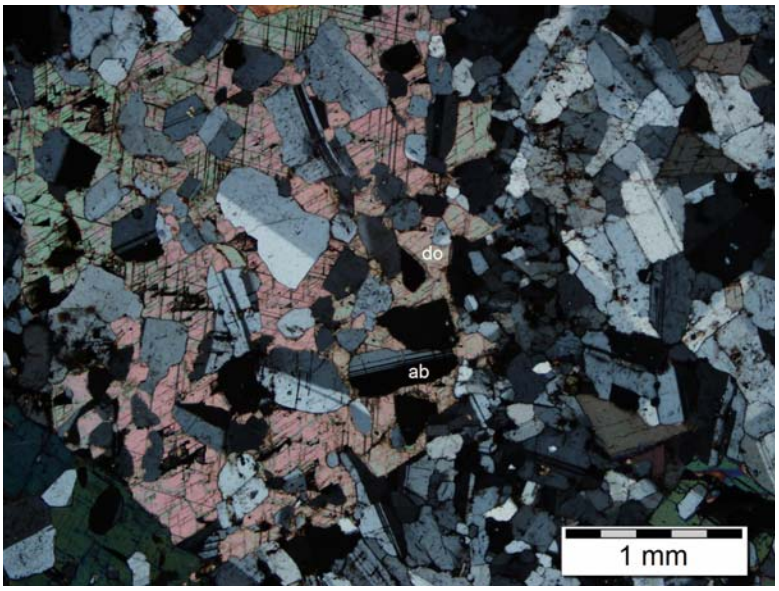

***Photomicrograph 22**: Medium-grained albite (ab) is intergrown with subordinate and poikiloblastic dolomite (do). Crossed Nicols transmitted light.*

Sample 23: JFM023-1

Metamudstone

Alteration: moderate–white mica-albite

Albite-dolomite/ankerite-iron oxide vein

A very fine-grained aggregate of muscovite, albite, and probable quartz is overprinted by irregular flame-like domains of fine-grained albite. In the upper part of the polished thin section, the very fine-grained aggregate is crosscut by an inequigranular vein of albite-dolomite/ankerite-iron oxide.

Mineral	*Modal %*	*Main Size Range (mm)*
mudstone (93% of PTS)		
muscovite	40 – 42	up to 0.04
plagioclase (albite)	35 – 37	up to 0.2
quartz(?)	15 – 18	up to 0.04
rutile	tr	up to 0.02
apatite(?)	tr	up to 0.02
albite-dolomite/ankerite-iron oxide vein (7% of PTS)		
plagioclase (albite)	4	up to 0.7
dolomite/ankerite	2	up to 1.5
iron oxides	1	cryptocrystalline
Mg-chlorite	tr	up to 0.05

Plagioclase (albite?) forms very fine-grained crystals that are intergrown with very fine-grained **muscovite**[1] and probable **quartz** within most of the polished thin section. The very fine-grained aggregate is overprinted by inequigranular (up to 0.2 mm) interlobate aggregates of plagioclase. Due to the very fine-grained nature of the albite-white mica-quartz(?), the presence of the plagioclase is indicated by some albite twinning, while the presence of quartz is highly hypothetical and should be verified by electron optic analysis. The plagioclase finally filled in the inequigranular vein as xenoblastic crystals of up to 0.7 mm. In this case, the albitic

1 Determined by SWIR Spectroscopy. See Table 2.

composition is supported by the presence of albite twinning in most of the crystals, and the measurement of small angles (less than 14°) between the adjacent twinning lamellae [a′: (010)].

Dolomite/ankerite forms xenoblastic crystals of up to 1.5 mm within the vein and is characterized by very fine-grained dispersion of iron oxides that may be related to its ankeritic composition; however, another possibility that must be considered is that fine-grained iron oxides are also present within the vein and completely replaced an unknown mineral of up to 1 mm. Limonitic stains permeated the interstices of most of the crystals within the vein.

Very rare fine-grained lamellae of **Mg-chlorite** are hosted within an interstitial replacement aggregate of iron oxides. The magnesium-rich composition of the chlorite is indicated by its negative elongation.

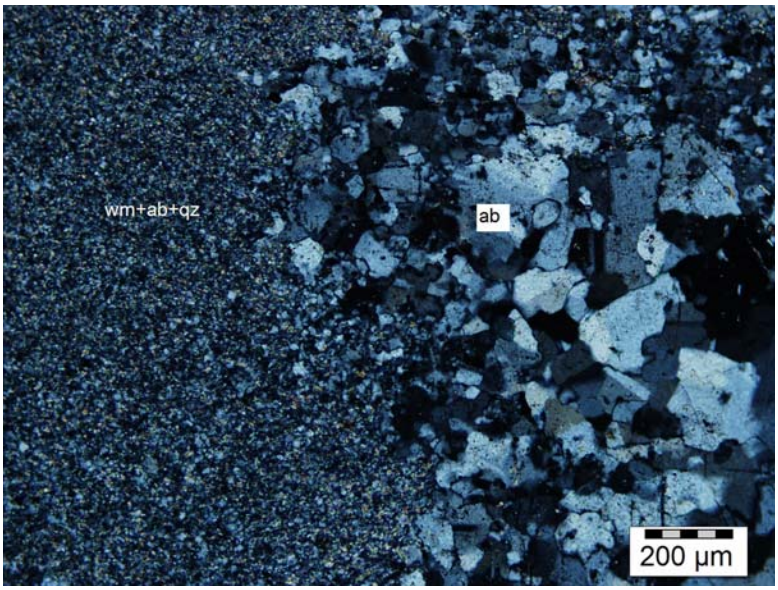

***Photomicrograph 23a**: A very fine-grained aggregate of white mica, albite, and quartz (wm+ab+qz) is overprinted by fine-grained replacement patches of albite (ab). Crossed Nicols transmitted light.*

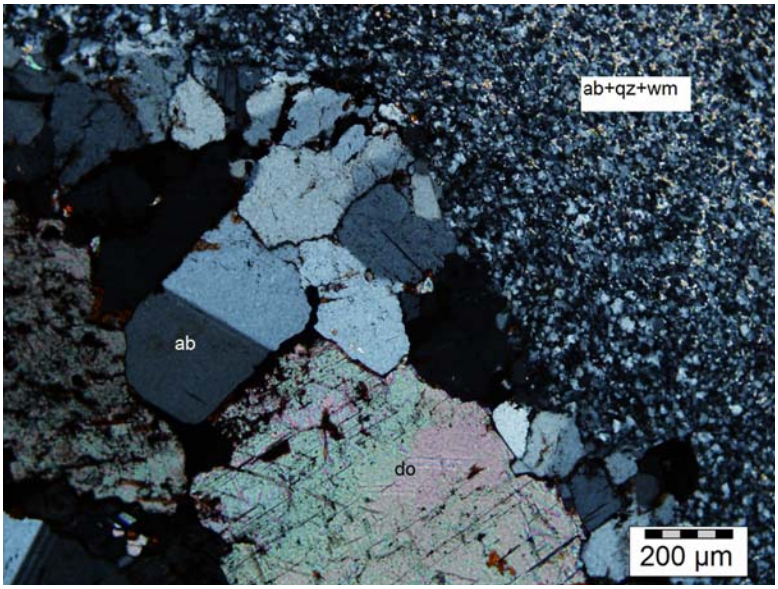

***Photomicrograph 23b**: The very fine-grained mudstone shows a lower white mica content close to the vein walls and is made up of albite, probable quartz, and lesser white mica (ab+qz+wm in the upper right part of this photomicrograph). The vein is made up of albite (ab), dolomite (do), and interstitial iron oxides (opaque). Crossed Nicols transmitted light.*

Sample 24: JFM028-1

Meta-basalt; Alteration: strong–albite-actinolite-rutile-chlorite

Fine-grained xenoblastic crystals of actinolite and albite completely replaced the probable magmatic protolith and are associated with fine-grained crystals of rutile and subordinate chlorite.

Mineral	*Modal %*	*Main Size Range (mm)*
albite	47 – 50	uo to 0.2
actinolite	38 – 38	up to 0.2
rutile	5 – 6	up to 0.2
chlorite	5 – 6	up to 0.05
quartz	tr	up to 0.1
apatite	tr	up to 0.2
titanite	tr	up to 0.1

Plagioclase (albite) forms very fine- to fine-grained xenoblastic crystals that partially to completely replaced the magmatic plagioclase. Some of the plagioclase crystals show albite twinning, and the albitic composition of the plagioclase is indicated by the small angles (less than 10°) between the adjacent twinned lamellae. Some of the fine-grained crystals show relict growth zoning, which indicates a magmatic origin.

Actinolite forms fine-grained xenoblastic crystals of up to 0.2 mm that overprinted the magmatic microstructure and probably overprinted the ferromagnesian minerals. The actinolite is distinguished by its moderate relief, distinct pleochroism (X: pale yellow green; Y: light green; Z: light brownish green) and extinction angles (c:Z) smaller than 15°.

Fine-grained xenoblastic crystals of **rutile** are relatively abundant and are heterogeneously dispersed within the fine-grained albite-actinolite replacement aggregate.

Mg-Chlorite forms fine-grained (up to 0.05 mm) crystals that are randomly oriented within irregularly shaped replacement patches. Chlorite is heterogeneously distributed within the strongly altered sample and partially replaced the actinolite.

Very rare replacement patches of polygonal **quartz** and **titanite** overprinted the strongly altered rock.

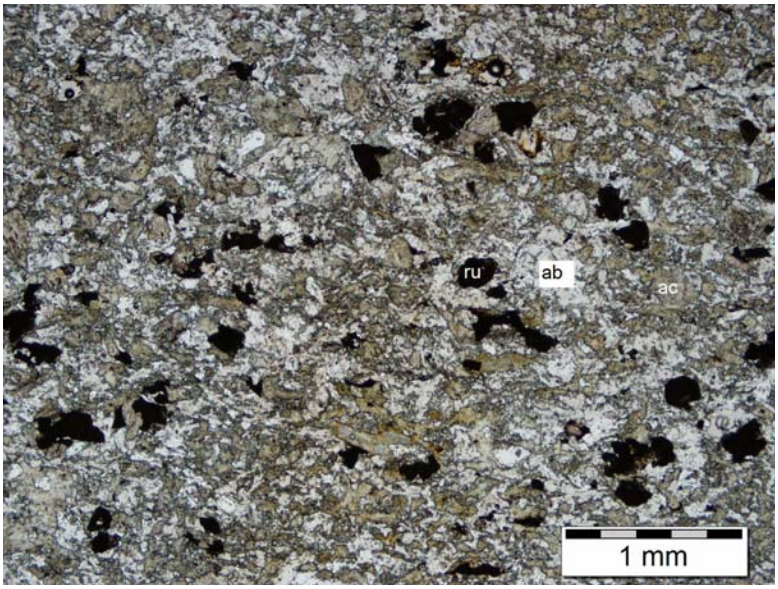

***Photomicrograph 24**: Fine-grained actinolite (ac), chlorite, and rutile (ru) completely replaced the ferromagnesian minerals. The albite (ab) partially replaced the magmatic plagioclase. Plane-polarized transmitted light.*

Sample 25: JFM031-1

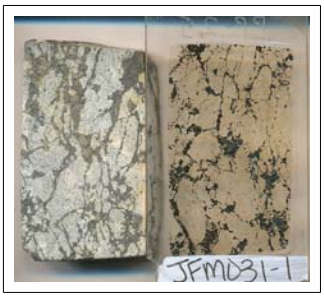

Brecciated (mosaic-breccia) albite-rich alteration-zone

Pyrrhotite-quartz-white mica-pyrite-tourmaline-chalcopyrite infill

The mesostructure of this sample is very similar to the one of Sample 16; however, in this sample the elongate fragments are made up of inequigranular (up to 0.1 mm and in some cases up to 1 mm) plagioclase, which is weakly altered by a cryptocrystalline dispersion of clay and/or epidote. The brecciated (mosaic breccia) fragments are filled in by moderately to strongly altered pyrrhotite, which is partially replaced by pyrite, white mica, and tourmaline.

Mineral	*Modal %*	*Main Size Range (mm)*
plagioclase (albite)	75 – 78	up to 0.1; rare up to 1
pyrrhotite	13 – 15	up to 3
quartz	3 – 3.5	up to 0.5
white mica	2.5 – 3	up to 0.2
clay	1 – 2	cryptocrystalline
pyrite	0.5 – 0.7	up to 1
rutile	0.3 – 0.5	up to 0.05
tourmaline	tr	up to 0.3
chalcopyrite	tr	up to 0.1

Plagioclase (albite) forms inequigranular (up to 0.1 mm) and interlobate crystal aggregates that dominate the composition of this polished thin section. The fine-grained albite-rich aggregates were overprinted by inequigranular and coarser-grained (up to 1 mm) replacement domains of albite. The albite hosts abundant dispersions of a cryptocrystalline to very fine-grained clay, probable epidote, fine-grained rutile, and close to the infill domains, fine- to medium-grained tourmaline. Most of the plagioclase shows albite twinning with small (less than 10°) angles between the twinned lamellae, indicating that the composition of the plagioclase is albitic. In some cases, the undulose extinction of some of the albite crystals indicates that they crystallized during the brittle-ductile deformation that is responsible for the brecciation. The albite-rich aggregate was fractured by an incipient brittle-ductile deformation event that produced a mosaic-breccia microstructure. The albite-rich fragments are sub-angular and are generally elongate with a negligible amount of reciprocal rotation.

Pyrrhotite filled in the interstices between the sub-angular albite-rich fragments and forms

moderately to strongly altered and fractured massive domains (up to 3 mm) that in some cases are partially replaced by **pyrite** (see Photomicrograph 25b). Very rare fine-grained **chalcopyrite** overprinted the strongly altered pyrrhotite within the infill.

Quartz is heterogeneously distributed within the infill domains and is intergrown with the pyrrhotite as anhedral crystals of up to 0.5 mm. The quartz shows moderate to strong undulose extinction. The crosscutting relationship between the quartz-pyrrhotite infill domains and the medium-grained albite indicates that the quartz-pyrrhotite post-dated the crystallization of albite during the brittle-ductile deformation event. The quartz and pyrrhotite are intergrown with subordinate **white mica**, which is concentrated within the infill domains as fine-grained (up to 0.2 mm) randomly oriented lamellae, and subordinate **tourmaline**, which is concentrated within the infill domains. In some cases, the tourmaline reaches 0.3 mm. It forms sub-idioblastic prisms showing strong pleochroism with brown tints, and oscillating growth zonation. Fine-grained tourmaline is also dispersed within the albite-rich fragments.

Rutile forms subidioblastic crystal clusters (up to 0.3 mm; rare up to 0.5 × 0.25 mm) and fine-grained crystals. The rutile is heterogeneously distributed within the albite-rich fine-grained domains, within the white mica-rich aggregates within the infill, and within the strongly altered pyrrhotite. One crystal cluster of rutile shows a lozenge shape (0.5 × 0.25 mm) that indicates the replacement of a titanium-bearing mineral such as hornblende or titanite.

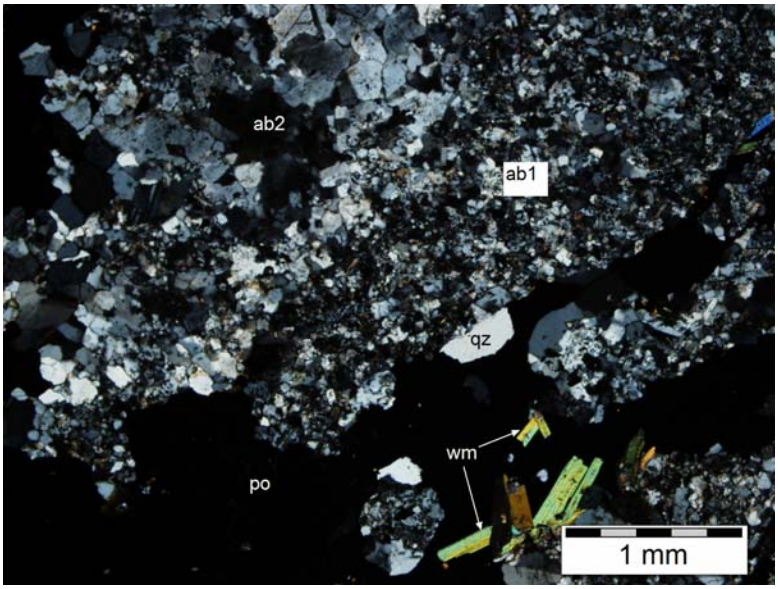

***Photomicrograph 25a**: The albite-rich fragments are made up of a fine-grained aggregate of albite (ab1) that was probably overprinted by a second generation of coarser albite (ab2). The albite-rich aggregate was fractured and filled in by pyrrhotite (po), quartz (qz), and white mica (wm). Crossed Nicols transmitted light.*

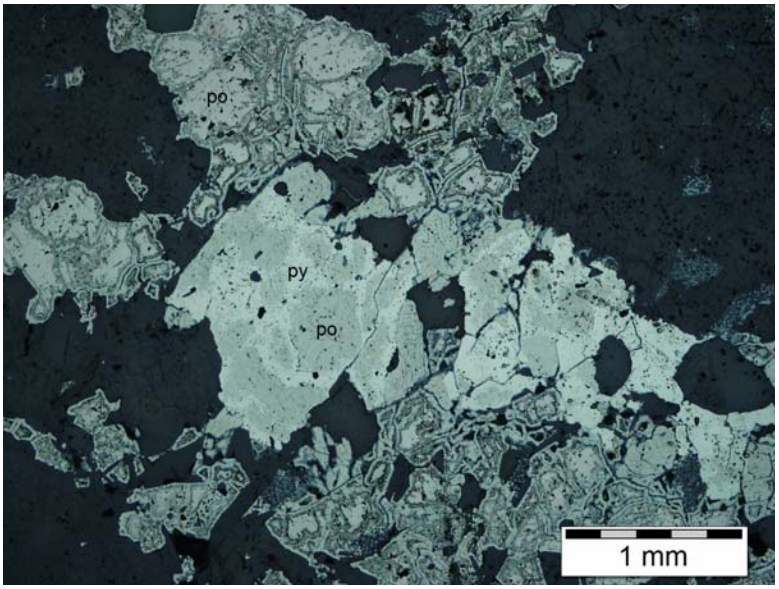

***Photomicrograph 25b**: The interstices between the sub-angular albite-rich fragments were filled in by pyrrhotite-rich infill domains. The pyrrhotite (po) is moderately to strongly altered and is partially replaced by pyrite (py). Plane-polarized reflected light.*

Sample 26: JFM032

Brecciated albite-quartz-biotite granofels

Chlorite-quartz-calcite-albite-titanite infill

Fine-grained interlobate crystal aggregates of albite, quartz, and biotite form angular fragments that are filled in by chlorite (probably after biotite), quartz, calcite, albite, and titanite.

Mineral	*Modal %*	*Main Size Range (mm)*
albite-quartz-biotite granofels (75% of PTS)		
plagioclase (albite)	40 – 45	up to 0.2
quartz	30 – 33	up to 0.2
biotite	2 – 2.5	up to 0.2
calcite	0.5 – 1	up to 0.2
chlorite-quartz-calcite-albite-titanite infill (25% of PTS)		
Mg-chlorite	15 – 17	up to 0.2
quartz	5 – 6	up to 0.2
calcite	2 – 2.5	up to 0.5
albite	1 – 2	up to 0.2
titanite	tr	up to 0.25
pyrite	tr	~0.5
pyrrhotite	tr	up to 0.05
chalcopyrite	tr	up to 0.01

Plagioclase (albite) forms fine-grained (up to 0.2 mm) interlobate crystal aggregates that are intergrown with quartz, calcite, and subordinate biotite. The plagioclase shows albite twinning and lower refractive indexes than those of the quartz; therefore, it is albitic. The plagioclase is subtly altered by very fine-grained to cryptocrystalline dispersions that are unresolved under the microscope; however, they facilitate the distinction between the albite and quartz, which is free of inclusions, under plane-polarized transmitted light. The plagioclase also occurs as fine-grained irregular aggregates within the infill domains, indicating its stability during the brittle deformation event and the infill emplacement.

Quartz is fine grained and is intergrown with and subordinate to the albite within the fragments. The quartz is subordinate to the chlorite within the infill domains, where it forms fine-grained interlobate to blocky crystals.

Biotite is fine grained and is heterogeneously distributed within the albite-rich fragments. The relative amount of biotite increases in the fragments located in the lower part of the polished thin section. This can be interpreted as a primary feature, or can be the consequence of a stronger alteration, as the fragments were more abundantly permeated by potassium- and iron-rich fluids during and after the brittle deformation event. The subordinate relicts of the biotite hosted within that abundant chlorite infill indicate that the biotite was stable during the crystallization of the infill domains and was partially replaced by chlorite at a later stage.

Mg-chlorite is concentrated within the infill domains and is intergrown with fine-grained quartz, fine-grained xenoblastic titanite, and fine-grained biotite, which in some cases is partially replaced by the chlorite. The chlorite shows negative elongation, which shows that it is magnesium rich.

Fine- to medium-grained **calcite** forms interlobate, quasi-monomineralic domains that are concentrated within the infill domains. Fine-grained calcite is also distributed within the fine-grained albite-rich fragments. The calcite was distinguished by its high relief, its extreme birefringence, and the presence of twinning lamellae parallel to the edges of the rhomb. On the offcut, the calcite shows a brisk reaction to cold dilute (10%) HCl.

In this polished thin section, only one subhedral crystal of **pyrite** (~0.5 mm) crystallized within an irregular replacement patch of quartz and subordinate biotite, which in turn is within the albite-rich fragment. Three fine-grained (up to 0.05 mm) crystals of **pyrrhotite** are armoured within the quartz close to the edge of the pyrite, and the pyrite hosts very rare fine-grained inclusions of **chalcopyrite**.

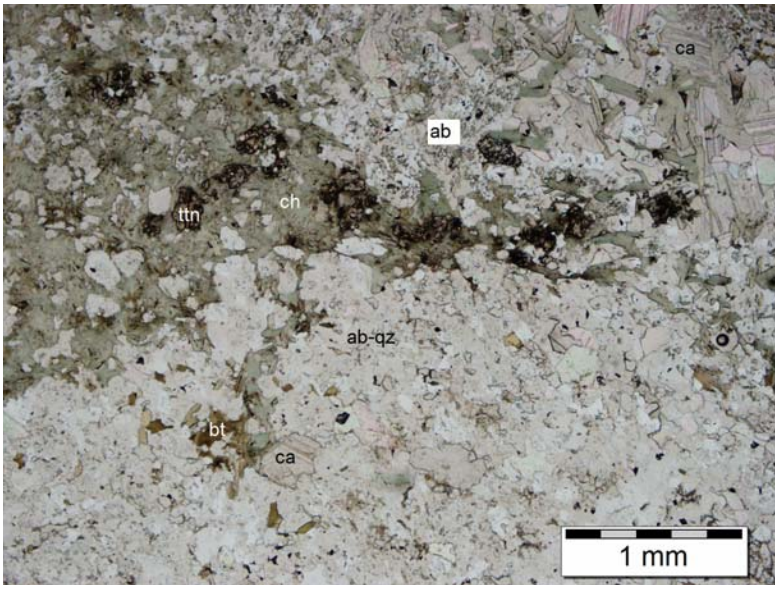

***Photomicrograph 26**: A fine-grained aggregate of albite and quartz (ab-qz) and subordinate calcite (ca) is filled in by fine-grained chlorite (ch), albite (ab), titanite (ttn), and calcite (ca). Relicts of the biotite (bt) are partially to completely replaced by the chlorite within the infill domain (upper part of the photomicrograph). Plane-polarized transmitted light.*

Sample 27: JFM033-1

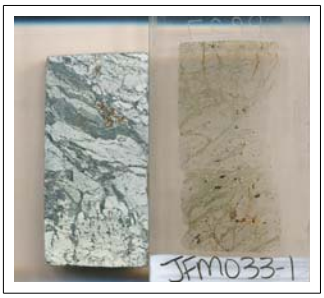

Albite schist

Actinolite-albite-chlorite-chalcopyrite-pyrite infill

Fine-grained recrystallized aggregates of albite and fine-grained clustered aggregates of clay, titanite, and actinolite define a spaced foliation within fractured fragments that are filled in by a fine-grained heterogeneous aggregate of actinolite, albite, chlorite, and subordinate pyrite, iron oxides, and rare chalcopyrite.

Mineral	*Modal %*	*Main Size Range (mm)*
albite-rich schist (80% of PTS)		
plagioclase (albite)	70 – 74	0.01–01
clay	5 – 6	up to 0.02
titanite	1	up to 0.1
actinolite	1	up to 0.1
actinolite-albite-chlorite-chalcopyrite-pyrite infill (20% of PTS)		
actinolite	10 – 15	up to 0.3
plagioclase (albite)	2.5 – 3	up to 0.3
Fe-chlorite	2.5 – 3	up to 0.3
chalcopyrite	1	up to 1 × 0.3 mm
pyrite	1	up to 0.25
iron oxides	tr	cryptocrystalline

Plagioclase (albite) forms fine-grained recrystallized aggregates that are intergrown with fine-grained clay and define irregular and subparallel microlithons within the fragments. The albite-rich microlithons are wrapped by fine-grained clustered aggregates of **clay**, titanite, and actinolite. The plagioclase occurs as fine- to medium-grained xenoblastic crystals within the infill domains, where it is intergrown with quartz and actinolite. Within the infill, most of the plagioclase crystals show albite twinning and lower refractive indexes than those of quartz, indicating its albite-rich composition.

Actinolite is fine grained and forms xenoblastic to prismatic crystals that are randomly oriented within the infill domains. Very fine- to fine-grained prismatic actinolite is subordinate

to the albite within the fragments and tends to occur with a preferred dimensional iso-orientation. The actinolite within the infill is distinguished by its distinct pleochroism and extinction angles (c:Z) up to 15°. The occurrence of idioblastic crystals that are immersed and intergrown with the plagioclase and quartz within the infill domains indicates that these three minerals were in equilibrium during the infill stage. Some of the actinolite is partially replaced by fine-grained **chlorite**, which shows positive elongation and is iron rich.

Chalcopyrite crystallized as xenoblastic crystals (up to 1 × 0.3 mm) within the infill domains. The chalcopyrite is coarser grained and more abundant within the fine-grained actinolite-chlorite-rich part of the infill.

Pyrite forms fine-grained (up to 0.25 mm) anhedral crystals that are concentrated within the infill domains and in some cases are rimmed and partially replaced by iron oxides.

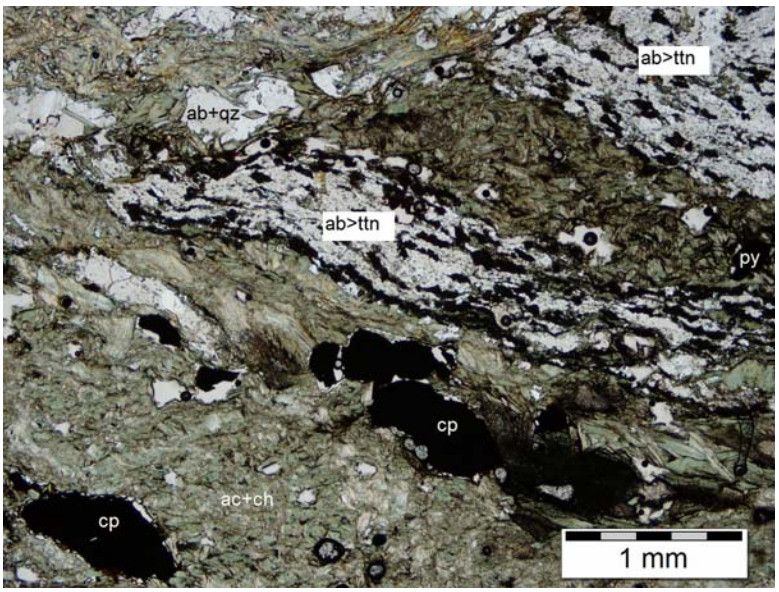

***Photomicrograph 27**: Fine-grained albite-rich domains host clustered aggregates of titanite (ab>ttn), are deformed by a brittle-ductile deformation, and are filled in by actinolite, which is partially replaced by chlorite (ac+ch), albite, quartz (ab+qz), chalcopyrite (cp), and pyrite (py). Plane-polarized transmitted light.*

Sample 28: JFM033-1.5

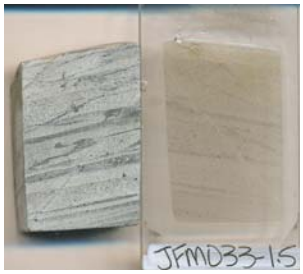

Metamudstone; Albite-quartz-chlorite veinlets

A very fine-grained and interlobate aggregate of albite and subordinate quartz is intergrown with very fine- to fine-grained flakes of white mica and chlorite. The slightly different grain size and the differences in the relative amount of chlorite and albite define a rhythmic sub-parallel compositional layering that is likely to be inherited from the sedimentary protolith. The layered sample is tightly folded during a ductile deformation event. Fish-hook folds occur in some of the layers, which are crosscut by sub-parallel albite-quartz-chlorite veinlets (0.3 mm and 0.07 mm thick).

Mineral	*Modal %*	*Main Size Range (mm)*
metamudstone (~98% of PTS)		
plagioclase (albite)	85 – 87	0.01–0.1
white mica	3.5 – 7	up to 0.02
quartz	3 – 6	up to 0.02
Mg-chlorite	2 – 3	up to 0.1
titanite?	1	up to 0.01
tourmaline	tr	up to 0.1
Albite-quartz-chlorite veinlets (~2% of PTS)		
plagioclase (albite)	1.5	up to 0.2
quartz	0.3	up to 0.15
Mg-chlorite	0.2	up to 0.1

Plagioclase (albite) forms a very fine- to fine-grained (0.01–0.1 mm) interlobate crystal aggregate that dominates the composition of this sample. The albite is intergrown with subordinate quartz and very fine-grained flakes of white mica, lesser chlorite, and very fine-grained to cryptocrystalline dispersions a high-relief mineral that I tentatively interpret as titanite and/or rutile. The grain size of the albite-rich aggregate is inversely proportional to the amount of dispersed phyllosilicate (white mica and chlorite), and these variations define a sub-planar compositional layering that is probably inherited from the sedimentary protolith. Within the more albite-rich layer, the average grain size reaches 0.1 mm, and the albite hosts subordinate amounts of fine-grained chlorite, rare very fine-grained white mica, and very rare

crystals of **tourmaline**.

Within the veinlets, fine-grained xenoblastic albite is distinguished by its albite twinning from the subordinate quartz and is associated with subordinate fine-grained crystals of chlorite.

White mica forms very fine-grained lamellae that show a preferred dimensional iso-orientation. Their differential distribution within the different albite-rich layers defines a continuous cleavage and a mesoscopically visible compositional layering.

Mg-chlorite forms very fine- to fine-grained xenoblastic crystals up to 0.1 mm. The chlorite shows negative elongation, indicating its magnesium-rich composition. In some cases, the chlorite hosts very fine-grained crystals of titanite and/or rutile, which may indicate that the chlorite completely replaced pre-existing biotite.

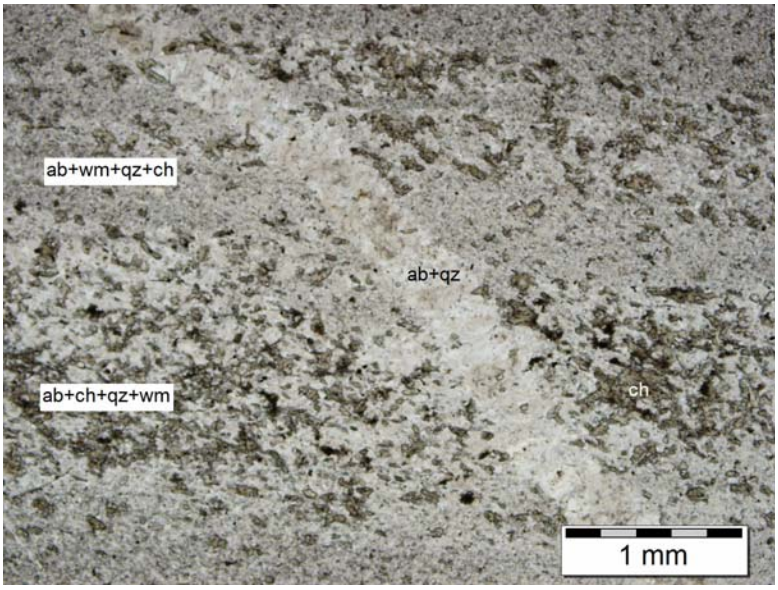

Photomicrograph 28*: The subparallel compositional layering is defined by fine- to very fine-grained albite-rich aggregates with different amounts of phyllosilicates. Very fine-grained albite-white mica-quartz-chlorite (ab+wm+qz+ch) layers alternate rhythmically with albite-chlorite-quartz-white mica layers (ab+ch+qz+wm), and are crosscut by albite-quartz veinlets. Plane-polarized transmitted light.*

Sample 29: JFM033-2a

Albite-dolomite-chlorite schist

A compositional layering is defined by fine-grained (up to 0.05 mm) granoblastic aggregates of albite, dolomite, quartz, and chlorite, and a coarser-grained (0.1–0.5 mm) and granoblastic aggregate of dolomite, albite, chlorite, and quartz. This aggregate is inequigranular and shows sub-tabular shapes. Tabular crystals of chlorite up to 1.2 mm long are preferentially iso-oriented parallel to the layering. They are concentrated along the inside borders of the medium-grained granoblastic aggregate and are less abundant within the fine-grained aggregates.

Mineral	*Modal %*	*Main Size Range (mm)*
plagioclase (albite)	40 – 44	0.05–1
dolomite	35 – 37	0.05–1
Mg-chlorite	12 – 15	up to 2.5 × 0.2
quartz	10 – 14	0.05–0.2
biotite	tr	up to 0.15
rutile?	tr	up to 0.02

Plagioclase (albite) forms fine-grained (up to 0.05 mm) granoblastic crystals that are intergrown with comparable amounts of fine-grained dolomite and subordinate **quartz** within the fine-grained layers. The plagioclase is inequigranular and granoblastic within the medium-grained layer, and in this case some of the plagioclase crystals form xenoblastic and slightly elongated crystals up to 1 mm long. These porphyroblasts host abundant inclusions of dolomite, chlorite, and biotite. The albitic composition of the plagioclase is determined by its refractive indexes, which are lower than those of quartz.

Dolomite is intergrown with the albite and subordinate quartz within the fine-grained layers. Within the medium-grained layer, the dolomite prevails over the albite and the quartz. In some cases, it forms quasi-monomineralic aggregates with a size comparable to the albite porphyroblasts. The dolomite was distinguished by its high relief, extreme birefringence, and slow reaction to cold dilute (10%) HCl. The absence of undulose extinction within the dolomite, the albite, and the subordinate quartz indicates that these three minerals recrystallized after the end of the ductile deformation event.

Medium-grained **Mg-chlorite** occurs as a tabular crystals up to 2.5 mm long with an aspect ratio of up to 10 to 1. The medium-grained chlorite is concentrated within the medium-grained layer and is less abundant within the fine-grained layers. Most of the crystals are oriented

parallel to the layering and show a strong undulose extinction. Some of the crystals form radial aggregates or are decussate. These microstructural features indicate that the chlorite crystallized during the waning stages of the ductile deformation event and post-dated the deformation. The chlorite is pale green and negatively elongated, which indicates its magnesium-rich composition.

Very rare **biotite** forms fine-grained crystals that are iso-oriented within the medium- and fine-grained layers.

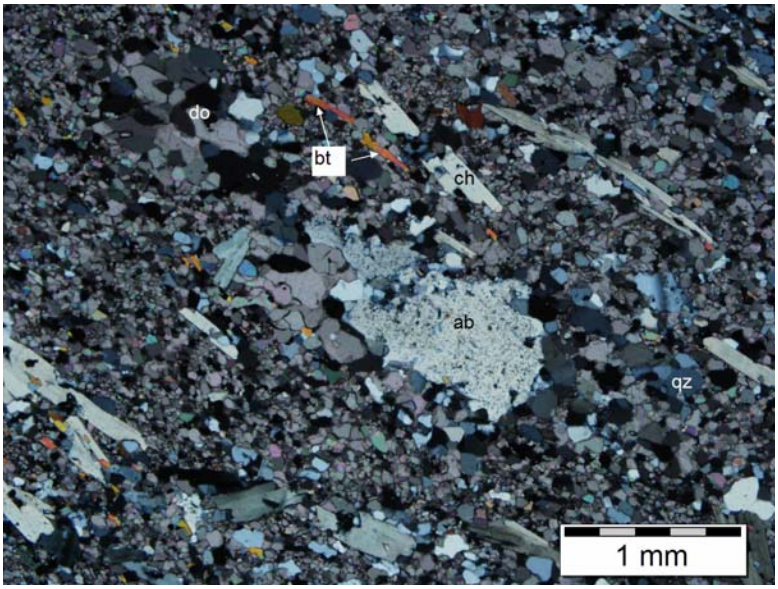

Photomicrograph 29*: Medium-grained chlorite (ch) and fine-grained biotite (bt) are iso-oriented and define a weak foliation within an inequigranular granoblastic aggregate of dolomite (do), albite (ab), and quartz (qz). Crossed Nicols transmitted light.*

Sample 30: JFM033-2b

Quartz-albite-chlorite schist;

Chalcopyrite-quartz-white mica-chlorite-pyrite infill

Coarse-grained interlobate, poikiloblastic quartz crystals host fine-grained blocky to subidioblastic albite. The quartzofeldspathic aggregate is crosscut by irregular cleavage domains of chlorite. In the upper and lower parts of the polished thin section, the quartz is coarse-grained and interlobate, and the albite inclusions are rare or absent. Amoeboid chalcopyrite preferentially precipitated within the interstices of the interlobate quartz within one of the transition zones between the quartz-albite aggregate and the quartz-rich domain. The chalcopyrite is spatially associated and intergrown with fine-grained white mica and chlorite.

Mineral	*Modal %*	*Main Size Range (mm)*
quartz-albite-chlorite schist (~95% of PTS)		
quartz	75 – 77	up to 4
plagioclase (albite)	15 – 17	up to 0.2
Mg-chlorite	1.5 – 2	up to 0.2
white mica	tr	up to 0.25
rutile	tr	up to 0.1
zircon	tr	up to 0.001
chalcopyrite-quartz-white mica-chlorite-pyrite infill (~5% of PTS)		
chalcopyrite	2.5 – 3	up to 1.5
quartz	1 – 2	up to 0.5
white mica	1 – 2	up to 0.25
pyrite	0.2 – 0.5	up to 1.2
Mg-chlorite	tr –	up to 0.2
zircon	tr	up to 0.001

Quartz forms coarse-grained (up to 4 mm) interlobate and poikiloblastic crystals that host abundant fine-grained crystals of albite within the central part of the polished thin section. The quartz occurs as coarse-grained interlobate crystals within the upper and lower parts of the

polished thin section. All the quartz crystals show strong undulose extinction, which I interpret as a consequence of the brittle-ductile deformation that generated the irregular subparallel cleavage domains of chlorite. The fractures are filled in by chalcopyrite, white mica, chlorite, and pyrite.

Plagioclase (albite) is fine grained (up to 0.3 mm) and forms subidioblastic crystals randomly oriented within the coarse-grained interlobate quartz. The plagioclase shows albite twinning and lower refractive indexes than those of quartz, indicating its albitic composition. The distribution of the abundant albite inclusions within the quartz defines an irregular vein-like domain on the offcut; however, because of the transitional nature of the quartz-albite and the quartz-rich domains, their relative ages must be verified in the field. In this polished thin section, I tentatively interpret the albite inclusions as post-dating the quartz-rich domains as a consequence of the induced strain within the quartz, as the fine-grained albite crystals in some cases are preferentially crystallized along the interlobate crystal boundaries of quartz.

Mg-chlorite forms subparallel and irregular cleavage domains (up to 0.5 mm thick) that define a weak spaced foliation. The chlorite shows a preferred dimensional orientation; however, some of the crystals are randomly oriented within the cleavage domains. The chlorite forms fine-grained crystals and replacement patches that are heterogeneously distributed within the quartz-albite and the quartz-rich domains. In most cases, these replacement patches are spatially associated with the cleavage domains, and I interpret them as having been generated during the shear. Chlorite shows a negative elongation, hence it is magnesium-rich and hosts metamictic halos, which are generated by very fine-grained inclusions of zircon. Finally, the chlorite is spatially associated and intergrown with the chalcopyrite crystals.

Chalcopyrite precipitated as amoeboid crystals (up to 1.5 mm) that occupy the interstices and fractures between the quartz. The medium-grained crystals are irregularly concentrated at the boundary between a quartz-albite and a quartz-rich domain. The chalcopyrite is spatially associated with fine-grained randomly oriented crystals of **white mica** and lesser chlorite. The fine-grained tabular crystals of white mica are preferentially associated with the chlorite; in some cases the white mica shows a preferred dimensional orientation, and in others it forms randomly oriented crystals that overprinted the chlorite.

Rare idioblastic **pyrite** (up to 1.2 mm) is spatially associated with the chalcopyrite.

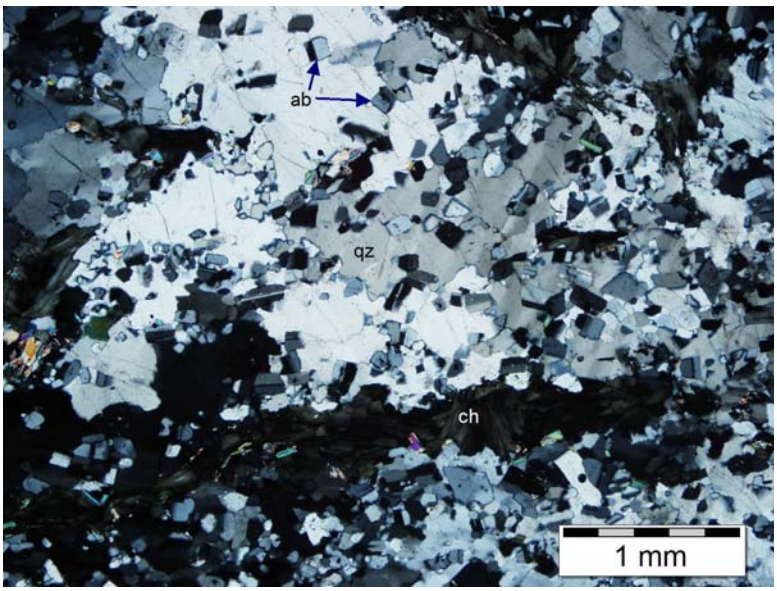

***Photomicrograph 30a**: Coarse-grained poikiloblastic quartz (qz) hosts fine-grained crystals of albite (ab) and is crosscut by chlorite-rich cleavage domains (ch). Crossed Nicols transmitted light.*

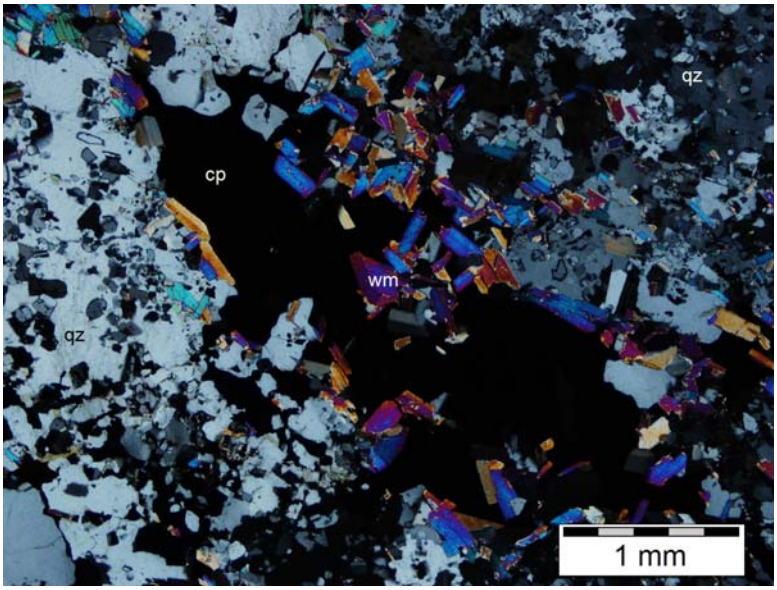

***Photomicrograph 30b**: Amoeboid chalcopyrite (cp) filled in the fractures between the poikiloblastic quartz (qz) and is intergrown with randomly oriented and tabular white mica (wm). The inclusions within the quartz are made up of albite and lesser chlorite and white mica. Crossed Nicols transmitted light.*

Vancouver Petrographics Ltd.
8080 GLOVER ROAD, LANGLEY, B.C. V1M 3S3
PHONE: 604-888-1323 • FAX: 604-888-3642
email: vanpetro@vanpetro.com
Website: www.vanpetro.com

Report for: Energizer Resources Inc.
141 Adelaide Street West Suite 520
Toronto, Ontario, Canada, M5H 3L5

Sent to: Craig Scherba <cscherba@energizerresources.com>
Jean-François Montreuil <montreuil.jean.francois@gmail.com>
Quentin Yarie <qyarie@macdonaldmines.com>

Report 130645

October 9, 2013

Petrographic Report on 54 Samples from Sagar Property Part 2 (Samples 31–54)

Fabrizio Colombo, Ph.D., P.Geo.

Table of Contents (Part 2)

5. Petrographic Descriptions (continued).....83
Sample 31: JFM033-3.....83
Sample 32: JFM033-5.....85
Sample 33: JFM033-6.....87
Sample 34: JFM033-7.....89
Sample 35: JFM035-1.....91
Sample 36: JFM037.....93
Sample 37: JFM039-1.....95
Sample 38: JFM039-2.....97
Sample 39: JFM042-1.....99
Sample 40: JFM042-2.....101
Sample 41: JFM042-3.....103
Sample 42: JFM042-5.....105
Sample 43: JFM043-2.....107
Sample 44: JFM044-1.....109
Sample 45: JFM049.....112
Sample 46: SGR-02-440m.....114
Sample 47: SUS-07-15-275'.....117
Sample 48: SUS-07-44-234'.....120
Sample 49: WP-253.....122
Sample 50: WP282.....124
Sample 51: WP284.....126
Sample 52: 1272227.....128
Sample 53: WP-292.....130
Sample 54: WP535-CaRB-3 132

5. Petrographic Descriptions (continued)

Sample 31: JFM033-3

Chlorite granofels

Fine-grained and randomly oriented chlorite flakes dominate the composition of this sample. A subtle compositional heterogeneity is defined by fine-grained dispersions of pyrrhotite, quartz, and lesser chalcopyrite and pyrite in the lower part of the polished thin section. Irregular crystal aggregates (up to 2.5 × 1 mm) of poikiloblastic quartz and fine-grained inclusions of chlorite and rare dolomite are heterogeneously dispersed within the chlorite-rich isotropic domain.

Mineral	*Modal %*	*Main Size Range (mm)*
Mg-chlorite	94 – 95	up to 0.3
quartz	3 – 5	up to 0.2
pyrrhotite	1 – 2	up to 0.5
chalcopyrite	tr	up to 0.5
pyrite	tr	up to 0.2
rutile	tr	up to 0.01; rare up to 0.1
dolomite	tr	up to 0.05
apatite	tr	up to 0.1
zircon	tr	0.001–0.02
pentlandite	tr	up to 0.01

Mg-chlorite forms fine-grained and randomly oriented flakes that dominate the composition of this sample. The chlorite hosts very fine-grained inclusions of rutile and zircon, as indicated by the rounded metamictic halos within the chlorite host. The chlorite is magnesium rich, as indicated by its negative elongation, and crystallized in equilibrium with the quartz, as suggested by some straight boundaries between the quartz and chlorite.

Quartz is dispersed within the chlorite as fine-grained xenoblastic to amoeboid crystals that in some cases are poikiloblastic, fine-grained and recrystallized, and include fine-grained flakes of chlorite and rare **dolomite**.

Anhedral **pyrrhotite**, pyrite, and chalcopyrite preferentially precipitated within and are intergrown with the quartz. The pyrrhotite is characterized by a distinct bireflectance and in some cases is partially replaced by **chalcopyrite**. The pyrite is xenoblastic and is intergrown

with the pyrrhotite. Very rare, very fine-grained flame-like exsolutions of **pentlandite** are hosted within the pyrrhotite.

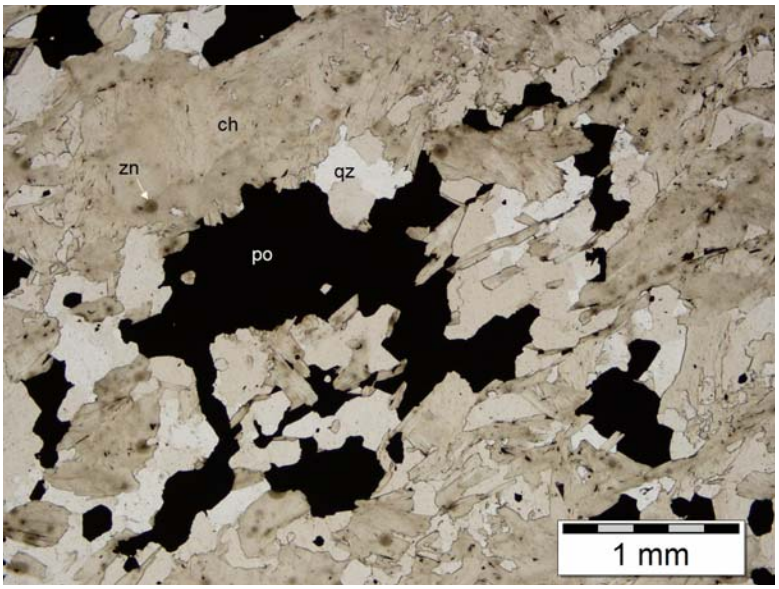

Photomicrograph 31*: Amoeboid pyrrhotite (po) is intergrown with quartz (qz) and is immersed within randomly oriented fine-grained chlorite (ch), which includes very fine-grained crystals of zircon (zn) highlighted by the metamictic halos produced within the chlorite host. Plane-polarized transmitted light.*

Sample 32: JFM033-5

Chlorite-pyrrhotite-quartz granofels

Similarly to Sample 31, this sample is made up of a fine-grained aggregate of chlorite and subordinate quartz. However, in this sample the pyrrhotite is more abundant and is concentrated in the upper left part of the polished thin section as xenoblastic, fractured, moderately altered coarse-grained crystals.

Mineral	*Modal %*	*Main Size Range (mm)*
Mg-chlorite	74 – 78	up to 0.3; rare up to 0.5 mm long
pyrrhotite	15 – 17	up to 4
quartz	7 – 8	up to 1; rare up to 4
chalcopyrite	0.1 – 0.2	up to 1
rutile	tr	up to 0.1
limonite and iron oxide	tr	cryptocrystalline
zircon	tr	up to 0.01

Within half of the polished thin section, the **Mg-chlorite** forms a randomly oriented fine-grained aggregate in association with subordinate and fine-grained quartz. This aggregate is very similar to the chlorite aggregate described in Sample 31. In the other part of the polished thin section, the fine-grained chlorite is intergrown with abundant medium- to coarse-grained pyrrhotite, medium-grained quartz, and in some cases the chlorite, and it forms lamellae up to 0.5 mm long. The negative elongation of the chlorite indicates its magnesium-rich composition, and the chlorite hosts fine- to coarse-grained poikiloblastic quartz, in which the chlorite is enclosed as randomly oriented fine-grained flakes.

Pyrrhotite is concentrated in the upper left part of the polished thin section (see the image in the upper right part of this page) as fine- to coarse-grained (up to 4 mm) xenoblastic crystals. The coarser crystals are poikiloblastic and enclose fine- to medium-grained crystals of quartz, quartz and chlorite, chlorite, **chalcopyrite** (up to 1 mm), and unresolved oxidized minerals.

Quartz is dispersed as fine-grained xenoblastic crystals that are intergrown with the chlorite within the chlorite-rich part of this sample. The quartz is more abundant and forms amoeboid crystals (up to 1 mm, and in rare cases up to 4 mm) that are spatially associated and intergrown with the pyrrhotite.

Rutile is dispersed within the chlorite and forms columnar crystals of up to 0.1 mm.

Iron oxides and limonitic stains permeate the fractures and in rare instances form irregular

boxwork that is likely to replace intensely altered pyrrhotite.

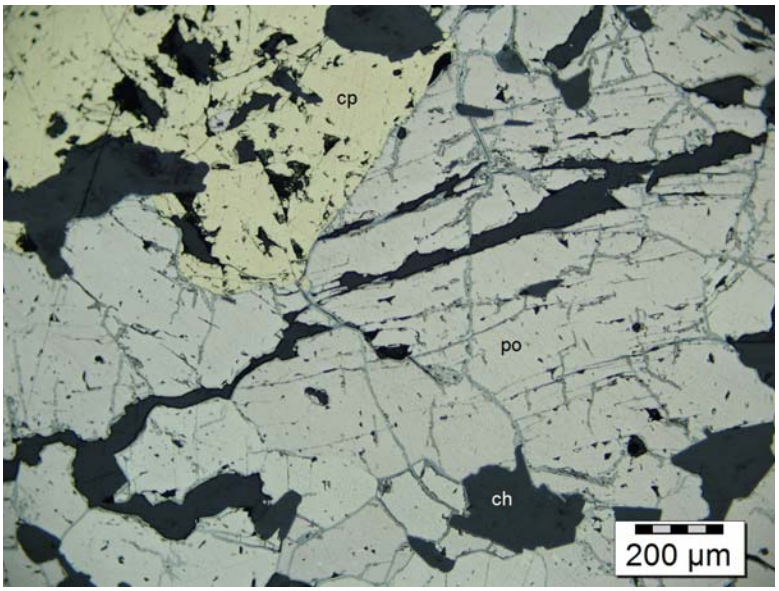

***Photomicrograph 32**: Coarse-grained poikiloblastic pyrrhotite (po) hosts xenoblastic chalcopyrite (cp) and chlorite (ch). It is weakly to moderately altered. Plane-polarized reflected light.*

Sample 33: JFM033-6

Clay-quartz alteration-zone

This polished thin section is made up of a very fine-grained felt-like aggregate of clay, quartz, very fine- to fine-grained sub-rounded to sub-tabular crystals of hematite(?), and fine-grained replacement patches of dolomite.

Mineral	*Modal %*	*Main Size Range (mm)*
clay	63 – 66	up to 0.02
quartz	25 – 27	up to 0.02
hematite(?)	5 – 6	up to 0.05; rare up to 0.1
dolomite(?)	2 – 2.5	up to 0.15
limonite	tr	cryptocrystalline
rutile	tr	up to 0.02

Clay is very fine grained and forms a felt-like aggregate that is characterized by low birefringence (up to first-order grey) and hosts very fine-grained and randomly oriented lamellae with higher birefringence (third-order blue). I tentatively interpret it as illite or white mica flakes. The mineral composition of the very fine-grained aggregate should be tested by spectroscopic analysis (short-wave infrared spectroscopy).

Quartz forms very fine-grained (up to 0.02 mm) crystals that are subordinate to the clay and in some cases form granoblastic aggregates.

Hematite(?) forms very fine- to fine-grained (up to 0.04 mm) sub-rounded to sub-tabular crystals that are homogeneously dispersed within the clay-rich aggregates. The crystals are bireflectant and anisotropic, and show a moderate reflectance.

Fine-grained (up to 0.15 mm) patches of carbonate overprinted the clay-rich aggregate and are distinguished by their high relief and extreme birefringence; however, due to the very fine-grained nature of the aggregate, no visible reaction to cold dilute (10%) HCl was observed on the offcut, and the nature of the carbonate is only tentatively interpreted as **dolomite**.

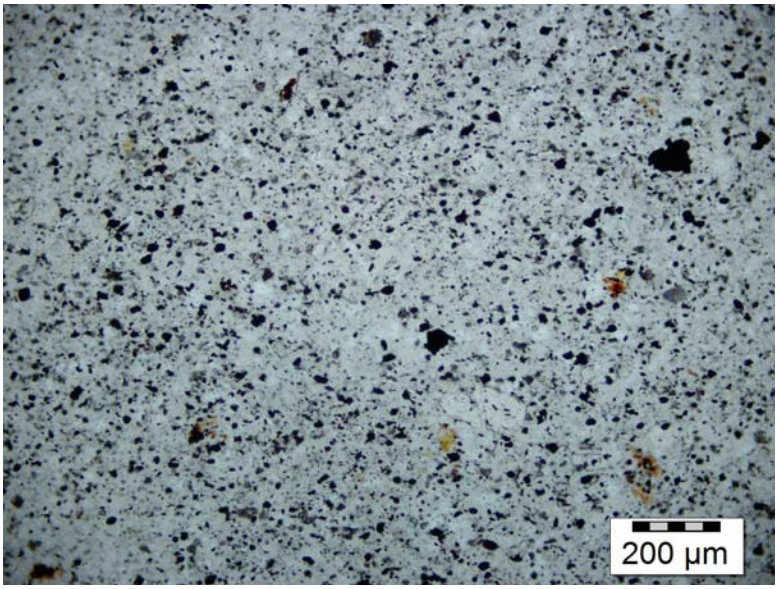

***Photomicrograph 33**: The very fine-grained aggregate is made up of clay, quartz (transparent minerals), and very fine- to fine-grained hematite (opaque). Plane-polarized transmitted light.*

Sample 34: JFM033-7

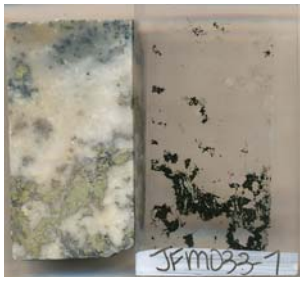

Dolomite-chalcopyrite-quartz vein[1]

An inequigranular granoblastic aggregate of dolomite hosts interstitial to amoeboid chalcopyrite, rare quartz, and very rare pyrite.

Mineral	*Modal %*	*Main Size Range (mm)*
dolomite	85 – 87	0.05–0.5; rare up to 8
chalcopyrite	10 – 12	massive; up to 10 × 4 mm
quartz	0.2 – 0.5	up to 1.5
pyrite	tr	up to 0.4
Mg-chlorite	tr	up to 0.1
rutile	tr	up to 0.03

Dolomite forms an inequigranular and granoblastic crystal aggregate that dominates the composition of this polished thin section. The dolomite aggregate is fine grained (0.1–0.25 mm) in the upper part of the polished thin section and gradually increases its grain size in the lower part, in which the coarse-grained (up to 8 mm) and inequigranular crystals tend to form interlobate aggregate and are intergrown with abundant chalcopyrite.

Chalcopyrite is concentrated in the lower part of the polished thin section as interstitial to amoeboid crystals that in some cases are poikiloblastic and host fine- to coarse-grained crystals of dolomite, rare and medium-grained subhedral pyrite, and fine-grained crystal aggregates of **Mg-chlorite**. The chalcopyrite forms heterogeneously dispersed crystal clusters in the fine- to medium-grained dolomitic aggregates in the upper part of the polished thin section.

Quartz is rare. It forms fine- to medium-grained crystals that are heterogeneously distributed in the upper part of the polished thin section; in this part of the sample, they are intergrown with the medium-grained dolomite and in some cases with the chalcopyrite.

1 As indicated in the sample description.

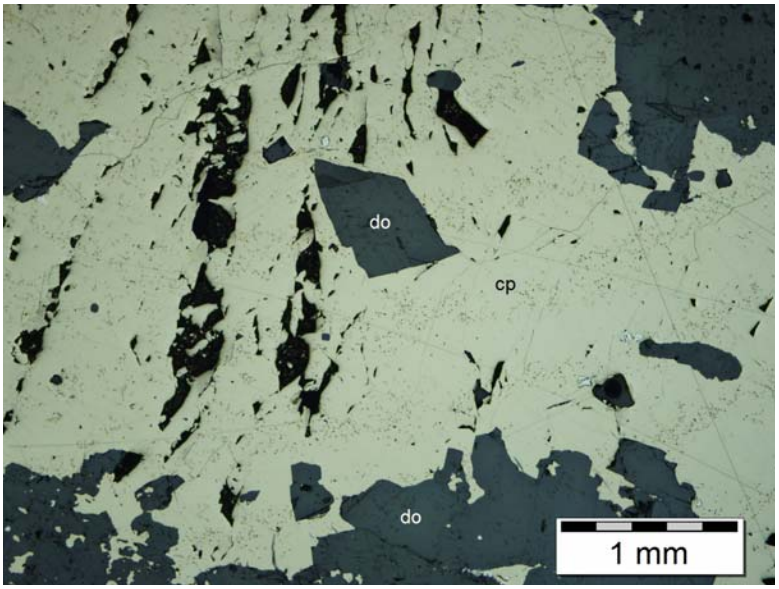

***Photomicrograph 34**: Massive chalcopyrite (cp) is intergrown with the dolomite (do) and hosts idioblastic crystals of dolomite as inclusions. Plane-polarized transmitted light.*

Sample 35: JFM035-1

Dolomite-quartz-white mica schist

Irregular, anastomosing cleavage domains are made up of preferentially iso-oriented fine-grained white mica and quartz, and crosscut an inequigranular and interlobate aggregate of dolomite, and lesser quartz and chlorite.

Mineral	*Modal %*	*Main Size Range (mm)*
dolomite	80 – 82	up to 0.3; rare up to 1
quartz	10 – 12	up to 0.7
white mica	5 – 6	up to 0.2
chlorite	2 – 4	up to 0.5
pyrite	tr	up to 0.2
iron oxides	tr	cryptocrystalline

Dolomite is inequigranular (up to 0.3; rare up to 1) and forms interlobate crystal aggregates intergrown with subordinate blocky to granoblastic quartz. Some of the dolomite crystals show the distinctive twinning parallel to the short diagonal of the cleavage rhombs, and by its slow reaction to cold dilute (10%) HCl.

Quartz is heterogeneously distributed within the dolomite-rich aggregates as blocky crystals (up to 0.3 mm) and granoblastic crystal aggregates with a moderate undulose extinction. The inequigranular dolomite-quartz aggregate is crosscut by irregular subparallel anastomosing cleavage domains (up to ~1 mm thick) made up of fine-grained iso-oriented **white mica** and subordinate quartz. The cleavage domains define a weak, rough spaced foliation.

Medium-grained tabular **Mg-chlorite** occurs as randomly oriented crystals that overprinted the dolomite-quartz aggregate. In some cases, it shows kink bands and bent crystals. The negative extension of the chlorite indicates its magnesium-rich composition. The microstructural relationships between Mg-chlorite and the preferentially iso-oriented white mica indicate that most of the Mg-chlorite crystallization post-dated the ductile deformation event.

Rare fine-grained (up to 0.2 mm) subhedral **pyrite** preferentially crystallized within the white mica-rich cleavage domains. In some cases, the pyrite crystals are surrounded by quartz-rich strain shadows, and for this reason I interpret their crystallization as syn- to post-tectonic. The pyrite crystals are weakly altered by iron oxide rims.

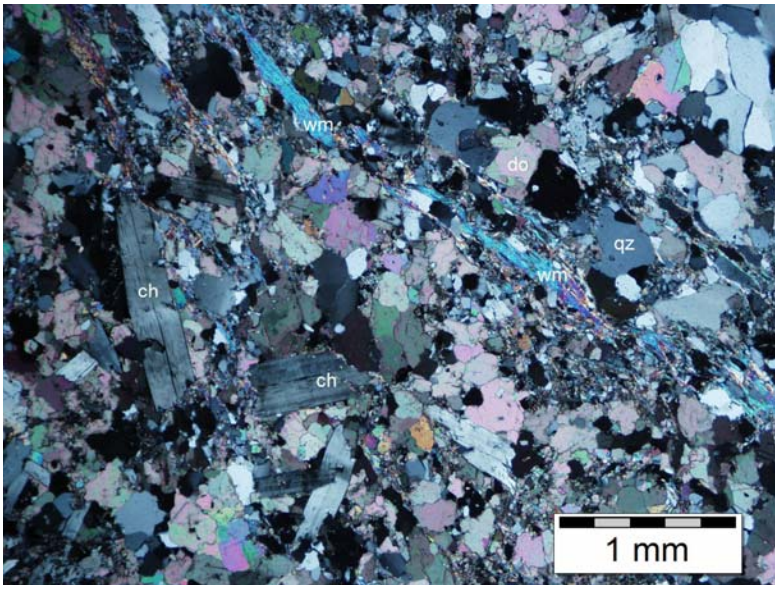

***Photomicrograph 35**: An inequigranular aggregate of dolomite (do) and quartz (qz) is crosscut by irregular cleavage domains of white mica (wm) and is overprinted by a medium-grained chlorite (ch). Crossed Nicols transmitted light.*

Sample 36: JFM037

Quartz-chlorite schist

An inequigranular and granoblastic microstructure is defined by quartz. Fine-grained chlorite defines thin (less than 0.1 mm thick), discontinuous subparallel cleavage domains and filled in the interstices between the subtly fractured quartz-rich aggregates.

Mineral	*Modal %*	*Main Size Range (mm)*
quartz	98 – 99	up to 0.2; rare up to 0.4
Mg-chlorite	1 – 1.5	up to 0.1
dolomite(?)	tr	up to 0.3
pyrite	tr	up to 0.25
iron oxides	tr	cryptocrystalline

Quartz is inequigranular (up to 0.2; rare up to 0.4 mm) and forms a granoblastic aggregate that dominates the composition of this polished thin section. The quartz-rich aggregate is subtly fractured and the irregular network of fractures are filled in by fine-grained chlorite. The quartz shows moderate undulose extinction, and in most cases fine-grained quartz nucleated along the edges of the fine-grained crystals as a consequence of the brittle-ductile deformation.

Mg-chlorite is fine grained and is concentrated within thin (less than 0.1 mm) cleavage domains that roughly define a spaced foliation. The presence of chlorite within the cleavage domains and as infill mineral within the fractures that crosscut the quartz-rich aggregate suggests that the brittle deformation was coeval with the ductile deformation that generated the incipient foliation. The fine-grained chlorite flakes show negative elongation; therefore, their composition is magnesium rich.

Dolomite(?) forms fine-grained blocky to xenoblastic crystals (up to 0.3 mm) that form irregular clusters filling in irregular fractures. The presence of dolomite is tentatively interpreted by its high relief, extreme birefringence, and slow reaction to cold dilute (10%) HCl along partially filled fractures on the offcut.

Rare fine-grained (up to 0.25 mm) **pyrite** is spatially associated with the chlorite-bearing fracture infills and cleavage domains, and I interpret its occurrence as syn- to post-kinematic. Most of the pyrite is coated by a thin rim of **iron oxides**.

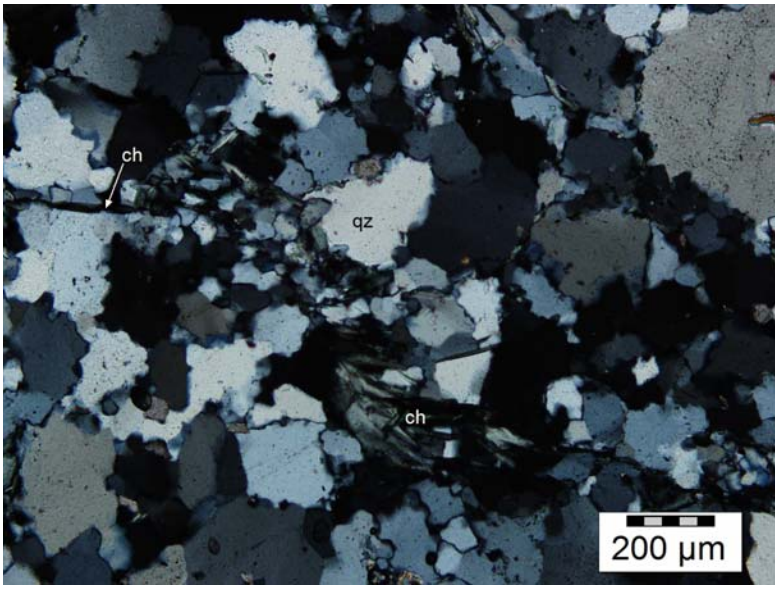

***Photomicrograph 36**: Thin, discontinuous cleavage domains of chlorite (ch) crosscut a granoblastic aggregate of quartz (qz) in which some of the crystals show the development of sub-grain boundaries. Crossed Nicols transmitted light.*

Sample 37: JFM039-1

Hematite-dolomite-quartz-albite vein[1]

Coarse-grained lamellar to massive hematite is intergrown with coarse-grained dolomite, fine- to medium-grained quartz, and fine-grained clustered aggregates of albite.

Mineral	*Modal %*	*Main Size Range (mm)*
hematite	54 – 56	lamellar: up to 8 mm long; massive: up to 10 × 8
dolomite	–	up to 3
quartz	–	up to 0.8
plagioclase (albite)		up to 0.2

Hematite forms tabular lamellae up to 8 mm long and massive aggregates up to 10 × 8 mm. The lamellae are bent and fractured and are intergrown with dolomite, quartz, and albite (see Photomicrograph 37). Hematite is distinguished by its deep red streak, moderate reflectance, grey-white colour with bluish tints, weak bireflectance, and distinct anisotropy.

Dolomite occurs as coarse-grained (up to 3 mm) crystals intergrown with the abundant hematite. Fine-grained xenoblastic crystals of dolomite occupy the interstices between the lamellar hematite. The dolomite shows moderate undulose extinction. Under the microscope, it can be distinguished by the presence of twinning parallel to the short and long diagonals of the cleavage rhombs. On the offcut, the coarse crystals slowly reacted to cold dilute (10%) HCl.

Fine- to medium-grained xenoblastic **quartz** is intergrown with the hematite and the dolomite, and forms fine-grained crystal clusters in association with subordinate plagioclase (see Photomicrograph 37).

Plagioclase (albite) is fine grained (up to 0.2 mm). It is distinguished by its typical albite twinning, and the albitic composition is indicated by its refractive indexes, which are lower than those of quartz.

1 As indicated in the sample description.

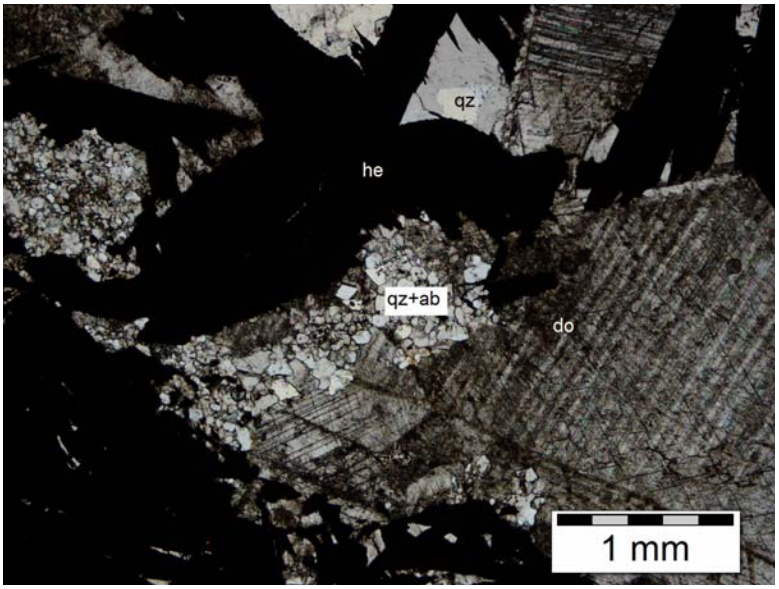

***Photomicrograph 37**: Coarse-grained lamellae of hematite (he) are intergrown with coarse-grained dolomite (do), medium-grained quartz (qz), and fine-grained clusters of quartz and albite (qz+ab). Plane-polarized transmitted light.*

Sample 38: JFM039-2

Dolomite-albite granofels

Fine-grained granoblastic dolomite, subordinate blocky albite, and quartz dominate the composition of this sample. A sub-planar compositional layering is defined by subtle variations in the relative proportion and grain size of these two main components with the addition of fine-grained clustered hematite and rare rutile.

Mineral	*Modal %*	*Main Size Range (mm)*
dolomite	75 – 78	0.02–0.4; rare up to 2
albite	15 – 16	0.1–0.5
quartz	5 – 6	up to 0.02
hematite	tr	up to 0.04
rutile	tr	up to 0.01

Dolomite forms fine-grained (0.02–0.4 mm) granoblastic crystal aggregates. The dolomite is intergrown with varying amounts of plagioclase and lesser quartz. In some cases the boundaries between the dolomite, plagioclase, and quartz are straight to slightly curved, indicating that they were in equilibrium during a strain-free recrystallization. Within rare monomineralic aggregates, the dolomite occurs as interlobate crystals of up to 2 mm. The dolomite forms irregular (up to 2.5 mm thick) medium-grained interlobate aggregates that I tentatively interpret as dolomite-rich infills.

Plagioclase (albite) occurs as inequigranular (0.1–0.5 mm) blocky, subidioblastic to xenoblastic crystals that are heterogeneously dispersed within the inequigranular dolomite-rich aggregate. In many instances, the plagioclase shows albite twinning and where the plagioclase is in contact with the quartz, the latter shows higher refractive indexes, indicating that the plagioclase is albitic.

Quartz forms fine-grained xenoblastic crystals that are subordinate to and preferentially associated with the plagioclase.

Hematite is very fine to fine grained (up to 0.04 mm) and is concentrated within thin (up to 0.2 mm) sub-planar clusters that are parallel to the compositional layering.

Very rare fine-grained **rutile** is preferentially associated with the hematite, from which it is distinguished by its lower reflectance, presence of internal reflections, and anisotropy under crossed Nicols transmitted light.

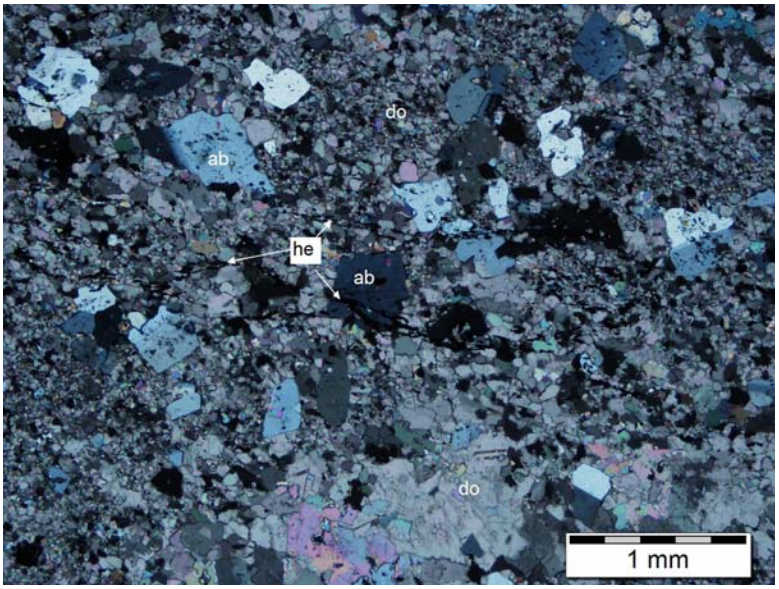

***Photomicrograph 38**: Inequigranular dolomite (do) is intergrown with medium-grained albite (ab) and lesser quartz. Thin crystal clusters of hematite (he) are parallel to the compositional layering defined by the variation in grain size and relative abundance of dolomite and plagioclase. Crossed Nicols transmitted light.*

Sample 39: JFM042-1

Dolomite-albite granofels

Inequigranular (0.1–0.5 mm) granoblastic dolomite is intergrown with subordinate plagioclase and lesser quartz. A planar compositional layering is defined by the distribution of plagioclase, which is proportional to the grain size of the dolomite.

Mineral	*Modal %*	*Main Size Range (mm)*
dolomite	95 – 98	0.1–0.5
plagioclase (albite)	2 – 2.5	up to 0.4
quartz	1 – 1.5	up to 0.2
hematite	tr	up to 0.05

Dolomite forms fine- to medium-grained granoblastic aggregates in which the average grain size of the dolomite crystals oscillates between 0.1 mm and 0.5 mm, defining a microstructural anisotropy. The coarser domains preferentially host medium-grained euhedral plagioclase. The dolomite was distinguished by its slow reaction to cold dilute (10%) HCl.

Plagioclase (albite) is medium grained and occurs as blocky crystals preferentially dispersed within the medium-grained doleritic aggregates. Only in rare cases was it possible to measure the angle between the adjacent twinning lamellae (according to the albite law), and in these cases the extinction angles [a′:(010)] reached a maximum of 10°, indicating the albitic composition of the plagioclase.

Quartz is fine grained. It forms blocky crystals intergrown with the dolomite and fine-grained granoblastic aggregates. It is subordinate to the plagioclase, and along with the plagioclase, the quartz is preferentially dispersed within the medium-grained dolomitic aggregate.

Rare fine-grained (up to 0.05 mm) **hematite** is dispersed within the dolomite and forms xenoblastic to sub-tabular crystals with moderate reflectance and a grey-white colour with bluish tints.

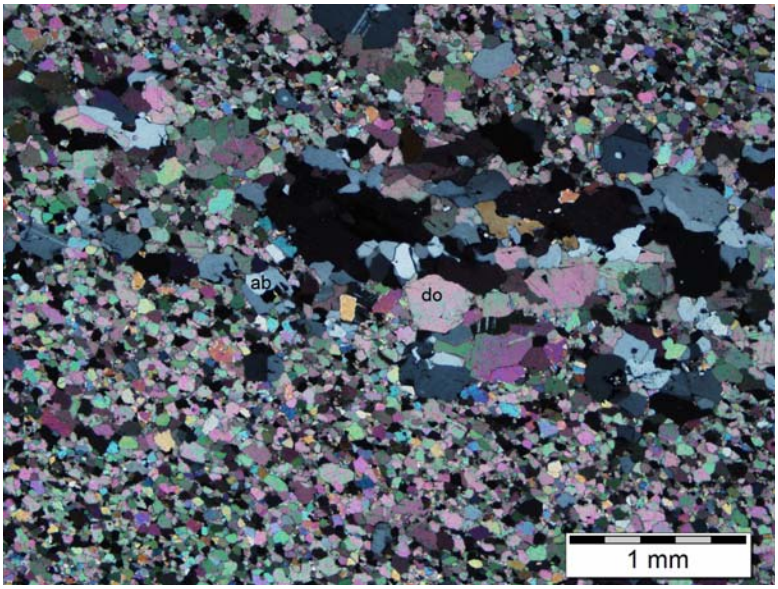

***Photomicrograph 39**: The dolomite (do) forms medium-grained granoblastic aggregates in association with subordinate albite (ab) and lesser quartz. It forms a fine-grained granoblastic aggregate with rare plagioclase and quartz (in the lower and upper part of the photomicrograph). Crossed Nicols transmitted light.*

Sample 40: JFM042-2

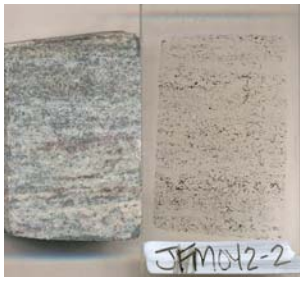

Dolomite-hematite-albite granofels

Inequigranular and granoblastic dolomite is intergrown with randomly oriented lamellae of hematite and subordinate albite and quartz.

Mineral	*Modal %*	*Main Size Range (mm)*
dolomite	90 – 92	0.05–0.5
hematite	5 – 7	up to 1.2 × 0.1
plagioclase (albite)	1 – 2	up to 0.2
quartz	0.5 – 1	up to 0.2

Dolomite occurs as inequigranular (0.05–0.5 mm) granoblastic to interlobate crystal aggregates. The dolomite forms medium-grained subparallel domains in which the hematite is preferentially concentrated and coarser grained. The dolomite was distinguished by its slow reaction to cold dilute (10%) HCl.

Hematite forms tabular crystals up to 1.2 mm long with an aspect ratio of up to 15 to 1. The hematite crystals are randomly oriented and are concentrated within the medium-grained dolomite-rich sub-parallel domains. The concentration of the hematite varies between 4% and 23% in different layers of the polished thin section (see image in the upper right part of this page and Photomicrograph 40). Fine-grained xenoblastic hematite is dispersed within the dolomite-rich granoblastic aggregate.

Plagioclase (albite) and subordinate **quartz** are heterogeneously dispersed within the dolomitic aggregate as fine-grained (up to 0.2 mm) crystals. The plagioclase is distinguished by its typical albite twinning, and by its refractive indexes, which are lower than those of quartz.

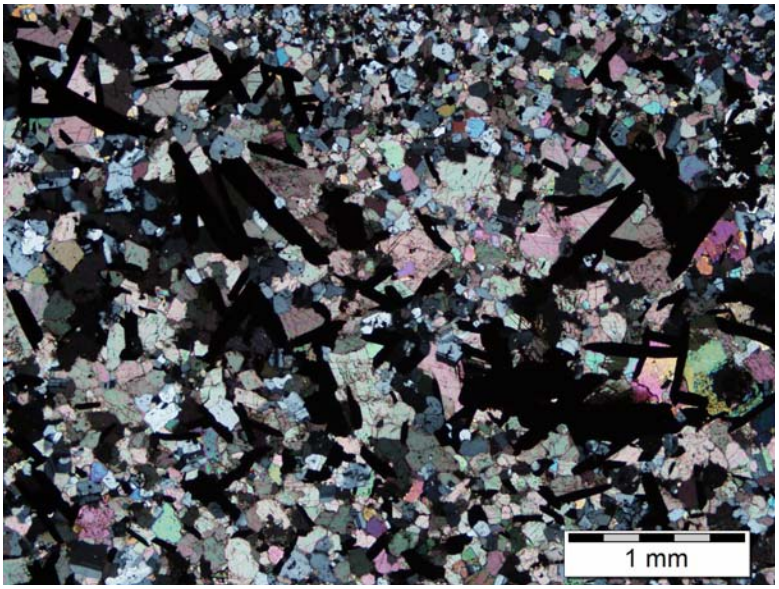

***Photomicrograph 40a**: Inequigranular dolomite (higher birefringence) is intergrown with tabular crystals of hematite (opaque) and fine-grained albite and quartz (grey to white). Crossed Nicols transmitted light.*

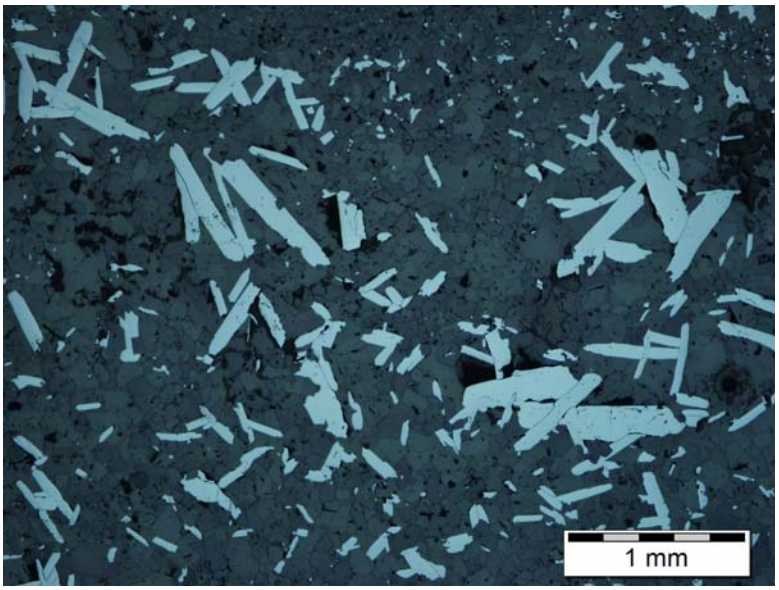

***Photomicrograph 40b**: Same area shown in Photomicrograph 40a. Tabular hematite (moderately reflective) crystals are randomly oriented within the dolomite-rich aggregate and are coarser grained within the medium-grained dolomitic domain. Plane-polarized reflected light.*

Sample 41: JFM042-3

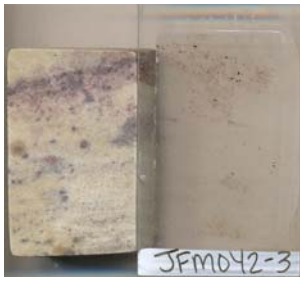

Dolomite-albite-hematite alteration-zone

An inequigranular interlobate to granoblastic aggregate of dolomite is intergrown with subordinate albite. Interstitial iron oxides and very fine- to fine-grained hematite form irregular clusters and dark patches within the dolomitic aggregate. In most cases, they are spatially associated with coarser-grained (up to 0.5 mm) crystal aggregates of dolomite.

Mineral	*Modal %*	*Main Size Range (mm)*
dolomite (and rare calcite)	97 – 99	0.02–0.5
plagioclase (albite)	1 – 2	up to 0.15
iron oxides	0.2 – 0.3	cryptocrystalline
hematite	tr	up to 0.07

Dolomite is inequigranular (0.02–0.5 mm) and defines an interlobate to granoblastic aggregate in which the coarser crystals form irregular elongate domains that are subparallel. I tentatively interpret these as recrystallized domains or dolomite-rich infill domains. The dolomite was distinguished by its slow reaction to cold dilute (10%) HCl on the offcut. Very rare **calcite** is also present, as indicated by rare spots that reacted briskly to the acid.

Plagioclase (albite) occurs as fine-grained blocky crystals of up to 0.15 mm. The plagioclase shows albite twinning and is heterogeneously distributed within the dolomitic aggregate, with curved boundaries between the fine-grained plagioclase crystals and the inequigranular dolomite. The low extinction angles (~10°) between the albite twinning lamellae indicate that the plagioclase is albite rich.

Iron oxides define irregular clusters as cryptocrystalline interstitial dispersions within the dolomite-rich aggregates. The iron oxides are spatially associated with the rare fine-grained sub-tabular to xenoblastic crystals of **hematite**. The iron-bearing minerals are more abundant within and near the coarser-grained dolomitic domains.

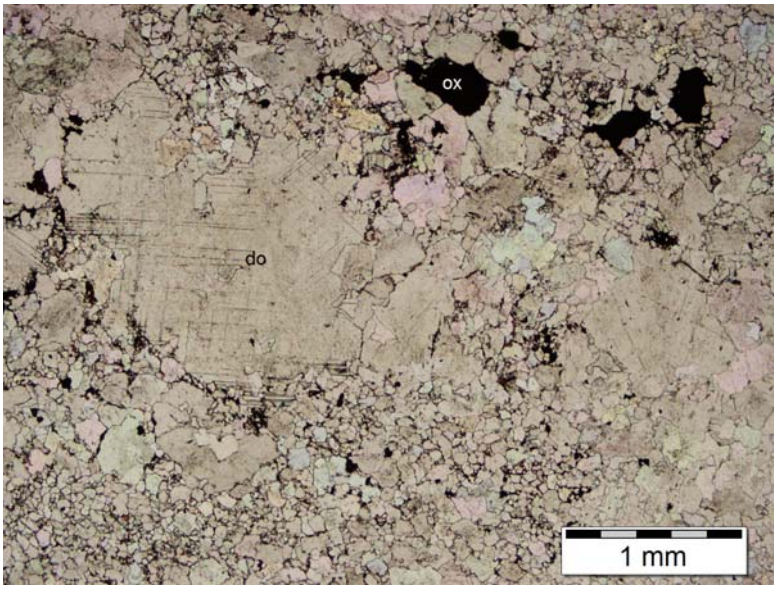

***Photomicrograph 41**: The iron oxides (ox) are dispersed within the dolomite-rich inequigranular aggregate and are spatially associated with the coarser-grained dolomite crystals (do). Plane-polarized transmitted light.*

Sample 42: JFM042-5

Albite-illite alteration-zone

Very fine-grained interlobate albite-quartz domains and very fine-grained illite-albite-rutile-quartz(?) domains define a subparallel, rhythmic compositional layering. A thin (0.05 mm) quartz veinlet crosscut, at low angle (~10°), both the compositional layering and the foliation defined by the iso-orientation of the phyllosilicates. Iron oxides overprinted the layered sample as sub-rounded spots up to 0.06 mm across.

Mineral	*Modal %*	*Main Size Range (mm)*
plagioclase (albite)	50 – 53	up to 0.05
illite	35 – 37	up to 0.02
quartz(?)	10 – 15	up to 0.04
iron oxides	0.5 – 1	cryptocrystalline
rutile	tr	up to 0.02

Plagioclase (albite) forms very fine-grained interlobate to granoblastic aggregates in association with **quartz**. The plagioclase was distinguished by the albite twinning seen in some of the crystals, and the quartz was distinguished by its refractive indexes, which were higher than those of the plagioclase. The very fine grain size of the aggregate makes it hard to estimate the relative proportions of the two minerals. I tentatively interpret the albite as the prevailing phase, as most of the crystals show the same relief. The very fine-grained quartzofeldspathic aggregates host very fine-grained dispersions of clay, iron oxides, and rutile.

Illite[1] forms very fine-grained flakes that are oriented parallel to the layering and define a continuous foliation within the clay/white mica-bearing layers. In most cases, the interference colours of the flakes reach second-order yellow; only in rare cases do they reach blue. The very fine-grained flakes are less abundant and interstitial within the albite-quartz-rich aggregate. The compositional layering is probably inherited from the sedimentary protolith, but the iso-orientation of the phyllosilicate was generated by a pure shear or simple shear dynamic event.

Iron oxides completely replaced sub-rounded crystals (up to 0.06 mm) that are evenly distributed within the illite-bearing and the albite-quartz-rich layers.

1 As determined by SWIR spectroscopy.

Very fine-grained **rutile** is preferentially distributed within the phyllosilicate-rich layers.

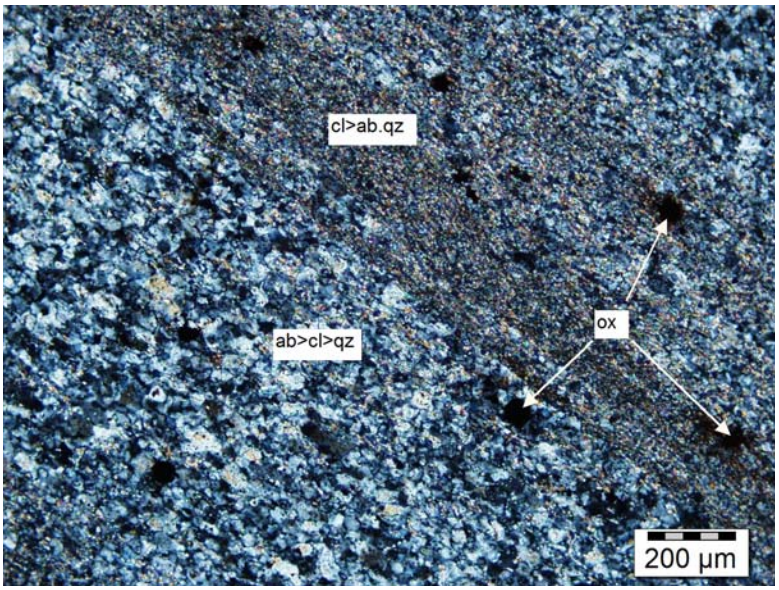

***Photomicrograph 42**: Very fine-grained albite-rich layers (ab>cl>qz) alternate with illite-rich (cl>ab>qz) layers. The iron oxides overprinted the sub-planar compositional layering (ox). Crossed Nicols transmitted light.*

Sample 43: JFM043-2

Dolomite-albite granofels

Quartz vein

This polished thin section shows the contact between a very coarse-grained quartz vein (~18 mm thick) and a coarse-grained dolomite selvage. The grain size of the interlobate dolomitic selvage decreases toward the lower part of the polished thin section, in which fine- to medium-grained dolomite is intergrown with subordinate and sub-prismatic albite.

Mineral	*Modal %*	*Main Size Range (mm)*
dolomite-albite granofels (~55% of PTS)		
dolomite	45 – 50	up to 0.3
plagioclase (albite)	5 – 7	up to 1 mm long
quartz	1	up to 0.3 within the selvage
rutile	tr	up to 0.1
pyrite	tr	up to 0.01
iron oxides	tr	cryptocrystalline
quartz vein (45% of PTS)		
quartz	45	15 × 21

Dolomite forms coarse-grained interlobate crystals (up to 6 mm) within the irregular (1–17 mm thick) vein selvage. The dolomite abruptly decreases its grain size and forms a medium-grained (~0.3 mm) interlobate aggregate, which hosts subordinate plagioclase and rare rutile and shows a moderate to strong undulose extinction. The dolomite is distinguished under the microscope by the typical twinning lamellae parallel to the short diagonal of the cleavage rhombs observed in some of the coarse-grained crystals, which show moderate to strong undulose extinction. The coarse-grained and medium-grained domains react slowly to cold dilute (10%) HCl.

Quartz filled in a monomineralic vein in which a crystal exceeding 18 × 20 mm shows strong undulose extinction and the incipient development of conjugated sets of sub-grain boundaries. The strong undulose extinction observed within the vein and the selvage shows that the quartz infill and the dolomite re-crystallization within the selvages and the host rock occurred during a deformation event. Fine-grained interstitial quartz permeated the fractures

of the coarse-grained selvage.

Plagioclase (albite) occurs as sub-prismatic crystals (up to 1 mm long) that are finely intergrown with the dolomite. The medium-grained aggregate of blocky crystals of plagioclase seen in the lower right part of the polished thin section hosts subordinate interstitial dolomite. The plagioclase shows albite twinning. The albitic composition of the plagioclase is suggested by the low angles (less than 15°) between the adjacent twinning lamellae. Very rare albite occurs within a quartz-dolomite irregular infill that reactivated the contact between the quartz vein and the dolomite-rich selvage.

Very rare, very fine-grained (~0.01 mm) **pyrite** is dispersed within the medium-grained dolomite-albite domain and is partially replaced by **iron oxides**.

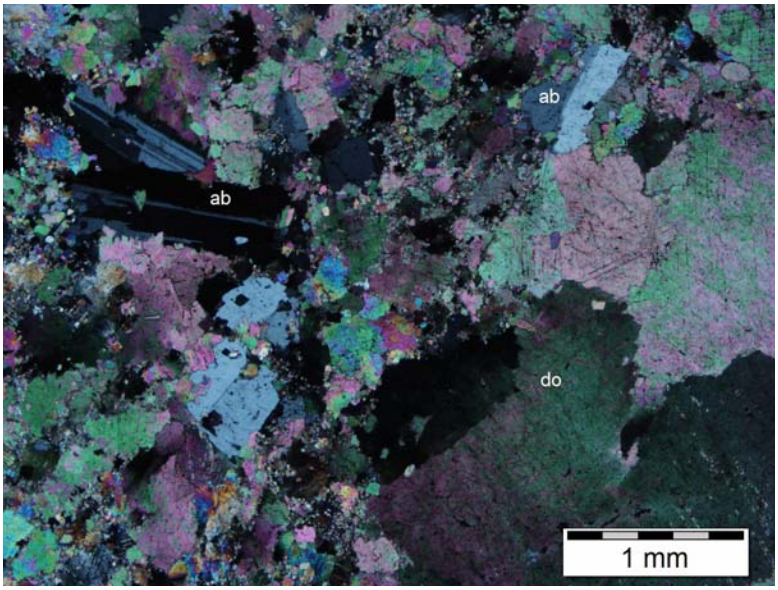

Photomicrograph 43*: Sub-prismatic albite (ab) is randomly oriented within a medium-grained interlobate aggregate of dolomite (in the middle and upper left part of the photomicrograph). Dolomite is coarser in the monomineralic selvage (do in the lower right). Crossed Nicols transmitted light.*

Sample 44: JFM044-1

Brecciated clay-rutile alteration-zone

Dolomite-chalcopyrite-pyrite-quartz infill

Sub-angular fragments of a very fine-grained aggregate of clay, rutile, and quartz are filled in by dolomite, chalcopyrite, pyrite, and quartz. Some of the fragments show a fine-grained clustering defined by very fine-grained dispersions of rutile and probable clay.

Mineral	*Modal %*	*Main Size Range (mm)*
clay-rutile alteration-zone (75% of PTS)		
clay	65 – 70	up to 0.02
rutile	7 – 9	up to 0.01
dolomite	tr	up to 0.1
quartz	tr	up to 0.02
dolomite-chalcopyrite-pyrite-quartz infill (~25% of PTS)		
dolomite	8 – 10	up to 0.6
plagioclase (albite)	7 – 9	up to 0.7
chalcopyrite	5 – 6	up to 1
pyrite	1	up to 0.4
quartz	1	up to 0.2

Clay dominates the composition of the sub-angular fragments as very fine-grained and interlobate crystal aggregates. The very fine-grained clay hosts very fine-grained clustered crystals of **rutile** that impart an irregular compositional layering to some of the fragments (see Photomicrograph 44a). Fine- to medium-grained xenoblastic crystals of plagioclase are associated and intergrown with dolomite, chalcopyrite, and pyrite within the infill that occupies the interstices of the fragments; therefore, the infill post-dated an albite-bearing alteration event.

Dolomite forms medium-grained xenoblastic crystals that are concentrated within the infill domains and overprinted the albite-rich fragments as fine-grained idioblastic crystals. The dolomite is distinguished by its slow reaction to cold dilute (10%) HCl, and some of the crystals show the typical twinning parallel to the short diagonal of the cleavage rhombs.

Fine- to medium-grained xenoblastic crystals of **plagioclase (albite)** are associated and intergrown with dolomite, chalcopyrite, and pyrite within the infill that occupies the interstices of the fragments; therefore, the infill post-dated an albite-bearing alteration event. The albitic composition of the plagioclase is indicated by its refractive indexes, which are lower than those of quartz.

Chalcopyrite occurs as medium-grained amoeboid to interstitial crystals. It is concentrated within the infill domains, where it is intergrown with dolomite, plagioclase, pyrite, and subordinate **quartz**.

Fine- to medium-grained (up to 0.4 mm) xenoblastic **pyrite** is concentrated within the infill domains and is partially replaced by the chalcopyrite (see Photomicrograph 44b). In many instances, the pyrite is rimmed and partially replaced by a cryptocrystalline aggregate of **iron oxides**.

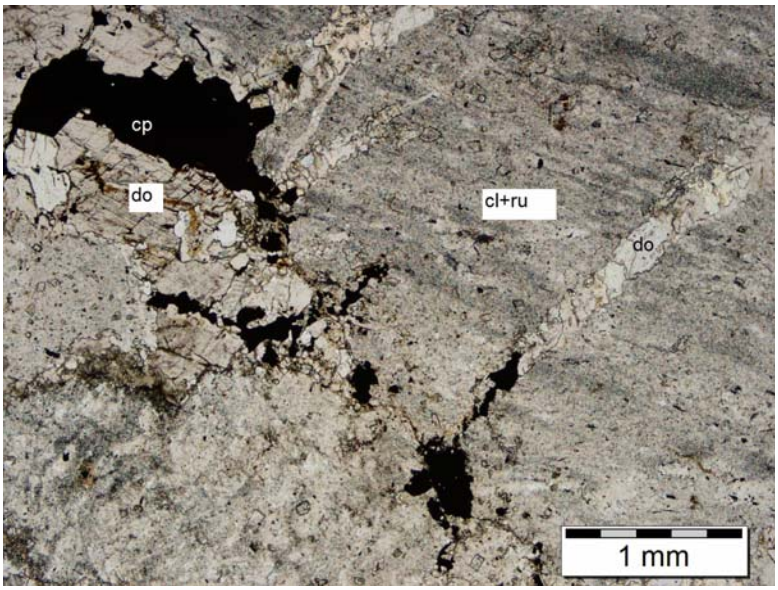

***Photomicrograph 44a**: Very fine-grained clay is intergrown with very fine-grained clusters of rutile (ab+ru) within the fragments that are filled in by dolomite (do) and chalcopyrite (cp). Plane-polarized transmitted light.*

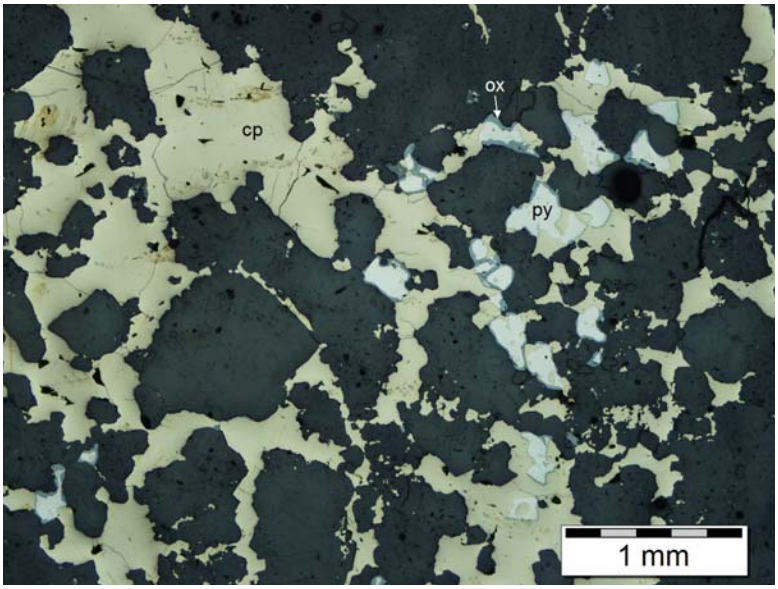

***Photomicrograph 44b**: Within the infill domains, the chalcopyrite (cp) prevails over and partially replaced the pyrite (py), which is also partially replaced and rimmed by iron oxides (ox). Plane-polarized reflected light.*

Sample 45: JFM049

Quartz-rutile-calcite alteration-zone

Medium-grained sub-rounded crystals of quartz are immersed within a fine-grained aggregate of albite, calcite, quartz, and very fine-grained dispersions of rutile. Rare pyrite overprinted this sample as coarse-grained euhedral crystals (up to 5 mm), and it forms coarse-grained pseudomorphs in association with calcite and quartz.

Mineral	*Modal %*	*Main Size Range (mm)*
quartz	45 – 47	up to 1
calcite	23 – 10	up to 0.2; up to 1 within the pseudomorphs
plagioclase (albite)	15 – 16	up to 0.25
rutile	10 – 12	up to 0.01
pyrite	3.5 – 4	up to 5
pyrrhotite	tr	up to 0.1
chalcopyrite	tr	up to 0.02

Quartz occurs as inequigranular (up to 1 mm) sub-rounded crystals immersed within a fine-grained and heterogeneous matrix of albite, rutile, calcite, and quartz. Most of the quartz crystals are free of inclusions; only in some cases do they host rare euhedral inclusions of pyrite and pyrrhotite. The edges of the crystals are finely interlobate within the fine-grained minerals of the matrix. Subordinate fine-grained quartz is intergrown within the matrix as interlobate crystals; these quartz crystals are also devoid of inclusions. Fine-grained quartz and medium-grained calcite form irregular coronae around anhedral pyrite (see Photomicrograph 45). These microstructures indicate the coexistence of these three minerals during the hydrothermal recrystallization.

Calcite is fine grained and is concentrated within the matrix. The calcite does not host the very fine-grained, heterogeneously distributed rutile; therefore, I interpret the crystallization of calcite as post-dating the rutile-bearing alteration event.

Rutile is very fine grained. It is dispersed within the matrix as irregular clusters that I interpret as the product of a strong alteration event.

Plagioclase (albite?) forms fine-grained xenomorphic crystals within the matrix. The plagioclase is intergrown with very fine-grained rutile and probable quartz, and for this reason, I interpret the plagioclase as having crystallized, probably with very fine- to fine-grained

quartz, during the abundant rutile-bearing alteration. The plagioclase is distinguished by its typical albite twinning and its refractive indexes, which are lower than those of quartz.

Very rare fine-grained **pyrrhotite** forms anhedral crystals within the medium-grained quartz. The pyrrhotite is moderately altered, and in some cases it is partially replaced by very fine-grained, very rare **chalcopyrite**.

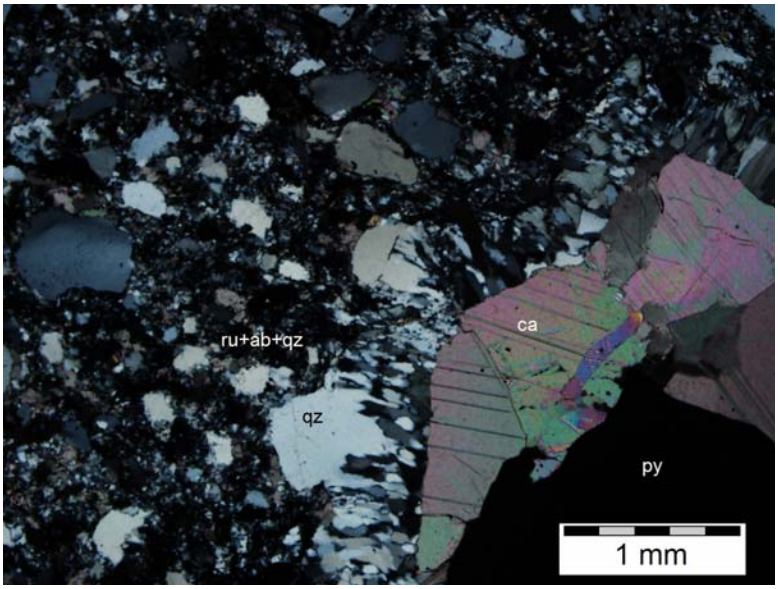

Photomicrograph 45*: Anhedral pyrite (py) is mantled by a corona of calcite (ca) and quartz (qz). The quartz within the corona in some cases is crystallized from the medium-grained quartz that is immersed within the matrix. The matrix is made up of a fine- to very fine-grained aggregate of rutile, albite, and quartz (ru+ab+qz). Crossed Nicols transmitted light.*

Sample 46: SGR-02-440m

Basalt

Alteration: moderate–magnetite-actinolite-titanite-epidote-chlorite

A fine-grained intergranular microstructure is defined by fine-grained magnetite, biotite, and actinolite, all of which occupy the interstitial spaces between subhedral plagioclase. Fine-grained epidote overprinted the interstitial ferromagnesian minerals, and rare medium-grained epidote crystals overprinted the magmatic microstructure. A sub-rounded aggregate (~3 mm) is made up of medium-grained Mg-chlorite, magnetite, and epidote, and I tentatively interpret it as a recrystallized xenolith.

Mineral	*Modal %*	*Main Size Range (mm)*
plagioclase (oligoclase)	55 – 57	up to 0.2; rare up to 0.5 mm long
biotite	17 – 20	up to 0.15
actinolite	12 – 15	up to 0.15
magnetite	4 – 5	0.05–0.1
epidote	3 – 4	up to 0.4
Mg-chlorite	2 – 3	up to 1
titanite	2	up to 0.02
hematite	tr	up to 0.05

Plagioclase forms fine-grained (up to 0.2 mm) elongate subhedral crystals that are randomly oriented and define a magmatic intergranular microstructure. The plagioclase shows albite twinning and is weakly altered by a very fine-grained dispersion of unresolved minerals (epidote and actinolite?). The plagioclase forms rare medium-grained (up to 0.6 mm) euhedral phenocrysts forming glomeroporphyritic aggregates. The measurement of the extinction angle between adjacent albite twinning lamellae [a′:(010) perpendicular to the zone (010) = 15°] indicates a 23% anorthite content (oligoclase) within the medium-grained crystal. The plagioclase phenocrysts host abundant inclusions that are iso-oriented parallel to the albite twinning. Most of the inclusions are oxidized; however, they could be interpreted as epitaxial inclusions of magnetite.

Magnetite is fine grained (0.05–0.1 mm), and the anhedral to subhedral crystals are concentrated within the interstices between the subhedral plagioclase. Only in very few cases

is that magnetite weakly altered and rimmed by **hematite**. The magnetite is slightly more abundant and coarser-grained close to the chlorite-epidote alteration patches, and I tentatively interpret its crystallization as coeval with the chlorite-epidote alteration event.

Biotite is fine grained, and the anhedral crystals are concentrated within the interstices between the plagioclase. The biotite is intergrown with and probably overprinted by fine-grained (up to 0.2 mm) anhedral to sub-prismatic crystals of **actinolite**, which is distinguished by its oblique extinction (c:Z up to 15°), and its pleochroism with green tints. Very fine-grained crystals and crystal clusters of **titanite** preferentially populate the actinolite crystals. The distribution of titanite suggests that the actinolite may have been produced by the alteration of biotite. Fine-grained crystals of biotite are associated with the chlorite-epidote alteration patches. It is not clear whether some of the biotite represents a mineralogic relict of the magmatic phase. The occurrence of fine-grained biotite intergrown with chlorite and epidote indicates that at least some of the biotite crystallized during the moderate alteration phase and replaced most of the interstitial ferromagnesian minerals. It was then overprinted by actinolite, titanite, and chlorite in the waning stages of the alteration.

Rare medium-grained **Mg-chlorite** partially replaced sub-rounded domains that I tentatively interpret as xenoliths. Lamellae up to 1 mm long are intergrown with epidote, magnetite, and subordinate biotite within irregular and heterogeneously distributed alteration patches. Fine-grained **chlorite** partially replaced the biotite. The negative extinction angle indicates the chlorite is magnesium rich.

Rare **epidote** is heterogeneously distributed within the magmatic microstructure as fine- to medium-grained anhedral to skeletal crystals associated with rare medium-grained Mg-chlorite.

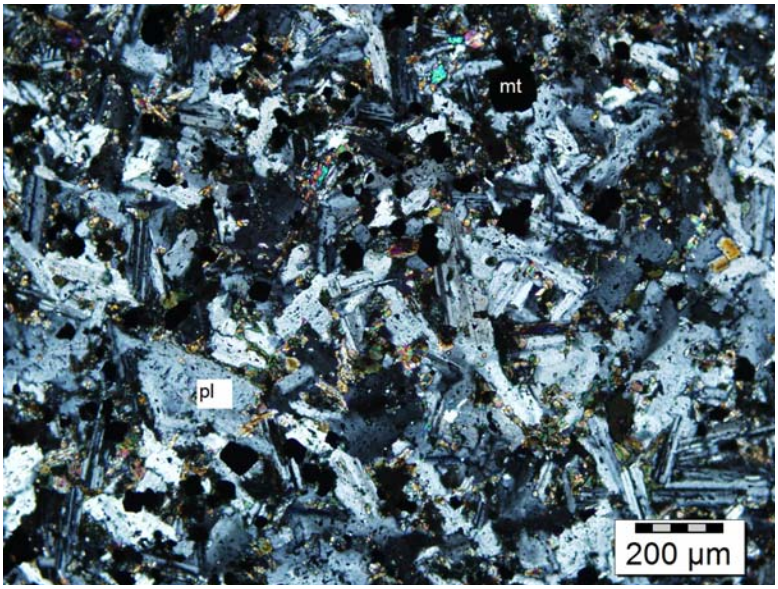

***Photomicrograph 46a**: Fine-grained subhedral plagioclase (pl) forms an intergranular microstructure in which the interstices between the sub-prismatic crystals of plagioclase are occupied by magnetite (mt), biotite, and actinolite. Crossed Nicols transmitted light.*

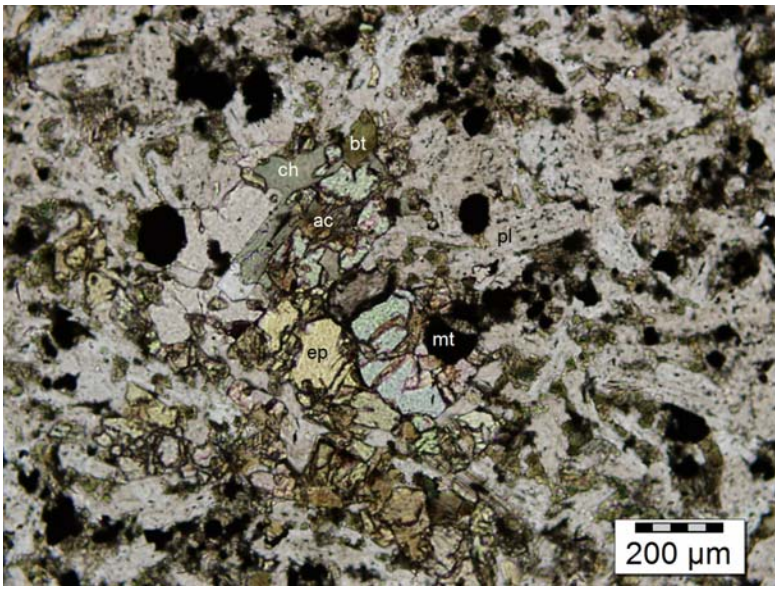

***Photomicrograph 46b**: Irregular and heterogeneously distributed alteration patches are made up of epidote (ep), chlorite (ch), magnetite (mt), and subordinate biotite (bt). Plane-polarized transmitted light.*

Sample 47: SUS-07-15-275'

Brecciated(?) dolomite granofels

Quartz-dolomite infill(?)

Dolomite-sphalerite-pyrite infill

This polished thin section is made up of two compositionally different domains. The first domain (A) is a fine-grained granoblastic aggregate of dolomite/ankerite with rare, randomly oriented lamellae of white mica. Domain B occurs in the lower left part of the polished thin section and is made up of fine- to medium-grained xenoblastic to interlobate quartz immersed within a fine-grained interlobate aggregate of dolomite. The contact between the two domains is crosscut by irregular and sub-parallel infill domains. The infill domains are made up of dolomite-sphalerite and subordinate pyrite and quartz; however, the sphalerite and the pyrite crystallized only in the infill segment contained within the dolomite-rich domain (Domain A).

Mineral	*Modal %*	*Main Size Range (mm)*
Domain A: dolomite granofels (68% of PTS)		
dolomite/ankerite	68	up to 0.1
white mica	tr	up to 0.1 × 0.04
Domain B: quartz-dolomite (infill?) (~20% of PTS)		
quartz	10	up to 0.25
dolomite/ankerite	10	up to 0.2
white mica	tr	up to 0.05
dolomite-sphalerite-pyrite infill (~12% of PTS)		
dolomite	8	up to 3
sphalerite	4	up to 6 × 2
pyrite	tr	up to 0.3
quartz	tr	up to 0.3
chalcopyrite	tr	up to 0.02

Dolomite/ankerite occurs as fine-grained (up to 0.1 mm) granoblastic aggregates within Domain A. This domain hosts rare fine-grained lamellae of white mica and shows an irregular contact with Domain B, in which the fine-grained (up to 0.25 mm) carbonate forms an interlobate grain aggregate that is intergrown with medium-grained crystals of quartz. Finally, the dolomite is the most abundant mineral within the irregular sub-parallel infill domains. In one case, the infill domain is pinched and offset at the contact between the fine-grained dolomite-rich domain and the quartz-dolomite domain (Domain B). Within the infill, the dolomite is inequigranular (up to 3 mm) and is intergrown with sphalerite, pyrite, and lesser fine-grained quartz. Dolomite was distinguished by its slow reaction to cold dilute (10%) HCl. The possibility that the carbonate domains also include ankerite should be investigated by electron optic analysis.

Quartz is medium grained and is abundant only within Domain B, where it forms slightly elongate and interlobate crystals. The moderate undulose extinction of quartz may indicate that the quartz crystallized during a brittle-ductile deformation event, probably related to a brecciation event. In this case, Domain B represents the result of an earlier infill emplacement related to the fragmentation of Domain A. Only mesoscopic and field relationships could offer more evidence about whether Domain A is a fragmented domain and Domain B is its associated infill material.

Sphalerite is intergrown with the dolomite within the infill domain as amoeboid crystals up to 6 × 2 mm. Fine-grained sphalerite occupies interstitial positions within the dolomite in the infill domain.

Medium-grained subhedral **pyrite** crystallized around the coarse-grained sphalerite in the infill domain. In some cases, the pyrite is intergrown with and enclosed within the sphalerite (see Photomicrograph 47b).

Very rare, very fine-grained chalcopyrite occurs as inclusions/exsolutions within the sphalerite only.

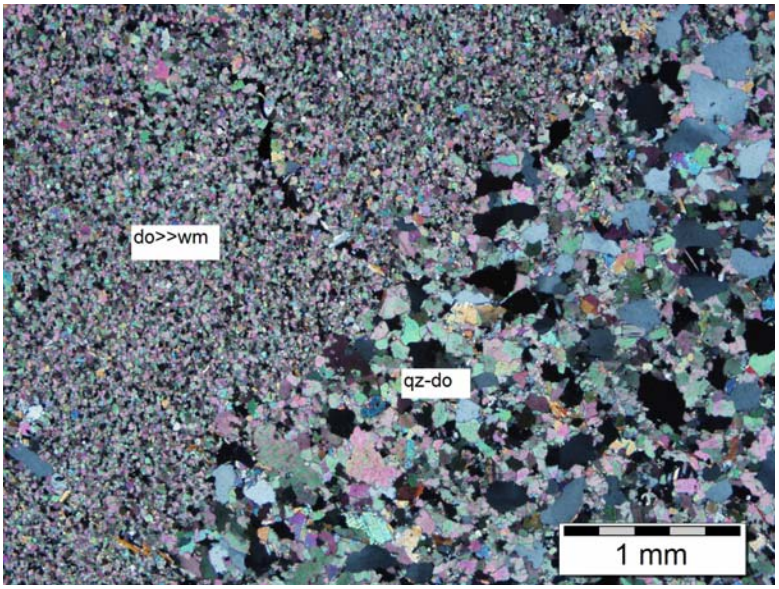

***Photomicrograph 47a**: Domain A (in the upper left of the photomicrograph) is made up of fine-grained dolomite and rare white mica (do+wm) and shows an irregular contact with a coarser-grained domain (B) with quartz and dolomite (qz+do). Crossed Nicols transmitted light.*

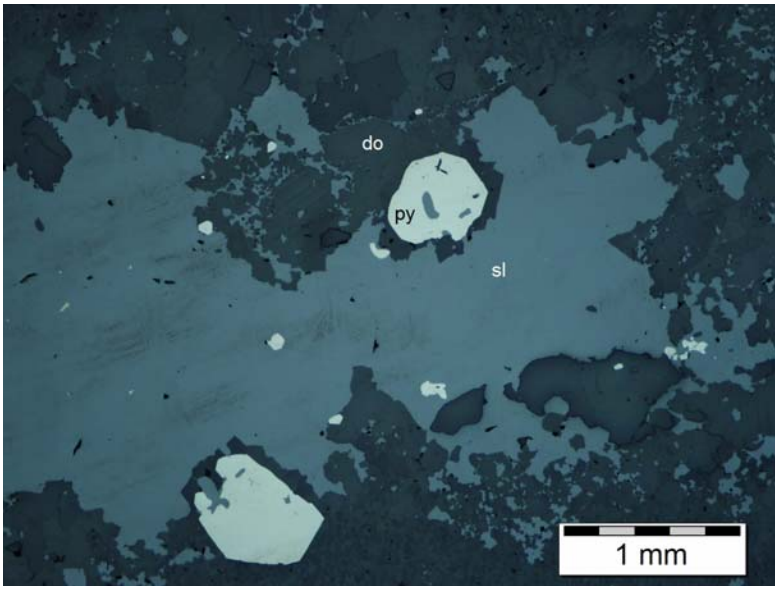

***Photomicrograph 47b**: Sphalerite (sl) dominates some segments of the irregular infill domains and is intergrown with dolomite (do) and subordinate pyrite (py). Plane-polarized reflected light.*

Sample 48: SUS-07-44-234'

Layered dolomite-white mica-albite schist

Dolomite/ankerite dominates the composition of this polished thin section and forms inequigranular and granoblastic aggregates. A sub-planar and probably folded compositional layering is defined by fine-grained (~0.05 mm) layers of dolomite and iso-oriented white mica alternating with slightly coarser (0.2–0.3 mm) layers of dolomite, albite, and white mica. Fine-grained clusters of hematite are preferentially dispersed within the coarser dolomite-rich layers.

Mineral	*Modal %*	*Main Size Range (mm)*
dolomite/ankerite	90 – 92	0.05–0.3
plagioclase (albite)	4 – 5	up to 0.1; rare up to 0.2
white mica	3 – 4	up to 0.1 long
hematite	1	up to 0.1 long
quartz	tr	up to 0.2

Dolomite/anhydrite defines a subparallel layering by varying its grain size from an average of 0.05 mm to 0.2–0.3 mm. A weak compositional layering is associated with the grain size variation of dolomite. Within some of the finer-grained granoblastic aggregate, the dolomite is associated with subordinate iso-oriented lamellae of white mica. Within the coarser (0.2–0.3 mm) inequigranular granoblastic aggregate, the dolomite is intergrown with subordinate blocky crystals and crystal aggregates of albite.

White mica is fine grained (up to 0.1 mm long, with an aspect ratio of 10:1 or higher) and iso-oriented parallel to the layering. Within some of the layers, it defines a continuous foliation (as defined in Passchier and Trouw 1998).

Plagioclase (albite) occurs as fine-grained xenoblastic to blocky crystals and crystal aggregates. The plagioclase is distinguished by its typical albite twinning, and the low angles between adjacent twinning lamellae suggest that the composition of the plagioclase is albitic.

Hematite is fine grained and forms sub-tabular crystals that are concentrated within sub-planar crystal clusters that preferentially occur within the coarser-grained dolomitic layers. The hematite is distinguished by its lamellar shape, moderate reflectance, weak bireflectance, and grey colour. Similarly to the white mica, the hematite is iso-oriented parallel to the layering, and some of its crystals show an aspect ratio of 10:1.

Rare **quartz** forms fine-grained crystals associated with albite within slightly elongated granoblastic domains that I interpret as dismembered infill domains.

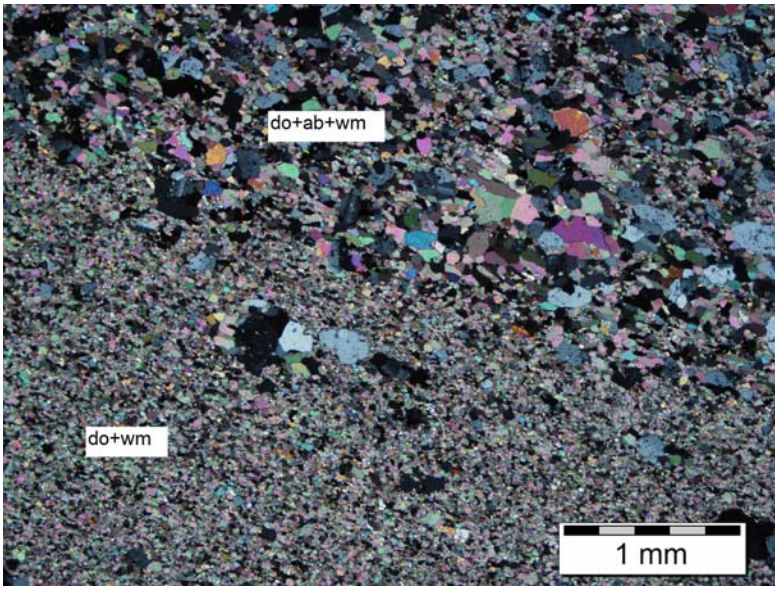

***Photomicrograph 48a**: A fine-grained layer of dolomite and white mica (do+wm) is in contact with a slightly coarser and inequigranular layer of dolomite, albite, and white mica (do+ab+wm, in the upper part). Crossed Nicols transmitted light.*

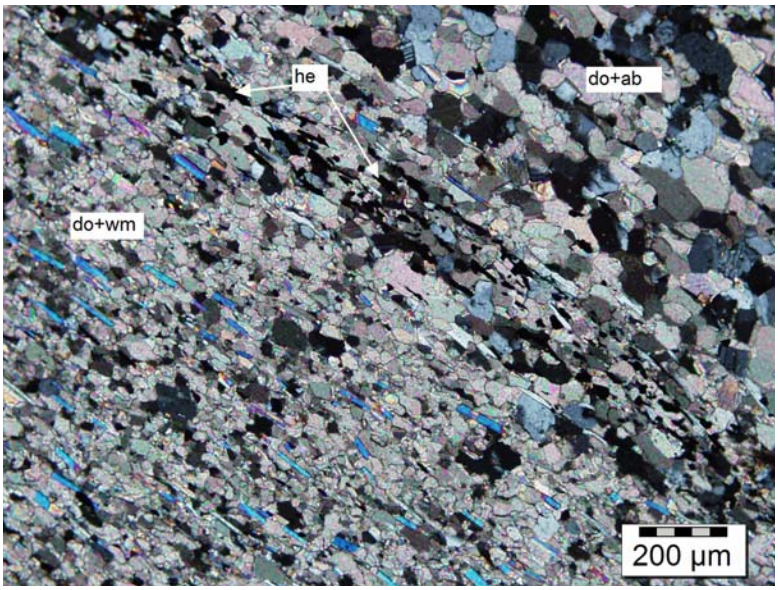

***Photomicrograph 48b**: Iso-oriented white mica defines a continuous foliation within the fine-grained granoblastic aggregate of dolomite (do+wm in the lower left of the photomicrograph). Hematite is iso-oriented parallel to the layering and the foliation and forms thin crystal clusters (he) within the granoblastic aggregate of dolomite and albite (do+ab). Crossed Nicols transmitted light.*

Sample 49: WP-253

Dolomite-chlorite-tremolite alteration-zone

Idioblastic crystals of chlorite (dark blade-like crystals on the offcut) and tremolite (colourless on the offcut) are randomly oriented within a fine-grained granoblastic aggregate of dolomite.

Mineral	*Modal %*	*Main Size Range (mm)*
dolomite	87 – 90	up to 0.2
Mg-chlorite	6 – 7	up to 1.5 × 0.5
tremolite	5 – 6	up to 3.5 × 0.1

Dolomite dominates the composition of this sample as an inequigranular (up to 0.2 mm) granoblastic to interlobate aggregate, which hosts randomly oriented crystals of chlorite and tremolite. The dolomite forms vein-like domains in which it occurs as slightly coarser (~0.2 mm) aggregate. It is distinguished by its slow reaction to cold dilute (10%) HCl.

Mg-chlorite forms medium-grained tabular crystals (up to 1.5 × 0.5 mm, with aspect ratio up to 10:1) that are randomly oriented within the dolomitic aggregate. The magnesium-rich composition is indicated by its negative elongation and very pale green colour in plane-polarized transmitted light. The chlorite is slightly deformed and shows kink bands and weak undulose extinction. The chlorite is heterogeneously distributed within the dolomitic aggregate and is intergrown with idioblastic tremolite. The chlorite probably pre-dated the blastesis of tremolite, as the latter shows idioblastic shapes at the contact with the chlorite.

Tremolite occurs as randomly oriented medium-grained (up to 3.5 × 0.1 mm, with aspect ratio up to 35:1) idioblastic prisms with a columnar to acicular shape. In the middle to upper part of the polished thin section, the tremolite shows a preferred dimensional orientation. The tremolite is distinguished by its oblique extinction (c:Z up to 20°) and very weak to absent pleochroism.

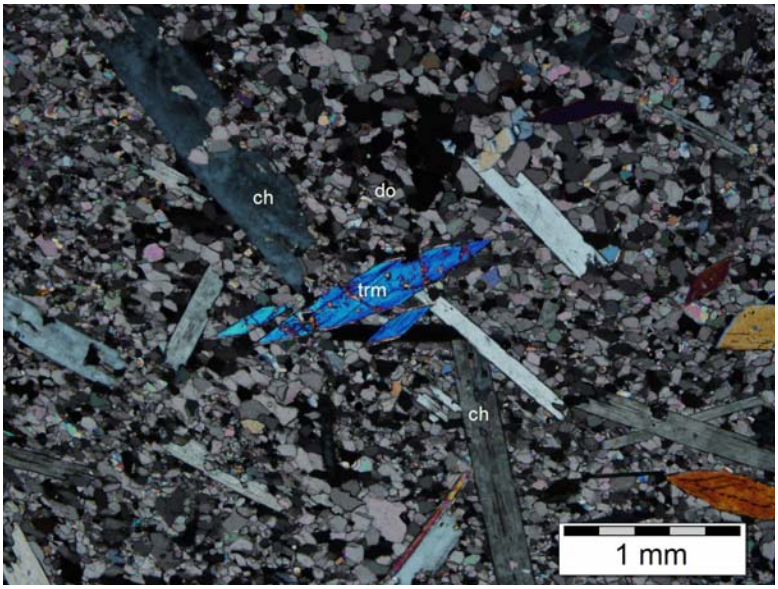

***Photomicrograph 49**: Randomly oriented chlorite (ch) and tremolite (trm) are immersed within a fine-grained granoblastic aggregate of dolomite (do). Crossed Nicols transmitted light.*

Sample 50: WP282

Actinolite-clinozoisite alteration-zone

Xenomorphic crystals of actinolite and clinozoisite/epidote overprinted a probable magmatic microstructure of which only rare prisms of moderately to strongly altered plagioclase are preserved after the strong alteration.

Mineral	*Modal %*	*Main Size Range (mm)*
actinolite	55 – 57	up to 0.5
clinozoisite	35 – 37	up to 0.5
titanite/rutile?	3 – 3.5	up to 0.1
plagioclase	2 – 4	up to 0.1; rare relict prism up to 0.5 m long
chlorite	1	up to 0.1
pyrite	tr	up to 0.03

Actinolite forms medium-grained (up to 0.5 mm) xenomorphic to skeletal crystals that are randomly oriented and overprinted the relict magmatic microstructure. The actinolite is distinguished by its moderate relief, high birefringence, oblique extinction (c:Z up to 15°), and weak pleochroism with green to bluish-green tints. In some cases, the actinolite shows undulose extinction that was probably generated during the intense alteration event.

Clinozoisite occurs as medium-grained (up to 0.5 mm) equant xenomorphic crystals that are intergrown with the actinolite and subordinate titanite, chlorite, and plagioclase. The clinozoisite was distinguished by its high relief and anomalous blue interference colours.

An unresolved mineral forms xenomorphic to subidiomorphic crystals (up to 0.1 mm) with high relief, a deep brown colour under plane-polarized transmitted light, high birefringence, and low to moderate reflectance. I tentatively interpret this mineral as altered rutile (leucoxene?) or altered carbonate (ankerite?).

Plagioclase forms fine-grained xenomorphic interstitial crystals that are intergrown with the actinolite, clinozoisite, and chlorite. In rare cases, the plagioclase forms relict prisms that are partially replaced by the actinolite and the clinozoisite. These prismatic crystals represent the only mineralogic and microstructural relicts of the magmatic protolith. Despite the presence of rare albite twinning, it was not possible to optically determine the composition of the plagioclase. It is only assumed that the plagioclase is albitic.

Mg-chlorite occurs as fine-grained interstitial replacement patches that are finely intergrown with the actinolite, clinozoisite, and fine-grained plagioclase. The chlorite shows negative

extinction, and therefore is magnesium rich.

Very rare, very fine-grained **pyrite** is preferentially associated with the clinozoisite replacement patches.

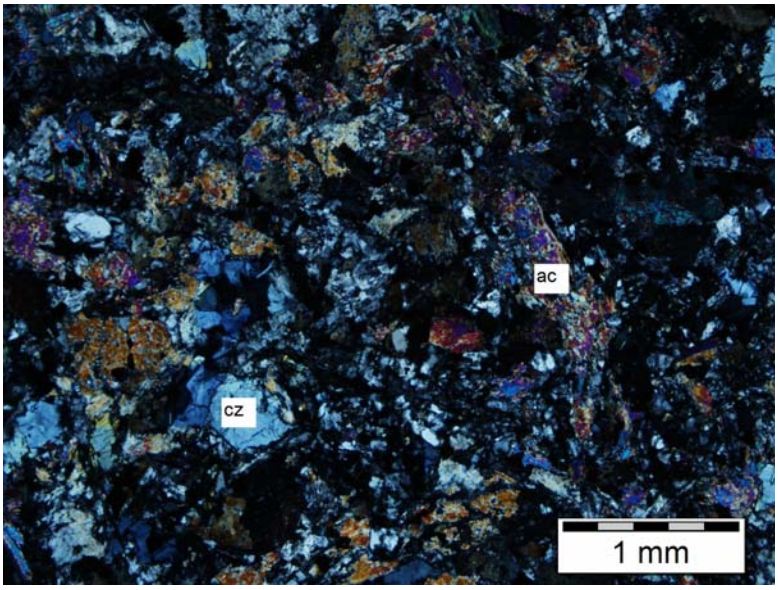

***Photomicrograph 50**: Xenomorphic actinolite (ac) and clinozoisite (cz) strongly overprinted this sample. Crossed Nicols transmitted light.*

Sample 51: WP284

Basalt(?)

Alteration: strong–actinolite-epidote-titanite(?)-calcite

Elongate prisms of actinolite are randomly oriented. In association with fine-grained epidote, titanite(?) and chlorite, the actinolite overprinted a fine-grained magmatic microstructure, of which rare and fine-grained prismatic plagioclase (up to 0.2 mm) represents the mineralogic relict.

Mineral	*Modal %*	*Main Size Range (mm)*
actinolite-epidote replacement-zone (98% of PTS)		
actinolite	68 – 70	up to 0.5 mm long
epidote	24 – 27	up to 0.1
titanite(?)	3 – 4	up to 0.1
plagioclase	1	up to 0.2
epidote-calcite-pyrrhotite-chalcopyrite vein (2% of PTS)		
epidote	1.5	up to 0.3
calcite	0.5	up to 0.1
pyrrhotite	tr	up to 0.15
iron oxides	tr	cryptocrystalline
chalcopyrite	tr	up to 0.03

Actinolite overprinted this sample as elongated prisms (up to 0.5 mm) that are randomly oriented within the fine-grained aggregate of xenomorphic actinolite, epidote, and mineral X. The actinolite was distinguished by its weak pleochroism with green tints and its oblique extinction (c:Z up to 15°).

Fine-grained xenomorphic **epidote** is intergrown with the actinolite. It is concentrated within irregular and intersecting veinlets (up to 0.16 mm thick), where it forms medium-grained (up to 0.5 mm) crystals intergrown with calcite, pyrrhotite, chalcopyrite, and rare clinozoisite. The epidote is distinguished by its high relief and very high birefringence.

Titanite(?) is characterized by high relief and a brown colour under plane-polarized

transmitted light. I tentatively interpret it as titanite or leucoxene. Electron optic analysis is required in order to determine its nature.

Plagioclase forms rare fine-grained prisms that are partially preserved in some rare areas of the polished thin section. I interpreted these crystals as the only mineralogic relict of a probable basaltic protolith.

Calcite forms fine-grained crystals that are intergrown with the epidote within the veinlets. It was distinguished by its brisk reaction to cold dilute (10%) HCl.

Fine-grained clusters of moderately altered **pyrrhotite** precipitated within one of the veinlets and are finely intergrown with the epidote and subordinate calcite.

Very rare **chalcopyrite** (up to 0.03 mm) is intergrown with and partially replaced the pyrrhotite within the veinlet.

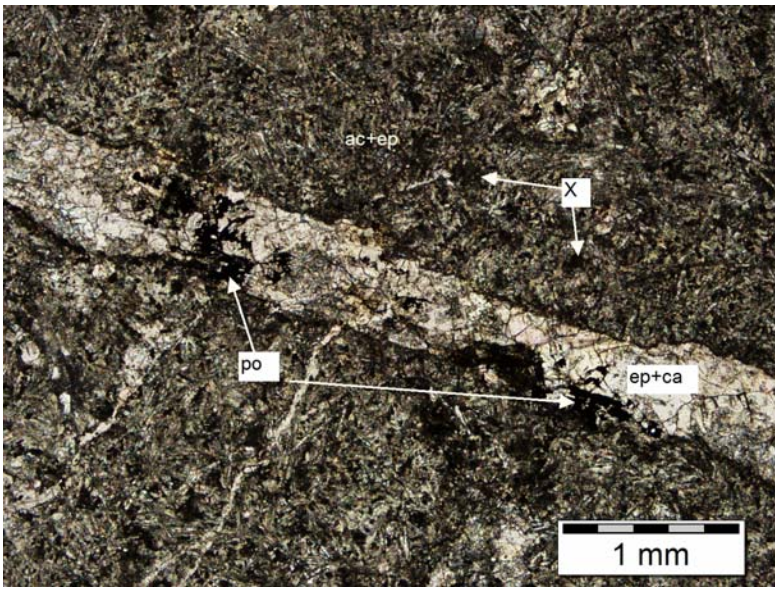

Photomicrograph 51*: An epidote and calcite veinlet (ep+ca) hosts rare pyrrhotite (po) and crosscut a strongly altered host rock made up of actinolite and epidote (ep+ep) and probable titanite (X). Plane-polarized transmitted light.*

Sample 52: 1272227

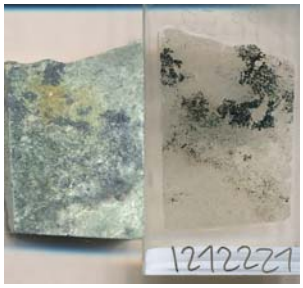

Tremolite-calcite-chalcocite alteration-zone

This compositionally heterogeneous sample is made up of a relatively homogeneous domain of randomly oriented elongate prisms of tremolite; subordinate chlorite and epidote; and coarser-grained domains calcite, tremolite, and chalcocite.

Mineral	*Modal %*	*Main Size Range (mm)*
tremolite	80 – 84	up to 2.5 mm long
calcite	8 – 10	up to 1
chalcocite	7 – 9	up to 1
epidote	1	up to 0.1
chlorite	tr	up to 0.1
iron oxides	tr	cryptocrystalline

Tremolite forms elongate prisms and aciculae (up to 1.2 mm long, with aspect ratio of 10:1) that are randomly oriented and dominate the composition of the lighter part of the offcut (see image in the upper right of this page). Within these irregular domains, the tremolite is intergrown with subordinate fine-grained crystals of epidote, and interstitial chlorite. The tremolite was distinguished by its moderate relief, absence of pleochroism, and extinction angles up to 23°. Coarser-grained (up to 2.5 mm long) crystals of tremolite are randomly oriented and intergrown with chalcocite and calcite.

Calcite forms medium- to coarse-grained crystals and crystal aggregates that are concentrated within and close to the chalcocite-rich domains. Calcite is fine grained and dispersed within irregularly distributed replacement patches within the tremolite-rich replacement zone. The calcite was distinguished by its brisk reaction to cold dilute (10%) HCl.

Chalcocite is concentrated within irregular alteration “fronts” up to 5 mm thick that overprinted the tremolite-rich aggregate. The chalcocite forms amoeboid and poikilitic crystals that are intergrown with and include the prismatic tremolite and the calcite. Finer-grained (up to 0.3 mm) equant chalcocite crystals form an irregular clustering that I interpret as a more far-reaching alteration front up to 10 mm away from the chalcocite-rich front.

Epidote is fine grained and heterogeneously distributed within the tremolite-rich replacement-zone.

Mg-chlorite forms fine-grained interstitial crystals that are intergrown with the tremolite within the tremolite-rich domain. The magnesium-rich composition is indicated by the negative

elongation of the xenomorphic and in some cases radial crystals.

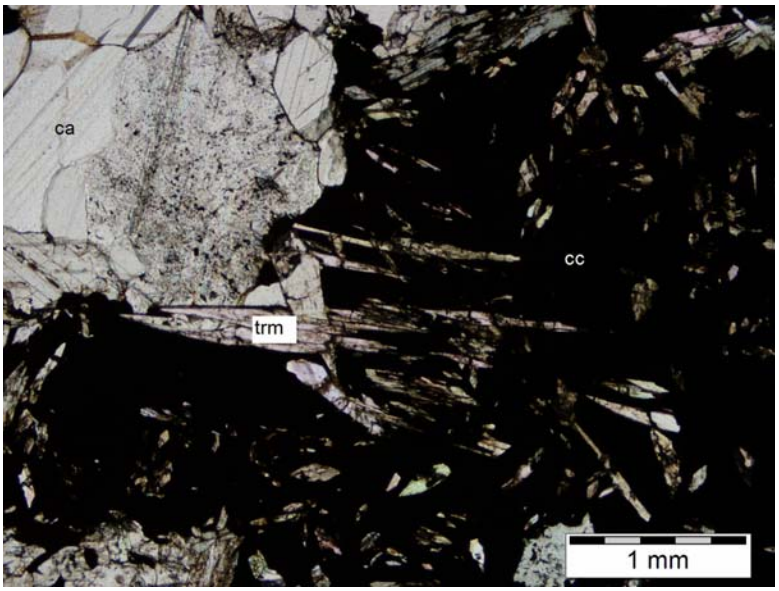

***Photomicrograph 52**: Poikilitic chalcocite (cc) is intergrown with and includes idiomorphic crystals of tremolite (trm) and xenomorphic calcite (ca). Plane-polarized transmitted light.*

Sample 53: WP-292

Basalt(?)

Alteration: strong–actinolite-clinozoisite-chlorite-titanite(?)-albite

A medium-grained intergranular microstructure is strongly altered by a fine-grained replacement aggregate of actinolite, chlorite, and titanite(?), all of which replaced the ferromagnesian minerals, and by elongate prisms of clinozoisite after plagioclase.

Mineral	*Modal %*	*Main Size Range (mm)*
actinolite	50 – 52	up to 0.3
clinozoisite/epidote	35 – 37	up to 0.15; up to 0.7 mm long
chlorite	7 – 9	up to 0.1
titanite or rutile(?)	3 – 4	up to 0.04
plagioclase (albite)	2 – 3	up to 0.2 mm long
pyrrhotite	tr	up to 0.04
pyrite	tr	up to 0.02
chalcopyrite	tr	up to 0.02

Actinolite occurs as fine-grained xenomorphic to skeletal crystals that are randomly oriented within a fine-grained matrix made up of chlorite, clinozoisite, fine-grained titanite (or rutile?), and interstitial albite. The actinolite is characterized by a distinct pleochroism with green tints, and extension angles (c:Z) of up to 15°. Most of the pseudomorphic crystals show a moderate to strong undulose extinction.

Mg-chlorite forms sub-rounded to subhedral pseudomorphs of up to 1 mm, in which it is associated with subordinate iron oxides and very rare, very fine-grained **pyrite** and **chalcopyrite**. One pseudomorph shows a subhedral shape that I tentatively interpret as a replacement after olivine. The chlorite also forms a fine- to very fine-grained aggregate that occupies the interstices between the actinolite and the clinozoisite.

Elongate prisms (up to 0.7 mm long, with an aspect ratio of up to 10:1) are made up of a fine-grained pseudomorphic aggregate of **clinozoisite/epidote**, chlorite, and **albite**. These pseudomorphs replaced and probably overgrew the plagioclase that in some rare cases is preserved as shorter prisms (up to 0.2 mm long) within this strongly altered sample. The skeletal relicts of plagioclase are distinguished by the presence of their typical albite twinning.

Fine-grained crystals with an earthy appearance and high relief are interpreted as altered titanite (or rutile?).

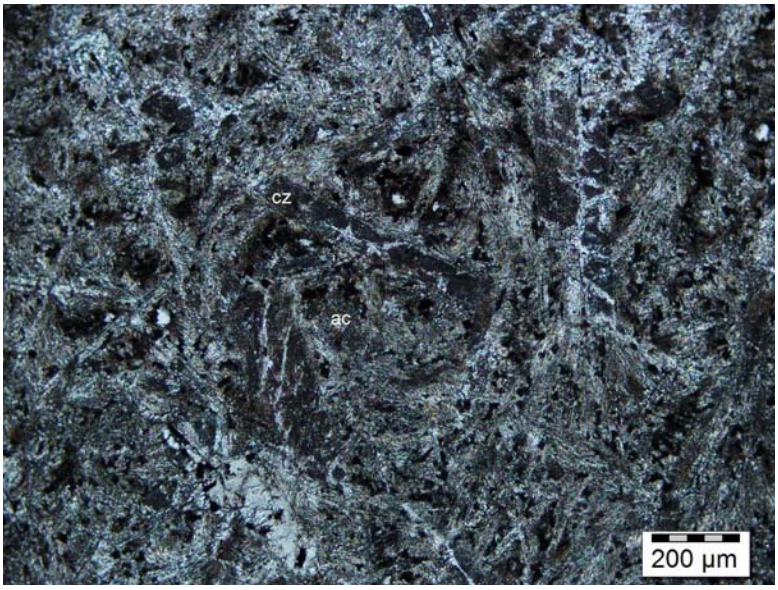

Photomicrograph 53*: Elongate prisms are mostly made up of clinozoisite (cz) replacing euhedral plagioclase. Xenomorphic actinolite (ac) is associated with fine-grained chlorite and fine-grained titanite(?) and replaced the interstitial ferromagnesian minerals. Plane-polarized transmitted light.*

Sample 54: WP535-CaRB-3

Micro-brecciated plagioclase-phyric microdiorite

Alteration: moderate–biotite-magnetite-titanite-dolomite(?)

Rare phenocrysts (2.5 × 0.5 mm) of plagioclase are immersed within an inequigranular groundmass of subhedral plagioclase. The groundmass is slightly brecciated (crackle breccia) and filled in by fine-grained biotite and fine-grained magnetite.

Mineral	*Modal %*	*Main Size Range (mm)*
plagioclase	72 – 74	up to 0.5; rare phenocrysts up to 2.5 × 0.5
biotite	16 – 18	up to 0.05; rare up to 0.1
magnetite	7 – 8	up to 0.25
titanite	0.2 – 0.5	up to 0.1
carbonate (dolomite?)	tr	up to 0.2
white mica	tr	up to 0.03

Plagioclase forms rare euhedral phenocrysts (2.5 × 0.5 mm), which are immersed within a groundmass of fine- to medium-grained plagioclase (up to 0.5 mm). The plagioclase-rich groundmass probably ended its crystallization with a microbrecciation episode during which the interstices between the plagioclase were filled in by fine-grained biotite (see photomicrograph 54). Some of the plagioclase crystals show undulose extinction and the effect of a ductile deformation that probably pre-dated the brittle event. Most of the plagioclase hosts abundant dispersions of very fine-grained biotite flakes and very rare white mica.

Biotite forms fine-grained anhedral flakes that filled in the interstices between the subhedral plagioclase. In some cases the biotite forms fine-grained replacements of larger crystals that I tentatively interpret as magmatic biotite. In some cases, the biotite aggregates host subordinate amounts of fine-grained **titanite**.

Magnetite is fine grained and occupies interstitial positions between the subhedral plagioclase within the groundmass. In some cases, the magnetite is intergrown with titanite, and these intergrowths are spatially associated with the fine-grained domains of biotite (*shreddy* biotite).

Fine-grained crystal clusters of **titanite** occur within the fine-grained domains of biotite and are probably the product of the replacement of a magmatic, more titanium-rich biotite by the

fine-grained biotite.

Rare fine-grained (up to 0.2 mm) idiomorphic crystals of carbonate are spatially associated with the biotite-titanite replacement aggregates. The absence of a reaction to cold dilute (10%) HCl on the offcut probably indicates that the rare and fine-grained crystals of carbonate are dolomitic; however, I put forward this interpretation as highly tentative, as the carbonate occurs in very small amounts and the reaction to the acid may not have been properly detected with the hand lens.

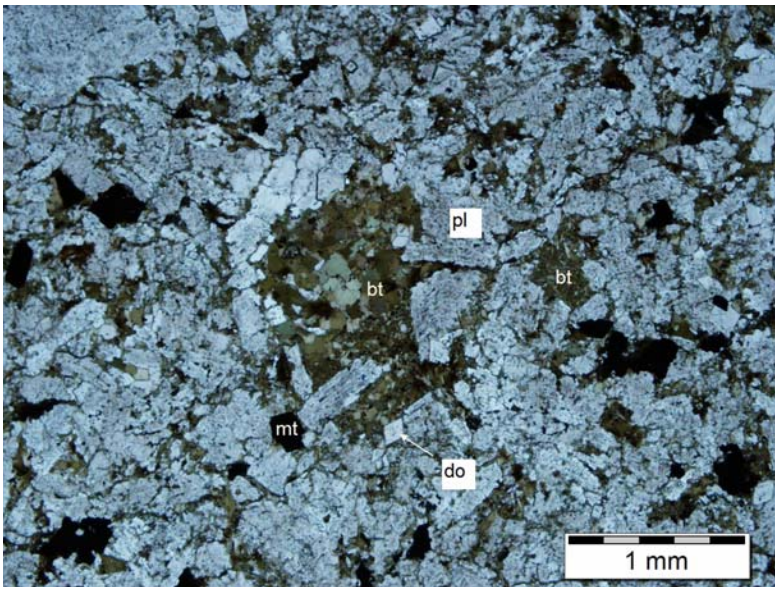

***Photomicrograph 54**: Fine-grained biotite (bt), magnetite (mt), and rare dolomite (do) filled in the interstices between subhedral plagioclase (pl). Plane-polarized transmitted light.*

Appendix E

List of Project Personnel

Name	Position	
Energizer Resources		
Craig Sherba	President	
Quentin Yarie	Vice-President	
James Master	Geologist	
Blake McLaughlin	Geologist	
Robert Dyer	Prospector	
Peter Olafson	Prospector	
Georgeen Saint-Pierre	Cook	
Martin Saint-Pierre	Camp manager	
Eric Steffler	Geomatic	
Jacob McKinnon	Logistics	
External Consultants		
Jean-Francois Montreui	Geochemist	
Rogerio Monteiro	Vectore	
Martin King	Geologist	
University of Manitoba		
Mostafa Fayek	Researcher	
Alfredo Camacho	Researcher	
Brandi Schabaga	Field assistant	
Additional Personnel		
Mike Ellis	Helicoper Pilot	